

ISSN 0390-6078

Volume 104

NOVEMBER

2019 - 11

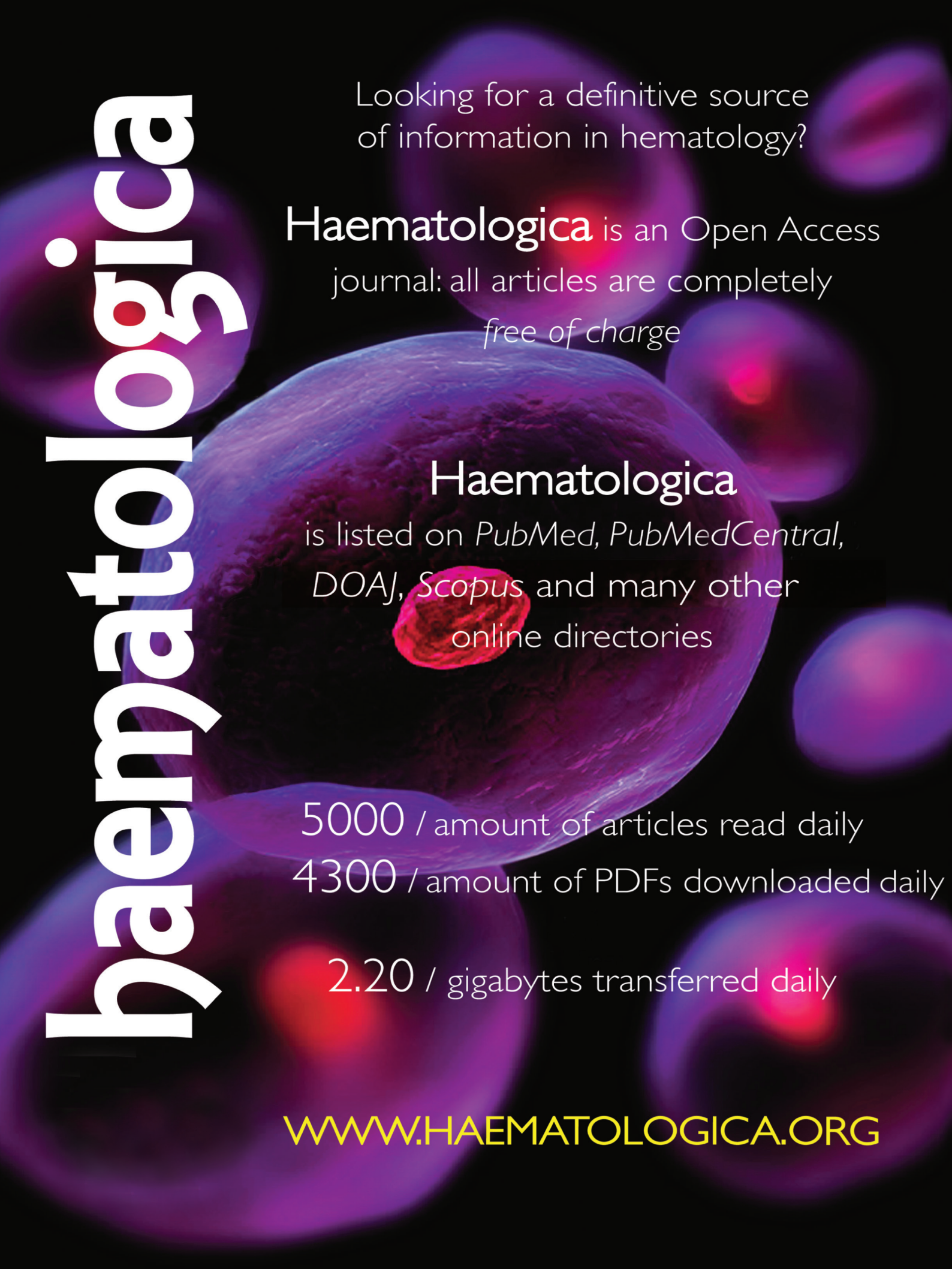


 **haematologica**

Journal of The Ferrata Storti Foundation

[www.haematologica.org](http://www.haematologica.org)

# haematologica

The background of the advertisement features a dark, almost black, field populated with various microscopic cells. A large, central cell is the most prominent, showing a textured, purple and blue surface. Surrounding it are several smaller, more rounded cells, some with bright red or pink centers, suggesting nuclei or specific organelles. The overall aesthetic is scientific and focused on hematology.

Looking for a definitive source  
of information in hematology?

**Haematologica** is an Open Access  
journal: all articles are completely  
*free of charge*

**Haematologica**  
is listed on *PubMed, PubMedCentral,*  
*DOAJ, Scopus* and many other  
online directories

5000 / amount of articles read daily

4300 / amount of PDFs downloaded daily

2.20 / gigabytes transferred daily

[WWW.HAEMATOLOGICA.ORG](http://WWW.HAEMATOLOGICA.ORG)

### **Editor-in-Chief**

Luca Malcovati (Pavia)

### **Managing Director**

Antonio Majocchi (Pavia)

### **Associate Editors**

Omar I. Abdel-Wahab (New York), H el ene Cav e (Paris), Simon Mendez-Ferrer (Cambridge), Pavan Reddy (Ann Arbor), Andreas Rosenwald (Wuerzburg), Monika Engelhardt (Freiburg), Davide Rossi (Bellinzona), Jacob Rowe (Haifa, Jerusalem), Wyndham Wilson (Bethesda), Paul Kyrle (Vienna), Swee Lay Thein (Bethesda), Pieter Sonneveld (Rotterdam)

### **Assistant Editors**

Anne Freckleton (English Editor), Cristiana Pascutto (Statistical Consultant), Rachel Stenner (English Editor), Kate O'Donohoe (English Editor), Ziggy Kennell (English Editor)

### **Editorial Board**

Jeremy Abramson (Boston); Paolo Arosio (Brescia); Raphael Bejar (San Diego); Erik Berntorp (Malm o); Dominique Bonnet (London); Jean-Pierre Bourquin (Zurich); Suzanne Cannegieter (Leiden); Francisco Cervantes (Barcelona); Nicholas Chiorazzi (Manhasset); Oliver Cornely (K oln); Michel Delforge (Leuven); Ruud Delwel (Rotterdam); Meletios A. Dimopoulos (Athens); Inderjeet Dokal (London); Herv e Dombret (Paris); Peter Dreger (Hamburg); Martin Dreyling (M unchen); Kieron Dunleavy (Bethesda); Dimitar Efremov (Rome); Sabine Eichinger (Vienna); Jean Feuillard (Limoges); Carlo Gambacorti-Passerini (Monza); Guillermo Garcia Manero (Houston); Christian Geisler (Copenhagen); Piero Giordano (Leiden); Christian Gisselbrecht (Paris); Andreas Greinacher (Greifswald); Hildegard Greinix (Vienna); Paolo Gresele (Perugia); Thomas M. Habermann (Rochester); Claudia Haferlach (M unchen); Oliver Hantschel (Lausanne); Christine Harrison (Southampton); Brian Huntly (Cambridge); Ulrich Jaeger (Vienna); Elaine Jaffe (Bethesda); Arnon Kater (Amsterdam); Gregory Kato (Pittsburg); Christoph Klein (Munich); Steven Knapper (Cardiff); Seiji Kojima (Nagoya); John Koreth (Boston); Robert Kralovics (Vienna); Ralf K uppers (Essen); Ola Landgren (New York); Peter Lenting (Le Kremlin-Bicetre); Per Ljungman (Stockholm); Francesco Lo Coco (Rome); Henk M. Lokhorst (Utrecht); John Mascarenhas (New York); Maria-Victoria Mateos (Salamanca); Giampaolo Merlini (Pavia); Anna Rita Migliaccio (New York); Mohamad Mohty (Nantes); Martina Muckenthaler (Heidelberg); Ann Mullally (Boston); Stephen Mulligan (Sydney); German Ott (Stuttgart); Jakob Passweg (Basel); Melanie Percy (Ireland); Rob Pieters (Utrecht); Stefano Pileri (Milan); Miguel Piris (Madrid); Andreas Reiter (Mannheim); Jose-Maria Ribera (Barcelona); Stefano Rivella (New York); Francesco Rodeghiero (Vicenza); Richard Rosenquist (Uppsala); Simon Rule (Plymouth); Claudia Scholl (Heidelberg); Martin Schrappe (Kiel); Radek C. Skoda (Basel); G erard Soci e (Paris); Kostas Stamatopoulos (Thessaloniki); David P. Steensma (Rochester); Martin H. Steinberg (Boston); Ali Taher (Beirut); Evangelos Terpos (Athens); Takanori Teshima (Sapporo); Pieter Van Vlierberghe (Gent); Alessandro M. Vannucchi (Firenze); George Vassiliou (Cambridge); Edo Vellenga (Groningen); Umberto Vitolo (Torino); Guenter Weiss (Innsbruck).

### **Editorial Office**

Simona Giri (Production & Marketing Manager), Lorella Ripari (Peer Review Manager), Paola Cariati (Senior Graphic Designer), Igor Ebuli Poletti (Senior Graphic Designer), Marta Fossati (Peer Review), Diana Serena Ravera (Peer Review)

### **Affiliated Scientific Societies**

SIE (Italian Society of Hematology, [www.siematologia.it](http://www.siematologia.it))

SIES (Italian Society of Experimental Hematology, [www.siesonline.it](http://www.siesonline.it))

## Information for readers, authors and subscribers

Haematologica (print edition, pISSN 0390-6078, eISSN 1592-8721) publishes peer-reviewed papers on all areas of experimental and clinical hematology. The journal is owned by a non-profit organization, the Ferrata Storti Foundation, and serves the scientific community following the recommendations of the World Association of Medical Editors ([www.wame.org](http://www.wame.org)) and the International Committee of Medical Journal Editors ([www.icmje.org](http://www.icmje.org)).

Haematologica publishes editorials, research articles, review articles, guideline articles and letters. Manuscripts should be prepared according to our guidelines ([www.haematologica.org/information-for-authors](http://www.haematologica.org/information-for-authors)), and the Uniform Requirements for Manuscripts Submitted to Biomedical Journals, prepared by the International Committee of Medical Journal Editors ([www.icmje.org](http://www.icmje.org)).

Manuscripts should be submitted online at <http://www.haematologica.org/>.

**Conflict of interests.** According to the International Committee of Medical Journal Editors (<http://www.icmje.org/#conflicts>), "Public trust in the peer review process and the credibility of published articles depend in part on how well conflict of interest is handled during writing, peer review, and editorial decision making". The ad hoc journal's policy is reported in detail online ([www.haematologica.org/content/policies](http://www.haematologica.org/content/policies)).

**Transfer of Copyright and Permission to Reproduce Parts of Published Papers.** Authors will grant copyright of their articles to the Ferrata Storti Foundation. No formal permission will be required to reproduce parts (tables or illustrations) of published papers, provided the source is quoted appropriately and reproduction has no commercial intent. Reproductions with commercial intent will require written permission and payment of royalties.

Detailed information about subscriptions is available online at [www.haematologica.org](http://www.haematologica.org). Haematologica is an open access journal. Access to the online journal is free. Use of the Haematologica App (available on the App Store and on Google Play) is free.

For subscriptions to the printed issue of the journal, please contact: Haematologica Office, via Giuseppe Belli 4, 27100 Pavia, Italy (phone +39.0382.27129, fax +39.0382.394705, E-mail: [info@haematologica.org](mailto:info@haematologica.org)).

Rates of the International edition for the year 2019 are as following:

	<i>Institutional</i>	<i>Personal</i>
<i>Print edition</i>	<i>Euro 700</i>	<i>Euro 170</i>

**Advertisements.** Contact the Advertising Manager, Haematologica Office, via Giuseppe Belli 4, 27100 Pavia, Italy (phone +39.0382.27129, fax +39.0382.394705, e-mail: [marketing@haematologica.org](mailto:marketing@haematologica.org)).

**Disclaimer.** Whilst every effort is made by the publishers and the editorial board to see that no inaccurate or misleading data, opinion or statement appears in this journal, they wish to make it clear that the data and opinions appearing in the articles or advertisements herein are the responsibility of the contributor or advisor concerned. Accordingly, the publisher, the editorial board and their respective employees, officers and agents accept no liability whatsoever for the consequences of any inaccurate or misleading data, opinion or statement. Whilst all due care is taken to ensure that drug doses and other quantities are presented accurately, readers are advised that new methods and techniques involving drug usage, and described within this journal, should only be followed in conjunction with the drug manufacturer's own published literature.

## Table of Contents

Volume 104, Issue 11: November 2019

### Cover Figure

---

Bone marrow smear from a patient with pure red cell aplasia showing marked erythroid hypoplasia with almost exclusive presence of early erythroid precursors. Courtesy of Prof. Rosangela Invernizzi.

### Editorials

---

- 2117** Notch in the niche: new insights into the role of Notch signaling in the bone marrow  
*Ashley N. Vanderbeck and Ivan Maillard*
- 2119** Time for revival of the red blood cell count and red cell mass in the differential diagnosis between essential thrombocythemia and polycythemia vera?  
*Hans Carl Hasselbalch*
- 2125** Standing at odds: mutated RAS and hematopoietic stem cells  
*Monica Nafria and Constanze Bonifer*
- 2128** Carfilzomib combination treatment as first-line therapy in multiple myeloma: where do we go from the Carthadex (KTd)-trial update?  
*Monika Engelhardt et al.*
- 2132** The child with immune thrombocytopenia: to treat or not to treat, is that still the question?  
*Nichola Cooper and Douglas B. Cines*

### Review Articles

---

- 2135** How I diagnose and manage Philadelphia chromosome-like acute lymphoblastic leukemia  
*Avraham Frisch and Yishai Ofran*
- 2144** Sequential and combination treatments with novel agents in chronic lymphocytic leukemia  
*Moritz Fürstenau et al.*

### Guideline Article

---

- 2155** Guidelines from the 2017 European Conference on Infections in Leukaemia for management of HHV-6 infection in patients with hematologic malignancies and after hematopoietic stem cell transplantation  
*Katherine N Ward et al.*

### Articles

---

#### *Hematopoiesis*

- 2164** A Tie2-Notch1 signaling axis regulates regeneration of the endothelial bone marrow niche  
*Lijian Shao et al.*

#### *Red Cell Biology & its Disorders*

- 2178** Deubiquitylase USP7 regulates human terminal erythroid differentiation by stabilizing GATA1  
*Long Liang et al.*
- 2189** Altered parasite life-cycle processes characterize *Babesia divergens* infection in human sickle cell anemia  
*Jeny R. Cursino-Santos et al.*

#### *Myeloproliferative Neoplasms*

- 2200** Distinguishing essential thrombocythemia *JAK2V617F* from polycythemia vera: limitations of erythrocyte values  
*Richard T. Silver and Spencer Krichevsky*

#### *Chronic Myeloid Leukemia*

- 2206** MR4 sustained for 12 months is associated with stable deep molecular responses in chronic myeloid leukemia  
*Simone Claudiani et al.*



## EMPOWER HIM TO STEP UP TO THE CHALLENGE

Jivi: a new rFVIII with  
the proven power to  
protect for up to 7 days

▼ **THIS MEDICINAL PRODUCT IS SUBJECT TO ADDITIONAL MONITORING.** Adverse events should be reported. Please report any suspected adverse reaction to the applicable national authority.

**JIVI 250 / 500 / 1000 / 2000 / 3000 IU POWDER AND SOLVENT FOR SOLUTION FOR INJECTION**  
(Refer to full SmPC before prescription.)

**COMPOSITION:** site specifically PEGylated recombinant human coagulation factor VIII, 250/500/1000/2000/3000 IU/vial (100/200/400/800/1200 IU/ml after reconstitution). **Excipients:** Powder: Sucrose, Histidine, Glycine, Sodium chloride, Calcium chloride dihydrate, Polysorbate 80, glacial acetic acid (for pH adjustment). Solvent: Water for injections. **INDICATION:** Treatment and prophylaxis of bleeding in previously treated patients  $\geq 12$  years of age with haemophilia A (congenital factor VIII deficiency). **CONTRAINDICATIONS:** Hypersensitivity to the active substance or to any of the excipients. Known allergic reactions to mouse or hamster proteins. **WARNINGS AND PRECAUTIONS:** Allergic type hypersensitivity reactions are possible. Hypersensitivity reactions could also be related to antibodies against polyethylene glycol (PEG). If symptoms of hypersensitivity occur, patients should be advised to discontinue the use of the medicinal product immediately and contact their physician. The formation of neutralising antibodies (inhibitors) to FVIII is a known complication in the

management of individuals with haemophilia A. A clinical immune response associated with anti-PEG antibodies, manifested as symptoms of acute hypersensitivity and/or loss of drug effect has been observed primarily within the first 4 exposure days. In patients with existing cardiovascular risk factors, substitution therapy with factor VIII may increase the cardiovascular risk. If a central venous access device (CVAD) is required, risk of CVAD-related complications including local infections, bacteraemia and catheter site thrombosis should be considered. **UNDESIRABLE EFFECTS:** *very common:* headache; *common:* hypersensitivity, insomnia, dizziness, cough, abdominal pain, nausea, vomiting, erythema (incl. erythema and erythema multiforme), rash (incl. rash and rash popular), injection site reactions (incl. injection site pruritus/rash and vessel puncture site pruritus), pyrexia; *uncommon:* FVIII inhibition (previously treated patients), dysgeusia, flushing, pruritus.

**ON PRESCRIPTION ONLY.**

**MARKETING AUTHORISATION HOLDER:**  
Bayer AG, 51368 Leverkusen, Germany.

**DATE OF REVISION OF THE UNDERLYING PRESCRIBING INFORMATION:**  
November 2018

PP-JIV-ALL-0215-1  
February 2019

  
Recombinant Factor VIII (damoctocog alfa pegol)

**LET'S GO**

*Acute Myeloid Leukemia*

**2215** Cell-intrinsic depletion of Aml1-ETO-expressing pre-leukemic hematopoietic stem cells by K-Ras activating mutation  
*Cristina Di Genua et al.*

**2225** Antileukemic activity and mechanism of action of the novel PI3K and histone deacetylase dual inhibitor CUDC-907 in acute myeloid leukemia  
*Xinyu Li et al.*

*Non-Hodgkin Lymphoma*

**2241** Prolonged survival in the absence of disease-recurrence in advanced-stage follicular lymphoma following chemo-immunotherapy: 13-year update of the prospective, multicenter randomized GITMO-IIL trial  
*Riccardo Bruna et al.*

*Chronic Lymphocytic Leukemia*

**2249** High prognostic value of measurable residual disease detection by flow cytometry in chronic lymphocytic leukemia patients treated with front-line fludarabine, cyclophosphamide, and rituximab, followed by three years of rituximab maintenance  
*José A. García-Marco et al.*

**2258** Utility of positron emission tomography-computed tomography in patients with chronic lymphocytic leukemia following B-cell receptor pathway inhibitor therapy  
*Anthony R. Mato et al.*

*Plasma Cell Disorders*

**2265** Phase II study of carfilzomib, thalidomide, and low-dose dexamethasone as induction and consolidation in newly diagnosed, transplant eligible patients with multiple myeloma; the carthadex trial  
*Ruth Wester et al.*

**2274** Bortezomib-based induction followed by stem cell transplantation in light chain amyloidosis: results of the multicenter HOVON 104 trial  
*Monique C. Minnema et al.*

*Platelet Biology & its Disorders*

**2283** Long-term treatment with romiplostim and treatment-free platelet responses in children with chronic immune thrombocytopenia  
*Michael D. Tarantino et al.*

**2292** Differences and similarities in the effects of ibrutinib and acalabrutinib on platelet functions  
*Jennifer Series et al.*

*Hemostasis*

**2300** Dynamic prediction of bleeding risk in thrombocytopenic preterm neonates  
*Susanna F. Fustolo-Gunnink et al.*

*Coagulation & its Disorders*

**2307** Christmas disease in a Hovawart family resembling human hemophilia B Leyden is caused by a single nucleotide deletion in a highly conserved transcription factor binding site of the *F9* gene promoter  
*Bertram Brenig et al.*

*Stem Cell Transplantation*

**2314** Role of interferon- $\gamma$  in immune-mediated graft failure after allogeneic hematopoietic stem cell transplantation  
*Pietro Merli et al.*

## Letters to the Editor

Letters are available online only at [www.haematologica.org/content/104/11.toc](http://www.haematologica.org/content/104/11.toc)

**e494** Clinical and morphological predictors of outcome in older aplastic anemia patients treated with eltrombopag  
*Bruno Fattizzo et al.*  
<http://www.haematologica.org/content/104/11/e494>

**e497** Correction of IVS I-110(G>A)  $\beta$ -thalassemia by CRISPR/Cas- and TALEN-mediated disruption of aberrant regulatory elements in human hematopoietic stem and progenitor cells  
*Petros Patsali et al.*  
<http://www.haematologica.org/content/104/11/e497>

**The origin of a name that reflects Europe's cultural roots.**

**Ancient Greek**

αἷμα [haima] = blood  
αἵματος [haimatos] = of blood  
λόγος [logos] = reasoning

**Scientific Latin**

haematologicus (adjective) = related to blood

**Scientific Latin**

haematologica (adjective, plural and neuter,  
used as a noun) = hematological subjects

**Modern English**

The oldest hematology journal,  
publishing the newest research results.  
2018 JCR impact factor = 7.570

- e502** Autoimmunity associated with Erdheim-Chester disease improves with BRAF/MEK inhibitors  
*Anais Roeser et al.*  
<http://www.haematologica.org/content/104/11/e502>
- e506** Evidence for prevention of renal dysfunction associated with primary myelofibrosis by cytoreductive therapy  
*Yasutaka Fukuda et al.*  
<http://www.haematologica.org/content/104/11/e506>
- e510** Response assessment in acute myeloid leukemia by flow cytometry supersedes cytomorphology at time of aplasia, amends cases without molecular residual disease marker and serves as an independent prognostic marker at time of aplasia and post-induction  
*Thomas Köhnke et al.*  
<http://www.haematologica.org/content/104/11/e510>
- e514** Increased neonatal level of arginase 2 in cases of childhood acute lymphoblastic leukemia implicates immunosuppression in the etiology  
*Amalie B. Nielsen et al.*  
<http://www.haematologica.org/content/104/11/e514>
- e517** Impact of corticosteroid pretreatment in pediatric patients with newly diagnosed B-lymphoblastic leukemia: a report from the Children's Oncology Group  
*Elizabeth A. Raetz et al.*  
<http://www.haematologica.org/content/104/11/e517>
- e521** PD-1 blockade as bridge to allogeneic stem cell transplantation in relapsed/refractory Hodgkin lymphoma patients: a retrospective single center case series  
*Beatrice Casadei et al.*  
<http://www.haematologica.org/content/104/11/e521>
- e523** Possibilities and limitations of an *in vitro* three-dimensional bone marrow model for the prediction of clinical responses in patients with relapsed multiple myeloma  
*Maaïke V.J. Braham et al.*  
<http://www.haematologica.org/content/104/11/e523>
- e527** Variation of rs3754689 at lactase gene and inhibitors in admixed Brazilian patients with hemophilia A  
*Luciana W. Zuccherato et al.*  
<http://www.haematologica.org/content/104/11/e527>

## Case Reports

Case Reports are available online only at [www.haematologica.org/content/104/11.toc](http://www.haematologica.org/content/104/11.toc)

- e530** Erdheim-Chester disease associated with chronic myelomonocytic leukemia harboring the same clonal mutation  
*Pauline Bonnet et al.*  
<http://www.haematologica.org/content/104/11/e530>
- e534** ALK-positive histiocytosis with *KIF5B-ALK* fusion in an adult female  
*Gaurav K. Gupta et al.*  
<http://www.haematologica.org/content/104/11/e534>
- e537** Clonally related duodenal-type follicular lymphoma and *in situ* follicular neoplasia  
*Dominik Nann et al.*  
<http://www.haematologica.org/content/104/11/e537>

## Comments

Comments are available online only at [www.haematologica.org/content/104/11.toc](http://www.haematologica.org/content/104/11.toc)

- e540** Acquisition of the recurrent Gly101Val mutation in *BCL2* confers resistance to venetoclax in patients with progressive chronic lymphocytic leukemia (Comment to Tausch *et al.*)  
*Jonathan Weiss et al.*  
<http://www.haematologica.org/content/104/11/e540>
- e541** Response to Comment by Amato T. *et al.*  
*Ilaria Del Giudice and Robin Foà*  
<http://www.haematologica.org/content/104/11/e541>
- e542** Response to Comment by Jonathan Weiss *et al.*  
*Eugen Tausch and Stephan Stilgenbauer*  
<http://www.haematologica.org/content/104/11/e541>

## ANNOUNCING THE AWARDEE 2019

**Dr. Ilaria Pagani**

*Leukaemia Research Group, Cancer Program, SAHMRI, Adelaide, Australia*



for her two year project on  
*'Use of machine learning to integrate clinical data and biomarkers to optimise prediction of TFR'*

"It is an honour and a pleasure to be the first John Goldman Research Prize Awardee. Receiving funding support from the European School of Haematology (ESH) is a privilege. It represents a critical step in my career towards becoming an independent investigator and provides the opportunity to build new collaborations.

My project aims to identify bioassays that can be integrated with clinical data in a machine learning system to develop a personalized predictive model for treatment free remission (TFR). I expect it will bring novel insights into the biology of TFR, opening new horizons toward the discovery of targeted therapies and improving TFR patient outcome."

## **APPLY FOR THE JOHN GOLDMAN AWARD 2020**

### **Submitted projects must:**

- aim to develop a method, algorithm or test to reliably identify patients able to benefit from treatment discontinuation, thereby significantly improving the probability of TFR success,
- demonstrate potential to improve healthcare standards for Chronic Myeloid Leukaemia (CML) patients or for patients suffering from other haematological malignancies.

The recipient of this annual award will receive a total of 80 000€ to finance or co-finance a research project on **Treatment Free Remission (TFR)**.

## **DEADLINE FOR SUBMISSION: MARCH 1, 2020**

**For further information:** Didi.jasmin@univ-paris-diderot.fr  
European School of Haematology (ESH)  
Saint-Louis Research Institute, Saint-Louis Hospital, Paris 75010, France  
[www.esh.org](http://www.esh.org)

## Notch in the niche: new insights into the role of Notch signaling in the bone marrow

Ashley N. Vanderbeck<sup>1-3</sup> and Ivan Maillard<sup>2-4</sup>

<sup>1</sup>VMD-PhD program at University of Pennsylvania School of Veterinary Medicine; <sup>2</sup>Immunology Graduate Group, University of Pennsylvania; <sup>3</sup>Abramson Family Cancer Research Institute, University of Pennsylvania and <sup>4</sup>Division of Hematology-Oncology, Department of Medicine, University of Pennsylvania, Philadelphia, PA, USA

E-mail: IVAN MAILLARD - [imaillard@penncmedicine.upenn.edu](mailto:imaillard@penncmedicine.upenn.edu)

doi:10.3324/haematol.2019.230854

In the bone marrow, specialized non-hematopoietic cells form unique microenvironmental niches that support and regulate the functions of hematopoietic stem and progenitor cells (HSPC).<sup>1</sup> Although many niche factors are well defined, the role of Notch signaling remains controversial (see Figure 1). Notch signaling in HSPC has been reported to regulate hematopoietic stem cell maintenance, suppress myelopoiesis, and promote megakaryocyte/erythroid cell development.<sup>2-7</sup> Mechanistically, most previous reports have been built on the concept that Notch receptors in HSPC interact with Notch ligands expressed in niche endothelial cells, or alternatively in other components of the bone marrow (including other non-hematopoietic and hematopoietic cells) (Figure 1, ① and ③). In contrast, several genetic models that inhibit all transcriptional effects of Notch signaling only in HSPC indicated that canonical Notch signaling is dispensable for HSPC maintenance, as well as myelo-erythropoiesis, under both homeostatic and stress conditions.<sup>8,9</sup> In this issue of *Haematologica*, Shao *et al.* bring a new perspective to this debate: perhaps Notch signaling is critical for stress hematopoiesis, but indirectly so by promoting niche cell regeneration through Notch ligand-receptor interactions that remain confined to the bone marrow endothelium<sup>10</sup> (Figure 1, ②).

Unlike secreted niche factors, Notch signaling is a juxtacrine communication pathway between signal-sending cells expressing agonistic Notch ligands (Dll1, Dll4, Jagged1, or Jagged2), and signal-receiving cells expressing Notch receptors (Notch1-4).<sup>11</sup> Ligand-receptor interactions induce regulated proteolytic cleavage of the Notch receptor, releasing the Notch intracellular domain which is then free to translocate to the nucleus and alter gene transcription in signal-receiving cells. Notch receptor and ligand expression has been reported in HSPC, osteoblasts, as well as key constituents of the perivascular niche, such as bone marrow endothelial cells.<sup>2,3,5,6,12,13</sup> Because Notch ligands and receptors are expressed by a variety of hematopoietic and non-hematopoietic cells, defining specific interactions that are biologically and functionally relevant for the HSPC microenvironment is a difficult task. For example, Notch signaling could be an important aspect of either endothelial-hematopoietic cell cross-talk (Figure 1, ①), or communication directly between endothelial niche cells (Figure 1, ②). Likewise, tight control of Notch signaling between hematopoietic cells is essential, as de-repression of *Dll4* in erythroblasts leads to premature differentiation of HSPC into T cells (Figure 1, ③).<sup>14</sup>

Shao *et al.* provide compelling new data indicating that activation of Notch signaling between endothelial cells is a key component of HSPC niche restoration after bone marrow injury. Hematopoietic cell recovery after chemotherapy

or radiation-induced myelosuppression relies heavily on regeneration of the endothelial cell network in order to support the hematopoietic compartment.<sup>6,15,16</sup> By examining the role of Notch signaling after injury using bone marrow chimeras and genetic models of cell type-specific Notch inactivation, Shao *et al.* dissected the functional importance of two possible routes of communication: cross-talk between endothelial cells and HSPC (Figure 1, ①), as well as Notch signaling between endothelial cells (Figure 1, ②) that indirectly affects HSPC. First, the authors demonstrated that endothelial restoration after bone marrow injury relied on activation of Notch signaling through the Notch1 receptor. Myeloablative stress induced by chemotherapy or irradiation caused lethal pancytopenia in mice harboring a hypomorphic *Notch1* allele. This phenotype was linked to a reduction in the number and frequency of HSPC after injury. Depletion of lymphoid-primed progenitors was also apparent. However, transplantation of *Notch1* hypomorphic HSPC into wildtype hosts revealed that the hematopoietic recovery defect was extrinsic to HSPC. Moreover, ablation of the *Notch1* receptor gene specifically in bone marrow endothelial cells using a tamoxifen-inducible VE-cadherin Cre<sup>ERT2</sup> transgene recapitulated the pancytopenia, morbidity and hematopoietic failure observed after injury in *Notch1* hypomorphic mice. Together, these data suggest a role for Notch signaling during endothelial cell recovery. To further investigate this hypothesis, the authors found that Notch signaling was promptly activated in bone marrow endothelial cells after injury. Tie2 activation, which is critical for endothelial cell regeneration, appeared to enhance Notch signaling by inducing expression of both Notch receptors and ligands in bone marrow endothelial cells.<sup>16</sup> Thus, Notch signals could be induced in bone marrow endothelial cells via a cross-talk involving expression of both Notch ligands and receptors in the endothelial compartment, with subsets of cells functioning as signal-sending and others as signal-receiving cells (Figure 1, ②).

When considering the impact of Notch signaling in the bone marrow, it has often been assumed that the only functionally significant signals for hematopoiesis are mediated directly between niche cells and HSPC. However, it is also possible that non-cell-autonomous signals regulate HSPC function indirectly, while cell-autonomous Notch signals are dispensable. This concept has been entertained previously, as transplantation of wildtype bone marrow cells into recipient mice lacking the capacity to undergo Notch-driven signals in the radioresistant host compartment led to altered hematopoietic differentiation, and eventually to myeloproliferative disease.<sup>17</sup> Likewise, Shao *et al.* highlight an often overlooked potential mechanism of HSPC regulation by showing that disruption of Notch signaling among endothe-

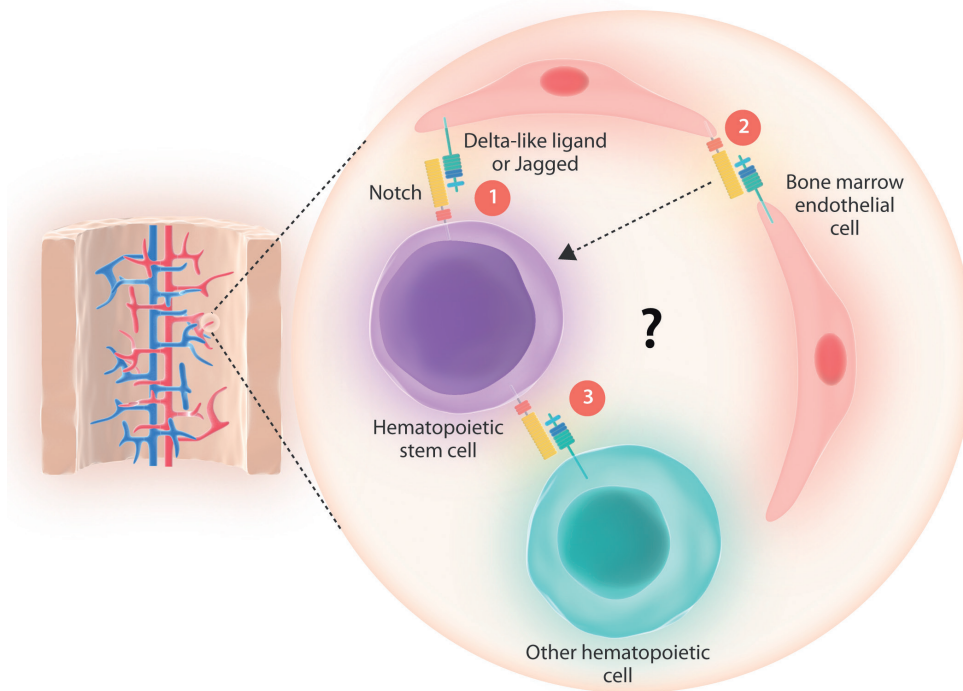


**Figure 1. Potential routes of Notch signaling in the bone marrow.** Notch ligands and receptors are expressed by both non-hematopoietic and hematopoietic cellular elements in the bone marrow. Potential routes of Notch signaling that influence the function of hematopoietic stem and progenitor cells (HSPC) include: (1) interaction of Notch ligands in endothelial cells with Notch receptors in HSPC; (2) Notch ligand-receptor interactions between endothelial cells, with indirect effects on HSPC; (3) interaction of Notch receptors in HSPC with Notch ligands expressed by other hematopoietic cells. In this issue, Shao *et al.* provide new data in support of Notch signaling within the endothelium (2) as a critical regulator of hematopoietic recovery after bone marrow injury.

lial cells impaired hematopoietic recovery (Figure 1, ②).

While the authors identified Notch signaling as an essential component of the response to injury in the bone marrow, the mechanisms underlying Notch's impact in this context remain unclear. The bone marrow injury response includes a complex interplay of signaling cues secreted from multiple cellular sources. For example, VEGF-A, as well as Angiopoietin-1, are thought to control regeneration and reassembly of the bone marrow vasculature.<sup>15,16</sup> Importantly, the cellular source, role and regulation of individual factors may differ markedly between steady-state conditions and after bone marrow injury.<sup>18</sup> Shao *et al.* found that lack of Notch activation after injury increased apoptosis among endothelial cells, suggesting that Notch functions as a pro-survival cue. During angiogenesis, Notch inhibits proliferation of endothelial cells and ultimately allows for proper formation of functional blood vessels.<sup>19</sup> Thus, Notch signaling may restrict bone marrow endothelial cell activation and entry into the cell cycle, ultimately protecting the endothelium from the DNA damage induced by chemotherapy and irradiation. Alternatively, Notch may have a more direct role in re-establishing the niche, analogous to its involvement in "tip/stalk" cell crosstalk during neoangiogenesis.<sup>19</sup> Sprouting of new vessels requires a delicate balance of tip/stalk cell differentiation in which tip endothelial cells lead new vessel sprouting for invasion and migration. Tip cells are highly responsive to VEGF, require a high glycolytic flux and, although they express Dll4, do not

actively engage Notch signaling. On the other hand, stalk cells undergo high levels of Notch signaling which reduces expression of VEGFR2/3 and glycolytic enzymes, ultimately helping to repress the tip cell fate while maintaining stalk cell identity.<sup>19</sup> Thus, Notch activity may be important during early stages of bone marrow vasculature reassembly by regulating pathways similar to tip/stalk cell differentiation and by integrating angiogenic cues with the metabolic status of the endothelium. Finally, it is possible that Notch acts through yet to be discovered mechanisms unique to the bone marrow vasculature, whose regulation during steady-state conditions and after injury remains only partially understood.

Notch signaling may also have roles in hematopoiesis beyond its functions in the HSPC niche. *Dll4* inactivation in mesenchymal progenitor cells was reported to decrease bone marrow common lymphoid progenitor numbers and impair thymopoiesis.<sup>12</sup> Similarly, endothelial *Dll4* inactivation was recently linked to decreased lymphoid progenitors and enhanced myelopoiesis.<sup>5</sup> Consistent with these data, Shao *et al.* reported a cell-autonomous hematopoietic cell defect in T-cell production by mice that received transplanted *Notch1* hypomorphic HSPC, which was associated with decreased numbers of lymphoid progenitors in the bone marrow. Altogether, these data leave room for the possibility of a bone marrow niche that provides prethymic Notch signals during early lymphoid development, in addition to the effects of Notch signaling in niche regeneration.

As another important consideration, individual Notch ligand/receptor pairs may have unique effects on hematopoietic function. Shao *et al.* focus on signaling through the Notch1 receptor, which is the predominant receptor expressed in endothelial cells. However, both Notch1 and Notch2 are present in HSPC, and a specific role for Notch2 in HSPC differentiation following bone marrow injury has been reported.<sup>5</sup> Recent advances in the biophysics of Notch signaling could provide explanations as to how engagement of distinct receptor-ligand pairs can lead to divergent functions.<sup>20</sup> Nandagopal *et al.* showed that Dll1/Notch1 signaling induced pulsatile Notch activation whereas Dll4/Notch1 signaling resulted in sustained Notch activation during myogenesis, allowing for ligand discrimination. Additional differences in the signaling potential of specific ligand-receptor pairs may also exist.<sup>21</sup> Whether similar biophysical and functional differences apply to the effects of individual Notch receptors in hematopoietic progenitors remains to be investigated.

Altogether, Shao *et al.* provide compelling data indicating that activation of Notch signaling between bone marrow endothelial cells is necessary for niche regeneration, as well as efficient and timely hematopoietic recovery after bone marrow injury. With a panoply of Notch receptors and ligands expressed throughout the bone marrow, Notch has the potential to regulate a number of communication channels between and among bone marrow cellular compartments. Future research should parse these cellular conversations to fully understand how Notch signaling helps to orchestrate hematopoiesis.

## References

- Crane GM, Jeffery E, Morrison SJ. Adult haematopoietic stem cell niches. *Nat Rev Immunol.* 2017;17(9):573-590.
- Poulos MG, Guo P, Kofler NM, et al. Endothelial Jagged-1 is necessary for homeostatic and regenerative hematopoiesis. *Cell Rep.* 2013;4(5):1022-1034.
- Varnum-Finney B, Halasz LM, Sun M, Gridley T, Radtke F, Bernstein ID. Notch2 governs the rate of generation of mouse long- and short-term repopulating stem cells. *J Clin Invest.* 2011;121(3):1207-1216.
- Oh P, Lobry C, Gao J, et al. In vivo mapping of notch pathway activity in normal and stress hematopoiesis. *Cell Stem Cell.* 2013;13(2):190-204.
- Tikhonova AN, Dolgalev I, Hu H, et al. The bone marrow microenvironment at single-cell resolution. *Nature.* 2019;569(7755):222-228.
- Butler JM, Nolan DJ, Vertes EL, et al. Endothelial cells are essential for the self-renewal and repopulation of Notch-dependent hematopoietic stem cells. *Cell Stem Cell.* 2010;6(3):251-264.
- Klinakis A, Lobry C, Abdel-Wahab O, et al. A novel tumour-suppressor function for the Notch pathway in myeloid leukaemia. *Nature.* 2011;473(7346):230-233.
- Maillard I, Koch U, Dumortier A, et al. Canonical notch signaling is dispensable for the maintenance of adult hematopoietic stem cells. *Cell Stem Cell.* 2008;2(4):356-366.
- Duarte S, Woll PS, Buza-Vidas N, et al. Canonical Notch signaling is dispensable for adult steady-state and stress myelo-erythropoiesis. *Blood.* 2018;131(15):1712-1719.
- Shao L, Sottoriva K, Palasiewicz K, et al. A Tie2-Notch1 signaling axis regulates regeneration of the endothelial bone marrow niche. *Haematologica.* 2019;104(11):2164-2177.
- Kopan R, Ilagan MX. The canonical Notch signaling pathway: unfolding the activation mechanism. *Cell.* 2009;137(2):216-233.
- Yu VW, Saez B, Cook C, et al. Specific bone cells produce DLL4 to generate thymus-seeding progenitors from bone marrow. *J Exp Med.* 2015;212(5):759-774.
- Guo P, Poulos MG, Palikuqi B, et al. Endothelial jagged-2 sustains hematopoietic stem and progenitor reconstitution after myelosuppression. *J Clin Invest.* 2017;127(12):4242-4256.
- Lee SU, Maeda M, Ishikawa Y, et al. LRF-mediated Dll4 repression in erythroblasts is necessary for hematopoietic stem cell maintenance. *Blood.* 2013;121(6):918-929.
- Hooper AT, Butler JM, Nolan DJ, et al. Engraftment and reconstitution of hematopoiesis is dependent on VEGFR2-mediated regeneration of sinusoidal endothelial cells. *Cell Stem Cell.* 2009;4(3):263-274.
- Kopp HG, Avezilla ST, Hooper AT, et al. Tie2 activation contributes to hemangiogenic regeneration after myelosuppression. *Blood.* 2005;106(2):505-513.
- Wang L, Zhang H, Rodriguez S, et al. Notch-dependent repression of miR-155 in the bone marrow niche regulates hematopoiesis in an NF- $\kappa$ B-dependent manner. *Cell Stem Cell.* 2014;15(1):51-65.
- Himburg HA, Termini CM, Schluskel L, et al. Distinct bone marrow sources of pleiotrophin control hematopoietic stem cell maintenance and regeneration. *Cell Stem Cell.* 2018;23(3):370-381.e5.
- Tetzlaff F, Fischer A. Control of blood vessel formation by notch signaling. *Adv Exp Med Biol.* 2018;1066:319-338.
- Nandagopal N, Santat LA, LeBon L, Sprinzak D, Bronner ME, Elowitz MB. Dynamic ligand discrimination in the notch signaling pathway. *Cell.* 2018;172(4):869-880.e19.
- Tveriakhina L, Schuster-Gossler K, Jarrett SM, et al. The ectodomains determine ligand function in vivo and selectivity of DLL1 and DLL4 toward NOTCH1 and NOTCH2 in vitro. *Elife.* 2018;7.

## Time for revival of the red blood cell count and red cell mass in the differential diagnosis between essential thrombocythemia and polycythemia vera?

Hans Carl Hasselbalch

Department of Hematology, Zealand University Hospital, Roskilde, Denmark

E-mail: HANS CARL HASSELBALCH - hans.hasselbalch@gmail.com

doi:10.3324/haematol.2019.229039

### Red blood cell indices, red blood cell mass and bone marrow biopsy in the differential diagnosis between essential thrombocythemia and polycythemia vera?

The correct diagnostic classification of the Philadelphia-negative chronic myeloproliferative neoplasms (MPN) in the three subcategories, essential thrombocythemia (ET), polycythemia vera (PV) and primary myelofibrosis (PMF), relies upon diagnostic criteria that aim at minimizing misclassification.<sup>1</sup> Several reports have addressed the issue that *JAK2V617F* positive "ET"

patients are frequently misclassified since they actually have a diagnosis of PV.<sup>2-8</sup> This misclassification is partly based upon the use of the hemoglobin (Hb) concentration as a surrogate marker for the red cell mass (RCM), irrespective of the fact that the Hb concentration is influenced by iron deficiency, which is prevalent in PV patients. Indeed, these concerns have been addressed and confirmed in several studies showing that a high proportion of ET patients (approx. 45-65%) did not meet the World Health Organization (WHO) diagnostic criterion

of an elevated Hb, despite an increased Cr-51 RCM.<sup>5,7</sup> However, despite the convincing data published in 2005 by Johansson *et al.*,<sup>5</sup> these concerns were not translated into the revised 2007 WHO diagnostic recommendations. These recommendations, therefore, remained unchanged<sup>9</sup> and were addressed and met by alternative diagnostic approaches in ET, PV and PMF patients.<sup>2</sup> In their 2013 study,<sup>3</sup> Silver *et al.* for the first time prospec-

tively evaluated the accuracy of the 2007 WHO criteria for diagnosing PV, especially in “early-stage” patients. This and other studies support the latest updated WHO criteria (2016) for diagnosing MPN,<sup>19</sup> which included these novel data with regard to the inaccuracy of the Hb-concentration, and even the hematocrit (HCT), in the differential diagnosis between ET and PV patients by lowering the Hb/HCT thresholds (> 16.5 g/dL/0.49 in men and > 16 g/dL/0.48 in women).<sup>1</sup> Thus, the 2013 Silver study in a prospective setting and with a median 5-year follow up time convincingly demonstrated that the surrogate markers Hb and HCT are inadequate in the assessment of an increased RCM for early PV cases, since 64.3%, 28.5%, and 28.5% of their patients would not have been diagnosed as PV using Hb, HCT, and either Hb or HCT values, respectively.<sup>3</sup> Importantly, of the 28 patients with an increased RCM in their study, 18 did not meet the WHO 2007 criteria for an increased Hb value. For the four women, the median Hb count was 15.2 g/dL (range: 14.4-16.4 g/dL) and for the 14 men 17.2 g/dL (range: 15.6-18.1 g/dL), respectively. Similarly, eight patients (1 woman and 7 men) did not meet the WHO criteria for an increased HCT value, being 44.3% for the woman, and for the seven men the median HCT was 48.5% (range: 45.7-49.4 %).<sup>3</sup> Silver *et al.* also highlighted the value of bone marrow (BM) morphology<sup>3</sup> as emphasized in the WHO classification. Accordingly, this study supported previous reports by Johansson *et al.*,<sup>5</sup> Cassinat *et al.*,<sup>6</sup> and Alvarez-Larran *et al.*<sup>7</sup> which all revived ancient knowledge, written by the Polycythemia Vera Study Group (PVSG), and underscoring the inaccuracy of the Hb and the HCT values for diagnosing PV and the need for RCM measurement instead.<sup>10</sup> This has since fostered intense debate in several reviews and perspective papers expressing conflicting opinions. On the one hand, some authors believe that only RCM measurements can reliably distinguish PV from other MPN,<sup>2-4,11</sup> while others would disregard RCM measurements,<sup>12-15</sup> arguing that Hb/HCT thresholds should be used as surrogate markers for RCM measurements. This lively debate has recently been further fueled by a comprehensive and scholarly review on MPN, emphasizing the urgent need for RCM investigations to distinguish PV from other MPN,<sup>16</sup> adding that BM morphology has no place in the distinction of PV from other MPN subtypes.<sup>16</sup> Others have highlighted the importance of BM morphology in PV and its usefulness in distinguishing between ET and PV.<sup>3,17-21</sup> A very recent study has established a clear-cut distinction between ET and PV, and, therefore, also the reproducibility of BM morphology in so-called masked polycythemia vera (mPV) and its differentiation from ET.<sup>21</sup> The disease entity mPV will be further addressed below.

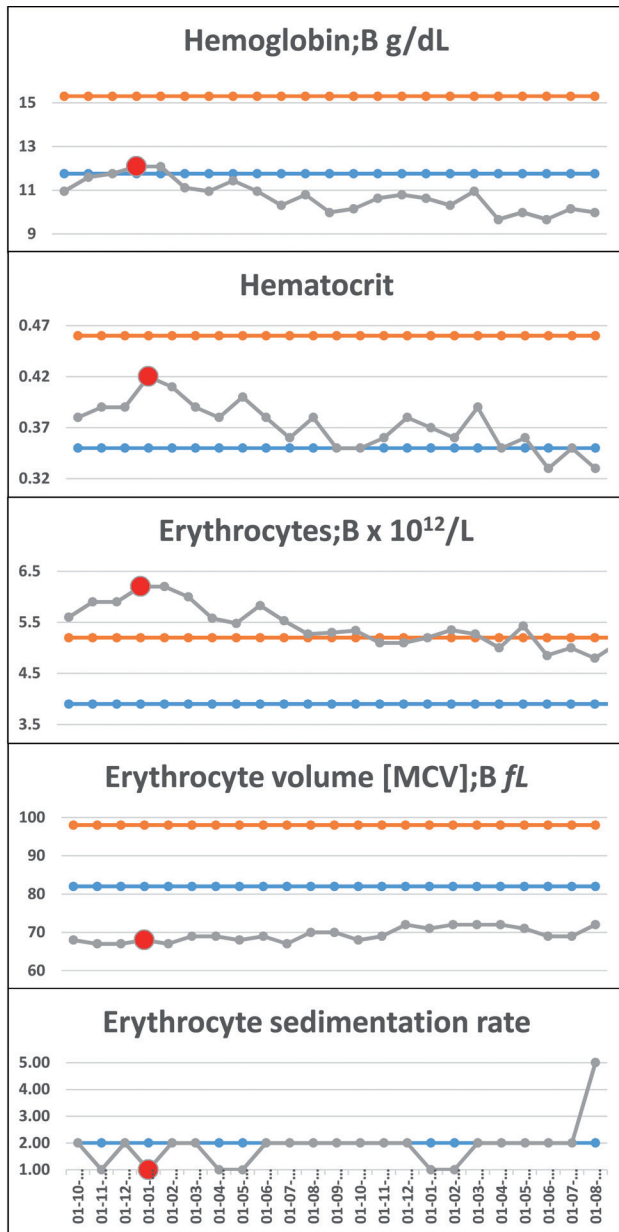


**Figure 1.** Association between the hemoglobin (Hb)-concentration, hematocrit, red blood cell (RBC) count and mean corpuscular volume (MCV) values in a 76-year old woman with polycythemia vera. The Figure illustrates that: (i) the RBC count is a more accurate indicator of erythrocytosis than the Hb-concentration and the hematocrit; (ii) that this dissociation is consequent to iron deficiency as evidenced by a lowered MCV; and (iii) the hyperviscosity state due to the raised RBC count is reflected in a low erythrocyte sedimentation rate (SR) (< 1 or 2 mm/h) (normal range: 2-20 mm/h). The need for phlebotomies in this patient was monitored by the elevated RBC count and the lowered SR, and tightly associated with the emergence of headache, which immediately resolved after phlebotomy.

**Do the revised and lowered thresholds for Hb/HCT levels unmask undiagnosed PV patients in the general population when “potential PV patients” are being referred?**

In 2014, the issue as to which of the three red cell parameters, Hb, HCT or RCM, to use as the diagnostic hallmark of PV was thoroughly reviewed by Barbui *et al.* They also critically addressed the validity and applicability of the three major diagnostic classification systems for

PV as proposed by the PVSG, the British Committee for Standards in Hematology (BCSH), and the WHO.<sup>13</sup> It was suggested either to reduce the thresholds for the Hb-concentration, or to include the HCT as a major diagnostic criterion in association with the *JAK2V617F* mutation. In this review, the existence of prodromal (latent PV-disease), named “masked” PV and defined by Barbui *et al.*,<sup>13</sup> was also addressed, covering patients not meeting the required Hb or HCT threshold levels as defined in the WHO and BCSH criteria.<sup>22,23</sup> With regards to the impact of lowering the Hb and the HCT thresholds for PV, influenced by the above studies,<sup>3,5-8,22,23</sup> the 2016 revised WHO criteria have not resolved the conflicting opinions,<sup>24,25</sup> as recently addressed and discussed in depth.<sup>26,27</sup> However, very interestingly, applying the lower Hb thresholds as reported by the WHO 2016 criteria in the Canadian population, Ethier *et al.* found an Hb value at or above the threshold in 4.1% of all complete blood counts from unselected males and in 0.35% of females. These figures increased the incidence of “potential PV patients” by up to 12-fold in males and 3-fold in females. The same pattern was demonstrated when including the neutrophil and platelet count, implying that up to 60 times more males and three times more women would be suspected of suffering from MPN and would accordingly require diagnostic investigations.<sup>24</sup> According to the screening procedure in clinical practice as described by Rumi and Cazzola,<sup>25</sup> the best compromise between the need for an early diagnosis of PV patients and the risk of excessively expanding the number of potential PV patients would be a threshold of 17 g/dL in men. Applying this Hb cut-off value, Barbui *et al.* found that 14% of their 375 patients presenting with WHO-defined PV did not meet the 2016 criteria.<sup>26</sup> In the context of screening procedures in clinical practice and which blood cell counts to use, according to the Canadian data, the Hb/HCT thresholds as defined in the 2016 WHO criteria will markedly increase the number of individuals with suspected PV in the general population.<sup>24</sup> Given this, it is important to note that a very recent Danish study has found MPN to be massively underdiagnosed with an estimate of 10,000 undiagnosed MPN in Denmark, corresponding to approximately 550,000 US citizens having an undiagnosed MPN and accordingly being at a considerable risk of thrombosis.<sup>28</sup> In this perspective, it might be much more cost-effective to screen high-risk MPN individuals and obtain a diagnosis earlier rather than later when the individual has already suffered one or more potentially life-invalidating thrombotic events before being diagnosed with ET or PV.<sup>28</sup>

### Consequences of misclassification of PV as ET

There are several consequences of misclassifying PV patients as ET.

1) Misclassification of *JAK2V617F* positive ET patients as ET instead of PV implies that these patients are not phlebotomized and are, therefore, exposed to an increased risk of potentially life-invalidating or life-threatening thrombotic complications due to the increased RCM. This is not a trivial risk, in particular in those patients aged <60 years without a prior thrombosis but with leukocytosis and platelet counts < 1500 × 10<sup>9</sup>/L, since these patients are categorized as “low-risk” accord-

ing to international guidelines and are not offered cytoreductive treatment, irrespective of the fact that both leukocytes and platelets are deeply involved in the development of atherothrombosis,<sup>29-33</sup> the *JAK2V617F* mutation promotes atherothrombosis, being associated with e.g. transitory cerebral ischemia, completed stroke and ischemic heart disease, and leukocytosis *per se* is considered a risk factor for thrombosis in the background population,<sup>34</sup> and a causative factor for thrombosis in ET and PV patients.<sup>35</sup> Importantly, the most recent studies, including a meta analysis study, have provided evidence that leukocytosis is a risk factor for thrombosis in the MPN-population as well.<sup>36,37</sup>

2) Misclassifying *JAK2V617F* positive “ET” patients as “ET” instead of PV has a huge impact on any prognostic model that compares the prognosis of ET and PV patients, the potential outcome being that *JAK2V617F* positive ET patients have an inferior prognosis as compared to those who are *JAK2V617F* negative or *CALR*-positive.<sup>38</sup> In several published studies these differences might be explained by the fact that PV patients - not being phlebotomized - have been included in the ET-cohorts. This may also hold true for mPV patients who have an increased risk of thrombosis (young patients)<sup>39</sup> and poorer survival than PV patients. This is likely explained by the fact that several mPV patients have not been phlebotomized despite an expanded RCM.

3) Results from studies on safety and efficacy of any drug, both those conventionally used [e.g. hydroxyurea (HU), interferon- $\alpha$ 2 (IFN) and anagrelide] and novel agents such as ruxolitinib or experimental drugs (in clinical trials for future approval for the indication of ET or PV) may be severely undermined, impossible to interpret, and therefore not credible.

4) Building future therapeutic recommendations and prognostic models on a diagnostic platform that does not take into account the true nature of a disease (e.g. a higher rate of thrombosis in PV than ET, a higher rate of transformation to myelofibrosis and acute myelogenous leukemia in PV than in ET, a reduced life expectancy in PV as compared to ET) due to diagnostic misclassification undermines our current understanding and concepts on MPN in highly important issues. These include pathogenetic mechanisms for disease evolution both in terms of molecular phenotypes, clinical phenotypes and associations between them, diagnostic classification in the biological continuum from early cancer stages (ET, PV) to the advanced myelofibrosis stage, and, not least, when and how to treat MPN. The cornerstone treatment of PV is phlebotomies, carried out to alleviate the hyperviscosity state due to an expanded RCM and thereby to reduce the risk of the deadly thrombosis seen in median survival figures for PV patients of 18 months without such treatment. This approach may, however, be misguided by using only the Hb concentration and the HCT as these are profoundly influenced by the iron-deficient state in patients with PV and also in *JAK2V617F* positive ET patients in whom erythropoietin (Epo) and ferritin levels and the mean corpuscular volume (MCV) values have been repeatedly reported to be lower than in *JAK2V617F* negative ET patients.<sup>40</sup>

5) Without an estimation of RCM and plasma volume

in the diagnostic setting of *JAK2V617F* positive ET and PV, the transitional stage between ET and PV may be wrongly described as a new disease entity within MPN.<sup>22</sup> Thus, it is tempting to speculate whether the “novel” disease entity (mPV) would ever have been born, if arguing that a large proportion of these mPV patients are only “masked” as long as RCM is not being estimated. As discussed above, reports on masked PV<sup>22,25</sup> were influential in lowering the Hb/HCT thresholds in the 2016 WHO classification of MPN.<sup>1,27</sup> This was defined as a new *JAK2V617F*-positive entity with a phenotype mimicking ET (isolated thrombocytosis) but, as in PV, associated to endogenous erythroid colony formation (EEC) or the BM features of PV, which had previously been described as latent or inapparent PV.<sup>41,42</sup> The revised WHO 2016 classification was, among others, based upon the mPV studies, which defined threshold values as optimal cut-off levels for distinguishing *JAK2V617F* ET from mPV (Hb 16.5 g/dL/HCT 0.49 in men and 16 g/dL/HCT 48 % in women, respectively)<sup>43</sup> and were subsequently validated in larger cohort studies.<sup>15,44</sup>

Very recently, the notion that mPV may not be a novel disease entity but has emerged consequent to the inaccuracy of diagnosing PV in the absence of an estimation of RCM has been supported by a large French single center study of 2,480 RCM estimations in patients with *JAK2V617F* positive ET, “masked PV”, and PV.<sup>45</sup> This study showed that patients with mPV actually have an increased RCM and are, therefore, easily “unmasked” and revealed to be true PV once RCM is estimated.<sup>45</sup> Thus, these mPV patients share clinical and biological features with both ET and PV, with a median age, platelet, Hb and leukocyte levels comparable to those of ET patients, and at the same time classic PV features, (which, in addition to the increased RCM, also include lower Epo level and lower MCV), and have splenomegaly more frequently than ET patients.<sup>45</sup> Accordingly, patients being described as mPV nicely present a picture of a diagnosis of MPN as a moving target that is highly dependent on the time point for diagnosis in the biological continuum from early *JAK2V617F* positive ET to overt PV.

The mPV story underscores the urgent need for a renaissance of the RCM and plasma volume assessment in these patients, since otherwise *JAK2V617F* positive “ET” patients and mPV patients will not receive adequate treatment by phlebotomies and so will obviously also have an increased risk of thrombosis.<sup>38,39</sup> The French and other studies, including those pioneered by Silver and Spivak, also put into perspective the view that it is indeed possible to incorporate RCM estimations into ‘good clinical practice’ in the differential diagnosis between *JAK2V617F* positive ET and PV.<sup>2-8,16,45</sup> However, as noted above, there are still conflicting opinions as to the need for RCM measurements in distinguishing between patients with *JAK2V617F* positive ET, mPV and overt PV.<sup>2,4,11-15</sup> Of note, a very recent study showed that when applying the 2016 WHO criteria, increased RCM was significantly associated with increased Hb/HCT (93.8%/94.6%),<sup>15</sup> thus supporting the 2016 WHO criteria for PV, implying Hb/HCT values should be used as surrogate markers for RCM measurements.<sup>15</sup> In this study, the importance of BM morphology for a diagnosis of PV was also highlighted.<sup>15</sup>

### Red blood cell count as a surrogate marker for red cell mass?

Recently, Michiels *et al.* underscored the importance of RBC count in addition to a BM biopsy as a powerful tool to differentiate between ET and PV.<sup>8</sup> In their study, the diagnostic value of RCM in relation to RBC count, Hb and HCT in discriminating between *JAK2V617F* ET and PV was assessed. The best correlation was found between RBC count and RCM. Thus, at RCM above 30 mL/kg the RBC count was above  $5.8 \times 10^{12}/L$ , and this diagnosed PV in all their patients. All *JAK2V617F* ET patients had a normal RCM and a RBC count below  $5.8 \times 10^{12}/L$ . It was concluded that a RBC count within the normal range ( $< 5.8 \times 10^{12}/L$  in males and  $< 5.6 \times 10^{12}/L$  in females) enables *JAK2V617F* ET to be distinguished from prodromal PV and overt PV. Thus, they also concluded that the RBC count and a BM biopsy might obviate the need for RCM measurement.<sup>8</sup>

### Are hemoglobin and hematocrit values imperfect surrogate markers for red cell mass?

In this issue of *Haematologica*, Silver *et al.* convincingly confirm the urgent need to investigate *JAK2V617F* positive ET patients using RCM estimations,<sup>46</sup> repeating the important message that a normal Hb or HCT value does not signify a normal RCM in MPN.<sup>2-8,10,11,16</sup> Based upon *JAK2V617F* positivity, chromium-51 RCM, and BM biopsy morphology, 83 and 39 patients were diagnosed with PV and ET, respectively. Chromium-51 RCM separated PV from ET *JAK2V617F*, whereas red cell values (Hb, HCT, RBC count) overlapped in 25.0-54.7%. The authors concluded that a significant proportion of PV patients may be underdiagnosed by using only red cell values. Of note, using ROC analyses, the authors found threshold values for the Hb / HCT coincidentally similar to the WHO 2016 criteria. Furthermore, it was concluded that (without isotope studies) BM biopsies and serum erythropoietin values should become mandatory since they improve diagnostic accuracy. In this perspective, the paper by Silver *et al.* is highly relevant and timely. It carries a novel approach into the future and will hopefully promote an optimal classification of MPN by a renaissance of the use of RCM estimations (the “gold standard” for discriminating *JAK2V617F* ET from PV) as a highly important tool to ensure a correct diagnostic classification of MPN. This will be a major scientific step forward in improving good clinical practice in MPN patients. It will reintroduce RCM and plasma volume estimations as essential for correct diagnostic classification of MPN, at least in *JAK2V617F* positive “ET” patients. In patients with huge splenomegaly but still a low normal or even lowered HCT, in the transitional stages between PV and post-polycythemic myelofibrosis, a RCM estimation may reveal the true nature of the disease as PV and accordingly a need for phlebotomies due to an expanded RCM in patients who still present a normal Hb-concentration and normal HCT consequent to hemodilution due to an expanded plasma volume. As previously noted, RCM estimation in *JAK2V617F* positive ET patients will likely reduce the risk of thrombosis in a substantial proportion of “ET” patients since they will be correctly classified as PV and will, therefore, receive treatment with phle-

botomies. Additionally, these patients will then also have the opportunity to be treated with IFN in cases in which the institution does not include ET patients as an indication for being treated with IFN but does so if the patient has PV. This will be even more important when the new IFN-drug, ropeginterferon  $\alpha$ -2b, has been licensed for use in newly diagnosed PV in Europe, and hopefully soon in the US as well.<sup>47</sup> Based upon the above considerations, the paper by Silver *et al.* is also of utmost importance since by diagnosing many more *JAK2V617F* ET patients correctly as PV, their findings may offer more patients the opportunity to be treated with IFN, which is the only agent that has shown to be disease modifying. In fact, in a subset of patients with early MPN disease (ET and PV), after approximately five years of IFN therapy it was seen that this approach may induce minimal residual disease (MRD), with normal cell counts, normal spleen size, a normal BM, and no detectable *JAK2V617F* mutation, representing an MRD stage that may even be sustained after interrupting IFN for up to three years.<sup>48</sup>

Considering the findings by Silver *et al.* and Michiels *et al.*, in some of their previous papers the RBC count is the most valuable parameter and is better than Hb-concentration and hematocrit when considering the equation:  $HCT = RBC \text{ count} \times MCV$ , and taking into account that several PV patients have lowered MCV which accordingly lowers the HCT and wrongly dictates that a phlebotomy is not needed, irrespective of the fact that the RBC count is increased<sup>49</sup> (Figure 1). In this context, it is also important to note that erythrocytosis in PV usually induces plasma volume expansion<sup>4,16,50</sup> which may mask the true HCT, implying that the HCT in many PV patients, especially women, appears to be normal.<sup>2,4,16,41,50</sup>

These considerations are not only relevant at the time of diagnosis but also during the course of PV when several patients may not be phlebotomized when only using HCT and elevated RBC count is not taken into consideration (Figure 1). On the contrary, hydroxyurea (HU)-treated patients may be unnecessarily phlebotomized due to an HU-induced increase in MCV and accordingly also an increase in the HCT, although the RBC count is normal.

Hopefully, based upon previous reports on the need of the RCM in the diagnosis of MPN,<sup>2,7,10,11,16,49,50</sup> and the most recent studies by Silver *et al.* and the French study discussed above, consideration of the RCM will be revived at many more MPN centers worldwide. Such efforts are not only expected to improve quality of life of the large proportion of undiagnosed PV patients amongst *JAK2V617F* positive ET patients, but likely prognosis as well, since they will be correctly diagnosed as PV and accordingly receive the cornerstone treatment of PV (phlebotomy) to reduce the HCT  $<0.42$  in women and  $<0.45$  in men.<sup>2-4,11,16,50-53</sup>

The important distinction between different HCT levels for women and men when deciding the need for phlebotomies has been addressed in several papers.<sup>2,4,16,50-53</sup> The rationales for this distinction are several and obvious, including the simple fact that women and men have different red blood cell volumes as reflected in different ranges for red cell indices. This common knowledge dictates that a woman's normal RCM is approximately 600 mL lower than that for men.<sup>4,53</sup> Accordingly, a female

patient with a hematocrit of 45% has at least an excess of approximately 600 mL blood<sup>4</sup> which associates with an increased risk of major thrombosis.<sup>54</sup> Indeed, the study by Marchioli *et al.* clearly showed that allowing HCT between 0.45 and 0.50 is associated with a significant risk of death from cardiovascular causes or major thrombotic events<sup>54</sup> - also in the general population.<sup>55</sup> These are lessons that we learnt from Pearson 30 years ago<sup>51,52</sup> and which have been repeated since then in several other studies: an elevated HCT is associated with an increased risk of thrombosis. In fact, in the general population the risk of thrombosis at elevated HCT values has previously been reported to be driven by smoking,<sup>56</sup> which has recently been associated with an increased risk of MPN.<sup>57</sup>

The excess blood volume is even larger in PV-patients with hepatic vein thrombosis,<sup>16</sup> who often have a normal HCT due to an expanded plasma volume.<sup>4</sup> Importantly, the thrombosis risk in *JAK2V617F* positive "ET" patients will likely be markedly reduced simply due to normalization of the expanded RCM by phlebotomies. Additionally, without a RCM estimation, some patients with *JAK2V617F* positive "ET" may be erroneously classified as "early prefibrotic myelofibrosis" while actually having undiagnosed PV for several years and then being referred with an enlarged spleen, a normal Hb-concentration and a normal HCT, red cell values that are in the normal range due to hemodilution consequent to the expanded plasma volume associated with the enlarged spleen. Accordingly, in such patients, a RCM estimation may reveal an expanded RCM requiring phlebotomies to omit thrombotic complications, often at unusual sites such as portal thrombosis, mesenteric thrombosis and thrombosis of hepatic veins.<sup>58</sup> Indeed, similar to mPV as a transitional stage in the biological continuum from ET to overt PV, one might speculate as to whether a proportion of *JAK2V617F* positive patients with a normal Hb /HCT and splenomegaly classified as "early prefibrotic myelofibrosis" may actually have PV with an expanded RCM and expanded plasma volume in a transitional stage towards classic myelofibrosis.

Today, we still need to go over the important lessons from the history of MPN. Back in 1908, Osler taught us that the RBC count is superior to the Hb concentration as an indicator of erythrocytosis.<sup>2,4,16,50,59,60</sup> This should, therefore, be used in the diagnosis of PV, and the lesson from the PV study group and from several authorities thereafter is that the RCM is "the gold standard" for an accurate diagnosis of PV in patients with mPV and its precursor stage: *JAK2V617F* positive ET.<sup>2-8,16</sup> In the paper by Silver *et al.* in this issue of *Haematologica* and in other papers, the importance of these lessons have been repeatedly highlighted. These will hopefully stimulate research into MPN towards additional comparative and correlative studies on the value of RCM estimations, the RBC count, and BM morphology in the diagnosis of MPN. Such studies are even more urgent taking into consideration a most recent review challenging and critically discussing the role of the hematocrit as a determinant risk factor for thrombosis in erythrocytosis.<sup>61</sup> It is to be hoped that such studies may promote a consensus amongst MPN experts that the RCM is essential for a correct classification of *JAK2V617F* positive ET patients, mPV and PV patients.

This will ensure timely treatment with phlebotomies in those patients who otherwise will be classified as ET and who would then carry an increased risk of potentially life-threatening or life-invalidating thrombotic complications. Future studies should also address whether the RBC count in addition to the erythrocyte SR may be simple but highly robust and reproducible indicators of an increased RCM and the hyperviscosity state, respectively, to be used in the diagnosis of PV and when monitoring PV patients for the need for phlebotomy.<sup>62</sup>

## References

- Arber DA, Orazi A, Hasserjian R, et al. The 2016 revision to the World Health Organization classification of myeloid neoplasms and acute leukemia. *Blood*. 2016;127(20):2391-2405.
- Spivak JL, Silver RT. The revised World Health Organization diagnostic criteria for polycythemia vera, essential thrombocytosis, and primary myelofibrosis: an alternative proposal. *Blood*. 2008;112(2):231-239.
- Silver RT, Chow W, Orazi A, Arles SP, Goldsmith SJ. Evaluation of WHO criteria for diagnosis of polycythemia vera: a prospective analysis. *Blood*. 2013;122(11):1881-1886.
- Spivak JL. How I treat polycythemia vera. *Blood*. 2019;134(4):341-352.
- Johansson PL, Safai-Kutti S, Kutti J. An elevated venous haemoglobin concentration cannot be used as a surrogate marker for absolute erythrocytosis: a study of patients with polycythaemia vera and apparent polycythaemia. *Br J Haematol*. 2005;129(5):701-705.
- Cassinat B, Laguillier C, Gardin C, et al; PV-Nord Group. Classification of myeloproliferative disorders in the JAK2 era: is there a role for red cell mass? *Leukemia*. 2008;22(2):452-453.
- Alvarez-Larran A, Ancochea A, Angona A, et al. Red cell mass measurement in patients with clinically suspected diagnosis of polycythemia vera or essential thrombocythemia. *Haematologica*. 2012;97(11):1704-1707.
- Michiels JJ, Medinger M, Raevé HD, et al. Increased Erythrocyte Count on Top of Bone Marrow Histology but not Serum EPO Level or JAK2 Mutation Load Discriminates between JAK2V617F Mutated Essential Thrombocythemia and Polycythemia Vera. *J Hematol Thromb Dis*. 2015;3:S1-001.
- Tefferi A, Thiele J, Orazi A, et al. Proposals and rationale for revision of the World Health Organization diagnostic criteria for polycythemia vera, essential thrombocythemia, and primary myelofibrosis: recommendations from an ad hoc international expert panel. *Blood*. 2007;110(4):1092-1097.
- Najejan Y, Dresch C, Rain J, Chomienne C. Radioisotope investigations for the diagnosis and follow-up of polycythemic patients. In: Wasserman LR, Berk PD, Berlin NI, eds. *Polycythemia Vera and the Myeloproliferative Disorders*. Philadelphia, PA: Saunders; 1995:79-90.
- Spivak JL. Polycythemia vera: myths, mechanisms, and management. *Blood*. 2002;100(13):4272-4290.
- Tefferi A. The rise and fall of red cell mass measurement in polycythemia vera. *Curr Hematol Rep*. 2005;4(4):213-217.
- Barbui T, Thiele J, Vannucchi AM, Tefferi A. Rethinking the diagnostic criteria of polycythemia vera. *Leukemia*. 2014;28(6):1191-1195.
- Tefferi A, Barbui T. Polycythemia vera and essential thrombocythemia: 2017 update on diagnosis, risk-stratification, and management. *Am J Hematol*. 2017;92(1):94-108.
- Jakovic L, Gotic M, Gisslinger H, et al. The WHO diagnostic criteria for polycythemia vera—role of red cell mass versus hemoglobin/hematocrit level and morphology. *Ann Hematol*. 2018;97(9):1581-1590.
- Spivak JL. Myeloproliferative Neoplasms. *N Engl J Med*. 2017;376(22):2168-2181.
- Thiele J, Kvasnicka HM. Diagnostic impact of bone marrow histopathology in polycythemia vera (PV). *Histol Histopathol*. 2005;20(1):317-328.
- Kvasnicka HM. WHO classification of myeloproliferative neoplasms (MPN): a critical update. *Curr Hematol Malig Rep*. 2013;8(4):333-341.
- Madelung AB, Bondo H, Stamp I, et al. World Health Organization-defined classification of myeloproliferative neoplasms: morphological reproducibility and clinical correlations—the Danish experience. *Am J Hematol*. 2013;88(12):1012-1016.
- Gianelli U, Iurlo A, Cattaneo D, Lambertenghi-Deliliers G. Cooperation between pathologists and clinicians allows a better diagnosis of Philadelphia chromosome-negative myeloproliferative neoplasms. *Expert Rev Hematol*. 2014;7(2):255-264.
- Kvasnicka HM, Orazi A, Thiele J, et al. European leukemia net study on the reproducibility of bone marrow features in masked polycythemia vera and differentiation from essential thrombocythemia. *Am J Hematol*. 2017;92(10):1062-1067.
- Barbui T, Thiele J, Gisslinger H, et al. Masked polycythemia vera (mPV): results of an international study. *Am J Hematol*. 2014;89(1):52-54.
- Barbui T, Thiele J, Carobbio A, et al. Masked polycythemia vera diagnosed according to WHO and BCSH classification. *Am J Hematol*. 2014;89(2):199-202.
- Ethier V, Sirhan S, Olney HJ, et al. The 2016 WHO criteria for the diagnosis of polycythemia vera: benefits and potential risks. [e-letters]. *Blood*. 2016. Available at: <http://www.bloodjournal.org/content/127/20/2391/tab-e-letters>.
- Rumi E, Cazzola M. Diagnosis, risk stratification, and response evaluation in classical myeloproliferative neoplasms. *Blood*. 2017;129(6):680-692.
- Barbui T, Thiele J, Gisslinger H, et al. Diagnostic impact of the revised WHO criteria for polycythemia vera. *Am J Hematol*. 2017;92(5):417-419.
- Barbui T, Thiele J, Gisslinger H, et al. The 2016 WHO classification and diagnostic criteria for myeloproliferative neoplasms: document summary and in-depth discussion. *Blood Cancer J*. 2018;8(2):15.
- Cordua S, Kjaer L, Skov V, et al. Prevalence and phenotypes of JAK2 V617F and calreticulin mutations in a Danish general population. *Blood*. 2019;134(5):469-479.
- Ross R. Atherosclerosis – an inflammatory disease. *N Engl J Med*. 1999;340(2):115-126.
- Davi G, Patrono C. Platelet activation and atherothrombosis. *N Engl J Med*. 2007;357(24):2482-2494.
- Totani L, Evangelista V. Platelet-leukocyte interactions in cardiovascular disease and beyond. *Arterioscler Thromb Vasc Biol*. 2010;30(12):2357-2361.
- Hoogeveen RM, Nahrendorf M, Riksen NP, et al. Monocyte and haematopoietic progenitor reprogramming as common mechanism underlying chronic inflammatory and cardiovascular diseases. *Eur Heart J*. 2018;39(38):3521-3527.
- Nahrendorf M. Myeloid cell contributions to cardiovascular health and disease. *Nat Med*. 2018;24(6):711-720.
- Coller BS. Leukocytosis and ischemic vascular disease morbidity and mortality: is it time to intervene? *Arterioscler Thromb Vasc Biol*. 2005;25(4):658-670.
- Barbui T, Carobbio A, Rambaldi A, Finazzi G. Perspectives on thrombosis in essential thrombocythemia and polycythemia vera: is leukocytosis a causative factor? *Blood*. 2009;114(4):759-763.
- Buxhofer-Ausch V, Steurer M, Sormann S, et al. Impact of white blood cells on thrombotic risk in patients with optimized platelet count in essential thrombocythemia. *Eur J Haematol*. 2018 Mar 30. [Epub ahead of print]
- Carobbio A, Ferrari A, Masciulli A, Ghirardi A, Barosi G, Barbui T. Leukocytosis and thrombosis in essential thrombocythemia and polycythemia vera: a systematic review and meta-analysis. *Blood Adv*. 2019;3(11):1729-1737.
- Rumi E, Pietra D, Ferretti V, et al. JAK2 or CALR mutation status defines subtypes of essential thrombocythemia with substantially different clinical course and outcomes. *Blood*. 2014;123(10):1544-1551.
- Lussana F, Carobbio A, Randi ML, et al. A lower intensity of treatment may underlie the increased risk of thrombosis in young patients with masked polycythemia vera. *Br J Haematol*. 2014;2014;167(4):541-546.
- Campbell PJ, Scott LM, Buck G, et al. ; United Kingdom Myeloproliferative Disorders Study Group; Medical Research Council Adult Leukaemia Working Party; Australasian Leukaemia and Lymphoma Group. Definition of subtypes of essential thrombocythemia and relation to polycythaemia vera based on JAK2 V617F mutation status: a prospective study. *Lancet*. 2005;366(9501):1945-1953.
- Lamy T, Devillers A, Bernard M, et al. Inapparent polycythemia vera: an unrecognized diagnosis. *Am J Med*. 1997;102(1):14-20.
- Thiele J, Kvasnicka HM, Diehl V. Initial (latent) polycythemia vera with thrombocytosis mimicking essential thrombocythemia. *Acta Haematol*. 2005;113(4):213-219.
- Barbui T, Thiele J, Carobbio A, et al. Discriminating between essential thrombocythemia and masked polycythemia vera in JAK2 mutated patients. *Am J Hematol*. 2014;89(6):588-590.
- Barbui T, Thiele J, Kvasnicka HM, et al. Essential thrombocythemia

- with high hemoglobin levels according to the revised WHO classification. *Leukemia*. 2014;28(10):2092-2094.
45. Maslah N, Soret J, Dosquet C Sr, et al. Masked polycythemia vera: analysis of a single center cohort of 2480 red cell masses. *Haematologica*. 2019 Aug 14. [Epub ahead of print]
  46. Silver RT, Krichevsky S. Distinguishing essential thrombocythemia JAK2V617F from polycythemia vera: limitations of erythrocyte values. *Haematologica*. 2019;104(11):2200-2205.
  47. Gisslinger H, Zagrijtschuk O, Buxhofer-Ausch V, et al. Ropeginterferon alfa-2b, a novel IFN $\alpha$ -2b, induces high response rates with low toxicity in patients with polycythemia vera. *Blood*. 2015;126(15):1762-1769.
  48. Hasselbalch HC, Holmström MO. Perspectives on interferon-alpha in the treatment of polycythemia vera and related myeloproliferative neoplasms: minimal residual disease and cure? *Semin Immunopathol*. 2019;41(1):5-19.
  49. Silver RT, Gjoni S. The hematocrit value in polycythemia vera: caveat utilitor. *Leuk Lymphoma*. 2015;56(5):1540-1541.
  50. Spivak JL. Polycythemia vera: myths, mechanisms, and management. *Blood*. 2002;100(13):4272-4290.
  51. Pearson TC, Wetherley-Mein G. Vascular occlusive episodes and venous haematocrit in primary proliferative polycythaemia. *Lancet*. 1978;2(8102):1219-1222.
  52. Pearson TC. Hemorheologic considerations in the pathogenesis of vascular occlusive events in polycythemia vera. *Semin Thromb Hemost*. 1997;23(5):433-439.
  53. Pearson TC, Guthrie DL, Simpson J, et al. Interpretation of measured red cell mass and plasma volume in adults: Expert Panel on Radionuclides of the International Council for Standardization in Haematology. *Br J Haematol*. 1995;89(4):748-756.
  54. Marchioli R, Finazzi G, Specchia G, et al. ; CYTO-PV Collaborative Group. Cardiovascular events and intensity of treatment in polycythemia vera. *N Engl J Med*. 2013;368(1):22-33.
  55. Warny M, Helby J, Birgens HS, et al. Arterial and venous thrombosis by high platelet count and high hematocrit: 108 521 individuals from the Copenhagen General Population Study. *J Thromb Haemost*. 2019 Jul 15. [Epub ahead of print]
  56. Kannel WB, Gordon T, Wolf PA, McNamara P. Hemoglobin and the risk of cerebral infarction: the Framingham study. *Stroke*. 1972;3(4):409-420.
  57. Pedersen KM, Bak M, Sørensen AL, et al. Smoking is associated with increased risk of myeloproliferative neoplasms: A general population-based cohort study. *Cancer Med*. 2018;7(11):5796-5802.
  58. Barosi G, Buratti A, Costa A, et al. An atypical myeloproliferative disorder with high thrombotic risk and slow disease progression. *Cancer*. 1991;68(10):2310-2318.
  59. Osler W. A clinical lecture on erythremia. *Lancet*. 1908;171(1):143-146.
  60. Weber FP. Polycythaemia, erythrocytosis and erythraemia. *Q J Med*. 1908;2:85-134.
  61. Gordeuk VR, Key NS, Prchal JT. Re-evaluation of hematocrit as a determinant of thrombotic risk in erythrocytosis. *Haematologica*. 2019 Apr;104(4):653-8.
  62. Nersesjan V, Zervides KA, Sørensen AL, Kjær L, Skov V, Hasselbalch HC. The red blood cell count and the erythrocyte sedimentation rate in the diagnosis of polycythemia vera. *Eur J Haematol* 2019 . Accepted for publication.

## Standing at odds: mutated RAS and hematopoietic stem cells

Monica Nafria and Constanze Bonifer

*Institute of Cancer and Genomic Sciences, College of Medicine and Dentistry, University of Birmingham, Birmingham, UK*

*E-mail: CONSTANZE BONIFER - c.bonifer@bham.ac.uk*

*doi:10.3324/haematol.2019.230029*

Acute myeloid leukemia (AML) is the most common acute leukemia in adults and is characterized by the accumulation of myeloid leukemic blasts unable to complete differentiation. However, AML is a complex disease with variable outcomes and prognoses.<sup>1</sup> Underlying these heterogeneous phenotypes is the fact that each sub-type of AML is defined by a different set of mutations and is controlled by a specific transcriptional and signaling network distinct to that of normal stem and progenitor cells.<sup>2</sup> Genes mutated in AML are involved in gene regulation and include transcription factors, chromatin modifiers / remodelers, splicing regulators, DNA methyltransferases and signaling regulators that control the activity of inducible transcription factors. The result is a profound deviation from the normal differentiation trajectory, with each AML sub-type taking a different path and establishing its own cellular identity.<sup>2,3</sup> Most AML sub-types carry more than one mutation and, with the exception of MLL-translocations (which are a hallmark of pediatric AML<sup>4</sup>), for a number of sub-types it has been shown that the first oncogenic hit is not sufficient to cause overt leukemia. In AML patients, mutations in genes from different functional categories co-exist, and data from sequencing studies as well as mouse models support this notion.<sup>5,6</sup>

The t(8;21) translocation, occurring in 7% of adult *de novo* patients, is one of the most frequent cytogenetic

aberrations in AML.<sup>7</sup> This translocation fuses the DNA-binding domain coding region of the hematopoietic master regulator RUNX1 (*AML1*) to the Eight-twenty-One (*ETO*, *RUNX1T1* or *MTG8*) gene, which encodes a nuclear co-repressor. The result is the formation of the AML1-ETO (alternatively named RUNX1-ETO) chimeric protein, which retains the ability to bind to RUNX1 binding motifs but lacks the transactivation domain of RUNX1.<sup>8,9</sup> Germline expression of full-length AML1-ETO in mice causes embryonic lethality,<sup>10,11</sup> but conditional expression in hematopoietic stem cells (HSC) leads to an initial expansion of myeloid progenitor cells, including HSC and granulocyte-macrophage progenitors (GMP). Such expansion was also seen with *AML1-ETO*-transduced human cord blood-derived HSC *in vitro*.<sup>12</sup> Fusion t(8;21) transcripts have been detected *in utero* and in post-natal blood samples<sup>13</sup> and remain expressed at low levels in blood samples from t(8;21) AML patients in long-term remission.<sup>14</sup> Furthermore, several *AML1-ETO*-expressing mouse models have failed to fully develop t(8;21) AML unless challenged by mutagenesis or aging,<sup>15-18</sup> indicating the necessity of additional secondary mutations. These findings suggest that this chromosomal rearrangement is the driver mutation establishing a pre-leukemic clone. This notion is supported by the finding that t(8;21) patients present with a number of different secondary mutations.<sup>19</sup> The most prominent of these mutations

occur in genes encoding for the growth factor receptors KIT and FLT3,<sup>20,21</sup> rendering these receptors chronically active, together with activating RAS mutations such as the K-RAS (G12D), all of which co-operate with AML1-ETO. Interestingly, K-RAS activating mutations occur late during leukemia development and are rarely detectable within the leukemic stem cell compartment<sup>21</sup> (Figure 1A). In myelodysplastic syndromes (MDS), it was shown that the order of acquisition of mutations makes a profound difference on the disease phenotype,<sup>22</sup> but whether the same stands true for t(8;21) AML is not known.

In this issue of *Haematologica*, Di Genua *et al.*<sup>23</sup> uncovered the mechanistic explanation for the absence of signaling pathway mutations, such as K-RAS activating mutations, within the t(8;21) pre-leukemic HSC compart-

ment by analyzing hematopoietic development and gene expression in conditional murine knock-in models expressing human *AML1-ETO* and *K-RAS(G12D)* individually or in combination, resulting in the generation of an *Aml1<sup>ETO/+</sup>* (AM), a *K-Ras<sup>G12D/+</sup>* (KM), and a double-targeted *Aml1<sup>ETO/+</sup>; K-Ras<sup>G12D/+</sup>* (AKM) mouse lines. Prior studies had shown that mice expressing *K-Ras(G12D)* from its endogenous locus develop MDS but not AML.<sup>24</sup> When combined with AML1-ETO in human hematopoietic cells, K-RAS(G12D) promoted leukemic transformation in murine transplantation models.<sup>25</sup> However, here expression levels were likely to be non-physiological and it had not been defined whether the presence of mutated RAS was compatible with the maintenance of *AML1-ETO*-expressing HSC. Di Genua *et al.* addressed these

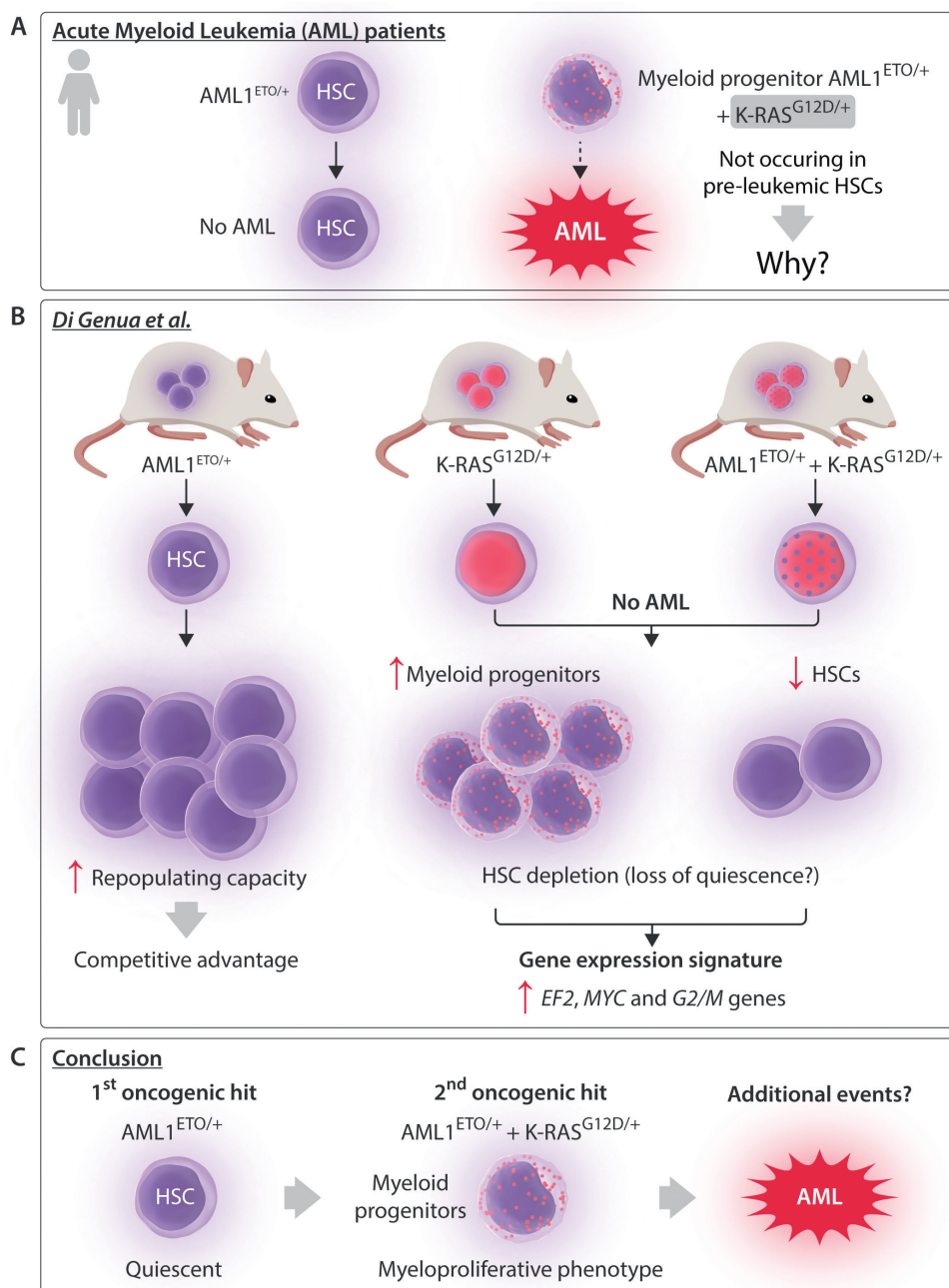


**Figure 1. Co-expression of AML1-ETO and mutant RAS is incompatible with hematopoietic stem cell (HSC) maintenance.** (A) In acute myeloid leukemia (AML) patients, HSC express AML1-ETO, but this is not sufficient to cause overt disease. AML leukemic blasts represent myeloid progenitors harboring the translocation that have undergone secondary oncogenic events, including mutations in signaling pathway genes such as the K-RAS<sup>G12D/+</sup>. However, prior to Di Genua *et al.*,<sup>23</sup> the molecular explanation for the lack of mutations in signaling pathway genes in the pre-leukemic stem cells was unknown. HSC (purple cells), myeloid progenitors (purple cells with pink dots). (B) Di Genua *et al.*<sup>23</sup> generated conditional murine knock-in models expressing human AML1-ETO and K-RAS(G12D) individually or in combination: *Aml1<sup>ETO/+</sup>* (purple nuclei), *K-Ras<sup>G12D/+</sup>* (pink nuclei), and *Aml1<sup>ETO/+</sup>; K-Ras<sup>G12D/+</sup>* (pink and dotted nuclei), respectively, and performed competitive transplantation assays to compare wild-type and transgenic stem cell activity and measure global gene expression as indicated. (C) Model of step-wise oncogenesis in t(8;21) patients: the presence of t(8;21) in HSC results in a quiescent phenotype. Acquisition of K-RAS(G12D) occurs at later stages and results in increased proliferation. However, the double oncogenic event is not sufficient to develop overt AML, and the nature and order of acquisition of additional oncogenic events remains unknown.

issues by conditionally introducing both mutant genes from the respective genomic loci in mice in order to reproduce physiological oncogene expression levels. They then subsequently performed competitive transplantation assays to be able to directly compare stem cell activity in wild-type and transgenic cells (Figure 1B).

AML1-ETO expression on its own affected platelet, B- and T-cell development, and led to an increased number of functional HSC together with enhanced myeloid reconstitution in secondary recipients. Expression of mutant K-RAS on its own resulted in a myeloproliferative phenotype, led to a lack of HSC expansion, decreased engraftment and diminished *in vitro* re-plating potential, which, importantly, was seen regardless of the presence of AML1-ETO. Interestingly, co-expression of both oncoproteins led to a milder myeloproliferative phenotype but not overt AML, as seen in patients, and only aggravated the defect in platelet development. The authors suggest that the competitive advantage observed in AML1-ETO-expressing HSC was due to an enhanced self-renewal capacity. To further elucidate the mechanisms behind the functional impairment of *K-Ras(G12D)*-expressing HSC, they compared gene expression in HSC from genetically modified and control cells using transplantation assays. The presence of mutant K-RAS conferred increased cell cycle activity as well as upregulation of the expression of checkpoint associated genes, such as *E2F*, *Myc* and G2M-associated genes, as compared to HSC harboring the AML1-ETO transgene only. Moreover, the presence of mutated K-RAS protein resulted in the downregulation of gene expression signature associated with self-renewal activity and acquisition of a GMP-associated transcriptional signature. Overall, the transcriptional profiles of K-RAS(G12D)-expressing HSC resembled those of myeloid progenitors. Gene expression changes in double mutant cells were distinct from those of cells carrying the individual mutations. For example, two genes, *Gja1* and *Gzmb*, were up-regulated in the double mutant HSC and the authors suggest that they regulate the p53 pathway and oxidative phosphorylation, respectively, both increasing cell death and apoptosis.

Taken together, Di Genua *et al.*<sup>23</sup> show that expression of a mutant K-RAS is not compatible with a pre-leukemic state of murine AML1-ETO-expressing HSC. Although AML1-ETO alone confers a competitive advantage to HSC, the additional presence of K-RAS(G12D) results in loss of HSC function, most likely by exhaustion. The study shows that this phenomenon is explained by an increase in cell cycle activity leading to a loss of quiescence in HSC co-expressing both mutations. Therefore, they hypothesize that acquisition of mutant K-RAS in t(8;21) AML occurs at the myeloid progenitor stage rather than within pre-leukemic HSC compartment harboring the t(8;21) translocation. Overall, this study demonstrates that the order of appearance of each class of mutations is also relevant for leukemic transformation in AML.

Additional questions arise from this and previous work (Figure 1C). Firstly, Di Genua *et al.* show that, even in the presence of K-RAS(G12D), AML1-ETO is unable to cause an overt leukemic phenotype *in vivo*. The same was found in xenotransplantation experiments with retrovirally transduced human CD34<sup>+</sup> cord blood cells expressing

AML1-ETO together with *N-RAS(G12D)*.<sup>26</sup> This notion ties in with the observation of Cabezas-Wallscheid *et al.*<sup>16</sup> that the development of AML in an AML1-ETO mouse model is a slow process, probably requiring multiple mutations or epigenetic reprogramming events, which were not examined in their study. Moreover, it has been previously shown that expression of AML1-ETO in an inducible transgenic mouse model leads to a block in differentiation, but not to an enhanced proliferation.<sup>17</sup> Di Genua *et al.*<sup>23</sup> add to this result that AML1-ETO-expressing pre-leukemic stem cells have a quiescent phenotype, leading to an accumulation of cells with high re-plating activity that are capable of going into cycle in a transplantation setting. Given that the double oncogenic event studied here is not enough to cause AML, the question that is now apparent is which additional events cause AML in patients. This work demonstrates that, even with a type of AML that has been studied in fine molecular detail for decades, the players of selection and clonal evolution in patients still have additional cards up their sleeve.

## References

1. De Kouchkovsky I, Abdul-Hay M. Acute myeloid leukemia: a comprehensive review and 2016 update. *Blood Cancer J.* 2016;6(7):e441.
2. Assi SA, Imperato MR, Coleman DJL, et al. Subtype-specific regulatory network rewiring in acute myeloid leukemia. *Nat Genet.* 2019;51(1):151-162.
3. Valk PJ, Verhaak RG, Beijen MA, et al. Prognostically useful gene-expression profiles in acute myeloid leukemia. *N Engl J Med.* 2004;350(16):1617-1628.
4. Szczepanski T, Harrison CJ, van Dongen JJ. Genetic aberrations in paediatric acute leukaemias and implications for management of patients. *Lancet Oncol.* 2010;11(9):880-889.
5. Papaemmanuil E, Gerstung M, Bullinger L, et al. Genomic Classification and Prognosis in Acute Myeloid Leukemia. *N Engl J Med.* 2016;374(23):2209-2221.
6. Wang M, Yang C, Zhang L, Schaar DG. Molecular Mutations and Their Cooccurrences in Cytogenetically Normal Acute Myeloid Leukemia. *Stem Cells Int.* 2017;2017:6962379.
7. Grimwade D, Hills RK, Moorman AV, et al. Refinement of cytogenetic classification in acute myeloid leukemia: determination of prognostic significance of rare recurring chromosomal abnormalities among 5876 younger adult patients treated in the United Kingdom Medical Research Council trials. *Blood.* 2010;116(3):354-365.
8. Miyoshi H, Shimizu K, Kozu T, Maseki N, Kaneko Y, Ohki M. t(8;21) breakpoints on chromosome 21 in acute myeloid leukemia are clustered within a limited region of a single gene, AML1. *Proc Natl Acad Sci U S A.* 1991;88(23):10431-10434.
9. Erickson P, Gao J, Chang KS, et al. Identification of breakpoints in t(8;21) acute myelogenous leukemia and isolation of a fusion transcript, AML1/ETO, with similarity to *Drosophila* segmentation gene, runt. *Blood.* 1992;80(7):1825-1831.
10. Yergeau DA, Hetherington CJ, Wang Q, et al. Embryonic lethality and impairment of haematopoiesis in mice heterozygous for an AML1-ETO fusion gene. *Nat Genet.* 1997;15(3):303-306.
11. Cai Z, Yang S, Okuda T, et al. Expression of a knocked-in AML1-ETO leukemia gene inhibits the establishment of normal definitive hematopoiesis and directly generates dysplastic hematopoietic progenitors. *Blood.* 1998;91(9):3134-3143.
12. Mulloy JC, Cammenga J, MacKenzie KL, Berguido FJ, Moore MA, Nimer SD. The AML1-ETO fusion protein promotes the expansion of human hematopoietic stem cells. *Blood.* 2002;99(1):15-23.
13. Wiemels JL, Xiao Z, Buffler PA, et al. In utero origin of t(8;21) AML1-ETO translocations in childhood acute myeloid leukemia. *Blood.* 2002;99(10):3801-3805.
14. Miyamoto T, Weissman IL, Akashi K. AML1/ETO-expressing non-leukemic stem cells in acute myelogenous leukemia with 8;21 chromosomal translocation. *Proc Natl Acad Sci U S A.* 2000;97(13):7521-7526.
15. Higuchi M, O'Brien D, Kumaravelu P, Lenny N, Yeoh EJ, Downing JR. Expression of a conditional AML1-ETO oncogene bypasses

- embryonic lethality and establishes a murine model of human t(8;21) acute myeloid leukemia. *Cancer Cell*. 2002;1(1):63-74.
16. Cabezas-Wallscheid N, Eichwald V, de Graaf J, et al. Instruction of haematopoietic lineage choices, evolution of transcriptional landscapes and cancer stem cell hierarchies derived from an AML1-ETO mouse model. *EMBO Mol Med*. 2013;5(12):1804-1820.
  17. Rhoades KL, Hetherington CJ, Harakawa N, et al. Analysis of the role of AML1-ETO in leukemogenesis, using an inducible transgenic mouse model. *Blood*. 2000;96(6):2108-2115.
  18. Yuan Y, Zhou L, Miyamoto T, et al. AML1-ETO expression is directly involved in the development of acute myeloid leukemia in the presence of additional mutations. *Proc Natl Acad Sci U S A*. 2001;98(18):10398-10403.
  19. Christen F, Hoyer K, Yoshida K, et al. Genomic landscape and clonal evolution of acute myeloid leukemia with t(8;21): an international study on 331 patients. *Blood*. 2019;133(10):1140-1151.
  20. Kuchenbauer F, Schnittger S, Look T, et al. Identification of additional cytogenetic and molecular genetic abnormalities in acute myeloid leukaemia with t(8;21)/AML1-ETO. *Br J Haematol*. 2006;134(6):616-619.
  21. Corces-Zimmerman MR, Majeti R. Pre-leukemic evolution of hematopoietic stem cells: the importance of early mutations in leukemogenesis. *Leukemia*. 2014;28(12):2276-2282.
  22. Shima T, Miyamoto T, Kikushige Y, et al. The ordered acquisition of Class II and Class I mutations directs formation of human t(8;21) acute myelogenous leukemia stem cell. *Exp Hematol*. 2014;42(11):955-965.e1-5.
  23. Di Genua C, Norfo R, Rodriguez-Meira A, et al. Cell-intrinsic depletion of Aml1-ETO-expressing pre-leukemic hematopoietic stem cells by K-Ras activating mutation. *Haematologica*. 2019;104(11):2215-2224.
  24. Braun BS, Tuveson DA, Kong N, et al. Somatic activation of oncogenic Kras in hematopoietic cells initiates a rapidly fatal myeloproliferative disorder. *Proc Natl Acad Sci U S A*. 2004;101(2):597-602.
  25. Zhao S, Zhang Y, Sha K, et al. KRAS (G12D) cooperates with AML1/ETO to initiate a mouse model mimicking human acute myeloid leukemia. *Cell Physiol Biochem*. 2014;33(1):78-87.
  26. Chou FS, Wunderlich M, Griesinger A, Mulloy JC. N-Ras(G12D) induces features of stepwise transformation in preleukemic human umbilical cord blood cultures expressing the AML1-ETO fusion gene. *Blood*. 2011;117(7):2237-2240.

## Carfilzomib combination treatment as first-line therapy in multiple myeloma: where do we go from the Carthadex (KTd)-trial update?

Monika Engelhardt,<sup>1,2</sup> Kwee Yong,<sup>3</sup> Sara Brin ghen<sup>4</sup> and Ralph Wäsch<sup>1,2</sup>

<sup>1</sup>Hematology and Oncology, Faculty of Medicine, University of Freiburg, Freiburg, Germany; <sup>2</sup>Comprehensive Cancer Center Freiburg (CCCF), Freiburg, Germany; <sup>3</sup>University College London, London, UK and <sup>4</sup>UNITO Dipartimento di Oncologia, University of Turin, Turin, Italy

E-mail: MONIKA ENGELHARDT - monika.engelhardt@uniklinik-freiburg.de

doi:10.3324/haematol.2019.228684

The prognosis and treatment of multiple myeloma (MM) patients have substantially changed in the last decade due to a better understanding of the disease and the introduction of novel agents (NA) with new mechanisms of action against malignant plasma cells.<sup>1-3</sup> In parallel with the improved understanding of myeloma biology, the field has witnessed a flood of NA, including immunomodulatory drugs (IMiD: thalidomide, lenalidomide, pomalidomide); proteasome inhibitors (PI: bortezomib, carfilzomib, ixazomib), monoclonal antibodies (mAb: daratumumab, elotuzumab),<sup>4</sup> and histone deacetylase inhibitors, which have substantially improved progression-free survival (PFS) and overall survival (OS). Other NA in clinical trials (selinexor, venetoclax, novel immunotherapeutics, iberdomide, and others) are being intensively tested, and specifically immunotherapeutics beyond mAb, such as bispecific T-cell engager (BITE) molecules and chimeric antigen receptor (CAR)-T cells will expand anti-myeloma therapy options.<sup>1-4</sup> Concomitantly, the application of tools that reliably assess “frailty” of patients is also helping with decision making, given that many patients with MM are elderly and often have significant comorbidities.<sup>5-10</sup> Sustained disease response is crucial in fit and in frail patients, since disease response can significantly improve quality of life and may reduce MM-induced comorbidity. Optimizing tolerability for timely treatment delivery has also proved beneficial.<sup>11</sup> However, this may prove challenging with triplet or quadruplet regimens that are being developed for continued therapy, where adverse events (AE) may lead to treatment interruptions and discontinuation.

After the introduction of the first PI bortezomib (Btz/V), second- and third-generation PI were developed, with the aim of providing therapy that would be potentially more efficacious and less toxic, including an improved polyneuropathy (PNP) side effect profile. Carfilzomib (Cfz/K) is a second-in-class, epoxyketone-based, irreversibly binding PI, which is approved in combination with dexamethasone (Kd) or lenalidomide and dexamethasone (KRd) for the treatment of relapsed/refractory MM (RRMM) patients.<sup>12,13</sup> The ENDEAVOR study compared Kd *versus* Btz plus dexamethasone (Vd) and reported a longer PFS and OS, with lower risk of painful PNP with Kd.<sup>15</sup> The ASPIRE study demonstrated the superiority of KRd over Rd, with unprecedented PFS benefit, as well as OS benefit in RRMM.<sup>14</sup> These studies have established the place of Cfz in treating RRMM.

Dyspnea, hypertension and cardiac toxicities stand out as clinically relevant side effects, and a widening experience of these has led to published guidance for the use of Cfz, as well as a re-appraisal of the baseline cardiovascular morbidity present in this patient group.<sup>15</sup> Such guidance provides a helpful description of expected events, as well as suggestions for subsequent monitoring, detection and management.<sup>16,17</sup> The analysis of cardiovascular adverse events (CVAE) in Cfz-treated patients revealed that, in those with CVAE, 91% had uncontrolled hypertension, with acute coronary syndrome or cardiac arrhythmias each present in 4.5%. Subjects with CVAE also had significantly higher blood pressure, left ventricular mass, and pulse wave velocity at baseline evaluation, compared to those without. Baseline uncontrolled blood

pressure, left ventricular hypertrophy, and pulse wave velocity  $\geq 9$  m/s identified patients at higher risk of developing CVAE during follow up. These findings indicated that careful monitoring, strict blood pressure control and identification of early symptoms suggestive of cardiac dysfunction, are crucial to ensure safe administration of Cfz.<sup>16-18</sup>

In newly diagnosed MM (NDMM), Cfz has been investigated in several studies, and the updated results of the

Carthadex trial of Cfz-thalidomide-dexamethasone (KTd) are now available. In this issue of the Journal, Wester *et al.* report on these findings.<sup>19</sup> With longer median follow up (58.7 months) of this multicenter phase II trial, impressive overall responses (ORR: 93%), with a high rate of CR (63% after consolidation) and substantial PFS and OS results (median: 58 and 83 months, respectively) were obtained.<sup>19</sup> Cfz was escalated from 20/27 (n=50), to 20/36 (n=20), 20/45 (n=21) and 20/56 mg/m<sup>2</sup>

**Table 1. Carthadex-(KTd) results compared to selected other carfilzomib combinations in newly diagnosed multiple myeloma.**

First author	Study phase	# pts	Median age (range)	Cfz-dose	Combination treatment	ORR	PFS	OS	Notable findings	FDA/EMA approval
Wester R, Haematologica 2019 <sup>19</sup>	II (#NTR2422) Follow-up report (median: 58.7 ms)	111	58 (29-66), Tx-eligible	20/27 (n=50), 20/36 (n=20), 20/45 (n=21) 20/56 (n=20)	Cfz 20-> 56mg/m <sup>2</sup> Thal: 200mg/d Dex 40mg weekly, 4 induction C -> ASCT->4 consolidation C	93%; CR: 18%	58 ms	83 ms	Grade 3/4 AE: Infections: 11% Respiratory: 8% Skin: 9%, Vascular: 9% Cardiac 5%	-
Sonneveld P, Blood 2015 <sup>20</sup>	II (#NTR2422) Initial report (median: 23 ms)	91	58 (29-66), Tx-eligible	20/27 (n=50), 20/36 (n=20), 20/45 (n=21)	Cfz 20-> 45mg/m <sup>2</sup> Thal: 200mg/d Dex 40mg weekly	86%	36-ms-PFS: 72%	Not given	Grade 3/4 AE: Respiratory: 15%, GI: 12%, Skin: 10%	-
Mikhael JR, Br J Haematol 2015 <sup>21</sup>	Cyklone: I/II, median follow-up 17.5ms	64	62.5 (27-82), Tx-eligible	20->45	Cfz: 20->45mg/m <sup>2</sup> 1x/w Cyclo: 300mg/m <sup>2</sup> d1,8,15, Thal 100mg d1-28, Dex 40,g d1,8,15,22, MTD: 36, 9 C -> maint.	91%	2y-PFS: 76%	2y-OS: 96%	G3/4 hypertension 6% Cardiac events: 6% Renal events: 5% Thromboembolic events: 5%, Dyspnea: 3%	-
Jackson, Blood (Suppl) 2018 <sup>22</sup>	III	526	61 (33-75), Tx-eligible	20/36	Cfz 36mg/m <sup>2</sup> d1, 2, 8, 9, 15, 16 Cyclo: 500mg d1,8,15, Len 25mg d1-21 Dex 40mg d1,8,15,22,	$\geq$ VGPR: 82.3%	36-ms-PFS: 64.5%	Not given	All grade cardiac: 4% All grade VTE: 12.5% Discont. 4.8%	-
Gay F, Blood (Suppl.) 2018 <sup>23</sup>	III, median follow-up 20 ms	474	57 (52-62), Tx-eligible	20/36	KRd-ASCT-KRd vs. KRd12 vs. KCd-ASCT-KCd	$\geq$ VGPR: 89:87:76%	Not given	Not given	G3/4 cardiac AE:3:2:4%, Thrombosis: 1:2:2% Discont. 6:8:7%	-
Moreau P, Blood 2015 <sup>24</sup>	I/II	68	72 (66-86), Tx-inelegible	20, 27, 36, 45; MTD: 36	Cfz: 20-45mg/m <sup>2</sup> M 9mg/m <sup>2</sup> , P 60mg/m <sup>2</sup> d1-4, 9 C	90%	Median: 21 ms	3y-OS: 80%	Death in n=12: PD (n=7), infection (n=2) cardiac failure (n=1) respiratory distress (n=1) urothelial ca (n=1)	-
Brighen S, Blood 2014 <sup>25</sup>	II, Median follow-up: 18ms	58	71 (68-75), Tx-inelegible	20->36 2x/w	Cfz: 20->36mg/m <sup>2</sup> Cyclo: 300mg/m <sup>2</sup> d1,8,15, Dex 40,g d1,8,15,22, 9 C $\geq$ maint.	95%	2y-PFS: 76%	2y-OS: 87%	AE 3-5: cardiopulmonary: 7% Discontinuation: 14% Cfz-dose reductions: 21%	-
Brighen S, Leukemia 2018 <sup>27</sup>	I/II, Median follow-up: 18ms	63	72 (69-74), Tx-inelegible	45,56,70 $\geq$ 70 1x/w	Cfz: 45->70mg/m <sup>2</sup> 1x/w Cyclo: 300mg/m <sup>2</sup> d1,8,15, dex 40,g d1,8,15,22, 9 C $\geq$ maint.	89%	2y-PFS: 53.2%	2y-OS: 81%	AE 3-5: cardiopulmonary: 9%, Discontinuation: 22% Cfz-dose reductions: 9% 6 pts died: 2 PD + AE (pulm. thromboembolism, resp. failure, pneumonia, sudden death)	-
Facon T, Blood 2019 <sup>25</sup>	III, Clarion	955	72 (42-91), Tx-inelegible	KMP (n=478) 20 $\geq$ 36 VMP (n=477)	Cfz: 20->36mg/m <sup>2</sup> M 9mg/m <sup>2</sup> , P 60mg/m <sup>2</sup> d1-4, 9 C V 1.3mg/m <sup>2</sup> d1,4,8,11,22,25,29,32 $\geq$ d4,11,25,32, C5-9	84.3% 78.8%	22.3 22.1	HR 1.08 (0.82-1.43)	Renal failure: 13.9 : 6.2% Cardiac failure: 10.8 : 4.3% >G3 AE rates: 74.7 : 76.2% >G2 PNP: 2.5% : 35.1%	- +

#: number, pts: patients; ND: newly diagnosed; RR: relapsed/refractory; MM: multiple myeloma; Cfz: carfilzomib; T: thalidomide; d: day; Dex: dexamethasone; M: melphalan; P: prednisone; v: bortezomib; L: lenalidomide; ORR: overall response rate; PFS: progression free survival; OS: overall survival; AE: adverse events; pts: patients; ms: months; C: cycle; MTD: max. tolerated dose; maint: maintenance therapy; FDA: Food and Drug Administration; CR: complete remission; GI: gastrointestinal; Tx: transplantation; VTE: venous thrombo-embolism; discontin.: discontinuation; PD: disease progression; ca: carcinoma; pulm.: pulmonary; resp: respiratory; HR: hazard risk.

(n=20 patients), given twice weekly combined with daily thalidomide [200 mg day (d) 1-28] and weekly dexamethasone for four KTD induction cycles before autologous stem cell transplantation (ASCT) was performed. These promptly induced responses allowed peripheral blood stem cell (PBSC) mobilization in 92%, and were followed by ASCT in 88% and Cfz-consolidation in 85% of patients. Since this was an updated study report,<sup>20</sup> with a last cohort of further escalated Cfz (20/56), a specific aim of the study had been to compare tolerability and efficacy between the various Cfz doses. This objective is clinically highly relevant; however, the small patient numbers allowed only preliminary observations to be made on this. Nevertheless, increasing Cfz doses beyond 20/36 did not seem to improve efficacy in terms of CR rates. Of note, CVAE did not seem to increase with Cfz dose escalation and were generally low (12% all grade, 5% grade  $\geq 3$ ), while infection rates, particularly pneumonia, did. The authors comment that their previous experience with this regimen likely contributed to the low incidence of SAE.<sup>19</sup>

With the usual caveats of conducting cross-trial comparisons, Table 1 summarizes selected Cfz-combination trials in NDMM, with the Carthadex results shown first.<sup>19</sup>

As compared to the Carthadex-trial with KTD, the Cyklone trial<sup>21</sup> investigated Cfz in quadruplet-combination in 64 transplant-eligible NDMM patients and was similar in its treatment combination: patients were treated with Cfz (d1, 2, 8, 9, 15, and 16), 300 mg/m<sup>2</sup> cyclophosphamide (d1, 8, and 15), 100 mg thalidomide (d1-28), and 40 mg dexamethasone (d1, 8, 15, and 22) in 28-day cycles. Cfz was dose-escalated at four dose levels to determine the maximum tolerated dose (MTD), which was 20/36 mg/m<sup>2</sup>. OS was similar as that reported by Wester *et al.* and Sonneveld *et al.*,<sup>19,20</sup> as were the 2-year PFS (76%) and OS (96%) (Table 1). Similar to the Carthadex trial, the Cyklone-quadruplet led to rapid and deep responses with limited PNP, cardiac or pulmonary toxicity.<sup>21</sup> Although due to PNP risks thalidomide is less used in Europe, and particularly in the US, than lenalidomide or pomalidomide, both Carthadex and Cyklone results illustrate the safety and efficacy of combining novel PI with IMiD, steroids and cyclophosphamide to a quadruplet. The UK Myeloma XI+ study evaluated a similar quadruplet, but with lenalidomide instead of thalidomide, KCRd (Cfz 20/36) as induction prior to ASCT, followed by randomization to lenalidomide maintenance or no further treatment.<sup>22</sup> This quadruplet was well tolerated, and response rates and PFS rates were remarkably similar to those in the Carthadex study (Table 1).<sup>22</sup>

In transplant-eligible patients, the combination of Cfz with lenalidomide (KRd) or cyclophosphamide (KCD), with or without ASCT (KRd-ASCT-KRd vs. KRd12 vs. KCD-ASCT-KCD), is also being assessed in the Forte trial.<sup>23</sup> The three Forte trial arms show high and deep very good partial response (VGPR) rates of 89%, 87% and 76%, respectively, with so far well manageable SAE signals, especially low grade 3/4 cardiac AE, thrombosis or discontinuation rates (Table 1).

In transplant-ineligible patients, Moreau *et al.* showed tolerability and efficacy of Cfz-melphalan-prednisone (KMP) in a phase I/II trial.<sup>24</sup> MTD of Cfz was 36 mg/m<sup>2</sup>,

the combination of KMP was feasible and ORR, PFS and 3-year OS were remarkable with 90%, 21 months, and 80%, respectively. This led to the randomized Clarion study of KMP *versus* VMP for nine 6-week cycles, the results of which showed that both regimens resulted in similar PFS and response rates, while PNP rates were higher with VMP, and acute renal failure and cardiac failure were higher with KMP (Table 1).<sup>25</sup> The reason for the lack of superior results with KMP may be the high level of experience of physicians managing VMP-treatment, the lower tolerability of KMP than VMP in elderly patients, and the much lower than anticipated PNP rate of VMP, so that the study endurance in both groups were similar.

Since cyclophosphamide is better tolerated than melphalan and a useful backbone for numerous MM protocols, Brinthen *et al.* assessed the safety and efficacy of Cfz in combination with cyclophosphamide and dexamethasone (KCD) in NDMM patients  $\geq 65$  years, ineligible for ASCT, both in twice- and once-weekly schedules.<sup>26-28</sup> In the twice-weekly Cfz-study, 58 patients were enrolled and received KCD for up to nine cycles, followed by maintenance with Cfz until progression or intolerance. Patients received oral cyclophosphamide 300 mg/m<sup>2</sup> and dexamethasone 40 mg on d1, 8 and 15; Cfz (20/36) was administered as 30-minute infusions on d1, 2, 8, 9, 15, and 16. In the maintenance phase, patients were treated with 36 mg/m<sup>2</sup> Cfz on d1, 2, 15, and 16 every 28 days. After a median of nine cycles of KCD, 71% of patients achieved  $\geq$  VGPR and the 2-year PFS and OS after a median follow up of 18 months were 76% and 87%, respectively. The rate of  $\geq$  grade 3 AE was low, and the most common toxicities were neutropenia (20%), anemia (11%), and cardiopulmonary events (7%).<sup>26</sup>

The once-weekly KCD-combination escalated Cfz initially from 45 to 56 and 70 mg/m<sup>2</sup>. Patients were treated with Cfz on d1, 8 and 15 of a 28-day cycle. A total of 63 patients were enrolled in the phase I and II of the study; 54 of them received recommended phase II dose 70 mg/m<sup>2</sup>. At least VGPR was achieved in 36 (66%). The frequency of hematologic and non-hematologic AE was similar or lower than that reported in previous studies with twice weekly Cfz.<sup>26-28</sup>

Several triplet and quadruplet schedules of KRd, KCD, e.g. with both elotuzumab and daratumumab antibodies, are being assessed in phase II/III clinical trials (e.g. the Deutsche Studiengruppe Multiples Myelom, the German-Speaking Multiple Myeloma Group, and others). The results of these studies are eagerly awaited, and preliminary safety and efficacy results have been highly promising.

The Carthadex trial investigating KTD in transplant-eligible NDMM is also of interest in the light of the Cassiopeia (VTd-Dara) transplant-eligible NDMM study that was presented at the recent 2019 ASCO and EHA meetings.<sup>29</sup> Although Cassiopeia is a randomized phase III trial and Carthadex was not, the responses in both are impressive and remarkably similar. In Carthadex, the sCR after induction and consolidation therapy for the triplet was 30%; in Cassiopeia the sCR for the experimental arm (VTd-Dara: quadruplet) was 28.9% after induction and consolidation. While such comparisons should be made

with caution, it may be that an antibody containing quadruplet with VRD will prove to have similar activity to a Cfz triplet without antibody.

In conclusion, given the updated Carthadex results,<sup>19,20</sup> Cfz proves to be a potent PI and important component of anti-myeloma treatment in a variety of regimens (KTd, KRd, KCd, Kd) (Table 1). Cfz has been investigated with other IMiD, such as pomalidomide, with different alkylators (e.g. Cfz-Bendamustin-Dex) and antibodies like daratumumab or elotuzumab in clinical trials. Due to its substantial efficacy and good tolerability it is used in doublets, triplets and quadruplets, both in younger and older, fit and frail patients, and in ASCT-eligible and -ineligible patients. Cfz is considered a potent relapse option in MM patients who have relapsed after and/or are refractory to both Btz and IMiD. Unfortunately, for NDMM patients, Cfz has not yet been approved, and all clinical trials, including the Carthadex trial, have not yet led to a change in Cfz registration status (Table 1). The findings from ongoing phase II and multiple phase III studies will help to determine optimum dosing regimens, to establish the position of Cfz in relapse, first-line and subsequent therapies, and for consolidation and maintenance approaches. The evidence from clinical trials should be supplemented by reports of real-world evidence in the near future, as experience with managing the toxicity profile continues to grow.<sup>30</sup>

## References

- Moreau P. How I treat myeloma with new agents. *Blood*. 2017;130(13):1507-1513.
- Chim CS, Kumar SK, Orłowski RZ, et al. Management of relapsed and refractory multiple myeloma: novel agents, antibodies, immunotherapies and beyond. *Leukemia*. 2018;32(2):252-262.
- Mikhael J, Ismaila N, Cheung MC, et al. Treatment of Multiple Myeloma: ASCO and CCO Joint Clinical Practice Guideline. *J Clin Oncol*. 2019;37(14):1228-1263.
- Köhler M, Greil C, Hudecek M, et al. Current developments in immunotherapy in the treatment of multiple myeloma. *Cancer*. 2018;124(10):2075-2085.
- Abel GA, Klepin HD. Frailty and the management of hematologic malignancies. *Blood*. 2018;131(5):515-524.
- Engelhardt M, Dold SM, Ihorst G, et al. Geriatric assessment in multiple myeloma patients: validation of the International Myeloma Working Group (IMWG) score and comparison with other common comorbidity scores. *Haematologica*. 2016;101(9):1110-1119.
- Engelhardt M, Domm A-S, Dold SM, et al. A concise revised Myeloma Comorbidity Index as a valid prognostic instrument in a large cohort of 801 multiple myeloma patients. *Haematologica*. 2017;102(5):910-921.
- Larocca A, Dold SM, Zweegman S, et al. Patient-centered practice in elderly myeloma patients: an overview and consensus from the European Myeloma Network (EMN). *Leukemia*. 2018;32(8):1697-1712.
- Ludwig H, Delforge M, Facon T, et al. Prevention and management of adverse events of novel agents in multiple myeloma: a consensus of the European Myeloma Network. *Leukemia*. 2018;32(7):1542-1560.
- Facon T, Anderson K. Treatment approach for the older, unfit patient with myeloma from diagnosis to relapse: perspectives of a European hematologist. *Hematol Am Soc Hematol Educ Program*. 2018;2018(1):83-87.
- Palumbo A, Gay F, Cavallo F, et al. Continuous Therapy Versus Fixed Duration of Therapy in Patients With Newly Diagnosed Multiple Myeloma. *J Clin Oncol*. 2015;33(30):3459-3466.
- Stewart AK, Rajkumar SV, Dimopoulos MA, et al. Carfilzomib, lenalidomide, and dexamethasone for relapsed multiple myeloma. *N Engl J Med*. 2015;372(2):142-152.
- Dimopoulos MA, Moreau P, Palumbo A, et al. Carfilzomib and dexamethasone versus bortezomib and dexamethasone for patients with relapsed or refractory multiple myeloma (ENDEAVOR): a randomised, phase 3, open-label, multicentre study. *Lancet Oncol*. 2016;17(1):27-38.
- Stewart AK, Siegel D, Ludwig H, et al. Overall Survival (OS) of Patients with Relapsed/Refractory Multiple Myeloma (RRMM) Treated with Carfilzomib, Lenalidomide, and Dexamethasone (KRd) Versus Lenalidomide and Dexamethasone (Rd): Final Analysis from the Randomized Phase 3 Aspire Trial. *Blood*. 2017;130(Suppl 1):743-743.
- Rajkumar SV, Kumar S. Multiple Myeloma: Diagnosis and Treatment. *Mayo Clin Proc*. 2016;91(1):101-119.
- Bringhen S, Milan A, D'Agostino M, et al. Prevention, monitoring and treatment of cardiovascular adverse events in myeloma patients receiving carfilzomib A consensus paper by the European Myeloma Network and the Italian Society of Arterial Hypertension. *J Intern Med*. 2019;286(1):63-74.
- Bringhen S, Milan A, Ferri C, et al. Cardiovascular adverse events in modern myeloma therapy - Incidence and risks. A review from the European Myeloma Network (EMN) and Italian Society of Arterial Hypertension (SIIA). *Haematologica*. 2018;103(9):1422-1432.
- Bruno G, Bringhen S, Maffei I, et al. Cardiovascular Organ Damage and Blood Pressure Levels Predict Adverse Events in Multiple Myeloma Patients Undergoing Carfilzomib Therapy. *Cancers (Basel)*. 2019;11(5).
- Wester R, van der Holt B, Asselbergs E, et al. Phase 2 study of carfilzomib, thalidomide, and low-dose dexamethasone as induction and consolidation in newly diagnosed, transplant eligible patients with multiple myeloma, the carthadex trial. *Haematologica*. 2019;104(11):2265-2273.
- Sonneveld P, Asselbergs E, Zweegman S, et al. Phase 2 study of carfilzomib, thalidomide, and dexamethasone as induction/consolidation therapy for newly diagnosed multiple myeloma. *Blood*. 2015;125(3):449-456.
- Mikhael JR, Reeder CB, Libby EN, et al. Phase Ib/II trial of CYK-LONE (cyclophosphamide, carfilzomib, thalidomide and dexamethasone) for newly diagnosed myeloma. *Br J Haematol*. 2015;169(2):219-227.
- Jackson GH, Davies FE, Pawlyn C, et al. A Quadruplet Regimen Comprising Carfilzomib, Cyclophosphamide, Lenalidomide, Dexamethasone (KCRD) Vs an Immunomodulatory Agent Containing Triplet (CTD/CRD) Induction Therapy Prior to Autologous Stem Cell Transplant: Results of the Myeloma XI Study. *Blood*. 2018;132(Suppl 1):302.
- Gay F, Cerrato C, Scalabrini DR, et al. Carfilzomib-lenalidomide-dexamethasone (KRd) induction-autologous-transplant (ASCT)-Krd consolidation vs. Krd 12 cycles vs. carfilzomib-cyclophosphamide-dexamethasone (Kcd) induction-ASCT-Kcd-consolidation: analysis of the randomized Forte trial in newly diagnosed multiple myeloma (NDMM). *Blood*. 2018;132(Suppl):121.
- Moreau P, Kolb B, Attal M, et al. Phase 1/2 study of carfilzomib plus melphalan and prednisone in patients aged over 65 years with newly diagnosed multiple myeloma. *Blood*. 2015;125(20):3100-3104.
- Facon T, Lee JH, Moreau P, et al. Carfilzomib or bortezomib with newly diagnosed multiple myeloma. *Blood*. 2019;133(18):1953-1963.
- Bringhen S, Petrucci MT, Larocca A, et al. Carfilzomib, cyclophosphamide, and dexamethasone in patients with newly diagnosed multiple myeloma: a multicenter, phase 2 study. *Blood*. 2014;124(1):63-69.
- Bringhen S, D'Agostino M, De Paoli L, et al. Phase 1/2 study of weekly carfilzomib, cyclophosphamide, dexamethasone in newly diagnosed transplant-ineligible myeloma. *Leukemia*. 2018;32(4):979-985.
- Bringhen S, Mina R, Petrucci MT, et al. Once-weekly versus twice-weekly carfilzomib in patients with newly diagnosed multiple myeloma: a pooled analysis of two phase 1/2 studies. *Haematologica*. 2019 Feb 7. [Epub ahead of print]
- Moreau P, Attal M, Hulin C. Phase 3 randomized study of daratumumab (DARA) + bortezomib/thalidomide/dexamethasone (D-VTd) vs VTD in transplant-eligible (TE) newly diagnosed multiple myeloma (NDMM): CASSIOPEIA Part 1 results. *Am Soc Clin Oncol ASCO*. 2019;8003.
- Auner HW, Yong KL. More convenient proteasome inhibition for improved outcomes. *Lancet Oncol*. 2018;19(7):856-858.

## The child with immune thrombocytopenia: to treat or not to treat, is that still the question?

Nichola Cooper<sup>1</sup> and Douglas B. Cines<sup>2</sup>

<sup>1</sup>Centre for Haematology, Department of Medicine, Imperial College, Hammersmith Hospital, London, UK and <sup>2</sup>Departments of Pathology and Laboratory Medicine and Medicine, University of Pennsylvania-Perelman School of Medicine, Philadelphia, PA, USA

E-mail: DOUGLAS B. CINES - [dcines@pennmedicine.upenn.edu](mailto:dcines@pennmedicine.upenn.edu)

doi:10.3324/haematol.2019.229179

In this issue of the Journal, Tarantino *et al.*<sup>1</sup> describe their experience with the use of romiplostim to treat children with persistent immune thrombocytopenia (ITP). The results of this study also have implications for management of children who present with ITP.<sup>1</sup>

Eighty to 90% of children who present with ITP go into remission within 12 months and life-threatening bleeding is rare.<sup>2,3</sup> However, this means that 10-20% do not go into remission, and even those whose disease eventually remits can experience bleeding symptoms and limitations in quality of life until this occurs. There is considerable heterogeneity in symptomatology and responsiveness that makes treatment decisions challenging for patients, families and clinicians alike.<sup>4</sup> ITP presenting in very young children, with a peak around 3-4 years, is somewhat more likely to be self-limiting, whereas ITP presenting in the teen years is more likely to follow the more prolonged course seen in adults.<sup>2</sup> Treatment decisions are further complicated by the fact that standard therapies are associated with burdensome adverse effects. Steroids cause metabolic and behavior problems that limit dosing and duration of treatment. Intravenous immunoglobulin (IVIg) can cause severe headaches, requires children to miss school, and its beneficial effects are transient. Splenectomy and immunosuppressive treatment, including rituximab, are used with caution in children because of the potential for increased risk of infection in an immature immune system and the unknown potential for late effects such as secondary malignancies if immunosuppressants are used persistently.<sup>5</sup> In view of these adverse effects of treatment, the low incidence of internal bleeding, the high likelihood of remission, and the absence of data indicating an effect on durable remission, many guidelines recommend not treating children with ITP unless bleeding is severe (Figure 1, left).<sup>6,7</sup> However, this clinical situation is not ideal. Episodic and unpredictable bleeding along with low platelet counts can lead to child and parental anxiety, restrictions on activities, and a significant negative impact on social and emotional development. Children with ITP and significant thrombocytopenia can have reduced school attendance, fail to participate in athletic activities, and families may be reluctant to travel far from home.<sup>5,8</sup>

Therefore, there is an unmet need for less toxic and less invasive approaches to managing children with: a) symptomatic persistent/chronic ITP; b) those at significant risk of bleeding based on platelet count and/or comorbidities; and c) those with impaired health care related quality of life (HRQoL) due to the need for considerable medical attention or because of the emotional impact associated with bleeding, the fear of bleeding, and the side effects of current treatments.

Thrombopoietin receptor agonists (TRA) have been

used successfully for these purposes in adults with ITP for approximately ten years.<sup>9</sup> From 80% to 90% of adults show a response, almost all of which are durable with continued treatment. Response rates are even higher when crossovers from either agent to the other are included and less stringent response criteria, e.g. attaining a patient-specific hemostatic platelet count, are employed. There is now less concern over the risk of thrombosis and marrow fibrosis based on long-term safety studies,<sup>10,11</sup> and 20-30% of adult patients are able to discontinue therapy by 2-3 years of treatment (reviewed by Ghanima *et al.*<sup>9</sup>).

Following upon from this track record in adults, it became important to assess whether similar efficacy and safety profiles would be seen in children with ITP. Smaller randomized studies showing efficacy and no major safety concerns led to the approval of romiplostim in 2018 for use in children with ITP who are over one year of age with ITP  $\geq 6$  months duration.<sup>12,13</sup> Treatment was associated with improvement in child self-reported HRQoL and reduced parental burden.<sup>14</sup> However, there continued to be a need to establish whether efficacy was sustained, to investigate the long-term safety, and to assess the impact of romiplostim on the natural history of ITP in children.

In this issue, Tarantino *et al.* report the outcomes of an open-label extension study of romiplostim in 65 children with ITP of  $\geq 6$  months duration,<sup>1</sup> 15 of whom were receiving this treatment for the first time. Median duration of disease was 3 years (range: 1-13 years) and median baseline age was 11 years (range: 3-18 years). Median duration of treatment was 2.6 years (range: 1-7 years), median average weekly dose 4.8  $\mu\text{g}/\text{kg}$  (but was as low as 0.1  $\mu\text{g}/\text{kg}$  in some), and the median response rate using previously published strict criteria (72% at  $\geq 75\%$  of visits; 58% at  $\geq 90\%$  of visits) was comparable to outcomes in adults. Fifty-nine (91%) of the 65 children or their caregivers “self-administered” treatment at home at least once starting at median study week 7. Fifty-seven reported miscellaneous bleeding adverse effects (AE) as would be expected in a trial in this population, but no thrombosis or other major drug-related AE were identified, although bone marrow examinations that might have revealed fibrosis were performed in only two subjects. Of note, 23 (35%) required rescue treatment on at least one occasion. Also, 29 (44%) left the study for a variety of reasons, including withdrawal of consent for unspecified reasons, non-compliance, need for other treatment, and two for AE unrelated to treatment. Treatment-free responses were observed in 15 children (23%) who had ITP for a median of four years (range: 1-12 years), had received romiplostim for two years (range: 1-6 years), and the response was maintained in 14 for a median of one

## Time for new approach to early management of children with ITP?

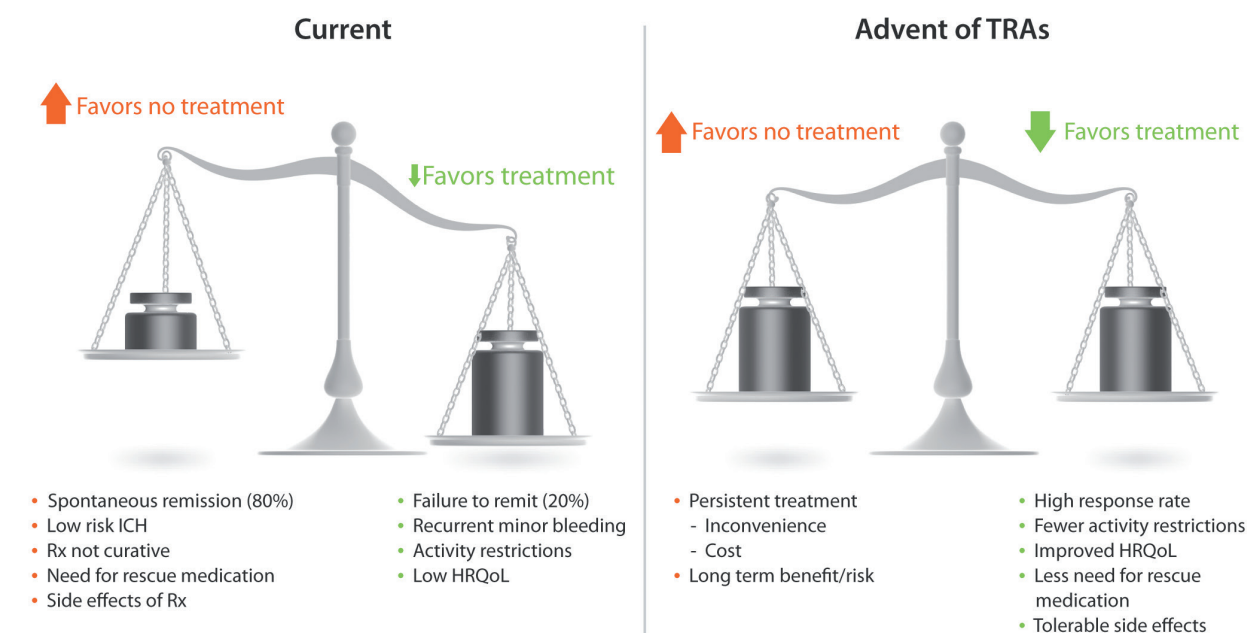


Figure 1. (Left) Currently, children who present with immune thrombocytopenia (ITP) are followed without therapy in the absence of significant bleeding. Life-threatening bleeding is rare, remission is common, and no therapy has been shown to alter the natural history of the disorder. The decision not to treat is therefore dominated by the side effects of therapy. The side effects of corticosteroids and intravenous immunoglobulin (IVIg) and the risk of infection after splenectomy and perhaps rituximab mitigate in favor of observation. Indeed, treatment may worsen health care related quality of life (HRQoL). (Right) With the advent of thrombopoietin receptor agonists (TRA), the proper balance has become less clear. TRA provide a therapeutic option with a high response rate and fewer concerns about side effects, as described in Tarentino *et al.*<sup>1</sup> Improvement in platelet counts may reduce nuisance bleeding and the need for rescue therapy and hospital attendance, increase participation in physical and social activities, reduce anxiety around low platelet counts, and improve HRQoL. ICH: intracranial hemorrhage; Rx: treatment.

year (range: 0.4-2.1 years); younger age at first dose was associated with treatment-free responses.

This is the most comprehensive placebo-controlled study of TRA in pediatric ITP. The data show that romiplostim is a highly effective maintenance therapy for children with ITP of at least six months duration who did not respond to, or perhaps were intolerant of, prior therapies and who experienced bleeding or are at risk of bleeding because of low platelet counts. Romiplostim was well tolerated, no significant drug-related AE were observed at two years of study, and, importantly, treatment could be given at home by trained patients or family members. The high rate of withdrawal complicates delineating sustained reduction in bleeding events, use of concurrent medications, and the need for rescue interventions that might occur with more extended use in practice. Also, the implication that romiplostim induces remission is less compelling in the absence of a control population.

Eltrombopag has also been approved for use in the pediatric population in a similar setting and with similar outcomes.<sup>15-18</sup> Iron deficiency and transaminitis have been reported in some children treated with eltrombopag.<sup>16,19</sup> One as yet theoretical concern when contemplating long-term use is that eltrombopag acts on bone marrow stem cells as well as on megakaryocytes.<sup>20</sup> In the absence of a head-to-head study, the choice between agents often comes down to the requirement for dietary restrictions and daily administration with eltrombopag *versus* parenteral administration with more frequent medical visits

with romiplostim, as well as differences in cost and insurance coverage.

One important issue raised by this study is whether consideration should be given to starting romiplostim or eltrombopag in children with ITP without the need to wait six months from diagnosis. This is particularly relevant for children who experience extensive bruising, epistaxis, menorrhagia, or other symptoms that require frequent medical interventions or that lead to loss of school days, withdrawal from competitive sports or otherwise reduce HRQoL (Figure 1, right). If durable safety is established, TRA may also be advantageous for those with less severe symptoms but significant anxiety related to low platelet counts. Indeed, this trend in treatment is becoming apparent, as approximately 20% of the children treated with romiplostim in the ICON2 analysis had severe, refractory, but newly diagnosed ITP, and a few were treated to resume physical activities or to improve QoL.<sup>17</sup> Improvements in platelet count and HRQoL have been reported with this approach, although the number of patients studied is small and the duration of follow up is short.<sup>18,21</sup>

In addition to continued surveillance relating to safety in the pediatric population, future studies are needed to determine if initiating treatment earlier in the disease reduces bleeding, the need for other treatment, medical visits, and lost school days while improving the emotional well-being of the child and the family. Therefore, studies such as the one reported here by Tarentino *et al.* could

have a major impact on the way in which pediatric hematologists approach the long standing “To treat or not to treat” question when evaluating children with suspected ITP at the time of or soon after presentation<sup>22</sup> (Figure 1). This study also highlights a compelling need for careful study of children now receiving TRA for other indications, including hereditary thrombocytopenia and associated qualitative platelet disorders, neonatal thrombocytopenia, and thrombocytopenia following chemotherapy or bone marrow transplantation (reviewed by Neunert and Rose<sup>23</sup>).

## References

1. Tarantino MD, Bussel JB, Blanchette VS, et al. Long-term treatment with romiplostim and treatment-free platelet responses in children with chronic immune thrombocytopenia. *Haematologica*. 2019; 104(11):2283-2291.
2. Bennett CM, Neunert C, Grace RF, et al. Predictors of remission in children with newly diagnosed immune thrombocytopenia: Data from the Intercontinental Cooperative ITP Study Group Registry II participants. *Pediatr Blood Cancer*. 2018;65(1).
3. Neunert CE, Buchanan GR, Imbach P, et al. Bleeding manifestations and management of children with persistent and chronic immune thrombocytopenia: data from the Intercontinental Cooperative ITP Study Group (ICIS). *Blood*. 2013;121(22):4457-4462.
4. Shaw J, Kilpatrick K, Eisen M, Tarantino M. The incidence and clinical burden of immune thrombocytopenia in pediatric patients in the United States. *Platelets*. 2019;1-8.
5. Cooper N. A review of the management of childhood immune thrombocytopenia: how can we provide an evidence-based approach? *Br J Haematol*. 2014;165(6):756-767.
6. Provan D, Stasi R, Newland AC, et al. International consensus report on the investigation and management of primary immune thrombocytopenia. *Blood*. 2010;115(2):168-186.
7. Neunert C, Lim W, Crowther M, Cohen A, Solberg L Jr, Crowther MA; American Society of Hematology. The American Society of Hematology 2011 evidence-based practice guideline for immune thrombocytopenia. *Blood*. 2011;117(16):4190-4207.
8. Klaassen RJ, Blanchette V, Burke TA, et al. Quality of life in childhood immune thrombocytopenia: international validation of the kids' ITP tools. *Pediatr Blood Cancer*. 2013;60(1):95-100.
9. Ghanima W, Cooper N, Rodeghiero F, Godeau B, Bussel JB. Thrombopoietin receptor agonists: ten years later. *Haematologica*. 2019;104(6):1112-1123.
10. Saleh MN, Bussel JB, Cheng G, et al. Safety and efficacy of eltrombopag for treatment of chronic immune thrombocytopenia: results of the long-term, open-label EXTEND study. *Blood*. 2013;121(3):537-545.
11. Cines DB, Gernsheimer T, Wasser J, et al. Integrated analysis of long-term safety in patients with chronic immune thrombocytopenia (ITP) treated with the thrombopoietin (TPO) receptor agonist romiplostim. *Int J Hematol*. 2015;102(3):259-270.
12. Bussel JB, Buchanan GR, Nugent DJ, et al. A randomized, double-blind study of romiplostim to determine its safety and efficacy in children with immune thrombocytopenia. *Blood*. 2011;118(1):28-36.
13. Tarantino MD, Bussel JB, Blanchette VS, et al. Romiplostim in children with immune thrombocytopenia: a phase 3, randomised, double-blind, placebo-controlled study. *Lancet*. 2016;388(10039):45-54.
14. Mathias SD, Li X, Eisen M, Carpenter N, Crosby RD, Blanchette VS. A Phase 3, Randomized, Double-Blind, Placebo-Controlled Study to Determine the Effect of Romiplostim on Health-Related Quality of Life in Children with Primary Immune Thrombocytopenia and Associated Burden in Their Parents. *Pediatr Blood Cancer*. 2016;63(7):1232-1237.
15. Tumaini Massaro J, Chen Y, Ke Z. Efficacy and safety of thrombopoietin receptor agonists in children with chronic immune thrombocytopenic purpura: meta-analysis. *Platelets*. 2019;30(7):828-835.
16. Kim TO, Despotovic J, Lambert MP. Eltrombopag for use in children with immune thrombocytopenia. *Blood Adv*. 2018;2(4):454-461.
17. Neunert C, Despotovic J, Haley K, et al. Thrombopoietin Receptor Agonist Use in Children: Data From the Pediatric ITP Consortium of North America ICON2 Study. *Pediatr Blood Cancer*. 2016;63(8):1407-1413.
18. Grainger JD, Blanchette VS, Grotzinger KM, Roy A, Bussel JB. Health-related quality of life in children with chronic immune thrombocytopenia treated with eltrombopag in the PETIT study. *Br J Haematol*. 2019;185(1):102-106.
19. Lambert MP, Witmer CM, Kwiatkowski JL. Therapy induced iron deficiency in children treated with eltrombopag for immune thrombocytopenia. *Am J Hematol*. 2017;92(6):E88-E91.
20. Kao YR, Chen J, Narayanagari SR, et al. Thrombopoietin receptor-independent stimulation of hematopoietic stem cells by eltrombopag. *Sci Transl Med*. 2018;10(458).
21. Grace RF, Shimano KA, Bhat R, et al. Second-line treatments in children with immune thrombocytopenia: Effect on platelet count and patient-centered outcomes. *Am J Hematol*. 2019;94(7):741-750.
22. Neunert CE, Cooper N. Evidence-based management of immune thrombocytopenia: ASH guideline update. *Hematology Am Soc Hematol Educ Program*. 2018;2018(1):568-575.
23. Neunert CE, Rose MJ. Romiplostim for the management of pediatric immune thrombocytopenia: drug development and current practice. *Blood Adv*. 2019;3(12):1907-1915.

# How I diagnose and manage Philadelphia chromosome-like acute lymphoblastic leukemia

Avraham Frisch<sup>1</sup> and Yishai Ofran<sup>1,2</sup>

<sup>1</sup>Department of Hematology and Bone Marrow Transplantation, Rambam Health Care Campus, Haifa, and <sup>2</sup>Bruce Rappaport Faculty of Medicine, Technion, Israel Institute of Technology, Haifa, Israel



## ABSTRACT

Advances in our understanding of mechanisms of leukemogenesis and driver mutations in acute lymphoblastic leukemia (ALL) lead to a more precise and informative sub-classification, mainly of B-cell ALL. In parallel, in recent years, novel agents have been approved for the therapy of B-cell ALL, and many others are in active clinical research. Among the newly recognized disease subtypes, Philadelphia-chromosome-like ALL is the most heterogeneous and thus, diagnostically challenging. Given that this subtype of B-cell ALL is associated with a poorer prognosis, improvement of available therapeutic approaches and protocols is a burning issue. Herein, we summarize, in a clinically relevant manner, up-to-date information regarding diagnostic strategies developed for the identification of patients with Philadelphia-chromosome-like ALL. Common therapeutic dilemmas, presented as several case scenarios, are also discussed. It is currently acceptable that patients with B-cell ALL, treated with an aim of cure, irrespective of their age, be evaluated for a Philadelphia-chromosome-like signature as early as possible. Following Philadelphia-chromosome-like recognition, a higher risk of resistance or relapse must be realized and treatment should be modified based on the patient's specific genetic driver and clinical features. However, while active targeted therapeutic options are limited, there is much more to do than just prescribe a matched inhibitor to the identified mutated driver genes. In this review, we present a comprehensive evidence-based approach to the diagnosis and management of Philadelphia-chromosome-like ALL at different time-points during the disease course.

## Introduction

In recent years several new agents have been approved for the treatment of acute lymphoblastic leukemia (ALL), resulting in a tremendous improvement in long-term survival of patients. Concurrently, refinements in risk stratification have enabled escalation and de-escalation of therapy, thus minimizing treatment-related mortality, while maintaining high response rates. While the traditional method for subgrouping B-cell ALL (B-ALL) is based on cytogenetic and mutation analyses, it has been demonstrated that each of the known subgroups has a unique gene expression profile. Subsequent studies identified a B-ALL group which expresses the *BCR/ABL* signature in the absence of the *BCR/ABL* fusion, and hence this group was defined as Philadelphia chromosome-like (Ph-like) ALL.

Surprisingly, a search for genetic alterations driving these types of leukemia has revealed multiple mutations and/or aberrations, involving different signal transduction pathways. Clinically, patients with Ph-like ALL have been recognized as being at a high risk for a poor response to therapy or relapse.<sup>1-3</sup> Herein we describe the challenges in the diagnosis and appropriate treatment selection for this heterogeneous group of patients.

**Haematologica** 2019  
Volume 104(11):2135-2143

## Correspondence:

YISHAI OFRAN  
y\_ofran@rambam.health.gov.il

Received: April 29, 2019.

Accepted: September 3, 2019.

Pre-published: October 3, 2019.

doi:10.3324/haematol.2018.207506

Check the online version for the most updated information on this article, online supplements, and information on authorship & disclosures: [www.haematologica.org/content/104/11/2135](http://www.haematologica.org/content/104/11/2135)

©2019 Ferrata Storti Foundation

Material published in *Haematologica* is covered by copyright. All rights are reserved to the Ferrata Storti Foundation. Use of published material is allowed under the following terms and conditions:

<https://creativecommons.org/licenses/by-nc/4.0/legalcode>.

Copies of published material are allowed for personal or internal use. Sharing published material for non-commercial purposes is subject to the following conditions:

<https://creativecommons.org/licenses/by-nc/4.0/legalcode>, sect. 3. Reproducing and sharing published material for commercial purposes is not allowed without permission in writing from the publisher.



## Driver mutations and aberrations in Philadelphia chromosome-like acute lymphoblastic leukemia

In their landmark analysis of 1,725 ALL patients, Roberts *et al.* found kinase-activating mutations in more than 90% of patients with Ph-like expression.<sup>4</sup> The large variability of genetic alterations recognized in patients with Ph-like ALL makes further sub-categorization a challenge. For the purpose of a clinically oriented discussion, we believe clustering Ph-like ALL into the following four subgroups would be helpful.

### CRLF2-associated Philadelphia chromosome-like acute lymphoblastic leukemia

The CRLF2 protein is a cytokine receptor which heterodimerizes with interleukin-7 receptor (IL7R)- $\alpha$ , and upon binding to its ligand (thymic stromal lymphopoietin) activates the JAK-STAT pathway. This activation leads to cell proliferation without concomitant differentiation.<sup>5</sup> In ALL, high expression of CRLF2 has been shown to correlate with reduced survival.<sup>4,6,7</sup> Several genotypes are associated with high CRLF2 expression, including a chromosomal translocation with *IGH-CRLF2* fusion, a cryptic interstitial deletion which results in a *P2RY8-CRLF2* fusion and *CRLF2* point mutations engendering uncontrolled receptor activation.

The *IGH-CRLF2* translocation is an early event in leukemogenesis and remains stable in relapse, while the *P2RY8-CRLF2* translocation takes place later during disease development, is often subclonal and cannot be recognized in one-third to one-half of relapsed patients.<sup>8,9</sup> Additionally, CRLF2 expression is 10-100-fold higher in patients with *IGH-CRLF2* than in those with the *P2RY8-CRLF2*.<sup>5,10,11</sup> With regard to the prognostic impact, the relapse risk of *IGH-CRLF2* ALL patients has been shown to be twice as high as that of *P2RY8-CRLF2* ALL patients.<sup>12</sup>

Deregulation of *CRLF2* expression is likely to require additional players to drive the leukemic process. In an ALL cell line with the *IGH-CRLF2* translocation, knock-down of *CRLF2* was not found to reduce proliferation of leukemic cells dramatically.<sup>5</sup> About half of ALL patients with deregulated *CRLF2* also have mutations in the JAK-STAT pathway<sup>4,7</sup> and these latter are associated with a worse prognosis.<sup>4,13</sup> In an analysis by the German Multicenter Study Group for Adult ALL (GMALL), one-third of adult patients with high CRLF2 expression were not found to harbor translocations or point mutations involving *CRLF2*.<sup>14</sup> Similarly, in a recently published study, the *CRLF2* translocation was identified in only 80% of Ph-like ALL patients demonstrating high CRLF2 expression.<sup>15</sup> In fact, high CRLF2 immunophenotypic expression does not *per se* confer a worse prognosis, if it is not accompanied by *CRLF2* genetic aberrations.<sup>11</sup> Notably, high CRLF2 expression is reported to be significantly more frequent among patients of Hispanic ethnicity.<sup>12,16</sup>

Mutations/deletions in the *IKZF1* gene are prevalent in patients with Ph-like ALL<sup>1,17,18</sup> and the presence of these mutations may be a better predictor of a poor prognosis than a high level of CRLF2 expression *per se*.<sup>17</sup> Interestingly, a Chinese group recently demonstrated that *IKZF1* is an epigenetic regulator of *CRLF2*, and *IKZF1* mutations/deletions can lead to overexpression of *CRLF2*.<sup>19</sup>

### ABL-class translocations

Translocations involving the pro-oncogenes *ABL1*, *ABL2*, *CSF1A* and *PGDFRB* are evident in about 15% of Ph-like ALL cases.<sup>4,20</sup> Due to the translocations, these genes lose their normal regulatory control; however, no specific partner genes, among the many reported, have been identified as being of particular prognostic significance. The presence of any of these translocations is considered sufficient for the diagnosis of Ph-like ALL.<sup>20</sup> The translocations in question are mutually exclusive with *CRLF2* and *JAK-STAT* mutations but, as in other Ph-like subgroups, are often concomitantly present with *IKZF1* mutations/deletions.<sup>4,20</sup> Patients with *ABL*-activating translocations usually respond poorly to therapy, continue to have measurable residual disease (MRD) after induction<sup>20</sup> and should be treated with *ABL* inhibitors, as discussed later.

### EPOR and JAK2 translocations

*EPOR* translocations, capable of partnering with multiple different genes, are grouped together with *JAK2* translocations as they share the same mechanism of inducing cell proliferation through constitutive activation of the JAK pathway. These translocations are easy to recognize by fluorescence *in situ* hybridization (FISH) analysis and they are associated with a poor prognosis.<sup>4,21,22</sup> *EPOR*-involving translocations lead to truncation of the erythropoietin receptor (EPO-R), its stabilization and overexpression, resulting in downstream activation of the *JAK2* pathway.<sup>23</sup> These chromosomal aberrations comprise about 10% of Ph-like ALL alterations, are associated with *IKZF1* mutations or deletions and could potentially be targeted with JAK inhibition.<sup>17</sup>

### JAK/STAT or RAS mutations:

This subgroup accounts for about 15-20% of Ph-like ALL cases. It includes genetic alterations of *IL7R*, *FLT3*, *SH2B3*, *JAK1*, *JAK3*, *IL2RB* and *RAS* genes.<sup>24</sup> These mutations are all subclonal<sup>4</sup> and there is paucity of data regarding the dynamics of their alterations in relapse. Remarkably, *IKZF1* is less common in this subtype of Ph-like ALL than in the above-mentioned ones.<sup>4,20,22</sup> The prognosis of these patients is believed to be better than that of patients with other subtypes of Ph-like ALL.<sup>4,22</sup> Individuals presenting with a *RAS* mutation as their sole driver mutation share both biological and clinical characteristics with the above-delineated *JAK/STAT*-derived group. Biologically, *JAK/STAT* and *RAS* signaling pathways are closely connected. Notably, other kinase mutations, i.e., *NRAS*, *KRAS*, *PTPN11*, and *NF1*<sup>4</sup> are observed not only in Ph-like ALL but also in hyperploid ALL.<sup>25,26</sup> They are also found, with different prevalences, in all other subgroups of Ph-like ALL.<sup>4,20,22</sup>

## Clinical presentation and diagnostic approaches to Philadelphia chromosome-like acute lymphoblastic leukemia

The prevalence of Ph-like ALL in cohorts of newly diagnosed pediatric patients is about 10-20%,<sup>1,3,4,18</sup> and rises to 20-30% in adults.<sup>13,14,27</sup> Ph-like cases are by definition *BCR/ABL*-negative, and are also always *MLL*-, *ETV/RUNX1*- and *TCF3/PBX1*-negative. Thus, they constitute a subgroup within the B cell other ALL.<sup>17,28</sup> It has been previously reported that some patients may present

with an overlapping group of hyperploid cytogenetics and Ph-like ALL.<sup>11,28</sup> A recent comprehensive and integrative genomic classification of B-ALL categorized 23 leukemia subclasses, clearly defined by a specific genetic aberration, thus minimizing overlaps with the Ph-like phenotype.<sup>29</sup>

There is no consensus approach to the diagnosis of patients who express a Ph-like gene signature.<sup>30</sup> These patients usually present with a higher white blood cell count<sup>1,4,17,22,27,31</sup> and are likely to remain MRD-positive following standard induction regimens.<sup>4,13,14,22,28,31</sup> Selecting an optimal screening method and defining the patient population to be screened are still moving targets.

When first recognized, Ph-like ALL were retrospectively identified based upon gene expression profiling of a very wide array of genes.<sup>1,4,32</sup> Notably, two large gene arrays,<sup>1,4</sup> using a 257-gene probe set and a 110-gene set<sup>2</sup> shared only a minimal number of genes. Application of both arrays to each of two different cohorts of patients resulted in low concordance.<sup>2</sup> Remarkably, kinase fusion cases in the two cohorts were identified by both methods in complete concordance, while there were many cases of high expression of *CRLF2* and *JAK/STAT* mutations that were recognized with the 257-gene probe set and not with the 110-gene set.<sup>2</sup> Thus, while the evaluation of newly diagnosed "B-cell other" ALL patients should include an attempt to identify the Ph-like phenotype,<sup>33</sup> a definitive diagnosis should not rely on the gene expression phenotype but rather on the identification of a genetic aberration in the cell signaling related gene. RNA sequencing enables both identification of a Ph-like phenotype and comprehensive analysis of aberrant translocations. As this method is technically complicated and unavailable in most centers, a routine diagnosis of Ph-like ALL requires a combination of a simple screening test and an ultimate method to identify the culprit leukemia driver in each patient.

One screening approach is to search for a specific phenotype using limited sets of genes.<sup>34</sup> Alternatively, a panel of FISH probes or polymerase chain reaction (PCR) tests covering the most common *ABL*, *JAK/EPOR* and *CRLF2* translocations can be employed as a screening tool.<sup>27,35</sup> Low density microarrays (LDA), using a limited number of genes were first employed by Harvey *et al.*<sup>36</sup> With an array of only 15 genes the tests were highly sensitive and specific (93% and 89%, respectively) for the identification of Ph-like ALL. The concordance between this assay and the result of the original 257-gene set analysis was only 87%, mainly due to over-diagnosis of cases of high *CRLF2* expression by the LDA. Application of this method in high-risk pediatric ALL patients failed to detect mutations in about 15% of LDA-positive patients.<sup>15</sup> Interestingly, the study identified nine patients with *CRLF2* translocations who were LDA-negative, which translated into a false negative value of less than 1%. Other LDA with fewer genes were developed by Heatley *et al.*<sup>18</sup> and Roberts *et al.*<sup>37</sup> To simplify this approach, Chiaretti *et al.* used quantitative real-time PCR to assess expression levels of ten genes and create a Ph-like ALL predictor.<sup>27</sup> Expression-based screening methods identify a phenotype and should be followed by a search for a targetable genotype, either by RNA sequencing, whole exome or targeted PCR panel sequencing, or by multiple-probe FISH analysis. As mentioned above, false negative results are rare; however, there are a substantial number of cases presenting with an overexpression signature but with no detectable driver

genetic aberration. The actual risk and clinical implications in such cases are unknown.

It is also possible to screen for Ph-like ALL by searching directly for specific translocations and mutations. In a study conducted by the research group from the Munich Leukemia Laboratory in Germany<sup>38</sup> screening by multiple FISH probes and targeted PCR (*ABL1*, *ABL2*, *CSF1R*, *PDGFRB* along with quantitative PCR for *CRLF2*) successfully identified all patients who had a Ph-like gene expression profile according to the aforementioned 257-gene set. Another advantage of this method is the option of using quantitative PCR of the found driver mutation for MRD detection, although the negative predictive value of each aberration should be evaluated separately. Cooperative groups and leading centers around the world use different methods for the identification of Ph-like ALL. In Europe, some groups employ multiplex PCR or commercially available targeted RNA sequencing kits, while others use a FISH panel for primary screening. In the USA, the Children's Oncology Group (COG) uses LDA as the screening approach. Comprehensive RNA sequencing is conducted only in specific centers such as the St. Jude Medical Center.

The variability of the methods available makes the diagnosis of a Ph-like expression signature in a patient with no defined genetic alteration a challenge. Figure 1 presents a suggested clinical screening algorithm for Ph-like ALL to be applied outside of clinical trials.

## Treatment of Philadelphia chromosome-like acute lymphoblastic leukemia

To illustrate some of the key therapeutic issues and dilemmas in Ph-like ALL, we present and discuss several case scenarios. The discussion focuses on possible benefits of induction therapy intensification for these patients, post-induction treatment in MRD-positive and -negative patients as well as management of the most challenging cases of relapsed and elderly patients.

### Is there any preferred induction regimen for patients presenting with Philadelphia chromosome-like acute lymphoblastic leukemia?

*Case presentation.* A 57-year old previously healthy man diagnosed with pre-B ALL has just been transferred from a rural hospital to your center. His peripheral blast count at diagnosis was  $32 \times 10^9$  cells/L which dropped significantly after 1 week of steroid therapy. FISH panel analysis identified the *EPOR* translocation as the sole cytogenetic aberration. What are preferable induction therapy options?

Remission induction protocols commonly employed in ALL are variations of a consensus basic paradigm, combining four or five of the following drugs: anthracyclines, vincristine, cyclophosphamide, L/PEG-asparaginase and steroids. Differences between the protocols lie in their intensity, schedule and the addition of 6-mercaptopurine, cytarabine and rituximab. Data derived from randomized comparisons are scanty and inconclusive regarding survival superiority following any induction regimen, despite variations in remission rates in specific subgroups.<sup>39-41</sup> In current clinical practice, appropriate treatment intensity and chemotherapy doses are usually determined based on the risk of adverse events and not on disease characteristics. Thus, a patient's advanced age, co-morbidities and/or fragility would lead most physicians to prescribe

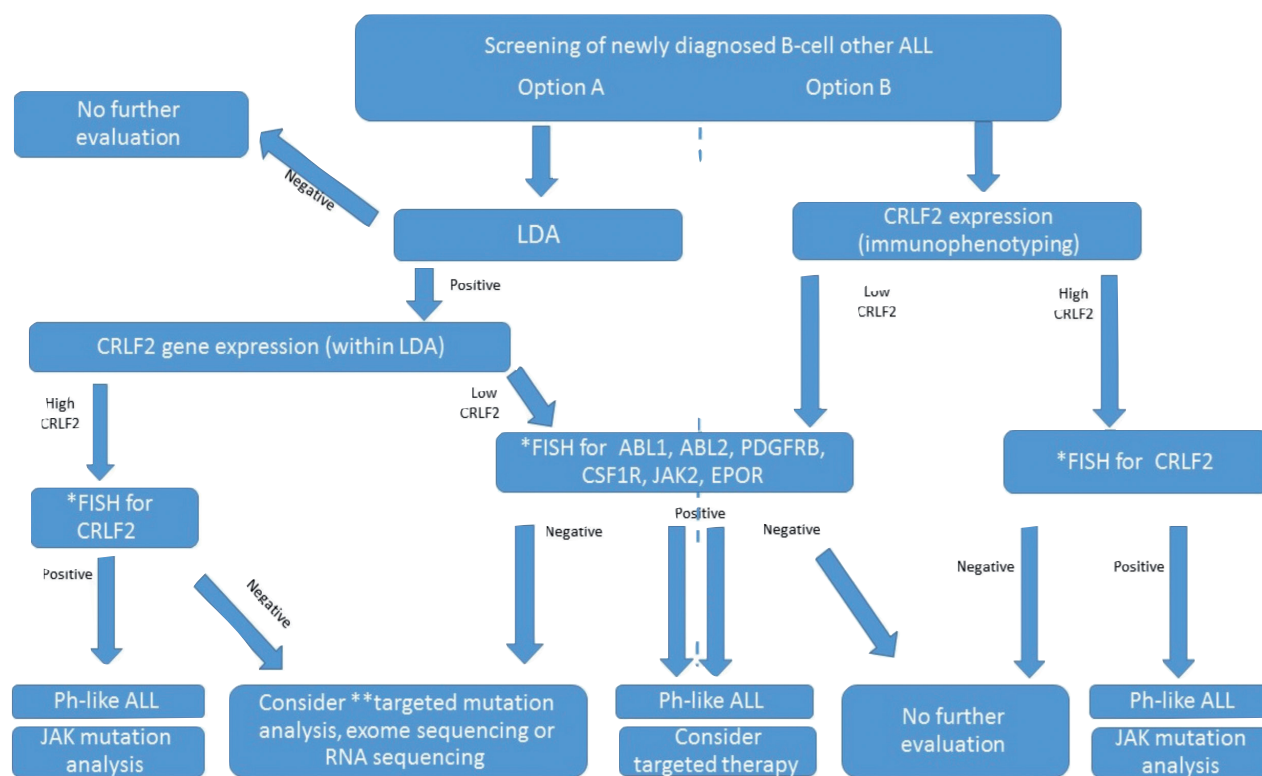


**Figure 1. Screening of newly diagnosed cases of B-cell other acute lymphoblastic leukemia.** \*FISH-break-apart. \*\*Targeted sequencing for mutations in *JAK*, *IL7R*, *FLT3*, *SH2B3*, *RAS* and *PTPN11*. ALL: acute lymphoblastic leukemia; LDA: low density microarray; FISH: fluorescence *in situ* hybridization; Ph-like: Philadelphia chromosome like.

low/moderate-intensity regimens, such as mini-Hyper-CVAD (cyclophosphamide and dexamethasone at 50% dose reduction, no anthracycline, methotrexate at 75% dose reduction, cytarabine at 0.5 g/m<sup>2</sup> x 4 doses) or other similar protocols.<sup>42-44</sup>

Until recently, the majority of Ph-like ALL patients were identified late during the course of treatment, usually after the completion of induction. Yet, with the implementation of CRLF2 immunophenotyping tests and routine application of wide-spectrum, rapid FISH panels and LDA, it is reasonable that a patient could be diagnosed with a Ph-like aberration early during induction. Clinical trials, such as the COG AALL1521, examining the benefit of adding ruxolitinib to standard induction, are currently recruiting patients. However, should the identification of an *EPOR* or *JAK* translocation entail alteration of the selected induction regimen for patients treated outside clinical trials? Ph-like ALL patients tend to remain MRD-positive after induction<sup>13,14</sup> and are therefore planned for intensification of consolidation therapy by most pediatric protocols.<sup>45-47</sup> Pediatric-oriented intensification regimens are extremely toxic and difficult to administer to high-risk adult patients. The presence of the *EPOR* translocation is an established adverse prognostic feature,<sup>5,23</sup> but due to its rarity, randomized studies to assess a potential benefit of different induction or intensification regimens will probably never be conducted. In the absence of such clinical trials, intensified induction seems reasonable.

Among 148 recently reported adults with ALL, the achievement of MRD negativity did not translate into a better outcome in the 49 patients who were diagnosed

with a Ph-like disease.<sup>13</sup> These patients were treated with Hyper-CVAD or augmented BFM (Berlin-Frankfurt-Munich) protocols with no specific intensification or modification for their high-risk ALL. In a pediatric series of 488 patients, those from the very high-risk group remained at a high risk of relapse even if MRD negativity was achieved.<sup>48</sup> A new comprehensive study from the United Kingdom has suggested that the cutoff level for clinically relevant MRD is different for various genetic subtypes of ALL.<sup>49</sup> Thus, it is reasonable to consider all Ph-like ALL patients as high risk, regardless of their MRD status. Some data from 344 pediatric patients suggest that therapy intensification for Ph-like MRD-positive patients can lead to MRD eradication and improve outcome.<sup>28</sup> However, confirmation from additional, large studies is required to feel confident about adopting chemotherapy intensification as a suitable therapeutic approach to be used as induction in Ph-like ALL patients. Notably, a randomized trial testing the value of enhancing therapy for MRD-positive patients, regardless of their genetic background, showed only a moderate improvement in event-free survival. However, even such benefit cannot be readily extrapolated to genetically very high-risk groups.<sup>50</sup>

As to practical suggestions for the patient in question, although not specifically tested in the context of Ph-like ALL, addition of rituximab if leukemic cells are CD20<sup>+</sup> and the use of L-asparaginase or PEG-asparaginase, known to be active in high-risk ALL, may be recommended. At the same time, the risk of asparaginase-related complications at his age needs to be considered.<sup>51-53</sup>

Blinatumomab, a bispecific antibody targeting CD19

and CD3, has not yet been tested as an agent for Ph-like ALL treatment intensification. However, it has been proven to be effective in MRD eradication, and is currently being incorporated in clinical trials as part of front-line treatment for other high-risk ALL patients.

### Should targeted agents be added to induction regimens if the diagnosis of Philadelphia chromosome-like acute lymphoblastic leukemia is confirmed?

*Case presentation.* A 23-year old woman with a recent diagnosis of B-ALL is being treated at your institution according to a GMALL protocol.<sup>54</sup> On day 15 of induction, results of molecular tests reveal an IGH-CRLF2 translocation and a JAK2-activating mutation at R683G in the pseudo-kinase domain. Should JAK inhibitors be included in the treatment plan?

Most aberrations identified in patients with Ph-like ALL lead to kinase activation in the JAK2 pathway.<sup>55,56</sup> Preclinical studies support the rationale that JAK inhibition would potentially counteract the aberrant, proliferation signal derived from the mutation.<sup>57,58</sup> Early-phase clinical trials have shown that the combination of JAK inhibitors with chemotherapy is safe and tolerable.<sup>59-61</sup> However, the clinical benefit of the addition of currently available JAK inhibitors, such as ruxolitinib, to chemotherapy in ALL is questionable. Unlike myeloproliferative neoplasms, in which JAK2 inhibition with low/intermediate-dose ruxolitinib is sufficient to yield a clinical response,<sup>62</sup> in leukemia, the use of ruxolitinib has not yet been approved. In addition, the proliferation signal in Ph-like ALL is derived from several kinases and parallel blockage of JAK 1&2, RAS and mTOR is probably needed for leukemia cell elimination.<sup>30,58,63-65</sup> Thus, high ruxolitinib doses of at least 50 mg twice daily<sup>60,66</sup> could be required to achieve clinical benefit. Phase II studies exploring the role of incorporating ruxolitinib in induction regimens for Ph-like ALL are ongoing.

For the minority of Ph-like patients presenting with BCR-activating aberrations, data are accumulating that kinase inhibition by BCR/ABL specific tyrosine kinase inhibitors (TKI) may be beneficial.<sup>67-70</sup> Most reports claiming the benefit of TKI present results of patients diagnosed with a *PDGFRB* translocation; so far, only a few cases of successful TKI use in patients with *ABL1* aberrations have been reported.<sup>4,71,72</sup> Although no generalized conclusion can be made regarding the value of TKI in all ABL-activating cases, we feel that, given the established safety of these drugs and the data provided in the above-mentioned reports, arguments for off-label TKI use when considering targeted therapies for Ph-like ALL are much stronger than those for the use of JAK inhibitors. At the same time, one should bear in mind that Ph-like leukemia is a genetically complex disease and resistance to TKI, related to clonal evolution and appearance of additional mutations, has been reported.<sup>73-75</sup> Therefore, the addition of targeted therapy to first-line chemotherapy in Ph-like ALL is currently considered experimental.

### Approaches to post-remission therapy in patients with Philadelphia chromosome-like acute lymphoblastic leukemia with measurable residual disease

*Case presentation.* A 63-year old man with B-ALL achieved complete remission after two cycles of Hyper-CVAD therapy. MRD analysis by fluorescence activated cell sorting identified leukemic cells at a level of  $4 \times 10^{-3}$  in the bone marrow. Results of

*molecular tests revealed the P2RY8-CRLF2 translocation. How should this patient be treated?*

MRD monitoring is currently incorporated in ALL treatment protocols and decisions on the intensity of the first-line regimen and upfront allogeneic stem cell transplantation (SCT) rely mainly on the results of MRD evaluation. The likelihood of Ph-like ALL patients remaining MRD-positive after standard induction is high. MRD positivity at the end of induction is considered to be associated with a high risk of relapse in patients with Ph-like ALL as well as any other type of ALL. In such case, in adults, allogeneic SCT is strongly recommended, while some pediatric protocols would mandate intensification, not necessarily followed by allogeneic SCT.<sup>47,76</sup> A retrospective study found no survival benefit from allogeneic SCT compared to chemotherapy intensification for high-risk pediatric patients.<sup>77</sup> However, since results of allogeneic SCT are superior in patients who are MRD-negative prior to the transplant,<sup>78,79</sup> intensification of therapy aiming to eradicate residual disease is logical even prior to allogeneic SCT. An analysis of the outcomes of 81 children treated in the ALL8 trial of the Australian and New Zealand Children's Haematology/Oncology Group (ANZCHOG) showed that even if considering only patients who achieved MRD negativity after allogeneic SCT, those who started conditioning with detectable MRD had a worse outcome.<sup>80</sup> Although patients included in this study were not tested for the Ph-like signature, most of them were classified as "high-risk B-other" which probably overlaps with Ph-like ALL. A recent analysis of results of the ALL2008 study by the Nordic Society of Pediatric Hematology and Oncology (NOPHO) suggested that high-risk pediatric patients who remain MRD-positive at the end of consolidation will have a better outcome if residual disease is eradicated with intensive chemotherapy blocks prior to allogeneic SCT.<sup>81</sup> Evidence supporting the administration of blinatumomab prior to transplant in an attempt to eliminate MRD is accumulating. Remarkably, based on a single-arm study, the Food and Drug Administration specifically approved the use of blinatumomab for high-risk B-ALL patients who achieve remission but remain MRD-positive. In a prospective trial, MRD was eliminated in 78% of patients following blinatumomab treatment at a daily dose of 15  $\mu\text{g}/\text{m}^2$ .<sup>82</sup> The poor outcome of ALL patients older than 15 years, who remain MRD-positive after initial therapy and receive no blinatumomab prior to allogeneic SCT, was confirmed in a large European retrospective analysis.<sup>83</sup> Apart from the recommendation of using this drug, additional treatment intensification may also be considered. For instance, idarubicin administration (for 3 days) just prior to busulfan/cyclophosphamide conditioning has been reported to improve post-SCT survival in MRD-positive patients.<sup>84</sup>

As far as concerns the issue of MRD elimination in the Ph-like ALL setting, there are case reports demonstrating complete eradication or significant reduction of MRD at the time of allogeneic SCT resulting from pre-transplant intensification with ruxolitinib.<sup>61,85</sup> However, the addition of targeted therapy, such as JAK or BCR/ABL inhibitors, should not substitute MRD eradication with blinatumomab or intensive chemotherapy prior to transplantation. Currently, no data are available to support maintenance with JAK2 inhibitors following allogeneic SCT in Ph-like ALL patients. While ruxolitinib has an immune

suppressive effect and is suggested to be active against graft-versus-host disease,<sup>86,87</sup> its routine use may prevent the benefit of the graft-versus-leukemia effect. For many years the association of graft-versus-host disease with graft-versus-leukemia activity has been considered questionable in ALL; yet, a currently published large retrospective study has confirmed an association between the presence of graft-versus-host disease and lower relapse rates.<sup>88</sup> Moreover, a preclinical animal model challenges the effectiveness of ruxolitinib maintenance in prevention of leukemia relapse.<sup>89</sup> Thus, ruxolitinib maintenance after allogeneic SCT should be considered experimental.

For patients with Ph-like ALL who carry an *ABL*-activating mutation the question of post-transplant TKI maintenance is unlikely to be answered in prospective clinical trials, mainly because of the rarity of this condition. However, safety data of post-transplant TKI maintenance can be extrapolated from the Philadelphia chromosome-positive ALL setting and encourage the use of this approach.

Persistence of MRD even after allogeneic SCT or failure to eradicate it prior to transplantation is a poor prognostic marker and a sign of impending relapse. In these circumstances, patients should be aggressively treated with intensive therapy individualized according to their treatment history and should be considered for chimeric antigen receptor T-cell therapy. Preclinical data suggest that for this very high-risk population, if *IKZF1* mutations or deletions are present, a clinical trial with focal adhesion kinase (FAK) inhibitors could be an appropriate option.<sup>90,91</sup>

#### Patients with Philadelphia chromosome-like acute lymphoblastic leukemia who achieve measurable residual disease-negative remission

*Case presentation.* A 42-year old woman presented with B-ALL with *CRFL2* overexpression and a peripheral blood white blood cell count of  $105 \times 10^9/L$ . Molecular evaluation identified the *IGH-CRLF2* translocation. Following two cycles of HyperCVAD + PEG-asparaginase she achieved molecular remission [MRD-negativity ( $<10^{-4}$ ), not detected by multicolor flow cytometry assay]. How should this patient be further treated?

MRD is currently recognized as the most powerful risk factor in ALL patients. Absence of MRD, as evaluated by the tests capable of detecting even a low concentration ( $10^{-4}$ ) of leukemic cells, is associated with a superior outcome irrespective of molecular subtypes, patient's age and treatment protocols used.<sup>77,92,95</sup> However, in patients carrying high-risk molecular aberrations, such as Ph-like ALL patients, achievement of molecular remission does not completely abrogate the risk of a relapse. In the pediatric Australian ALL8 trial, among 666 recruited patients, the relapse risk was significantly higher in Ph-like patients with *CRFL2* translocations than that in all non-Ph-like ALL patients (57.8% vs. 16%, respectively;  $P < 0.0001$ ).<sup>80</sup> Notably, ten of 14 (71.4%) relapses in Ph-like ALL patients occurred despite the achievement of MRD negativity by day 79.<sup>18</sup> Similar results were reported in the AIEOP-BFM ALL2000/R2006 study, in which a higher cumulative incidence of relapse was observed in Ph-like ALL patients (33.9% vs. 14.9% in non-Ph-like ALL;  $P = 0.009$ ) even though a poor prednisone response and MRD positivity rates were identical in both groups.<sup>94</sup> Similarly, data on adult patients demonstrated a high relapse rate in Ph-like ALL patients, including those who achieved molecular remission, regardless of whether BFM-based or HyperCVAD regimens were used.<sup>13</sup>

A study by Roberts *et al.* suggested that risk-adapted therapy assigning patients with a high MRD level to allogeneic SCT could overcome the substantial risk of relapse.<sup>28</sup> However, due to the lack of evidence supporting routine assignment to allogeneic SCT, a recent expert review and the updated recommendations from the European Working Group for Adult Acute Lymphoblastic Leukemia (EWALL) and the Acute Leukemia Working Party of the European Society for Blood and Marrow Transplantation (EBMT) advocated the use of allogeneic SCT during first complete remission only in MRD-positive pediatric and adult patients with Ph-like ALL.<sup>95,96</sup> Relapse rates in MRD-negative adults are higher than in pediatric patients with identical MRD kinetics of eradication. Therefore, in our opinion, a more liberal allogeneic SCT referral policy should be considered in adults with Ph-like ALL even if they achieve molecular remission. Additional risk factors, such as an *IKZF1* alteration, have the potential to identify patients at the highest risk of relapse.<sup>97-99</sup> However, we are unaware of any available prospective data on patients' outcome following therapy stratification by *IKZF1* alteration.

#### Relapse in patients with Philadelphia chromosome-like acute lymphoblastic leukemia

*Case presentation.* A 7-year old child presented with B-ALL and an *IGH-CRLF2* translocation. After COG-based induction, MRD was detected at a level of  $10^{-2}$  and high-risk intensive chemotherapy blocks were administered. Two weeks after the last chemotherapy the child had a full-blown hematologic relapse. How should this patient be managed?

Leukemia in patients presenting with early relapse right after intensive therapy is a devastating disease and prescribing additional chemotherapy seems futile. As described above, an anticipated effect of JAK inhibitors is modest and therefore in patients at a high risk of disease relapse immunotherapy should be the selected option. In CD19<sup>+</sup> ALL, blinatumomab is an acceptable option for both adult<sup>100</sup> and pediatric patients.<sup>101,102</sup> For adult patients, inotuzumab ozogamicin is also a valid option.<sup>103</sup> Although still not widely available, chimeric antigen receptor T-cell therapy is a powerful strategy to be used in such high-risk patients. A remission achieved with chimeric antigen receptor T-cell therapy should be followed by allogeneic SCT.<sup>104-106</sup> To minimize the risk of CD19<sup>-</sup> escape and relapse, there is a rationale for combining CD19 with CD22-directed therapies and this combination should be evaluated against the risk of developing veno-occlusive disease during subsequent allogeneic SCT.<sup>107</sup> Targeted therapy based on a patient's classification as having Ph-like ALL and/or identification of a specific genetic aberration should not replace the use of other efficient agents available for the relapse setting.

#### Patients of advanced age with Philadelphia chromosome-like acute lymphoblastic leukemia

*Case presentation.* A 78-year old man who until recent days had been healthy with no chronic diseases, was admitted to hospital because of ALL. At presentation his white blood cell count was  $55 \times 10^9/L$ , his hemoglobin concentration was 8.5 g/dL and a spontaneous tumor lysis syndrome was diagnosed. Cytogenetic evaluation revealed an *IGH-CRLF2* translocation and a molecular test identified an activating *JAK2* mutation at the R683G position. How should this patient be treated?

Patients of advanced age diagnosed with ALL may

achieve remission with intensive therapy but despite that are anticipated to experience a poorer survival mainly due disease relapse.<sup>108</sup> The Ph-like signature was reported in 24% of ALL patients over the age of 65<sup>22</sup> but no prospective studies have included these patients, considering their genetic profile. Given that in most patients of advanced age, prolonged intensive chemotherapy followed by allogeneic SCT is not feasible, all such patients should be considered at high risk of relapse, regardless of their gene expression profile. The most promising approach thus far, which provided a considerable long-term survival in Ph-negative ALL patients older than 60 years, was reported by Kantarjian *et al.*<sup>109</sup> In their protocol, researchers from MD Anderson Cancer Center replaced a significant portion of chemotherapy with inotuzumab ozogamicin, hence creating a less toxic first-line regimen.<sup>109</sup> With a median follow-up of 29 months, the 2-year progression-free survival rate of 52 patients with a median age of 68 years was 59%. Blinatumomab can also be safely added to such a protocol.<sup>110</sup> We consider such a modified induction an acceptable approach for all Ph-negative ALL patients of advanced age. As previously discussed, the addition of targeted agents is rational only if *BCR/ABL*-activating genetic aberrations are identified and thus, for patients treated on such protocols molecular evaluation can be limited to *BCR/ABL*-activating lesions only. Outside of clinical trials, the patient in question should be treated with a less toxic regimen. Assuming that such regimen will not result in MRD eradication, blinatumomab should be added as early

as possible, and inclusion of inotuzumab ozogamicin should be encouraged, if its off-label use is possible.

## Summary

Patients with the Ph-like gene expression pattern are at a high risk of relapse and theoretically could be offered treatment considering specific genetics of their disease. However, given that this group of patients is heterogeneous, it is unlikely that prospective studies will be conducted for each specific mutation to identify optimal treatment protocols. Moreover, no consensus exists regarding the preferred approach to be used for the diagnosis of Ph-like ALL and management of a specific patient. Under these circumstances, the following three principles should guide the management of these patients. Screening for the Ph-like pattern should be adopted in routine practice in all patients. Patients should be informed that current screening methods may miss rare gene mutations that could be subject to off-label use of available targeted therapies (e.g., crizotinib); nevertheless, the effect of targeted therapy on such rare leukemic mutations has not been reported. If the *ABL*-activating aberration is identified, adding TKI to therapy is advised. All patients with identified kinase-activating aberrations should be defined as high risk; hence, intensification of chemotherapy, treatment with kinase targeting agents and/or antibody-derived novel agents may be considered.

## References

- Den Boer ML, van Slegtenhorst M, De Menezes RX, et al. A subtype of childhood acute lymphoblastic leukaemia with poor treatment outcome: a genome-wide classification study. *Lancet Oncol.* 2009;10(2):125-134.
- Boer JM, Koenders JE, van der Holt B, et al. Expression profiling of adult acute lymphoblastic leukemia identifies a BCR-ABL1-like subgroup characterized by high non-response and relapse rates. *Haematologica.* 2015;100(7):e261-264.
- Mullighan CG, Su X, Zhang J, et al. Deletion of IKZF1 and prognosis in acute lymphoblastic leukemia. *N Engl J Med.* 2009;360(5):470-480.
- Roberts KG, Li Y, Payne-Turner D, et al. Targetable kinase-activating lesions in Ph-like acute lymphoblastic leukemia. *N Engl J Med.* 2014;371(11):1005-1015.
- Russell LJ, Capasso M, Vater I, et al. Deregulated expression of cytokine receptor gene, CRLF2, is involved in lymphoid transformation in B-cell precursor acute lymphoblastic leukemia. *Blood.* 2009;114(13):2688-2698.
- Yoda A, Yoda Y, Chiaretti S, et al. Functional screening identifies CRLF2 in precursor B-cell acute lymphoblastic leukemia. *Proc Natl Acad Sci U S A.* 2010;107(1):252-257.
- Chiaretti S, Brugnoletti F, Messina M, et al. CRLF2 overexpression identifies an unfavourable subgroup of adult B-cell precursor acute lymphoblastic leukemia lacking recurrent genetic abnormalities. *Leuk Res.* 2016;41:36-42.
- Tsai AG, Yoda A, Weinstock DM, Lieber MR. t(X;14)(p22;q32)/t(Y;14)(p11;q32) CRLF2-IGH translocations from human B-lineage ALLs involve CpG-type breaks at CRLF2, but CRLF2/P2RY8 intrachromosomal deletions do not. *Blood.* 2010;116(11):1993-1994.
- Vesely C, Frech C, Eckert C, et al. Genomic and transcriptional landscape of P2RY8-CRLF2-positive childhood acute lymphoblastic leukemia. *Leukemia.* 2017;31(7):1491-1501.
- Morak M, Attarbaschi A, Fischer S, et al. Small sizes and indolent evolutionary dynamics challenge the potential role of P2RY8-CRLF2-harboring clones as main relapse-driving force in childhood ALL. *Blood.* 2012;120(26):5134-5142.
- Palmi C, Vendramini E, Silvestri D, et al. Poor prognosis for P2RY8-CRLF2 fusion but not for CRLF2 over-expression in children with intermediate risk B-cell precursor acute lymphoblastic leukemia. *Leukemia.* 2012;26(10):2245-2253.
- Enser HM, Schwab C, Russell LJ, et al. Demographic, clinical, and outcome features of children with acute lymphoblastic leukemia and CRLF2 deregulation: results from the MRC ALL97 clinical trial. *Blood.* 2011;117(7):2129-2136.
- Jain N, Roberts KG, Jabbour E, et al. Ph-like acute lymphoblastic leukemia: a high-risk subtype in adults. *Blood.* 2017;129(5):572-581.
- Herold T, Schneider S, Metzeler KH, et al. Adults with Philadelphia chromosome-like acute lymphoblastic leukemia frequently have IGH-CRLF2 and JAK2 mutations, persistence of minimal residual disease and poor prognosis. *Haematologica.* 2017;102(1):130-138.
- Reshmi SC, Harvey RC, Roberts KG, et al. Targetable kinase gene fusions in high-risk B-ALL: a study from the Children's Oncology Group. *Blood.* 2017;129(25):3352-3361.
- Konoplev S, Lu X, Konopleva M, et al. CRLF2-positive B-cell acute lymphoblastic leukemia in adult patients: a single-institution experience. *Am J Clin Pathol.* 2017;147(4):357-363.
- van der Veer A, Waanders E, Pieters R, et al. Independent prognostic value of BCR-ABL1-like signature and IKZF1 deletion, but not high CRLF2 expression, in children with B-cell precursor ALL. *Blood.* 2013;122(15):2622-2629.
- Heatley SL, Sadras T, Kok CH, et al. High prevalence of relapse in children with Philadelphia-like acute lymphoblastic leukemia despite risk-adapted treatment. *Haematologica.* 2017;102(12):e490-e493.
- Ge Z, Gu Y, Zhao G, et al. High CRLF2 expression associates with IKZF1 dysfunction in adult acute lymphoblastic leukemia without CRLF2 rearrangement. *Oncotarget.* 2016;7(31):49722-49732.
- Boer JM, Steeghs EM, Marchante JR, et al. Tyrosine kinase fusion genes in pediatric BCR-ABL1-like acute lymphoblastic leukemia. *Oncotarget.* 2017;8(3):4618-4628.
- Jaso JM, Yin CC, Lu VW, et al. B acute lymphoblastic leukemia with t(14;19)(q32;p13.1) involving IGH/EPOR: a clinically aggressive subset of disease. *Mod Pathol.* 2014;27(3):382-389.
- Roberts KG, Gu Z, Payne-Turner D, et al. High frequency and poor outcome of Philadelphia chromosome-like acute lymphoblastic leukemia in adults. *J Clin Oncol.* 2017;35(4):394-401.
- Iacobucci I, Li Y, Roberts KG, et al.

- Truncating erythropoietin receptor rearrangements in acute lymphoblastic leukemia. *Cancer Cell*. 2016;29(2):186-200.
24. Roberts KG, Mullighan CG. Genomics in acute lymphoblastic leukaemia: insights and treatment implications. *Nat Rev Clin Oncol*. 2015;12(6):344-357.
  25. Paulsson K, Horvat A, Strombeck B, et al. Mutations of FLT3, NRAS, KRAS, and PTPN11 are frequent and possibly mutually exclusive in high hyperdiploid childhood acute lymphoblastic leukemia. *Genes Chromosomes Cancer*. 2008;47(1):26-33.
  26. Wiemels JL, Kang M, Chang JS, et al. Backtracking RAS mutations in high hyperdiploid childhood acute lymphoblastic leukemia. *Blood Cells Mol Dis*. 2010;45(3):186-191.
  27. Chiaretti S, Messina M, Grammatico S, et al. Rapid identification of BCR/ABL1-like acute lymphoblastic leukaemia patients using a predictive statistical model based on quantitative real time-polymerase chain reaction: clinical, prognostic and therapeutic implications. *Br J Haematol*. 2018;181(5):642-652.
  28. Roberts KG, Pei D, Campana D, et al. Outcomes of children with BCR-ABL1-like acute lymphoblastic leukemia treated with risk-directed therapy based on the levels of minimal residual disease. *J Clin Oncol*. 2014;32(27):3012-3020.
  29. Gu Z, Churchman ML, Roberts KG, et al. PAX5-driven subtypes of B-progenitor acute lymphoblastic leukemia. *Nat Genet*. 2019;51(2):296-307.
  30. Ofran Y, Izraeli S. BCR-ABL (Ph)-like acute leukemia-Pathogenesis, diagnosis and therapeutic options. *Blood Rev*. 2017;31(2):11-16.
  31. Harvey RC, Mullighan CG, Wang X, et al. Identification of novel cluster groups in pediatric high-risk B-precursor acute lymphoblastic leukemia with gene expression profiling: correlation with genome-wide DNA copy number alterations, clinical characteristics, and outcome. *Blood*. 2010;116(23):4874-4884.
  32. Loh ML, Zhang J, Harvey RC, et al. Tyrosine kinase sequencing of pediatric acute lymphoblastic leukemia: a report from the Children's Oncology Group TARGET Project. *Blood*. 2013;121(3):485-488.
  33. Ofran Y. Activated kinases in ALL: time to act. *Blood*. 2017;129(25):3280-3282.
  34. Maese L, Tasian SK, Raetz EA. How is the Ph-like signature being incorporated into ALL therapy? *Best Pract Res Clin Haematol*. 2017;30(3):222-228.
  35. Robin AJ, Peterson JF, Grignon JW Jr, et al. Identification of high-risk cryptic CRLF2 rearrangements in B-cell acute lymphoblastic leukemia utilizing an FGFR3/IGH dual-color dual-fusion DNA probe set. *J Pediatr Hematol Oncol*. 2017;39(4):e207-e210.
  36. Harvey RC, Kang H, Roberts KG, et al. Development and validation of a highly sensitive and specific gene expression classifier to prospectively screen and identify B-precursor acute lymphoblastic leukemia (ALL) patients with a Philadelphia chromosome-like ("Ph-like" or "BCR-ABL1-like") signature for therapeutic targeting and clinical intervention. *Blood*. 2013;122(21):826.
  37. Roberts KG, Reshmi SC, Harvey RC, et al. Genomic and outcome analyses of Ph-like ALL in NCI standard-risk patients: a report from the Children's Oncology Group. *Blood*. 2018;132(8):815-824.
  38. Fasan A, Kern W, Nadarajah N, et al. Three steps to the diagnosis of adult Ph-like ALL. *Blood*. 2015;126(23):2610.
  39. Lamanna N, Heffner IT, Kalaycio M, et al. Treatment of adults with acute lymphoblastic leukemia: do the specifics of the regimen matter? Results from a prospective randomized trial. *Cancer*. 2013;119(6):1186-1194.
  40. El-Cheikh J, El Dika I, Massoud R, et al. Hyper-CVAD compared with BFM-like chemotherapy for the treatment of adult acute lymphoblastic leukemia. A retrospective single-center analysis. *Clin Lymphoma Myeloma Leuk*. 2017;17(3):179-185.
  41. Erkut N, Akidan O, Selim Batur D, Karabacak V, Sonmez M. Comparison between Hyper-CVAD and PETHEMA ALL-93 in adult acute lymphoblastic leukemia: a single-center study. *Chemotherapy*. 2018;63(4):207-213.
  42. Garcia-Manero G, Kantarjian HM. The hyper-CVAD regimen in adult acute lymphocytic leukemia. *Hematol Oncol Clin North Am*. 2000;14(6):1381-1396, x-xi.
  43. Offidani M, Corvatta L, Malerba L, et al. Comparison of two regimens for the treatment of elderly patients with acute lymphoblastic leukaemia (ALL). *Leuk Lymphoma*. 2005;46(2):233-238.
  44. Sancho JM, Ribera JM, Xicoy B, et al. Results of the PETHEMA ALL-96 trial in elderly patients with Philadelphia chromosome-negative acute lymphoblastic leukemia. *Eur J Haematol*. 2007;78(2):102-110.
  45. Schmiegelow K, Forestier E, Hellebostad M, et al. Long-term results of NOPHO ALL-92 and ALL-2000 studies of childhood acute lymphoblastic leukemia. *Leukemia*. 2010;24(2):345-354.
  46. Moricke A, Zimmermann M, Reiter A, et al. Long-term results of five consecutive trials in childhood acute lymphoblastic leukemia performed by the ALL-BFM study group from 1981 to 2000. *Leukemia*. 2010;24(2):265-284.
  47. Seibel NL, Steiner PG, Sather HN, et al. Early postinduction intensification therapy improves survival for children and adolescents with high-risk acute lymphoblastic leukemia: a report from the Children's Oncology Group. *Blood*. 2008;111(5):2548-2555.
  48. Pui CH, Pei D, Raimondi SC, et al. Clinical impact of minimal residual disease in children with different subtypes of acute lymphoblastic leukemia treated with response-adapted therapy. *Leukemia*. 2017;31(2):333-339.
  49. O'Connor D, Enshaei A, Bartram J, et al. Genotype-specific minimal residual disease interpretation improves stratification in pediatric acute lymphoblastic leukemia. *J Clin Oncol*. 2018;36(1):34-43.
  50. Vora A, Goulden N, Mitchell C, et al. Augmented post-remission therapy for a minimal residual disease-defined high-risk subgroup of children and young people with clinical standard-risk and intermediate-risk acute lymphoblastic leukaemia (UKALL 2003): a randomised controlled trial. *Lancet Oncol*. 2014;15(8):809-818.
  51. Maury S, Chevret S, Thomas X, et al. Rituximab in B-lineage adult acute lymphoblastic leukemia. *N Engl J Med*. 2016;375(11):1044-1053.
  52. Clavell LA, Gelber RD, Cohen HJ, et al. Four-agent induction and intensive asparaginase therapy for treatment of childhood acute lymphoblastic leukemia. *N Engl J Med*. 1986;315(11):657-663.
  53. Faderl S, Thomas DA, O'Brien S, et al. Augmented hyper-CVAD based on dose-intensified vincristine, dexamethasone, and asparaginase in adult acute lymphoblastic leukemia salvage therapy. *Clin Lymphoma Myeloma Leuk*. 2011;11(1):54-59.
  54. Hoelzer D, Walewski J, Dohner H, et al. Improved outcome of adult Burkitt lymphoma/leukemia with rituximab and chemotherapy: report of a large prospective multicenter trial. *Blood*. 2014;124(26):3870-3879.
  55. Mullighan CG, Zhang J, Harvey RC, et al. JAK mutations in high-risk childhood acute lymphoblastic leukemia. *Proc Natl Acad Sci U S A*. 2009;106(23):9414-9418.
  56. Harvey RC, Mullighan CG, Chen IM, et al. Rearrangement of CRLF2 is associated with mutation of JAK kinases, alteration of IKZF1, Hispanic/Latino ethnicity, and a poor outcome in pediatric B-progenitor acute lymphoblastic leukemia. *Blood*. 2010;115(26):5312-5321.
  57. Maude SL, Tasian SK, Vincent T, et al. Targeting JAK1/2 and mTOR in murine xenograft models of Ph-like acute lymphoblastic leukemia. *Blood*. 2012;120(17):3510-3518.
  58. Tasian SK, Teachey DT, Li Y, et al. Potent efficacy of combined PI3K/mTOR and JAK or ABL inhibition in murine xenograft models of Ph-like acute lymphoblastic leukemia. *Blood*. 2017;129(2):177-187.
  59. Tasian SK, Assad A, Hunter DS, Du Y, Loh ML. A phase 2 study of ruxolitinib with chemotherapy in children with Philadelphia chromosome-like acute lymphoblastic leukemia (INCB18424-269/AALL1521): dose-finding results from the part 1 safety phase. *Blood*. 2018;132(1):555.
  60. Loh ML, Tasian SK, Rabin KR, et al. A phase 1 dosing study of ruxolitinib in children with relapsed or refractory solid tumors, leukemias, or myeloproliferative neoplasms: A Children's Oncology Group phase 1 consortium study (ADVL1011). *Pediatr Blood Cancer*. 2015;62(10):1717-1724.
  61. Mayfield JR, Czuchlewski DR, Gale JM, et al. Integration of ruxolitinib into dose-intensified therapy targeted against a novel JAK2 F694L mutation in B-precursor acute lymphoblastic leukemia. *Pediatr Blood Cancer*. 2017;64(5).
  62. Bose P, Verstovsek S. JAK2 inhibitors for myeloproliferative neoplasms: what is next? *Blood*. 2017;130(2):115-125.
  63. Nikolaev SI, Garneri M, Santoni F, et al. Frequent cases of RAS-mutated Down syndrome acute lymphoblastic leukaemia lack JAK2 mutations. *Nat Commun*. 2014;5:4654.
  64. Suryani S, Bracken LS, Harvey RC, et al. Evaluation of the in vitro and in vivo efficacy of the JAK inhibitor AZD1480 against JAK-mutated acute lymphoblastic leukemia. *Mol Cancer Ther*. 2015;14(2):364-374.
  65. Zhang Q, Shi C, Han L, et al. Inhibition of mTORC1/C2 signaling improves anti-leukemia efficacy of JAK/STAT blockade in CRLF2 rearranged and/or JAK driven Philadelphia chromosome-like acute B-cell lymphoblastic leukemia. *Oncotarget*. 2018;9(8):8027-8041.
  66. Pemmaraju N, Kantarjian H, Kadia T, et al. A phase I/II study of the Janus kinase (JAK)1 and 2 inhibitor ruxolitinib in patients with relapsed or refractory acute myeloid leukemia. *Clin Lymphoma Myeloma Leuk*. 2015;15(3):171-176.
  67. Lengline E, Beldjord K, Dombret H, et al. Successful tyrosine kinase inhibitor therapy in a refractory B-cell precursor acute lymphoblastic leukemia with EBF1-PDGFRB fusion. *Haematologica*. 2013;98(11):e146-148.
  68. Weston BW, Hayden MA, Roberts KG, et al.

- Tyrosine kinase inhibitor therapy induces remission in a patient with refractory EBF1-PDGFRB-positive acute lymphoblastic leukemia. *J Clin Oncol.* 2013;31(25):e413-416.
69. Kobayashi K, Miyagawa N, Mitsui K, et al. TKI dasatinib monotherapy for a patient with Ph-like ALL bearing ATF7IP/PDGFRB translocation. *Pediatr Blood Cancer.* 2015;62(6):1058-1060.
  70. Zhang G, Zhang Y, Wu J, Chen Y, Ma Z. Acute lymphoblastic leukemia patient with variant ATF7IP/PDGFRB fusion and favorable response to tyrosine kinase inhibitor treatment: a case report. *Am J Case Rep.* 2017;18:1204-1208.
  71. Perwein T, Strehl S, Konig M, et al. Imatinib-induced long-term remission in a relapsed RCSD1-ABL1-positive acute lymphoblastic leukemia. *Haematologica.* 2016;101(8):e332-335.
  72. Frech M, Jehn LB, Stabla K, et al. Dasatinib and allogeneic stem cell transplantation enable sustained response in an elderly patient with RCSD1-ABL1-positive acute lymphoblastic leukemia. *Haematologica.* 2017;102(4):e160-e162.
  73. Zhang Y, Gao Y, Zhang H, et al. PDGFRB mutation and tyrosine kinase inhibitor resistance in Ph-like acute lymphoblastic leukemia. *Blood.* 2018;131(20):2256-2261.
  74. Yeung DT, Moulton DJ, Heatley SL, et al. Relapse of BCR-ABL1-like ALL mediated by the ABL1 kinase domain mutation T315I following initial response to dasatinib treatment. *Leukemia.* 2015;29(1):230-232.
  75. Zimmermannova O, Doktorova E, Stuchly J, et al. An activating mutation of GNB1 is associated with resistance to tyrosine kinase inhibitors in ETV6-ABL1-positive leukemia. *Oncogene.* 2017;36(43):5985-5994.
  76. Stary J, Zimmermann M, Campbell M, et al. Intensive chemotherapy for childhood acute lymphoblastic leukemia: results of the randomized intercontinental trial ALL IC-BFM 2002. *J Clin Oncol.* 2014;32(3):174-184.
  77. Conter V, Valsecchi MG, Parasole R, et al. Childhood high-risk acute lymphoblastic leukemia in first remission: results after chemotherapy or transplant from the AIEOP ALL 2000 study. *Blood.* 2014;123(10):1470-1478.
  78. Knechtli CJ, Goulden NJ, Hancock JP, et al. Minimal residual disease status before allogeneic bone marrow transplantation is an important determinant of successful outcome for children and adolescents with acute lymphoblastic leukemia. *Blood.* 1998;92(11):4072-4079.
  79. Sramkova L, Muzikova K, Fronkova E, et al. Detectable minimal residual disease before allogeneic hematopoietic stem cell transplantation predicts extremely poor prognosis in children with acute lymphoblastic leukemia. *Pediatr Blood Cancer.* 2007;48(1):93-100.
  80. Sutton R, Shaw PJ, Venn NC, et al. Persistent MRD before and after allogeneic BMT predicts relapse in children with acute lymphoblastic leukaemia. *Br J Haematol.* 2015;168(3):395-404.
  81. Iversen M, Turkiewicz D, Marquart HV, et al. Low burden of minimal residual disease prior to transplantation in children with very high risk acute lymphoblastic leukaemia: The NOPHO ALL2008 experience. *Br J Haematol.* 2019;184(6):982-993.
  82. Gokbuget N, Dombret H, Bonifacio M, et al. Blinatumomab for minimal residual disease in adults with B-cell precursor acute lymphoblastic leukemia. *Blood.* 2018;131(14):1522-1531.
  83. Gokbuget N, Dombret H, Giebel S, et al. Minimal residual disease level predicts outcome in adults with Ph-negative B-precursor acute lymphoblastic leukemia. *Hematology.* 2019;24(1):337-348.
  84. Zhang R, Lu X, Wang H, et al. Idarubicin-intensified hematopoietic cell transplantation improves relapse and survival of high-risk acute leukemia patients with minimal residual disease. *Biol Blood Marrow Transplant.* 2019;25(1):47-55.
  85. Ding YY, Stern JW, Jubelirer TF, et al. Clinical efficacy of ruxolitinib and chemotherapy in a child with Philadelphia chromosome-like acute lymphoblastic leukemia with GOLGA5-JAK2 fusion and induction failure. *Haematologica.* 2018;103(9):e427-e431.
  86. Mori Y, Ikeda K, Inomata T, et al. Ruxolitinib treatment for GvHD in patients with myelofibrosis. *Bone Marrow Transplant.* 2016;51(12):1584-1587.
  87. Zeiser R, Burchart A, Lengerke C, et al. Ruxolitinib in corticosteroid-refractory graft-versus-host disease after allogeneic stem cell transplantation: a multicenter survey. *Leukemia.* 2015;29(10):2062-2068.
  88. Yeshurun M, Weisdorf D, Rowe JM, et al. The impact of the graft-versus-leukemia effect on survival in acute lymphoblastic leukemia. *Blood Adv.* 2019;3(4):670-680.
  89. Kim SK, Knight DA, Jones LR, et al. JAK2 is dispensable for maintenance of JAK2 mutant B-cell acute lymphoblastic leukemias. *Genes Dev.* 2018;32(11-12):849-864.
  90. Churchman ML, Evans K, Richmond J, et al. Synergism of FAK and tyrosine kinase inhibition in Ph(+) B-ALL. *JCI Insight.* 2016;1(4).
  91. Kurmasheva RT, Gorlick R, Kolb EA, et al. Initial testing of VS-4718, a novel inhibitor of focal adhesion kinase (FAK), against pediatric tumor models by the Pediatric Preclinical Testing Program. *Pediatr Blood Cancer.* 2017;64(4).
  92. Conter V, Bartram CR, Valsecchi MG, et al. Molecular response to treatment redefines all prognostic factors in children and adolescents with B-cell precursor acute lymphoblastic leukemia: results in 3184 patients of the AIEOP-BFM ALL 2000 study. *Blood.* 2010;115(16):3206-3214.
  93. Gokbuget N, Kneba M, Raff T, et al. Adult patients with acute lymphoblastic leukemia and molecular failure display a poor prognosis and are candidates for stem cell transplantation and targeted therapies. *Blood.* 2012;120(9):1868-1876.
  94. te Kronnie G, Silvestri D, Vendramini E, et al. Philadelphia-like signature in childhood acute lymphoblastic leukemia: the AIEOP experience. *Blood.* 2013;122(21):353.
  95. Bhatt NS, Phelan R, Burke MJ. The role of hematopoietic stem-cell transplantation in first remission in pediatric acute lymphoblastic leukemia: a narrative review. *J Pediatr Rev.* 2017;5(2):e10831.
  96. Giebel S, Marks DI, Boissel N, et al. Hematopoietic stem cell transplantation for adults with Philadelphia chromosome-negative acute lymphoblastic leukemia in first remission: a position statement of the European Working Group for Adult Acute Lymphoblastic Leukemia (EWALL) and the Acute Leukemia Working Party of the European Society for Blood and Marrow Transplantation (EBMT). *Bone Marrow Transplant.* 2019;54(6):798-809.
  97. Sutton R, Venn NC, Law T, et al. A risk score including microdeletions improves relapse prediction for standard and medium risk precursor B-cell acute lymphoblastic leukaemia in children. *Br J Haematol.* 2018;180(4):550-562.
  98. Olsson L, Ivanov Ofverholm I, Noren-Nystrom U, et al. The clinical impact of IKZF1 deletions in paediatric B-cell precursor acute lymphoblastic leukaemia is independent of minimal residual disease stratification in Nordic Society for Paediatric Haematology and Oncology treatment protocols used between 1992 and 2013. *Br J Haematol.* 2015;170(6):847-858.
  99. Li JF, Dai YT, Lilljebjorn H, et al. Transcriptional landscape of B cell precursor acute lymphoblastic leukemia based on an international study of 1,223 cases. *Proc Natl Acad Sci U S A.* 2018;115(50):E11711-E11720.
  100. Kantarjian H, Stein A, Gokbuget N, et al. Blinatumomab versus chemotherapy for advanced acute lymphoblastic leukemia. *N Engl J Med.* 2017;376(9):836-847.
  101. Gore L, Locatelli F, Zugmaier G, et al. Survival after blinatumomab treatment in pediatric patients with relapsed/refractory B-cell precursor acute lymphoblastic leukemia. *Blood Cancer J.* 2018;8(9):80.
  102. von Stackelberg A, Locatelli F, Zugmaier G, et al. Phase I/phase II study of blinatumomab in pediatric patients with relapsed/refractory acute lymphoblastic leukemia. *J Clin Oncol.* 2016;34(36):4381-4389.
  103. Kantarjian HM, DeAngelo DJ, Stelljes M, et al. Inotuzumab ozogamicin versus standard therapy for acute lymphoblastic leukemia. *N Engl J Med.* 2016;375(8):740-753.
  104. Park JH, Riviere I, Gonen M, et al. Long-term follow-up of CD19 CAR therapy in acute lymphoblastic leukemia. *N Engl J Med.* 2018;378(5):449-459.
  105. Maude SL, Frey N, Shaw PA, et al. Chimeric antigen receptor T cells for sustained remissions in leukemia. *N Engl J Med.* 2014;371(16):1507-1517.
  106. Maude SL, Laetsch TW, Buechner J, et al. Tisagenlecleucel in children and young adults with B-cell lymphoblastic leukemia. *N Engl J Med.* 2018;378(5):439-448.
  107. Jabbour EJ, Sasaki K, Ravandi F, et al. Inotuzumab ozogamicin in combination with low-intensity chemotherapy (mini-HCVAD) with or without blinatumomab versus standard intensive chemotherapy (HCVAD) as frontline therapy for older patients with Philadelphia chromosome-negative acute lymphoblastic leukemia: a propensity score analysis. *Cancer.* 2019;125(15):2579-2586.
  108. Miller KC, Al-Kali A, Shah MV, et al. Elderly acute lymphoblastic leukemia: a Mayo Clinic study of 124 patients. *Leuk Lymphoma.* 2019;60(4):990-999.
  109. Kantarjian H, Ravandi F, Short NJ, et al. Inotuzumab ozogamicin in combination with low-intensity chemotherapy for older patients with Philadelphia chromosome-negative acute lymphoblastic leukaemia: a single-arm, phase 2 study. *Lancet Oncol.* 2018;19(2):240-248.
  110. Jabbour E, Sasaki K, Ravandi F, et al. Chemoimmunotherapy with inotuzumab ozogamicin combined with mini-hyper-CVD, with or without blinatumomab, is highly effective in patients with Philadelphia chromosome-negative acute lymphoblastic leukemia in first salvage. *Cancer.* 2018;124(20):4044-4055.



# Sequential and combination treatments with novel agents in chronic lymphocytic leukemia

Moritz Fürstenau,<sup>1</sup> Michael Hallek<sup>1,2</sup> and Barbara Eichhorst<sup>1</sup>

<sup>1</sup>University of Cologne, Department I of Internal Medicine, Center for Integrated Oncology Aachen Bonn Cologne Duesseldorf, German CLL Study Group, University Hospital Cologne and <sup>2</sup>Cologne Cluster of Excellence in Cellular Stress Responses in Aging-associated Disease (CECAD), University of Cologne, Cologne, Germany

Haematologica 2019  
Volume 104(11):2144-2154

## ABSTRACT

Chemoimmunotherapy has been the standard of care for patients with chronic lymphocytic leukemia for a long time. However, over the last few years, novel agents have produced unprecedented outcomes in treatment-naïve and relapsed/refractory chronic lymphocytic leukemia. With the advent of these targeted agents, treatment options have diversified very considerably and new questions have emerged. For example, it is unclear whether these novel agents should be used as sequential monotherapies until disease progression or whether they should preferably be combined in time-limited treatment regimens aimed at achieving deep and durable remissions. While both approaches yield high response rates and long progression-free and overall survival, it remains challenging to identify patients individually for the optimal concept. This review provides guidance in this decision process by presenting evidence on sequential and combined use of novel agents and discussing the advantages and drawbacks of these two approaches.

## Correspondence:

BARBARA EICHHORST  
barbara.eichhorst@uk-koeln.de

Received: April 15, 2019.

Accepted: May 22, 2019.

Pre-published: October 4, 2019.

doi:10.3324/haematol.2018.208603

Check the online version for the most updated information on this article, online supplements, and information on authorship & disclosures: [www.haematologica.org/content/104/11/2144](http://www.haematologica.org/content/104/11/2144)

©2019 Ferrata Storti Foundation

Material published in Haematologica is covered by copyright. All rights are reserved to the Ferrata Storti Foundation. Use of published material is allowed under the following terms and conditions:

<https://creativecommons.org/licenses/by-nc/4.0/legalcode>.

Copies of published material are allowed for personal or internal use. Sharing published material for non-commercial purposes is subject to the following conditions:

<https://creativecommons.org/licenses/by-nc/4.0/legalcode>,

sect. 3. Reproducing and sharing published material for commercial purposes is not allowed without permission in writing from the publisher.



## Introduction

Chemoimmunotherapy has been the standard first-line treatment of choice for patients with chronic lymphocytic leukemia (CLL) for many years.<sup>1,2</sup> However, with the advent of novel, targeted agents, the survival of CLL patients has improved markedly and treatment options have diversified, especially for patients with high-risk CLL.<sup>3-7</sup> Recently published studies directly comparing standard chemoimmunotherapy against novel agents have demonstrated the superiority of the latter in various groups of patients.<sup>8-10</sup> Chemoimmunotherapy still plays a role in the treatment of patients with mutated IGHV genes, in whom the combination of fludarabine, cyclophosphamide and rituximab produces a remarkably long progression-free survival (PFS) in nearly half of the patients, with the possibility of cure in those who have not relapsed beyond 10 years.<sup>11,12</sup>

With ibrutinib pushing into first-line treatment algorithms and other novel agents such as venetoclax and idelalisib proving their efficacy as monotherapy as well as in various combinations, new challenges are emerging. Information is needed to determine whether novel agents should be used in combination or as sequential monotherapies. Another burning issue is how to manage patients who are refractory to or relapse after treatment with novel agents.

In this review, we discuss currently approved treatment options as well as new approaches using novel agents and address optimal sequencing of single agents and the most promising combination treatments. Furthermore, we debate the concepts of time-limited versus indefinite treatment and offer guidance for treatment decisions in routine care of patients.

## Approved targeted agents in chronic lymphocytic leukemia

### BTK inhibitors

Ibrutinib is an inhibitor of Bruton tyrosine kinase (BTK), which is an intracellular protein downstream of the B-cell receptor. Ibrutinib has been approved for and implemented in the treatment of previously untreated and relapsed/refractory (r/r)

CLL patients following the impressive results of the pivotal RESONATE-2 trial.<sup>5,13,14</sup> The phase III trial demonstrated markedly prolonged PFS and overall survival (OS) in ibrutinib-treated patients compared to patients treated with chlorambucil monotherapy. The superiority of ibrutinib was shown independently of genetic subgroups and a recent follow-up documented an overall response rate (ORR) of 92% and a 2-year PFS of 89% in the ibrutinib arm.<sup>15</sup> Data from the first trial investigating indefinite ibrutinib treatment in young, fit CLL patients *versus* the standard of care in these patients (fludarabine, cyclophosphamide and rituximab) were published recently.<sup>9</sup> The ECOG-ACRIN E1912 intergroup trial showed significant PFS and OS advantages for patients treated with ibrutinib plus rituximab (Table 1). Improved survival was observed across all analyzed subgroups except for IGHV-mutated patients. In another recently published study, Woyach and colleagues evaluated the efficacy of ibrutinib alone or in combination with rituximab in CLL patients ≥65 years and compared it to that of bendamustine plus rituximab.<sup>10</sup> The study showed a clear PFS advantage for both ibrutinib and ibrutinib plus rituximab compared with bendamustine plus rituximab. Due to the planned cross-over no significant survival differences were seen in the IGHV-mutated group or with regards to OS. The addition of rituximab to ibrutinib did not result in an improved survival.

Consequently, the place of ibrutinib in the first-line

treatment of most groups of patients with CLL has been consolidated and the responses seem to be durable as well. A 5-year follow-up of a phase II trial initiated by the National Institutes of Health evaluating ibrutinib as first-line therapy in CLL showed a 5-year PFS of 74.4% in treatment-naïve patients with *TP53* mutations or deletions and 100% in treatment-naïve patients without *TP53* mutations.<sup>16</sup> Although ibrutinib monotherapy is currently the most and best evaluated novel substance and indisputably yields impressive outcomes, its continued administration is associated with several problems. In the above-mentioned study in patients with high-risk CLL, the cumulative incidence of resistance-conferring BTK or PLCγ2 mutations at 5 years ranged between 22.6% and 66.7% depending on the risk group.<sup>16,17</sup> Similar rates were observed in a French real world cohort: after a median of 3.5 years of ibrutinib treatment, BTK mutations were found in 57% of the patients.<sup>18</sup> The same study showed that 3 years after initiation of ibrutinib treatment, only 31% of the patients remained on the drug. The incidence of ibrutinib-related toxicities and associated treatment discontinuation vary significantly between clinical trials and so-called real world experiences. A retrospective analysis reported toxicity-related treatment discontinuations in 128 of 616 patients (21%) with a median follow-up of 17 months in their comprehensive real-world analysis while the toxicity-related treatment discontinuation rate in the

**Table 1. Trials using chemotherapy-free combination treatments in chronic lymphocytic leukemia**

Treatment	TN, r/r	Age ‡	ORR	CR %	PR %	uMRD %	PFS*	2 y-PFS	2 y-OS	Reference
<b>Novel agents + anti-CD20 antibodies</b>										
Ibrutinib + rituximab	TN (n=354)	58	96%	17%	NA	8%	NA	3 y: 89%	3 y: 99%	Shanafelt <i>et al.</i> 2019 <sup>9</sup>
FCR	TN (n=175)	57	81%	30%	NA	59%	NA	3 y: 73%	3 y: 92%	
Ibrutinib	TN (n=182)	71	93%	7%	NA	1%	NR	87%	90%	Woyach <i>et al.</i> 2018 <sup>10</sup>
Ibrutinib + rituximab	TN (n=182)	71	94%	12%	NA	4%	NR	88%	94%	
Bendamustine + rituximab	TN (n=183)	70	81%	26%	NA	8%	41.0	74%	95%	
Ibrutinib + obinutuzumab	TN (n=113)	70	88%	19%	69%	35%	NR	30 m: 79%	30 m-OS: 86%	Moreno <i>et al.</i> 2018 <sup>8</sup>
Chlorambucil + obinutuzumab	TN (n=116)	72	73%	8%	66%	25%	19.0	30 m: 31%	30 m-OS: 85%	
Idelalisib + rituximab	r/r (n=110)	71	81%	0	81%	NA	NR	6 m: 93%	1 y-OS: 92%	Furman <i>et al.</i> 2014 <sup>4</sup>
Rituximab	r/r (n=110)	71	13%	0	13%	NA	5.5	6 m: 46%	1 y-OS: 80%	
Acalabrutinib + obinutuzumab	TN (n=19) r/r (n=26)	61	TN: 95% r/r: 92%	TN: 16% r/r: 8%	TN: 79% r/r: 85%	NA	NR	NA	NA	Woyach <i>et al.</i> 2017 <sup>64</sup>
Venetoclax + rituximab	r/r (n=194)	65	92%	8%	84%	62%	NR	85%	92%	Seymour <i>et al.</i> 2018 <sup>31</sup>
Bendamustine + rituximab	r/r (n=195)	65	72%	4%	69%	13%	17.0	63%	87%	
Venetoclax + obinutuzumab	TN (n=216)	72	85%	50%	35%	76%	NR	88%	92%	Fischer <i>et al.</i> 2019 <sup>69</sup>
CLB + obinutuzumab	TN (n=216)	71	71%	23%	48%	35%	NR	64%	93%	
Venetoclax + obinutuzumab	TN (n=32) r/r (n=50)	63 61	TN: 100% r/r: 95%	TN: 78% r/r: 37%	TN: 22% r/r: 58%	TN: 91% r/r: 64%	NR	TN: 91% r/r: 85%	NA	Flinn <i>et al.</i> 2019 <sup>70</sup>
<b>Novel-novel combinations</b>										
Venetoclax + ibrutinib	r/r (n=50)	NA	100%	58%	42%	58%	NR	NA	NA	Hillmen <i>et al.</i> 2018 <sup>71</sup>
Venetoclax + ibrutinib	TN (n=80)	65	100%	96%	4%	69%	NR	1 y: 98%	1 y: 99%	Jain <i>et al.</i> 2018 <sup>72</sup>
Venetoclax + ibrutinib + obinutuzumab	TN (n=25)	59	100%	50%	50%	70%	NR	NA	NA	Rogers <i>et al.</i> 2018 <sup>73</sup>
Umbralisib + ibrutinib	r/r (n=21)	67	90%	29%	62%	NA	NR	90%	95%	Daivids <i>et al.</i> 2019 <sup>74</sup>
Umbralisib + ibrutinib + ublituximab	r/r (n=22)	62	100%	36%	64%	78%	NR	NA	NA	Nastoupil <i>et al.</i> 2019 <sup>75</sup>

‡median, years; \*median, months; TN: treatment-naïve; r/r: relapsed or refractory; ORR: overall response rate; CR %: complete response rate; PR %: partial response rate; uMRD %: rate of patients with undetectable minimal residual disease (<10<sup>4</sup>) in peripheral blood; PFS: progression-free survival; y: year; m: month; OS: overall survival; FCR: fludarabine, cyclophosphamide, rituximab; NR: not reached, NA: not available.

above-mentioned phase II trial in high-risk CLL was only 6%.<sup>16,19</sup> Atrial fibrillation has been reported in several trials as a cause of treatment interruption. In a retrospective analysis, the 5-year incidence of atrial fibrillation was 21%.<sup>16</sup> Another pooled analysis of multiple clinical trials estimated a 3-year cumulative incidence of atrial fibrillation of 13.8% among ibrutinib-treated patients.<sup>20</sup>

Other BTK inhibitors have been developed to overcome these commonly encountered difficulties, such as the development of resistance mutations and the discontinuation of treatment due to adverse drug effects. While second-generation inhibitors such as substance ARQ 531 promise efficacy in the context of BTK C481S mutations, more specific inhibitors, including acalabrutinib and zanubrutinib, appear to cause fewer adverse off-target effects.<sup>21-24</sup> Direct, randomized comparisons of acalabrutinib (NCT02477696) and zanubrutinib (NCT03734016) against ibrutinib are currently ongoing.

### PI3K inhibitors

Phosphoinositide 3-kinase (PI3K) $\gamma$  is the target of the kinase inhibitor idelalisib and a downstream kinase of the B-cell receptor that stimulates the proliferation and survival of CLL cells (Figure 1). The combination of idelalisib with rituximab is approved for the treatment of r/r CLL as well as for the first-line treatment of patients with del(17p)

and/or *TP53* mutations for whom no other therapies are appropriate. Idelalisib has shown some activity as a single agent in r/r CLL and was combined with rituximab in a prospective randomized study against rituximab monotherapy.<sup>4,25</sup> The median PFS in the placebo group was 5.5 months and was not reached in the rituximab-idelalisib arm [hazard ratio (HR) for disease progression or death 0.15,  $P < 0.001$ ]; the ORR was 81% with idelalisib, but only 13% in the rituximab arm. Following these encouraging results, the combination was investigated in the first-line setting. In a phase II study, 64 patients were treated with rituximab and idelalisib with a median treatment duration of 22.4 months.<sup>26</sup> The ORR was 97%, including 19% complete responses (CR) and the estimated 3-year PFS was 83%. However, significant severe adverse events of this regimen were reported. Diarrhea and colitis occurred in 61% of patients, skin rash in 58%, fever in 42%, nausea in 38% and transaminitis in 67%.<sup>27</sup> In large phase III trials, an increased mortality was observed in the idelalisib-containing arms which led to premature discontinuation of other trials and a re-evaluation of the substance by regulatory authorities.<sup>28</sup>

Other kinase inhibitors targeting the PI3K pathway are umbralisib and the dual PI3K inhibitor duvelisib. While umbralisib treatment is not yet approved, the use of duvelisib has been approved by the Food and Drug

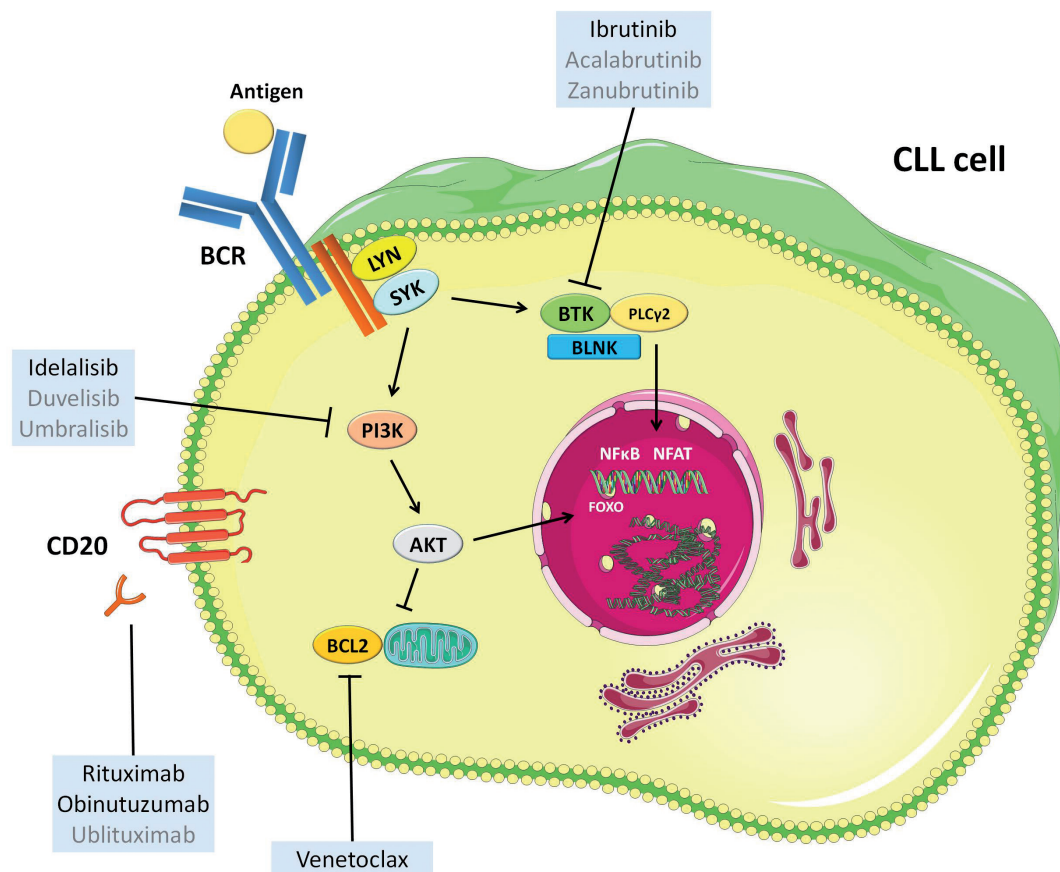


**Figure 1. Targets of currently approved (black) and investigated (gray) novel agents.** CLL: chronic lymphocytic leukemia; BCR: B-cell receptor. This figure was produced by M. Fürstenau using servier medical art ([smart.servier.com](http://smart.servier.com)).

Administration (FDA). The efficacy of duvelisib, an oral inhibitor of PI3K $\delta$  and PI3K $\gamma$ , was demonstrated in a phase I study that included 55 r/r CLL patients of whom 56% responded to treatment.<sup>29</sup> The results of the phase III DUO study, which tested the efficacy and safety of duvelisib versus ofatumumab, were recently published: duvelisib was associated with a significantly prolonged PFS compared to ofatumumab (13.3 vs. 9.9 months, HR=0.52,  $P<0.0001$ ) and a superior ORR (74 % vs. 45 %,  $P<0.0001$ ). The PI3K $\delta$  inhibitor umbralisib demonstrated promising activity in an initial phase I trial while showing a more favorable safety profile than other PI3K inhibitors with a lower incidence of autoimmune-like adverse events.<sup>30</sup>

### BCL2 inhibitors

Venetoclax is an oral B-cell lymphoma 2 (BCL2) inhibitor and was recently approved for the treatment of patients with r/r CLL in combination with rituximab.<sup>31</sup> Before the approval of the combination therapy, venetoclax was used as an indefinite monotherapy in patients who relapsed after ibrutinib treatment and patients with *TP53* aberrations.<sup>7</sup> With the universal approval of venetoclax plus rituximab as second-line therapy, indefinite venetoclax monotherapy will be less relevant in the near future. Nonetheless, it is worthwhile looking at extended follow-up data of venetoclax monotherapy trials.

The results of a phase II study evaluating venetoclax in 158 mostly r/r CLL patients with 17p deletions was recently published.<sup>32</sup> The median duration of venetoclax treatment was 23.1 months (range, 0-44.2 months) and the ORR was 77% (122 of 158 patients; 20% CR) while the 2-year PFS was 54% [95% confidence interval (95% CI): 45% to 62%]. Forty-eight (30%) of the 158 patients achieved a minimal residual disease (MRD) status below  $10^{-4}$  at least once in the course of the study. More detailed MRD data showed that, in patients receiving venetoclax monotherapy, MRD status was closely associated with PFS. Patients who achieved undetectable MRD during treatment had significantly longer PFS than patients with intermediate or high MRD levels.<sup>33</sup> This association had previously only been reported for chemoimmunotherapy

regimens.<sup>34</sup> While these results demonstrate the relevance of venetoclax for patients with 17p deletions, venetoclax monotherapy is still only approved in the first-line setting in patients ineligible for ibrutinib treatment.

In relapsed CLL, venetoclax was approved in combination with rituximab based on the data from the MURANO study that tested this 24-month long combination treatment against bendamustine plus rituximab in a population of 389 CLL patients.<sup>31</sup> With a median follow-up of 23.8 months, PFS among the patients treated with venetoclax plus rituximab was clearly superior to that of patients treated with bendamustine plus rituximab (HR=0.17; 95% CI: 0.11-0.25;  $P<0.0001$ ): the estimated 2-year PFS was 84.9% for patients treated with venetoclax plus rituximab and 36.3% for those treated with bendamustine plus rituximab. Venetoclax plus rituximab also produced a significantly prolonged OS (HR=0.48; 95% CI: 0.25-0.90) and an impressive ORR of 93.3% compared to 67.7% with bendamustine plus rituximab (difference= 25.6%; 95% CI: 17.9-33.3%). Venetoclax plus rituximab also led to higher rates of undetectable MRD in peripheral blood (62.4% vs. 13.3% after 9 months). Most importantly, the MURANO study established the feasibility of a time-limited chemotherapy-free treatment regimen by demonstrating that the majority of MRD-negative remissions were sustained after the end of the study treatment.<sup>35</sup> With an extended median follow-up of 36 months, 130 (67%) of 194 patients completed the 2-year treatment and with a median observation time of 9.9 months after completion of treatment with venetoclax plus rituximab, only 16 of 130 patients (12%) showed disease progression.

While the occurrence of clinical tumor lysis syndromes was a dreaded and common event in the early experiences with venetoclax, the risk of these syndromes has now been successfully mitigated by introducing a ramp-up schedule and repeated testing of tumor lysis syndrome parameters within the first 24 h after each ramp-up.<sup>7</sup> A recent comprehensive safety analysis of three trials using venetoclax monotherapy showed an incidence of laboratory tumor lysis syndrome of only 1.4% while no clinical tumor lysis syndrome occurred.<sup>36</sup> Most adverse events

**Table 2.** Trials using novel agents in combination with chemoimmunotherapy as first or further line therapy for CLL.

Treatment	TN, r/r	Age ‡	ORR	CR %	PR %	uMRD %	PFS*	2 y-PFS	2 y-OS	Reference
BR + ibrutinib	r/r (n=289)	64	83%	10%	72%	26%	NR	18 m: 79%	3 y-OS: 82%	Chanan-Khan <i>et al.</i> 2016 <sup>56</sup>
BR	r/r (n=289)	63	68%	3%	65%	6%	13.3	18 m: 24%	3 y-OS: 73%	
BR + idelalisib	r/r (n=207)	62	70%	1%	69%	NA	20.8	NA	NA	Zelenetz <i>et al.</i> 2017 <sup>58</sup>
BR	r/r (n=209)	64	45%	0	44%	NA	11.1	NA	NA	
Ibrutinib + FCR	TN (n=85)	55	96%	36%	61%	78%	NR	100%	100%	Daids <i>et al.</i> 2019 <sup>59</sup>
Duvelisib + FCR	TN (n=32)	55	97%	28%	69%	67%	NR	97%	97%	Daids <i>et al.</i> 2018 <sup>62</sup>
Ibrutinib + FCG	TN (n=42)	60	100%	40%	60%	100%	NR	NA	NA	Jain <i>et al.</i> 2018 <sup>60</sup>
Bendamustine + ibrutinib + ofatumumab	TN (n=40), r/r (n=25)	60	93%	31%	62%	7%	NR	NA	NA	Cramer <i>et al.</i> 2017 <sup>65</sup>
Bendamustine + ibrutinib + obinutuzumab	TN (n=30), r/r (n=31)	67	100%	46%	54%	48%	NR	15 m: 96%	NA	Von Tresckow <i>et al.</i> 2018 <sup>66</sup>
Bendamustine + venetoclax + obinutuzumab	TN (n=35), r/r (n=31)	59	95%	38%	56%	87%	NR	15 m: 92%	15 m: 95%	Cramer <i>et al.</i> 2018 <sup>67</sup>

‡median, years; \*median, months; TN: treatment-naïve; r/r: relapsed or refractory; ORR: overall response rate; CR %: complete response rate; PR %: partial response rate; uMRD %: rate of patients with undetectable minimal residual disease ( $<10^{-4}$ ) in peripheral blood; PFS: progression-free survival; y: year; m: month; OS: overall survival; BR: bendamustine, rituximab; FCR: fludarabine, cyclophosphamide, rituximab; FCG: fludarabine, cyclophosphamide, obinutuzumab; NR: not reached; NA: not available.

were hematologic toxicities such as neutropenia (40% of all patients) and thrombocytopenia (21%), gastrointestinal disorders including diarrhea (41%) and nausea (39%) as well as upper respiratory tract infections (25%).

As previously reported for ibrutinib, continued drug exposure may result in the development of specific resistance mutations in the context of indefinite venetoclax treatment. A venetoclax-specific resistance mutation in the *BCL2* gene was recently reported.<sup>37</sup> Of 15 patients whose disease progressed during venetoclax treatment, seven showed a heterozygous nucleotide variant (Gly101Val) in *BCL2* that impaired binding of venetoclax to the protein. The mutation was detected as early as 25 months before clinically apparent CLL progression. Another study showed various other molecular aberrations in patients who developed resistance upon BCL2-inhibition by venetoclax, including cancer-related genes such as *TP53*, *BRAF* and *CD274*.<sup>38</sup>

### Sequential use of novel agents

Despite the long PFS that novel agents have produced, most patients will probably require a second-line treatment after the first novel agent either because of disease progression or because of toxicity-related treatment discontinuation. As novel agents have only been approved recently, there is limited evidence on how best to sequence these agents and how to treat patients who relapse after these therapies. Available data are largely based on retrospective cohort studies and registry data.

Mato *et al.* systematically assessed treatment sequences in a large cohort of patients treated with ibrutinib or venetoclax.<sup>39</sup> Ibrutinib given as a first kinase inhibitor yielded better outcomes than idelalisib, while in the setting of ibrutinib failure, venetoclax produced superior survival compared with idelalisib and chemoimmunotherapy. Jones and colleagues confirmed this observation in their analysis of 127 patients who received venetoclax after kinase inhibitor failure with a median PFS of 24.7 months for venetoclax treatment after ibrutinib and an estimated 1-year PFS of 79% for venetoclax after idelalisib failure.<sup>40</sup> Within another analysis, Mato and colleagues assessed outcomes in patients who had previously been treated with idelalisib or ibrutinib with regard to the reason of prior treatment discontinuation.<sup>19</sup> The main reason for discontinuation of treatment with a kinase inhibitor was toxicity (51%), followed by disease progression (29%) and Richter transformation. Patients who were retreated due to intolerance of the previously used kinase inhibitor had significantly better outcomes than patients whose disease had progressed during the kinase inhibitor treatment.

Patients in whom venetoclax treatment fails have not yet been extensively analyzed. In a recently published analysis, 204 venetoclax-treated patients were evaluated of whom about 47% discontinued treatment due to progressive disease, 21% due to Richter transformation and 11% because of mostly hematologic adverse events.<sup>41</sup> Nineteen patients who were subsequently treated with a kinase inhibitor showed a good ORR of 69% and a median PFS that was not reached after a median follow-up of 7 months. First data from patients progressing on the MURANO trial who were subsequently treated with ibrutinib indicate that this kinase inhibitor can be successfully used after venetoclax.<sup>42</sup> Of eight patients who were

included in this analysis, seven responded to ibrutinib (6 partial responses, 1 complete response).

Furthermore, alternate kinase inhibitors were investigated in patients who were intolerant to either ibrutinib or idelalisib.<sup>43,44</sup> Thirty-three patients who discontinued ibrutinib treatment due to toxicities were treated with acalabrutinib and showed an ORR of 76%. The median PFS had not been reached after a median follow-up of 9.5 months. During this time only 6% of the ibrutinib-intolerant patients discontinued treatment with acalabrutinib due to adverse events.<sup>43</sup> In a similar study, 36 BTK inhibitor-intolerant and four PI3K inhibitor-intolerant patients were treated with umbralisib; four of these patients discontinued treatment due to an adverse event within a median follow-up of 7 months.<sup>44</sup>

Prospective clinical trials including long-term follow-ups are urgently needed to establish an optimal sequencing strategy. Nonetheless, some conclusions on the sequence of therapy can be drawn based on the limited, existing data. Venetoclax-containing regimens appear to be superior after ibrutinib failure while ibrutinib seems the best option after venetoclax.<sup>39-41</sup> Patients in whom idelalisib fails can be treated equally with either ibrutinib or venetoclax. When ibrutinib treatment is discontinued due to toxicities, changing to an alternative BTK inhibitor, such as acalabrutinib, can be considered, where available. However, other factors must also be taken into account when deciding on a treatment sequence. These factors include the genetic risk profile, specific co-morbidities and co-medications as well as the expected compliance and personal treatment preference of the patient. Figures 2 and 3 show proposed treatment algorithms based on the available evidence and current approval status of the drugs.

### Limitations of monotherapy with novel agents

Optimal sequencing of single agents ideally leads to durable remissions with each new substance while other effective substances are saved for the next line of treatment. In reality, however, this is often not the case.

Retrospective and registry data show markedly higher discontinuation rates of monotherapy with ibrutinib or venetoclax than those documented in the pivotal clinical trials, either due to disease progression, toxicities or other long-term adherence issues.<sup>3,15,16,19,45</sup> After several years of exposure to ibrutinib, the incidence of BTK and PLC $\gamma$ 2 mutations appears to increase drastically and certain toxicities, such as cardiac arrhythmias, seem to occur at a constant frequency during ibrutinib treatment.<sup>16,18-20,37,46,47</sup> In the long-term follow-up of the RESONATE trial, atrial fibrillation occurred in 11% of the ibrutinib-treated patients with a median follow-up of 44 months. While hematologic toxicities and infections occurred mostly in the first year of ibrutinib treatment and decreased afterwards, hypertension and rare major hemorrhages were seen constantly during the following years.<sup>48</sup>

Another crucial drawback of indefinite monotherapy is the financial burden, as all novel agents approved for use in CLL are extremely costly compared to established treatment options such as chemoimmunotherapy.<sup>49</sup> Furthermore, kinase inhibitor monotherapy rarely leads to complete and deep molecular remissions due to various mechanisms of adaptation that have recently been described.<sup>50</sup>

For these reasons, efforts have been made to design time-limited combination treatments that, despite their

limited duration, achieve deep and long-lasting remissions. The only approved treatment concepts that meet these criteria and show a favorable safety profile are the 24-month fixed-duration combination of venetoclax and rituximab and the 12-month fixed-duration combination of venetoclax and obinutuzumab.<sup>31</sup> A multitude of different combination treatments containing novel agents are currently being investigated.

### Undetectable minimal residual disease as a treatment goal of new combination therapies

In 2016, the European Medicines Agency accepted the use of undetectable MRD as a surrogate for PFS and as an intermediate endpoint in CLL trials. This decision was based on large analyses of chemoimmunotherapy studies that demonstrated a strong association between MRD status and PFS and established undetectable MRD as an independent prognostic factor for PFS and OS.<sup>34,51-55</sup> Recently the predictive value of undetectable MRD was confirmed in the context of treatment with several new substances.

An analysis of venetoclax monotherapy showed that 2-year PFS rates were significantly higher in patients who achieved undetectable ( $<10^{-4}$ ) or intermediate MRD ( $\geq 10^{-4}$  to  $<10^{-2}$ ) than in patients who never achieved MRD  $<10^{-2}$  (92.8%, 84.3%, and 63.2%, respectively).<sup>33</sup> Similarly, the recently published follow-up of the MURANO study underscored the predictive value of MRD status in the context of venetoclax plus rituximab treatment.<sup>35</sup> In con-

trast, the complete remission rate with ibrutinib monotherapy increased with a significant delay over time and reached 28% after a median time of 60 months. Undetectable MRD is still rarely achieved and in clinical trials evaluating ibrutinib therapy no correlation between MRD status and survival has been established so far.<sup>16</sup>

Since low MRD levels promise longer PFS and, presumably, treatment-free survival, the achievement of the lowest possible MRD level represents a desirable treatment goal. With chemoimmunotherapy the eradication of MRD below the detection limit of one CLL cell per 10,000 normal leukocytes ( $<10^{-4}$ ) could only be reliably achieved by intensive treatment regimens (e.g. fludarabine, cyclophosphamide and rituximab), which were not tolerable for the majority of elderly CLL patients with comorbidities.<sup>12</sup> With the increasing availability of new substances, high rates of MRD-negative CR can also be achieved in older patients with comorbidities (Table 1).

### Combinations

#### Chemoimmunotherapy plus novel agents

As undetectable MRD and CR are not commonly achieved with ibrutinib alone, several studies have combined the BTK inhibitor with chemoimmunotherapy to increase efficacy (Table 2). In the recently published follow-up of the HELIOS trial evaluating ibrutinib together

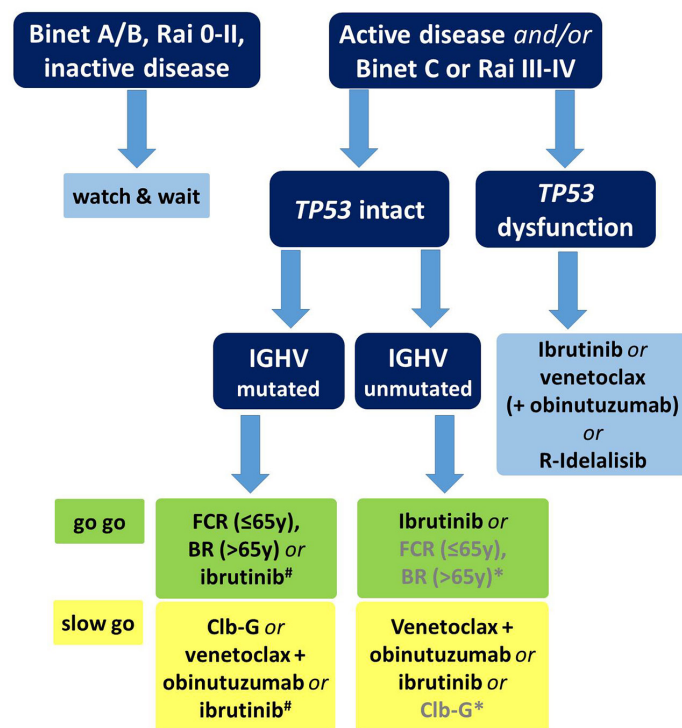


Figure 2. Proposed algorithm for first-line treatment using approved options in clinical practice. y: years; R: rituximab; FCR: fludarabine, cyclophosphamide, rituximab; BR: bendamustine, rituximab; Clb-G: chlorambucil, obinutuzumab.

#consider and discuss with patient: long-term vs. fixed-duration therapy, specific side effects of each therapeutic option (myelosuppression, infections, secondary malignancies, cardiac toxicities, bleeding, autoimmune disorders);

\*Chemoimmunotherapy as alternative treatment only if no TP53 dysfunction and reasons against continuous treatment with ibrutinib or non-availability

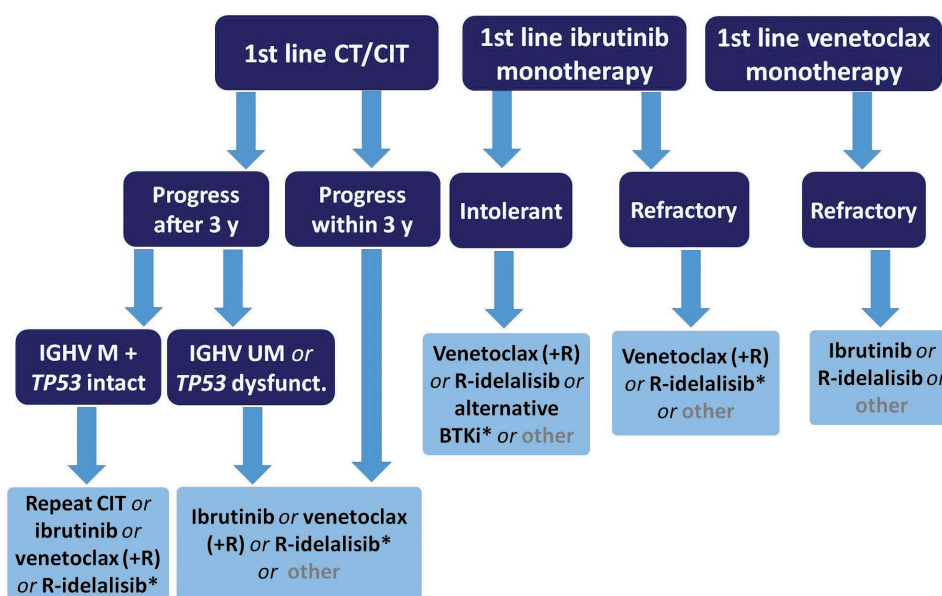
with bendamustine plus rituximab *versus* bendamustine plus rituximab only, the reported rate of undetectable MRD at 36 months was 26.3% in the ibrutinib, bendamustine and rituximab arm and increased over time.<sup>56,57</sup> Undetectable MRD status was associated with significantly improved PFS (3-year PFS rate: 88.6% for patients with undetectable MRD *vs.* 60.1% for patients with MRD  $\geq 10^{-4}$ ). However, no termination of ibrutinib therapy was planned according to the study protocol, even when MRD was no longer detectable.

A similar concept was tested with the PI3K $\delta$  inhibitor idelalisib in combination with bendamustine plus rituximab.<sup>58</sup> While idelalisib together with bendamustine plus rituximab produced a significantly improved PFS compared with bendamustine plus rituximab only (median PFS 20.8 *vs.* 11.1 months), the triple combination was associated with an increased risk of severe infections, limiting its use in clinical practice.

Various phase II studies have evaluated the addition of kinase inhibitors to chemoimmunotherapy in young and fit, treatment-naïve CLL patients. Davids and colleagues reported an impressive rate of undetectable MRD in bone marrow of 78% and a CR rate of 36% after six cycles of fludarabine, cyclophosphamide and rituximab and 2 years of continuous ibrutinib.<sup>59</sup> Another trial evaluated the MRD-guided use of frontline therapy with ibrutinib, fludarabine, cyclophosphamide and obinutuzumab in patients with a favourable genetic risk profile (IGHV-mutated, no *TP53* aberrations).<sup>60</sup> After three courses of the quadruple combination, treatment was continued with

either nine cycles of ibrutinib plus obinutuzumab or three cycles of ibrutinib plus obinutuzumab and six cycles of ibrutinib only, depending on post-chemoimmunotherapy MRD status. Undetectable MRD at 1 year led to the discontinuation of all therapy. All 28 patients who completed 12 months of treatment had undetectable MRD and stopped therapy per protocol: the CR rate was 86% at that time point. Michallet *et al.* evaluated a similar scheme in a larger study including previously untreated CLL patients with mutated or unmutated IGHV. Induction treatment consisted of 6 months of ibrutinib plus obinutuzumab followed by 3 months of ibrutinib.<sup>61</sup> After this treatment, MRD was tested and patients with MRD-negative CR or CR with incomplete hematologic recovery (CRi) continued treatment with ibrutinib for another 6 months while all other patients received an intensified regimen with four cycles of the quadruple combination (ibrutinib, fludarabine, cyclophosphamide and obinutuzumab) and ibrutinib until month 16. With this approach, only 12% of the patients were in MRD-negative CR or CRi: after 9 months and could avoid intensive chemoimmunotherapy.

The dual PI3K inhibitor duvelisib was also evaluated in combination with fludarabine, cyclophosphamide and rituximab therapy. However, this regimen induced a slightly lower CR rate of 26% and a rate of undetectable MRD in bone marrow of 67%.<sup>62</sup> Although the most frequent adverse events were hematologic toxicities, several immune-mediated toxicities, including transaminitis (grade 3: 34%), arthritis (9%), colitis (6%), pericarditis and pancreatitis (both 3%), were also reported.



**Other options:** Alemtuzumab (+fludarabine), FCR (after BR), BR (after FCR), Lenalidomide (+R), discuss cellular therapy (allogeneic hematopoietic stem cell transplantation or chimeric antigen receptor (CAR) T-cell therapy) in fit patients

\*consider and discuss with patient: long-term *vs.* fixed-duration (CIT: 6 months; venetoclax+R: 24 months) therapy, specific side effects of each therapeutic option (myelosuppression, infections, secondary malignancies, cardiac toxicities, bleeding, autoimmune disorders).

**Figure 3. Proposed sequencing of therapy according to first-line treatment; approved options.** CT: chemotherapy; CIT: chemoimmunotherapy; y: years; M: mutated; UM: unmutated; R: rituximab; BTKi: Bruton tyrosine kinase inhibitor.

Although the addition of kinase inhibitors to conventional chemoimmunotherapy regimens yields significant undetectable MRD and CR rates in selected populations of patients, these combinations have not yet been tested against kinase inhibitor monotherapy. This limits the practical relevance of these observations in the light of the impressive outcomes of single agent ibrutinib. In addition, toxicity rates with these more intensive combinations cannot be neglected. Treatment of elderly patients with comorbid conditions, in particular, is probably more difficult due to the toxicity rates.

### Novel agents plus anti-CD20 antibodies

While idelalisib is specifically approved in combination with anti-CD20 antibodies, ibrutinib has so far not been approved as part of a combination treatment due to ambiguous study results.<sup>4,10,65</sup> The combination of ibrutinib plus rituximab has been tested in randomized settings in phase II and phase III trials.<sup>10,63</sup> Burger and colleagues conducted a randomized trial of ibrutinib *versus* ibrutinib plus rituximab in 208 CLL patients of whom 181 had r/r CLL.<sup>63</sup> The other 27 patients included were treatment-naïve, but had high-risk, unfavorable genetics, defined by del(17p) or TP53 mutation. The study showed no difference between ibrutinib plus rituximab and ibrutinib in either PFS (3-year PFS: 86.9% *vs.* 86%), ORR (92.3% for both) or CR rate (26% *vs.* 20.2%). However, patients treated with ibrutinib plus rituximab showed higher rates of undetectable MRD and achieved their remissions faster than patients treated with ibrutinib only. A phase III trial (ALLIANCE) that tested ibrutinib and ibrutinib plus rituximab against bendamustine plus rituximab in older patients showed almost identical efficacy data for both ibrutinib-containing arms.<sup>10</sup> While these data support the conclusion that there is no clear benefit of adding rituximab to ibrutinib, no randomized comparison has been performed so far comparing obinutuzumab plus ibrutinib *versus* ibrutinib monotherapy. The iLLUMINATE trial evaluated ibrutinib plus obinutuzumab in comparison to chlorambucil plus obinutuzumab. The combination of ibrutinib plus obinutuzumab was significantly superior to the chemoimmunotherapy regimen with a PFS at 30 months of 79% *versus* 31% ( $P < 0.0001$ ), but unfortunately a third arm with ibrutinib monotherapy was missing. Hence the benefit of the addition of obinutuzumab is not clear, particularly because no treatment stop was planned in the case of CR, which was achieved in 19% of the patients receiving ibrutinib plus obinutuzumab. First data from a phase Ib/II study combining acalabrutinib and obinutuzumab were impressive with an ORR of 93%, but also in this trial there was no direct comparison to acalabrutinib monotherapy.<sup>64</sup>

Two identically designed phase II trials evaluated the use of ibrutinib plus obinutuzumab and ibrutinib plus ofatumumab after an optional debulking with bendamustine including a planned termination of treatment if peripheral blood samples showed undetectable MRD at two consecutive time-points. While 48% of all ibrutinib plus obinutuzumab-treated patients had undetectable MRD at the final restaging, only 14% achieved this status after ibrutinib plus ofatumumab treatment.<sup>65,66</sup>

In contrast to ibrutinib, the addition of rituximab to venetoclax has produced unprecedented MRD-negative response rates in r/r CLL leading to its broad approval in the r/r setting.<sup>31</sup> In the pivotal MURANO trial comparing bendamustine plus rituximab *versus* 24 months of veneto-

clax plus rituximab 64% of the patients treated with the latter combination had no detectable MRD after 24 months of treatment and this status was sustained in the majority, with a median follow-up of approximately 10 months.<sup>35</sup> This study was the first to establish a chemotherapy-free time-limited treatment regimen in CLL.

Even higher response rates were observed when venetoclax was combined with obinutuzumab. The CLL2-BAG trial combined an optional upfront debulking with bendamustine with an 8-month induction treatment and a MRD-guided maintenance phase, both consisting of venetoclax and obinutuzumab.<sup>67</sup> At the end of induction treatment, 60 of 63 patients (95%) had responded to treatment and 87% of the patients had no detectable MRD below  $10^{-4}$ . The remissions seem durable after undetectable MRD-triggered end of treatment even in patients with high-risk genetic features.<sup>68</sup> The recently published phase III CLL14 trial confirmed the efficacy of this combination treatment in a comorbid patient collective when tested against chlorambucil plus obinutuzumab. A 12 month fixed-duration treatment with venetoclax and obinutuzumab produced an unprecedented uMRD rate of 76% and an estimated 2-year PFS of 88%.<sup>69</sup> In a recent phase Ib study, venetoclax and obinutuzumab were combined for 6 months and followed by venetoclax treatment for either 1 year in the first-line cohort or until disease progression in the r/r cohort.<sup>70</sup> The overall best response rate was 95% in r/r CLL patients and 100% in those treated first-line. Undetectable MRD rates in the peripheral blood were 64% and 91%, respectively,  $\geq 3$  months after the last dose of obinutuzumab.

### Inhibitors in combination, including triple combinations

Considering the impressive single agent activity of kinase inhibitors and venetoclax in CLL and their ability to induce deep and durable remissions when combined with an anti-CD20 antibody, it seems obvious to test novel combinations to further increase efficacy by synergistically tackling the CLL cell in different vital pathways (Figure 1).

The phase II CLARITY trial tested a time-limited and MRD-guided oral combination treatment of ibrutinib and venetoclax in 40 patients with r/r CLL.<sup>71</sup> After 8 weeks of ibrutinib treatment, venetoclax was added with the established 5-week dose escalation scheme. All patients responded to treatment (CR/CRi rate: 58%) and 23 of 40 patients (58%) had no detectable MRD in peripheral blood after 12 months of combined therapy. The same combination in a fixed-duration 24-month strategy was investigated in 80 treatment-naïve patients with CLL.<sup>72</sup> After 12 months of combined venetoclax and ibrutinib the CR/CRi rate was 96% and 69% of the patients had no detectable MRD in the bone marrow. In both trials, the rates of undetectable MRD increased during the course of treatment, promising higher rates with longer follow-up.

Rogers and colleagues recently reported the preliminary outcomes of their phase II trial investigating the triple combination of obinutuzumab, ibrutinib and venetoclax in treatment-naïve and r/r CLL.<sup>73</sup> In the first month of treatment, only obinutuzumab was administered. Ibrutinib was added in month 2 and venetoclax was added in month 3. After 12 months of combined treatment, the

ORR was 88% in the r/r patients and 84% in the treatment-naïve cohort while 67% of treatment-naïve patients and 50% of all r/r patients had no detectable MRD in bone marrow and peripheral blood.

The first study successfully using two novel agents that directly target the B-cell receptor pathway combined umbralisib with ibrutinib and produced an ORR of 90% (CR: 29%) and a 2-year PFS of 90%.<sup>74</sup> In contrast to prior studies that combined multiple kinase inhibitors, this combination was well-tolerated and no dose-limiting toxicities were observed. The same combination plus ublituximab was assessed safe and active in a phase I study in which the ORR was 100% among 22 previously treated patients with CLL or small lymphocytic lymphoma. The median duration of response was 22.7 months.<sup>75</sup>

Checkpoint inhibitor monotherapy has shown limited efficacy in CLL but promising activity in Richter transformation.<sup>76</sup> A phase II study investigated the combination of ibrutinib and nivolumab in patients with high-risk CLL or Richter transformation.<sup>77</sup> While the combination showed promising efficacy in Richter transformation, it produced an ORR of 61% in the high-risk CLL group, which is comparable to that achieved with single-agent ibrutinib.

## Discussion

Ibrutinib monotherapy has produced unprecedented PFS and OS in various groups of CLL patients.<sup>5,9,10,13,14</sup> Being the only novel agent that has been broadly approved in the first-line setting, it remains the most widely used novel agent in clinical routine. For the consequently increasing number of patients relapsing after ibrutinib, current evidence indicates that optimal sequencing of novel agents can lead to long PFS and OS with an overall favorable safety profile.<sup>39-41,78</sup> The bar in terms of PFS has been raised high by the sequence of frontline ibrutinib followed by venetoclax.

However, continued monotherapy is associated with some drawbacks including the development of resistance mutations, an increased financial burden, cumulative toxicities, and long-term adherence issues.<sup>18,19,36,38,45,47,50,79</sup> These factors underscore the need for further development of time-limited treatment concepts that lead to deep and durable remissions, ideally with long treatment-free intervals.

With the broad approval of venetoclax plus rituximab for r/r CLL, a first chemotherapy-free fixed-duration regimen has pushed into clinical practice and the even shorter combination treatment of venetoclax and obinutuzumab that has proven its striking efficacy in treatment-naïve patients has just followed. Based on the CLL14 data comparing chlorambucil plus obinutuzumab *versus* fixed-duration venetoclax plus obinutuzumab for 12 months another venetoclax combination therapy has been approved by the FDA for the frontline treatment of patients with CLL.

The essential question of how durable achieved remissions are after stopping combination treatment was in part answered by two recently published long-term follow-ups. In the MURANO trial, the majority of MRD-negative remissions were sustained with a median follow-up of 9.9 months after the end of study treatment.<sup>35</sup> Furthermore, Cramer *et al.* documented that 13 of 17 high-risk CLL patients (17p deletion/*TP53* mutation) who achieved undetectable MRD after a time-limited treatment with either venetoclax plus obinutuzumab or ibrutinib plus

obinutuzumab had ongoing remissions after a median observation time of 16 months after the end of study treatment.<sup>68</sup>

While these treatment-free phases are certainly desirable from a patient's point of view, their effect on clonal evolution of CLL remains largely unknown. It is conceivable though that shorter exposure to ibrutinib and venetoclax might be associated with a lower incidence of drug-specific resistance mutations as most of these seem to appear later in the course of monotherapy.<sup>16,18,37,38,47,80,81</sup> The absence of resistance mutations and treatment-free intervals could allow for re-exposure of patients to the same combination treatment, potentially with a similar efficacy as before.

Comprehensive safety analyses are much needed, particularly in the context of novel-novel combinations to detect treatment-specific toxicities that might not be detected in smaller phase II trials.<sup>27,36,82</sup> As ibrutinib alone seems to be associated with an increased incidence of certain opportunistic infections, it is conceivable that this specific risk might be even higher when this drug is combined with additional substances that influence the immune system.<sup>83,84</sup>

Detailed pharmacokinetic analyses are also warranted to optimize combination treatments as kinase inhibitors and venetoclax might interact due to their CYP-dependent metabolism.<sup>85</sup> A recent study found that even reduced doses of ibrutinib lead to complete BTK occupancy, possibly clearing the way for lower dosed treatment with fewer off-target effects.<sup>17</sup>

Results from the currently recruiting phase III FLAIR (2013-001944-76) and GAIA/CLL13 (NCT02950051) trials are eagerly awaited to see whether time-limited combinations of novel agents prove themselves superior in a direct comparison with standard first-line regimens. While the GAIA/CLL13 trial is investigating various venetoclax-based combinations in young and fit patients, the FLAIR study will show, in a similar group of patients, whether the promising oral combination of ibrutinib plus venetoclax is superior to the current standards, ibrutinib monotherapy and fludarabine, cyclophosphamide and rituximab.

However, it will probably take more well-designed, randomized trials and particularly long-term follow-up data as well as detailed analyses of PFS2 or 3 after combination treatments in order to determine conclusively whether sequential single-agent therapy or novel combination therapy is superior to the other.

With upcoming combination therapies in contrast to continuous monotherapies, the optimal selection of individual treatment for each patient is challenging. For instance, patients with a complex karyotype who might be more susceptible to the development of resistance mutations under single-agent monotherapy could be eligible for novel combinations.<sup>86</sup> Ahn and colleagues recently presented a risk score that predicts survival and the occurrence of resistance mutations in the context of ibrutinib monotherapy, whereas Visentin and colleagues developed a score that predicts atrial fibrillation during ibrutinib treatment.<sup>17,87</sup> These are just two examples of how more available information will lead to a further diversification and personalization of treatment options. It is, therefore, crucial to work on identifying additional risk factors and understanding disease biology and clonal evolution of CLL in the context of novel agents.

## References

- Eichhorst B, Fink AM, Bahlo J, et al. First-line chemoimmunotherapy with bendamustine and rituximab versus fludarabine, cyclophosphamide, and rituximab in patients with advanced chronic lymphocytic leukaemia (CLL10): an international, open-label, randomised, phase 3, non-inferiority trial. *Lancet Oncol.* 2016;17(7):928-942.
- Hallek M, Fischer K, Fingerle-Rowson G, et al. Addition of rituximab to fludarabine and cyclophosphamide in patients with chronic lymphocytic leukaemia: a randomised, open-label, phase 3 trial. *Lancet.* 2010;376(9747):1164-1174.
- Burger JA, Tedeschi A, Barr PM, et al. Ibrutinib as initial therapy for patients with chronic lymphocytic leukemia. *N Engl J Med.* 2015;373(25):2425-2437.
- Furman RR, Sharman JP, Coutre SE, et al. Idelalisib and rituximab in relapsed chronic lymphocytic leukemia. *N Engl J Med.* 2014;370(11):997-1007.
- Hallek M, Cheson BD, Catovsky D, et al. iwCLL guidelines for diagnosis, indications for treatment, response assessment, and supportive management of CLL. *Blood.* 2018;131(25):2745-2760.
- Hallek M, Shanafelt TD, Eichhorst B. Chronic lymphocytic leukaemia. *Lancet.* 2018;391(10129):1524-1537.
- Roberts AW, Davids MS, Pagel JM, et al. Targeting BCL2 with venetoclax in relapsed chronic lymphocytic leukemia. *N Engl J Med.* 2016;374(4):311-322.
- Moreno C, Greil R, Demirkan F, et al. Ibrutinib plus obinutuzumab versus chlorambucil plus obinutuzumab in first-line treatment of chronic lymphocytic leukaemia (iLLUMINATE): a multicentre, randomised, open-label, phase 3 trial. *Lancet Oncol.* 2019;20(1):43-56.
- Shanafelt TD, Wang XV, Kay NE, et al. Ibrutinib-rituximab or chemoimmunotherapy for chronic lymphocytic leukemia. *N Engl J Med.* 2019 Aug 1;381(5):432-43.
- Woyach JA, Ruppert AS, Heerema NA, et al. Ibrutinib regimens versus chemoimmunotherapy in older patients with untreated CLL. *N Engl J Med.* 2018;379(26):2517-2528.
- Fischer K, Bahlo J, Fink AM, et al. Long-term remissions after FCR chemoimmunotherapy in previously untreated patients with CLL: updated results of the CLL8 trial. *Blood.* 2016;127(2):208-215.
- Thompson PA, Tam CS, O'Brien SM, et al. Fludarabine, cyclophosphamide, and rituximab treatment achieves long-term disease-free survival in IGHV-mutated chronic lymphocytic leukemia. *Blood.* 2016;127(3):303-309.
- Byrd JC, Brown JR, O'Brien S, et al. Ibrutinib versus ofatumumab in previously treated chronic lymphoid leukemia. *N Engl J Med.* 2014;371(3):213-223.
- Byrd JC, Furman RR, Coutre SE, et al. Targeting BTK with ibrutinib in relapsed chronic lymphocytic leukemia. *N Engl J Med.* 2013;369(1):32-42.
- Barr PM, Robak T, Owen C, et al. Sustained efficacy and detailed clinical follow-up of first-line ibrutinib treatment in older patients with chronic lymphocytic leukemia: extended phase 3 results from RESONATE-2. *Haematologica.* 2018;103(9):1502-1510.
- Ahn IE, Farooqui MZH, Tian X, et al. Depth and durability of response to ibrutinib in CLL: 5-year follow-up of a phase 2 study. *Blood.* 2018;131(21):2357-2366.
- Ahn IE, Tian X, Albitar M, et al. Validation of clinical prognostic models and integration of genetic biomarkers of drug resistance in CLL patients treated with ibrutinib. *Blood.* 2018;132(Suppl 1):186.
- Quinquenel A, Fornecker LM, Letestu R, et al. High Prevalence of BTK Mutations on ibrutinib therapy after 3 years of treatment in a real-life cohort of CLL patients: a study from the French Innovative Leukemia Organization (FILO) Group. *Blood.* 2018;132(Suppl 1):584.
- Mato AR, Nabhan C, Thompson MC, et al. Toxicities and outcomes of 616 ibrutinib-treated patients in the United States: a real-world analysis. *Haematologica.* 2018;103(5):874-879.
- Brown JR, Moslehi J, O'Brien S, et al. Characterization of atrial fibrillation adverse events reported in ibrutinib randomized controlled registration trials. *Haematologica.* 2017;102(10):1796-1805.
- Byrd JC, Harrington B, O'Brien S, et al. Acalabrutinib (ACP-196) in relapsed chronic lymphocytic leukemia. *N Engl J Med.* 2016;374(4):323-332.
- Tam C. Pooled analysis of safety data from zanubrutinib (BGB-3111) monotherapy studies in hematologic malignancies. EHA Annual Meeting. 2018;214907.
- Byrd JC, Smith S, Wagner-Johnston N, et al. First-in-human phase 1 study of the BTK inhibitor GDC-0853 in relapsed or refractory B-cell NHL and CLL. *Oncotarget.* 2018;9(16):13023-13035.
- Reiff SD, Mantel R, Smith LL, et al. The BTK inhibitor ARQ 531 targets ibrutinib-resistant CLL and Richter transformation. *Cancer Discov.* 2018;8(10):1300-1315.
- Brown JR, Byrd JC, Coutre SE, et al. Idelalisib, an inhibitor of phosphatidylinositol 3-kinase p110delta, for relapsed/refractory chronic lymphocytic leukemia. *Blood.* 2014;123(22):3390-3397.
- O'Brien SM, Lamanna N, Kipps TJ, et al. A phase 2 study of idelalisib plus rituximab in treatment-naïve older patients with chronic lymphocytic leukemia. *Blood.* 2015;126(25):2686-2694.
- Lampson BL, Kasar SN, Matos TR, et al. Idelalisib given front-line for treatment of chronic lymphocytic leukemia causes frequent immune-mediated hepatotoxicity. *Blood.* 2016;128(2):195-203.
- European Medicines Agency. EMA reviews cancer medicine Zydelig. <https://www.ema.europa.eu/en/news/ema-reviews-cancer-medicine-zydelig> 2016. (accessed: 11/02/2019). 2016.
- Flinn IW, Hillmen P, Montillo M, et al. The phase 3 DUO trial: duvelisib vs ofatumumab in relapsed and refractory CLL/SLL. *Blood.* 2018;132(23):2446-2455.
- Burris HA 3rd, Flinn IW, Patel MR, et al. Umbralisib, a novel PI3Kdelta and casein kinase-1epsilon inhibitor, in relapsed or refractory chronic lymphocytic leukaemia and lymphoma: an open-label, phase 1, dose-escalation, first-in-human study. *Lancet Oncol.* 2018;19(4):486-496.
- Seymour JF, Kipps TJ, Eichhorst B, et al. Venetoclax-rituximab in relapsed or refractory chronic lymphocytic leukemia. *N Engl J Med.* 2018;378(12):1107-1120.
- Stilgenbauer S, Eichhorst B, Schetelig J, et al. Venetoclax for patients with chronic lymphocytic leukemia with 17p deletion: results from the full population of a phase II pivotal trial. *J Clin Oncol.* 2018;36(19):1973-1980.
- Wierda WG, Roberts AW, Ghia P, et al. Minimal residual disease status with venetoclax monotherapy is associated with progression-free survival in chronic lymphocytic Leukemia. *Blood.* 2018;132(Suppl 1):3134.
- Dimier N, Delmar P, Ward C, et al. A model for predicting effect of treatment on progression-free survival using MRD as a surrogate end point in CLL. *Blood.* 2018;131(9):955-962.
- Kater AP, Seymour JF, Hillmen P, et al. Fixed duration of venetoclax-rituximab in relapsed/refractory chronic lymphocytic leukemia eradicates minimal residual disease and prolongs survival: post-treatment follow-up of the MURANO phase III study. *J Clin Oncol.* 2019;37(4):269-277.
- Davids MS, Hallek M, Wierda W, et al. Comprehensive safety analysis of venetoclax monotherapy for patients with relapsed/refractory chronic lymphocytic leukemia. *Clin Cancer Res.* 2018;24(18):4371-4379.
- Blombery P, Anderson MA, Gong JN, et al. Acquisition of the recurrent Gly101Val mutation in BCL2 confers resistance to venetoclax in patients with progressive chronic lymphocytic leukemia. *Cancer Discov.* 2019;9(3):342-353.
- Herling CD, Abedpour N, Weiss J, et al. Clonal dynamics towards the development of venetoclax resistance in chronic lymphocytic leukemia. *Nat Commun.* 2018;9(1):727.
- Mato AR, Hill BT, Lamanna N, et al. Optimal sequencing of ibrutinib, idelalisib, and venetoclax in chronic lymphocytic leukemia: results from a multicenter study of 683 patients. *Ann Oncol.* 2017;28(5):1050-1056.
- Jones JA, Mato AR, Wierda WG, et al. Venetoclax for chronic lymphocytic leukaemia progressing after ibrutinib: an interim analysis of a multicentre, open-label, phase 2 trial. *Lancet Oncol.* 2018;19(1):65-75.
- Mato AR, Tam CS, Allan JN, et al. Disease and patient characteristics, patterns of care, toxicities, and outcomes of chronic lymphocytic leukemia (CLL) patients treated with venetoclax: a multicenter study of 204 patients. *Blood.* 2017;130(Suppl 1):4315.
- Greil R, Fraser G, Leber B, et al. Efficacy and safety of ibrutinib (IBR) after venetoclax (VEN) treatment in IBR-naïve patients with relapsed/refractory (R/R) chronic lymphocytic leukemia (CLL): follow-up of patients from the MURANO study. *Blood.* 2018;132(Suppl 1):5548.
- Awan FT, Schuh A, Brown JR, et al. Acalabrutinib monotherapy in patients with ibrutinib intolerance: results from the phase 1/2 ACE-CL-001 clinical study. *Blood.* 2016;128(22):638.
- Mato AR, Schuster SJ, Lamanna N, et al. A phase 2 study to assess the safety and efficacy of umbralisib (TGR-1202) in pts with CLL who are intolerant to prior BTK or PI3Kδ inhibitor therapy. *J Clin Oncol.* 2018;36(15\_suppl):7530.
- Barr PM, Brown JR, Hillmen P, et al. Impact of ibrutinib dose adherence on therapeutic efficacy in patients with previously treated CLL/SLL. *Blood.* 2017;129(19):2612-2615.
- Ahn IE, Underbayev C, Albitar A, et al. Clonal evolution leading to ibrutinib resistance in chronic lymphocytic leukemia. *Blood.* 2017;129(11):1469-1479.
- Woyach JA, Ruppert AS, Guinn D, et al. BTK(C481S)-mediated resistance to ibruti-

- nib in chronic lymphocytic leukemia. *J Clin Oncol.* 2017;35(13):1437-1443.
48. Byrd JC, Hillmen P, O'Brien S, et al. Long-term follow-up of the RESONATE™ phase 3 trial of ibrutinib versus ofatumumab. *Blood.* 2019;133(19):2031-2042.
  49. Chen Q, Jain N, Ayer T, et al. Economic Burden of chronic lymphocytic leukemia in the era of oral targeted therapies in the United States. *J Clin Oncol.* 2017;35(2):166-174.
  50. Spina V, Forestieri G, Zucchetto A, et al. Mechanisms of adaptation to ibrutinib in high risk chronic lymphocytic leukemia. *Blood.* 2018;132(Suppl 1):585.
  51. EMA. (European Medicines Agency). Appendix 4 to the guideline on the evaluation of anticancer medicinal products in man - condition specific guidance. <https://www.ema.europa.eu/en/appendix-4-guideline-evaluation-anticancer-medicinal-products-man-condition-specific-guidance>. 2016.
  52. Bottcher S, Ritgen M, Fischer K, et al. Minimal residual disease quantification is an independent predictor of progression-free and overall survival in chronic lymphocytic leukemia: a multivariate analysis from the randomized GCLLSG CLL8 trial. *J Clin Oncol.* 2012;30(9):980-988.
  53. Goede V, Fischer K, Busch R, et al. Obinutuzumab plus chlorambucil in patients with CLL and coexisting conditions. *N Engl J Med.* 2014;370(12):1101-1110.
  54. Kovacs G, Robrecht S, Fink AM, et al. Minimal residual disease assessment improves prediction of outcome in patients with chronic lymphocytic leukemia (CLL) who achieve partial response: comprehensive analysis of two phase III studies of the German CLL Study Group. *J Clin Oncol.* 2016;34(31):3758-3765.
  55. Langerak AW, Ritgen M, Goede V, et al. Prognostic value of MRD in CLL patients with comorbidities receiving chlorambucil plus obinutuzumab or rituximab. *Blood.* 2019;133(5):494-497.
  56. Chanan-Khan A, Cramer P, Demirkan F, et al. Ibrutinib combined with bendamustine and rituximab compared with placebo, bendamustine, and rituximab for previously treated chronic lymphocytic leukaemia or small lymphocytic lymphoma (HELIOS): a randomised, double-blind, phase 3 study. *Lancet Oncol.* 2016;17(2):200-211.
  57. Fraser G, Cramer P, Demirkan F, et al. Updated results from the phase 3 HELIOS study of ibrutinib, bendamustine, and rituximab in relapsed chronic lymphocytic leukemia/small lymphocytic lymphoma. *Leukemia.* 2019;33(4):969-980.
  58. Zelenetz AD, Barrientos JC, Brown JR, et al. Idelalisib or placebo in combination with bendamustine and rituximab in patients with relapsed or refractory chronic lymphocytic leukaemia: interim results from a phase 3, randomised, double-blind, placebo-controlled trial. *Lancet Oncol.* 2017;18(3):297-311.
  59. Davids MS, Brander DM, Kim HT, et al. Ibrutinib plus fludarabine, cyclophosphamide, and rituximab as initial treatment for younger patients with chronic lymphocytic leukaemia: a single-arm, multicentre, phase 2 trial. *Lancet Haematol.* 2019;6(8):e419-e28.
  60. Jain N, Thompson PA, Burger JA, et al. Ibrutinib, fludarabine, cyclophosphamide, and obinutuzumab (IFCG) for firstline treatment of patients with CLL with mutated IGHV and without TP53 aberrations. *Blood.* 2018;132(Suppl 1):695.
  61. Michallet A-S, Dilhuydy M-S, Subtil F, et al. High rate of complete response (CR) with undetectable bone marrow minimal residual disease (MRD) after chemo-sparing and MRD-driven strategy for untreated fit CLL patients: final results of the Icll 07 FILO trial. *Blood.* 2018;132(Suppl 1):1858.
  62. Davids MS. A Phase Ib/II study of duvelisib in combination with FCR (dFCR) for front-line therapy of younger CLL patients. EHA Annual Meeting; oral presentation. 2018.
  63. Burger JA, Sivina M, Jain N, et al. Randomized trial of ibrutinib versus ibrutinib plus rituximab in patients with chronic lymphocytic leukemia. *Blood.* 2019;133(10):1011-1019.
  64. Woyach JA, Awan FT, Jianfar M, et al. Acalabrutinib with obinutuzumab in relapsed/refractory and treatment-naive patients with chronic lymphocytic leukemia: the phase 1b/2 ACE-CL-003 study. *Blood.* 2017;130(Suppl 1):432.
  65. Cramer P, von Tresckow J, Robrecht S, et al. Bendamustine followed by ofatumumab and ibrutinib in patients with chronic lymphocytic leukemia (CLL): CLL2-BIO trial of the German CLL Study Group (GCLLSG). *Blood.* 2017;130(Suppl 1):494.
  66. von Tresckow J, Cramer P, Bahlo J, et al. CLL2-BIG: sequential treatment with bendamustine, ibrutinib and obinutuzumab (GA101) in chronic lymphocytic leukemia. *Leukemia.* 2019;33(5):1161-1172.
  67. Cramer P, von Tresckow J, Bahlo J, et al. Bendamustine followed by obinutuzumab and venetoclax in chronic lymphocytic leukaemia (CLL2-BAG): primary endpoint analysis of a multicentre, open-label, phase 2 trial. *Lancet Oncol.* 2018;19(9):1215-1228.
  68. Cramer P, von Tresckow J, Bahlo J, et al. Durable remissions after discontinuation of combined targeted treatment in patients with chronic lymphocytic leukemia (CLL) harbouring a high-risk genetic lesion (del(17p)/TP53 mutation). *Blood.* 2018;132(Suppl 1):694.
  69. Fischer K, Al-Sawaf O, Bahlo J, et al. Venetoclax and Obinutuzumab in Patients with CLL and Coexisting Conditions. *The N Engl J Med.* 2019;380(23):2225-2236.
  70. Flinn IW, Gribben JG, Dyer MJS, et al. Phase 1b study of venetoclax-obinutuzumab in previously untreated and relapsed/refractory chronic lymphocytic leukemia. *Blood.* 2019 Mar 12. [Epub ahead of print]
  71. Hillmen P, Rawstron A, Brock K, et al. Ibrutinib plus venetoclax in relapsed/refractory CLL: results of the Bloodwise TAP Clarity Study. *Blood.* 2018;132(Suppl 1):182.
  72. Jain N, Keating M, Thompson P, et al. Ibrutinib and Venetoclax for First-Line Treatment of CLL. *N Engl J Med.* 2019;380(22):2095-2103.
  73. Rogers KA, Huang Y, Ruppert AS, et al. Phase 2 study of combination obinutuzumab, ibrutinib, and venetoclax in treatment-naive and relapsed/refractory chronic lymphocytic leukemia. *Blood.* 2018;132(Suppl 1):693.
  74. Davids MS, Kim HT, Nicotra A, et al. Umbralisib in combination with ibrutinib in patients with relapsed or refractory chronic lymphocytic leukaemia or mantle cell lymphoma: a multicentre phase 1-1b study. *Lancet Haematol.* 2019;6(1):e38-e47.
  75. Nastoupil LJ, Lunning MA, Vose JM, et al. Tolerability and activity of ublituximab, umbralisib, and ibrutinib in patients with chronic lymphocytic leukaemia and non-Hodgkin lymphoma: a phase 1 dose escalation and expansion trial. *Lancet Haematol.* 2019;6(2):e100-e109.
  76. Ding W, LaPlant BR, Call TG, et al. Pembrolizumab in patients with CLL and Richter transformation or with relapsed CLL. *Blood.* 2017;129(26):3419-3427.
  77. Younes A, Brody J, Carpio C, et al. Safety and activity of ibrutinib in combination with nivolumab in patients with relapsed non-Hodgkin lymphoma or chronic lymphocytic leukaemia: a phase 1/2a study. *Lancet Haematol.* 2019;6(2):e67-e78.
  78. Mato AR, Thompson M, Allan JN, et al. Real-world outcomes and management strategies for venetoclax-treated chronic lymphocytic leukemia patients in the United States. *Haematologica.* 2018;103(9):1511-1517.
  79. Chen Q, Jain N, Ayer T, et al. Economic burden of chronic lymphocytic leukemia in the era of oral targeted therapies in the United States. *J Clin Oncol.* 2017;35(2):166-174.
  80. Kadri S, Lee J, Fitzpatrick C, et al. Clonal evolution underlying leukemia progression and Richter transformation in patients with ibrutinib-relapsed CLL. *Blood Adv.* 2017;1(12):715-727.
  81. Landau DA, Sun C, Rosebrock D, et al. The evolutionary landscape of chronic lymphocytic leukemia treated with ibrutinib targeted therapy. *Nat Commun.* 2017;8(1):2185.
  82. Lampson BL, Yu L, Glynn RJ, et al. Ventricular arrhythmias and sudden death in patients taking ibrutinib. *Blood.* 2017;129(18):2581-2584.
  83. Ghez D, Calleja A, Protin C, et al. Early-onset invasive aspergillosis and other fungal infections in patients treated with ibrutinib. *Blood.* 2018;131(17):1955-1959.
  84. Bercusson A, Colley T, Shah A, Warris A, Armstrong-James D. Ibrutinib blocks Btk-dependent NF- $\kappa$ B and NFAT responses in human macrophages during *Aspergillus fumigatus* phagocytosis. *Blood.* 2018;132(18):1985-1988.
  85. Waldron M, Winter A, Hill BT. Pharmacokinetic and pharmacodynamic considerations in the treatment of chronic lymphocytic leukemia: ibrutinib, idelalisib, and venetoclax. *Clin Pharmacokinet.* 2017;56(11):1255-1266.
  86. Baliakas P, Jeromin S, Iskas M, et al. Cytogenetic complexity in chronic lymphocytic leukemia: definitions, associations and clinical impact. *Blood.* 2019;133(11):1205-1216.
  87. Visentin A, Deodato M, Mauro FR, et al. A Scoring system to predict the risk of atrial fibrillation in chronic lymphocytic leukemia and its validation in a cohort of ibrutinib-treated patients. *Blood.* 2018;132(Suppl 1):3118.

# Guidelines from the 2017 European Conference on Infections in Leukaemia for management of HHV-6 infection in patients with hematologic malignancies and after hematopoietic stem cell transplantation



Katherine N Ward,<sup>1</sup> Joshua A Hill,<sup>2</sup> Petr Hubacek,<sup>3</sup> Rafael de la Camara,<sup>4</sup> Roberto Crocchiolo,<sup>5</sup> Hermann Einsele,<sup>6</sup> David Navarro,<sup>7</sup> Christine Robin,<sup>8</sup> Catherine Cordonnier,<sup>8</sup> and Per Ljungman,<sup>9</sup> for the 2017 European Conference on Infections in Leukaemia (ECIL)\*

**Haematologica** 2019  
Volume 104(11):2155-2163

<sup>1</sup>Division of Infection and Immunity, University College London, London, UK; <sup>2</sup>Fred Hutchinson Cancer Research Center, Seattle, WA, USA; <sup>3</sup>Department of Medical Microbiology and Department of Paediatric Haematology and Oncology 2<sup>nd</sup> Medical Faculty of Charles University and Motol University Hospital, Prague, Czech Republic; <sup>4</sup>Department of Haematology, Hospital de la Princesa, Madrid, Spain; <sup>5</sup>SIMT, ASST di Bergamo Ovest, Treviglio, Italy; <sup>6</sup>Medizinische Klinik und Poliklinik II, Julius Maximilians Universität, Würzburg, Germany; <sup>7</sup>Microbiology Service, Hospital Clínico Universitario, Instituto de Investigación INCLIVA and Department of Microbiology, School of Medicine, University of Valencia, Valencia, Spain; <sup>8</sup>Department of Haematology, Henri Mondor Hospital, Assistance Publique-Hopitaux de Paris, Université Paris-Est Créteil, Créteil, France and <sup>9</sup>Department of Cellular Therapy and Allogeneic Stem Cell Transplantation, Karolinska University Hospital, Division of Haematology, Department of Medicine Huddinge, Karolinska Institutet, Stockholm, Sweden

\*A joint project of the European Organization for Research and Treatment of Cancer - Infectious Diseases Group, European Society for Blood and Marrow Transplantation - Infectious Diseases Working Party, European Leukaemia Net-Project 15: Supportive Care and the International Immunocompromised Host Society

## ABSTRACT

Of the two human herpesvirus 6 (HHV-6) species, human herpesvirus 6B (HHV-6B) encephalitis is an important cause of morbidity and mortality after allogeneic hematopoietic stem cell transplant. Guidelines for the management of HHV-6 infections in patients with hematologic malignancies or post-transplant were prepared a decade ago but there have been no other guidelines since then despite significant advances in the understanding of HHV-6 encephalitis, its therapy, and other aspects of HHV-6 disease in this patient population. Revised guidelines prepared at the 2017 European Conference on Infections in Leukaemia covering diagnosis, preventative strategies and management of HHV-6 disease are now presented.

## Introduction

Over the past ten years, it has been recognized that human herpesvirus 6A (HHV-6A) and HHV-6B are distinct species,<sup>1</sup> HHV-6B not HHV-6A is the most frequent cause of encephalitis post-hematopoietic stem cell transplant (HSCT) and that chromosomally integrated HHV-6 (CIHHV-6) is clinically significant. Revised European Conference on Infections in Leukemia (ECIL) HHV-6 guidelines were prepared after a literature review by a group of experts, and discussed at a plenary session on September 22<sup>nd</sup>, 2017 until consensus. Those guidelines specifically applying to treatment were graded according to pre-ordained criteria (Table 1) for level of evidence and strength of recommendation; participants were hematologists, microbiologists and infectious disease specialists with expertise on infectious complications in hematology. (A list of ECIL meeting participants is provided in the *Online Supplementary Appendix*.) A final slide set was posted on the ECIL website ([www.ecil-leukaemia.com](http://www.ecil-leukaemia.com)) on October 2<sup>nd</sup>, 2017 and made available for open consultation.

## Correspondence:

KATHERINE N WARD  
k.n.ward@ucl.ac.uk

Received: April 1, 2019.

Accepted: August 27, 2019.

Pre-published: August 29, 2019.

doi:10.3324/haematol.2019.223073

Check the online version for the most updated information on this article, online supplements, and information on authorship & disclosures: [www.haematologica.org/content/104/11/2155](http://www.haematologica.org/content/104/11/2155)

©2019 Ferrata Storti Foundation

Material published in *Haematologica* is covered by copyright. All rights are reserved to the Ferrata Storti Foundation. Use of published material is allowed under the following terms and conditions:

<https://creativecommons.org/licenses/by-nc/4.0/legalcode>.  
Copies of published material are allowed for personal or internal use. Sharing published material for non-commercial purposes is subject to the following conditions:  
<https://creativecommons.org/licenses/by-nc/4.0/legalcode>, sect. 3. Reproducing and sharing published material for commercial purposes is not allowed without permission in writing from the publisher.



### Human herpesvirus 6A and human herpesvirus 6B

The two species of HHV-6, HHV-6A and HHV-6B infect and establish latency in different cell types including CD4 positive T lymphocytes, monocytes, and other epithelial, fibroblastic and neuronal cells.<sup>2</sup> No disease has been causally linked to HHV-6A, and its natural history is unknown. In contrast, HHV-6B primary infection is ubiquitous in the first two years of life sometimes causing *exanthema subitum*; subsequent viral latency gives the potential for reactivation and disease.

### Chromosomally integrated human herpesvirus 6

As well as the almost universal postnatal acquisition of HHV-6B, in approximately 1% of humans the complete genome of HHV-6A or HHV-6B is integrated into a chromosomal telomere in every nucleated cell in the body and is transmitted through Mendelian inheritance.<sup>3,4</sup> Although HHV-6A is rare in the general population, HHV-6A and HHV-6B are encountered in approximately one-third and two-thirds of individuals with CIHHV-6, respectively.<sup>5</sup> Telomeric integration sites have been identified on different chromosomes using fluorescence *in situ* hybridization (FISH).<sup>6</sup> Integration is normally restricted to a particular chromosome per individual but very rarely two sites, if inherited from both parents.<sup>3</sup>

Human herpesvirus 6 DNA detected in blood usually indicates virus replication. However, in individuals with CIHHV-6, viral DNA in latent form originating from human chromosomal DNA is persistently detected at high levels in whole blood as well as in "cell free" samples such as serum and cerebrospinal fluid (CSF), since the latter contain cellular DNA released from damaged cells during sample preparation.<sup>7,8</sup> Although HHV-6B encephalitis is an accepted, albeit rare, complication of primary HHV-6B infection in young children, HHV-6 DNA in the CSF of older immunocompetent children and adults is most likely due to latent virus originating from CIHHV-6 rather than central nervous system (CNS) infection.<sup>8,9</sup>

### Chromosomally integrated human herpesvirus 6 and potential for disease post-hematopoietic stem cell transplantation

There is limited evidence of symptomatic reactivation of CIHHV-6. One report demonstrated CIHHV-6A reactivation

in a child with severe combined immunodeficiency and hemophagocytic syndrome pre-HSCT and thrombotic microangiopathy post-HSCT.<sup>10</sup> Two other reports from settings other than HSCT give evidence for symptomatic reactivation in a patient treated with a histone deacetylase inhibitor<sup>11</sup> and a patient who received a liver transplant from a donor with CIHHV-6A.<sup>12</sup>

Despite the above case of reactivation with accompanying morbidity post-HSCT,<sup>10</sup> this has not been reported in the few other cases where CIHHV-6 was identified in the donor or recipient,<sup>13-16</sup> and the frequency and type of diseases caused by CIHHV-6 in HSCT recipients remain unknown. A recent study of 87 patients with CIHHV-6 in HSCT donors and/or recipients demonstrated an association with acute graft-versus-host disease (GvHD) and cytomegalovirus (CMV) reactivation, but there was no effect on overall or non-relapse mortality.<sup>17</sup> Neither has an increased frequency of CIHHV-6 been identified in a range of hematologic malignancies.<sup>17,21</sup> None of these studies was designed to address the likelihood that integration into different chromosomal sites might have different pathological consequences and vary according to HHV-6 species.

### Human herpesvirus 6 and disease in patients with hematologic malignancies or post-hematopoietic stem cell transplantation

In patients with hematologic malignancies without HSCT, there is little evidence that HHV-6 causes disease. Post-HSCT the high frequency of HHV-6B reactivation, plus the difficulty of identifying CIHHV-6, causes substantial challenges in determining the pathogenic role of HHV-6 in disease. For autologous transplants, there are insufficient data for a causal association with end-organ disease. However, after allogeneic HSCT, HHV-6B is associated with several syndromes and is a well recognized cause of encephalitis with high morbidity and mortality.

### Definitions

#### Primary human herpesvirus 6 infection

This is defined as the first detection of HHV-6 replication in an individual with no evidence of previous infection

**Table 1.** European Society of Clinical Microbiology and Infectious Diseases (ESCMID) grading system.

Strength of a recommendation	
Grade A	ESCMID strongly supports a recommendation for use
Grade B	ESCMID moderately supports a recommendation for use
Grade C	ESCMID marginally supports a recommendation for use
Grade D	ESCMID supports a recommendation against use
Quality of evidence	
Level I	Evidence from at least one properly designed randomized, controlled trial
Level II *	Evidence from at least one well-designed clinical trial, without randomization; from cohort or case-controlled analytical studies (preferably from more than one center); from multiple time series; or from dramatic results of uncontrolled experiments
Level III	Evidence from opinions of respected authorities, based on clinical experience, descriptive case studies, or reports of expert committees

\*Added index for level II quality of evidence. · r: meta-analysis or systematic review of randomized controlled trials. · t: transferred evidence, i.e. results from different patient cohorts, or similar immune-status situation. · h: comparator group is a historical control. · u: uncontrolled trial. · a: published abstract (presented at an international symposium or meeting).

tion. Normally this would be accompanied by HHV-6 seroconversion, but severely immunocompromised HSCT recipients may not develop antibodies. Donor-derived CIHHV-6 must be excluded.

### Human herpesvirus 6 reactivation

Given the difficulty distinguishing between reactivation of latent virus (endogenous) and reinfection (exogenous), in clinical practice the term HHV-6 reactivation is applied to both scenarios and is defined as new detection of HHV-6 in individuals with evidence of previous infection; this latter can be assumed in individuals older than two years. The diagnosis usually relies on the presence of HHV-6 DNA in peripheral blood but other methods and samples are sometimes used. Reactivation is not proven if newly detected HHV-6 DNA is due to donor- or recipient-derived CIHHV-6 since latently-integrated viral DNA cannot be distinguished from replicating virus DNA. See below for tests for CIHHV-6 and its reactivation.

### Human herpesvirus 6 diagnostic testing

Antibody tests cannot distinguish between HHV-6A and HHV-6B and are not indicated in HSCT patients. Table 2 gives an overview of possible diagnostic tests.

#### DNA tests

Polymerase chain reaction (PCR) is the mainstay of HHV-6 diagnosis and a variety of real-time PCR assays for HHV-6 DNA load are available.<sup>22,23</sup> Not all differentiate

between HHV-6A and HHV-6B, and agreement between laboratories for HHV-6 DNA levels is poor.<sup>22,24</sup> However, a World Health Organization standard for HHV-6B DNA is now available (<http://www.nibsc.org/documents/ifu/15-266.pdf>).

- Quantitative PCR that distinguishes between HHV-6A and HHV-6B DNA is recommended for diagnosis of infection.

- For a given patient, repeat HHV-6 DNA testing should be performed using the same DNA extraction method, quantitative PCR and type of specimen.

### Interpretation of DNA testing post-hematopoietic stem cell transplantation in the presence of chromosomally integrated human herpesvirus 6

If a HSCT donor has CIHHV-6, HHV-6 DNA load in blood will increase post-HSCT in parallel with leukocyte engraftment,<sup>13,16,25</sup> and antivirals will have no effect on the quantity of the latently integrated viral DNA.<sup>26</sup> Alternatively, if the recipient has CIHHV-6, high levels of HHV-6 DNA will be detected pre-HSCT in blood and will decrease alongside recipient leukocytes post-transplant.<sup>14,27</sup> Importantly, in this latter situation, HHV-6 DNA will continue to be detected at high levels in non-hematopoietic tissue throughout the body<sup>28</sup> (Table 3).

#### Tests for chromosomally integrated human herpesvirus 6

Currently there is no indication for routine testing of HSCT donors or recipients for CIHHV-6. However, in clinically ambiguous cases, such testing can be important

**Table 2.** Human herpesvirus 6 (HHV-6) diagnostic tests.

Method	Use and limitations
Virus culture*	Diagnosis of infection: gold standard, specialized, labor-intensive
Viral antigen test (immunohistochemical staining)*	Diagnosis of infection: limited sensitivity, slow turn-around time
Detection of viral mRNA by reverse transcription PCR*	Late gene transcripts to confirm virus replication. No international standardization or specific thresholds for virus replication, especially for CIHHV-6
Quantitative viral DNA PCR	Longitudinal studies, comparison of HHV-6 DNA levels in blood <i>vs.</i> organs. Can discriminate between HHV-6A and HHV-6B*
Droplet digital PCR*	Precise method for DNA levels, identification of CIHHV-6
Fluorescence <i>in situ</i> hybridization*	Confirmation of CIHHV-6

\*Not available to most diagnostic laboratories. PCR: polymerase chain reaction; CIHHV6: chromosomally integrated HHV-6.

**Table 3.** Human herpesvirus 6 (HHV-6) test results after allogeneic hematopoietic stem cell transplantation that indicate naturally acquired HHV-6 infection *versus* chromosomally integrated HHV-6 (CIHHV-6).

Laboratory observations	HHV-6 status			
	Prior childhood infection*	Donor CIHHV-6 positive	Recipient CIHHV-6 positive	Donor and recipient CIHHV-6 positive
One HHV-6 copy/leukocyte	No	Yes**	No	Yes **
One HHV-6 copy/non-hematopoietic cell	No	No	Yes <sup>§</sup>	Yes <sup>§</sup>
HHV-6 species	B	A or B	A or B	A or B
Persistent HHV-6 DNA in blood	No	Yes	+/-***	Yes
Response of HHV-6 DNA level to antiviral drugs	Yes	No	No	No

\*Human herpesvirus 6B (HHV-6B) primary infection usually occurs in childhood. \*\*HHV-6 found persistently in hematopoietic tissue, e.g. blood, bone marrow, spleen. <sup>§</sup>HHV-6 found persistently at extremely high levels in all nucleated non-hematopoietic cells. \*\*\*A low level in peripheral blood in cases of organ damage and cell death or hematologic malignancy relapse.

to avoid unnecessary, potentially toxic, antiviral therapy.

Chromosomally integrated human herpesvirus 6 should be suspected in the donor and/or recipient if HHV-6 DNA detection follows one of the patterns described in Table 3 or if HHV-6A is detected. Where necessary, CIHHV-6 can easily be excluded by a negative HHV-6 DNA test on a blood/serum sample taken pre-transplant from the recipient or at any time from the donor. Individuals with CIHHV-6 have characteristic persistently high levels of HHV-6 DNA in whole blood (>5.5 log<sub>10</sub> copies/mL) and in serum (100-fold lower than that in whole blood for a given patient).<sup>5,7</sup> The level of DNA detected in plasma varies depending on the timing of separation from whole blood.<sup>29</sup>

A ratio of one copy of HHV-6 DNA/cellular genome confirms the diagnosis of CIHHV-6. Droplet digital PCR<sup>29</sup> is the most accurate method as it gives an absolute number. Comparison of two quantitative real-time PCR results (one for HHV-6 and one for a human gene present in all nucleated cells) is also acceptable albeit with a significant margin of error due to inherent assay imprecision.<sup>7</sup> HHV-6 DNA is present in hair follicles and nails exclusively in persons with CIHHV-6.<sup>4,19</sup>

- If CIHHV-6 is suspected, whole blood or serum or cellular samples or leftover DNA taken from donor and/or recipient pre-HSCT should be tested by quantitative PCR that distinguishes between HHV-6A and HHV-6B DNA. Testing plasma is not recommended.

- CIHHV-6 can be confirmed by evidence of one copy of viral DNA/cellular genome, or viral DNA in hair follicles/nails, or by FISH demonstrating HHV-6 integrated into a human chromosome.

### Tests for chromosomally integrated human herpesvirus 6 reactivation

This must be confirmed by virus culture plus viral genome sequencing to confirm identity of the viral isolate with the integrated virus.

## Human herpesvirus 6B end-organ disease and other outcomes post-hematopoietic stem cell transplantation

### Human herpesvirus 6B primary infection versus reactivation

Only two cases of primary HHV-6B infection after allogeneic HSCT have been reported; these were in very young children and were accompanied by fever and rash.<sup>30,31</sup> In contrast, various end-organ diseases and other complications post-HSCT have been associated with HHV-6B reactivation. But apart from encephalitis and fever with rash, the evidence for causation is moderate or weak (Table 4).

### Human herpesvirus 6B encephalitis and its definition

The first described encephalitis case<sup>32</sup> was followed by many confirmatory reports.<sup>33</sup> Zerr and Ogata analyzed the accumulated published data and provided evidence for a causal association between HHV-6 and encephalitis using the Bradford Hill criteria.<sup>34</sup>

The most frequent cause of encephalitis after allogeneic transplant is HHV-6. When the species is identified, it is

almost invariably HHV-6B. Of the only three reported patients with HHV-6A encephalitis, one had an atypical presentation and the other two had unrecognized CIHHV-6.<sup>9</sup> In one of these two, testing of archived samples confirmed CIHHV-6A pre-HSCT,<sup>35</sup> but the question remained as to whether reactivation of the virus causing encephalitis or an alternative unidentified cause was responsible. Whether CIHHV-6B can reactivate causing encephalitis is theoretically possible, but requires viral culture and sequencing to distinguish childhood-acquired HHV-6B from integrated virus.

Human herpesvirus 6B encephalitis typically presents early as post-transplant acute limbic encephalitis (PALE). CSF protein and cell counts are often unremarkable (see Table 5 for further clinical features). Although magnetic resonance imaging (MRI) may be negative at the start of the disease, changes in the temporal lobe are demonstrated in approximately 60% of cases.<sup>36</sup> However, similar observations occur in limbic encephalitis caused by other infectious agents.<sup>37</sup> Extrahippocampal abnormalities may

**Table 4. Human herpesvirus 6B reactivation after allogeneic hematopoietic stem cell transplantation: disease associations.**

Epidemiological associations	Level of <i>in vitro</i> or <i>in vivo</i> support for causation
<b>HHV-6B end-organ disease</b>	
Encephalitis (predominantly limbic)	Strong
Non-encephalitic central nervous system dysfunction e.g. delirium, myelitis	Moderate
Myelosuppression, allograft failure	Moderate
Pneumonitis	Weak
Hepatitis	Weak
<b>Other</b>	
Fever and rash	Strong
Acute graft-versus-host disease	Moderate
CMV reactivation	Moderate
Increased all-cause mortality	Weak

HHV-6B: human herpesvirus 6B; CMV: cytomegalovirus. Adapted from Table 29.2 in Hill and Zerr.<sup>36</sup>

**Table 5. Clinical features of human herpesvirus 6B encephalitis.**

Disease onset	Usually 2-6 weeks post HSCT, but can be later
Symptoms/signs	Confusion, encephalopathy, short-term memory loss, SIADH, seizures, insomnia
Brain MRI <sup>a</sup>	Often normal. Typically but not exclusively, circumscribed, non-enhancing, hyperintense lesions in the medial temporal lobes (especially hippocampus and amygdala)
Cerebrospinal fluid	HHV-6B DNA, +/- mild protein elevation, +/-mild lymphocytic pleocytosis
Prognosis	Memory defects and neuropsychological sequelae in 20-60%. Death due to progressive encephalitis in up to 25% of all HSCT recipients and up to 50% of cord blood recipients

HSCT: hematopoietic stem cell transplantation; SIADH: syndrome of inappropriate antidiuretic hormone secretion; MRI: magnetic resonance imaging; HHV-6B: human herpesvirus 6B. <sup>a</sup>Features of T2, fluid attenuation, inversion recovery (FLAIR) and diffusion weighted-imaging sequences. Modified from Hill and Zerr.<sup>36</sup>

occur in areas such as the entorhinal cortex or amygdala.<sup>38</sup> Temporal lobe seizures are relatively frequent but focal neurological deficits are rare. Computed tomography of the brain is often normal. Electroencephalograms are usually diffusely abnormal sometimes involving the temporal region. Autopsy reveals hippocampal disease with HHV-6 protein in astrocytes and neurons suggesting local virus reactivation<sup>32</sup> rather than an indirect effect of viral-induced neuroinflammation. Notably, a retrospective study<sup>39</sup> showed that only one-third of HHV-6 encephalitis patients had the typical features of PALE.

Different studies have used different definitions of HHV-6 encephalitis.<sup>40</sup> Ideally the definition would require proof of HHV-6 infection in tissue samples from the affected part of the brain. However, given the impracticality of such an approach and the epidemiological evidence, the definition below can replace the need for brain biopsy.

- Diagnosis of HHV-6B encephalitis should be based on HHV-6 DNA in CSF coinciding with acute-onset altered mental status (encephalopathy), or short-term memory loss, or seizures.
- Other likely infectious or non-infectious causes must be excluded.
- CIHHV-6 in donor and recipient should be excluded.
- If CIHHV-6 is detected, evidence for CIHHV-6 reactivation in the CSF or brain tissue is necessary to implicate CIHHV-6.

#### Other central nervous system dysfunction

Apart from encephalitis post-HSCT, HHV-6 has been associated with CNS disease ranging from headache to delirium and neurocognitive decline;<sup>41-43</sup> patients whose donors or recipients had CIHHV-6 were excluded in two of these studies.<sup>42,43</sup> HHV-6 has also been associated with myelitis, pruritis and dysesthesia in Japanese patients.<sup>44</sup> Notably, HHV-6 DNA can be found in CSF in patients without CNS symptoms.<sup>42</sup>

#### Risk factors for human herpesvirus 6B encephalitis

Human herpesvirus 6B reactivation in blood (i.e. viremia) is a major risk factor and occurs in approximately half of allogeneic transplant recipients in the first few weeks post-HSCT.<sup>45,46</sup> The highest rates are seen after umbilical cord blood transplantation (CBT); in a prospective cohort of 125 cord blood recipients, HHV-6B reactivation was documented in 94%.<sup>47</sup> In a multicenter prospective study, Ogata *et al.*<sup>48</sup> showed that reactivation precedes or coincides with HHV-6 encephalitis and that  $\geq 10,000$  copies/mL in plasma correlated with onset of disease with 100% sensitivity and 64.6% specificity. Similar values of 100% and 81% respectively were obtained in a much larger retrospective study.<sup>49</sup>

However, not all patients develop encephalitis when the plasma HHV-6 DNA level is high, and other factors are involved, usually related to poor T-cell function, such as T-cell depleted allografts, CBT, a mismatched or unrelated donor, acute GvHD and treatment with glucocorticoids.<sup>50</sup> A retrospective cohort study of 1,344 patients showed CBT is a major risk factor [adjusted hazard ratio (aHR) 20.0;  $P < 0.001$ ], as well as acute GvHD grades II-IV (aHR 7.5;  $P < 0.001$ ) and use of mismatched unrelated donors (aHR 4.3;  $P < 0.04$ ).<sup>49</sup> A subsequent systematic review and meta-analysis of all relevant HSCT studies also demonstrated the incidence of HHV-6 encephalitis

was significantly higher post-CBT than other stem cell sources (8.3% vs. 0.5%;  $P < 0.001$ ).<sup>40</sup> Ogata *et al.*<sup>56</sup> used the Japanese Adult Transplant Registry and identified 145 patients with HHV-6 encephalitis; the relative risk for CBT was 11.09 ( $P < 0.001$ ) and 9.48 ( $P < 0.001$ ) for HLA-mismatched unrelated donors. Haploidentical transplant recipients may also be at high risk of HHV-6B encephalitis based on a combined report of two small studies<sup>51</sup> where, in an attempt to improve engraftment and reduce GvHD, donor cells were depleted of naive T cells and natural killer (NK) cells, but memory T cells remained. Finally, pre-engraftment syndrome might be a risk factor for HHV-6 encephalitis.<sup>50</sup>

#### Prognosis of human herpesvirus 6B encephalitis

Zerr<sup>53</sup> reviewed the outcome in the many previous detailed descriptions of individual patients; 11 of 44 (25%) died within 1-4 weeks of diagnosis, 6 (14%) showed improvement but died with various unrelated medical problems, 8 (18%) improved but with lingering neurological compromise, and 19 (43%) appeared to make a full recovery. In a single retrospective study, Hill *et al.*<sup>49</sup> reported 19 patients with PALE; attributable mortality was higher after CBT (5 of 10) than in recipients of adult donor stem cells (0 of 9). In a much larger number of allogeneic HSCT recipients,<sup>56</sup> neuropsychological sequelae were reported in 57% of encephalitic patients with an overall survival rate of 58.3% in those with encephalitis as opposed to 80.5% in those without.

Other retrospective surveys of small numbers of patients have reported variable outcomes in terms of mortality and neurological sequelae including temporal lobe epilepsy (TLE).<sup>50</sup> Long-term consequences of HHV-6 encephalitis post-HSCT in children may include a new syndrome, involving generalized epilepsy (as opposed to TLE in adults) together with cognitive regression and delayed intellectual development.<sup>52,53</sup>

#### Human herpesvirus 6B myelosuppression and allograft failure

Evidence for a causal association is moderate (Table 4). HHV-6B infects hematologic progenitor cells *in vitro* thereby reducing colony formation.<sup>54</sup> Virus reactivation post-HSCT has been frequently associated with myelosuppression and delayed engraftment, particularly involving platelets<sup>46,55,56</sup> and also allograft failure.<sup>57,58</sup>

- If there is failed engraftment, blood or bone marrow should be tested for HHV-6B DNA.
- Other likely infectious or non-infectious causes must be excluded.
- CIHHV-6 in donor and recipient should be excluded.

#### Other end-organ diseases

Evidence for a causal association of HHV-6 with other disease post-HSCT is weak (Table 4). Viral DNA in tissue is not diagnostic as it may reflect HHV-6 DNAemia or inflammation with consequent infiltrating HHV-6 infected lymphocytes.

Pneumonitis remains a leading cause of morbidity and mortality post-HSCT, and HHV-6 has been implicated as a potential cause.<sup>59</sup> Studies using heterogeneous populations and methods, including patients with hematologic malignancies with and without HSCT, have produced variable results.<sup>60-62</sup> A recent study applied molecular testing for 28 pathogens in bronchoalveolar lavage samples

from HSCT recipients previously diagnosed with idiopathic pneumonia syndrome. HHV-6 was the most common pathogen (29% of cases) identified, and it was the only pathogen in approximately half of these.<sup>65</sup> However, the clinical significance of this finding remains to be determined.

Although there are many reports of HHV-6B-associated hepatitis after liver transplantation, this has only been well documented in two cases post-HSCT,<sup>64,65</sup> both of which describe acute hepatitis successfully treated with ganciclovir. HHV-6B DNA was demonstrated in hepatic tissue by immunohistochemistry.

- In suspected end-organ disease other than failed engraftment or encephalitis, tissue from the affected organ should be tested for HHV-6 infection by culture, immunochemistry, *in situ* hybridization or reverse transcription PCR for mRNA.

- PCR for HHV-6 DNA in tissue is not recommended for documentation of HHV-6 disease.

- Other likely infectious or non-infectious causes must be excluded.

- CIHHV-6 in donor and recipient should be excluded.

### Human herpesvirus 6B and cytomegalovirus reactivation

Human herpesvirus 6B reactivation has been associated with an increased risk of subsequent CMV reactivation and disease post-HSCT,<sup>45,66</sup> although this was not replicated in another study.<sup>67</sup> One study suggests that HHV-6 reactivation may indicate cellular immunosuppression which also predisposes to CMV reactivation.<sup>68</sup> *In vitro* studies of HHV-6 reactivation demonstrate that HHV-6B infection might contribute to CMV reactivation through inhibition of IL-12 production.<sup>69,70</sup>

### Human herpesvirus 6B - acute graft-versus-host disease and increased all-cause mortality

A well-designed study established an association between HHV-6B reactivation and subsequent acute GvHD.<sup>71</sup> A meta-analysis of 11 such studies demonstrated a statistically significant association between HHV-6B and subsequent grade II-IV acute GvHD (HR: 2.65; 95% CI: 1.89-3.72;  $P < 0.001$ ).<sup>72</sup>

Human herpesvirus 6B reactivation has also been associated with increased all-cause mortality post-HSCT.<sup>45,46,73,74</sup> However, whether HHV-6B directly or indirectly impacts on mortality in the absence of clinically apparent end-organ disease remains unclear.

## Treatment strategies

### Antiviral drugs and immunotherapy

Ganciclovir, foscarnet, and cidofovir inhibit HHV-6 replication *in vitro*.<sup>75</sup> Whilst *in vitro* studies support the potential for HHV-6 to develop resistance to the above antiviral agents, very few case reports have described the emergence of drug-resistant isolates, specifically to ganciclovir, and after lengthy exposure in the clinical setting.<sup>76</sup>

<sup>79</sup> Additionally, the use of valganciclovir or ganciclovir treatment for CMV disease did not result in the emergence of drug-resistant HHV-6 mutants in a large prospective trial of solid organ transplant patients.<sup>80</sup>

New treatment modalities for HHV-6 are needed due to the nephrotoxic and myelosuppressive properties of the

available agents. Brincidofovir (or CMX-001) has high *in vitro* activity against HHV-6 species<sup>81</sup> but has significant gastrointestinal toxicity;<sup>82</sup> an intravenous formulation under development may be better tolerated.<sup>83</sup> However, this drug is not currently available for clinical use. Adoptive immunotherapy with virus-specific T cells is an exciting new therapeutic approach for HHV-6.<sup>84,85</sup> This approach appears to be safe and potentially effective in small, uncontrolled studies.

### Prevention of human herpesvirus 6B encephalitis

Human herpesvirus 6B DNA screening during the high-risk period post-HSCT is impractical as HHV-6 reactivation often coincides with the onset of disease.<sup>46</sup> Effective pre-emptive or prophylactic strategies have not been identified. Three prospective, non-randomized studies of prophylactic foscarnet (pre- or post-engraftment) did not significantly lower the incidence of encephalitis.<sup>86-88</sup> Similarly, two prospective, non-randomized studies of pre-emptive ganciclovir or foscarnet did not reduce the incidence of HHV-6B encephalitis.<sup>89,90</sup> Failure of these approaches may be a result of inadequate dosing due to concerns about toxicity and resultant insufficient drug penetration into the CSF. Thus, routine HHV-6 DNA screening is not recommended for pre-emptive or prophylactic therapy, in any context.

- Routine screening of HHV-6 DNA in blood post-HSCT is not recommended (DIIu)

- Anti-HHV-6 prophylactic or pre-emptive therapy is not recommended for the prevention of HHV-6B reactivation or encephalitis post-HSCT (DIIu)

### Treatment of human herpesvirus 6B encephalitis

Zerr *et al.*<sup>91</sup> demonstrated a response of HHV-6 to ganciclovir or foscarnet as measured by DNA in the CSF or serum of allogeneic HSCT patients. Ljungman *et al.*<sup>92</sup> reported reductions in the HHV-6 load in saliva in patients receiving ganciclovir for pre-emptive therapy of CMV. Vu *et al.*<sup>93</sup> described positive responses in 4 of 5 patients treated with foscarnet.

On the basis of the above results, foscarnet or ganciclovir were recommended for treatment of HHV-6 encephalitis post-HSCT.<sup>94</sup> Since then a substantial amount of additional evidence supports the use of ganciclovir and foscarnet. Hill *et al.*<sup>49</sup> treated 18 patients with HHV-6 PALE with foscarnet 180 mg/kg/day and symptoms improved in most. Schmidt-Hieber *et al.*<sup>95</sup> reported a response rate of 63% with either foscarnet or ganciclovir therapy for HHV-6 encephalitis. More recently, data comparing the use of ganciclovir with foscarnet in Japanese patients<sup>96</sup> showed response rates of neurological symptoms were 83.8% and 71.4% with foscarnet monotherapy and ganciclovir monotherapy, respectively ( $P = 0.10$ , Fisher's exact test). Full-dose therapy with foscarnet ( $\geq 180$  mg/kg) or ganciclovir ( $\geq 10$  mg/kg) was associated with a better response rate than treatment with lower doses (foscarnet, 93% vs. 74%,  $P = 0.044$ ; ganciclovir, 84% vs. 58%,  $P = 0.047$ ). The response rate of ten patients receiving combination therapy with various doses of foscarnet and ganciclovir was 100%. However, the small sample size limits conclusions regarding whether combination therapy is superior to monotherapy, and drug toxicity is an important consideration. Death from any cause within 30 days after development of HHV-6 encephalitis was significantly lower in patients

who received foscarnet and significantly higher in patients who received ganciclovir, but this was in unadjusted descriptive analyses.

Information on the clinical use of cidofovir for the treatment of HHV-6 encephalitis is limited to two case reports;<sup>96,97</sup> in one cidofovir was interrupted due to drug toxicity and in the other the drug was combined with foscarnet.

- Intravenous foscarnet or ganciclovir are recommended for treatment of HHV-6B encephalitis. Drug selection should be dictated by the drug's side effects and the patient's comorbidities (AIIu).

- The recommended doses are 90 mg/kg b.d. for foscarnet and 5 mg/kg b.d. for ganciclovir (AIIu).

- Antiviral therapy should be for at least three weeks and until testing demonstrates clearance of HHV-6 DNA from blood and, if possible, CSF (CIII).

- Combined ganciclovir and foscarnet therapy can be considered (CIII).

- Immunosuppressive medications should be reduced if possible (BIII).

- There are insufficient data on the use of cidofovir to make a recommendation.

### Treatment of human herpesvirus 6B associated end-organ diseases other than encephalitis

Since the strength of associations with other end-organ diseases is moderate or weak, there are insufficient data to guide a recommendation for antiviral treatment.

- No recommendation can be made.

## Conclusions

Human herpesvirus 6B is the primary cause of infectious encephalitis after allogeneic HSCT. Studies of prevention and treatment strategies for this disease are urgently required to improve outcomes using novel therapeutic approaches, such as new antiviral drugs and immunotherapy.

As regards other possible HHV-6B end-organ diseases post-HSCT, improved RNA diagnostic tests are necessary to demonstrate active viral replication (*in situ* hybridization and/or reverse transcription PCR).

Understanding the pathogenic potential of HHV-6 and CIHHV-6 requires that all prospective studies on HSCT patients and health outcomes use tests on both donor and recipient that distinguish HHV-6A from HHV-6B.

### Funding

The ECIL meeting (Sept 21-23, 2017) was supported by unrestricted grants from Astellas, Basilea, Chimerix, Clinigen, Gilead, MSD, Pfizer and Shire. None of these pharmaceutical companies had any role in the selection of experts and the scope and purpose of the guidelines, or the collection, analysis, and interpretation of the data and editing the guidelines.

### Acknowledgments

The authors would like to thank Thierry Calandra for chairing the ECIL HHV-6 session and the ECIL participants. We also thank GL events, Lyon, France for organizing the meeting.

## References

- Ablashi D, Agut H, Alvarez-Lafuente R, et al. Classification of HHV-6A and HHV-6B as distinct viruses. *Arch Virol*. 2014;159(5):863-870.
- De Bolle L, Naesens L, De Clercq E. Update on human herpesvirus 6 biology, clinical features, and therapy. *Clin Microbiol Rev*. 2005;18(1):217-245.
- Daibata M, Taguchi T, Nemoto Y, Taguchi H, Miyoshi I. Inheritance of chromosomally integrated human herpesvirus 6 DNA. *Blood*. 1999;94(5):1545-1549.
- Tanaka-Taya K, Sashihara J, Kurahashi H, et al. Human herpesvirus 6 (HHV-6) is transmitted from parent to child in an integrated form and characterization of cases with chromosomally integrated HHV-6 DNA. *J Med Virol*. 2004;73(3):465-473.
- Pellet PE, Ablashi DV, Ambros PE, et al. Chromosomally integrated human herpesvirus 6: questions and answers. *Rev Med Virol*. 2012;22(3):144-155.
- Nacheva EP, Ward KN, Brazma D, et al. Human herpesvirus 6 integrates within telomeric regions as evidenced by five different chromosomal sites. *J Med Virol*. 2008;80(11):1952-1958.
- Ward KN, Leong HN, Nacheva EP, et al. Human herpesvirus 6 chromosomal integration in immunocompetent patients results in high levels of viral DNA in blood, sera, and hair follicles. *J Clin Microbiol*. 2006;44(4):1571-1574.
- Ward KN, Leong HN, Thiruchelvam AD, Atkinson CE, Clark DA. Human herpesvirus 6 DNA levels in cerebrospinal fluid due to primary infection differ from those due to chromosomal viral integration and have implications for diagnosis of encephalitis. *J Clin Microbiol*. 2007;45(4):1298-1304.
- Ward KN. Child and adult forms of human herpesvirus 6 encephalitis: looking back, looking forward. *Curr Opin Neurol*. 2014;27(3):349-355.
- Endo A, Watanabe K, Ohye T, et al. Molecular and virological evidence of viral activation from chromosomally integrated human herpesvirus 6A in a patient with X-linked severe combined immunodeficiency. *Clin Infect Dis*. 2014;59(4):545-548.
- Politikos I, McMasters M, Bryke C, Avigan D, Boussiotis VA. Possible reactivation of chromosomally integrated human herpesvirus 6 after treatment with histone deacetylase inhibitor. *Blood Adv*. 2018;2(12):1367-1370.
- Bonnafous P, Marlet J, Bouvet D, et al. Fatal outcome after reactivation of inherited chromosomally integrated HHV-6A (iciHHV-6A) transmitted through liver transplantation. *Am J Transplant*. 2018;18(6):1548-1551.
- Clark DA, Nacheva EP, Leong HN, et al. Transmission of integrated human herpesvirus 6 through stem cell transplantation: implications for laboratory diagnosis. *J Infect Dis*. 2006;193(7):912-916.
- Hubacek P, Hyncicova K, Muzikova K, Cinek O, Zajac M, Sedlacek P. Disappearance of pre-existing high HHV-6 DNA load in blood after allogeneic SCT. *Bone Marrow Transplant*. 2007;40(8):805-806.
- Yagasaki H, Shichino H, Shimizu N, et al. Nine-year follow-up in a child with chromosomal integration of human herpesvirus 6 transmitted from an unrelated donor through the Japan Marrow Donor Program. *Transpl Infect Dis*. 2015;17(1):160-161.
- Yamada Y, Osumi T, Imadome KI, et al. Transmission of chromosomally integrated human herpesvirus 6 via cord blood transplantation. *Transpl Infect Dis*. 2017;19(1):e12636.
- Hill JA, Magaret AS, Hall-Sedlak R, et al. Outcomes of hematopoietic cell transplantation using donors or recipients with inherited chromosomally integrated HHV-6. *Blood*. 2017;130(8):1062-1069.
- Hubacek P, Muzikova K, Hrdlickova A, et al. Prevalence of HHV-6 integrated chromosomally among children treated for acute lymphoblastic or myeloid leukemia in the Czech Republic. *J Med Virol*. 2009;81(2):258-263.
- Hubacek P, Hrdlickova A, Spacek M, et al. Prevalence of chromosomally integrated HHV-6 in patients with malignant disease and healthy donors in the Czech Republic. *Folia Microbiol (Praha)*. 2013;58(1):87-90.
- Gravel A, Sinnett D, Flamand L. Frequency of chromosomally-integrated human herpesvirus 6 in children with acute lymphoblastic leukemia. *PLoS One*. 2013;8(12):e84322.
- Bell AJ, Gallagher A, Mottram T, et al. Germ-line transmitted, chromosomally integrated HHV-6 and classical Hodgkin lymphoma. *PLoS One*. 2014;9(11):e112642.
- Flamand L, Gravel A, Boutolleau D, et al. Multicenter comparison of PCR assays for

- detection of human herpesvirus 6 DNA in serum. *J Clin Microbiol.* 2008;46(8):2700-2706.
23. Cassina G, Russo D, De BD, Broccolo F, Lusso P, Malnati MS. Calibrated real-time polymerase chain reaction for specific quantitation of HHV-6A and HHV-6B in clinical samples. *J Virol Methods.* 2013;189(1):172-179.
  24. de Pagter PJ, Schuurman R, de Vos NM, Mackay W, van Loon AM. Multicenter external quality assessment of molecular methods for detection of human herpesvirus 6. *J Clin Microbiol.* 2010;48(7):2536-2540.
  25. Purev E, Winkler T, Danner RL, et al. Engraftment of donor cells with germ-line integration of HHV6 mimics HHV6 reactivation following cord blood/haplo transplantation. *Blood.* 2014;124(7):1198-1199.
  26. Hubacek P, Maalouf J, Zajickova M, et al. Failure of multiple antivirals to affect high HHV-6 DNAemia resulting from viral chromosomal integration in a case of severe aplastic anaemia. *Haematologica.* 2007;92(10):e98-e100.
  27. Jeulin H, Guery M, Clement L, et al. Chromosomally integrated HHV-6: slow decrease of HHV-6 viral load after hematopoietic stem-cell transplantation. *Transplantation.* 2009;88(9):1142-1143.
  28. Hubacek P, Virgili A, Ward KN, et al. HHV-6 DNA throughout the tissues of two stem cell transplant patients with chromosomally integrated HHV-6 and fatal CMV pneumonitis. *Br J Haematol.* 2009;145(3):394-398.
  29. Sedlak RH, Cook L, Huang ML, et al. Identification of chromosomally integrated human herpesvirus 6 by droplet digital PCR. *Clin Chem.* 2014;60(5):765-772.
  30. Lau YL, Peiris M, Chan GC, Chan AC, Chiu D, Ha SY. Primary human herpes virus 6 infection transmitted from donor to recipient through bone marrow infusion. *Bone Marrow Transplant.* 1993;21(10):1063-1066.
  31. Muramatsu H, Watanabe N, Matsumoto K, et al. Primary infection of human herpesvirus-6 in an infant who received cord blood SCT. *Bone Marrow Transplant.* 2009;43(1):83-84.
  32. Drobyski WR, Knox KK, Majewski D, Carrigan DR. Brief report: fatal encephalitis due to variant B human herpesvirus-6 infection in a bone marrow-transplant recipient. *N Engl J Med.* 1994;330(19):1356-1360.
  33. Zerr DM. Human herpesvirus 6 and central nervous system disease in hematopoietic cell transplantation. *J Clin Virol.* 2006;37 Suppl 1:S52-S56.
  34. Zerr DM, Ogata M. HHV-6A and HHV-6B in Recipients of Hematopoietic Cell Transplantation. In: Flaman L, Lautenschlager I, Krueger G, Ablashi D, editors. *HHV-6A, HHV-6B & HHV-7 Diagnosis and Clinical Management.* 3rd ed. San Francisco: Elsevier; 2014.
  35. Hill JA, Sedlak RH, Zerr DM, et al. Prevalence of chromosomally integrated human herpesvirus 6 in patients with human herpesvirus 6-central nervous system dysfunction. *Biol Blood Marrow Transplant.* 2015;21(2):371-373.
  36. Ogata M, Oshima K, Ikebe T, et al. Clinical characteristics and outcome of human herpesvirus-6 encephalitis after allogeneic hematopoietic stem cell transplantation. *Bone Marrow Transplant.* 2017;52(11):1563-1570.
  37. Noguchi T, Yoshiura T, Hiwatashi A, et al. CT and MRI findings of human herpesvirus 6-associated encephalopathy: comparison with findings of herpes simplex virus encephalitis. *AJR Am J Roentgenol.* 2010;194(3):754-760.
  38. Provenzale JM, van LK, White LE. Clinical and imaging findings suggesting human herpesvirus 6 encephalitis. *Pediatr Neurol.* 2010;42(1):32-39.
  39. Bhanushali MJ, Kranick SM, Freeman AF, et al. Human herpes 6 virus encephalitis complicating allogeneic hematopoietic stem cell transplantation. *Neurology.* 2013;80(16):1494-1500.
  40. Scheurer ME, Pritchett JC, Amirian ES, Zemke NR, Lusso P, Ljungman P. HHV-6 encephalitis in umbilical cord blood transplantation: a systematic review and meta-analysis. *Bone Marrow Transplant.* 2013;48(4):574-580.
  41. Zerr DM, Fann JR, Breiger D, et al. HHV-6 reactivation and its effect on delirium and cognitive functioning in hematopoietic cell transplantation recipients. *Blood.* 2011;117(19):5243-5249.
  42. Hill JA, Boeckh MJ, Sedlak RH, Jerome KR, Zerr DM. Human herpesvirus 6 can be detected in cerebrospinal fluid without associated symptoms after allogeneic hematopoietic cell transplantation. *J Clin Virol.* 2014;61(2):289-292.
  43. Hill JA, Boeckh M, Leisenring WM, et al. Human herpesvirus 6B reactivation and delirium are frequent and associated events after cord blood transplantation. *Bone Marrow Transplant.* 2015;50(10):1348-1351.
  44. Ueki T, Hoshi K, Hiroshima Y, et al. Analysis of five cases of human herpesvirus-6 myelitis among 121 cord blood transplantations. *Int J Hematol.* 2018;107(3):363-372.
  45. Zerr DM, Boeckh M, Delaney C, et al. HHV-6 reactivation and associated sequelae after hematopoietic cell transplantation. *Biol Blood Marrow Transplant.* 2012;18(11):1700-1708.
  46. Dulery R, Salleron J, Dewilde A, et al. Early human herpesvirus type 6 reactivation after allogeneic stem cell transplantation: a large-scale clinical study. *Biol Blood Marrow Transplant.* 2012;18(7):1080-1089.
  47. Olson AL, Dahi PB, Zheng J, et al. Frequent human herpesvirus-6 viremia but low incidence of encephalitis in double-unit cord blood recipients transplanted without antithymocyte globulin. *Biol Blood Marrow Transplant.* 2014;20(6):787-793.
  48. Ogata M, Satou T, Kadota J, et al. Human herpesvirus 6 (HHV-6) reactivation and HHV-6 encephalitis after allogeneic hematopoietic cell transplantation: a multicenter, prospective study. *Clin Infect Dis.* 2013;57(5):671-681.
  49. Hill JA, Koo S, Guzman Suarez BB, et al. Cord-blood hematopoietic stem cell transplant confers an increased risk for human herpesvirus-6-associated acute limbic encephalitis: a cohort analysis. *Biol Blood Marrow Transplant.* 2012;18(11):1638-1648.
  50. Ogata M, Fukuda T, Teshima T. Human herpesvirus-6 encephalitis after allogeneic hematopoietic cell transplantation: what we do and do not know. *Bone Marrow Transplant.* 2015; 50(8):1030-1036.
  51. Perruccio K, Sisinni L, Perez-Martinez A, et al. High Incidence of Early Human Herpesvirus-6 Infection in Children Undergoing Haploidentical Manipulated Stem Cell Transplantation for Hematologic Malignancies. *Biol Blood Marrow Transplant.* 2018;24(12):2549-2557.
  52. Howell KB, Tiedemann K, Haessler G, et al. Symptomatic generalized epilepsy after HHV6 posttransplant acute limbic encephalitis in children. *Epilepsia.* 2012;53(7):e122-e126.
  53. Raspall-Chaure M, Armangue T, Elorza J, Sanchez-Montanez A, Vicente-Rasoamalala M, Macaya A. Epileptic encephalopathy after HHV6 post-transplant acute limbic encephalitis in children: confirmation of a new epilepsy syndrome. *Epilepsy Res.* 2013;105(3):419-422.
  54. Isomura H, Yoshida M, Namba H, et al. Suppressive effects of human herpesvirus-6 on thrombopoietin-inducible megakaryocytic colony formation in vitro. *J Gen Virol.* 2000;81(Pt 3):663-673.
  55. Ljungman P, Wang FZ, Clark DA, et al. High levels of human herpesvirus 6 DNA in peripheral blood leucocytes are correlated to platelet engraftment and disease in allogeneic stem cell transplant patients. *Br J Haematol.* 2000;111(3):774-781.
  56. Zerr DM, Corey L, Kim HW, Huang ML, Nguy L, Boeckh M. Clinical outcomes of human herpesvirus 6 reactivation after hematopoietic stem cell transplantation. *Clin Infect Dis.* 2005;40(7):932-940.
  57. Lagadinou ED, Marangos M, Liga M, et al. Human herpesvirus 6-related pure red cell aplasia, secondary graft failure, and clinical severe immune suppression after allogeneic hematopoietic cell transplantation successfully treated with foscarnet. *Transpl Infect Dis.* 2010;12(5):437-440.
  58. Le Bourgeois A, Labopin M, Guillaume T, et al. Human herpesvirus 6 reactivation before engraftment is strongly predictive of graft failure after double umbilical cord blood allogeneic stem cell transplantation in adults. *Exp Hematol.* 2014;42(11):945-954.
  59. Carrigan DR, Drobyski WR, Russler SK, Tapper MA, Knox KK, Ash RC. Interstitial pneumonitis associated with human herpesvirus-6 infection after marrow transplantation. *Lancet.* 1991;338(8760):147-149.
  60. Cone RW, Hackman RC, Huang ML, et al. Human herpesvirus 6 in lung tissue from patients with pneumonitis after bone marrow transplantation. *N Engl J Med.* 1993; 329(3):156-161.
  61. Buchbinder S, Elmaagacli AH, Schaefer UW, Roggendorf M. Human herpesvirus 6 is an important pathogen in infectious lung disease after allogeneic bone marrow transplantation. *Bone Marrow Transplant.* 2000;26(6):639-644.
  62. Nishimaki K, Okada S, Miyamura K, et al. The possible involvement of human herpesvirus type 6 in obliterative bronchiolitis after bone marrow transplantation. *Bone Marrow Transplant.* 2003;32(11):1103-1105.
  63. Seo S, Renaud C, Kuypers JM, et al. Idiopathic pneumonia syndrome after hematopoietic cell transplantation: evidence of occult infectious etiologies. *Blood.* 2015;125(24):3789-3797.
  64. Hill JA, Myerson D, Sedlak RH, Jerome KR, Zerr DM. Hepatitis due to human herpesvirus 6B after hematopoietic cell transplantation and a review of the literature. *Transpl Infect Dis.* 2014;16(3):477-483.
  65. Kuribayashi K, Matsunaga T, Iyama S, et al. Human herpesvirus-6 hepatitis associated with cyclosporine-A encephalitis after bone marrow transplantation for chronic myeloid leukemia. *Intern Med.* 2006;45(7): 475-478.
  66. Crocchiolo R, Giordano L, Rimondo A, et al. Human Herpesvirus 6 replication predicts Cytomegalovirus reactivation after allogeneic stem cell transplantation from haploidentical donor. *J Clin Virol.* 2016;84: 24-26.
  67. Tormo N, Solano C, de la Camara R, et al. An assessment of the effect of human her-

- pesvirus-6 replication on active cytomegalovirus infection after allogeneic stem cell transplantation. *Biol Blood Marrow Transplant.* 2010;16(5):653-661.
68. Wang FZ, Larsson K, Linde A, Ljungman P. Human herpesvirus 6 infection and cytomegalovirus-specific lymphoproliferative responses in allogeneic stem cell transplant recipients. *Bone Marrow Transplant.* 2002;30(8):521-526.
  69. Smith AP, Paolucci C, Di Lullo G, Burastero SE, Santoro F, Lusso P. Viral replication-independent blockade of dendritic cell maturation and interleukin-12 production by human herpesvirus 6. *J Virol.* 2005;79(5): 2807-2813.
  70. Lusso P. HHV-6 and the immune system: mechanisms of immunomodulation and viral escape. *J Clin Virol.* 2006; 37 Suppl 1:S4-10.
  71. Admiraal R, de Koning CCH, Lindemans CA, et al. Viral reactivations and associated outcomes in the context of immune reconstitution after pediatric hematopoietic cell transplantation. *J Allergy Clin Immunol.* 2017;140(6):1643-1650.
  72. Phan TL, Carlin K, Ljungman P, et al. Human Herpesvirus-6B Reactivation Is a Risk Factor for Grades II to IV Acute Graft-versus-Host Disease after Hematopoietic Stem Cell Transplantation: A Systematic Review and Meta-Analysis. *Biol Blood Marrow Transplant.* 2018;24(11):2324-2336.
  73. de Pagter PJ, Schuurman R, Visscher H, et al. Human herpes virus 6 plasma DNA positivity after hematopoietic stem cell transplantation in children: an important risk factor for clinical outcome. *Biol Blood Marrow Transplant.* 2008;14(7):831-839.
  74. Hill JA, Mayer BT, Xie H, et al. Kinetics of Double-Stranded DNA Viremia After Allogeneic Hematopoietic Cell Transplantation. *Clin Infect Dis.* 2013;66(3):368-375.
  75. Prichard MN, Whitley RJ. The development of new therapies for human herpesvirus 6. *Curr Opin Virol.* 2019;148-153.
  76. Manichanh C, Olivier-Aubron C, Lagarde JP, et al. Selection of the same mutation in the U69 protein kinase gene of human herpesvirus-6 after prolonged exposure to ganciclovir in vitro and in vivo. *J Gen Virol.* 2001;82(Pt 11):2767-2776.
  77. Isegawa Y, Hara J, Amo K, et al. Human herpesvirus 6 ganciclovir-resistant strain with amino acid substitutions associated with the death of an allogeneic stem cell transplant recipient. *J Clin Virol.* 2009;44(1):15-19.
  78. Baldwin K. Ganciclovir-resistant human herpesvirus-6 encephalitis in a liver transplant patient: a case report. *J Neurovirol.* 2011;17(2):193-195.
  79. Piret J, Boivin G. Antiviral drug resistance in herpesviruses other than cytomegalovirus. *Rev Med Virol.* 2014;24(3):186-218.
  80. Bounaadja L, Piret J, Goyette N, Boivin G. Analysis of HHV-6 mutations in solid organ transplant recipients at the onset of cytomegalovirus disease and following treatment with intravenous ganciclovir or oral valganciclovir. *J Clin Virol.* 2013;58(1): 279-282.
  81. Williams-Aziz SL, Hartline CB, Harden EA, et al. Comparative activities of lipid esters of cidofovir and cyclic cidofovir against replication of herpesviruses in vitro. *Antimicrob Agents Chemother.* 2005;49(9):3724-3733.
  82. Marty FM, Winston DJ, Chemaly RF, et al. A Randomized, Double-Blind, Placebo-Controlled Phase 3 Trial of Oral Brinciclovir for Cytomegalovirus Prophylaxis in Allogeneic Hematopoietic Cell Transplantation. *Biol Blood Marrow Transplant.* 2019;25(2):369-381.
  83. Wire MB, Morrison M, Anderson M, Arumugham T, Dunn J, Naderer O. Pharmacokinetics (PK) and Safety of Intravenous (IV) Brinciclovir (BCV) in Healthy Adult Subjects. *Open Forum Infect Dis.* 2017;4(Suppl 1):S311.
  84. Becerra A, Gibson L, Stern LJ, Calvo-Calle JM. Immune response to HHV-6 and implications for immunotherapy. *Curr Opin Virol.* 2014;9:154-161.
  85. Tzannou I, Papadopoulou A, Naik S, et al. Off-the-Shelf Virus-Specific T Cells to Treat BK Virus, Human Herpesvirus 6, Cytomegalovirus, Epstein-Barr Virus, and Adenovirus Infections After Allogeneic Hematopoietic Stem-Cell Transplantation. *J Clin Oncol.* 2017;35(31):3547-3557.
  86. Ishiyama K, Katagiri T, Ohata K, et al. Safety of pre-engraftment prophylactic foscarnet administration after allogeneic stem cell transplantation. *Transpl Infect Dis.* 2012;14(1):33-39.
  87. Ogata M, Satou T, Inoue Y, et al. Foscarnet against human herpesvirus (HHV)-6 reactivation after allo-SCT: breakthrough HHV-6 encephalitis following antiviral prophylaxis. *Bone Marrow Transplant.* 2013;48(2):257-264.
  88. Ogata M, Takano K, Moriuchi Y, et al. Effects of Prophylactic Foscarnet on Human Herpesvirus-6 Reactivation and Encephalitis in Cord Blood Transplant Recipients: A Prospective Multicenter Trial with an Historical Control Group. *Biol Blood Marrow Transplant.* 2018;24(6):1264-1273.
  89. Ogata M, Satou T, Kawano R, et al. Plasma HHV-6 viral load-guided preemptive therapy against HHV-6 encephalopathy after allogeneic stem cell transplantation: a prospective evaluation. *Bone Marrow Transplant.* 2008;41(3):279-285.
  90. Ishiyama K, Katagiri T, Hoshino T, Yoshida T, Yamaguchi M, Nakao S. Preemptive therapy of human herpesvirus-6 encephalitis with foscarnet sodium for high-risk patients after hematopoietic SCT. *Bone Marrow Transplant.* 2011;46(6):863-869.
  91. Zerr DM, Gupta D, Huang ML, Carter R, Corey L. Effect of antivirals on human herpesvirus 6 replication in hematopoietic stem cell transplant recipients. *Clin Infect Dis.* 2002;34(3):309-317.
  92. Ljungman P, Dahl H, Xu YH, Larsson K, Brytting M, Linde A. Effectiveness of ganciclovir against human herpesvirus-6 excreted in saliva in stem cell transplant recipients. *Bone Marrow Transplant.* 2007; 39(8):497-499.
  93. Vu T, Carrum G, Hutton G, Heslop HE, Brenner MK, Kamble R. Human herpesvirus-6 encephalitis following allogeneic hematopoietic stem cell transplantation. *Bone Marrow Transplant.* 2007;39(11):705-709.
  94. Ljungman P, de la Camara R, Cordonnier C, et al. Management of CMV, HHV-6, HHV-7 and Kaposi-sarcoma herpesvirus (HHV-8) infections in patients with hematological malignancies and after SCT. *Bone Marrow Transplant.* 2008;42(4):227-240.
  95. Schmidt-Hieber M, Schwender J, Heinz WJ, et al. Viral encephalitis after allogeneic stem cell transplantation: a rare complication with distinct characteristics of different causative agents. *Haematologica.* 2011;96(1):142-149.
  96. Denes E, Magy L, Pradeau K, Alain S, Weinbreck P, Ranger-Rogez S. Successful treatment of human herpesvirus 6 encephalomyelitis in immunocompetent patient. *Emerg Infect Dis.* 2004;10(4):729-731.
  97. Pohlmann C, Schetelig J, Reuner U, et al. Cidofovir and foscarnet for treatment of human herpesvirus 6 encephalitis in a neutropenic stem cell transplant recipient. *Clin Infect Dis.* 2007;44(12):e118-e120.
  98. Hill JA, Zerr DM. Human herpesvirus 6A, 6B, 7 and 8 infections After Hematopoietic Stem Cell Transplantation. In: Ljungman P, Snydman D, Boeckh M, editors. Switzerland: Springer International. 2016. pp.547-562.
  99. Hill JA, Zerr DM. Roseoloviruses in transplant recipients: clinical consequences and prospects for treatment and prevention trials. *Curr Opin Virol.* 2014;9:53-60.



# A Tie2-Notch1 signaling axis regulates regeneration of the endothelial bone marrow niche

Lijian Shao,<sup>1</sup> Kilian Sottoriva,<sup>1</sup> Karol Palasiewicz,<sup>1</sup> Jizhou Zhang,<sup>2</sup> James Hyun,<sup>1</sup> Sweta S. Soni,<sup>1</sup> Na Yoon Paik,<sup>1</sup> Xiaopei Gao,<sup>1</sup> Henar Cuervo,<sup>3</sup> Asrar B. Malik,<sup>1</sup> Jalees Rehman,<sup>1</sup> Daniel Lucas<sup>2,4</sup> and Kostandin V. Pajcini<sup>1</sup>

<sup>1</sup>Department of Pharmacology, The University of Illinois College of Medicine, Chicago, IL

<sup>2</sup>Division of Experimental Hematology and Cancer Biology, Cincinnati Children's Medical Center, Cincinnati, OH; <sup>3</sup>Department of Physiology and Biophysics, The University of Illinois College of Medicine, Chicago, IL and <sup>4</sup>Department of Pediatrics, University of Cincinnati College of Medicine, Cincinnati, OH, USA

**Haematologica** 2019  
Volume 104(11):2164-2177

## ABSTRACT

Loss-of-function studies have determined that Notch signaling is essential for hematopoietic and endothelial development. By deleting a single allele of the Notch1 transcriptional activation domain we generated viable, post-natal mice exhibiting hypomorphic Notch signaling. These heterozygous mice, which lack only one copy of the transcriptional activation domain, appear normal and have no endothelial or hematopoietic phenotype, apart from an inherent, cell-autonomous defect in T-cell lineage development. Following chemotherapy, these hypomorphs exhibited severe pancytopenia, weight loss and morbidity. This phenotype was confirmed in an endothelial-specific, loss-of-function Notch1 model system. Ang1, secreted by hematopoietic progenitors after damage, activated endothelial Tie2 signaling, which in turn enhanced expression of Notch ligands and potentiated Notch1 receptor activation. In our heterozygous, hypomorphic model system, the mutant protein that lacks the Notch1 transcriptional activation domain accumulated in endothelial cells and interfered with optimal activity of the wildtype Notch1 transcriptional complex. Failure of the hypomorphic mutant to efficiently drive transcription of key gene targets such as *Hes1* and *Myc* prolonged apoptosis and limited regeneration of the bone marrow niche. Thus, basal Notch1 signaling is sufficient for niche development, but robust Notch activity is required for regeneration of the bone marrow endothelial niche and hematopoietic recovery.

## Correspondence:

KOSTANDIN V. PAJCINI  
kvp@uic.edu

Received: October 5, 2018.

Accepted: March 18, 2019.

Pre-published: March 28, 2019.

doi:10.3324/haematol.2018.208660

Check the online version for the most updated information on this article, online supplements, and information on authorship & disclosures: [www.haematologica.org/content/104/11/2164](http://www.haematologica.org/content/104/11/2164)

©2019 Ferrata Storti Foundation

Material published in *Haematologica* is covered by copyright. All rights are reserved to the Ferrata Storti Foundation. Use of published material is allowed under the following terms and conditions:

<https://creativecommons.org/licenses/by-nc/4.0/legalcode>.

Copies of published material are allowed for personal or internal use. Sharing published material for non-commercial purposes is subject to the following conditions:

<https://creativecommons.org/licenses/by-nc/4.0/legalcode>,

sect. 3. Reproducing and sharing published material for commercial purposes is not allowed without permission in writing from the publisher.



## Introduction

Chemotherapy and radiotherapy are widely used in the treatment of hematopoietic malignancies but broad cytotoxicity is an undesirable feature of these treatments.<sup>1</sup> These therapies damage multiple tissues including the bone marrow (BM) microvasculature.<sup>2-4</sup> The regeneration of the endothelial BM vascular niche is crucial for successful reconstitution of hematopoietic cells.<sup>5,6</sup> The interplay between the vascular and hematopoietic systems has multiple physiological and therapeutic implications. Endothelial cell (EC)-secreted growth factors such as vascular endothelial growth factor (VEGF)-A, enhance self-renewal and survival of hematopoietic stem cells (HSC) and mediate recovery of hematopoiesis.<sup>5,7,8</sup> Angiopoietin-1 (Ang1) signaling<sup>9,10</sup> via the activation of tyrosine kinase Tie2 has been proposed as the key endocrine mechanism mediating endothelial recovery and regeneration.<sup>2,11</sup> It is unknown whether paracrine signaling plays a role in the regeneration and reassembly of the BM endothelium.

Notch receptors are evolutionarily conserved transmembrane glycoproteins. Upon paracrine activation by neighboring cells through ligand interactions and proteolytic cleavage, they activate a transcriptional apparatus.<sup>12</sup> *Notch1* and *Notch4*

are highly expressed in the endothelium during embryonic development and control EC specification<sup>13</sup> and Notch1/Dll4 in coordination with VEGF-A/VEGFR2 signaling regulates sprouting angiogenesis.<sup>14,15</sup> The function of Notch signaling in the adult vasculature is less understood. Studies showed that Notch1 signaling in the adult endothelium regulates expression of inflammatory genes.<sup>16</sup> Notch1 is also known to be activated by blood flow and shear stress forces, which contribute to vascular homeostasis.<sup>17</sup> Important, unresolved questions are whether Notch activation has a role in post-injury endothelial regeneration and whether it promotes the recovery of hematopoiesis.

The intracellular domains of Notch receptors have distinct roles. The RAM domain has a high affinity for binding to RBPJ, while the Ankyrin repeat (ANK) domains interact with a Mastermind-like (MAML) protein factor and recruit other co-activators. The PEST domain localized at the C-terminal facilitates Notch degradation.<sup>18</sup> In between the ANK and PEST domains there is a transcriptional activation domain (TAD), which is capable of autonomous transcriptional activity and directly binds co-activators PCAF and GNC5.<sup>19,20</sup> The TAD is a region of significant divergence among the four mammalian Notch receptors.<sup>20,21</sup> These differences among the Notch receptor TAD may be important in the tissue-specific variability of Notch signaling.

We previously developed a transgenic knock-in model system which deleted the TAD of Notch1.<sup>22</sup> This model system was used to study the role of Notch1 TAD function during fetal development. The loss of TAD in both *Notch1* alleles ( $\Delta TAD/\Delta TAD$ ), allowed mice to develop to late gestation when they succumbed to multiple Notch-dependent cardiovascular anomalies.<sup>22-24</sup> While definitive HSC emerged from the aorta-gonad-mesonephros region, they failed to expand in the fetal liver of  $\Delta TAD/\Delta TAD$  embryos. Furthermore, when transplanted into irradiated adult recipients,  $\Delta TAD/\Delta TAD$  HSC underperformed in primary transplants and failed to reconstitute the hematopoietic system efficiently in secondary transplants.<sup>22</sup> In contrast, mice heterozygous for one allele of *Notch1* $\Delta TAD$  (*Notch1*<sup>+/ $\Delta TAD$</sup> ) survive to adulthood and exhibit no overt hematopoietic phenotype.

In the present study, we made use of hypomorphic Notch signaling in the *Notch1*<sup>+/ $\Delta TAD$</sup>  model to address whether the Notch pathway is crucial for the recovery of the adult BM niche and regeneration of hematopoietic cells after injury. We observed that high levels of Notch signaling were dispensable for the development of the endothelial niche and high Notch activity was not required during adult BM endothelial homeostasis. In the hematopoietic system, *Notch1*<sup>+/ $\Delta TAD$</sup>  only displayed cell-autonomous defects in the development of the T-cell lineage. However, following myelosuppressive injury, robust Notch signaling was critical for recovery of the BM endothelial niche and thereby the regeneration of HSC. Notch signaling was stimulated by a burst of Tie2-dependent activation, which induced expression of Notch1 ligands. Interestingly, expression of Notch1 $\Delta TAD$  protein in *Notch1*<sup>+/ $\Delta TAD$</sup>  EC decreased expression of Notch target genes and led to severe apoptosis. This phenotype could not be rescued by enhanced activation of Tie2 signaling. Our results suggest a crucial role for TAD-regulated Notch activity in mediating EC survival and promoting recovery of hematopoiesis following chemotherapeutic stress.

## Methods

### Animals

The following strains of mice were used in our studies under the guidelines and protocols approved by the Institutional Animal Care and Use Committees of University of Illinois at Chicago: C57BL/6J (or CD45.2), B6.SJL-*Ptprc*<sup>o</sup>*Pep3*<sup>o</sup>/BoyJ (or CD45.1), *Notch*<sup>+/ $\Delta TAD$</sup> , *Notch*<sup>+/+</sup>, *Notch1*<sup>fl</sup>, *RBPJ*<sup>fl</sup>, *PDGFR $\beta$ -Cre*<sup>ERT2</sup> and *VE-Cadherin Cre*<sup>ERT2</sup> mice. More details about the mice can be found in the *Online Supplementary Methods*.

### 5-Fluorouracil treatment and irradiation

5-Fluorouracil (5-FU, 150 mg/kg) was peritoneally injected into mice. For irradiation treatment, mice were exposed, on a rotating platform, to a lethal dose (9.0 Gy) of total body irradiation in a Mark I <sup>137</sup>Ce  $\gamma$ -irradiator (JL Shepherd, Glendale, CA, USA) at a dose rate of 6.38 Gy/min. More details about chemotherapy and radiotherapy can be found in the *Online Supplementary Methods*.

### Analysis of bone marrow and thymic mononuclear cells

Mononuclear cells from BM and thymus were prepared as described in the *Online Supplementary Methods*. The frequencies of LSK cells (Lin<sup>-</sup>Sca1<sup>+</sup>c-kit<sup>+</sup> cells), HSC (CD150<sup>+</sup>CD48<sup>-</sup>LSK cells), common lymphoid progenitors (CLP: Lin<sup>-</sup>Sca1<sup>low</sup>c-kit<sup>low</sup>CD135<sup>+</sup>CD127<sup>+</sup>), thymic early T-cell precursors (ETP: Lin<sup>-</sup>c-kit<sup>+</sup>CD25<sup>+</sup>CD44<sup>-</sup>) and double-negative 3 cells (DN3 cells: Lin<sup>-</sup>CD4<sup>+</sup>CD8<sup>+</sup>CD25<sup>+</sup>CD44<sup>-</sup>) were analyzed with a flow cytometer, Fortessa LSRII, after immunostaining with appropriate antibodies as described in the *Online Supplementary Methods*. All antibodies used are listed in *Online Supplementary Table S1*.

### Isolation of CD25<sup>+</sup> thymocytes and primary bone endothelial cells

Cell suspensions from the thymus or digested bones were incubated with dynabeads labeled with CD25 antibody and CD31 antibody (Invitrogen), respectively, for 30 min at 4°C. CD25<sup>+</sup> thymocytes and bone CD31<sup>+</sup> cells (pBEC) were isolated and used for western blot and quantitative reverse transcriptase polymerase chain reaction (RT-qPCR) analysis.

### Bone marrow-derived endothelial cell culture

Cultured bone marrow-derived endothelial cells (cBEC) were purchased from Cell Biologicals Inc (cat#, C57-6221) and cultured in EC medium. cBEC were treated with a  $\gamma$ -secretase inhibitor (1  $\mu$ M, Sigma), a Tie2 kinase inhibitor (1  $\mu$ M, Abcam), Ang1 (300 ng/mL, Peprotech) or 5-FU (100  $\mu$ M, Sigma). More detailed information can be found in the *Online Supplementary Methods*.

### Western blot analysis

Expression of cleaved/active Notch1 (Val1744), Notch1, VE-Cadherin, Tie2, and phosphorylated Tie2-Y992 was measured by western blot. The procedure is detailed in the *Online Supplementary Methods*.

### Quantitative reverse transcriptase polymerase chain reaction

Expression of various genes was measured by RT-qPCR and calculated using the comparative C<sub>T</sub> method. The sequences of all primers used in the RT-qPCR assay are listed in *Online Supplementary Table S2*.

### Chromatin immunoprecipitation assays

RBPJ binding sites at *Myc NDME*, *Hes1*, *Hey1* and *Dtx1* locus

were analyzed by chromatin immunoprecipitation assay. The procedure is described in detail in the *Online Supplement*. The sequences of primers are provided in *Online Supplementary Table S3*.

### Analysis of hematopoietic stem cell transplantation, apoptosis, luciferase activity, bone micro-computed tomography, sternum vasculature whole-mount imaging and immunostaining

These assays and methods are described in the *Online Supplementary Methods*.

### Statistical analysis

Details of the statistical analysis of the data are provided in the *Online Supplementary Methods*.

## Results

### Myelosuppression by 5-fluorouracil or $\gamma$ -irradiation causes pancytopenia in *Notch1*<sup>+/ $\Delta$ TAD</sup> mice

Myelosuppression by 5-FU is achieved by incorporating an analog of uracil into RNA or DNA of proliferating cells.<sup>25</sup> The result of 5-FU treatment during hematopoiesis is apoptosis of proliferating progenitors, followed by activation of HSC and reconstitution of the hematopoietic system.<sup>26</sup> To test for a possible hematopoietic defect in *Notch1*<sup>+/ $\Delta$ TAD</sup> mice, 5-week old wildtype (WT) and *Notch1*<sup>+/ $\Delta$ TAD</sup> littermates were treated with two doses of 5-FU, 14 days apart. Terminal hematopoietic analysis was performed 28 days after the first injection (Figure 1A). The condition of the *Notch1*<sup>+/ $\Delta$ TAD</sup> mice deteriorated rapidly after treatment. Analysis of peripheral blood from *Notch1*<sup>+/ $\Delta$ TAD</sup> mice revealed a sharp decrease in red blood cell and platelet counts, as well as hemoglobin concentration (Figure 1D). White blood cell and lymphocyte counts were also reduced in *Notch1*<sup>+/ $\Delta$ TAD</sup> mice (*Online Supplementary Figure S1A*). During the first 9 days after treatment, all *Notch1*<sup>+/ $\Delta$ TAD</sup> mice exhibited severe pancytopenia. For half of the *Notch1*<sup>+/ $\Delta$ TAD</sup> mice, the body-score condition index and body weight dropped below humane levels (body condition index = 2) (Figure 1B,C), and the animals were sacrificed.

We analyzed bone marrow LSK (Lin<sup>+</sup>Sca1<sup>+</sup>cKit<sup>+</sup>) progenitors and HSC (LSK<sup>+</sup>CD48<sup>+</sup>CD150<sup>+</sup>) after 5-FU treatment. *Notch1*<sup>+/ $\Delta$ TAD</sup> mice showed significant decreases in the numbers of BM progenitors and HSC (Figure 1E) 9 days after treatment. The BM-residing common lymphoid progenitors (CLP), thymic early T-cell precursors (ETP) and CD4<sup>+</sup>CD8<sup>-</sup> double negative 3 (DN3) T-cell progenitors were also significantly reduced in *Notch1*<sup>+/ $\Delta$ TAD</sup> mice after treatment (Figure 1F-H). Thymus size was reduced in 5-FU-treated *Notch1*<sup>+/ $\Delta$ TAD</sup> mice compared to controls (Figure 1I). These findings indicate that TAD-dependent Notch1 signaling plays a critical role in recovery of the hematopoietic system following myelosuppression.

To determine whether <sup>137</sup>Cs  $\gamma$  total body irradiation had a similar effect as 5-FU treatment, WT or *Notch1*<sup>+/ $\Delta$ TAD</sup> recipient mice (CD45.2<sup>+</sup>) were lethally irradiated and subsequently transplanted with 2.0x10<sup>6</sup> WT donor (CD45.1<sup>+</sup>) BM cells. Recipient mice were monitored for 90 days after irradiation/transplantation (*Online Supplementary Figure S2A*). We observed that the *Notch1*<sup>+/ $\Delta$ TAD</sup> mice suffered severe weight loss (*data not shown*) and 50% of them had low body-score condition leading to mortality 9 days following irradiation/transplantation (*Online Supplementary*

*Figure S2B*). Total body irradiation has a limited effect on enucleated erythroid cells<sup>1</sup> (*Online Supplementary Figure S2C*) but the numbers of white blood cells, neutrophils and lymphocytes were significantly lower in *Notch1*<sup>+/ $\Delta$ TAD</sup> mice than in controls (*Online Supplementary Figure S1B*). At the 9-day time point, the numbers of donor-derived HSC, ETP, and DN3 cells in the *Notch1*<sup>+/ $\Delta$ TAD</sup> recipient mice were markedly reduced (*Online Supplementary Figure S2D*), suggesting that the *Notch1*<sup>+/ $\Delta$ TAD</sup> BM microenvironment plays a critical role during hematopoietic recovery. However, 90 days after transplantation, the numbers of the donor-derived HSC, ETP, and DN3 populations were comparable between recipients (*Online Supplementary Figure S2E*) suggesting that in the surviving *Notch1*<sup>+/ $\Delta$ TAD</sup> recipients, hematopoietic homeostasis was normalized. Thus, early hematopoietic recovery following  $\gamma$  irradiation also depends on Notch1-TAD signaling.

### Transplantation with *Notch1*<sup>+/ $\Delta$ TAD</sup> hematopoietic stem cells reveals a cell-autonomous defect in T-cell development

We next investigated whether there was a pre-existing hematopoietic defect in *Notch1*<sup>+/ $\Delta$ TAD</sup> mice. Neither progenitors nor HSC were significantly affected in 6-week old *Notch1*<sup>+/ $\Delta$ TAD</sup> animals (*Online Supplementary Figure S3A*). No effect was seen in marginal zone B cells in the spleen or in B- and T-cell populations in the lymph nodes in *Notch1*<sup>+/ $\Delta$ TAD</sup> mice (*Online Supplementary Figure S3B, C*). The presence of a single *Notch1*- $\Delta$ TAD allele significantly reduced the frequency and number of thymic ETP and DN3 populations (*Online Supplementary Figure S3D, E*). This T-cell lineage defect could be traced to a reduction in the BM-residing CLP population (*Online Supplementary Figure S3F*). These findings show an inherent early role for Notch1-TAD signaling in the BM lymphoid progenitor population.

To investigate whether the effect of *Notch1*<sup>+/ $\Delta$ TAD</sup> on hematopoietic recovery is cell autonomous, 350 HSC from *Notch1*<sup>+/ $\Delta$ TAD</sup> or WT donors (CD45.2<sup>+</sup>) were transplanted into congenic (CD45.1<sup>+/2</sup>) recipients (Figure 2A). Reconstitution, defined by having 85-90% of blood cells in the recipients derived from *Notch1*<sup>+/ $\Delta$ TAD</sup> or WT donors, and multi-lineage potential was confirmed at 1, 2, and 3 months after transplantation (*Online Supplementary Figure S4A*). *Notch1*<sup>+/ $\Delta$ TAD</sup> HSC reconstituted recipients similarly to WT HSC. There were equal numbers of donor-derived LSK cells and HSC in recipient BM (*Online Supplementary Figure S4B*), indicating that *Notch1*<sup>+/ $\Delta$ TAD</sup> HSC were capable of homing and successfully engrafting into the WT recipient niche. In secondary transplants, mice receiving *Notch1*<sup>+/ $\Delta$ TAD</sup> BM cells had no defects in HSC reconstitution (*Online Supplementary Figure S4C, D*); however, the CLP, ETP, and DN3 populations were significantly reduced (*Online Supplementary Figure S4E, F*). This finding indicated an inherent T-cell defect resulting from loss of one *Notch1* TAD allele but also showed that HSC reconstitution was otherwise unaffected.

To test the effects of chemotherapy on the *Notch1*<sup>+/ $\Delta$ TAD</sup> hematopoietic system, we treated WT recipient mice reconstituted by *Notch1*<sup>+/ $\Delta$ TAD</sup> HSC with two rounds of 5-FU (Figure 2A). Recipients transplanted with *Notch1*<sup>+/ $\Delta$ TAD</sup> HSC exhibited no adverse effects when compared to those that received WT HSC (Figure 2B). Following treatment, comparable numbers of BM HSC were present in recipient mice (Figure 2C). Both sets of recipients had equivalent platelet, white blood cell, neutrophil, lymphocyte and red

blood cell counts as well as hemoglobin levels (*Online Supplementary Figure S4G*). 5-FU treatment continued to affect the recovery of the T-cell lineage populations originating from *Notch1<sup>+/-ΔTAD</sup>* donors (Figure 2D-F), which led to a 50% decrease in thymic mass (Figure 2G). Our findings showed that loss of a single *Notch1* TAD allele markedly impaired T-cell development in the reconstituted WT recipients, but had no other adverse effects on hematopoiesis.

### *Notch1* haploinsufficiency has no effect on hematopoietic recovery

To test whether *Notch1* haploinsufficiency can account for pancytopenia, weight loss and morbidity after chemotherapy, we treated *Notch1<sup>+/-</sup>* mice with 5-FU (*Online Supplementary Figure S5A*). *Notch1<sup>+/-</sup>* mice exhibited no significant difference in body score index compared to WT mice and had no discernable hematopoietic phenotype (*Online Supplementary Figure S5B, C*). Furthermore, no dif-

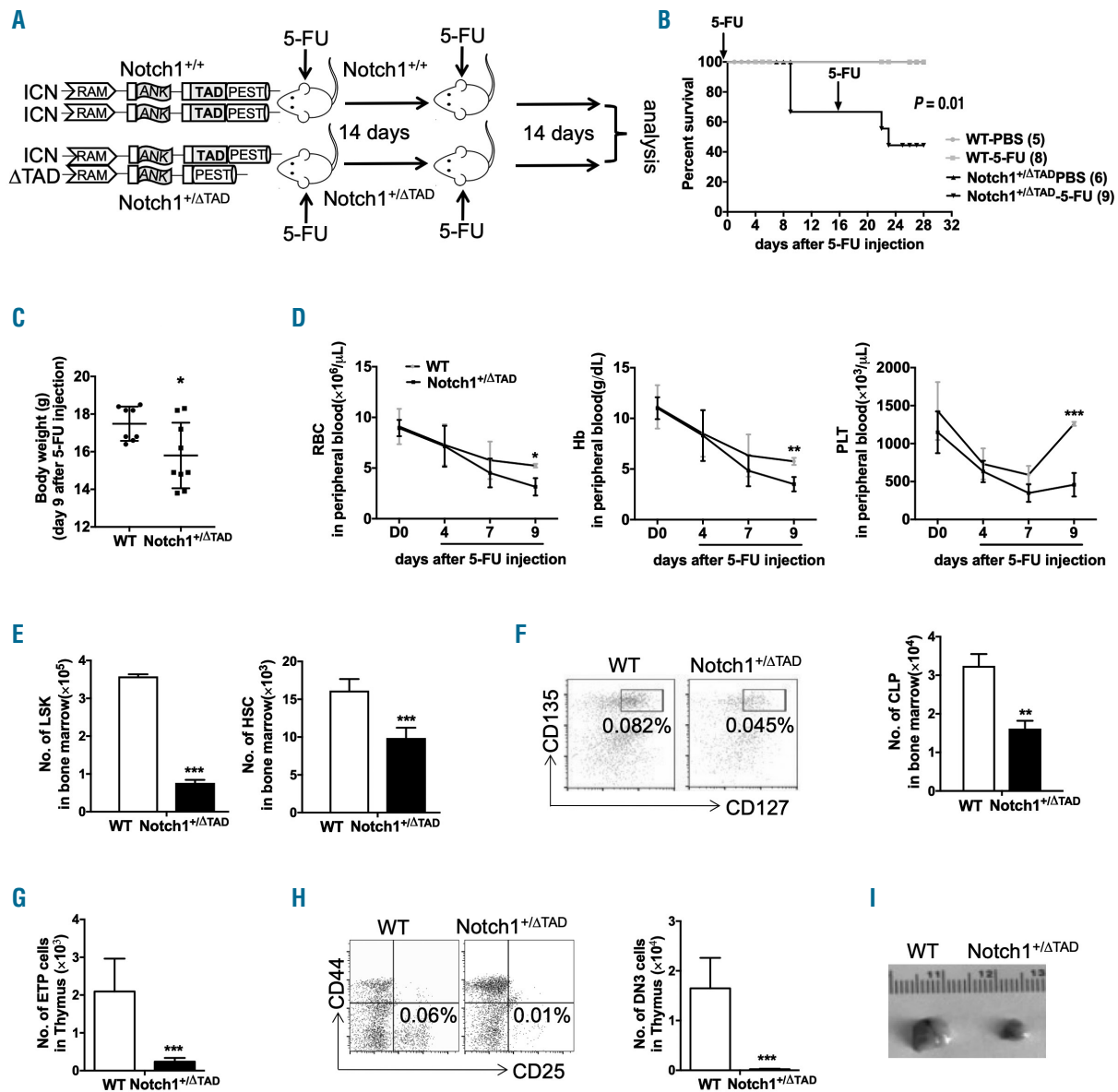


**Figure 1. Limited recovery of *Notch1<sup>+/-ΔTAD</sup>* mice after chemotherapeutic stress.** (A) Experimental design of 5-fluorouracil (5-FU) injection. 5-FU (150 mg/kg) was injected intraperitoneally into *Notch1<sup>+/+</sup>* (WT) and *Notch1<sup>+/-ΔTAD</sup>* 5-week old mice on days 1 and 14. (B) Kaplan-Meier plot indicating survival of WT and *Notch1<sup>+/-ΔTAD</sup>* mice after 5-FU injection. Mice ( $n=5-9$ ) were monitored daily until terminal analysis at day 28 after the first 5-FU injection. The statistical significance ( $P=0.01$ ) between WT and *Notch1<sup>+/-ΔTAD</sup>* 5-FU-treated littermates was determined by the Mantel-Cox test. (C) Body weight of WT and *Notch1<sup>+/-ΔTAD</sup>* mice 9 days after 5-FU injection. (D) Red blood cell (RBC) and platelet (PLT) counts and hemoglobin (Hb) concentration were determined from peripheral blood of WT and *Notch1<sup>+/-ΔTAD</sup>* mice ( $n=5-9$  mice/group) before (D0) and at days 4, 7 and 9 after 5-FU injection. (E) Numbers of hematopoietic stem cells (HSC) and LinSca1<sup>+</sup>cKit<sup>+</sup> (LSK) progenitors in the bone marrow were analyzed 9 days after 5-FU injection. HSC were defined as Lin<sup>+</sup>cKit<sup>+</sup>Sca1<sup>+</sup>CD150<sup>+</sup>CD48<sup>+</sup> cells. The numbers of each population are expressed as mean  $\pm$  standard deviation (SD). (F) Cytometric analysis of common lymphoid progenitors (CLP) in bone marrow from WT and *Notch1<sup>+/-ΔTAD</sup>* mice at day 14 after 5-FU injection. CLP were defined as Lin<sup>+</sup>cKit<sup>+</sup>Sca1<sup>+</sup>CD135<sup>+</sup>CD127<sup>+</sup> (left panel). Absolute numbers of CLP from each mouse are expressed as mean  $\pm$  SD (right panel). (G, H) Cytometric analysis of early T-cell precursors (ETP) and double-negative 3 (DN3) cells in the thymus from WT and *Notch1<sup>+/-ΔTAD</sup>* mice at day 14 after 5-FU injection. ETP and DN3 populations were defined as Lin<sup>+</sup>cKit<sup>+</sup>CD25<sup>+</sup>CD144<sup>+</sup> (G) and Lin<sup>+</sup>CD4<sup>+</sup>CD8<sup>+</sup>CD44<sup>+</sup>CD25<sup>+</sup> (H), respectively. Absolute numbers of ETP and DN3 cells from each mouse are expressed as mean  $\pm$  SD. (I) Representative images of the thymus from WT and *Notch1<sup>+/-ΔTAD</sup>* mice at day 14 after 5-FU injection. \* $P < 0.05$ , \*\* $P < 0.01$ , \*\*\* $P < 0.001$ . ICN: intracellular domains of Notch; TAD: transcriptional activation domain; RAM: RBP-J-associated molecule domain; ANK: ankyrin repeats.

ferences were observed between *WT* and *Notch1*<sup>+/-</sup> littermates in hematopoietic progenitors and lineages in the BM and thymus (*Online Supplementary Figure S5D-H*). These findings show that a single allele of the *Notch1* receptor

was sufficient for recovery of the hematopoietic system and development of the T-cell lineage following myelosuppression. Thus, the phenotype observed in *Notch1*<sup>+/ $\Delta$ TAD</sup> mice was unique and depended on the function of the TAD.

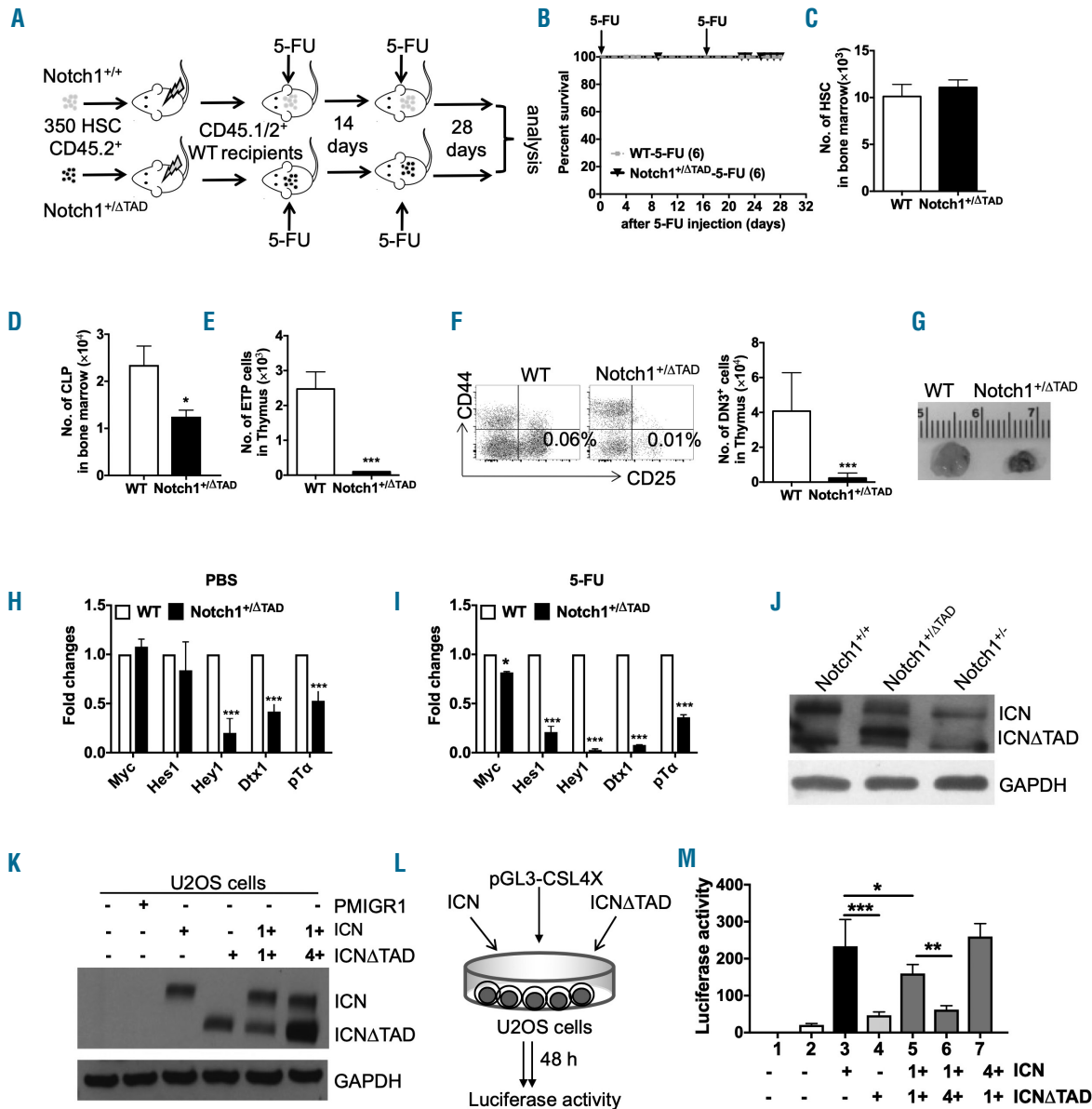


**Figure 2. Transcriptional defect in T-cell development induced by *Notch1*<sup>+/ $\Delta$ TAD</sup>.** (A) Experimental design of 5-fluorouracil (5-FU) treatment of recipient mice reconstituted with hematopoietic stem cells (HSC) from *Notch1*<sup>+/ $\Delta$ TAD</sup> mice. Three hundred and fifty HSC from 5-week old wildtype (*WT*) or *Notch1*<sup>+/ $\Delta$ TAD</sup> donors were sorted and transplanted into irradiated CD45.1/2<sup>+</sup> WT recipients. After transplantation, 5-FU (150 mg/kg) was injected intraperitoneally into recipient mice on days 1 and 14. (B) Kaplan-Meier plot after 5-FU injection of recipients reconstituted by either *WT* or *Notch1*<sup>+/ $\Delta$ TAD</sup> HSC. Mice (n=6/group) were monitored daily until day 28 after the first 5-FU injection. Statistical significance was determined using the Mantel-Cox test. (C) Absolute numbers of donor-derived HSC in the bone marrow 14 days after the 5-FU injection. (D) Absolute numbers of donor-derived common lymphoid progenitors (CLP) in bone marrow at day 14 after the 5-FU injection are shown as mean  $\pm$  standard deviation (SD). (E, F) Cytometric analysis and quantification of donor-derived early T-cell precursors (ETP) and double-negative 3 (DN3) cells from the thymus of reconstituted mice at day 14 after 5-FU injection. Absolute numbers are shown as mean  $\pm$  SD. (G) Representative images of the thymus from recipient mice at day 14 after 5-FU injection. (H, I) Expression of the indicated genes in the DN3 population from *WT* or *Notch1*<sup>+/ $\Delta$ TAD</sup> mice (n=3). Thymic DN3 cells collected by flow-activated cell sorting at day 9 after injection of phosphate-buffered saline (PBS) (H) or 5-FU (I). Fold changes in the relative gene expression in *Notch1*<sup>+/ $\Delta$ TAD</sup> DN3 cells are shown normalized to *WT* expression and GAPDH. (J) Expression of Notch1-ICN and Notch1-ICN $\Delta$ TAD in CD25<sup>+</sup> thymocytes (n=3). CD25<sup>+</sup> thymocytes from *WT*, *Notch1*<sup>+/ $\Delta$ TAD</sup> and *Notch1*<sup>-/-</sup> mice were isolated by anti-CD25 dynabead magnetic sorting and whole cells were lysed to measure protein expression of cleaved Notch1 ICN (val1744) by western blot. ICN is 100 kDa, ICN $\Delta$ TAD is 75 kDa, and a non-specific band of ~65kDa is seen in all three lanes. (K) U2OS cells transfected with pMIGR1 control vector, pMIGR1-Notch1 ICN and pMIGR1-Notch1 ICN $\Delta$ TAD. At 48 h, protein expression of Notch1 ICN and Notch1 ICN $\Delta$ TAD was measured by western blot. (L) Experimental design of the luciferase assay. U2OS cells were transfected with reporters pRL-TK, pGL3-CSL4X, and with either pMIGR1 control vector or ICN or ICN $\Delta$ TAD or both ICN and ICN $\Delta$ TAD at indicated ratios (n=3). (M) Firefly luciferase activity was measured relative to renilla luciferase activity. Values are shown relative to the empty vector. \**P*<0.05, \*\**P*<0.01, \*\*\**P*<0.001.

### Transcriptional defect in *Notch1*<sup>+/ΔTAD</sup> impairs T-cell development

Notch function in T-cell development has been well documented,<sup>27,28</sup> so to determine how lack of a single TAD allele affects T cells, we measured target expression in sorted WT and *Notch1*<sup>+/ΔTAD</sup> DN3 cells before and after 5-FU treatment. During resting conditions, no significant change was observed in the expression of *Hes1* or *Myc*, but a decrease in the levels of *Hey1* and *Dtx1* was seen in *Notch1*<sup>+/ΔTAD</sup> DN3 cells (Figure 2H). However, the expression of *Hes1*, *Hey1*, and *Dtx1* was severely reduced after 5-FU treatment, and expression of pre-T-cell receptor alpha ( $\nu T\alpha$ ) and *Myc* was moderately reduced (Figure 2I), suggesting that Notch1ΔTAD strongly impairs target gene expression in developing thymocytes during regeneration.

To determine whether production of active Notch1 was equal among our different model systems, CD25<sup>+</sup> thymocytes were isolated from WT, *Notch1*<sup>+/−</sup>, and *Notch1*<sup>+/ΔTAD</sup> mice. The abundance of cleaved, full-length intracellular domains of Notch (ICN) was comparable between *Notch1*<sup>+/−</sup> and *Notch1*<sup>+/ΔTAD</sup> samples; however, there was an accumulation and a nearly 3-fold increase of the levels of cleaved ICN ΔTAD protein (Figure 2J).

Next, we employed an *in vitro* U2OS-based Notch luciferase reporter assay to assess the effects of accumulated ICN ΔTAD on transcription.<sup>29</sup> We chose U2OS cells, a human osteosarcoma cell line, because they express very low levels of endogenous Notch signaling and are highly transfectable. Constructs expressing Notch1 WT or ΔTAD mutant were transfected into U2OS cells at various ratios of ICN to ICNΔTAD (Figure 2K, L). ICNΔTAD had a lower capacity of transcriptional activation compared to ICN (Figure 2M, lanes 3 and 4). Dose-dependent transcriptional inhibition was observed when ICNΔTAD was co-transfected with ICN. The presence of a 1:4 ratio of ICN:ICNΔTAD caused a 4-fold decrease in luciferase activity (Figure 2M, lane 6). This TAD-dependent regimen was rescued by inverting the ratio of ICN to ICNΔTAD (Figure 2M, lane 7). Our findings uncovered a role for the ΔTAD-mediated suppression of WT Notch signaling which we termed TAD transcriptional interference. These findings showed that the presence of a Notch1ΔTAD protein impaired Notch target expression. Since Notch signaling is crucial for T-lineage development, we conclude that this transcriptional interference negatively affected *in vivo* development of thymocytes.

### Chemotherapy severely damages bone marrow microvasculature and induces endothelial cell apoptosis in *Notch1*<sup>+/ΔTAD</sup> mice

Our findings suggest that the cell-intrinsic hematopoietic defect in *Notch1*<sup>+/ΔTAD</sup> is limited to the T-cell lineage, which cannot account for the pancytopenia, morbidity, and the eventual mortality observed in the *Notch1*<sup>+/ΔTAD</sup> mice (Figures 1 and 2). Thus, our attention turned to the BM microenvironment. First, to elucidate whether loss of one copy of TAD in the *Notch1* locus affects bone and mesenchymal cells, we performed micro-computed tomography analysis of femoral bones. This assay indicated comparable bone length, bone volume fraction (BV/TV) and cortical thickness in WT and *Notch1*<sup>+/ΔTAD</sup> mice (Online Supplementary Figure S6A-C). Furthermore, CD51 and Sca1 were used to identify osteoblasts and mesenchymal stem/precursor cells.<sup>30</sup> Flow cytometry analysis showed that there were similar numbers of osteoblasts

and mesenchymal stem/precursor cells in digested bones from WT and *Notch1*<sup>+/ΔTAD</sup> mice (Online Supplementary Figure S6D, E). These data indicate that loss of one copy of *Notch1* TAD does not significantly affect bone development in *Notch1*<sup>+/ΔTAD</sup> mice.

To test whether the presence of one *Notch1*ΔTAD allele affects formation of the bone vasculature network, whole-mount sternal imaging was conducted. Imaging of the vasculature labeled by CD31 and VE-cadherin showed comparable vessel number and vessel length between WT and *Notch1*<sup>+/ΔTAD</sup> mice under resting conditions (Figure 3A). Next, we wanted to determine the effect of chemotherapy on the recovery and regeneration of BM EC and specifically the sinusoidal EC, which have been shown to be crucial components of the adult hematopoietic niche.<sup>31–33</sup> Primary bone CD31<sup>+</sup> EC (pBEC) were harvested from WT mice 3 days after 5-FU treatment. Expression of the *Notch1* receptor and several Notch canonical gene targets were upregulated after the chemotherapy (Figure 3B). Target gene upregulation corresponded with Notch1 receptor cleavage (Figure 3B, inset), showing an increase in Notch activation which occurred in pBEC as early as 3 days after 5-FU treatment.

To determine the condition of the BM EC niche at the time point when the *Notch1*ΔTAD-expressing heterozygous hypomorphs succumb to myelosuppressive treatment, pBEC in WT or *Notch1*<sup>+/ΔTAD</sup> littermates were analyzed 9 days after 5-FU treatment (Figure 3C). Annexin V staining showed that 20% of the pBEC in *Notch1*<sup>+/ΔTAD</sup> mice were apoptotic compared to <7% of WT pBEC (Figure 3D). This sorted pBEC population from digested bones, over 90% of which expressed CD31<sup>+</sup> and less than 5% expressed CD45<sup>+</sup> (Figure 3E, left panel), was further analyzed for expression of pro-apoptotic genes. A corresponding 2-fold increase in the expression of *Puma* and *Bax*<sup>34</sup> was observed in sorted *Notch1*<sup>+/ΔTAD</sup> pBEC (Figure 3E, right panel). Absolute numbers of *Notch1*<sup>+/ΔTAD</sup> pBEC were markedly decreased, reflecting apoptosis (Figure 3F).

To visualize the BM microenvironment,<sup>35</sup> sections of the tibia of WT and *Notch1*<sup>+/ΔTAD</sup> littermates were analyzed before and after chemotherapy. Under resting conditions, as suggested by the whole mount imaging of the sternum (Figure 3A), there was no difference in the abundance of hematopoietic cells in the BM, and similar CD31<sup>+</sup> and endomucin<sup>+</sup> sinusoidal endothelial structures were present in WT and *Notch1*<sup>+/ΔTAD</sup> littermates (Figure 3G–I, top panels). After 5-FU treatment, retention of hematopoietic cells was markedly reduced in *Notch1*<sup>+/ΔTAD</sup> BM (Figure 3G, bottom panel). Severe damage to the BM niche following 5-FU treatment was evident by the lack of CD31<sup>+</sup> cells and irregular endomucin<sup>+</sup> endothelial staining in the *Notch1*<sup>+/ΔTAD</sup> mice following this treatment (Figure 3H–I, bottom panel). Overall, our findings indicate that the hematopoietic defect observed in *Notch1*<sup>+/ΔTAD</sup> mice can be attributed to the failure of endothelial regeneration after chemotherapy.

### Endothelial cell-specific deletion of Notch1 receptor confirms the requirement for endothelial Notch signaling during niche recovery

To specify a tissue-specific role for Notch signaling in the recovery and regeneration of BM EC, *Notch1*<sup>fl/VE-cadherin-Cre<sup>ERT2</sup>+</sup> mice were treated with tamoxifen 1 week prior to administration of 5-FU (Figure 4A). The tamoxifen regimen led to loss of Notch1 protein (Figure 4B) and a

decrease in Notch target expression (Figure 4C) in pBEC. The condition of *Notch1<sup>fl</sup>VE-cadherin-Cre<sup>ERT2+</sup>* mice deteriorated (body condition index = 2) within a week after treatment, and five of 13 mice succumbed between days 7-9 after treatment (Figure 4D). The morbidity of *Notch1<sup>fl</sup>VE-cadherin-Cre<sup>ERT2+</sup>* mice was reflected in the low peripheral blood counts (Figure 4E) as well as decreases in the numbers of BM HSC, progenitors and CLP (Figure 4F, G). Consistent with increased endothelial apoptosis after treatment, the absolute number of pBEC in *Notch1<sup>fl</sup>VE-cadherin-Cre<sup>ERT2+</sup>* mice was significantly reduced (Figure 4H, I).

Besides the endothelium, perivascular cells have been implicated in the regulation of HSC function.<sup>36</sup> We observed a decrease in numbers of BM PDGFRβ<sup>+</sup> pericytes after chemotherapy in *Notch1<sup>+/ΔTAD</sup>* mice. However, this effect was not due to increased apoptosis of the pericytes and may be attributed to a previously described loss of

BM EC (Online Supplementary Figure S7A). To determine whether Notch signaling in pericytes played a role in the recovery of the BM niche, *RBPJ<sup>fl</sup>-PDGFRβ-Cre<sup>ERT2+</sup>* and *RBPJ<sup>fl</sup>-PDGFRβ-Cre<sup>ERT2+</sup>* littermates were treated first with tamoxifen and then with 5-FU (Online Supplementary Figure S7B, C). We observed no significant hematopoietic differences between the two cohorts after 5-FU treatment (Online Supplementary Figure S7D-I). Overall these results show that robust Notch signaling in EC is essential for recovery of the BM niche following chemotherapeutic challenge.

### Loss of the transcriptional activation domain suppresses transcriptional activation of Notch1 targets in endothelial cells

To determine whether the ΔTAD-dependent transcriptional interference observed in T cells also occurred EC

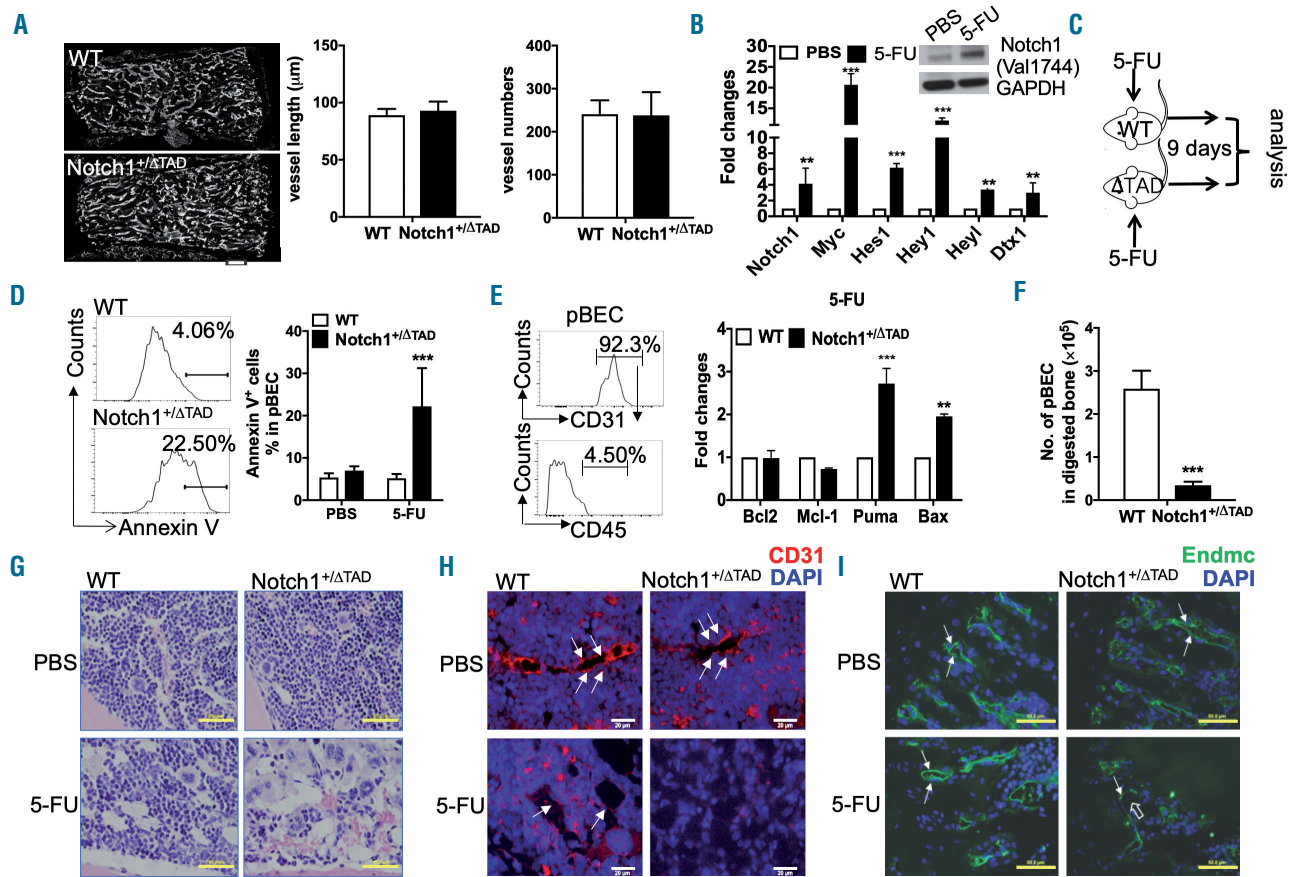


**Figure 3. Defective recovery of endothelial niche induced by *Notch1<sup>ΔTAD</sup>*.** (A) Whole mount imaging of the sternal vasculature after staining for CD31 and VE-cadherin was performed in WT and *Notch1<sup>ΔTAD</sup>* mice under resting conditions, including analysis of vessel length and vessel numbers (n=4). Scale bar=150 μm. (B) CD31<sup>+</sup> primary bone endothelial cells (pBEC) were isolated at day 3 after 5-fluorouracil (5-FU) injection and expression of the indicated genes was determined by quantitative reverse transcriptase polymerase chain reaction (RT-qPCR) normalized to expression of genes after injection of phosphate-buffered saline (PBS) (n=3). GAPDH was used as an internal expression control. Levels of active Notch1 protein in pBEC were measured by western blot at day 3 after 5-FU injection (insert). (C) Experimental design of 5-FU treatment for endothelial cell analysis in bone marrow (n=6). (D) pBEC harvested from long bones of WT and *Notch1<sup>ΔTAD</sup>* littermates gated for 4',6-diamidino-2-phenylindole (DAPI)CD45<sup>+</sup>TER119<sup>+</sup>CD31<sup>+</sup> and analyzed by flow cytometry for annexin V at day 9 after PBS or 5-FU injection (left panel). Percentages of annexin V<sup>+</sup> cells in CD31<sup>+</sup> endothelial cells (pBEC) are presented as mean±SD (right panel). (E) Isolated pBEC from digested bones were stained with DAPI/CD45/TER119/CD31<sup>+</sup>. The purity of CD31<sup>+</sup> cells as a percent of CD31<sup>+</sup>CD45<sup>+</sup> cells is demonstrated in the histogram analysis (left panel). The expression of indicated genes was determined by RT-qPCR in pBEC isolated from WT and *Notch1<sup>ΔTAD</sup>* mice at day 7 after 5-FU injection (right panel). Fold changes in the relative gene expression, normalized to WT samples with GAPDH used as an internal expression control, are shown as mean±SD. (F) Absolute numbers of pBEC (DAPI/CD45/TER119/CD31<sup>+</sup>) were analyzed at day 9 after 5-FU injection by flow cytometry. (G) Representative longitudinal bone sections from mice treated with PBS (upper panels) or 5-FU (lower panels) stained with hematoxylin and eosin-Y at day 9 after 5-FU treatment. Scale bar=50 μm. (H, I) Representative longitudinal bone section from mice treated with PBS (upper panels) or 5-FU (lower panel) fixed with formalin and stained for CD31 (H, red, scale bar=20 μm) or endomucin (endmC) (I, green, scale bar=100 μm) at day 9 after 5-FU injection. DAPI was used to stain nuclei (blue). Filled white arrows point to vascular structures representative of the bone marrow endothelium. The open white arrow points to discontinuous vascular structures. \*\**P*<0.01, \*\*\**P*<0.001.

and whether it affected the recovery of EC in the BM niche, we tested the expression of Notch target genes in pBEC. Under basal conditions, expression of *Hes1*, *Hey1* and *Dtx1* was downregulated in *Notch1<sup>ΔTAD</sup>* pBEC, while expression of *Myc* and *EphB2* was unaffected (Figure 5A). However, 9 days after 5-FU treatment, expression of the

Notch target genes *EphB2*, *Myc*, *Hes1*, *Hey1* and *Dtx1* was markedly downregulated in *Notch1<sup>ΔTAD</sup>* pBEC (Figure 5B). To determine how Notch target expression was affected by the *Notch1ΔTAD* mutant, a chromatin immunoprecipitation assay was performed on purified pBEC from WT or *Notch1<sup>ΔTAD</sup>* littermates after 5-FU treatment. The chromatin

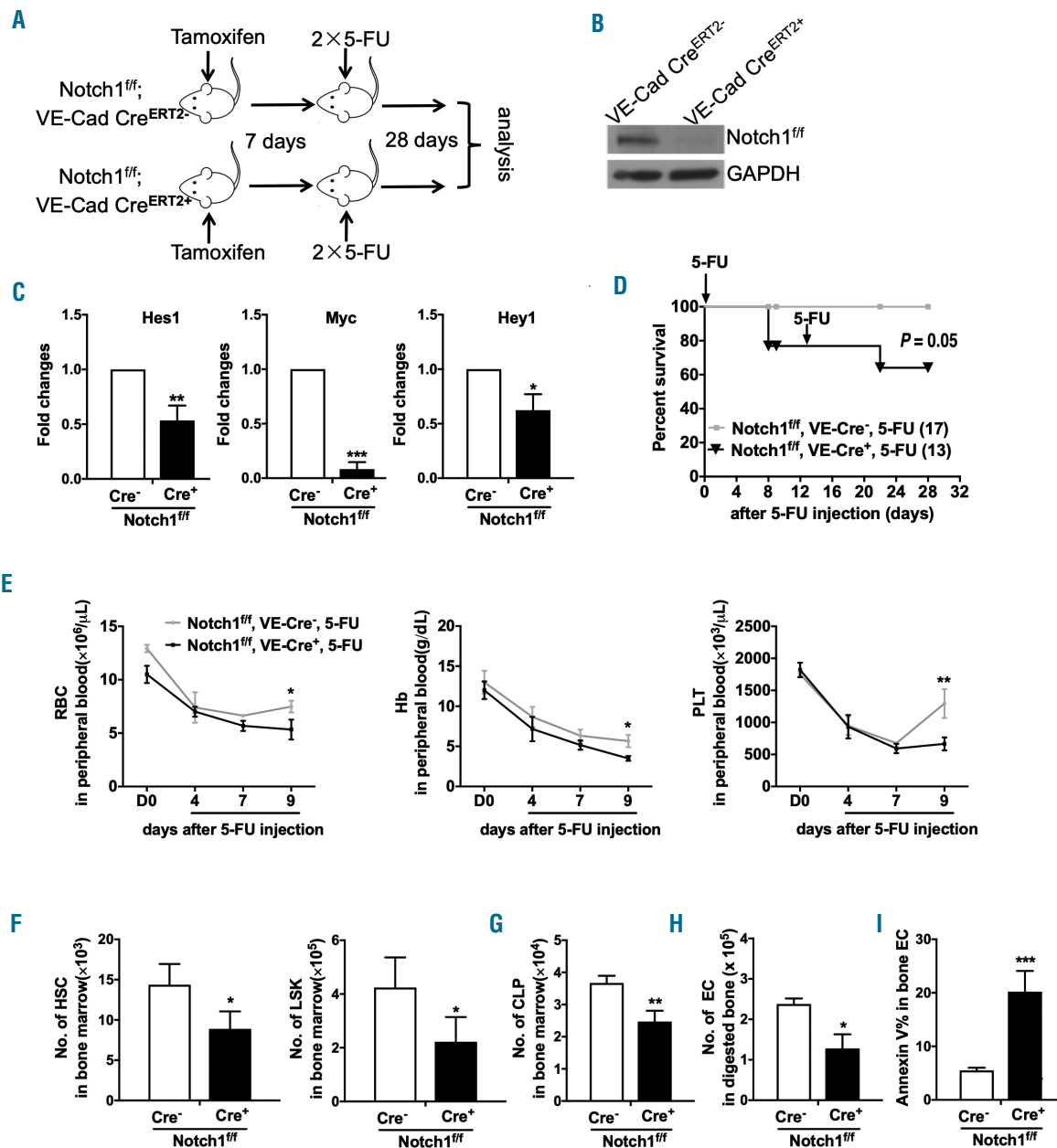


**Figure 4. Conditional deletion of *Notch1* in endothelial cells phenocopies *Notch1<sup>ΔTAD</sup>* mice after myelosuppression.** (A) Experimental design of 5-fluorouracil (5-FU) injection of *Notch1<sup>ff</sup>;VE-CadherinCre<sup>ERT2+</sup>* mice. Tamoxifen (80 mg/kg) was injected intraperitoneally (IP) into *Notch1<sup>ff</sup>;VE-CadherinCre<sup>ERT2+</sup>* mice for 5 consecutive days. One week later, 5-FU (150 mg/kg) was injected IP into *Notch1<sup>ff</sup>;VE-CadherinCre<sup>ERT2+</sup>* or *Cre<sup>ERT2+</sup>* littermates on days 1 and 14. (B) Protein expression of cleaved Notch1 in CD31<sup>+</sup> primary bone endothelial cells (pBEC) from *Notch1<sup>ff</sup>;VE-CadherinCre<sup>ERT2+</sup>* or *Cre<sup>ERT2+</sup>* littermates after tamoxifen treatment. GAPDH was used as a loading control. (C) Quantitative reverse transcriptase polymerase chain reaction (RT-qPCR) expression of *Hes1*, *Myc*, *Hey1* and *Dtx1* in pBEC harvested from *Notch1<sup>ff</sup>;VE-CadherinCre<sup>ERT2+</sup>* or *Cre<sup>ERT2+</sup>* littermates after tamoxifen and 5-FU treatment. (D) Kaplan-Meier plot of *Notch1<sup>ff</sup>;VE-CadherinCre<sup>ERT2+</sup>* and *Notch1<sup>ff</sup>;VE-CadherinCre<sup>ERT2+</sup>* littermates after tamoxifen and 5-FU treatment. Mice were monitored daily until day 28 after 5-FU injection (n=13-17 mice/group). Significance (P=0.05) was determined by the Mantel-Cox test. (E) Peripheral blood counts of red blood cells (RBC) and platelets (PLT), and concentration of hemoglobin (Hb) in *Notch1<sup>ff</sup>;VE-CadherinCre<sup>ERT2+</sup>* and *Cre<sup>ERT2+</sup>* littermates were conducted before (D0) and at days 4, 7 and 9 after 5-FU injection. (F) Absolute numbers of hematopoietic stem cells (HSC) and LinSca1<sup>+</sup>c-kit<sup>+</sup> (LSK) cells in bone marrow were analyzed 9 days after the 5-FU injection and expressed as mean ± standard deviation (SD). (G) Absolute numbers of common lymphoid progenitors (CLP) in bone marrow were analyzed at day 9 after the 5-FU injection and expressed as mean ± SD. (H) Absolute numbers of pBEC were analyzed at day 9 after the 5-FU injection by flow cytometry. (I) Percentages of annexin V<sup>+</sup> Lin-Sca1<sup>+</sup>c-Kit<sup>+</sup> pBEC 9 days after 5-FU injection are presented as mean ± SD. \*P<0.05, \*\*P<0.01, \*\*\*P<0.001.

immunoprecipitation assay showed reduction of Notch1 occupancy at the Notch-dependent Myc enhancer *NDME*<sup>37</sup> and at *Hes1*, *Hey1* and *Dtx1* promoters<sup>38</sup> in *Notch1*<sup>+ΔTAD</sup> pBEC (Figure 6C). In line with our findings in thymocytes (Figure 2J), we observed a 3-fold accumulation of Notch1 ICN ΔTAD protein in pBEC when compared to cleaved Notch1 WT protein (Figure 5D). These results indicate that ΔTAD interference occurred in pBEC and contributed to the decreased target gene expression in EC, thus limiting regeneration and recovery of the BM niche.

For further *in vitro* study of ΔTAD transcriptional interference, pBEC were sorted from the BM by expression of CD31<sup>+</sup> and VE-cadherin<sup>+</sup> (*Online Supplementary Figure S8A*). These cultured bone EC (cBEC) exhibited typical endothelial morphology, VE-cadherin<sup>+</sup> adherent junctions and active Notch signaling (*Online Supplementary Figure S8B, C*). To replicate the effects of ΔTAD interference, we transduced cBEC with a retroviral vector expressing GFP (PMIGR1) or ICNΔTAD (Figure 5E, left). Accumulation of ICNΔTAD protein in GFP<sup>+</sup> sorted cBEC

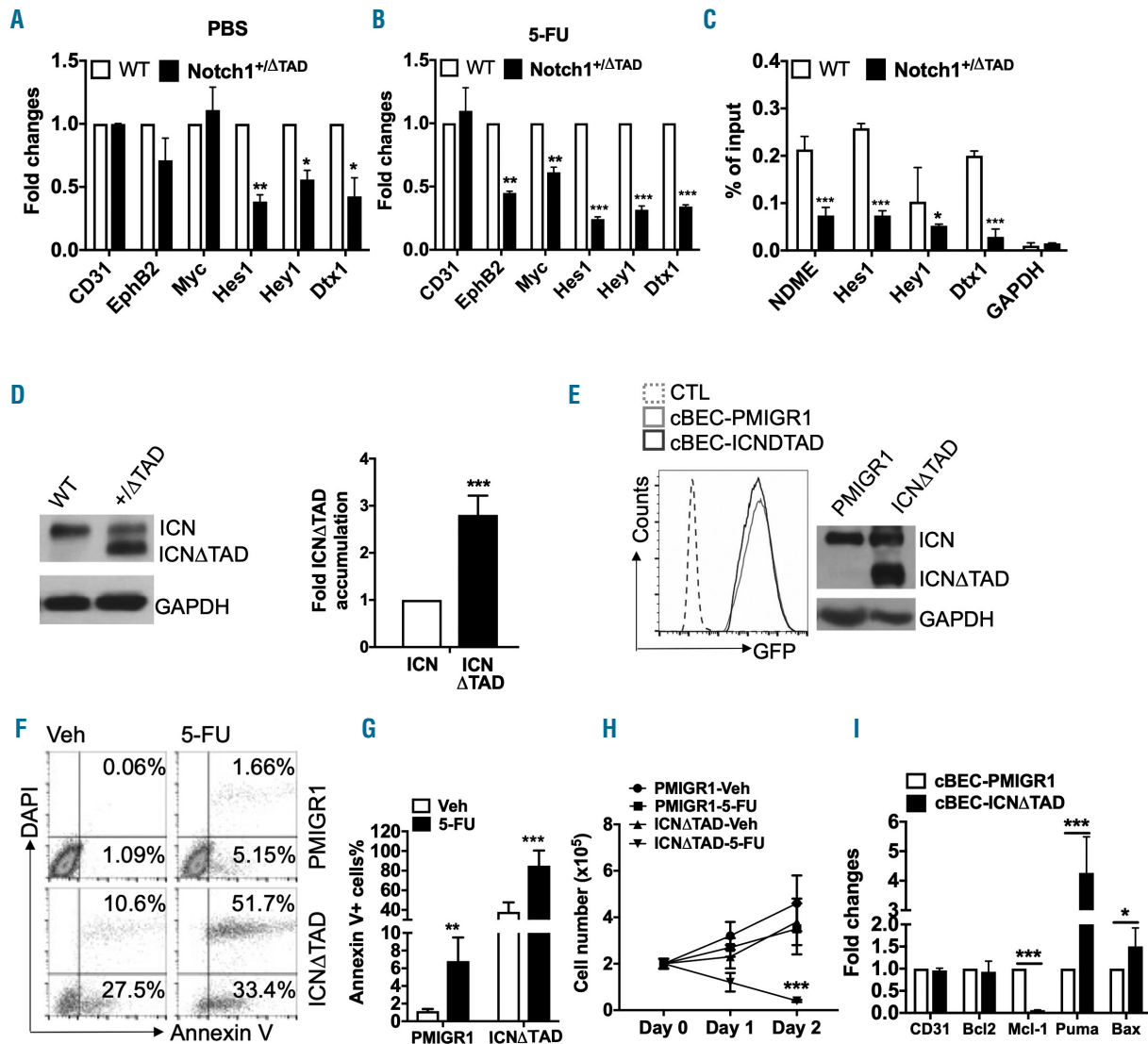


**Figure 5. Notch1 ICNΔTAD interference in bone marrow endothelial cells.** (A, B) The expression of the indicated genes was determined by quantitative reverse transcriptase polymerase chain reaction (RT-qPCR) in CD31<sup>+</sup> primary bone endothelial cells (pBEC) at day 9 after treatment of wildtype (WT) and *Notch1*<sup>+ΔTAD</sup> littermates (n=3) with phosphate-buffered saline (PBS) or 5-fluorouracil (5-FU). Values were normalized to expression of genes in WT littermates. *GAPDH* was used as an internal expression control. (C) Local chromatin immunoprecipitation (CHIP) assay to detect the occupancy of Notch1 complex on Rbpj DNA-binding sites of Notch-dependent Myc enhancer (*NDME*), *Hes1*, *Hey1*, *Dtx1* and *GAPDH* promoter elements. pBEC from WT and *Notch1*<sup>+ΔTAD</sup> mice were used for CHIP analysis at day 9 after 5-FU treatment (n=3). Values represent the mean of signal intensity relative to input DNA normalized to IgG. (D) pBEC from WT and *Notch1*<sup>+ΔTAD</sup> mice were harvested and used to measure protein levels of cleaved Notch1 and Notch1ΔTAD by western blot (left panel). The band intensities of Notch1 ICN and Notch1 ICNΔTAD in *Notch1*<sup>+ΔTAD</sup> pBEC were quantified by ImageJ software (n=3, right panel). (E) Flow cytometry analysis of cultured bone marrow-derived endothelial cells (cBEC) (untransduced control) or cBEC transduced with retrovirus expressing PMIGR1 or PMIGR1-ICNΔTAD (left panel). Western blot analysis for expression of Notch1 protein in transduced and sorted GFP<sup>+</sup> cBEC expressing PMIGR1 or PMIGR1-ICNΔTAD. *GAPDH* was used as a loading control (n=3, right panel). (F, G) cBEC transduced with PMIGR1 or PMIGR1-ICNΔTAD were treated with 5-FU or vehicle (Veh) for 24 h (n=3). Representative annexin V and 4',6-diamidino-2-phenylindole (DAPI) flow cytometry analysis (F) and quantified percentages of pro-apoptotic annexin V<sup>+</sup> cells (G). (H) Cell counts of cBEC-PMIGR1 and cBEC-ICNΔTAD after Veh or 5-FU treatment. Cell numbers were counted at day 1 and day 2 after a single 5-FU treatment (n=3). (I) RT-qPCR for the indicated genes in cBEC-PMIGR1 and cBEC-ICNΔTAD cells 24 h after 5-FU treatment. Values were normalized to PMIGR1 transduced cells. *GAPDH* was used as an internal expression control. \**P*<0.05, \*\**P*<0.01, \*\*\**P*<0.001.

was confirmed by western blot analysis (Figure 5E, right).

Increased ICNΔTAD in cBEC markedly impaired the expression of *Hey1* and *Dtx1* and significantly downregulated the expression of *Myc* (Online Supplementary Figure S8D). To mimic chemotherapy *in vitro*, cBEC were treated with 100 μM of 5-FU. After 24 h, the cells were analyzed for apoptosis by flow cytometry. We observed that 27% of cBEC-ICNΔTAD cells were pro-apoptotic (annexin V<sup>+</sup>) under resting conditions; furthermore, the apoptotic cells (annexin V<sup>+</sup>/DAPI<sup>+</sup>) cells increased to 50% in 5-FU-treated cBEC-ICNΔTAD (Figure 5F, G). Apoptosis of cBEC-ICNΔTAD led to a rapid decrease in cell numbers 48 h after 5-FU treatment (Figure 5H). This finding was validated by a decrease of Mcl-1 expression and an increase of Puma and Bax expression in cBEC-ICNΔTAD (Figure 5I). These findings corroborate the *in vivo* phenotype observed in freshly isolated BM EC and indicate the importance of Notch signaling in the recovery and survival of EC after chemotherapy.

### Both Notch1 and Tie2 signaling are activated during recovery of bone marrow endothelium

Tie2 signaling has been proposed to facilitate endothelial regeneration.<sup>2,39</sup> Thus, we compared the expression of the *Notch1* and *Tie2* receptors 3, 5, and 7 days after 5-FU treatment in the pBEC of WT mice. Tie2 expression was low in resting pBEC and rapidly increased by 10-fold at day 5 after 5-FU treatment (Figure 6A). This increase in Tie2 expression corresponded with a significant increase in the phosphorylation of Tie2 protein (p-Tie2) (Figure 6B, right panel). Expression of *Notch1* receptor was increased 4-fold after treatment, but *Notch1* receptor expression and activation remained high throughout until day 7 (Figure 6A, B). Previous work has suggested that activation of Tie2 signaling by Ang1 in human vascular EC results in increased induction of Notch ligand delta-like 4 (Dll4).<sup>40</sup> To test this *in vivo*, we treated WT mice with 5-FU (Figure 6C). Five days later, expression of *Dll4* and *Jag1*, determined by analysis of both mRNA (Figure 6D) and protein levels

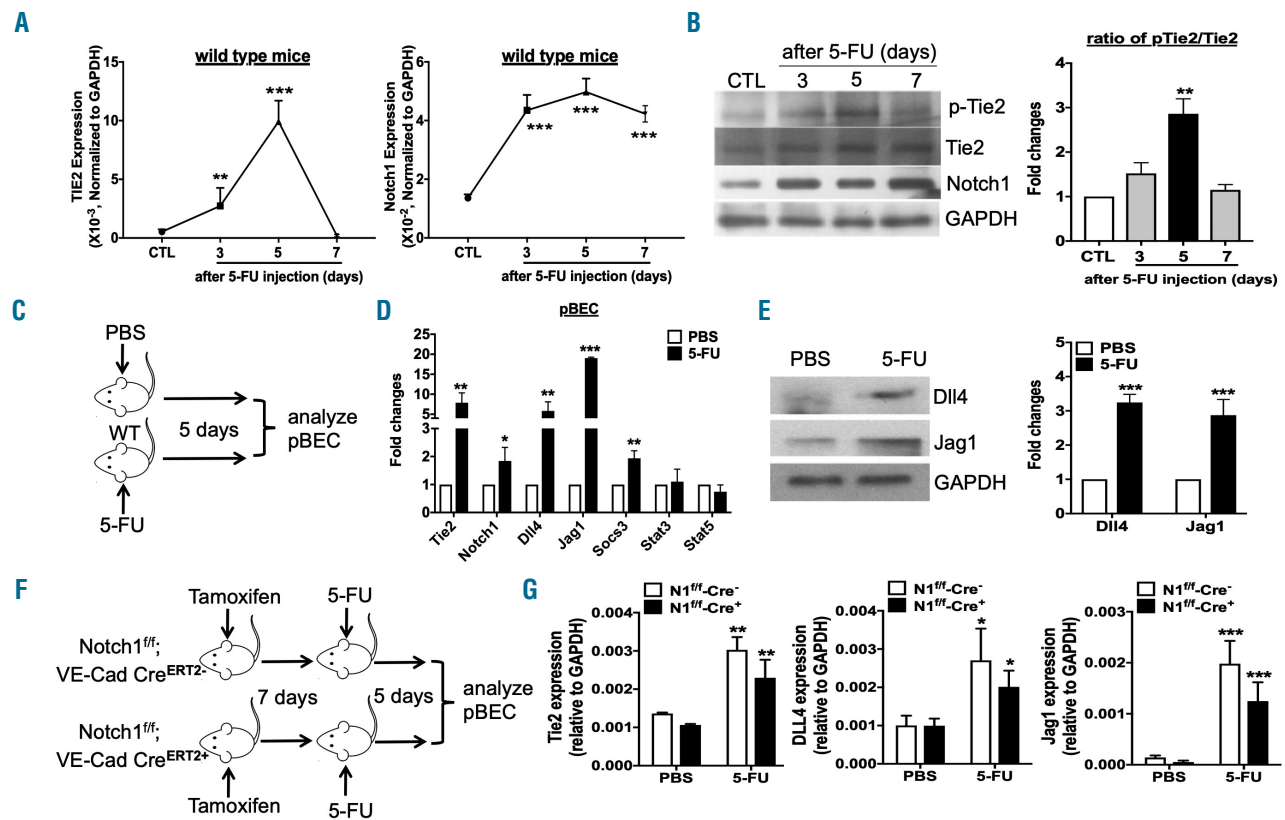


**Figure 6. Both Notch1 and Tie2 signaling are activated during endothelial niche recovery after chemotherapy.** (A) Expression kinetics of Tie2 and Notch1 after chemotherapy. Quantitative reverse transcriptase polymerase chain reaction (RT-qPCR) expression of *Tie2* and *Notch1* in sorted CD31<sup>+</sup> primary bone endothelial cells (pBEC) from wildtype (WT) mice before (CTL) and at days 3, 5 and 7 after 5-fluorouracil (5-FU) treatment. *GAPDH* was used as an internal expression control at each time-point. (B) Representative western blot of protein level analysis for phosphorylated Tie2 (p-Tie2), total Tie2, cleaved Notch1 and GAPDH from sorted pBEC before (CTL) and at days 3, 5 and 7 after 5-FU treatment (left panel). The band intensities of Tie2 and p-Tie2 in pBEC were quantified by ImageJ software. The ratios of pTie2/Tie2 at days 3, 5 and 7 after 5-FU treatment were normalized to that of the control (CTL) group. The fold changes of pTie2/Tie2 ratio are presented (n=3, right panel). (C) Experimental design of 5-FU treatment for pBEC analysis (phosphate-buffered saline, PBS, n=6; 5-FU, n=15). Five- to six-week old mice were treated intraperitoneally (IP) with PBS or 5-FU. CD31<sup>+</sup>Ter119<sup>+</sup>CD45<sup>+</sup> cells (pBEC) were sorted from digested bones 5 days after 5-FU treatment. (D) RT-qPCR expression of indicated genes from pBEC treated as described in (C). Values are normalized to PBS-treated pBEC. *GAPDH* was used as an internal expression control. (E) Protein expression of Dll4 and Jag1 was measured in pBEC from mice treated with PBS or 5-FU. *GAPDH* was used as a loading control (left panel). The band intensities of Dll4 and Jag1 in pBEC were quantitated by ImageJ software (n=3, right panel). (F) Experimental design of 5-FU injection of *Notch1<sup>fl/fl</sup>; VE-CadherinCre<sup>ERT2</sup>+* mice (left panel). *Notch1<sup>fl/fl</sup>; VE-CadherinCre<sup>ERT2</sup>+* mice were injected IP with tamoxifen daily for 5 days. One week later, 5-FU was injected IP into *Notch1<sup>fl/fl</sup>; VE-CadherinCre<sup>ERT2</sup>+* or *CreERT2* littermates. pBEC were analyzed at day 5 after 5-FU injection (n=3). (G) Expression of *Tie2*, *Dll4* and *Jag1* was measured by RT-qPCR in pBEC as described in (F). Absolute expression values were compared to those of PBS-injected mice of each genotype. *GAPDH* was used as an internal expression control.

(Figure 6E), was significantly increased in pBEC from both BM (*Online Supplementary Figure S8E*) and digested bone (Figure 6D, E). Notch ligand upregulation corresponded with the upregulation of *Tie2*, *Notch1* and the Tie2 signaling target *Socs3* (Figure 6D, E, *Online Supplementary Figure S8E*).

Our initial expression timeline (Figure 6A) indicated that *Notch1* expression is upregulated prior to *Tie2* upregulation. To determine whether the induction of *Tie2* and Notch ligands after chemotherapy depended on active Notch signaling, we employed the previously described *Notch1<sup>fl/fl</sup>VE-cadherin-Cre<sup>ERT2+</sup>* model system and analyzed freshly harvested pBEC from WT (*Cre*<sup>-</sup>) and *Notch1<sup>fl/fl</sup>VE-cadherin-Cre<sup>ERT2+</sup>* (*Cre*<sup>+</sup>) mice after tamoxifen and 5-FU treatment (Figure 6F). Our data indicate that 5-FU treatment significantly increased expression of *Tie2*, *Dll4* and *Jag1* in pBEC in WT and *Notch1<sup>fl/fl</sup>VE-cadherin-Cre<sup>ERT2+</sup>* mice. However, loss of endothelial *Notch1* expression did not significantly affect upregulation of *Tie2* after 5-FU treatment (Figure 6G, left panel). Furthermore, loss of Notch signaling did not significantly affect the expression of Notch ligands *Dll4* and *Jag1* (Figure 6G), upregulation of which coincided with the increase in *Tie2* expression and activity (Figure 6A, B). Taken together, we show that Tie2 signaling is independent of Notch1 signaling during BM endothelial regeneration and recovery.

### Notch1 functions downstream of Tie2 signaling during the recovery of bone marrow endothelium

Previous studies have shown that hematopoietic progenitors and mesenchymal cells are responsible for the secretion of Ang1 in the BM.<sup>10</sup> To test this, hematopoietic progenitor (Lin<sup>-</sup>Sca-1<sup>+</sup>) cells and bone osteoblasts (CD51<sup>+</sup>) were sorted from the BM 5 days after 5-FU treatment. Expression of *Ang1* was markedly increased in 5-FU-treated hematopoietic progenitors (up to 150-fold) and osteoblasts (up to 30-fold) when compared to the same untreated cell populations (Figure 7A). To further analyze any possible crosstalk between the Notch and Tie-2 signaling pathways, we supplemented cBEC culture media with Ang1, which caused an increase in the levels of p-Tie2 and cleaved Notch1 (Figure 7B). Ang1 stimulation also induced the expression of Notch ligands (*Dll4* and *Jag1*) and its targets, such as *Hes1*, *Hey1* and *Myc* (Figure 7C). To determine whether Tie2 stimulation by Ang1 was essential for Notch ligand upregulation, we treated cBEC with a Tie2 inhibitor. Our results show that increased expression of *Dll4* and *Jag1* by Ang1 stimulation was completely blocked by pre-treatment with the Tie2 kinase inhibitor (Figure 7D). Our findings support a role for the Tie2 signaling pathway in the induction of Notch signaling by enhancing expression of Notch ligands.

To determine whether Notch signaling also influenced *Tie2* expression, we inhibited Notch activity by addition of a  $\gamma$  secretase inhibitor for 48 h followed by a 3 h washout. Notch targets, inhibited by  $\gamma$  secretase inhibitors, are rapidly upregulated during washout. We observed that this was the case for *Hes1* in cBEC, but not for *Tie2* and *Ang2* (Figure 7E). Interestingly, *Myc* expression in cBEC was not entirely dependent on Notch activity; however, *Myc* levels markedly increased after the washout of the  $\gamma$  secretase inhibitor, indicating that in EC *Myc* is responsive to higher levels of Notch signaling (Figure 7E). These data showed that, in BM EC, Tie2 activation enhanced downstream Notch signaling while Notch activity had no effect on Tie2 signaling.

To test whether Notch functioned downstream of Tie2 activation, ICNΔTAD-cBEC cells were treated with 5-FU for 24 h and then the medium was supplemented with Ang1 (Figure 7F, left). Ang1 stimulated moderate growth of resting cBEC but had no effect on the ICNΔTAD-transduced cBEC. After 5-FU treatment, Ang1 significantly increased growth of control cBEC but did not rescue ICNΔTAD-cBEC (Figure 7F, right). Tie2 activation by Ang1 had the expected result of increasing *Socs3* expression.<sup>41</sup> However, Tie-2 activation had no effect on the Notch targets *Hes1* and *Hey1* in ICNΔTAD-expressing cells (Figure 7G). These results show that whereas Tie2 activation accelerates the recovery of the BM EC niche after chemotherapy by promoting Notch ligand expression, ultimately, the resolution of niche recovery depends on activation of robust Notch signaling.

## Discussion

The Notch1 receptor is crucial for the emergence of the first definitive HSC from the embryonic hemangioblast<sup>22</sup> and expansion of fetal liver HSC.<sup>22</sup> The role of Notch signaling in adult BM HSC is not well understood and mired in controversy.<sup>43-46</sup> It has been suggested that Notch signaling is essential for HSC self-renewal, specifically with regard to Jagged1 activation of Notch1 signaling in HSC.<sup>46</sup> Even so, pan-inhibition of Notch signaling in HSC by deletion of the key transcriptional complex member and DNA-binding factor RBPJ, showed no adverse effects in maintenance and expansion of the stem and progenitor pool.<sup>47</sup> A separate recent study showed depletion of HSC numbers after complete ablation of Notch signaling in the endothelium, thus suggesting that the Notch1 receptor participates in the development of the EC niche.<sup>48</sup> An even more recent article indicated a possible alternative to Notch1 BM signaling by suggesting that Jagged2 triggers Notch2 signaling in HSC after myelosuppression.<sup>49</sup>

Regardless of its proposed involvement during hematopoietic and endothelial development, the specific role of Notch signaling, its mechanistic interplay with other known regenerative pathways and its temporal activation during and following myelosuppression are not known. In the present study, we investigated Notch signaling in adult hematopoietic and endothelial tissues by deleting the TAD from a single allele of *Notch1*. This mutation has the capacity to interfere with the activity of the WT Notch1 transcriptional complex and created a hypomorphic signaling environment. Our *Notch1<sup>+ΔTAD</sup>* heterozygous model system matured to adulthood and under homeostatic conditions exhibited no adverse effects in the bone and vasculature. We show that this heterozygous hypomorphic model system is useful for determining the requirement for robust Notch signaling activation in adult tissues. Using the *Notch1<sup>+ΔTAD</sup>* mice we determined that basal Notch1 signaling was sufficient for development of the endothelial hematopoietic niche; however, robust activation of Notch1 was required for the regeneration of the hematopoietic system.

We observed increased Notch1 receptor expression and cleavage in BM EC following treatment with the chemotherapeutic agent 5-FU. The WT BM microenvironment began to recover at ~9 days after exposure to 5-FU. However, the BM niche was persistently disrupted in *Notch1<sup>+ΔTAD</sup>* mice as evidenced by the presence of few CD31<sup>+</sup>

and endomucin<sup>+</sup> microvessels and a high frequency of apoptotic EC. Defective regeneration of EC in these mice caused gaps in sinusoidal vessels leading to severe hemorrhage.<sup>5,50</sup> The occupancy of the Notch transcriptional complex and expression of Notch target genes associated with survival and proliferation, such as *Hes1* and *Myc*,<sup>51,52</sup> was markedly decreased in *Notch1*<sup>+ΔTAD</sup> BM EC, indicating that

the regeneration of niche EC following chemotherapy was dependent on high levels of Notch signaling. Validation was obtained using conditional deletion of the Notch1 receptor in the VE-cadherin<sup>+</sup> EC. Similar to the *Notch1*<sup>+ΔTAD</sup>, this EC-specific, conditional, loss-of-function Notch1 model exhibited defective regeneration of BM EC highlighted by increased EC apoptosis and limited hematopoietic recovery.

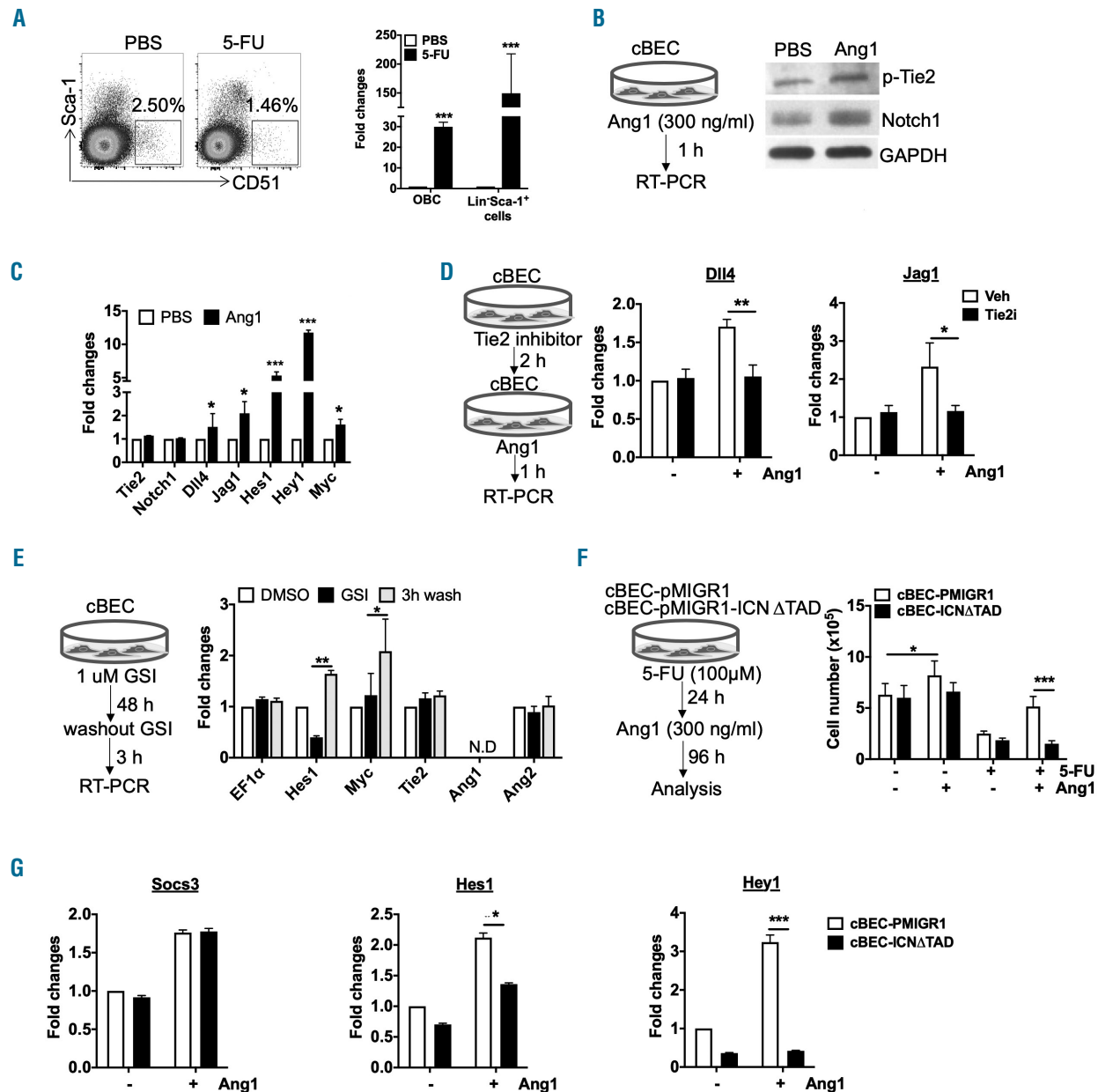


**Figure 7. Notch1 functions downstream of Tie2 signaling to mediate endothelial niche recovery.** (A) Representative gating strategy for osteoblasts (Ter119-CD45<sup>+</sup>CD31<sup>+</sup>Sca1<sup>+</sup>CD51<sup>+</sup> cells) in digested bones from mice treated with phosphate-buffered saline (PBS) and 5-fluorouracil (5-FU) (PBS, n=5; 5-FU, n=15; left panel). Expression of *Ang1* was determined by quantitative reverse transcriptase polymerase chain reaction (RT-qPCR) in osteoblasts and Lin<sup>+</sup>Sca-1<sup>+</sup> cells treated with PBS and 5-FU (right panel). GAPDH was used as an internal expression control. (B) Schematic of Ang1 treatment in serum-starved (16 h) cultured bone marrow-derived endothelial cells (cBEC) (left panel). Expression of p-Tie2, cleaved Notch1 and GAPDH protein levels in Ang1-treated cBEC was detected by western blot (right panel). (C) RT-qPCR expression of Notch target genes from cBEC treated as described in (B). Values are normalized to those in PBS-treated cBEC. GAPDH was used as an internal expression control. (D) Schematic of Tie2 inhibitor (Tie2i) and Ang1 treatment in serum-starved (16 h) cBEC (left panel). Expression of *Dll4* and *Jag1* was determined by RT-qPCR in Tie2i and/or Ang1-treated cBEC. The vehicle for the Tie2 inhibitor was dimethylsulfoxide (DMSO). Vehicle for Ang1 is PBS. (E) Schematic for treatment of cBEC with  $\gamma$  secretase inhibitors (GSI). RT-qPCR expression analysis of the indicated genes in cBEC treated with GSI/washout. Values were normalized to those of DMSO-treated cBEC. GAPDH was used as an internal expression control. (F) Schematic for treatment of control PMIGR1 or PMIGR1-ICN $\Delta$ TAD cBEC with 5-FU and Ang1. The indicated cBEC populations of cells were monitored for growth after 5-FU and Ang1 treatment. (G) RT-qPCR expression of Tie2 target *Socs3*, and Notch targets *Hes1* and *Hey1* was examined after cell growth analysis of cBEC in (F). Values were normalized to those of PMIGR1 cBEC without Ang1-treatment. GAPDH was used as an internal expression control. Unless indicated differently, n=3 were used for experiments in this figure. \**P*<0.05, \*\**P*<0.01, \*\*\**P*<0.001.

While further work is required to determine whether specific subsets of BM EC are more susceptible to loss of Notch signaling during niche regeneration, our work suggests that a majority of EC, which express CD31, VE-cadherin and endomucin, require robust Notch1 signaling to recovery after myelosuppressive injury.

Mediators of BM niche recovery include VEGF-A, Tie2, and the Tie2 agonist Ang1.<sup>2,53,54</sup> Initiation of regenerative signaling is believed to hinge upon VEGF-A produced by osteoblasts and osteocytes<sup>55,56</sup> and Ang1 produced by osteoprogenitors and hematopoietic precursors.<sup>10,57</sup> We observed that there was a short pulse of Tie2 phosphorylation after chemotherapeutic damage while Notch signaling remained at elevated levels for at least 7 days after chemotherapy. Tie2 activation increased Notch receptor cleavage and the Tie2 agonist, Ang1 stimulated Notch signaling and promoted the expression of two canonical Notch ligands: *Dll4* and *Jag1*. However, Tie2 stimulation, after 5-FU treatment failed to rescue the survival of Notch-deficient EC which expressed the hypomorphic *Notch1 $\Delta$ TAD* allele. These results indicate that Notch signaling functions downstream of Tie2 and that Notch1 signaling is ultimately responsible for the regeneration of the BM endothelium.

The *Notch1<sup>+/ $\Delta$ TAD</sup>* mice exhibited no inherent HSC defect in the absence of BM injury, corroborating reports that indicate a lack of involvement of Notch signaling in adult HSC expansion.<sup>44,45,47</sup> However, chemotherapy severely impaired the generation of HSC in *Notch1<sup>+/ $\Delta$ TAD</sup>* mice suggesting that Notch signaling is required for HSC self-renewal. Transplantation of *Notch1<sup>+/ $\Delta$ TAD</sup>* HSC reconstituted irradiated WT hosts which showed no pancytopenic symptoms after chemotherapy, indicating that there is no cell-intrinsic defect in HSC generation due to the presence of the Notch1 $\Delta$ TAD protein. In fact, the reverse experiment, in which WT HSC were transplanted into *Notch1<sup>+/ $\Delta$ TAD</sup>* recipients had the same severe phenotype as the constitutive *Notch1<sup>+/ $\Delta$ TAD</sup>* or *Notch1<sup>fl</sup>/VE-cadherin-Cre<sup>ERT2+</sup>* models, further supporting a specific role for Notch signaling in the regeneration of the BM EC niche. Thus, we attribute the loss of HSC and progenitor cells observed after 5-FU treatment to the destruction of the BM EC niche, a process which requires robust Notch activity for its recovery.

Previous work has established that successful T-cell development requires Notch signaling up until  $\beta$ -selection of  $\alpha\beta$  T cells in the thymus.<sup>27,58,59</sup> *Notch1<sup>+/ $\Delta$ TAD</sup>* mice exhibited a moderate decrease in developing T cells and had no defect in mature single-positive T cells (*data not shown*). This inherent defect was exacerbated by 5-FU treatment and extended to the BM-residing CLP population. These results suggest that the Notch-driven commitment of the T-cell lineage begins at an early stage in the BM. A recent study, in which genetic deletion of *Dll4* in the bone producing mesenchymal Ocn<sup>+</sup> cells decreased CLP numbers and limited the production of T cells in the thymus,<sup>60</sup> supports our observations. Thus, the present findings suggest an important role for Notch1 signaling in mediating the differentiation of early lymphoid hematopoietic progenitors and the existence of a specific Notch-signal-promoting niche in the BM for T-cell commitment prior to thymic migration.

In summary, we employed a novel strategy for physiological inhibition of Notch signaling in adult tissues using a hypomorphic *in vivo* model system. We demonstrated that high levels of Notch1 signaling are required for the regeneration of BM EC after myelosuppressive chemotherapy and radiotherapy. Optimal recuperation of the EC niche relies on several signaling pathways, but it is ultimately a Notch-dependent process that supports regeneration of the BM niche and hematopoietic recovery.

#### Acknowledgments

We thank Dr. Warren Pear for invaluable advice and for sharing the *Notch1<sup>+/ $\Delta$ TAD</sup>* murine model system. We also thank Dr. Kishore Wary for sharing the *Cdh5-CreERT2* mouse model. Drs. Jon Aster and Stephen Blacklow for advice and thoughtful discussion, Dr. Dawson Gerhardt for her help in generating the *Notch1- $\Delta$ TAD* plasmids and vector constructs, Dr. Jan Kitejewski for helpful advice on Notch mutant mice and Drs. Fotini Gounari and Linda Dagenstein of the University of Chicago transgenic mouse facility for help in maintaining the transgenic mouse colonies. The following cores at the University of Illinois at Chicago contributed to this study: RRC Histology Core and RRC Flow Cytometry Core. This study was funded by NIH grants 1R01HL134971 to KVP and 1R01HL136529 to DL.

#### References

- Li X, Slayton WB. Molecular mechanisms of platelet and stem cell rebound after 5-fluorouracil treatment. *Exp Hematol*. 2013;41(7):635-645 e633.
- Kopp HG, Avcilla ST, Hooper AT, et al. Tie2 activation contributes to hemangiogenic regeneration after myelosuppression. *Blood*. 2005;106(2):505-513.
- Soligo DA, Lambertenghi Delilieri G, Servida F, et al. Haematopoietic abnormalities after autologous stem cell transplantation in lymphoma patients. *Bone Marrow Transplant*. 1998;21(1):15-22.
- Wittels B. Bone marrow biopsy changes following chemotherapy for acute leukemia. *Am J Surg Pathol*. 1980;4(2):135-142.
- Hooper AT, Butler JM, Nolan DJ, et al. Engraftment and reconstitution of hematopoiesis is dependent on VEGFR2-mediated regeneration of sinusoidal endothelial cells. *Cell Stem Cell*. 2009;4(3):263-274.
- Islam A. Pattern of bone marrow regeneration following chemotherapy for acute myeloid leukemia. *J Med*. 1987;18(2):108-122.
- Ding L, Saunders TL, Enikolopov G, Morrison SJ. Endothelial and perivascular cells maintain haematopoietic stem cells. *Nature*. 2012;481(7382):457-462.
- Doan PL, Himburg HA, Helms K, et al. Epidermal growth factor regulates hematopoietic regeneration after radiation injury. *Nat Med*. 2013;19(3):295-304.
- Arai F, Hirao A, Ohmura M, et al. Tie2/angiopoietin-1 signaling regulates hematopoietic stem cell quiescence in the bone marrow niche. *Cell*. 2004;118(2):149-161.
- Zhou BO, Ding L, Morrison SJ. Hematopoietic stem and progenitor cells regulate the regeneration of their niche by secreting Angiopoietin-1. *Elife*. 2015;4:e05521.
- Doan PL, Russell JL, Himburg HA, et al. Tie2(+) bone marrow endothelial cells regulate hematopoietic stem cell regeneration following radiation injury. *Stem Cells*. 2013;31(2):327-337.
- Artavanis-Tsakonas S, Rand MD, Lake RJ. Notch signaling: cell fate control and signal integration in development. *Science*. 1999;284(5415):770-776.
- Phng LK, Gerhardt H. Angiogenesis: a team effort coordinated by notch. *Dev Cell*. 2009;16(2):196-208.
- Hellstrom M, Phng LK, Hofmann JJ, et al. Dll4 signalling through Notch1 regulates formation of tip cells during angiogenesis. *Nature*. 2007;445(7129):776-780.
- Pitulescu ME, Schmidt I, Giaimo BD, et al. Dll4 and Notch signalling couples sprouting angiogenesis and artery formation. *Nat Cell*

- Biol. 2017;19(8):915-927.
16. Briot A, Civelek M, Seki A, et al. Endothelial NOTCH1 is suppressed by circulating lipids and antagonizes inflammation during atherosclerosis. *J Exp Med.* 2015;212(12):2147-2163.
  17. Mack JJ, Mosqueiro TS, Archer BJ, et al. NOTCH1 is a mechanosensor in adult arteries. *Nat Commun.* 2017;8(1):1620.
  18. Andersson ER, Sandberg R, Lendahl U. Notch signaling: simplicity in design, versatility in function. *Development.* 2011;138(17):3593-3612.
  19. Kurooka H, Honjo T. Functional interaction between the mouse notch1 intracellular region and histone acetyltransferases PCAF and GCN5. *J Biol Chem.* 2000;275(22):17211-17220.
  20. Kurooka H, Kuroda K, Honjo T. Roles of the ankyrin repeats and C-terminal region of the mouse notch1 intracellular region. *Nucleic Acids Res.* 1998;26(23):5448-5455.
  21. Ong CT, Cheng HT, Chang LW, et al. Target selectivity of vertebrate notch proteins. Collaboration between discrete domains and CSL-binding site architecture determines activation probability. *J Biol Chem.* 2006;281(8):5106-5119.
  22. Gerhardt DM, Pajcini KV, D'Altri T, et al. The Notch1 transcriptional activation domain is required for development and reveals a novel role for Notch1 signaling in fetal hematopoietic stem cells. *Genes Dev.* 2014;28(6):576-593.
  23. High F, Epstein JA. Signalling pathways regulating cardiac neural crest migration and differentiation. *Novartis Found Symp.* 2007;283:152-161; discussion 161-154, 238-241.
  24. High FA, Jain R, Stoller JZ, et al. Murine Jagged1/Notch signaling in the second heart field orchestrates Fgf8 expression and tissue-tissue interactions during outflow tract development. *J Clin Invest.* 2009;119(7):1986-1996.
  25. Longley DB, Harkin DP, Johnston PG. 5-fluorouracil: mechanisms of action and clinical strategies. *Nat Rev Cancer.* 2003;3(5):330-338.
  26. Lerner C, Harrison DE. 5-Fluorouracil spares hemopoietic stem cells responsible for long-term repopulation. *Exp Hematol.* 1990;18(2):114-118.
  27. Radtke F, Wilson A, Stark G, et al. Deficient T cell fate specification in mice with an induced inactivation of Notch1. *Immunity.* 1999;10(5):547-558.
  28. Tanigaki K, Han H, Yamamoto N, et al. Notch-RBP-J signaling is involved in cell fate determination of marginal zone B cells. *Nat Immunol.* 2002;3(5):443-450.
  29. Pajcini KV, Xu L, Shao L, et al. MAFB enhances oncogenic Notch signaling in T cell acute lymphoblastic leukemia. *Sci Signal.* 2017;10(505).
  30. Schepers K, Pietras EM, Reynaud D, et al. Myeloproliferative neoplasia remodels the endosteal bone marrow niche into a self-reinforcing leukemic niche. *Cell Stem Cell.* 2013;13(3):285-299.
  31. Avicilla ST, Hattori K, Heissig B, et al. Chemokine-mediated interaction of hematopoietic progenitors with the bone marrow vascular niche is required for thrombopoiesis. *Nat Med.* 2004;10(1):64-71.
  32. Kiel MJ, Yilmaz OH, Iwashita T, et al. SLAM family receptors distinguish hematopoietic stem and progenitor cells and reveal endothelial niches for stem cells. *Cell.* 2005;121(7):1109-1121.
  33. Rafii S, Shapiro F, Pettengell R, et al. Human bone marrow microvascular endothelial cells support long-term proliferation and differentiation of myeloid and megakaryocytic progenitors. *Blood.* 1995;86(9):3353-3363.
  34. Shao L, Sun Y, Zhang Z, et al. Deletion of proapoptotic Puma selectively protects hematopoietic stem and progenitor cells against high-dose radiation. *Blood.* 2010;115(23):4707-4714.
  35. Zhao M, Perry JM, Marshall H, et al. Megakaryocytes maintain homeostatic quiescence and promote post-injury regeneration of hematopoietic stem cells. *Nat Med.* 2014;20(11):1321-1326.
  36. Mendelson A, Frenette PS. Hematopoietic stem cell niche maintenance during homeostasis and regeneration. *Nat Med.* 2014;20(8):833-846.
  37. Yashiro-Ohtani Y, Wang H, Zang C, et al. Long-range enhancer activity determines Myc sensitivity to Notch inhibitors in T cell leukemia. *Proc Natl Acad Sci U S A.* 2014;111(46):E4946-4953.
  38. Wang H, Zou J, Zhao B, et al. Genome-wide analysis reveals conserved and divergent features of Notch1/RBPJ binding in human and murine T-lymphoblastic leukemia cells. *Proc Natl Acad Sci U S A.* 2011;108(36):14908-14913.
  39. Hassanshahi M, Hassanshahi A, Khabbazi S, Su YW, Xian CJ. Bone marrow sinusoidal endothelium: damage and potential regeneration following cancer radiotherapy or chemotherapy. *Angiogenesis.* 2017;20(4):427-442.
  40. Zhang J, Fukuhara S, Sako K, et al. Angiopoietin-1/Tie2 signal augments basal Notch signal controlling vascular quiescence by inducing delta-like 4 expression through AKT-mediated activation of beta-catenin. *J Biol Chem.* 2011;286(10):8055-8066.
  41. Bourillot PY, Aksoy I, Schreiber V, et al. Novel STAT3 target genes exert distinct roles in the inhibition of mesoderm and endoderm differentiation in cooperation with Nanog. *Stem Cells.* 2009;27(8):1760-1771.
  42. Kumano K, Chiba S, Kunisato A, et al. Notch1 but not Notch2 is essential for generating hematopoietic stem cells from endothelial cells. *Immunity.* 2003;18(5):699-711.
  43. Karanu FN, Murdoch B, Gallacher L, et al. The notch ligand jagged-1 represents a novel growth factor of human hematopoietic stem cells. *J Exp Med.* 2000;192(9):1365-1372.
  44. Maillard I, Koch U, Dumortier A, et al. Canonical notch signaling is dispensable for the maintenance of adult hematopoietic stem cells. *Cell Stem Cell.* 2008;2(4):356-366.
  45. Mancini SJ, Mantei N, Dumortier A, et al. Jagged1-dependent Notch signaling is dispensable for hematopoietic stem cell self-renewal and differentiation. *Blood.* 2005;105(6):2340-2342.
  46. Poulos MG, Guo P, Kofler NM, et al. Endothelial Jagged-1 is necessary for homeostatic and regenerative hematopoiesis. *Cell Rep.* 2013;4(5):1022-1034.
  47. Duarte S, Woll PS, Buza-Vidas N, et al. Canonical Notch signaling is dispensable for adult steady-state and stress myelo-erythropoiesis. *Blood.* 2018;131(15):1712-1719.
  48. Kusumbe AP, Ramasamy SK, Itkin T, et al. Age-dependent modulation of vascular niches for haematopoietic stem cells. *Nature.* 2016;532(7599):380-384.
  49. Guo P, Poulos MG, Palikuqi B, et al. Endothelial jagged-2 sustains hematopoietic stem and progenitor reconstitution after myelosuppression. *J Clin Invest.* 2017;127(12):4242-4256.
  50. Shirota T, Tavassoli M. Cyclophosphamide-induced alterations of bone marrow endothelium: implications in homing of marrow cells after transplantation. *Exp Hematol.* 1991;19(5):369-373.
  51. Murata K, Hattori M, Hirai N, et al. Hes1 directly controls cell proliferation through the transcriptional repression of p27Kip1. *Mol Cell Biol.* 2005;25(10):4262-4271.
  52. Stine ZE, Walton ZE, Altman BJ, Hsieh AL, Dang CV. MYC, Metabolism, and cancer. *Cancer Discov.* 2015;5(10):1024-1039.
  53. Gale NW, Thurston G, Hackett SF, et al. Angiopoietin-2 is required for postnatal angiogenesis and lymphatic patterning, and only the latter role is rescued by Angiopoietin-1. *Dev Cell.* 2002;3(3):411-423.
  54. Yancopoulos GD, Davis S, Gale NW, et al. Vascular-specific growth factors and blood vessel formation. *Nature.* 2000;407(6801):242-248.
  55. Juffer P, Jaspers RT, Lips P, Bakker AD, Klein-Nulend J. Expression of muscle anabolic and metabolic factors in mechanically loaded MLO-Y4 osteocytes. *Am J Physiol Endocrinol Metab.* 2012;302(4):E389-395.
  56. Schlaeppli JM, Gutzwiller S, Finkenzeller G, Fournier B. 1,25-Dihydroxyvitamin D3 induces the expression of vascular endothelial growth factor in osteoblastic cells. *Endocr Res.* 1997;23(3):213-229.
  57. Sacchetti B, Funari A, Michienzi S, et al. Self-renewing osteoprogenitors in bone marrow sinusoids can organize a hematopoietic microenvironment. *Cell.* 2007;131(2):324-336.
  58. MacDonald HR, Wilson A, Radtke F. Notch1 and T-cell development: insights from conditional knockout mice. *Trends Immunol.* 2001;22(3):155-160.
  59. Wilson A, MacDonald HR, Radtke F. Notch 1-deficient common lymphoid precursors adopt a B cell fate in the thymus. *J Exp Med.* 2001;194(7):1003-1012.
  60. Yu VW, Saez B, Cook C, et al. Specific bone cells produce DLL4 to generate thymus-seeding progenitors from bone marrow. *J Exp Med.* 2015;212(5):759-774.



# Deubiquitylase USP7 regulates human terminal erythroid differentiation by stabilizing GATA1

Long Liang,<sup>1,2</sup> Yuanliang Peng,<sup>1</sup> Jieying Zhang,<sup>1,3</sup> Yibin Zhang,<sup>1,2</sup> Mridul Roy,<sup>1,2</sup> Xu Han,<sup>1</sup> Xiaojuan Xiao,<sup>1</sup> Shuming Sun,<sup>1</sup> Hong Liu,<sup>4</sup> Ling Nie,<sup>4</sup> Yijin Kuang,<sup>1</sup> Zesen Zhu,<sup>1</sup> Jinghui Deng,<sup>1</sup> Yang Xia,<sup>5</sup> Vijay G. Sankaran,<sup>6,7</sup> Christopher D. Hillyer,<sup>8</sup> Narla Mohandas,<sup>8</sup> Mao Ye,<sup>2</sup> Xiuli An<sup>3,9</sup> and Jing Liu<sup>1,10</sup>

**Haematologica** 2019  
Volume 104(11):2178-2188

<sup>1</sup>Molecular Biology Research Center & Center for Medical Genetics, School of Life Sciences, Central South University, Changsha, China; <sup>2</sup>Molecular Science and Biomedicine Laboratory, State Key Laboratory for Chemo/Biosensing and Chemometrics, College of Biology, College of Chemistry and Chemical Engineering, Hunan University, Changsha, China; <sup>3</sup>Laboratory of Membrane Biology, New York Blood Center, New York, NY, USA; <sup>4</sup>Xiangya Hospital, Central South University, Changsha, China; <sup>5</sup>Department of Biochemistry and Molecular Biology, The University of Texas Health Science Center at Houston, Houston, TX, USA; <sup>6</sup>Broad Institute of MIT and Harvard, Cambridge, MA, USA; <sup>7</sup>Division of Hematology/Oncology, Boston Children's Hospital and Department of Pediatric Oncology, Dana-Farber Cancer Institute, Harvard Medical School, Boston, MA, USA; <sup>8</sup>Red Cell Physiology Laboratory, New York Blood Center, New York, NY, USA; <sup>9</sup>School of Life Sciences, Zhengzhou University, Zhengzhou, China and <sup>10</sup>Erythropoiesis Research Center, Central South University, Changsha, China

## ABSTRACT

Ubiquitination is an enzymatic post-translational modification that affects protein fate. The ubiquitin-proteasome system (UPS) was first discovered in reticulocytes where it plays important roles in reticulocyte maturation. Recent studies have revealed that ubiquitination is a dynamic and reversible process and that deubiquitylases are capable of removing ubiquitin from their protein substrates. Given the fact that the UPS is highly active in reticulocytes, it is speculated that deubiquitylases may play important roles in erythropoiesis. Yet, the role of deubiquitylases in erythropoiesis remains largely unexplored. In the present study, we found that the expression of deubiquitylase USP7 is significantly increased during human terminal erythroid differentiation. We further showed that interfering with USP7 function, either by short hairpin RNA-mediated knockdown or USP7-specific inhibitors, impaired human terminal erythroid differentiation due to decreased GATA1 level and that restoration of GATA1 levels rescued the differentiation defect. Mechanistically, USP7 deficiency led to a decreased GATA1 protein level that could be reversed by proteasome inhibitors. Furthermore, USP7 interacts directly with GATA1 and catalyzes the removal of K48-linked polyubiquitylation chains conjugated onto GATA1, thereby stabilizing GATA1 protein. Collectively, our findings have identified an important role of a deubiquitylase in human terminal erythroid differentiation by stabilizing GATA1, the master regulator of erythropoiesis.

## Correspondence:

JING LIU  
jingliucs@hotmai.com or  
liujing2@sklmg.edu.cn

XIULI AN  
xan@nybc.org

MAO YE  
goldleaf@hnu.edu.cn

Received: September 8, 2018.

Accepted: March 13, 2019.

Pre-published: March 14, 2019.

doi:10.3324/haematol.2018.206227

Check the online version for the most updated information on this article, online supplements, and information on authorship & disclosures: [www.haematologica.org/content/104/11/2178](http://www.haematologica.org/content/104/11/2178)

©2019 Ferrata Storti Foundation

Material published in *Haematologica* is covered by copyright. All rights are reserved to the Ferrata Storti Foundation. Use of published material is allowed under the following terms and conditions:

<https://creativecommons.org/licenses/by-nc/4.0/legalcode>.

Copies of published material are allowed for personal or internal use. Sharing published material for non-commercial purposes is subject to the following conditions:

<https://creativecommons.org/licenses/by-nc/4.0/legalcode>,

sect. 3. Reproducing and sharing published material for commercial purposes is not allowed without permission in writing from the publisher.



## Introduction

Red blood cells, the most abundant of all circulating blood cells, facilitate gas exchange in the lungs and transporting oxygen to tissues. More than two million red blood cells are generated per second in a healthy adult through a process termed erythropoiesis. Mature red blood cells are produced from hematopoietic stem cells, which commit to erythroid progenitors followed by terminal erythroid differentiation. Terminal erythroid differentiation, driven by the glycoprotein hormone erythropoietin, begins with proerythroblasts, which sequentially divide into basophilic, polychromatic and orthochromatic erythroblasts that enucleate to generate reticulocytes.<sup>1,2</sup> Erythropoiesis is a tightly regulated process. Previous studies were primarily focused on the regulation of erythropoiesis by transcription factors and cytokines.<sup>3,4</sup>

In contrast, the regulation of erythropoiesis by other mechanisms has been less well studied. Notably, our knowledge on post-translational regulation of erythropoiesis is limited.

Ubiquitination is an enzymatic post-translational modification. Ubiquitinated proteins are degraded by the ubiquitin-proteasome system (UPS). The UPS controls the degradation of most intracellular proteins and plays important roles in many cellular processes.<sup>5</sup> Although the UPS was first discovered in reticulocytes over 40 years ago,<sup>6</sup> to date there are only limited studies on the roles of the UPS in erythropoiesis. These include the reported role of CUL4A-mediated degradation of p27 in cell proliferation in the early stages of erythropoiesis and cell cycle exit at a later stage of erythropoiesis.<sup>7,8</sup> A recent, exciting study demonstrated that UBE2O remodels the proteome during terminal erythroid differentiation, underscoring the importance of the UPS in erythropoiesis.<sup>9</sup>

Ubiquitination is a dynamic and reversible process.<sup>10</sup> It has been reported that deubiquitylases are capable of removing ubiquitin from their protein substrates and allow proteins to be salvaged from proteasomal degradation.<sup>11</sup> USP7 is a deubiquitylase that belongs to the ubiquitin-specific protease (USP) family, which constitutes the largest subgroup of deubiquitylases. Accumulated evidence has shown that USP7 plays diverse roles in genome stability, epigenetic regulation, the cell cycle, apoptosis, viral infection, immunity and stem cell maintenance.<sup>12-17</sup> Recently, USP7 was reported to be an important regulator of osteogenic differentiation and adipogenesis.<sup>18,19</sup> Our RNA-sequencing analyses revealed high-level expression of genes/pathways (including USP7) involved in the ubiquitin system during late stages of terminal erythroid differentiation.<sup>2</sup> Nevertheless, the function of USP7 in human erythropoiesis remains unexplored.

GATA1 is the key transcription factor for erythropoiesis, controlling the expression of a large series of erythroid genes, including erythropoietin receptor, globins and several membrane proteins.<sup>20</sup> GATA1-deficient mice die *in utero* due to severe anemia at embryonic day 10.5-11.5,<sup>21</sup> and chimeric mice lacking GATA1 fail to produce mature red blood cells, although the formation of cells of other hematopoietic lineages is normal.<sup>22</sup> In contrast, overexpression of GATA1 in erythroid cells inhibits their differentiation, leading to fatal anemia in mice.<sup>23</sup> GATA1 stability is finely regulated by multiple mechanisms,<sup>24</sup> since changes in its protein levels will exert a great influence on erythropoiesis. Although GATA1 degradation by the ubiquitin-proteasome pathway has been characterized,<sup>24</sup> how GATA1 recycles from the UPS is yet to be defined.

In this study, we demonstrated that USP7 deficiency impairs human terminal erythroid differentiation due to a decreased level of GATA1 protein. We further showed that USP7 interacts directly with GATA1 and catalyzes the removal of poly-ubiquitylation chains on GATA1, thus stabilizing GATA1. Our findings have thus not only documented the role of a deubiquitylase in erythropoiesis, but also enabled the identification of a novel mechanism by which deubiquitylases regulate GATA1 protein stability.

## Methods

### Reagents and antibodies

P5091 (S7132) and MG132 (S2619) were obtained from Selleckchem (TX, USA); P22077 (HY-13865) from MCE (NJ,

USA); and cycloheximide was purchased from Sigma-Aldrich (MO, USA). Antibodies used for western blot, immunoprecipitation and immunofluorescence studies are detailed in the *Online Supplementary Methods*. The antibodies used for flow cytometry analysis were glycoprotein A (GPA)-PE-Cy7, GPA-APC, and  $\alpha$ 4-integrin (CD49d)-PE from BD Pharmingen (NJ, USA). Band 3-APC and 4.1R antibodies were used as previously described.<sup>25</sup>

### Cell culture

Human cord blood samples were obtained from Xiangya Hospital of Central South University or New York Blood Center under Institutional Review Board approval and in accordance with the Declaration of Helsinki. The detailed composition of the culture medium and the cell culture protocol has been described previously.<sup>25</sup> HEK293T cells (American Type Culture Collection: CRL-11268) were cultured in Dulbecco modified Eagle medium (Gibco, MA, USA) supplemented with 10% fetal bovine serum (Gibco).

### Lentivirus packaging and infection

USP7-specific short hairpin (sh)RNA was purchased from GenePharma (Shanghai, China) (shRNA #1: 5'-AGTCGTTTCAGTCGTCGTAT-3' and #2: 5'-TGGATTTGTG-GTTACGTTACTC-3', constructed in pGLV3-H1-GFP or pGLV2-U6 vector). GATA1 overexpression (HMD-GATA1-IRES-GFP) and control plasmids have been described previously.<sup>26</sup> Lentiviruses were packaged in HEK293T cells according to the manufacturer's protocol (Invitrogen, MA, USA). A total of  $30 \times 10^7$  lentiviral particles were infected using polybrene with  $0.5 \times 10^7$  CD34<sup>+</sup> cells on day 3 or 4. Puromycin (1  $\mu$ g/mL) was used for selection of transduced cells.

### GATA1 rescue assay

For rescue experiments, erythroid cells were infected with USP7 shRNA or control shRNA lentiviruses for 3 days. On day 7 of culture, erythroid cells were transduced with the control or GATA1 lentivirus. Double-transduced cells were identified following puromycin (1  $\mu$ g/mL) selection and GFP expression from the HMD vector. The extent of terminal erythroid differentiation was monitored beginning on day 9.

### RNA isolation, quantitative real-time polymerase chain reaction and western blot analysis.

Standard protocols were used for RNA and protein isolation, polymerase chain reaction (PCR) and western blot analysis. Details are given in the *Online Supplementary Methods*. The GATA1 primer sequences were described previously.<sup>27</sup> USP7 primer sequences were: forward: 5'-AGCGTGGCATCACCATAATC-3' and reverse: 5'-CGAGGCAACCTTTTCAGTTCA-3'.

### Immunoprecipitation and glutathione-S-transferase pull-down

Immunoprecipitation studies were performed using M2/Flag or protein A/G-agarose beads. For the glutathione-S-transferase (GST) pull-down assay, purified Flag-USP7 and bacterial expressed GST or GST-GATA1 were used. The methods are described in detail in the *Online Supplementary Methods*.

### In vivo ubiquitylation and deubiquitylation assays

For cell-based deubiquitylation assays, Flag-GATA1 and HA-ubiquitin were co-transfected with an empty vector or a vector expressing USP7 (WT or CS) for 48 h. For USP7 knockdown, the cells were infected with the lentiviruses for 48 h. Additional details of the methods are given in the *Online Supplementary Methods*.

### **In vitro** deubiquitylation assays

*In vitro* ubiquitylation assays were performed as previously described<sup>28</sup> and additional details are provided in the *Online Supplement*.

### Statistical analysis

All data are presented as mean  $\pm$  standard deviation (SD), and the results were analyzed using the SPSS 18.0 software package. Significant differences between groups were determined using analysis of variance and the Tukey range test.

## Results

### Deficiency of USP7 impairs human terminal erythroid differentiation

To explore the roles of deubiquitylases during erythropoiesis, we first analyzed the expression patterns of deubiquitylases in human erythroblasts at different stages of differentiation from our RNA-sequencing data.<sup>2</sup> Figure 1A shows the expression patterns of USP family members and reveals that the expression levels of USP7 are significantly increased during erythropoiesis. Based on the previously identified important role of USP7 in cell differentiation in other cellular systems,<sup>17-19</sup> in the present study we focused our attention on the role of USP7 in erythroid differentiation. We confirmed the increased expression of USP7 during late stages of erythroid differentiation by both real-time PCR (Figure 1B) and by western blot analysis (Figure 1C). To examine the effect of USP7 on erythropoiesis, we employed a shRNA-mediated knockdown approach in human CD34<sup>+</sup> cells.<sup>27,29,30</sup> As shown in Figure 1D, USP7 knockdown impaired the terminal erythroid differentiation as demonstrated by the decreased surface expression of the erythroid marker GPA, delayed loss of  $\alpha$ 4-integrin expression in association with decreased surface expression of band 3. There was also a marked decrease in the extent of enucleation. USP7 knockdown also inhibited the expression of hemoglobin (Figure 1E). The significant impairment of the growth of late-stage erythroblasts caused by USP7 knockdown was accompanied by increased apoptosis (*Online Supplementary Figure S1A, B*). Similar to USP7 knockdown, USP7-specific inhibitors P5091 and P22077<sup>31,32</sup> also impaired human terminal erythroid differentiation, inhibited hemoglobin expression (Figure 1F, G) and cell proliferation (*Online Supplementary Figure S1C, D*). These results imply that USP7 plays an important role in human terminal erythroid differentiation.

### USP7 regulates erythroid differentiation by modulating GATA1 protein levels

We subsequently explored the molecular mechanism(s) of the altered erythropoiesis due to USP7 deficiency. Given the fact that USP7 functions in the nucleus,<sup>33,34</sup> we hypothesized that USP7 might affect erythropoiesis by regulating erythroid differentiation-related transcription factors. As shown in Figure 2A and *Online Supplementary Figure S2*, GATA1 was the transcription factor most significantly decreased after knockdown of USP7, although KLF1 levels also decreased. Since KLF1 expression is regulated by GATA1,<sup>35</sup> we suggest that the decreased expression of KLF1 is a consequence of GATA1 downregulation. Interestingly, mRNA levels of GATA1 were not affected by USP7 knockdown on day 9 (Figure 2B), suggesting that

the observed decrease in GATA1 levels is at the post-transcriptional level. We noted decreased levels of GATA1 mRNA levels on days 11 and 13 following USP7 knockdown (*Online Supplementary Figure S3A, B*), likely due to the fact that GATA1 mediates its own regulation at the late stages of erythropoiesis.<sup>36,37</sup> Similarly, inhibition of USP7 activity by the USP7-specific inhibitors P5091 and P22077 also resulted in significant decreases in GATA1 protein levels in a dose-dependent manner (Figure 2C, D), with no obvious effects on other transcription factors beside a slightly decreased expression of KLF1 (*Online Supplementary Figure S4*), implying that USP7-mediated regulation of GATA1 depends on the enzymatic activity of USP7. To further confirm that USP7 deficiency-induced defective erythropoiesis is due to downregulation of GATA1, we performed rescue experiments by ectopically expressing GATA1 in USP7 knockdown cells. Figure 2E shows that the delayed erythroid differentiation as well as impaired erythroblast enucleation could be rescued by restoring GATA1 levels. Furthermore, the expression of GATA1 target genes such as 4.1R and HBG were also rescued (Figure 2F). These results imply that USP7 regulates erythroid differentiation through GATA1.

### USP7 regulates the stability of the GATA1 protein

GATA1 protein levels are regulated by several proteins, including HSP70, a GATA1 chaperone<sup>38-40</sup> and RPS19, necessary for GATA1 translation.<sup>26,41</sup> To examine whether HSP70 and RPS19 are involved in the regulation of GATA1 mediated by USP7, we analyzed the effect of USP7 knockdown on their expression levels. As shown in *Online Supplementary Figure S5A, B*, USP7 knockdown or inhibition had no effects on HSP70 or RPS19 protein levels. Moreover, USP7 knockdown did not affect the translocation of HSP70 into the nucleus (*Online Supplementary Figure S5C, D*). The above findings strongly suggest that USP7 regulates the stability of GATA1 protein directly. We performed several additional studies to confirm this hypothesis and to define the underlying mechanisms. First, co-expression of wildtype USP7 (USP7-WT) with GATA1 increased the GATA1 level (Figure 3A). Importantly, catalytically inactive mutant USP7 (USP7-CS, C233S) did not increase GATA1 protein levels (Figure 3B). Second, downregulation of GATA1 by USP7 knockdown or the USP7 inhibitors P5091 and P22077 was reversed by the proteasome inhibitor MG132 (Figure 3C-E), implying that USP7 maintains the steady-state levels of GATA1 by blocking its proteasomal degradation. To further examine the relationship between USP7 and GATA1, we measured the half-life of intracellular GATA1 after cells had been treated with cycloheximide to inhibit protein biosynthesis. As shown in Figure 3F, knockdown of USP7 significantly shortened the half-life of the GATA1 protein. Conversely, overexpression of USP7-WT, but not USP7-CS, prolonged the half-life of GATA1 (Figure 3G). Taken together, our data demonstrate that USP7 stabilizes GATA1 by preventing its proteasomal degradation.

### USP7 interacts directly with GATA1

Having demonstrated that USP7 stabilizes GATA1, we then examined whether this effect is through their direct interaction by performing co-immunoprecipitation experiments. USP7 or GATA1 was separately immunoprecipitated from cultured primary erythroblasts and the reciprocal protein was detected by western blot analysis. As

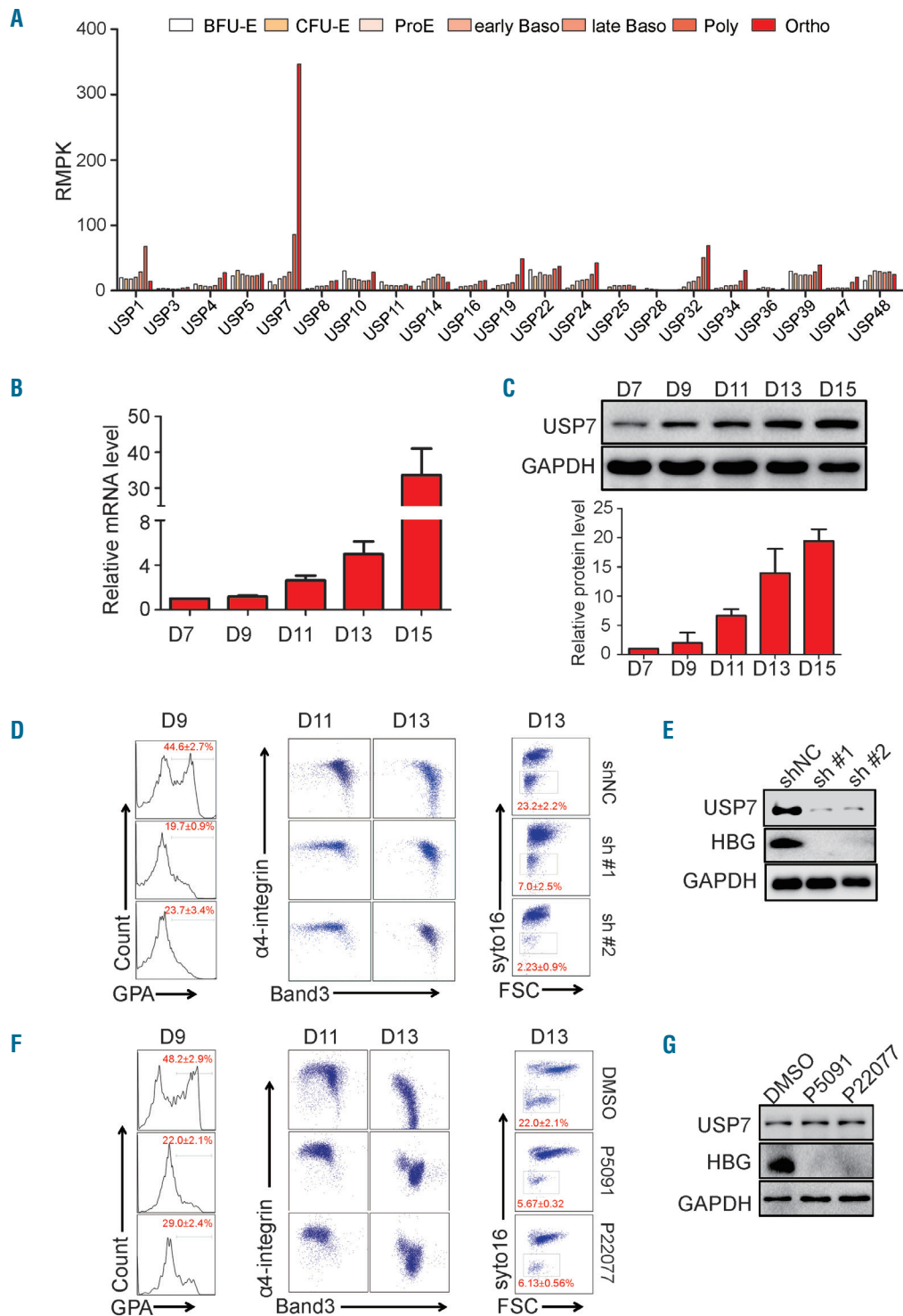


**Figure 1. Deficiency of USP7 impairs human terminal erythroid differentiation.** (A) RNA-sequencing data showing the expression of USP family members (fragments per kilobase of transcript per million) at each distinct stage of human terminal erythroid differentiation. (B) Real-time quantitative polymerase chain reaction results showing the expression of USP7 mRNA on the indicated days of human erythroid terminal differentiation. (C) Representative western blot analysis of the protein level of USP7 on the indicated days of human terminal erythroid differentiation. Quantitative analysis of data from three independent experiments of protein expression levels are shown (lower panel). (D) Left, representative profiles of flow cytometry-based detection of glycoprotein A (GPA) expression in erythroblasts infected with the control or USP7 shRNA on day 9. Middle, representative profiles of Band3/ $\alpha$ 4-integrin levels of GPA-positive erythroblasts transfected with the control or USP7 shRNA lentiviruses on days 11 and 13. Right, representative profiles of flow cytometry-based detection of enucleation by syto16 staining on day 13. Quantification from three independent experiments is indicated. (E) Representative western blot showing the protein level of  $\gamma$ -hemoglobin (HBG) and USP7 in erythroblasts transfected with either the control or USP7 shRNA on day 9. (F) Left, representative profiles of flow cytometry-based detection of GPA expression in erythroblasts treated with dimethylsulfoxide (DMSO) or USP7 inhibitor P5091 (5  $\mu$ M) or P22077 (7.5  $\mu$ M) on day 9. Middle, representative profiles of Band3/ $\alpha$ 4-integrin levels of GPA-positive erythroblasts treated with DMSO or USP7 inhibitor P5091 or P22077 on day 11 and day 13. Right, representative profiles of flow cytometry-based detection of enucleation by syto16 staining on day 13. Quantification from three independent experiments is shown. (G) Representative western blot showing the protein level of HBG and USP7 in erythroblasts treated with DMSO or USP7 inhibitors (P5091 or P22077) on day 9. For all western blot analyses, GAPDH was used as the loading control. BFU-E: burst-forming unit - erythroid; CFU-E: colony-forming unit - erythroid; ProE: proerythroblast; early Baso: early basophilic erythroblast; late Baso: late basophilic erythroblast; Poly: polychromatic erythroblast; Ortho: orthochromatic erythroblast; D: day; GPA: glycoprotein A; FSC: forward scatter; DMSO: dimethylsulfoxide.

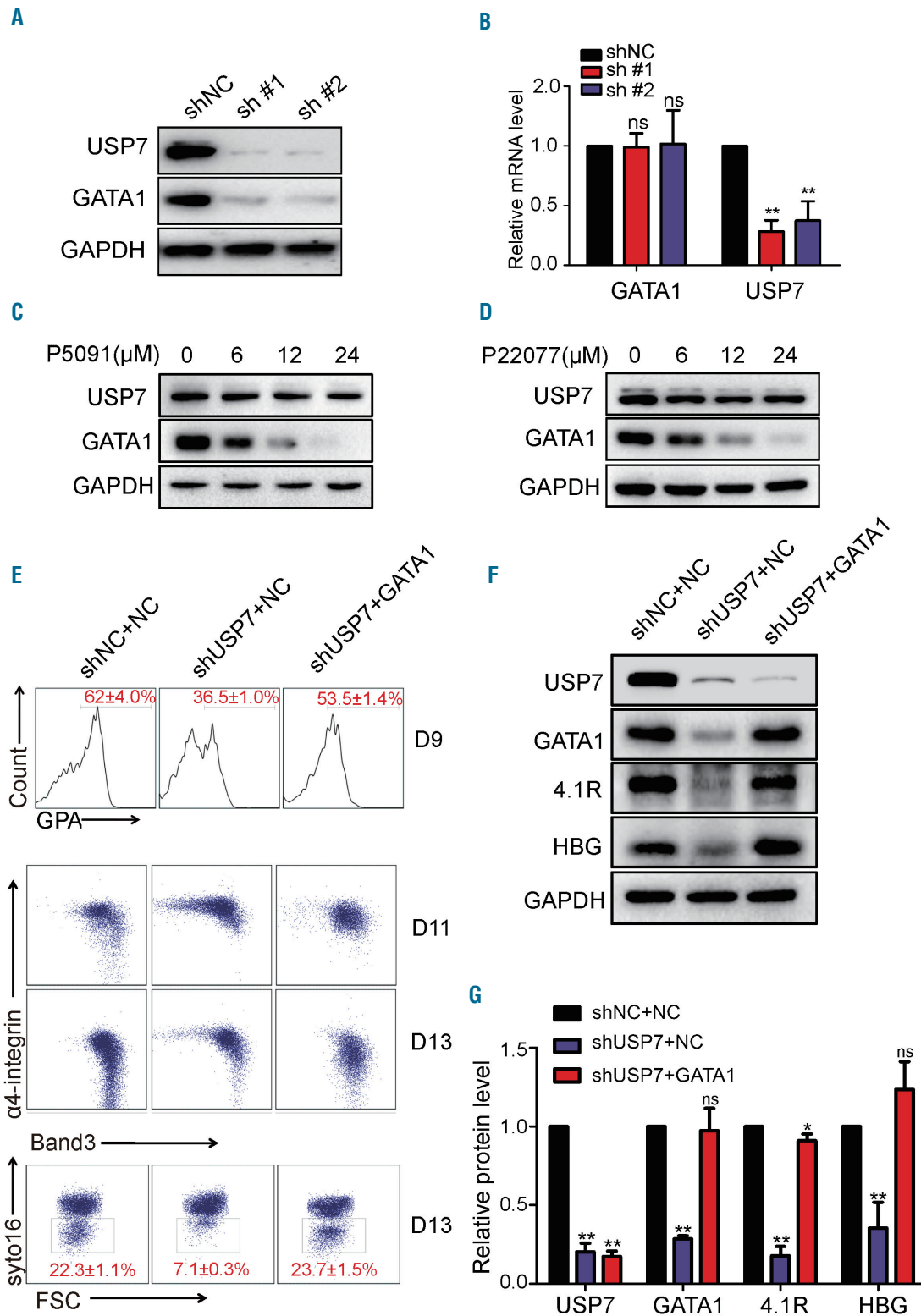


**Figure 2. USP7 regulates erythroid differentiation by affecting GATA1 protein levels.** (A) Representative western blot analysis of erythroblasts transfected with control or USP7 short hairpin (sh)RNA on day 9. GAPDH was used as a loading control. (B) Bar graph presentation of USP7 and GATA1 mRNA levels as determined by real-time quantitative polymerase chain reaction analysis of erythroblasts transfected with the negative control shRNA or USP7 shRNA #1 or #2, which were harvested on day 9. (C) Representative western blot analysis of the erythroblasts after treatment with indicated doses of P5091 on day 9. GAPDH was used as the loading control. (D) Representative western blot analysis of the erythroblasts after treatment with different doses of P22077 on day 9. GAPDH was used as the loading control. (E) The upper panel shows the representative profiles of flow cytometry analysis of GPA expression on day 9 in erythroblasts transfected with control shRNA and NC (HMD empty vector), USP7 shRNA and NC, or USP7 shRNA and GATA1 (GATA1-HMD). The middle panel shows the representative profiles of flow cytometry analysis of Band3/ $\alpha$ 4-integrin expression of the GPA-positive cells in the same groups on days 11 and 13. The bottom panel shows the representative profiles of flow cytometry-based detection of enucleation by syto16 staining on day 13. Quantification from three independent experiments is indicated. (F) Representative western blot analysis of erythroblasts transfected with control shRNA and NC (HMD empty vector), USP7 shRNA and NC, or USP7 shRNA and GATA1 (GATA1-HMD) on day 9. (G) Bar diagram presenting the quantitative analysis of protein expression data from (F). The plot was generated from three independent experiments and shows the means  $\pm$  standard deviations (\*\* $P < 0.01$ , \* $P < 0.05$ ).

shown in Figure 4A, endogenous USP7 was immunoprecipitated by anti-GATA1 antibodies but not by control IgG. Conversely, GATA1 was immunoprecipitated by anti-USP7 antibodies but not by control IgG (Figure 4B). To determine whether USP7 and GATA1 interact directly with each other, we performed GST pull-down assays under a cell-free condition by using purified recombinant GST-GATA1 and Flag-USP7 proteins. As shown in Figure 4C, the purified GST-GATA1 but not the control GST was able to pull down USP7. Furthermore, we mapped the detailed binding region of GATA1 and USP7 in

HEK293T cells, a non-erythroblast environment.<sup>38,42,43</sup> Truncation mutants of GFP-USP7 and Flag-GATA1 were co-transfected into HEK293T cells and co-immunoprecipitation analyses revealed that the N-terminal TRAF-like domain (1-208) of USP7 was critical for the interaction between GATA1 and USP7 (Figure 4D). Conversely, mapping the region of GATA1 required for USP7 binding showed that the DNA binding domain (200-290) of GATA1 was responsible for its interaction with USP7 (Figure 4E). Collectively, these results show that USP7 interacts with GATA1 directly.

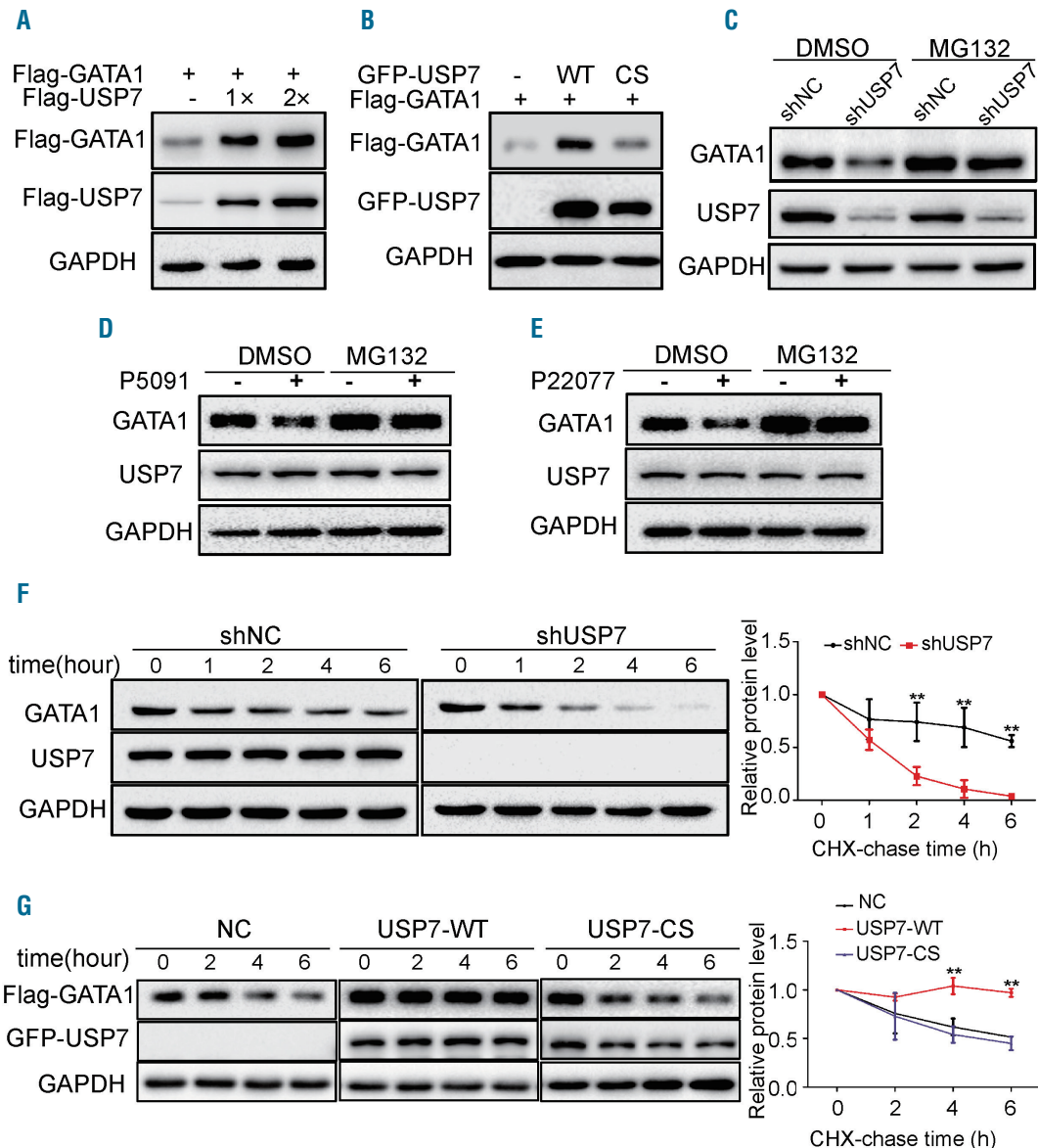


**Figure 3. USP7 regulates the stability of GATA1.** (A) Representative western blot analysis of HEK293T cells transfected with a GATA1-expressing plasmid and either an empty vector or increasing amounts of a GFP-USP7-expressing vector. (B) Representative western blot analysis of HEK293T cells that were transfected with a construct expressing Flag-GATA1 and an empty vector (-), a construct expressing wildtype USP7 (USP7-WT) or one expressing the USP7 (Cys223Ser) mutant (USP7-CS). (C) Representative western blot analysis of erythroblasts that were transfected with control (shNC) or USP7 shRNA treated with or without the proteasome inhibitor MG132 (20  $\mu$ M, 6 h). (D) Representative western blot analysis of erythroblasts that were treated for 6 h with dimethylsulfoxide (DMSO) (-) and/or 15  $\mu$ M P5091 (+) or with 15  $\mu$ M P5091 and 20  $\mu$ M MG132. (E) Representative western blot for the expression of GATA1 in erythroblasts treated for 6 h with DMSO (-) and/or 15  $\mu$ M P22077 (+) or with 15  $\mu$ M P22077 and 20  $\mu$ M MG132 on day 9. (F) Erythroblasts transfected with control or USP7 shRNA were treated with cycloheximide (CHX) (150  $\mu$ g/mL), and collected at the indicated times for western blot. Results are shown as mean  $\pm$  standard deviation (SD) (\*\* $P$ <0.01). (G) Representative western blot analysis of HEK293T cells that were transfected with a vector expressing Flag-GATA1 and an empty vector (NC), one expressing GFP-USP7-WT or one expressing GFP-USP7-CS, after treatment with CHX (150  $\mu$ g/mL) for the indicated amounts of time. Results are shown as mean  $\pm$  standard deviation (\*\* $P$ <0.01). For all western blot analyses, GAPDH was used as the loading control.

**USP7 stabilizes GATA1 protein through K48 deubiquitylation**

Since USP7 is a deubiquitylase, it is reasonable to speculate that USP7 regulates the stability of GATA1 via deubiquitylation. To test this hypothesis, we investigated the effect of USP7 on the poly-ubiquitylation of GATA1. As expected, knockdown of USP7 resulted in a significant increase in the poly-ubiquitylation of GATA1 (Figure 5A). In contrast, ectopic expression of USP7-WT but not the catalytic inactive mutant USP7-CS reduced the level of poly-ubiquitylation of GATA1 (Figure 5B and *Online Supplementary Figure S6A*). Moreover, USP7-mediated

decrease of GATA1 poly-ubiquitylation was blocked by the USP7 inhibitors P5091 and P22077 (Figure 5C and *Online Supplementary Figure S6B*), demonstrating that the enzymatic activity of USP7 is essential for the USP7-mediated deubiquitylation of GATA1. To verify that GATA1 is a direct substrate of USP7, the purified USP7 protein was incubated with ubiquitylated GATA1 in a cell-free system. As shown in Figure 5D, GATA1 poly-ubiquitylation was decreased in the presence USP7, indicating that USP7 deubiquitylates GATA1 directly. To determine which poly-ubiquitin chain on GATA1 is removed by USP7, we employed a series of ubiquitin mutants that contain only

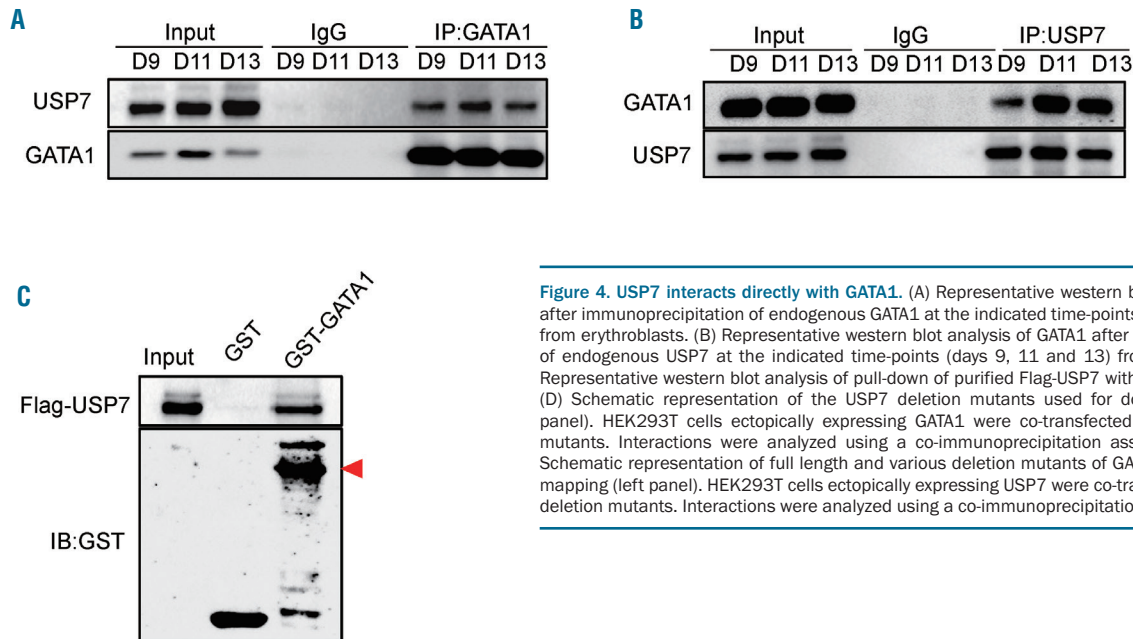
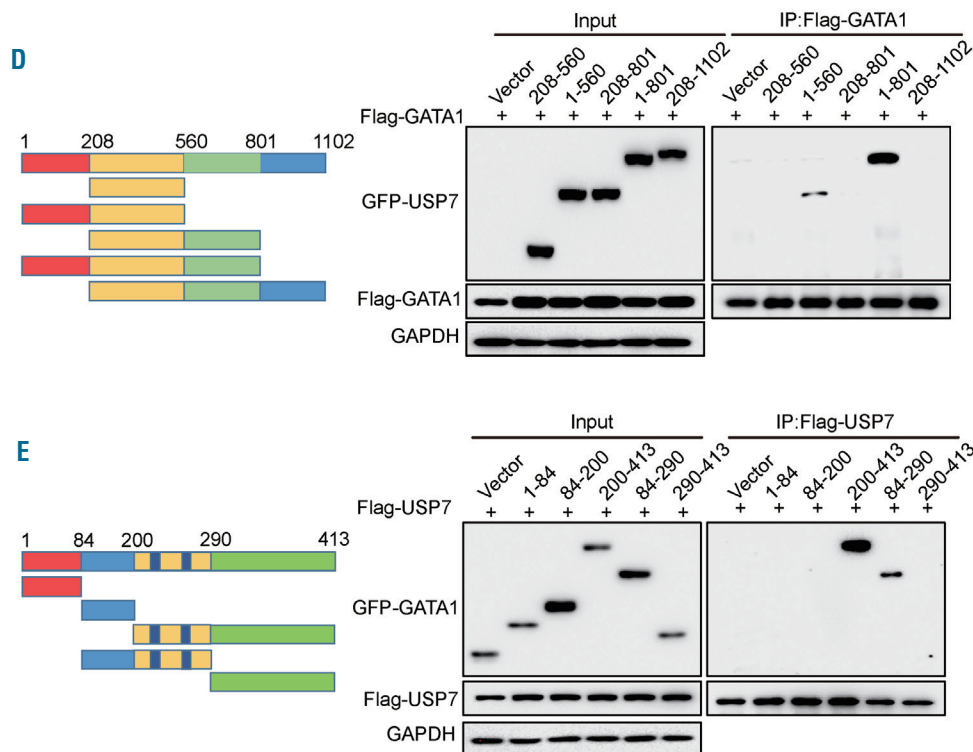


**Figure 4. USP7 interacts directly with GATA1.** (A) Representative western blot analysis of USP7 after immunoprecipitation of endogenous GATA1 at the indicated time-points (days 9, 11 and 13) from erythroblasts. (B) Representative western blot analysis of GATA1 after immunoprecipitation of endogenous USP7 at the indicated time-points (days 9, 11 and 13) from erythroblasts. (C) Representative western blot analysis of pull-down of purified Flag-USP7 with purified GST-GATA1. (D) Schematic representation of the USP7 deletion mutants used for domain mapping (left panel). HEK293T cells ectopically expressing GATA1 were co-transfected with USP7 deletion mutants. Interactions were analyzed using a co-immunoprecipitation assay (right panel). (E) Schematic representation of full length and various deletion mutants of GATA1 used for domain mapping (left panel). HEK293T cells ectopically expressing USP7 were co-transfected with GATA1 deletion mutants. Interactions were analyzed using a co-immunoprecipitation assay (right panel).



one lysine (K6, K11, K27, K29, K33, K48 or K63). As shown in *Online Supplementary Figure S7*, USP7 significantly decreased only the K48-linked poly-ubiquitin chain but not any other lysine isopeptide-linked poly-ubiquitin chains (K6, K11, K27, K29, K33 or K63). To further confirm that K48-linked poly-ubiquitin is removed by USP7, we replaced K48 or K63 lysine by arginine (R) and, as shown in Figure 5E, mutation of K48 but not K63 significantly impaired USP7-mediated deubiquitylation. Collectively, these results confirm that USP7 stabilizes GATA1 by removing the K48-linked poly-ubiquitin.

## Discussion

Erythropoiesis is a process by which hematopoietic stem cells proliferate and differentiate to eventually produce mature red blood cells. Many cellular and molecular changes occur during this process. Morphological changes include a progressive decrease in cell size, increase in chromatin condensation and enucleation. At the molecular level, high-throughput analyses revealed dramatic changes in both the transcriptome and the proteome.<sup>2,44</sup> In contrast to extensive studies on transcriptional networks, very little

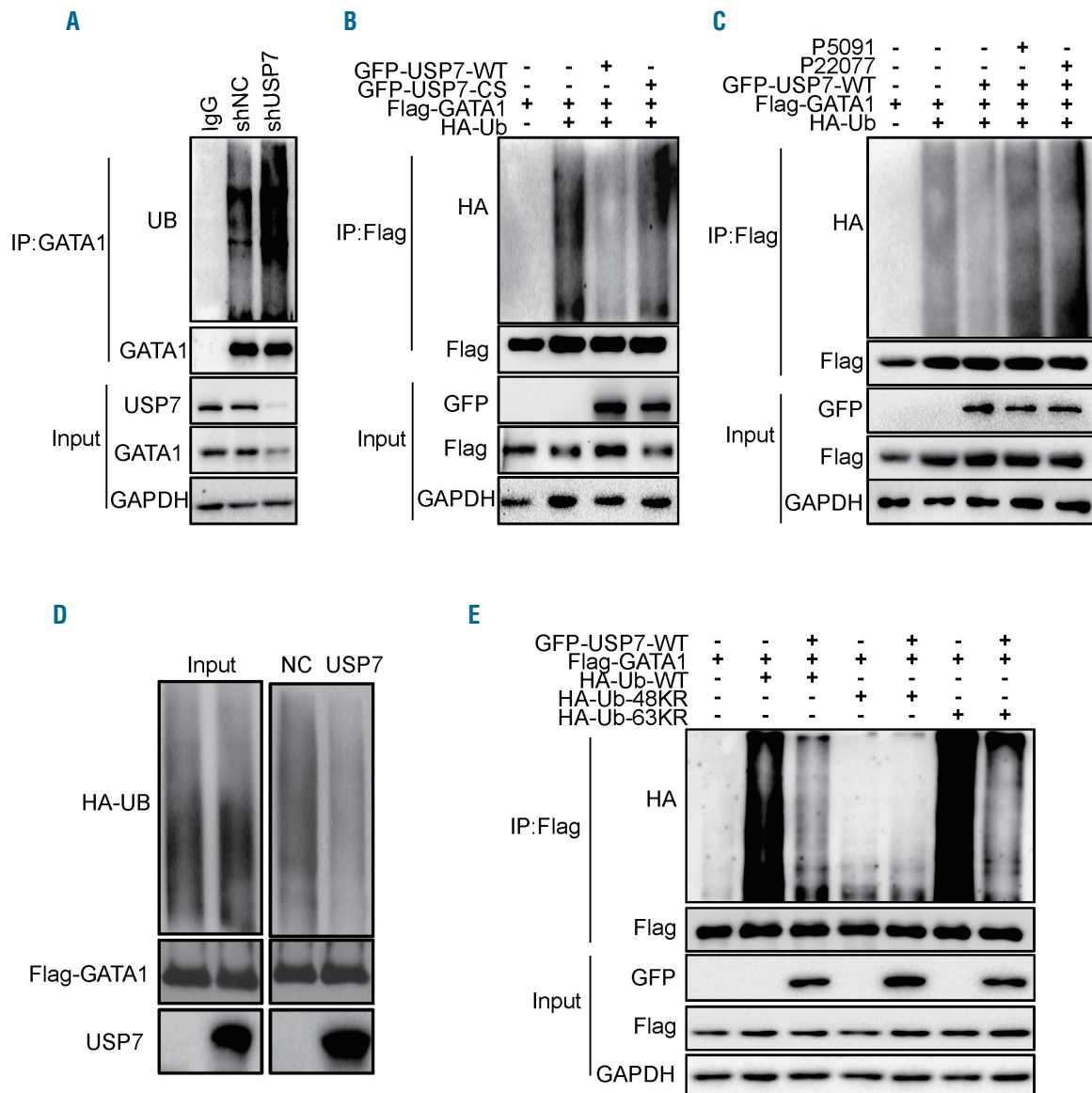


**Figure 5. USP7 stabilizes GATA1 protein through deubiquitination.** (A) Erythroblasts at day 7 transfected with control or USP7 shRNA (#1) lentivirus. GATA1 was immunoprecipitated with anti-GATA1 antibody and immunoblotted with anti-ubiquitin on day 9. (B) Representative western blot analysis of ubiquitin after incubation of anti-Flag-coated beads with lysates from HEK293T cells that were transfected with empty vectors (-) or those expressing Flag-GATA1 either alone or in combination with vectors expressing USP7-WT or USP7-CS, and HA-ubiquitin. (C) Representative western blot analysis for ubiquitin after anti-Flag immunoprecipitation of HEK293T cells ectopically expressing Flag-GATA1 either alone or in combination with USP7-WT. Cells expressing both Flag-GATA1 and USP7-WT were treated with 20  $\mu$ M P5091 or P22077 for 8 h before being harvested. (D) Representative western blot for the cell-free deubiquitylation assay. Ubiquitylated GATA1 was incubated with bacterial-expressed and purified USP7-WT for 2 h at 37  $^{\circ}$ C, followed by western blot with anti-HA antibody (right panel). The left panel is the input. (E) Representative western blot analysis for ubiquitin after anti-Flag immunoprecipitation of HEK293T cells ectopically expressing Flag-GATA1 either alone or in combination with USP7-WT, and ubiquitin WT or mutant (K48R or K63R).

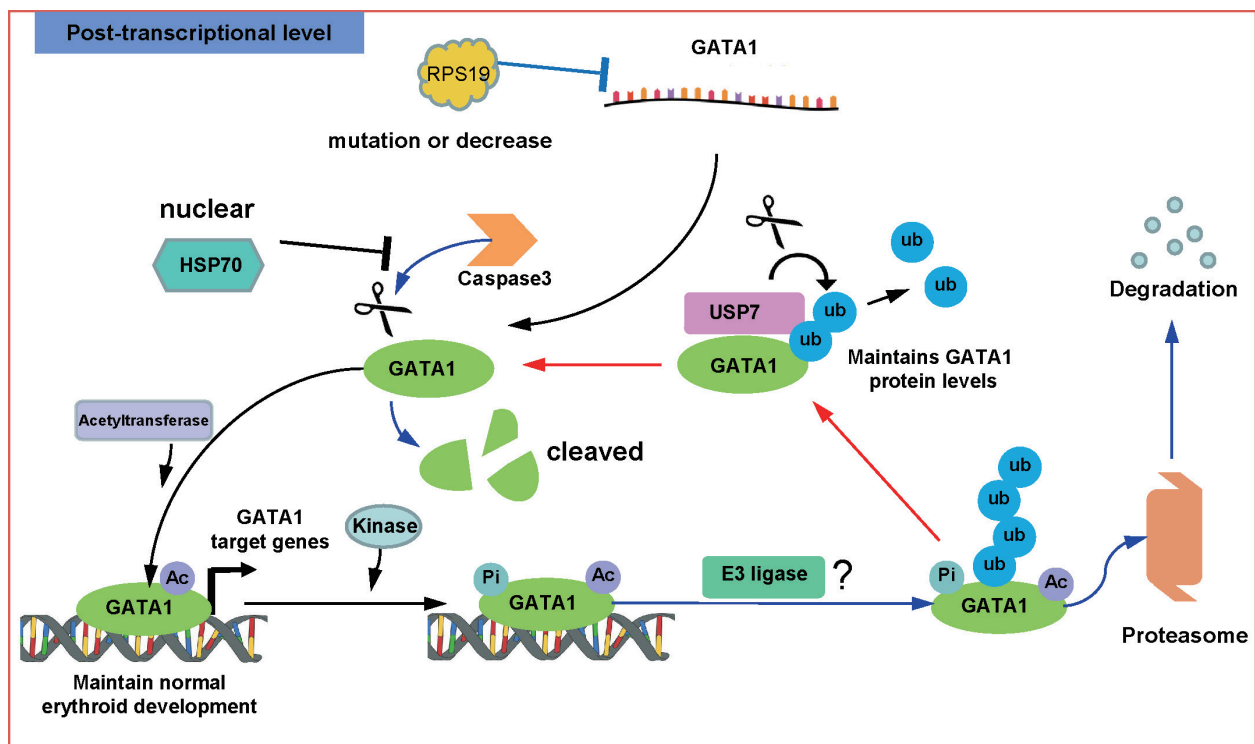


**Figure 6. A schematic model of post-transcriptional regulation of GATA1.** Post-transcriptional regulation of GATA1 includes the translational and post-translational levels. The translational level of GATA1 is mainly controlled by RPS19. Decrease or mutation of RPS19 results in reduced translation of GATA1. At the post-translational level, the nuclear HSP70 protects GATA1 from caspase 3 cleavage. In addition, acetylation and phosphorylation of GATA1 cooperate as the signal for ubiquitylation of GATA1 to degradation. USP7 interacts directly with GATA1 and maintains stability of GATA1 by removing the poly-ubiquitylation.

is known about the mechanisms by which the proteome is remodeled. Previous studies demonstrated that the balance between ubiquitination and deubiquitination plays important roles in homeostasis of cellular protein pools.<sup>45</sup> In the present study, we documented, for the first time, the role of a deubiquitylase, USP7, in erythroid differentiation. We further documented that the mechanism is stabilization of the erythropoiesis master regulator GATA1.

USP7 is a member of a deubiquitinating enzyme family that contains more than 90 genes.<sup>46</sup> USP7 expression is ubiquitous in different cell types: mice with knocked out USP7, which are homozygous for a null allele, show embryonic growth arrest and die between embryonic day 6.5 and 7.5.<sup>47</sup> Furthermore, conditional knockout mice showed that USP7 is required for development of the central nervous system and functional regulatory T cells.<sup>48,49</sup> We expect that deletion of USP7 in erythroid cells *in vivo* will lead to altered erythropoiesis. We are in the process of generating such conditional knockout mice to define the function of USP7 *in vivo*. Besides USP7, many other deubiquitinating enzymes are also expressed in erythroid cells, although at lower levels than USP7. It will be interesting in future studies to identify the functional roles of other deubiquitylases during erythroid differentiation. Since each deubiquitinating enzyme has different substrate specificity,<sup>47</sup> it is likely that members of the deubiquitinating enzyme family may regulate different aspects of erythropoiesis via different mechanisms.

As the key transcriptional factor for erythropoiesis, GATA1 protein expression is tightly regulated at several levels. These include translational control by ribosome lev-

els,<sup>26,41</sup> stabilization by HSP70 from caspase 3 cleavage,<sup>27,38-40</sup> and degradation by acetylation and phosphorylation-associated ubiquitination.<sup>24</sup> Here we show that knockdown of USP7 by shRNA or inhibition of USP7 activity by USP7-specific inhibitors led to dramatic decreases in GATA1 protein levels. Interestingly, USP7 knockdown or inhibition had no effects on the protein levels of RPS19 or HSP70, strongly suggesting that USP7 affects the stability of GATA1 in a direct manner. This notion is supported by our findings that USP7 binds GATA1 directly and stabilizes GATA1 by de-ubiquitination. Specifically, USP7 catalyzes the removal of K48-linked poly-ubiquitin which is a proteasome degradation signal for proteins. Based on our findings and that of others, we propose a schematic model for post-transcriptional regulation of GATA1 (Figure 6). GATA1 functions in the context of multi-protein complexes that include interacting proteins such as FOG1.<sup>50-53</sup> Although USP7 knockdown or inhibition did not affect the level of FOG1 or NuRD complex (Online Supplementary Figure S8), we cannot exclude the possibility that these important GATA1 cofactors or modifications can modulate GATA1-USP7 interactions during erythroid development. Further study is therefore warranted to investigate whether USP7 binds other cofactors such as FOG1 and/or different modifications of GATA1.

Altered expression of GATA1 has been reported in myelodysplastic syndromes<sup>39,54</sup> and  $\beta$ -thalassemia.<sup>40</sup> However, the mechanisms of the altered GATA1 expression remains to be fully defined. It has been reported that USP7 is associated with several human diseases.<sup>55-57</sup> Given the close relationship between USP7 and GATA1, demon-

strated in our present study, it will be interesting in future studies to examine whether the altered expression of GATA1 may be associated with changes in USP7 expression in certain blood disorders.

In summary, we have uncovered a previously unrecognized role for a deubiquitylase, USP7, in human terminal erythroid differentiation and have identified USP7 as a deubiquitylase of GATA1. Our findings provide new and novel insights into mechanisms of regulating human erythropoiesis.

### Acknowledgments

This work was supported by the National Key Research and Development Program of China (2018YFA0107800), the Natural Science Foundation of China (81770107, 81672760, 81920108004, 81270576, 81800125, 81470362 and 81530005), National Institutes of Health grants (DK100810 and DK32094), the Strategic Priority Research Program of Central South University (zLXD2017004) and the postgraduate innovation project of Central South University (2016zzts165).

### References

- Hattangadi SM, Wong P, Zhang L, et al. From stem cell to red cell: regulation of erythropoiesis at multiple levels by multiple proteins, RNAs, and chromatin modifications. *Blood*. 2011;118(24):6258-6268.
- An X, Schulz VE, Li J, et al. Global transcriptome analyses of human and murine terminal erythroid differentiation. *Blood*. 2014;123(22):3466-3477.
- Nandakumar SK, Ulirsch JC, Sankaran VG. Advances in understanding erythropoiesis: evolving perspectives. *Br J Haematol*. 2016;173(2):206-218.
- Dzierzak E, Philipsen S. Erythropoiesis: development and differentiation. *Cold Spring Harb Perspect Med*. 2013;3(4):a011601.
- Amm I, Sommer T, Wolf DH. Protein quality control and elimination of protein waste: the role of the ubiquitin-proteasome system. *Biochim Biophys Acta*. 2014;1843(1):182-196.
- Ciechanover A, Hod Y, Hershko A. A heat-stable polypeptide component of an ATP-dependent proteolytic system from reticulocytes. *Biochem Biophys Res Commun*. 1978;81(4):1100-1105.
- Li B, Jia N, Kapur R, Chun KT. Cul4A targets p27 for degradation and regulates proliferation, cell cycle exit, and differentiation during erythropoiesis. *Blood*. 2006;107(11):4291-4299.
- Waning DL, Li B, Jia N, et al. Cul4A is required for hematopoietic cell viability and its deficiency leads to apoptosis. *Blood*. 2008;112(2):320-329.
- Nguyen AT, Prado MA, Schmidt PJ, et al. UBE2O remodels the proteome during terminal erythroid differentiation. *Science*. 2017;357(6350).
- D'Andrea A, Pellman D. Deubiquitinating enzymes: a new class of biological regulators. *Crit Rev Biochem Mol Biol*. 1998;33(5):337-352.
- Hanpude P, Bhattacharya S, Dey AK, Maiti TK. Deubiquitinating enzymes in cellular signaling and disease regulation. *IUBMB Life*. 2015;67(7):544-555.
- Zlatanou A, Sabbioneda S, Miller ES, et al. USP7 is essential for maintaining Rad18 stability and DNA damage tolerance. *Oncogene*. 2016;35(8):965-976.
- Van der Knaap JA, Kumar BR, Moshkin YM, et al. GMP synthetase stimulates histone H2B deubiquitylation by the epigenetic silencer USP7. *Mol Cell*. 2005;17(5):695-707.
- Alonso-de Vega I, Martín Y, Smits VA. USP7 controls Chk1 protein stability by direct deubiquitination. *Cell Cycle*. 2014;13(24):3921-3926.
- Li M, Chen D, Shiloh A, et al. Deubiquitination of p53 by HAUSP is an important pathway for p53 stabilization. *Nature*. 2002;416(6881):648-653.
- Daubeuf S, Singh D, Tan Y, et al. HSV ICP0 recruits USP7 to modulate TLR-mediated innate response. *Blood*. 2009;113(14):3264-3275.
- Huang Z, Wu Q, Guryanova OA, et al. Deubiquitylase HAUSP stabilizes REST and promotes maintenance of neural progenitor cells. *Nat Cell Biol*. 2011;13(2):142-152.
- Tang Y, Lv L, Li W, et al. Protein deubiquitinase USP7 is required for osteogenic differentiation of human adipose-derived stem cells. *Stem Cell Res Ther*. 2017;8(1):186.
- Gao Y, Koppen A, Rakhshandehroo M, et al. Early adipogenesis regulated through USP7-mediated deubiquitylation of the histone acetyltransferase TIP60. *Nat Commun*. 2013;4:2656.
- Crispino JD. GATA1 in normal and malignant hematopoiesis. *Semin Cell Dev Biol*. 2005;16(1):137-147.
- Fujiwara Y, Browne CP, Cunniff K, et al. Arrested development of embryonic red cell precursors in mouse embryos lacking transcription factor GATA-1. *Proc Natl Acad Sci U S A*. 1996;93(22):12355-12358.
- Pevny L, Simon MC, Robertson E, et al. Erythroid differentiation in chimaeric mice blocked by a targeted mutation in the gene for transcription factor GATA-1. *Nature*. 1991;349(6303):257-260.
- Whyatt D, Lindeboom F, Karis A, et al. An intrinsic but cell-nonautonomous defect in GATA-1-overexpressing mouse erythroid cells. *Nature*. 2000;406(6795):519-524.
- Hernandez-Hernandez A, Ray P, Litos G, et al. Acetylation and MAPK phosphorylation cooperate to regulate the degradation of active GATA-1. *EMBO J*. 2006;25(14):3264-3274.
- Hu J, Liu J, Xue F, et al. Isolation and functional characterization of human erythroblasts at distinct stages: implications for understanding of normal and disordered erythropoiesis in vivo. *Blood*. 2013;121(16):3246-3253.
- Ludwig LS, Gazda HT, Eng JC, et al. Altered translation of GATA1 in Diamond-Blackfan anemia. *Nat Med*. 2014;20(7):748-753.
- Han X, Zhang J, Peng Y, et al. Unexpected role for p19INK4d in posttranscriptional regulation of GATA1 and modulation of human terminal erythropoiesis. *Blood*. 2017;129(2):226-237.
- Choo YS, Zhang Z. Detection of protein ubiquitination. *J Vis Exp*. 2009;(30).
- Yan H, Wang Y, Qu X, et al. Distinct roles for TET family proteins in regulating human erythropoiesis. *Blood*. 2017;129(14):2002-2012.
- Huang Y, Hale J, Wang Y, et al. SF3B1 deficiency impairs human erythropoiesis via activation of p53 pathway: implications for understanding of ineffective erythropoiesis in MDS. *J Hematol Oncol*. 2018;11(1):19.
- Chauhan D, Tian Z, Nicholson B, et al. A small molecule inhibitor of ubiquitin-specific protease-7 induces apoptosis in multiple myeloma cells and overcomes bortezomib resistance. *Cancer Cell*. 2012;22(3):345-358.
- Altun M, Kramer H B, Willems L I, et al. Activity-based chemical proteomics accelerates inhibitor development for deubiquitylating enzymes. *Chem Biol*. 2011;18(11):1401-1412.
- Morotti A, Panuzzo C, Crivellaro S, et al. BCR-ABL disrupts PTEN nuclear-cytoplasmic shuttling through phosphorylation-dependent activation of HAUSP. *Leukemia*. 2014;28(6):1326-1333.
- Song MS, Salmena L, Carracedo A, et al. The deubiquitylation and localization of PTEN are regulated by a HAUSP-PML network. *Nature*. 2008;455(7214):813-817.
- Crossley M, Tsang A P, Bieker J J, et al. Regulation of the erythroid Kruppel-like factor (EKLF) gene promoter by the erythroid transcription factor GATA-1. *J Biol Chem*. 1994;269(22):15440-15444.
- Kobayashi M, Yamamoto M. Regulation of GATA1 gene expression. *J Biol Chem*. 2007;282(1):1-10.
- Kaneko H, Shimizu R, Yamamoto M. GATA factor switching during erythroid differentiation. *Curr Opin Hematol*. 2010;17(3):163-168.
- Ribeil JA, Zermati Y, Vandekerckhove J, et al. Hsp70 regulates erythropoiesis by preventing caspase-3-mediated cleavage of GATA-1. *Nature*. 2007;445(7123):102-105.
- Frisan E, Vandekerckhove J, de Thonel A, et al. Defective nuclear localization of Hsp70 is associated with dyserythropoiesis and GATA-1 cleavage in myelodysplastic syndromes. *Blood*. 2012;119(6):1532-1542.
- Arlet JB, Ribeil JA, Guillem F, et al. HSP70 sequestration by free  $\alpha$ -globin promotes ineffective erythropoiesis in  $\beta$ -thalassaemia. *Nature*. 2014;514(7521):242-246.
- Khajuria RK, Munschauer M, Ulirsch JC, et al. Ribosome levels selectively regulate translation and lineage commitment in human hematopoiesis. *Cell*. 2018;173(1):90-103.
- de Thonel A, Vandekerckhove J, Lanneau D, et al. HSP27 controls GATA-1 protein

- level during erythroid cell differentiation. *Blood*. 2010;116(1):85-96.
43. Wu J, Zhou LQ, Yu W, et al. PML4 facilitates erythroid differentiation by enhancing the transcriptional activity of GATA-1. *Blood*. 2014;123(2):261-270.
  44. Gautier EF, Ducamp S, Leduc M, et al. Comprehensive proteomic analysis of human erythropoiesis. *Cell Rep*. 2016;16(5):1470-1484.
  45. Clague MJ, Heride C, Urbé S. The demographics of the ubiquitin system. *Trends Cell Biol*. 2015;25(7):417-426.
  46. Clague MJ, Barsukov I, Coulson JM, et al. Deubiquitylases from genes to organism. *Physiol Rev*. 2013;93(3):1289-1315.
  47. Kon N, Kobayashi Y, Li M, et al. Inactivation of HAUSP in vivo modulates p53 function. *Oncogene*. 2010;29(9):1270-1279.
  48. Kon N, Zhong J, Kobayashi Y, et al. Roles of HAUSP-mediated p53 regulation in central nervous system development. *Cell Death Differ*. 2011;18(8):1366-1375.
  49. van Loosdregt J, Fleskens V, Fu J, et al. Stabilization of the transcription factor Foxp3 by the deubiquitinase USP7 increases Treg-cell-suppressive capacity. *Immunity*. 2013;39(2):259-271.
  50. Crispino JD, Lodish MB, MacKay JP, Orkin SH. Use of altered specificity mutants to probe a specific protein-protein interaction in differentiation: the GATA-1:FOG complex. *Mol Cell*. 1999;3(2):219-228.
  51. Rodriguez P, Bonte E, Krijgsveld J, et al. GATA-1 forms distinct activating and repressive complexes in erythroid cells. *EMBO J*. 2005;24(13):2354-2366.
  52. Tsang AP, Visvader JE, Turner CA, et al. FOG, a multitype zinc finger protein, acts as a cofactor for transcription factor GATA-1 in erythroid and megakaryocytic differentiation. *Cell*. 1997;90(1):109-119.
  53. Miccio A, Wang Y, Hong W, et al. NuRD mediates activating and repressive functions of GATA-1 and FOG-1 during blood development. *EMBO J*. 2010;29(2):442-456.
  54. Hopfer O, Nolte F, Mossner M, et al. Epigenetic dysregulation of GATA1 is involved in myelodysplastic syndromes dyserythropoiesis. *Eur J Haematol*. 2012;88(2):144-153.
  55. Hao YH, Fountain MD Jr, Fontacer K, et al. USP7 acts as a molecular rheostat to promote WASH-dependent endosomal protein recycling and is mutated in a human neurodevelopmental disorder. *Mol Cell*. 2015;59(6):956-969.
  56. Nicholson B, Suresh Kumar KG. The multifaceted roles of USP7: new therapeutic opportunities. *Cell Biochem Biophys*. 2011;60(1-2):61-68.
  57. YeasminKhusbu F, Chen FZ, Chen HC. Targeting ubiquitin specific protease 7 in cancer: a deubiquitinase with great prospects. *Cell Biochem Funct*. 2018;36(5):244-254.

# Altered parasite life-cycle processes characterize *Babesia divergens* infection in human sickle cell anemia

Jeny R. Cursino-Santos,<sup>1</sup> Manpreet Singh,<sup>1</sup> Eric Senaldi,<sup>2</sup> Deepa Manwani,<sup>3</sup> Karina Yazdanbakhsh<sup>4</sup> and Cheryl A. Lobo<sup>1</sup>

<sup>1</sup>Department of Blood-Borne Parasites Lindsley F. Kimball Research Institute, New York Blood Center, New York, NY; <sup>2</sup>Medical Services New York Blood Center, New York, NY;

<sup>3</sup>Department of Pediatrics, Albert Einstein College of Medicine, Bronx, NY and

<sup>4</sup>Department of Complement Biology Lindsley F. Kimball Research Institute, New York Blood Center, New York, NY, USA



Haematologica 2019  
Volume 104(11):2189-2199

## ABSTRACT

*Babesia divergens* is an intra-erythrocytic parasite that causes malaria-like symptoms in infected people. As the erythrocyte provides the parasite with the infra-structure to grow and multiply, any perturbation to the cell should impact parasite viability. Support for this comes from the multitude of studies that have shown that the sickle trait has in fact been selected because of the protection it provides against a related Apicomplexan parasite, *Plasmodium*, that causes malaria. In this paper, we examine the impact of both the sickle cell anemia and sickle trait red blood cell (RBC) environment on different aspects of the *B. divergens* life-cycle, and reveal that multiple aspects of parasite biological processes are altered in the mutant sickle anemia RBC. Such processes include parasite population progression, caused potentially by defective merozoite infectivity and/or defective egress from the sickle cell, resulting in severely lowered parasitemia in these cells with sickle cell anemia. In contrast, the sickle trait RBC provide a supportive environment permitting *in vitro* infection rates comparable to those of wild-type RBC. The elucidation of these naturally occurring RBC resistance mechanisms is needed to shed light on host-parasite interaction, lend evolutionary insights into these related blood-borne parasites, and to provide new insights into the development of therapies against this disease.

## Introduction

The human erythrocyte serves as the common host cell for two major Apicomplexan parasites, *Plasmodium* and *Babesia*. Both species invade, develop and egress from the red blood cell (RBC) following specific developmental programs that contribute to the majority of clinical symptoms associated with these infections.<sup>1-3</sup> Shielded within the host RBC, these intra-erythrocytic parasites differentiate and multiply while concealing their presence from the immune system. After filling the available intra-cellular space, the resultant parasite progeny egress as merozoites, and invade new RBC, carrying on the cycle of growth and proliferation. This cycle depends on intricate interactions between host RBC and parasite molecules. Thus, any perturbations to either the composition or arrangement of proteins on or within the host RBC can impact the parasite's development and survival, and thus increase host resistance to parasite infection.

Much effort has been spent in determining the different means by which the human host can suppress this active parasite replication to limit the damage caused by the continuous destruction of the host RBC. One of the most commonly encountered mechanisms discovered is the genetic disorders that are found in the RBC.<sup>4</sup> As the *Plasmodium* parasites have long co-existed with the human host, they have exerted extraordinary adaptive pressure on the human species.<sup>5</sup> Consequently, in humans, multiple genetic polymorphisms have been selected for several hemoglobin disorders that provide intrinsic protection against severe malaria complications and are convincingly supported by clinical data.<sup>6,7</sup> Hemoglobin (Hb) is the oxy-

## Correspondence:

CHERYL A. LOBO  
CLobo@NYBloodcenter.org

Received: December 13, 2018.

Accepted: March 20, 2019

Pre-published: March 28, 2019

doi:10.3324/haematol.2018.214304

Check the online version for the most updated information on this article, online supplements, and information on authorship & disclosures: [www.haematologica.org/content/104/11/2189](http://www.haematologica.org/content/104/11/2189)

©2019 Ferrata Storti Foundation

Material published in *Haematologica* is covered by copyright. All rights are reserved to the Ferrata Storti Foundation. Use of published material is allowed under the following terms and conditions:

<https://creativecommons.org/licenses/by-nc/4.0/legalcode>. Copies of published material are allowed for personal or internal use. Sharing published material for non-commercial purposes is subject to the following conditions: <https://creativecommons.org/licenses/by-nc/4.0/legalcode>, sect. 3. Reproducing and sharing published material for commercial purposes is not allowed without permission in writing from the publisher.



gen-carrying component and major protein of the RBC and is normally formed as a tetramer of two  $\alpha$ -globins and two  $\beta$ -globins which constitute adult hemoglobin A (HbA). The major hemoglobinopathies result from mutations that either decrease the production of  $\alpha$ - or  $\beta$ -globins (in  $\alpha$ - and  $\beta$ -thalassemia) or sickling of the erythrocyte (in sickle HbS, HbC, and HbE diseases).<sup>8,9</sup> Remarkably, small genetic variations confer dramatic levels of protection from malaria.<sup>10,11</sup> HbS is the result of a single point mutation (Glu→Val) on the sixth codon of the  $\beta$ -globin gene. Homozygotes for hemoglobin S (HbSS) with two affected  $\beta$  chains develop sickle cell disease (SCD), in which polymerized Hb causes RBC to sickle and occlude blood vessels, and results in high morbidity and mortality.<sup>12</sup> Heterozygotes for sickle hemoglobin (HbAS) have sickle cell trait and are generally asymptomatic. Despite the obvious deleterious nature of HbSS, it is now widely accepted that the persistence of the sickle mutation in human populations is due to the protection from malaria afforded to heterozygous individuals.<sup>13,14</sup> Multiple divergent mechanisms have been put forward to explain this resistance to malaria, including enhanced macrophage uptake, impaired growth and maturation of parasite, and decreased deposition of parasitized RBC in deep post capillary beds, but no single convincing explanation has yet been given.<sup>1,15,16</sup>

Babesiosis has long been recognized as a veterinary problem of great significance, but only in the last 50 years has it been recognized as an important pathogen in man.<sup>2</sup> The four identified *Babesia* species that have so far been definitively confirmed to infect humans are *B. microti*,<sup>17</sup> *B. divergens*,<sup>18</sup> *B. dumcani*,<sup>19,20</sup> and *B. venatorum*.<sup>21-24</sup> As sampling has become expansive and techniques have become more sensitive, there is evidence that more *B. microti*-like and *B. divergens*-like *spp.* are able to cause human infection (as reported in detail by Yabsley and Shock).<sup>25</sup> However, the general life cycle within humans remains the same. *Babesia* parasites are intracellular obligates that target RBC, and the parasite's ability to first recognize and then invade host RBC is central to the disease pathology. Besides its natural route of transmission *via* the infected tick, the parasite is also transmitted by transfusion of infected blood as its RBC host provides an optimum vehicle to facilitate its transmission. In fact, as the frequency of clinical cases has risen, there has been an associated increase in transfusion-transmitted *Babesia* (TTB), mainly reported for *B. microti*,<sup>26-28</sup> making babesiosis the most frequent transfusion-transmitted infection in the US. Patients with sickle cell anemia, especially those on chronic transfusion therapy, are at high risk for severe TTB.<sup>29,30</sup> Whether the sickle red cells themselves are responsible for the increased susceptibility of these patients to TTB or whether this is due to other related factors, such as a compromised immune system, has not been investigated. In this paper, we focus on the ability of the *Babesia* parasite to invade, grow in and egress from sickle trait and sickle cell anemia erythrocytes. Use of *in vitro* invasion and development assays were developed in our laboratory,<sup>31</sup> as our primary outcome provided a rare opportunity to systematically examine the cellular determinants of parasite development in the sickle cell anemia setting. These enabled a comparison between various components of the parasite life-cycle in RBC obtained from various hemoglobin genotypes, HbAA, HbAS and HbSS, and revealed altered parasite population progres-

sion, parasite maturation and egress phenotypes in the HbSS cells.

## Methods

### Ethics statement

Human blood from healthy volunteer donors was used to culture *B. divergens* (Bd) *in vitro*. SCD patients' RBC were obtained from residual anticoagulated blood samples from same day collections from patients with sickle cell anemia (hemoglobin genotype SS) who had not been transfused for at least three months prior to sample draw. Patients provided consent for use of de-identified blood for research purposes on a Montefiore Medical Center Institutional Review Board (IRB) approved protocol. HbAA RBC and sickle trait RBC were identified from New York Blood Center (NYBC) blood donors and confirmed through genotypic analysis. All blood was used within a few hours of drawing. The blood was de-identified and approved for use by the NYBC IRB. All blood donors gave informed written consent for use of their blood for research purposes.

### *B. divergens in vitro* culture

*B. divergens* (Bd Rouen 1986 strain) were maintained in human RBC as previously described.<sup>32,33</sup> A<sup>+</sup> RBC were collected in 10% CPD and washed 3X with RPMI 1640 medium for the complete plasma and white cell removal.

### Free merozoites isolation

High concentration of viable free merozoites was isolated from unsynchronized cultures at high parasitemia (40%), as described previously.<sup>31,34</sup>

### Assessment of invasion, development and egress in various red blood cells

Fresh cultures were seeded with purified merozoite suspension at 20% (v/v) of culture volume. To define time points to accurately estimate invasion in the different RBC (HbAA, HbAS; HbSS), invasion was assayed in the first set of samples at 5 minutes (min), 1 hour (h) or 6 h post invasion. At additional time points (24-72 h), samples were collected to assess the culture progression and sub-population dynamics from the perspective of parasite development and egress. Analysis was carried out at specific intervals of 24 h, 48 h and 72 h for the majority of cultures (6 cultures were monitored for 48 h). The culture size (parasitemia) and the parasite proliferation analysis were carried out by FACS (described below). Characterization of parasite morphology and development was performed by light microscopy. Cells were obtained from three replicate cultures for each RBC sample.

### Light microscopy

Blood smears were fixed with methanol and stained with 20% Giemsa (Sigma-Aldrich, St. Louis, MO, USA) for the morphological analysis of parasites. A minimum of 2000 cells was scanned for assessment of changes in morphology using a Nikon Eclipse E 600 microscope.

### Flow cytometry

The dual-color staining protocol was used to monitor the parasite cycle within the RBC over 72 h, as previously described<sup>31</sup> with modifications.

### Statistical analysis

Parasitemia was defined as the total number of infected RBC (iRBC) in every 100 RBC, not taking into consideration the number of parasites seen in a given cell when measured by flow

cytometry. Sub-populations were identified as a function of the presence and their number of intra erythrocyte parasites / genome (intra erythrocyte parasite load) where “1 N” refers to one genome copy based on the method previously describe.<sup>34</sup> The percentage of inhibition mediated by the different Hb genotypes was determined by assuming that the parasitemia from control HbAA cells was equivalent to 0% inhibition or enhancement.

**Results**

**Response of *B. divergens* to the different host cell hemoglobin environments**

To assess the hosting ability of the sickle cell anemia cells, purified merozoite preparations were used to infect HbSS and HbAS RBC from sickle and sickle trait patients, respectively, in parallel with HbAA RBC as wild-type control. Multiple independent experiments were performed with each cell type and processes such as invasion, development and egress were chronologically observed during the asexual erythrocytic cycle of *B. divergens*.

The first indication that there were differences in parasite development in the RBC of different Hb genotypes was observed while defining the ideal time points to evaluate various aspects of the parasite life-cycle (Table 1). A single sample each of HbAA, HbAS and HbSS RBC was used in an invasion assay using purified merozoite preparations. One-hour post-mixing was found to be the ideal time point to evaluate invasion and monitor the initial parasitemia. At the 5 min time point, the parasitemia was too low to assess differences between the three cell types, although high synchronicity of parasites was achieved. At the 6 h time point, the initial synchronicity was lost by events of late merozoite invasion and the cultures were affected by the long exposure to the ruptured RBC remnants that were introduced by the inoculation (*data not shown*). Because of these factors, 1 h post- mixing of merozoite preparations and RBC was used as the time-point to assess invasion in the experiments that followed.

*B. divergens* was able to efficiently invade RBC of all three genotypes: HbAA, HbAS and HbSS. However, parasite culture expansion was drastically compromised in the sickle cell (SS) environment which can be seen by the comparison of parasitemia progression in the HbSS culture as compared to both HbAS and HbAA cultures (Table 1) (culture growth inhibition of 36%, 59% and 70% respectively at 24 h, 48 h and 72 h post invasion of the HbSS culture when compared to HbAA) (Figure1A). In contrast to the HbSS cultures, HbAS cells were found to provide a favorable environment for parasite progression, with only modest differences in parasitemia observed when compared with the wild-type HbAA (culture growth inhibition of 4.3%, 0% and 1% respectively at 24 h, 48 h and 72 h post invasion of HbAS culture compared to HbAA) (Table 1 and Figure 1A).

**HbSS red blood cells from diverse donors exhibit comparable degrees of impairment of parasitemia progression while HbAS red blood cells from diverse donors permit normal parasite progression**

To assess the effect of the individual variability in sickle cell anemia and sickle trait RBC from different individuals on the parasite response to these RBC environments, RBC from 11 different sickle cell (Table 2) and five sickle trait (Table 3) patients were infected with purified merozoite preparations. Each experiment was run together with several wild-type RBC controls (HbAA) originating from different individuals. The cultures were monitored from invasion to 48-72 h post invasion.

On monitoring the parasite population sizes over time, it was clear that, although there was individual variation among sickle cells from different sickle cell anemia patients, the HbSS cells in every tested culture did not support normal culture progression, as the parasitemia was drastically reduced in all 11 sickle cell cultures (Table 2). This inhibition of HbSS-culture expansion was statistically significant at 48 h ( $P<0.05$ ), when HbAA RBC controls exhibited a robust approximately 3-4-fold increase in parasitemia, compared to the HbSS cells which remained static, exhibiting parasitemia close to the initial starting values. Eight HbSS cultures continued to be monitored at 72 h post invasion, to confirm if significant inhibition ( $P<0.05$ ) was maintained. Inhibition was found to be sustained and, once again, all eight cultures showed a plateau in parasitemia, not appreciably changed from their 48 h parasitemia, unlike the HbAA cultures which approach 40-50% parasitemia at 72 h (Table 2). From the perspective of parasitemia progression, there was thus an increased inhibition over time; approximately 73-92% inhibition of growth in HbSS cultures when compared to HbAA controls at 72 h (Figure 1B). In contrast, all HbAS cultures were able to reach a similar parasite population size as the control HbAA cultures at 72 h, averaging 45% parasitemia, with no significant variations in parasitemia in individual HbAS donor cells at different time points ( $P>0.05$ ) (Table 3). Overall, all parasite cultures established in the HbAS-cells exhibited a similar increase in parasitemia when compared to the HbAA control (Tables 1 and 3), indicating the parasites capability for population progression in HbAS RBC, unlike the impaired culture growth phenotype observed in HbSS RBC. Table 4 shows the aggregate values of inhibition of parasite population progression in the HbSS cells and HbAS cells with reference to the parasitemias in HbAA cells at the three time points tested. Despite the HbSS cells and HbAS originating from diverse donors, the inhibition seen in the HbSS population is significantly higher than that seen in the HbAS population which has close to parasitemia values in the HbAA population, at the 48 h (68% inhibition in HbSS vs. 15% in HbAS) and 72 h (84% inhibition in HbSS vs. 4% in HbAS) time points in culture ( $P<0.05$ ) (Table 4).

**Table 1.** Parasitemia assessed from cultures grown in single samples of each hemoglobin (Hb) genotype-HbAA, HbSS, HbAS cultures (5 min-6 hours post inoculation of cultures with free merozoites) and at 24-hour intervals after inoculation (24-72 hours).

Sample	5 min	1 h	6 h	24 h	48 h	72 h
HbAA	0.6 [0.03]	2.1 [0.03]	3.0 [0.06]	4.7 [0.00]	14.4 [0.25]	43.2 [0.15]
HbSS	0.9 [0.01]	2.7 [0.02]	3.1 [0.06]	3.0 [0.00]	5.9 [0.06]	12.8 [0.10]
HbAS	0.4 [0.04]	2.8 [0.02]	3.3 [0.00]	4.5 [0.00]	15.1 [0.12]	42.9 [0.32]

Parasitemia values represent average percentage. [StDv]: Standard Deviation among triplicates; h: hours; min: minutes.

**Similar invasion efficiencies were obtained in HbAA, HbAS and HbSS red blood cells**

To understand the specific defect induced in the parasite life-cycle by the sickle environment, the population structure of cultures was analyzed based on the parasite load within the infected RBC (number of parasite genomes by FACS analysis). By monitoring the distribution of sub-populations of infected RBC, the life cycle processes of invasion, parasite development and egress were evaluated in sickle cell anemia compared with sickle trait and control cells.

The invasion of merozoites in all cell types was measured by the percent parasitemia in the different cultures at the 1 h time point, established earlier to be the optimum point to assess invasion efficiency. The sickle RBC were able to support efficient merozoite invasion (HbSS-1 h parasitemia ranged from 0.8% to 2.3%) (Tables 1 and 2). When the invasion efficiency of HbSS RBC was compared

to that of control HbAA RBC, no significant difference in parasite invasion was observed among cultures ( $P>0.05$ ). In fact, the subtle increase in initial infection rates of HbSS *versus* HbAA RBC was found to be an artefactual consequence of the presence of Howell-Jolly bodies (H-JB) in HbSS cells. These bodies, known as micronuclei, contain small erythrocyte DNA inclusions (approx. 1  $\mu\text{m}$ ) that are the consequence of cytogenetic damage.<sup>35,36</sup> To confirm that the higher DNA content in infected HbSS cells was indeed from H-J bodies, their quantification was first performed by their detailed counts on Giemsa stained smears of uninfected HbSS cells, followed by quantification of DNA content in uninfected HbSS cells (FACS analysis with Vybrant®DyeCycleTMGreen) (Figure 2). Our estimates of these bodies in all HbSS samples were in the range of 0.1-0.3% (shown for 3 independent HbSS samples in *Online Supplementary Table S1*), which when subtracted from the parasitemias found for the same infected

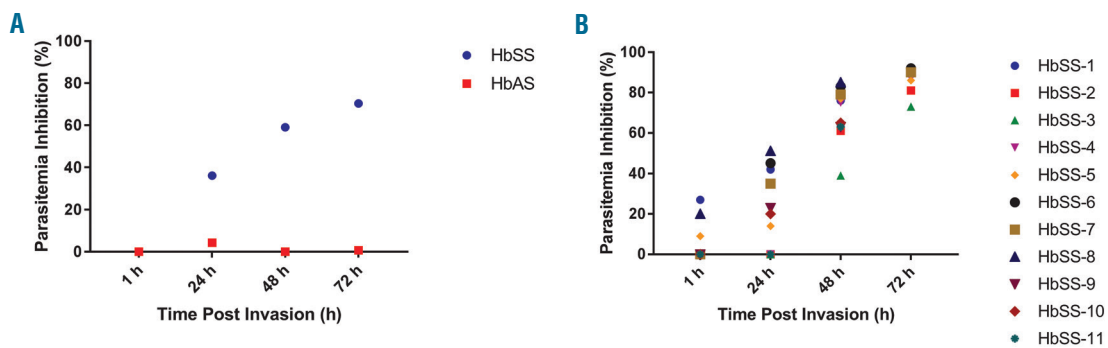


**Figure 1. The expansion of *B. divergens* population was inhibited in HbSS cultures.** Comparison of the growth inhibition rate between parasite cultures grown in HbSS cells and HbAS cells relative to growth in wild-type HbAA as measured by parasitemia. (A) Between cultures originating from a single HbSS and single HbAS donor. Values calculated based on data from Table 1. (B) Among HbSS cells from 11 different sickle cell disease patients, showing that, despite variation in parasitemia in individual cultures, all exhibit high degrees of inhibition of culture progression. Values calculated based on data from Table 2.

**Table 2. Parasitemia of *B. divergens* cultures measured 1-72 hours post-invasion in sickle (HbSS) and wild-type (HbAA) red blood cells from different donors.**

Sample*	1 h	24 h	48 h†	72 h†
HbAA-I	1.1 [0.01]	4.0 [0.40]	14.5 [0.35]	37.3 [1.35]
HbSS-1	0.8 [0.03]	2.3 [0.21]	3.4 [0.12]	3.9 [0.23]
HbSS-2	1.5 [0.01]	4.5 [1.18]	5.6 [0.12]	7.2 [0.21]
HbSS-3	1.9 [0.02]	5.1 [0.84]	8.9 [0.38]	9.9[0.10]
HbAA-II	1.1 [0.03]	4.1 [1.06]	20 [0.92]	43.4 [0.21]
HbSS-4	2.0 [0.02]	4.6 [1.56]	5.1 [0.07]	5.5 [0.28]
HbSS-5	1.0 [0.02]	3.5 [1.13]	4.8 [0.07]	5.9 [0.00]
HbAA-III	1.9 [0.02]	5.5 [0.26]	21 [0.15]	49.3 [0.75]
HbSS-6	2.3 [0.01]	3.0 [0.00]	3.5 [0.14]	4.1 [0.07]
HbSS-7	2.0 [0.03]	3.6 [0.06]	4.5 [0.20]	4.9 [0.12]
HbAA-IV	1.0 [0.03]	2.9 [0.06]	12 [0.25]	ND
HbSS-8	0.8 [0.03]	1.4 [0.10]	1.7 [0.12]	ND
HbSS-9	1.5 [0.02]	2.2 [0.07]	4.3 [0.03]	ND
HbSS-10	1.5 [0.04]	2.3 [0.02]	4.0 [0.10]	ND
HbSS-11	1.5 [0.01]	3.0 [0.35]	4.2 [0.15]	ND

\*Four independent experiments. (HbSS 1-11) sickle samples (HbAA I-IV) wild-type control samples. Parasitemia values represent average percentage. [StDv]: Standard Deviation among triplicates. †Significant difference between wild-type controls HbAA and tested HbSS samples.  $P<0.05$ . ND: not determined; h: hours.

HbSS cells, results in equivalent invasion efficiencies for HbSS and HbAA cells. Additionally, all the parasite cultures were followed a few hours later to ensure that parasite development could be recorded to yield comparable parasitemia. Images of invaded parasites can be very easily discriminated from that of the H-J bodies, with the parasite seen as a distinct ring *versus* the solid staining pattern of the body (Figure 2). Overall, all cells were found to support parasite invasion equally well.

**Effect of sickle Hb (HbSS) and sickle trait Hb (HbAS) on the intra-erythrocytic parasite development**

The relative differences in parasitemia in the cultures (Tables 1-3) and in the distribution of their infected RBC sub-populations (Figure 3) described not only parasite competence for population expansion in that cell type, but also their developmental and differentiation status when monitoring the chronological emergence of each sub-parasite population within the infected RBC. The supplementary histogram peaks detected at 24 h post invasion (Figure 3) indicating parasite proliferation showed that the HbSS sickle cells, permitted intra-erythrocytic proliferation and differentiation of the parasites; however, they

may not be providing an optimum environment for culture propagation as there was no appreciable increase in parasitemia after 24 h.

As mentioned before, at 1 h post invasion (1 h histograms) (Figure 3), all cultures exhibited similar FACS profiles, with the 1N population seen as the dominant sub-population as expected, as shown in the representative samples. The distribution over time of these sub-populations of iRBC (frequency of events acquired in the histogram peaks corresponding to 1N-; 2N-; 4N-; and >4N-iRBC sub-populations), when translated into the line charts as presented in *Online Supplementary Figure S1*, showed that the conventional pattern of population formation was adopted by *B. divergens* in all RBC, irrespective of genotype, during the first 24 h. During this first intra-erythrocytic cycle, with the intense intra-cellular proliferation (characterized by the emergence of infected RBC with higher intra-cellular parasite load) and the low ratio of invasion/egress (as evidenced by the relatively stable culture sizes over 24 h as expected, even for the control cultures) *Babesia* similarly built its populations in all three cell types, exhibiting the common gain of heterogeneity by the presence of different sub-populations of iRBC.

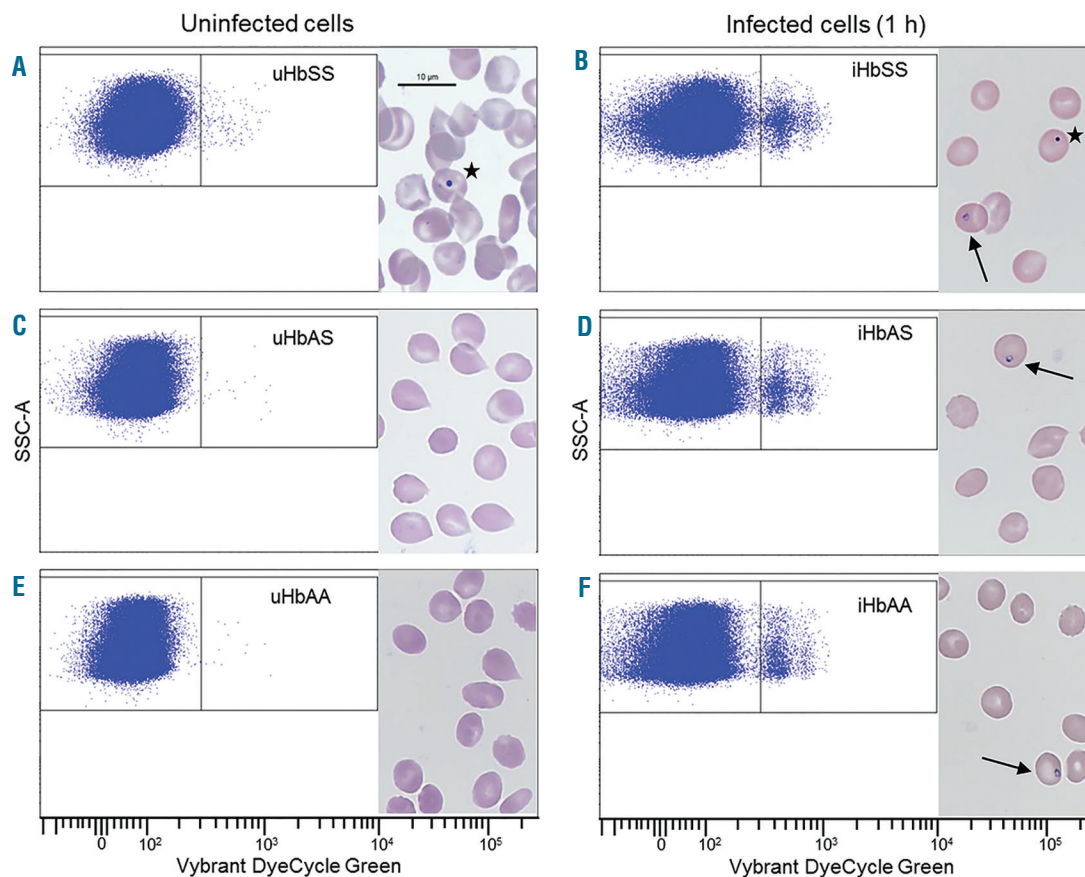


**Figure 2. Invasion efficiency is similar in HbAA, HbAS and HbSS cells.** FACS analysis of DNA content in representative (A,C,E) uninfected red blood cells (RBC) and (B,D,F) infected RBC, along with Giemsa stained smears. (A) HbSS cells reveal DNA positive population (0.1-0.3%) from Howell Jolly (H-J) Bodies in cells, Giemsa image shows a dense H-J body, (marked by asterisk). (C) HbAS cells and (E) HbAA cells do not have DNA positive population and Giemsa smear shows absence of bodies. (B) Parasite cultures in the same HbSS cells show higher Vybrant positive population than uninfected, being composed of both cells containing H-J bodies and parasites. The difference between panels (B) and (A) yields invasion parasitemias (see Table 4 for data). Giemsa smear shows distinct ring formed 1 hour (h) post invasion, presenting a clear difference from H-J body. (D and F) 1 h post-invasion cultures of (D) HbAS cells and (F) HbAA cells showing Vybrant positive population, and 1 h post-invasion Giemsa image showing newly invaded parasites (marked by arrows).

**Table 3.** Parasitemia of *B. divergens* cultures measured 1-72 hours post invasion in sickle trait (HbAS) and wild-type (HbAA) red blood cells from different donors.

Sample	1 h	24 h	48 h	72 h
HbAA-V	4.5 [0.50]	8.7 [0.15]	26.7 [0.82]	43.1 [2.35]
HbAA-VI	3.8 [0.22]	7.7 [0.15]	26.7 [0.38]	47.2 [1.25]
HbAA-VII	3.3 [0.12]	7.6 [0.21]	26.0 [0.26]	48.2 [0.70]
HbAS-1	2.8 [0.04]	6.7 [0.23]	23.8 [1.01]	41.8 [3.35]
HbAS-2	3.1 [0.01]	6.1 [0.06]	16.9 [0.32]	41.8 [2.95]
HbAS-3	3.6 [0.03]	7.5 [0.17]	22.2 [0.06]	44.7 [1.04]
HbAS-4	4.9 [0.03]	8.4 [0.00]	23.6 [0.10]	47.4 [2.35]
HbAS-5	3.9 [0.11]	7.4 [0.00]	21.2 [0.12]	45.8 [1.50]

Parasitemia values in percentage average. [StDv]: Standard Deviation among triplicates; h: hours.

During the second proliferative cycle (between 24-48 h post invasion) the emergence of >4N- and the increase of 4N-iRBC revealed the continued cellular proliferation over time. However, unlike the population seen in the control HbAA cells after 24 h, the parasite population in the HbSS RBC turned structurally stable, with the frequency of sub-populations remaining constant up to the last time point assayed at 72 h. The set of data from four representative HbSS cultures presented in *Online Supplementary Figure S1* illustrates that, despite the individual biological features of RBC from different individuals with SCD, a general common pattern of population structure was adopted by the parasite in sickle cells (HbSS). Once the heterogeneity of stages and sub-parasite populations was achieved at the 24 h time point in the HbSS cells, the proportion of sub-populations were kept relatively stable throughout the monitored 72 h period. Comparing these frequencies with those from control HbAA samples showed that the maintenance of relative proportions of sub-populations was not random. Although the parasitemia along with the sub-population structure varied among the sickle cell anemia samples, the specific proportions of 1N-, 2N-, 4N- and >4N-iRBC were built in the 11 samples that stayed constant from 24-72 h [frequency averages in HbSS iRBC: 1N-HbSS-iRBC dropped from approx. 68% at 1 h to 47% at 24 h; remained constant throughout 48 h as 44% and at 72 h as 51%; 2N-HbSS-iRBC from the initial 26% at 1 h slightly changed to 28% up to 72 h; 4N reached 20% at 24 h and then stayed relatively unchanged up to 48 h (21%) and 16% (72 h); >4N reached 7% at 24 h, 10% at 48 h and 5% at 72 h] (*data not shown*). Unlike the HbSS cultures, control HbAA cultures exhibited the typical fluctuating dynamics of parasite culture.

Unlike the parasites in the HbSS cell cultures, parasites grown in wild-type cells (HbAA-RBC) efficiently performed sequential cycles of invasion and egress, as evidenced by the increase in 1N-iRBC (invasion clearly identified by the arrow between 48-72 h) (*Online Supplementary Figure S1A*) and the decrease in 4N- and >4N-iRBC (egress identified by the decrease in quantified frequency 4N- and >4N-iRBC; *data not shown*) with a progressive increase in total parasite population size (levels of parasitemia over time HbAA-III; Table 2). This fluctuation among sub-populations of parasites in HbAA cultures proved that conditions in HbAA cells were conducive to parasite life-cycle processes that resulted in population growth. Similarly, parasite cultures in HbAS cells exhibited the variation in infected RBC-sub populations expected

**Table 4.** Inhibition of parasite culture expansion compared to wild-type (HbAA) measured 24-72 hours post invasion in sickle cell anemia (HbSS) and sickle trait (HbAS) from different donors.

Sample	24 h	48 h	72 h
HbSS (n=12)	22 [19]	69 [12]	84 [8]
HbAS (n=6)	10 [8]	15 [11]	4 [4]

Values expressed as average percentage of inhibition compared to control HbAA [StDv]: Standard Deviation among triplicates; h: hours.

over time, based on the sequential process of invasion, development and egress (*data not shown*). This normal equilibrium among the infected RBC hosting different intra-parasitic loads observed in HbAA and HbAS contrasted with the static proportions of the sub-populations among the HbSS cultures (*Online Supplementary Figure S1B-E*) observed after 24 h, and suggested a potential inhibitory environment in the HbSS cell may account for the low parasitemia found in HbSS cultures.

#### Effect of HbSS cell environment on the morphological differentiation of the parasite

As shown above, HbSS RBC did not interfere with the intra-erythrocytic parasite proliferation and differentiation since iRBC were seen carrying high intracellular parasite loads (4N and >4N) right from the first 24 h life cycle (Figure 3A). In addition, the analysis of the sequential appearance of the different morphological stages (light microscopy of Giemsa smears) in the HbAA, HbAS and HbSS cultures confirmed this successful intracellular proliferation, and showed that parasite differentiation into the different morphological stages occurred successfully in all three types of cultures (Figure 4). However, closer examination of parasite morphology in HbSS cells revealed some abnormalities. The heterogeneity of the sub-populations of iRBC reported from the FACS analysis of these cultures (Figure 3) was also observed by microscopic analysis and can be described as a change in frequency of infected RBC hosting different numbers of attached or detached parasites (Figure 4). The predominant parasite stages seen at later time points in sickle cells were of the detached variety and consisted of rings (describes any unattached intracellular parasite) present in single, double, quadruple and multiple forms. Many of the parasites were seen unattached to each other and assumed either circular, pear or deformed shapes (Figure 4). However, there were parasitized RBC that also assumed conventional morphological stages, seen as “paired-fig-

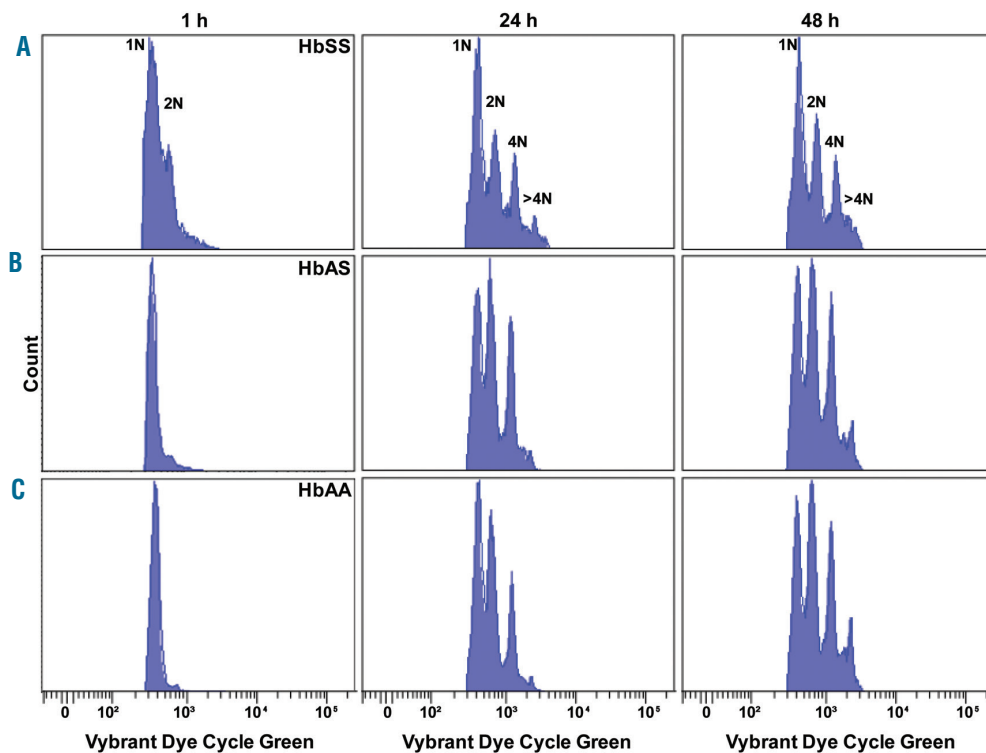


**Figure 3.** Distribution of parasite sub-populations cultured in three types of red blood cells (RBC), based on genome content reveals all sub-populations are represented in the cultures. (A) HbSS. (B) HbAS. (C) HbAA. Samples were collected at 1 hour (h), 24 h and 48 h and the percentage of each infected RBC sub-population was determined by FACS using VybrantRDyeCycleTMGreen dye to quantify the amount of parasitic DNA within infected cells, where (N) is the number of parasite genomes. (Top left) HbSS cells show higher numbers of 2N cells at 1 h time point compared to (left middle) HbAS and (left bottom) HbAA cells confirming a higher frequency of multiple invasion events in HbSS. (Middle and right panels) Parasite population structure at 24 and 48 h showing all sub-populations represented in all three cell genotypes.

ures" (2 attached parasites) and/or Maltese Cross (4 attached parasites) and/or double paired-figures (also as 4 parasites attached 2 by 2) and were seen co-existing with the detached ring parasites, showing that cellular division and differentiation of *B. divergens* followed the sequential transformation of stages from attached into unattached forms after completing cytokinesis before their egress. In addition, some of the infected RBC in HbSS cells hosted multiple parasites ( $\geq 4$ -8 or more) which were detected with variable frequency among HbSS cultures (Figure 4).

Thus, the morphological analysis supported the FACS analysis of population structures at the various sampled time points of the different cultures, HbAA, AS and SS. Importantly, the parasites in the HbSS RBC exhibited features that signaled they were ready for egress, i.e. the presence of both-infected RBC hosting multiple parasites as well as the presence of detached parasites in these cells. However, these parasites were not successful at starting new intra-erythrocytic cycles, as evidenced by the lack of increase in parasitemia.

#### Parasite infectivity is impaired in HbSS cells as the addition of fresh red blood cells does not rescue parasitemia in HbSS cultures

Success of the parasite culture propagation as measured by an increase in parasitemia requires successful invasion, successful production and maturation of merozoites which then need to successfully egress. This in turn depends on several factors involving host cells and para-

sites. Sickle cell anemia RBC are notorious for exhibiting increased fragility<sup>37</sup> as compared to HbAA RBC and this could be a factor in the inability of the cultures to support parasitemia after 24 h.

To test whether the lack of increase in parasitemia was a consequence of defective egress, sickle cell fragility or defective merozoite maturation, we examined progression of cultures in which the introduction of fresh RBC (either HbAA and HbSS) into 24 h HbSS parasite cultures was performed. After 1 h, all cells supported *Babesia* invasion equally well, as shown, following the mixing of merozoite inoculum and RBC (*Online Supplementary Table S2*). The cultures were then allowed to progress for 24 h at which point, the parasitemia in both the HbAA and HbSS cultures had risen slightly (HbAA-A: 3.2% vs. HbSS-A: 3.4%) (*Online Supplementary Table S2*), in line with the results reported for the 12 HbSS cultures above (Tables 1 and 2). The cultures were then split, either staying the same with only medium change (flasks A) or receiving fresh SS cells (flasks B) or AA cells (flasks C), maintaining hematocrits of 5%. At 48 h, the parasitemia in the original HbAA-A culture had doubled (from 3.2% to approx. 6.5%) while that of the original HbSS-A culture reported only a small increase in parasitemia (from 3.4% to approx. 4%), following the pattern reported for the original 12 HbSS cultures (Tables 1 and 2). The HbAA-B culture which was diluted with fresh HbAA RBC to receive half of the inoculum exhibited half the parasitemia of the undiluted HbAA-A culture, once again as expected (3.2%)

(*Online Supplementary Table S2*). The two HbSS cultures that received fresh RBC, either HbAA (HbSS-C) or HbSS (HbSS-B), had lower parasitemias (2.1% and 2.5%, respectively; 24 h time point) than that of HbAA-B culture, proving that the nature or condition of the host cells did not play a role in the inhibition of new cycles of parasitemia seen in the HbSS cultures (HbSS-C and HbSS-B). At later time points (48 h after addition of fresh cells), this result of non-rescue was further strengthened when cultures in HbAA-B exhibited a robust increase in parasitemia (16%), contrasting with HbSS-B and HbSS-C and the stable parasitemia of (3.6% and 2.3%, respectively). The original half culture which had only medium change (HbAA-A and HbSS-A) followed the previously reported inhibition patterns of in culture progression showing approximately 18% inhibition in HbSS-A culture growth, compared to the HbAA-A culture. Neither the addition of fresh HbSS RBC or HbAA RBC could significantly rescue the HbSS cultures, with the original HbSS-A parent culture at 4.7% and the culture receiving fresh HbSS cells at 3.6% parasitemia. Surprisingly, the culture that received

fresh HbAA cells was even lower demonstrating an infection rate of 2.3%, indicating that parasite development within the HbSS RBC was potentially impaired, resulting in the formation of merozoites unable to invade fresh RBC at frequencies typically seen *in vitro* parasite cultures. The formation of mature merozoites that egress from the RBC are critical to start new intra-erythrocytic cycles by invading new host cells, and these merozoites are required to be in an optimum invasive state to support new cycles.

#### Parasite egress from sickle red blood cells may also be compromised

One of the factors that may impact the progress in parasitemia in HbSS cells is the ability of the parasite to egress from the host sickle cell and invade new host cells. The FACS profile of the parasite population in the HbSS cells was carefully examined to look for this inhibition of egress. The typical pattern of parasite-holding within the RBC that we have reported for *B. divergens*,<sup>31</sup> when there is an egress defect, where the *B. divergens* parasite population builds its 4N and >4N populations to high levels that

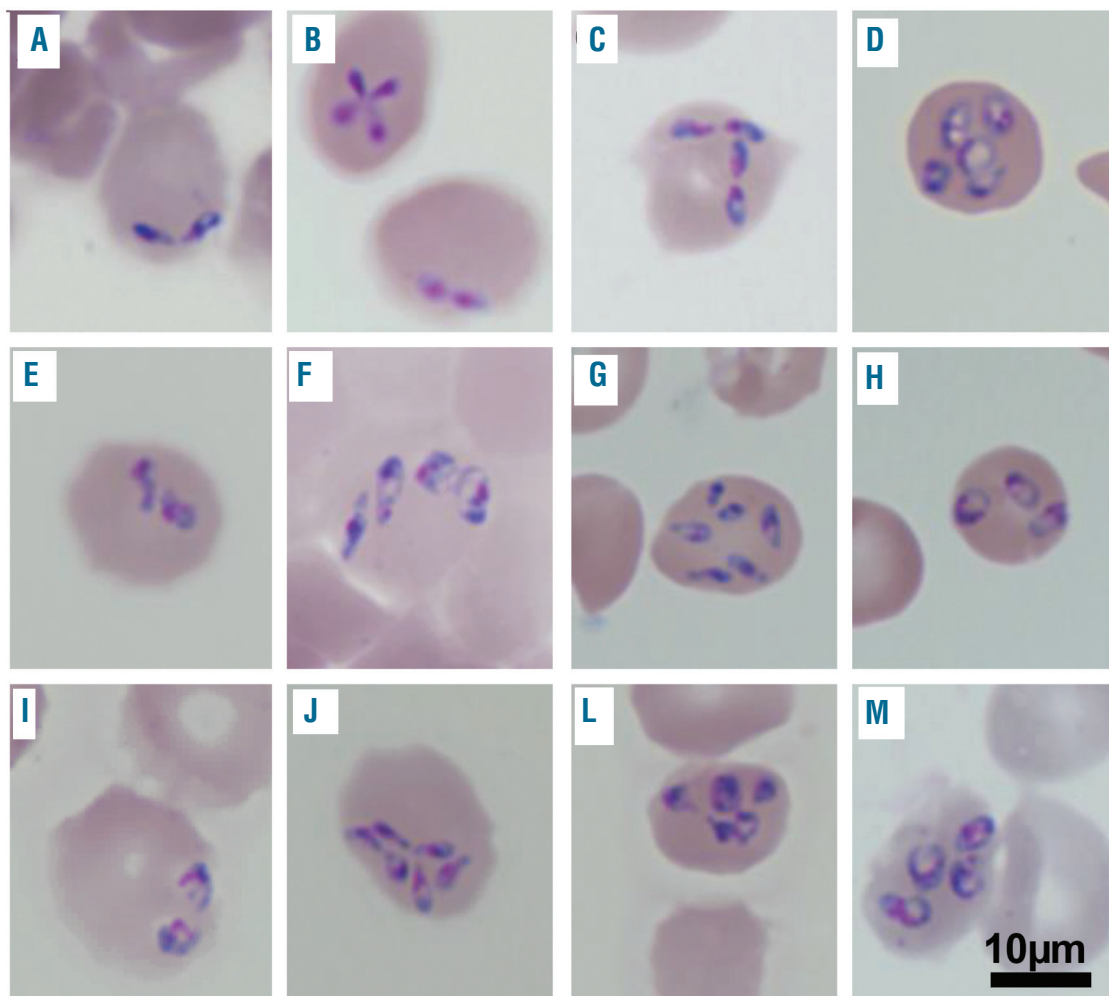


**Figure 4.** Parasites grown in HbSS cells exhibit atypical morphology although normal parasite forms are also seen in the same cultures. (A-C) Normal morphology of parasite seen as paired figures or Maltese Crosses or double paired figures (D-M) Unusually high numbers of detached rings seen at high frequency in all HbSS parasite cultures.

can be visualized by both FACS analysis and Giemsa stained smears, was not seen in these sickle cell cultures (Figures 3 and 4). In fact, the presence of free merozoites was noted in most culture supernatants (*data not shown*), although it is difficult to quantitatively estimate if these numbers are normal as compared to wild-type RBC. However, unlike the fluctuating proportions of the parasite sub-populations seen in both HbAA and HbAS cultures, relatively stable proportions of parasite sub-populations in the sickle RBC cultures, after the 24 h time point was a characteristic noted in all 12 HbSS cultures (*Online Supplementary Figure S1*). This novel holding pattern could potentially signify an inability of the parasites to egress, which in turn could cause the relatively static parasitemia observed in these cultures. Thus, inefficient parasite egress from the host HbSS cells infected in the first round of invasion may not permit new cycles of invasion to take place.

## Discussion

Variant RBC are produced from some of the most common human genetic polymorphisms, and their high incidence has been ascribed to the evolutionary selection by life-threatening falciparum malaria.<sup>38,39</sup> The sickle hemoglobin genotype (HbAS/HbSS) is the best-characterized human genetic polymorphism associated with malaria. In this paper, we have explored the effect of the sickle hemoglobin mutation on a related intra-erythrocytic apicomplexan parasite, *B. divergens*. There are several stages in the parasite's erythrocytic cycle at which RBC mutations can affect parasite infection. The first would be erythrocyte invasion by *Babesia* merozoites; the next stage susceptible to inhibition is the intra-erythrocytic parasite development. This category would include impairments in the parasite's ability to meet its nutritional requirements or changes in the host cell milieu that would be fatal to the parasite. Finally, impairment of red cell rupture and release of infective merozoites at parasite maturity could inhibit increase in infection. Use of *in vitro* growth assays as our primary outcome, along with a robust sample size of SCD RBC, provided a rare opportunity to systematically examine the cellular determinants of parasite growth in the sickle setting. We present here evidence for atypical population progression, a potential loss of merozoite infectivity, and defective egress of the parasite in these hemoglobinopathic cells (Tables 1-4 and *Online Supplementary Table S2*). Interestingly, using the Townes mouse model of SCD, and *B. microti*, we have shown that a similar inhibition results in dramatically low infection rates in HbSS mice as compared to HbAS and HBAA mice.<sup>40</sup>

Invasion of the human RBC is the central pathogenic step in the life-cycle of *Babesia*. When *Babesia* spp. sporozoites are first injected into the human host with a tick bite, they target the host RBC immediately, unlike *Plasmodium* spp. which are required to undergo an exo-erythrocytic phase in hepatic cells. It is the parasite's ability to first recognize and then invade host RBC that is central to symptomatic human babesiosis, and the parasites invade RBC using multiple complex interactions between parasite proteins and the host cell surface, which have not been fully elucidated.<sup>2,41,42</sup> Like *Plasmodium*, *B. divergens* has been shown to use GPA and GPB as invasion receptors.<sup>33</sup> *In vitro* studies with *P. falciparum* have suggested a

decreased invasion and growth of the parasite in sickle cells;<sup>43-45</sup> however, some of the older studies have not been able to differentiate between the various phases of the parasite lifecycle. Hence, a deficiency in egress or invasion would both be visualized as an overall decrease in parasitemia. The use of our platform combining *in vitro* invasion and growth assays with synchronized cultures monitored by both FACS analysis and Giemsa smears provided an excellent system to systematically dissect the phase of the erythrocytic cycle impacted by the HbSS environment. The increased DNA content of HbSS cells that contributed to the subtle higher invasion percentages was found to be due to the presence of the Howell-Jolly bodies which artefactually increased the DNA load of the cell. When the contribution of the bodies was subtracted, a similar rate of invasion was obtained in all Hb genotypes, indicating a potential difference between malaria and *Babesia* mechanisms of invasion in sickle cells.

The development of the parasite in HbSS cells in the first 24 h was normal and exhibited all conventional forms reported *in vitro* cultures by us earlier.<sup>34</sup> Thus, rings, paired figure and Maltese Cross forms were all documented in culture. However, a larger than expected proportion of cells hosted detached rings (Figure 4). The multiple unattached parasites feature assumed by parasites in HbSS cultures suggests that the parasite is able to complete cytokinesis shortly after the nuclear duplication, allowing the conclusion of cell division which may not allow the accumulation of attached morphological stages such as Maltese-Cross or paired-figures, as seen in HbAA cultures. After 24 h, the progression of cultures is stalled in HbSS cells as seen by FACS analysis (Figure 3A and *Online Supplementary Figure S1B-E*) where the sub-populations remain in static proportions unlike the dynamic movements seen among sub-populations in HbAA (Figure 3C and *Online Supplementary Figure S1A*) and AS cells (Figure 3B). As this profile is representative of the parasite population and not individual parasites, it is apparent that, overall, there is no growth in the population despite small increases seen in parasitemia, reflecting a minority of parasites successfully initiating new cycles of infection. Microscopic analysis of the parasites in HbSS cells reveals normal morphology in terms of size, shape and staining patterns. Ultra-structural analysis may shed more light on potential defects in these parasites, if present.

Egress is a phase of the cycle that, if impacted, can lead to disastrous outcomes for the parasite population progression. *In vitro* studies with *P. falciparum* suggest a link between the hydration status of the host RBC and parasite invasion and egress.<sup>46,47</sup> The high water-permeability of the RBC ensures their continued osmotic equilibrium in plasma so that they can shrink or swell by the loss or gain of a fluid isosmotic with surrounding plasma. This homeostatic balance is disrupted in HbSS cells, resulting in altered ion fluxes, ion content regulation, and hydration states in the circulation.<sup>48</sup> Malaria parasites have to breach both the parasitophorous vacuolar membrane (PVM) and erythrocyte membrane in order to egress. The altered exit of malaria merozoites from the dehydrated RBC was linked to the reduction of osmotic pressure within the parasitophorous vacuole that was needed to lyse the compartment prior to lysis of the RBC membrane. However, intra-erythrocytic *Babesia* parasites are free in the cytoplasm of the RBC without being enclosed in a vacuole as the PVM is a transient structure found fleetingly after

invasion of the *Babesia* merozoite. Thus, the lack of osmotic pressure in the infected sickle RBC may not impact *Babesia* parasite egress. Additionally, FACS analysis of the cultures at later time points do not support the typical loss of egress phenotype, which presents as a build-up of 4N and >4N populations in a single cell, as seen in our previous work with egress inhibitors.<sup>31</sup> Although there were cells that hosted multiple parasites (>4N), these appeared to be a result of the normal proliferative cycle to build the population structure, but they were not the majority of infected cells. However, the novel holding pattern reported here (*Online Supplementary Figure S1*), where the sub-populations are maintained after 24 h in the same ratios, indicate that egress may be compromised in these cells. Thus, it is possible that HbSS cells were not as efficient in supporting egress as HbAA cells, but other factors also contribute to the low infection rates seen in these cultures. Production of viable, infective merozoites within HbSS cell appeared to be another limitation of these cultures. Although free merozoites were seen in most HbSS culture supernatants, they did not appear to be able to successfully initiate new rounds of infection. Rescue experiments with both fresh HbSS and HbAA cells indicate that the defect may not lie in the unavailability of optimal host cells but rather with the merozoite, despite them presenting normal morphology (*Online Supplementary Table S2*). Detailed morphological examination of these zoites by electron microscopy may provide clues to their lack of infectivity.

Despite years of research effort, the mechanism of protection of the sickle trait in malaria remains unclear. A number of cellular, biochemical and immune-mediated mechanisms have been proposed, and it is likely that multiple complex mechanisms are responsible for the observed protection. Invasion and growth of *P. falciparum* *in vitro* within HbAS RBC is reduced in low oxygen tension growth conditions (<5% O<sub>2</sub>).<sup>43,49</sup> Some have proposed that the increased sickling of infected HbAS RBC, due to polymerization of sickle Hb, may be a mechanism for impaired growth under low O<sub>2</sub> conditions.<sup>50,51</sup> However, in our *in vitro* assays, which utilize micro-aerophilic conditions with 5% O<sub>2</sub>, no inhibition of *Babesia* growth was observed in the HbAS cells, in which all five samples yielded comparable support of parasite growth as that seen in control HbAA RBC. Unlike *Plasmodium*, which digests Hb to meet its nutritional needs, *Babesia* does not digest any of the Hb, which may account for the lack of

inhibition of intra-erythrocytic proliferation seen in the HbAS cells (no significant difference between HbAA and HbAS cells;  $P>0.05$ ) (Table 3). As the assays reported here are purely *in vitro* assays, the effect of *in vivo* parameters like increased cytoadhesion,<sup>52</sup> splenic retention,<sup>53</sup> and altered immune system response, as seen in enhanced phagocytosis and induction of inflammatory cytokines following endothelial activation, are not factored in, which may lead to an overall protection against the parasite *in vivo*, as seen in malaria. Future studies documenting the incidence of babesiosis in the sickle cell trait population compared to that in the HbAA individuals will confirm these findings.

In this paper, we present evidence for altered parasite population progression caused potentially by defective merozoite maturation and/or defective egress from the sickle cell anemia RBC. The latter two phenomena when present alone or together may explain the inability of HbSS cells to support high infection rates *in vitro*. It is not clear whether the parasite would behave similarly *in vivo*. We have recently shown in a mouse SCD model similar inhibition of parasite population progression, and the results presented in this study confirm the inability of the *Babesia* parasite to thrive in the sickle cell anemia setting.<sup>40</sup> In a significant contrast to malaria, sickle trait cells seemed to sustain parasite infection rates comparable to those of wild-type RBC, and, once again, these *in vitro* studies need to be supplemented by comparable *in vivo* analyses under conditions of differing oxygen tension, which has been shown to play a role in suppressing malaria parasitemia. Patients with SCD are on chronic transfusion therapy and may develop severe transfusion-associated *Babesia* infection.<sup>29</sup> Studies dissecting the cellular and molecular mechanisms of parasite growth within sickle cell patients that may impact the pathogenesis of babesiosis in sickle cell and other hemoglobinopathies are needed to define potential novel therapies against this disease.

#### Acknowledgments

We thank Vijay Nandi, PhD (Laboratory Data Analytic Services, NYBC) for help with the statistical analysis.

#### Funding

This research was funded by NIH grant to CL-HL140625 and Hugoton Foundation grant to JRCS-HUG575.

## References

- Lelliott PM, McMorran BJ, Foote SJ, Burgio G. The influence of host genetics on erythrocytes and malaria infection: is there therapeutic potential? *Malar J.* 2015;14:289.
- Ord RL, Lobo CA. Human Babesiosis: Pathogens, Prevalence, Diagnosis and Treatment. *Curr Clin Microbiol Rep.* 2015;2(4):173-181.
- Alaganan A, Singh P, Chitnis CE. Molecular mechanisms that mediate invasion and egress of malaria parasites from red blood cells. *Curr Opin Hematol.* 2017;24(3):208-214.
- Taylor SM, Fairhurst RM. Malaria parasites and red cell variants: when a house is not a home. *Curr Opin Hematol.* 2014;21(3):193-200.
- Goheen MM, Campino S, Cerami C. The role of the red blood cell in host defence against falciparum malaria: an expanding repertoire of evolutionary alterations. *Br J Haematol.* 2017;179(4):543-556.
- Williams TN. Human red blood cell polymorphisms and malaria. *Curr Opin Microbiol.* 2006;9(4):388-394.
- Kwiatkowski DP, Luoni G. Host genetic factors in resistance and susceptibility to malaria. *Parasitologia.* 2006;48(4):450-467.
- Weatherall DJ, Provan AB. Red cells I: inherited anaemias. *Lancet.* 2000;355(9210):1169-1175.
- Taylor SM, Cerami C, Fairhurst RM. Hemoglobinopathies: slicing the Gordian knot of *Plasmodium falciparum* malaria pathogenesis. *PLoS Pathog.* 2013;9(5):e1003327.
- May J, Evans JA, Timmann C, et al. Hemoglobin variants and disease manifestations in severe falciparum malaria. *JAMA.* 2007;297(20):2220-2226.
- Taylor SM, Parobek CM, Fairhurst RM. Haemoglobinopathies and the clinical epidemiology of malaria: a systematic review and meta-analysis. *Lancet Infect Dis.* 2012;12(6):457-468.
- Ingram VM. Abnormal human haemoglobins. III. The chemical difference between normal and sickle cell haemoglobins. *Biochim Biophys Acta.* 1959;36:402-411.

13. Macharia AW, Mochamah G, Uyoga S, et al. The clinical epidemiology of sickle cell anemia in Africa. *Am J Hematol*. 2018;93(3):363-370.
14. Aidoo M, Terlouw DJ, Kolczak MS, et al. Protective effects of the sickle cell gene against malaria morbidity and mortality. *Lancet*. 2002;359(9314):1311-1312.
15. Gong L, Parikh S, Rosenthal PJ, Greenhouse B. Biochemical and immunological mechanisms by which sickle cell trait protects against malaria. *Malar J*. 2013;12:317.
16. Beaudry JT, Krause MA, Diakite SA, et al. Ex-vivo cytoadherence phenotypes of *Plasmodium falciparum* strains from Malian children with hemoglobins A, S, and C. *PLoS One*. 2014;9(3):e92185.
17. Western KA, Benson GD, Gleason NN, Healy GR, Schultz MG. Babesiosis in a Massachusetts resident. *N Engl J Med*. 1970;283(16):854-856.
18. Skrabalo Z, Deanovic Z. Piroplasmosis in man; report of a case. *Doc Med Geogr Trop*. 1957;9(1):11-16.
19. Bloch EM, Herwaldt BL, Leiby DA, et al. The third described case of transfusion-transmitted *Babesia duncani*. *Transfusion*. 2012;52(7):1517-1522.
20. Conrad PA, Kjemtrup AM, Carreno RA, et al. Description of *Babesia duncani* n.sp. (Apicomplexa: Babesiidae) from humans and its differentiation from other piroplasms. *Int J Parasitol*. 2006;36(7):779-789.
21. Jiang JF, Zheng YC, Jiang RR, et al. Epidemiological, clinical, and laboratory characteristics of 48 cases of "*Babesia venatorum*" infection in China: a descriptive study. *Lancet Infect Dis*. 2015;15(2):196-203.
22. Sun Y, Li SG, Jiang JF, et al. *Babesia venatorum* infection in child, China. *Emerg Infect Dis*. 2014;20(5):896-897.
23. Haselbarth K, Tenter AM, Brade V, Krieger G, Hunfeld KP. First case of human babesiosis in Germany - Clinical presentation and molecular characterisation of the pathogen. *Int J Med Microbiol*. 2007;297(3):197-204.
24. Herwaldt BL, Caccio S, Gherlinzoni F, et al. Molecular characterization of a non-*Babesia divergens* organism causing zoonotic babesiosis in Europe. *Emerg Infect Dis*. 2003;9(8):942-948.
25. Yabsley MJ, Shock BC. Natural history of Zoonotic *Babesia*: Role of wildlife reservoirs. *Int J Parasitol Parasites Wildl*. 2013; 2:18-31.
26. Gubernot DM, Nakhasi HL, Mied PA, Asher DM, Epstein JS, Kumar S. Transfusion-transmitted babesiosis in the United States: summary of a workshop. *Transfusion*. 2009;49(12):2759-2771.
27. Leiby DA. Transfusion-associated babesiosis: shouldn't we be ticked off? *Ann Intern Med*. 2011;155(8):556-557.
28. Lobo CA, Cursino-Santos JR, Alhassan A, Rodrigues M. *Babesia*: an emerging infectious threat in transfusion medicine. *PLoS Pathog*. 2013;9(7):e1003387.
29. Karkoska K, Louie J, Appiah-Kubi AO, et al. Transfusion-transmitted babesiosis leading to severe hemolysis in two patients with sickle cell anemia. *Pediatr Blood Cancer* 2018;65(1).
30. Cushing M, Shaz B. Transfusion-transmitted babesiosis: achieving successful mitigation while balancing cost and donor loss. *Transfusion*. 2012;52(7):1404-1407.
31. Cursino-Santos JR, Singh M, Pham P, Lobo CA. A novel flow cytometric application discriminates among the effects of chemical inhibitors on various phases of *Babesia divergens* intraerythrocytic cycle. *Cytometry A*. 2017;91(3):216-231.
32. Gorenflot A, Brasseur P, Precigout E, L'Hostis M, Marchand A, Schrevel J. Cytological and immunological responses to *Babesia divergens* in different hosts: ox, gerbil, man. *Parasitol Res*. 1991;77(1):3-12.
33. Lobo CA. *Babesia divergens* and *Plasmodium falciparum* use common receptors, glycoporphins A and B, to invade the human red blood cell. *Infect Immun*. 2005; 73(1):649-651.
34. Cursino-Santos JR, Singh M, Pham P, Rodriguez M, Lobo CA. *Babesia divergens* builds a complex population structure composed of specific ratios of infected cells to ensure a prompt response to changing environmental conditions. *Cell Microbiol*. 2016;18(6):859-874.
35. Harrod VL, Howard TA, Zimmerman SA, Dertinger SD, Ware RE. Quantitative analysis of Howell-Jolly bodies in children with sickle cell disease. *Exp Hematol*. 2007; 35(2):179-183.
36. El Hoss S, Dussiot M, Renaud O, Brousse V, El Nemer W. A novel non-invasive method to measure splenic filtration function in humans. *Haematologica*. 2018; 103(10):e436-e439.
37. Rees DC, Williams TN, Gladwin MT. Sickle-cell disease. *Lancet*. 2010; 376(9757):2018-2031.
38. Bunn HF. The triumph of good over evil: protection by the sickle gene against malaria. *Blood*. 2013;121(1):20-25.
39. Elguero E, Delicat-Loembet LM, Rougeron V, et al. Malaria continues to select for sickle cell trait in Central Africa. *Proc Natl Acad Sci U S A*. 2015;112(22):7051-7054.
40. Yi W, Bao W, Rodriguez M, et al. Robust adaptive immune response against *Babesia microti* infection marked by low parasitemia in a murine model of sickle cell disease. *Blood Adv*. 2018;2(23):3462-3478.
41. Lobo CA, Rodriguez M, Cursino-Santos JR. *Babesia* and red cell invasion. *Curr Opin Hematol*. 2012;19(3):170-175.
42. Cursino-Santos JR, Halverson G, Rodriguez M, Narla M, Lobo CA. Identification of binding domains on red blood cell glycoporphins for *Babesia divergens*. *Transfusion*. 2014;54(4):982-989.
43. Friedman MJ. Erythrocytic mechanism of sickle cell resistance to malaria. *Proc Natl Acad Sci U S A*. 1978;75(4):1994-1997.
44. Pasvol G, Weatherall DJ, Wilson RJ. Cellular mechanism for the protective effect of haemoglobin S against *P. falciparum* malaria. *Nature*. 1978; 274(5672):701-703.
45. Pasvol G. The interaction between sickle haemoglobin and the malarial parasite *Plasmodium falciparum*. *Trans R Soc Trop Med Hyg*. 1980;74(6):701-705.
46. Tiffert T, Lew VL, Ginsburg H, Krugliak M, Croisille L, Mohandas N. The hydration state of human red blood cells and their susceptibility to invasion by *Plasmodium falciparum*. *Blood*. 2005;105(12):4853-4860.
47. Glushakova S, Humphrey G, Leikina E, Balaban A, Miller J, Zimmerberg J. New stages in the program of malaria parasite egress imaged in normal and sickle erythrocytes. *Curr Biol*. 2010;20(12):1117-1121.
48. Lew VL, Bookchin RM. Ion transport pathology in the mechanism of sickle cell dehydration. *Physiol Rev*. 2005;85(1):179-200.
49. Goheen MM, Wegmuller R, Bah A, et al. Anemia Offers Stronger Protection Than Sickle Cell Trait Against the Erythrocytic Stage of *Falciparum* Malaria and This Protection Is Reversed by Iron Supplementation. *EBioMedicine*. 2016; 14:123-130.
50. Luzzatto L, Nwachuku-Jarrett ES, Reddy S. Increased sickling of parasitised erythrocytes as mechanism of resistance against malaria in the sickle-cell trait. *Lancet*. 1970; 1(7642):319-321.
51. Archer NM, Petersen N, Clark MA, Buckee CO, Childs LM, Duraisingh MT. Resistance to *Plasmodium falciparum* in sickle cell trait erythrocytes is driven by oxygen-dependent growth inhibition. *Proc Natl Acad Sci U S A*. 2018;115(28):7350-7355.
52. Cholera R, Brittain NJ, Gillrie MR, et al. Impaired cytoadherence of *Plasmodium falciparum*-infected erythrocytes containing sickle hemoglobin. *Proc Natl Acad Sci U S A*. 2008;105(3):991-996.
53. Diakite SA, Ndour PA, Brousse V, et al. Stage-dependent fate of *Plasmodium falciparum*-infected red blood cells in the spleen and sickle-cell trait-related protection against malaria. *Malar J*. 2016;15(1):482.



# Distinguishing essential thrombocythemia *JAK2V617F* from polycythemia vera: limitations of erythrocyte values

Richard T. Silver<sup>1</sup> and Spencer Krichevsky<sup>1</sup>

<sup>1</sup>Richard T. Silver Myeloproliferative Neoplasm Center, Division of Hematology/Medical Oncology, Weill Cornell Medicine, New York, NY, USA

Haematologica 2019  
Volume 104(11):2200-2205

## ABSTRACT

Distinguishing essential thrombocythemia *JAK2V617F* from polycythemia vera is difficult because of shared mutation and phenotypic characteristics. The World Health Organization suggested hemoglobin and hematocrit values to diagnose polycythemia vera (PV), but their sensitivity and specificity were not tested. Moreover, red cell values do not accurately predict red cell mass, which we use to discriminate essential thrombocythemia *JAK2V617F* from PV. Eighty-three PV and 39 essential thrombocythemia *JAK2V617F* patients were diagnosed based on *JAK2V617F* positivity, chromium-51 red cell mass, and marrow biopsy findings. Red cell values used to construct a receiver operating characteristic analysis determined optimal thresholds for distinguishing essential thrombocythemia *JAK2V617F* from PV. Red cell value frequencies were plotted determining if overlap existed. Chromium-51 red cell mass separated PV from essential thrombocythemia *JAK2V617F*, but red cell values overlapped in 25.0-54.7%. Our data indicate that a significant proportion of PV patients may be underdiagnosed by using only red cell values. A bone marrow biopsy was performed in 199 of 410 (48.5%) and a serum erythropoietin value was measured in 225 of 410 (54.9%) of potential PV patients at our institution. Without isotope studies, marrow biopsies and serum erythropoietin values should improve diagnostic accuracy and become mandatory, but clinical data suggest these tests have not been routinely performed. Therefore, the clinical hematologist must be aware of imperfect accuracy when using only red cell values for distinguishing essential thrombocythemia *JAK2V617F* from PV.

## Correspondence:

RICHARD T. SILVER  
rtsilve@med.cornell.edu

SPENCER KRICHEVSKY  
spk2002@med.cornell.edu

Received: December 11, 2018.

Accepted: April 3, 2019.

Pre-published: April 4 2019.

doi:10.3324/haematol.2018.213108

Check the online version for the most updated information on this article, online supplements, and information on authorship & disclosures: [www.haematologica.org/content/104/11/2200](http://www.haematologica.org/content/104/11/2200)

©2019 Ferrata Storti Foundation

Material published in *Haematologica* is covered by copyright. All rights are reserved to the Ferrata Storti Foundation. Use of published material is allowed under the following terms and conditions:

<https://creativecommons.org/licenses/by-nc/4.0/legalcode>.

Copies of published material are allowed for personal or internal use. Sharing published material for non-commercial purposes is subject to the following conditions:

<https://creativecommons.org/licenses/by-nc/4.0/legalcode>,

sect. 3. Reproducing and sharing published material for commercial purposes is not allowed without permission in writing from the publisher.



## Introduction

The *JAK2V617F* and exon 12 mutations are critical for the diagnosis of polycythemia vera (PV); *JAK2V617F* is also the molecular marker of 50-60% of patients with essential thrombocythemia (ET<sup>*JAK2V617F*</sup>).<sup>1</sup> Distinguishing these illnesses in their early stages remains a clinical problem because of their shared mutation and phenotypic characteristics.<sup>2,3</sup>

In clinical situations when the hematocrit (HCT), hemoglobin (HGB), or red blood cell (RBC) count are relatively increased, we distinguish ET<sup>*JAK2V617F*</sup> from PV using chromium-51 (Cr-51) labeled RBC and iodine-135 (I135) to measure red cell mass (RCM) and plasma volume, respectively.<sup>4</sup> We include the latter to determine if an elevated HCT is attributed to reduced plasma volume when the Cr-51 determined RCM is normal. The distinction of these diagnoses has clinical significance: if a presumptive ET<sup>*JAK2V617F*</sup> patient in fact has PV, a significant risk for thrombosis may incur because therapeutic phlebotomy is not performed. Conversely, if a patient is misdiagnosed with PV, inappropriate phlebotomy treatment may cause significant iron deficiency and other related complications.<sup>5</sup> In addition, a misdiagnosis may also affect prognostic models comparing ET<sup>*JAK2V617F*</sup> with PV, ET<sup>CALR</sup>, or ET<sup>MPL</sup>.

The majority of hematology centers worldwide do not use isotope techniques but instead rely on arbitrarily defined World Health Organization (WHO) 2016

**Table 1.** Demographic and hematologic data of polycythemia vera (PV) and essential thrombocythemia (ET<sup>*JAK2V617F*</sup>) patients at diagnosis.

	PV Patients (n = 83)		ET Patients (n = 39)	
	Men (n = 45)	Women (n = 38)	Men (n = 12)	Women (n = 27)
Age median, range (yrs)	53.0 (28.0-80.0)	57.0 (27.0-78.0)	53.5 (29.0-77.0)	51.0 (24.0-76.0)
HCT mean ± SD (%)	50.9±4.4	51.2±5.8	43.5±4.4	42.8±2.2
HGB mean ± SD (g/dL)	17.1±1.7	16.7±1.8	14.9±1.6	14.4±0.8
RBC mean ± SD (x10 <sup>12</sup> /L)	5.8±0.6	6.0 ± 0.9	4.9±0.8	4.8±0.4
RCM mean ± SD (%)	141.7±14.4	149.4±24.5	91.8±15.9	96.1±14.8
Plasma volume mean ± SD (%)	(n=28) 105.1±15.0	(n=21) 99.4±15.3	91.2±9.4	(n=26) 99.1±11.5
SEV mean ± SD (mU/mL)	(n=41) 4.2±2.9	(n=35) 2.8±1.6	(n=9) 5.8±2.1	(n=14) 5.6±3.0

n: number; yrs: years; HCT: hematocrit; HGB: hemoglobin; RBC: red blood cell count; RCM: red cell mass; SD: standard deviation; SEV: serum erythropoietin values.

HCT and HGB threshold values<sup>6</sup> as surrogates for RCM to help diagnose and distinguish these diseases.<sup>7</sup> These unconfirmed values were derived from a retrospective study and do not discriminate all cases of ET<sup>*JAK2V617F*</sup> from PV.<sup>2,7</sup> For this reason, the WHO has advocated marrow biopsy and serum erythropoietin values (SEV), although it is not clear how frequently these tests are actually performed in clinical practices.

Since red cell values in ET<sup>*JAK2V617F*</sup> and PV can overlap, a proportion of both diseases may be misdiagnosed. Therefore, we decided to systematically study the sensitivity and specificity of distinguishing ET<sup>*JAK2V617F*</sup> with relatively high-normal red blood values from PV in patients when the RCM had been confirmed by isotope studies. Using a newly devised database-querying tool, we also determined the frequency of marrow biopsy and SEV testing, both of which we use at our own intuition.

## Methods

The Institutional Review Board of Weill Cornell Medicine (WCM) approved this study. Signed informed consent was obtained in accordance with the Declaration of Helsinki.

The diagnosis of PV in our patients was established according to our previously published criteria which included *JAK2V617F* positivity, a Cr-51 isotope measured RCM $\geq$ 125% of expected volume, and a marrow biopsy consistent with PV.<sup>4,8</sup> The diagnosis of ET<sup>*JAK2V617F*</sup> in our patients was established using *JAK2V617F* positivity, a Cr-51 isotope measured RCM<125% of expected volume, WHO 2007 criteria,<sup>1</sup> and a marrow biopsy consistent with ET.<sup>8</sup> ET<sup>*JAK2V617F*</sup> patients presenting with “high-normal” blood values (women: HCT>42.0%, HGB>14.0 g/dL; men: HCT>45.0%, HGB>15.0 g/dL) prompted an RCM study and were selected for this review.

We used a bioinformatics tool developed at WCM to search our electronic medical records for patients with an International Classification of Diseases (ICD) 9 or 10 code for PV or ET who had an RCM study performed from 2004-2017.<sup>9</sup>

Utilizing a receiver operating characteristic (ROC) analysis, we then determined threshold values for HCT, HGB, and RBC to establish limits of specificity and sensitivity. The ROC analysis calculates the optimal combination of sensitivity and specificity thresholds within a range of values to determine which one is the most accurate for diagnosis. We then plotted these ROC-derived threshold values and the frequencies of red cell values obtained at the time of isotope studies to ascertain whether there was any overlap between ET<sup>*JAK2V617F*</sup> and PV.

## Results

Of 157 patients who had an RCM study performed, 35 were excluded because of *JAK2V617F* and exon 12 negativity; of the remaining 122 patients, 83 PV and 39 ET<sup>*JAK2V617F*</sup> patients met study requirements. Relevant demographic and hematologic data of these patients, including age, HCT, HGB, RBC, RCM, and plasma volume are shown in Table 1. The blood values were recorded at the time of isotope study and prior to any treatment, including phlebotomy. The median age for male and female PV patients was 53.0 (28.0-80.0) and 57.0 (27.0-78.0) years, respectively. The median age for male and female ET<sup>*JAK2V617F*</sup> patients was 53.5 (29.0-77.0) and 51.0 (24.0-76.0) years, respectively. For male PV patients, the mean HCT was 50.9±4.4%, the mean HGB 17.1±1.7 g/dL, and the mean RBC count 5.8±0.6x10<sup>12</sup>/L. For female PV patients, the mean HCT was 51.2±5.8%, the mean HGB 16.7±1.8 g/dL, and the mean RBC count 6.0±0.9x10<sup>12</sup>/L. For male ET<sup>*JAK2V617F*</sup> patients, the mean HCT was 43.5±4.4%, the mean HGB 15.4±1.6 g/dL, and the mean RBC count 4.9±0.8x10<sup>12</sup>/L. For female ET<sup>*JAK2V617F*</sup> patients, the mean HCT was 42.8±2.2%, the mean HGB 14.4±0.8 g/dL, and the mean RBC count 4.8±0.4x10<sup>12</sup>/L. The mean Cr-51 RCM of all 83 PV patients was 145.3±20.1%, greater than 125% above the expected value and thus establishing polycythemia;<sup>4</sup> it was measured in 39 presumptive ET<sup>*JAK2V617F*</sup> and it was normal in all of them (mean: 94.8±15.3%). These RCM values show a clear distinction because unlike in red cell values, there was no overlap in values. The mean plasma volume was measured in 49 of 83 PV patients and it was 102.7±15.4%. The mean plasma volume was measured in 38 of 39 ET<sup>*JAK2V617F*</sup> patients and was 96.6±11.5%. The difference in plasma volume for all patients with PV and ET<sup>*JAK2V617F*</sup> was statistically significant ( $P=0.04$ ) due to differences for male patients ( $P=0.01$ ), but not for female patients ( $P=0.94$ ). In addition, there was a weak correlation between HCT and plasma volume ( $r=-0.05$ ). The mean serum erythropoietin value (SEV) was measured in 76 of 83 PV patients and was 3.5±2.5 mU/mL. The mean SEV was measured in 23 of 40 ET<sup>*JAK2V617F*</sup> patients and was 5.7±2.7 mU/mL.

Receiver operating characteristic (ROC) analyses were performed to determine optimal threshold values of HCT, HGB, and RBC to discriminate ET<sup>*JAK2V617F*</sup> from PV. The threshold values for distinguishing ET<sup>*JAK2V617F*</sup> from PV in men and women, respectively, are HCT: 49.3 and 47.9%, HGB: 16.8 and 15.3 g/dL, and RBC: 5.8 and 5.1x10<sup>12</sup>/L.

(Table 2). Figure 1A shows ROC curves for HCT in men and women with  $ET^{JAK2V617F}$  and PV; Figure 1B shows this for HGB concentration and Figure 1C shows this for RBC counts. The computer-calculated area under the curve (AUC) measures how well  $ET^{JAK2V617F}$  and PV patients are distinguished using HCT, HGB, or RBC. AUC ranges from 0 to 1, inclusive, with 1 representing a perfectly specific and sensitive test. For men, the AUC for HCT is 0.819 (specificity=100.0%, sensitivity=64.4%) indicating that by using this sole criterion, 100.0% of male  $ET^{JAK2V617F}$  patients, but only 64.4% of male PV patients, would be correctly diagnosed. For men, the AUC for HGB is 0.753

(specificity=100.0%, sensitivity=62.8%) indicating that 100.0% of male  $ET^{JAK2V617F}$  patients, but only 62.8% of male PV patients, would be correctly diagnosed. For men, the AUC for RBC is 0.761 (specificity=100.0%, sensitivity=52.5%) indicating that 100.0% of male  $ET^{JAK2V617F}$  and 52.5% of male PV patients would be correctly diagnosed. For women, the AUC for HCT is 0.957 (specificity=100.0%, sensitivity=71.1%), for HGB 0.875 (specificity=88.9%, sensitivity=75.0%), and for RBC 0.924 (specificity=81.5%, sensitivity=87.1%). The implications of these varying specificities and sensitivities are as previously noted above for men.

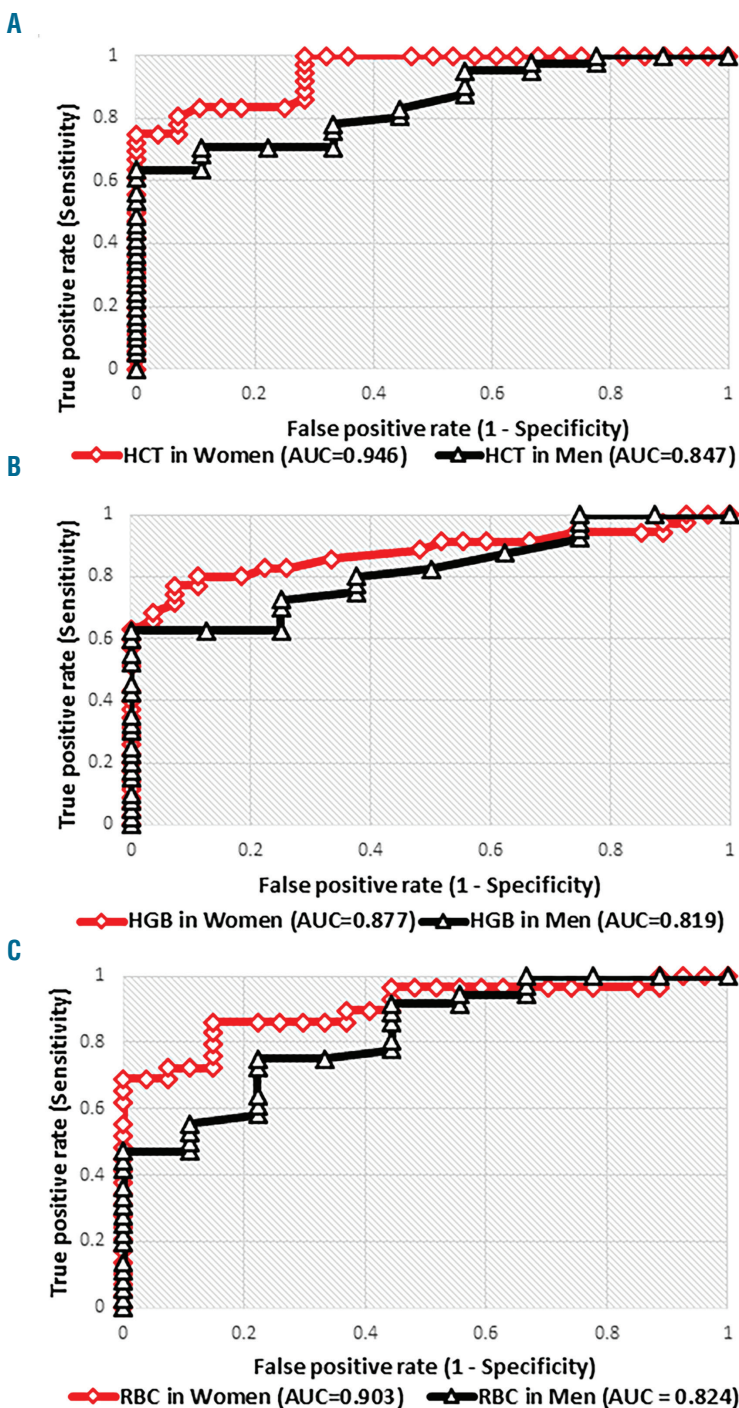


Figure 1. Receiver operating characteristic (ROC) analysis curves of red cell values in men with polycythemia vera (PV) versus men with essential thrombocythemia ( $ET^{JAK2V617F}$ ) (triangle markers) and women with PV versus women with  $ET^{JAK2V617F}$  (diamond markers). (A) For hematocrit (HCT), (B) for hemoglobin (HGB), and (C) for red blood cells (RBC).

For patients with either ET<sup>*JAK2V617F*</sup> or PV, the HCT values overlap in 36.0% of men and 25.0% of women (Figure 2A), the HGB values overlap in 40.0% of men and 54.7% of women (Figure 2B), and the RBC values overlap in 44.0% of men and 35.9% of women (*data not shown*). In these figures, the threshold values are shown in vertical, solid lines.

Querying our outpatient and inpatient electronic medical records with a bioinformatics tool provisioned by WCM showed that of 410 presumptive PV patients, 199 (48.5%) and 225 (54.9%) had a marrow biopsy performed and a SEV measured, respectively.

## Discussion

For more than half a century, it has been emphasized that a single HCT or HGB determination cannot be used as a surrogate for RCM.<sup>4,10,11</sup> Additional errors in blood count values are compounded by poor techniques of obtaining blood samples and other issues affecting plasma volume. We attempt to minimize these errors by collecting blood samples at the same time of the day insofar as possible and by using a standardized blood collection technique.<sup>12</sup> To attain an accurate RCM and plasma volume, we employ a dual isotope technique, using Cr-51 and I135 to measure these values simultaneously. In this study, as expected, the plasma volume was increased in PV.<sup>4,10</sup> We have no explanation for the gender differences, but insights may be learned from a larger sample size. The normal RCM and reduced plasma volume found in ET<sup>*JAK2V617F*</sup> patients accounted for the increased red cell values at the time of diagnosis.

An insufficient number of matched Cr-51 RCM and marrow results from our patients precluded comparison or correlation, which we plan to carry out as a future study. Discriminating ET<sup>*JAK2V617F*</sup> from PV is hierarchical with a dual isotope RCM study remaining the “gold standard”. We recognize that many institutions cannot perform the standard dual isotope technique;<sup>13</sup> in this situation, we espouse the use of marrow biopsy, which is now performed in all potential MPN patients at our institution at diagnosis, even in patients with a measured Cr-51 RCM to evaluate baseline fibrosis and cellularity to assess subsequent response to treatment.<sup>14</sup> It would be of interest to correlate marrow biopsy and Cr-51 RCM findings in the future. Despite the usefulness of a diagnostic marrow findings, as reported by us and others,<sup>4,8</sup> such findings have not been universally accepted<sup>15-17</sup> and even the value of marrow examination in general has been questioned.<sup>18</sup>

Although the SEV is a WHO 2016 minor criterion for the diagnosis of PV,<sup>6</sup> we emphasize that approximately 15% of PV patients have a normal SEV (4-27 mU/mL).<sup>19,20</sup> This fact and the availability of isotope studies may account for the relatively infrequent use of this test at our institution in the past. However, this laboratory value may be used in combination with abnormal red cell values to distinguish ET<sup>*JAK2V617F*</sup> from PV with higher accuracy than using red cell values exclusively.

There are no published data regarding the frequency with which marrow biopsy and SEV are currently performed in patients with PV at diagnosis by general hematologists. We reviewed marrow performance at our institution over the past decade and found that marrow biopsies were performed in 199 of 410 (48.5%) and an SEV

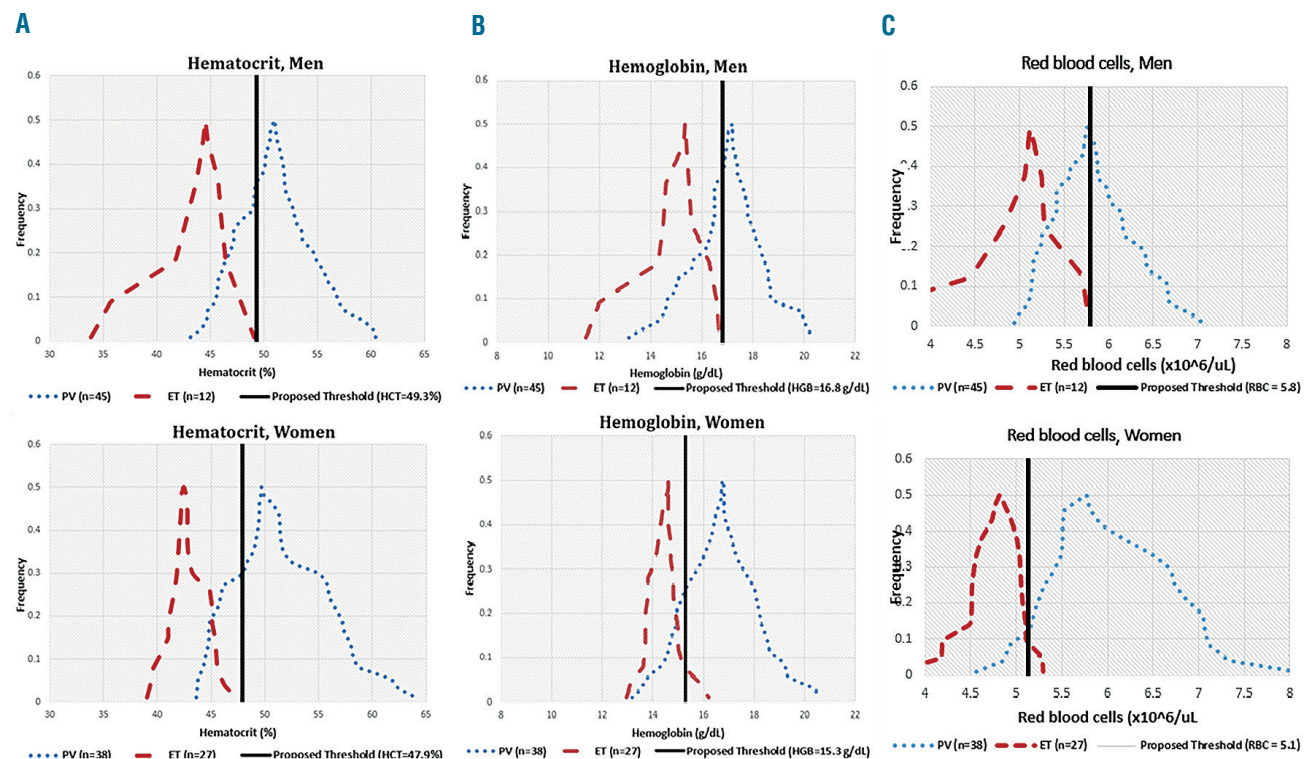


**Figure 2.** Frequencies of red cell values in men and women with polycythemia vera (PV) (dotted curve) and essential thrombocythemia (ET<sup>*JAK2V617F*</sup>) (dashed curve). Proposed thresholds shown in black, vertical line. (A) For hematocrit (HCT), (B) for hemoglobin (HGB), and (C) for red blood cells (RBC).

**Table 2.** Threshold values of hematocrit (HCT), hemoglobin (HGB), or red blood cell (RBC) count for men and women with associated area under the curve (AUC), specificity, and sensitivity.

	Value	Threshold	AUC	Specificity (%)	Sensitivity (%)
Men	HCT (%)	49.3	0.819	100.0	64.4
	HGB (g/dL)	16.8	0.753	100.0	62.8
	RBC (x10 <sup>12</sup> /L)	5.3	0.761	100.0	52.5
Women	HCT (%)	47.9	0.957	100.0	71.1
	HGB (g/dL)	15.3	0.875	88.9	75.0
	RBC (x10 <sup>12</sup> /L)	5.1	0.924	81.5	87.1

was measured in 225 of 410 (54.9%) PV patients. Of those that did not have a marrow biopsy, the majority had been encountered for only a single visit so that a marrow biopsy was not temporally feasible or the patient was advised to have it performed with their primary hematologist.

In the absence of isotope studies and an initial marrow biopsy or SEV, it is important to evaluate the accuracy, as defined statistically, of the HCT, HGB, and RBC threshold values that are advocated to distinguish ET<sup>JAK2V617F</sup> from PV. We found overlap in HCT, HGB, and RBC values ranging from 25.0-54.7% indicating that a single red cell value will not effectively distinguish ET<sup>JAK2V617F</sup> from PV.

Such considerations have been overlooked in other studies. For example, it has been suggested that ET<sup>JAK2V617F</sup> patients are at higher risk for thrombosis than those with a CALR mutation.<sup>21</sup> However, those patients diagnosed with ET<sup>JAK2V617F</sup> had a median SEV of 4.7 mU/mL (range: 0-47 mU/mL) compared with CALR+ ET patients who had a median SEV of 9.4 mU/mL (range: 1.2-27 mU/mL). An unspecified number of ET<sup>JAK2V617F</sup> patients had a SEV below normal (i.e. <4 mU/mL)<sup>22</sup> suggesting the possibility of PV. Since neither all red cell values, isotope studies, nor systematic marrow biopsies were reported, some of these ET<sup>JAK2V617F</sup> patients might have, in fact, had a higher risk of thrombotic events because they actually had PV.<sup>23</sup> Thus, they were incorrectly assigned to a disease with a decreased expected survival.<sup>24</sup> Of course, these issues do not occur in JAK2V617F wild-type, CALR+, or MPL+

patients because these mutations, with very rare exceptions, do not occur in PV.<sup>18</sup>

It is of interest that our threshold values are coincidentally similar to the WHO 2016 criteria,<sup>6</sup> which did not address the important topic of imperfect specificity and sensitivity. Although marrow biopsy and SEV are advantageous for distinguishing ET<sup>JAK2V617F</sup> from PV, it is unclear how frequently these examinations are being performed in actual clinical practice. Our data support their use even despite the discussed limitations. In the absence of resolving these discrepancies, isotope RCM studies remain the gold standard for discriminating ET<sup>JAK2V617F</sup> from PV.

In summary, the clinical hematologist must be warned of the varying specificity and sensitivity and the considerable limitations of discriminating ET<sup>JAK2V617F</sup> from PV solely when using red cell values, and the importance of isotope, marrow, and SEV studies as outlined by WHO 2016 criteria.<sup>6</sup> It remains undetermined how frequently any of these tests are performed in clinical practice.

#### Acknowledgments

We thank Dr. Paul Christos for statistical review. He was partially supported by the Clinical and Translational Science Center, Weill Cornell Medical College (UL1-TR000457-06).

#### Funding

This study was supported in part by the William and Judy Higgins Trust and the Johns Family Foundation of the Cancer Research and Treatment Fund Inc., New York, NY, USA.

## References

- Tefferi A, Thiele J, Orazi A, et al. Proposals and rationale for revision of the World Health Organization diagnostic criteria for polycythemia vera, essential thrombocythemia, and primary myelofibrosis: recommendations from an ad hoc international expert panel. *Blood*. 2007;110(4):1092-1097.
- Barbui T, Thiele J, Kvasnicka HM, Carobbio A, Vannucchi AM, Tefferi A. Essential thrombocythemia with high hemoglobin levels according to the revised WHO classification. *Leukemia*. 2014; 28(10):2092-2094.
- Spivak JL. Myeloproliferative Neoplasms. *N Engl J Med*. 2017;377(9):895-896.
- Silver RT, Chow W, Orazi A, Arles SP, Goldsmith SJ. Evaluation of WHO Criteria for Diagnosis of Polycythemia Vera: A Prospective Analysis. *Blood*. 2013; 22(11):1881-1886.
- Silver RT, Kiladjian JJ, Hasselbalch HC. Interferon and the treatment of polycythemia vera, essential thrombocythemia and myelofibrosis. *Exp Rev Hematol*. 2013;6(1):49-58.
- Arber DA, Orazi A, Hasserjian R, et al. The 2016 revision to the World Health Organization (WHO) classification of myeloid neoplasms and acute leukemia. *Blood*. 2016;127(20):2391-2405.
- Barbui T, Thiele J, Gisslinger H, et al. Masked polycythemia vera (mPV): Results of an international study. *Am J Hematol*. 2014;89(1):52-54.
- Kvasnicka HM, Orazi A, Thiele J, Barosi G, Bueso-Ramos CE, Vannucchi AM. European LeukemiaNet study on the reproducibility of bone marrow features in masked polycythemia vera and differentiation from essential thrombocythemia. *Am J Hematol*. 2017;92(1):1062-1067.
- Overhage JM, Ryan PB, Reich CG, Hartzema AG, Stang PE. Validation of a common data model for active safety surveillance research. *J Am Med Inform Assoc*. 2012;19(1):54-60.
- Alvarez-Larran A, Ancochea A, Angona A, et al. Red cell mass measurement in patients with clinically suspected diagnosis of polycythemia vera or essential thrombocythemia. *Haematologica*. 2012; 97(11): 1704-1707.
- Johansson PL, Safai-Kutti S, Kutti J. An elevated haemoglobin concentration cannot be used as a surrogate marker for absolute erythrocytosis: a study of patients with polycythaemia vera and apparent polycythaemia. *Br J Haematol*. 2005;129(5):701-705.
- Silver RT, Gjoni S. The hematocrit value in

- polycythemia vera: caveat utilitor. *Leuk Lymphoma*. 2015;56(6):1540-1541.
13. Margolske E, Orazi A, Krichevsky S, Silver RT. Evaluation of bone marrow morphology is essential for assessing disease status in interferon-treated polycythemia vera patients. *Haematologica*. 2017;102(3):e97-e99.
  14. Alvarez-Larran A, Ancochea A, Garcia M, et al. WHO-histological criteria for myeloproliferative neoplasms: reproducibility, diagnostic accuracy and correlation with gene mutations and clinical outcomes. *Br J Haematol*. 2014;166(6):911-919.
  15. Ellis JT, Silver RT, Coleman M, Geller SA. The bone marrow in polycythemia vera. *Semin Hematol*. 1975;12(4):433-444.
  16. Wilkins BS, Erber WN, Bareford D, et al. Bone marrow pathology in essential thrombocythemia: interobserver reliability and utility for identifying disease subtypes. *Blood*. 2008;111(1):60-70.
  17. Spivak J. Polycythemia Vera. *Curr Treat Options Oncol*. 2018;19(2):12.
  18. Silver RT, Krichevsky S, Cross NCP. Evaluation of serum erythropoietin values as defined by 2016 World Health Organization criteria for the diagnosis of polycythemia vera. *Leuk Lymphoma*. 2017;58(11):2768-2769.
  19. Ancochea A, Alvarez-Larran A, Morales-Indiano C, et al. The role of serum erythropoietin level and JAK2 v617f allele burden in the diagnosis of polycythemia vera. *Br J Haematol*. 2014;167(3):411-417.
  20. Rumi E, Pietra D, Ferretti V, et al. JAK2 or CALR mutation status defines subtypes of essential thrombocythemia with substantially different clinical course and outcomes. *Blood*. 2014;123(10):1544-1551.
  21. "Laboratory Testing Information - Erythropoietin." RSS 20 In Focus. ARUP Laboratories, Web. 28 Feb. 2013. <http://www.aruplab.com/guides/ug/tests/0050227.jsp>.
  22. Price GL, Davis KL, Karve S, Pohl G, Walgren RA. Survival Patterns in United States (US) Medicare Enrollees with Non-CML Myeloproliferative Neoplasms (MPN). *PLoS One*. 2014;9(3):e90299.
  23. Michiels JJ, Medinger M, Raeve HD, et al. Increased erythrocyte count on top of bone marrow histology but not serum EPO level or JAK2 mutation load discriminates between JAK2V617F mutated essential thrombocythemia and polycythemia vera. *J Hematol Thromb Dis*. 3:S1-001.
  24. Pearson TC, Guthrie DL, Simpson J, et al. Interpretation of measured red cell mass and plasma volume in adults: Expert Panel on Radionuclides of the International Council for Standardization in Haematology. *Br J Haematol*. 1995;89(4): 745-756.



Ferrata Storti Foundation

## MR4 sustained for 12 months is associated with stable deep molecular responses in chronic myeloid leukemia

Simone Claudiani,<sup>1,2</sup> Aoife Gatenby,<sup>2</sup> Richard Szydlo,<sup>2</sup> George Nesr,<sup>1,2</sup> Adi Shacham Abulafia,<sup>3</sup> Renuka Palanicawandar,<sup>1</sup> Georgios Nteliopoulos,<sup>2</sup> Jamshid Khorashad,<sup>2</sup> Letizia Foroni,<sup>2</sup> Jane F. Apperley<sup>1,2</sup> and Dragana Milojkovic<sup>1</sup>

<sup>1</sup>Department of Haematology, Hammersmith Hospital, Imperial College Healthcare NHS Trust, London, UK; <sup>2</sup>Centre for Haematology, Imperial College London, London, UK; <sup>3</sup>Institute of Hematology, Davidoff Cancer Centre, Beilinson Hospital, Rabin Medical Centre, Petah-Tiqva, Israel

Haematologica 2019  
Volume 104(11):2206-2214

### ABSTRACT

The majority of patients with newly diagnosed chronic myeloid leukemia (CML) will enjoy a life expectancy equivalent to that of unaffected individuals, but will remain on life-long treatment with a concomitant requirement for on-going hospital interactions for molecular monitoring and drug dispensing. In order to determine more accurately the frequency of monitoring required, we performed a 'real-life' retrospective single-center cohort study of 450 patients with CML in at least major molecular remission (MR3) to analyze the risk of loss of MR3 [defined as at least 2 consecutive real-time quantitative polymerase chain reaction (RT-qPCR) results >0.1% International Scale (IS)]. Patients who achieved sustained MR4 (sMR4, BCR-ABL1 RT-qPCR <0.01% IS for 12 months) had a probability of loss of MR3 at 1 and 5 years of 0 and 2.6% (95% CI: 1.2-5.4) respectively, compared to 4.4% (95% CI: 1.9-9.8) and 25.4% (95% CI: 16.7-36.7) respectively, in those who achieved sustained MR3 (sMR3) but not sMR4 ( $P < 0.001$ ). No patient who improved their response to a deep molecular level (at least MR4) lost MR3 if they were considered compliant, had no history of resistance and remained on standard dose tyrosine kinase inhibitor (TKI). MR4 maintained for at least one year represents a secure response threshold for patients with CML, after which no MR3 loss occurs if certain conditions are satisfied (standard TKI dose, full compliance, and lack of previous TKI resistance). This finding may justify reduction of the frequency of hospital interaction, with an associated positive impact on quality of life, survivorship, and economic burden to both patients and healthcare providers.

### Correspondence:

SIMONE CLAUDIANI  
simone.claudiani@nhs.net

Received: December 16, 2018.

Accepted: March 21, 2019.

Pre-published: March 28, 2019.

doi:10.3324/haematol.2018.214809

Check the online version for the most updated information on this article, online supplements, and information on authorship & disclosures: [www.haematologica.org/content/104/11/2206](http://www.haematologica.org/content/104/11/2206)

©2019 Ferrata Storti Foundation

Material published in *Haematologica* is covered by copyright. All rights are reserved to the Ferrata Storti Foundation. Use of published material is allowed under the following terms and conditions:

<https://creativecommons.org/licenses/by-nc/4.0/legalcode>.

Copies of published material are allowed for personal or internal use. Sharing published material for non-commercial purposes is subject to the following conditions:

<https://creativecommons.org/licenses/by-nc/4.0/legalcode>,

sect. 3. Reproducing and sharing published material for commercial purposes is not allowed without permission in writing from the publisher.



### Introduction

Since the advent of tyrosine kinase inhibitors (TKI), chronic myeloid leukemia (CML) has indeed become a 'chronic' disorder. With a life expectancy comparable to unaffected individuals,<sup>1,2</sup> management of CML typically involves daily oral TKI, together with regular hospital attendances for molecular monitoring, control of side effects and dispensing of prescription medicines. Whilst this dramatic change is a welcome testament to the power of molecularly targeted agents, further thought can now be given to decreasing the number of interactions between patient and healthcare professionals in order to restore patient autonomy and reduce the financial burden of long-term care.

In the first year of treatment, molecular monitoring at a minimum of 3-monthly intervals is recommended to assess response against international guidelines [European LeukemiaNet (ELN), National Comprehensive Cancer Network (NCCN)].<sup>3,4</sup> Several studies have shown the importance of early molecular responses (EMR) at 3, 6 and 12 months for their ability to predict the probability of achievement of deep molecular responses, progression-free survival (PFS) and overall sur-

vival (OS).<sup>5-10</sup> Indeed, the achievement of a major molecular response (MMR, MR3) is often used as a surrogate end point in clinical trials,<sup>11</sup> as failure to reach MR3 by 12 months is associated with lower rates of deeper molecular responses, PFS and OS.<sup>1, 11-13</sup>

Confirmed major molecular response (defined as MR3 on at least two consecutive occasions) has been described as a 'safe haven', in that patients who reach this level of response are highly unlikely to experience disease progression.<sup>14-19</sup> However, few studies have investigated the predictive value of a stable MR3 with respect to subsequent loss of MR and the requirement for a change in therapy. Furthermore, there are no studies addressing the requirement for, and frequency of, molecular monitoring in patients who have achieved a stable MR3. We interrogated our single center database to determine if we could identify a level of MR that is highly unlikely to be lost provided the patient remains on treatment, a molecular threshold that would render frequent molecular monitoring unnecessary.

## Methods

### Patient selection

We included all patients diagnosed with CML in chronic phase, treated with TKI from January 2000 until December 2015, who achieved sustained MR3 (sMR3). We excluded patients treated with chemotherapy and/or stem cell transplantation before TKI. TKI were commenced at standard doses and may have been dose reduced subsequently to manage adverse events. Because some of the patients were treated prior to the availability of second-generation TKI, doses of imatinib > 400 mg daily (HD) were prescribed for less than optimal responses in 15% of patients. Episode of non-compliance with treatment was recorded in our database when patients admitted to taking less than 100% of the prescribed therapy. The data cut-off was 31<sup>st</sup> October 2017. This retrospective observational study was approved by the research ethics committee, and all patients gave written informed consent for their data to be stored and analyzed in our institutional database.

### Response definitions

Standard definitions of response and resistance were used.<sup>3</sup> Sustained MR3 (sMR3) and sustained MR4 (sMR4) were defined as BCR-ABL1 real-time quantitative polymerase chain reaction (RT-qPCR) of  $\leq 0.1\%$  and  $< 0.01\%$  (on International Scale, IS), respectively, maintained for at least one year. The BCR-ABL1 RT-qPCR was performed according to our previously established methodology.<sup>20</sup> At least three consecutive assessments, at a frequency of 3-4 monthly, were required to define sustained response.

Single RT-qPCR results above MR3 or MR4 were considered fluctuations. The date of loss of MR3 and MR4 was the first of at least two consecutive RT-qPCR levels  $> 0.1\%$  and  $\geq 0.01\%$ , respectively.

A BCR-ABL1 RT-qPCR  $< 1\%$  was considered to be equivalent to complete cytogenetic response (CCyR).<sup>21</sup> The date of loss of CCyR was the first of two consecutive RT-qPCR determinations  $\geq 1\%$  (IS).

Patients were monitored every three months throughout the entire follow up, according to current guidelines.<sup>3</sup>

### Statistical analysis

Times to achievement of sMR3 and sMR4 were calculated from the date of starting TKI until the first day of RT-qPCR  $\leq 0.1\%$  and

$< 0.01\%$  IS, respectively, maintained for at least one year. The probabilities of loss of MR3, MR4 and CCyR after the first year of sustained response were calculated using the Kaplan-Meier method, with patients being censored at last follow up on treatment. Potential prognostic factors for loss of MR3 were investigated using the log-rank test, with continuous variables split into groups using either quartiles or median values. Variables significant at the  $P < 0.20$  level were then included in a Cox proportional hazard regression analysis to find the best model.

Baseline characteristics were compared using the Mann-Whitney test for continuous variables, and Fisher Exact test for categorical variables.

Overall survival (OS) and the event-free survival (EFS) were estimated using the Kaplan-Meier method. For the analysis of survival from CML-related deaths (CML-OS), patients dying from any cause other than CML progression were censored at the date of death; all the other subjects were censored at the date of last follow up. Both OS and CML-OS were calculated from the date of diagnosis, whereas EFS was calculated from the first year in MR3. For EFS, progression to either accelerated or blast phases and death from any cause were considered as events.

$P < 0.05$  was considered statistically significant. All analyses were performed with SPSS software (version 24; IBM, USA).

## Results

### Achievement of sustained MR3 and MR4

A total of 450 patients achieved sMR3 (Table 1) at a median time from start of TKI of 15.7 months (range: 2-184 months). The median number of RT-qPCR assays in the first year of MR3 was five (range: 3-12), with a median interval between samples of two months (range: 0.5-4 months). The majority of patients, 336 of 450 (74.7%), were on first-line therapy at the time of achievement of sMR3, and most of the remainder, 96 of 114 (84.2%) had changed treatment because of resistance. Of the total cohort, 324 achieved sMR4 at a median of 11.4 months (range: 0-120 months) from sMR3 and 29.1 months (range: 3.3-172.1 months) from start of TKI therapy. The median number of RT-qPCR assays in the first year of MR4 was four (range: 3-11), with a median interval among samples of 2.8 months (range: 0.5-4). After the achievement of sMR3, the median interval between RT-PCR assays was 2.7 months (range: 0.5-9 months) and was identical in both groups. The 5-year probability of sMR4 after the achievement of sMR3 was 74% (95%CI: 69.3-78.2).

*Online Supplementary Table S1* shows a comparison of clinical and CML-related characteristics between patients who achieved sMR3 only and those who reached sMR4. We observed a significant difference in the number of patients treated with high-dose imatinib and in the proportion of those with a history of resistance to first-line TKI ( $P = 0.02$  and  $P = 0.0002$ , respectively), both more common in the sMR3 only group.

Patients who achieved sMR4 reached sMR3 more rapidly (median 12.3 months, range: 1-135.2) than those whose best response was sMR3 only (median 24.5 months, range: 2.8-184.4;  $P < 0.001$ ). The median follow up of patients in sMR3 only was shorter (56.9 months, range: 12.3-155) than those in sMR4 (108.1 months, range: 14.6-199.7).

Patients expressing the BCR-ABL1 e14a2 transcript achieved sMR3 more rapidly at 12.2 months (range: 1-130 months) than those expressing e13a2 at 21.4 months

(range: 1-144 months;  $P=0.019$ ) and were more likely to achieve sMR4, with 5-year probabilities of 81% (range: 74-86.5%) compared to 72.8% (95%CI: 64.8-79.6;  $P=0.009$ ) for those with the e13a2 transcript (*Online Supplementary Figure S1A and B*).

### Loss of sustained responses

Among the total cohort of 450 patients, the 1- and 5-year probabilities of loss of MR3 were 1.1% (95%CI: 0.5-2.6) and 7.5% (95%CI: 5.2-10.7), respectively (Figure 1B), and of loss of CCyR 0.7% (95%CI: 0.2-2) and 5.9% (95%CI: 4-8.7), respectively. In univariate analysis, a history of resistance to any TKI, time to sMR3 longer than 7.7 months (corresponding to the 1<sup>st</sup> quartile of the time of achievement of sMR3 in the whole patient cohort), and failure to reach sMR4 were significantly associated with loss of MR3. In multivariate analysis, only failure to reach sMR4 remained statistically significant (Table 2). Patients who achieved sMR3 after an increase in the dose of imatinib were more likely to lose MR3 than patients who achieved sMR3 after a change to a 2GTKI (*Online Supplementary Table S2*).

Of the 324 patients in sMR4, 29 (8.9%) lost MR4 at a median of 49.9 months (range: 2.5-111.4 months) after the first year in MR4, of whom 15 also lost MR3 at a median of 41.3 months (range: 15.3-112.7 months) after the first year in MR4 and 2.1 months (range: 0-23.3 months) from loss of MR4. At the time of MR4 loss and MR3 loss, no patient had remained on standard dose of TKI throughout their disease course. Seven were known to be non-compliant with therapy, 18 were on lower doses of TKI, and four had previously received TKI doses greater than standard doses for resistance (Figure 2). The probabilities of loss of MR3 at 1 and 5 years were 0 and 4.6% (95%CI: 2.5-8.2), and of loss of MR4 were 1.3% (95%CI: 0.5-3.5) and 8.7% (95%CI: 5.6-13.2), respectively (Figure 1A).

Of the 126 patients who achieved sMR3 only, 21 (16.7%) lost MR3 at a median of 21.5 months (range: 1-60 months) after the first year in MR3. The probabilities of loss of MR3 at 1 and 5 years were 4.4% (95%CI: 1.9-9.8) and 25.4% (95%CI: 16.7-36.7), respectively, which were higher than in the sMR4 cohort ( $P<0.001$ ) (Figure 2B). At the time of MR3 loss, only one patient had remained on standard dose of TKI throughout their disease course. Five were known to be non-compliant with therapy, five were on lower doses of TKI, and ten had previously received TKI doses greater than standard doses for resistance (Figure 2).

### Durability of response in patients achieving sMR4

Of the 324 patients in sMR4, 107 patients (23.7%) had remained on standard dose TKI after the achievement of sMR3 and sMR4. None of these patients lost MR3. In order to address the subsequent pattern of BCR-ABL1 RT-qPCR responses after their achievement of sMR3, we plotted a total of 3,305 consecutive results, with a median number of tests per patient of 29 (range: 6-93 tests) and a median interval between tests of three months (range: 1-12 months). Most of the results (2,573, 77.8%) fell below the MR4 threshold, and demonstrated a continuing decline over time (Figure 3).

### Events subsequent to the loss of MR3 and of MR4

In 36 patients who lost MR3, the median follow up since the loss was 24.5 months (range: 1.3-135.4 months).

**Table 1. Study cohort characteristics (n=450).**

Variable	N (%)
Gender	
Male	224 (49.7%)
Female	226 (51.3%)
Age at diagnosis (median, range)	45 (19-86.4)
<40	172 (38.2%)
≥40 and <60	200 (44.4%)
≥60	78 (17.3%)
Date of 1 <sup>st</sup> line TKI start	
2000-2006	252 (56.0%)
2007-2011	120 (26.7%)
2012-2014	74 (16.4%)
2015	4 (0.9%)
Transcript type	
E14a2	222 (49.3%)
E13a2	159 (35.4%)
E14a2/e13a2	50 (11.1%)
Others	6 (1.3%)
Unknown	13 (2.9%)
Sokal score	
Low	135 (30%)
Intermediate	106 (23.5%)
High	109 (24.2%)
Unknown	100 (22.2%)
Previous interferon therapy	
Yes	90 (20%)
No	360 (80%)
BCR-ABL1 mutation detected before the achievement of MR3	24
T315I	3/24 (12.5%)
TKI 1 <sup>st</sup> line	
Imatinib	402 (89.3%)
Dasatinib	21 (4.7%)
Nilotinib	21 (4.7%)
Bosutinib	6 (1.3%)
TKI 1 <sup>st</sup> line at MR3	336 (100%)
Imatinib	226 (71.4%)
Imatinib higher dose	68 (16.1%)
-for resistance according to ELN	54
Nilotinib	21 (6.3%)
Dasatinib	16 (4.8%)
Bosutinib	5 (1.5%)
TKI ≥2 <sup>nd</sup> line at MR3 for previous resistance to at least 1 TKI	96 (100%)
Nilotinib	32 (33.3%)
Dasatinib	54 (56.3%)
Bosutinib	4 (4.2%)
Ponatinib	6 (6.3%)
TKI ≥2 <sup>nd</sup> line at MR3 for previous intolerance	18 (100%)
Imatinib	1 (5.6%)
Nilotinib	9 (50%)
Dasatinib	7 (38.9%)
Bosutinib	1 (5.6%)

n: number; TKI: tyrosine kinase inhibitor; ELN: European LeukemiaNet.

Of these, 14 also lost CCyR at a median of six months (range: 1.3-55.4 months) from loss of MR3. The 1- and 5-year probabilities of loss of CCyR were 1.9% (95%CI: 0.5-6.5) and 13.1% (95%CI: 6.5-24.2) for those who achieved only sMR3 and 0 and 1.2% (95%CI: 0.4-3.5) for those who reached sMR4 (Figure 1C). Three of these patients experienced progression to accelerated phase, of

whom two died subsequently in blast phase and one achieved MR4 on a different TKI. Of the remaining 11 patients, at last follow up four were in complete hematological response, two in CCyR, two in MR3, one in MR4, and two in MR4.5. The median follow up of the 22 patients who lost MR3 but not CCyR was 33.4 months (range: 5.4-135.4 months). At last follow up, ten had

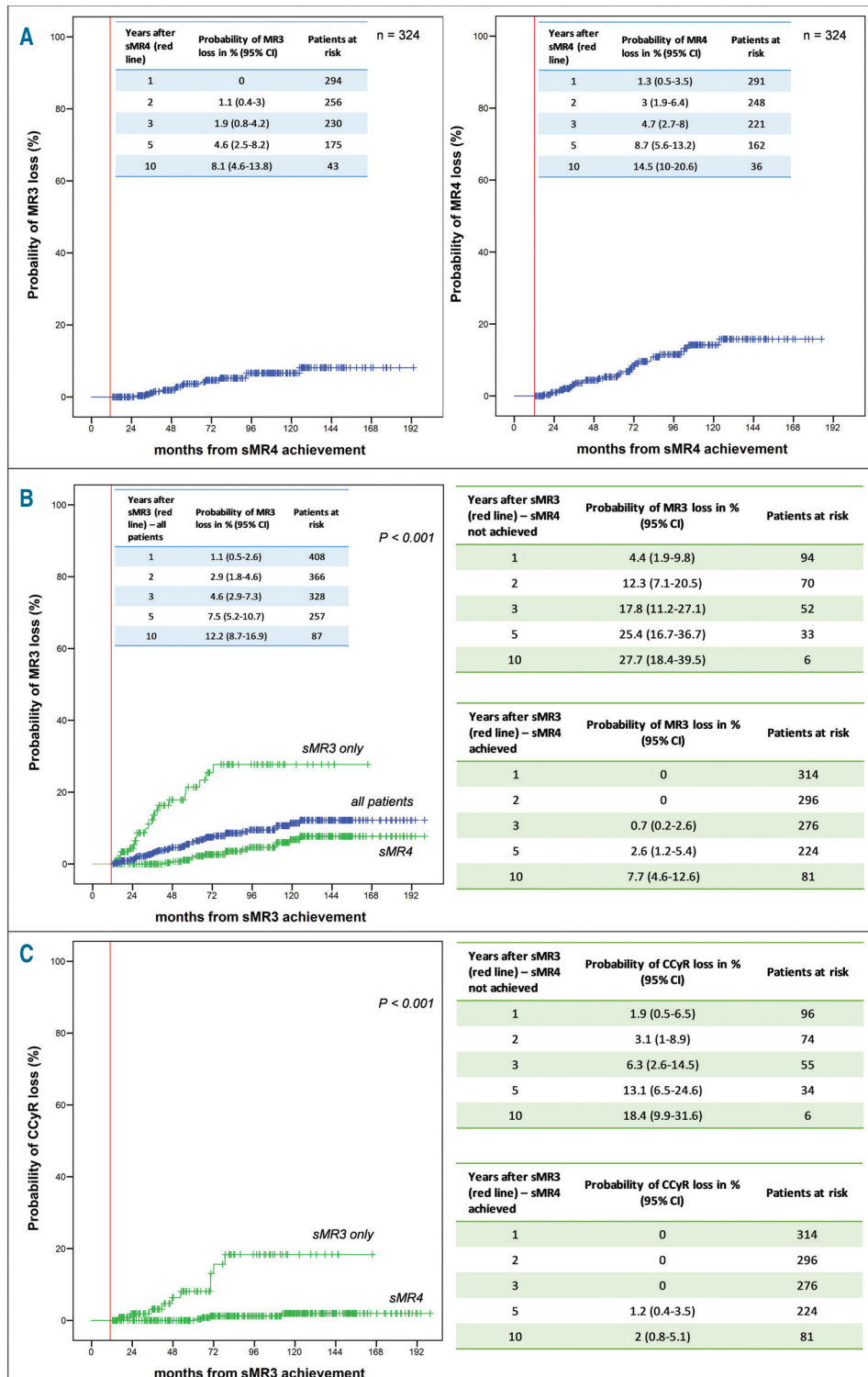


**Figure 1.** Probabilities of loss of responses after achieving sustained molecular response (MR)-3 (sMR3) and sMR4. (A) Probability of loss of MR3 and MR4 after the first year in MR4 (vertical line indicates time of sMR4, i.e. time at which MR4 was sustained for 12 months). (B) Probability of loss of MR3 for all 450 patients (vertical line indicates time of sMR3, i.e. time at which MR3 was sustained for 12 months) (blue curve); probability of loss of MR3 for patients who achieved sMR3 only (n=126) and those who achieved sMR4 (n=324) (green curves). (C) Probability of loss of complete cytogenetic response (CCyR) for patients who achieved sMR3 only (n=126) and those who achieved sMR4 (n=324). n: number; CI: Confidence Interval.

achieved MR3, five were in MR4, and seven in MR4.5. Of the 14 patients who lost MR4 but not MR3, none had lost CCyR at a median follow up of 39.2 months (range: 26-89.3 months). At last follow up, five patients were in MR3, five in MR4, and four in MR4.5.

The response status at last follow up on TKI and treatment status at last follow up are summarized in *Online Supplementary Figure S2*.

### Overall survival

The 5- and 10-year OS were 98.8% (95%CI: 98.7-98.9) and 96.8% (95%CI: 94.2-97.3), while CML-OS were 100% and 99.4% (95%CI: 98-99.8) (Figure 4A). The 5-year EFS after the first year in MR3 was 97.3% (95%CI: 95.2-98.5) (Figure 4B). Overall, 11 deaths were recorded at a median follow up from diagnosis of 122.5 months (range: 17.5-234 months). Of these, only two were directly related to CML. Other causes of death included chronic obstructive pulmonary disease (n=2), second cancer (n=5: non-Hodgkin lymphoma, glioblastoma, mesothelioma, colonic adenocarcinoma, esophageal adenocarcinoma), autoimmune disease (n=1), unknown (n=1).

### Discussion

One of the real-life outcomes of the successful use of TKI has been the increase in the number of patients living with CML. Estimates of prevalence of CML suggest that more than 100,000 individuals will be on TKI in the USA alone by 2020,<sup>22</sup> requiring in excess of 300,000 out-patient

interactions annually. Data from Phase III randomized studies of imatinib *versus* dasatinib<sup>12</sup> and imatinib *versus* nilotinib<sup>11</sup> show that the majority of patients achieve MR3 on at least one occasion by five years (imatinib 64%, dasatinib 76% in DASISION; imatinib 60.4%, nilotinib 77% in ENESTnd) and that many of these also reach MR4 or deeper.<sup>11,12</sup> Although the cumulative incidences of molecular responses by pre-defined time points are not identical to the achievement of sustained responses, it seems reasonable to assume that with continued treatment and changes of treatment for less than optimal responses, the number of patients achieving deep and durable responses will continue to increase.

We used our single center cohort of patients who had reached and sustained for 12 months the 'safe-haven' of MR3 to investigate the durability of this response,<sup>14</sup> in order to provide some evidence for recommendations for the frequency of PCR monitoring once these deep responses have been established. In using a 'real-life' patient cohort, we appreciate that there are complexities of decision-making that are confounding compared to the rigorous clinical trial environment. In clinical practice, many patients are managed on lower than standard doses of the various TKI because of intolerance, some admit to non-compliance so that actual dosing is difficult to estimate, and in the early TKI era when only imatinib was available and when the various milestones for response had not been established, some patients were given higher than standard doses to try to deepen their responses. These varying conditions should be taken into account during response monitoring, such that patients may

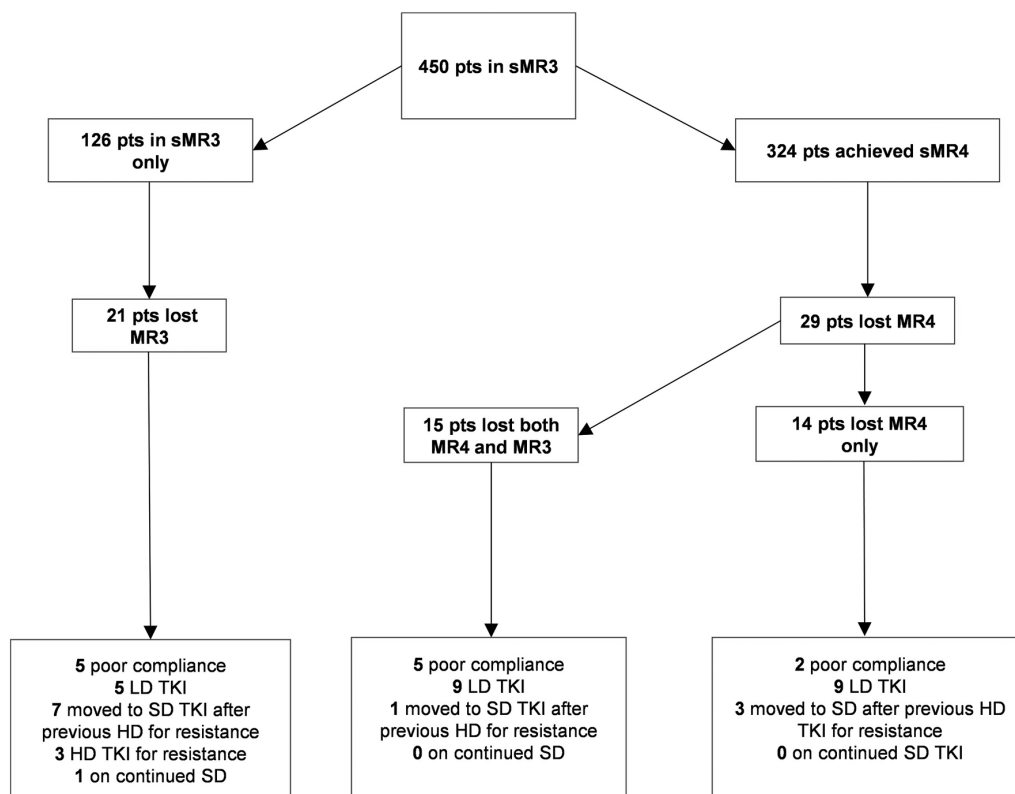


**Figure 2. Patient outcomes.** Flow diagram showing outcomes of 450 patients after the achievement of sustained molecular response (MR)-3 (sMR3). The boxes in the lower part of the image contain information about the tyrosine kinase inhibitor (TKI) dose at the time of response loss. LD: lower TKI dose (compared to the standard recommended doses for first or subsequent lines); SD: standard TKI dose; HD: higher TKI dose; sMR4: sustained MR4; pts: patients.

**Table 2.** Univariate and multivariate analysis of factors possibly associated with MR3 loss.

Factor	n	Probability of MR3 loss at 5 yrs % (95% CI)	P	Multivariate analysis HR (95% CI)	P
<b>Gender</b>					
Male	224	5.9 (3.4-10.2)	0.34		
Female	226	9 (5.6-14.3)			
<b>Age at diagnosis</b>					
< 45 yrs	225	9.1 (5.6-14.4)	0.84		
≥ 45 yrs	225	5.8 (3.3-10.1)			
<b>Transcript type</b>					
e14a2	222	8 (4.8-13.1)	0.65		
e13a2 or e14a2/e13a2	209	6.3 (3.5-11.1)			
<b>History of TKI resistance before MR3</b>					
Yes	150	10.5 (6.2-17.3)	0.05		
No	300	5.9 (3.6-9.6)			
<b>Time to MR3 achievement</b>					
< 7.7 months (1st q)	112	3.6 (1.2-10.3)	0.03		
≥ 7.7 months	338	8.6 (5.8-12.5)			
<b>MR4 achieved</b>					
Yes	324	2.6 (1.2-5.4)	<0.001	1.00	<0.001
No	126	25.4 (16.7-37.7)		4.21 (2-8.5)*	
<b>&gt;1<sup>st</sup> TKI line at MR3</b>					
Yes	114	5.8 (2.2-14.3)	0.62		
No	336	8.1 (5.5-11.8)			
<b>1GTKI at MR3</b>					
Yes	295	7.7 (5-11.7)	0.83		
No	155	7.6 (3.7-15)			

n: number; yrs: years; CI: confidence interval; HR: hazard ratio; TKI: tyrosine kinase inhibitor; q: quartile; 1GTKI: 1<sup>st</sup> generation TKI. \*Achievement of MR4 was modelled in a time-dependent fashion.

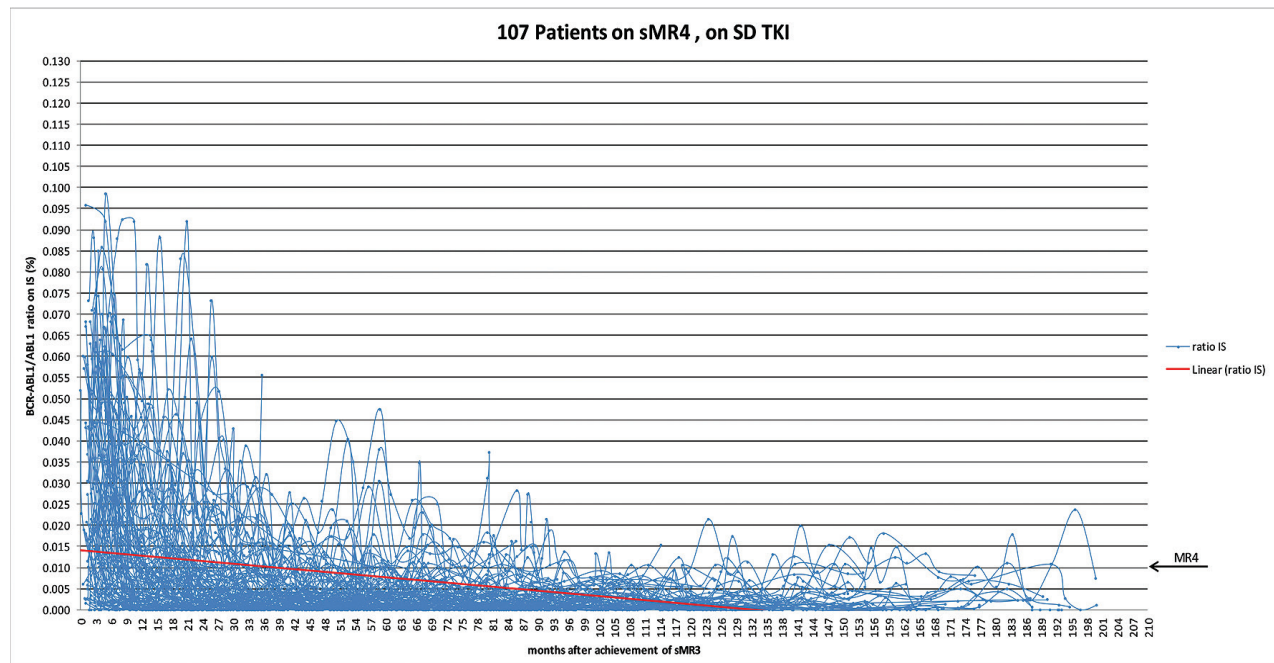


**Figure 3.** A total of 3,305 consecutive real-time quantitative polymerase chain reaction (RT-qPCR) results in patients achieving sustained molecular response (MR)-4 (sMR4) and on standard dose tyrosine kinase inhibitor (TKI) (n=107). The starting point is the date of achievement of sMR3. The red line depicts the linear trend-line of BCR-ABL1/ABL1 RT-qPCR values (expressed in % on International Scale, IS) over time. n: number.

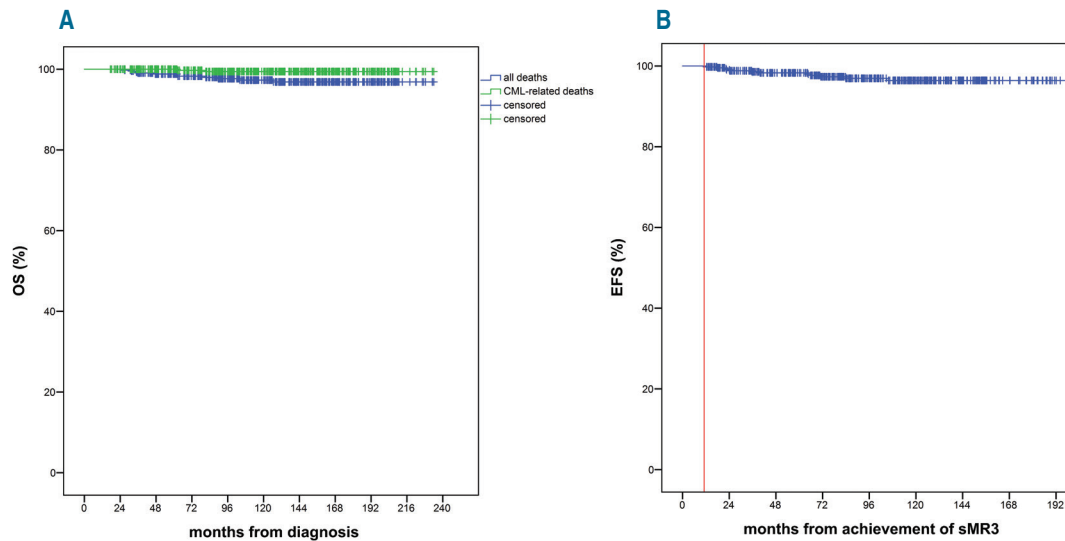


**Figure 4. Overall survival (OS) (A) and event-free survival (EFS) (B) for the entire patient cohort (n=450).** (A) The green line depicts the chronic myeloid leukemia (CML)-OS, whereas the blue line shows the OS. (B) EFS was calculated from the first year in sustained molecular response (MR)-3 (sMR3) (red vertical line indicates time of sMR3, i.e. time at which MR3 was sustained for 12 months).

require more frequent RTq-PCR testing if doses are reduced, patients admit to or are thought to be non-compliant or where there is previous evidence of resistance.

We found that patients who had achieved sMR3, who were known to be compliant and who were treated throughout their disease course with standard dose TKI had a low probability of loss of MR3. Furthermore, no patient satisfying these criteria and who achieved sMR4 experienced loss of MR3, and over time they gradually deepened their molecular responses. This leads us to suggest that the achievement of sMR4 in this group identifies patients at negligible risk of loss of molecular responses and that the frequency of molecular monitoring could be at 6-monthly intervals.

In contrast, the much higher rate of MR3 loss in the sMR3 only group (25.4% at 5 years) and the potential to subsequently lose CCyR, would favor continuation of molecular monitoring at a minimum frequency of 3-monthly in this group. Some of the patients who lost MR3 were on a reduced dose of their TKI and our observations are supported by the findings of the DESTINY study,<sup>23</sup> in which approximately 30% of patients in sMR3 who reduced their TKI dose by 50% subsequently lost MR3. Although only one patient in the sMR3 group who was on standard dose TKI and thought to be compliant lost MR3, we are aware that we can never be certain of individual patient compliance, and would not recommend reduced vigilance in this group. We have previously reported a close association between compliance and major molecular response.<sup>24</sup> We think it unlikely that there would be an unexpected and clinically significant degree of non-compliance in patients in sMR4. In contrast, lack of compliance might be a contributing factor to the failure of patients in sMR3 to gain deeper responses. In fact, this latter group are clearly responsive to TKI and the reasons for their failure to gain deeper responses are unclear.

It is possible that we have underestimated the probabil-

ity of loss of MR3 in the patients who achieved only sMR3 because this group may contain two distinct sub-populations: those who are destined to achieve sMR4 with longer follow up (and therefore have a better outcome) and those who do not have the biological potential to achieve deeper responses. We consider this unlikely because the median duration of follow up in patients who achieved sMR3 only was long (56.9 months), whereas the median time to sMR4 was 29.1 months (range: 3.3-172.1 months) from start of TKI therapy, such that sMR4 should have been observed had it been destined to occur.

We observed some differences between the patients who achieved sMR3 only and those who reached sMR4 in that the former group were more likely to express the e13a2 BCR-ABL1 transcript, more frequently demonstrated resistance to their first-line TKI and were more likely to have required a higher dose of imatinib before the achievement of sMR3. Moreover, the time to sMR3 was longer in patients in whom this was the best response than in those who achieved sMR4. Although these factors may be useful in identifying a group of patients with a lower probability of achieving sMR4 after reaching sMR3, the fact remains that once sMR4 is reached, it is highly unlikely to be lost if the patient remains on standard doses of TKI. The only factor predictive for loss of MR3 in multivariate analysis was the failure to achieve sMR4, leading us to conclude that sMR4 is a secure position for patients with CML.

The impact of the various levels of molecular response on patient outcome has been studied by others. For some time it was difficult to demonstrate an improvement in survival in patients who had achieved MR3 or better compared to those whose best response was CCyR.<sup>25-27</sup> Most recently, data from the German CML Study IV showed that there were no progressions among patients achieving MR4.5, as compared to one, nine and 13 events in patients whose deepest responses were MR4, MR3 and CCyR,

respectively.<sup>10</sup> Our results confirm the excellent outcome of patients who achieve sMR4 or better, but this was not the focus of our study; instead, we used our database of prolonged molecular monitoring to try to provide an evidence base for the frequency of molecular monitoring and a practical guide for clinical management.

One criticism of the use of our findings is that we are recommending reduced frequency of monitoring and hospital interactions in a group of patients who are candidates for trials of dose-reduction and/or discontinuation for treatment-free remission (TFR). We deliberately defined sMR4 as MR4 sustained for 12 months as this is identical to the criterion used to confirm eligibility for a trial of treatment discontinuation in the EURO-SKI study.<sup>28</sup> However, many patients are reluctant to discontinue therapy, and of those who do cease treatment, approximately half will have to recommence TKI because of loss of MR3,<sup>29-31</sup> resulting in the majority continuing to require life-long treatment and monitoring. These patients, who have responded well and durably to TKI, may welcome fewer hospital visits.

We acknowledge some limitations in our study. We are aware that it is a retrospective observational study. In addition, we included all patients who achieved sMR3, including those who had at some point received higher or lower than standard doses of TKI and those who were known to be non-compliant. However, we feel that this reflects the 'real-life' clinical situation, and it is not surprising that these groups are more likely to lose molecular responses. Our study does confirm the requirement to adhere to more rigorous monitoring in these vulnerable patient groups.

In summary, we have shown that risk of loss of MR3 is negligible in patients who have achieved sMR4, particularly in those who remain on standard dose TKI who have

not demonstrated prior resistance and who are known to be compliant. As a consequence, we suggest that sMR4 is regarded as a secure molecular threshold, representing a level of response that may justify less frequent monitoring in patients who are not considering, or who have failed, a trial of treatment discontinuation. For patients and healthcare providers, the identification of a secure level of molecular response has a number of direct and indirect benefits. For patients, the knowledge that they have reached a level of residual disease that is associated with a negligible risk of loss of response will not only be reassuring, improving morale and quality of life, but also facilitate the acceptance of alternative management styles, including remote care. The consequent reduction in hospital visits will be cost saving to both patients and healthcare providers.

There are, of course, reasons other than molecular monitoring, for continuing to provide close interactions between patients and healthcare professionals: continued close supervision may promote compliance, allow recognition and management of adverse events and co-morbidities, optimize the use of expensive medication, facilitate advice regarding parenting, and provide valuable reassurance of on-going response. Our results simply provide support for patients and healthcare professionals who wish to consider relaxing the need for hospital visits.

#### Acknowledgments

*JFA and DM acknowledge the support of the Imperial College NIHR Biomedical Research Centre. JFA is a NIHR Senior Investigator. SC acknowledges the support of Ariad (Incyte) and Pfizer. GN acknowledges the support of ARIAD (Incyte). The views expressed in this article are those of the author(s) and not necessarily those of the NHS, the NIHR, or the Department of Health.*

#### References

- Hochhaus A, Larson RA, Guilhot F et al. Long-Term Outcomes of Imatinib Treatment for Chronic Myeloid Leukemia. *N Engl J Med.* 2017;376(10):917-927.
- Bower H, Bjorkholm M, Dickman PW, Hoglund M, Lambert PC, Andersson TM. Life Expectancy of Patients With Chronic Myeloid Leukemia Approaches the Life Expectancy of the General Population. *J Clin Oncol.* 2016;34(24):2851-2857.
- Baccarani M, Deininger MW, Rosti G, et al. European LeukemiaNet recommendations for the management of chronic myeloid leukemia: 2013. *Blood.* 2013;122(6):872-884.
- Radich JE, Deininger M, Abboud CN, et al. Chronic Myeloid Leukemia, Version 1.2019, NCCN Clinical Practice Guidelines in Oncology. *J Natl Compr Canc Netw.* 2018;16(9):1108-1135.
- Hanfstein B, Muller MC, Hehlmann R, et al. Early molecular and cytogenetic response is predictive for long-term progression-free and overall survival in chronic myeloid leukemia (CML). *Leukemia.* 2012;26(9):2096-2102.
- Marin D, Ibrahim AR, Lucas C, et al. Assessment of BCR-ABL1 transcript levels at 3 months is the only requirement for predicting outcome for patients with chronic myeloid leukemia treated with tyrosine kinase inhibitors. *J Clin Oncol.* 2012;30(3):232-238.
- Branford S, Yeung DT, Ross DM, et al. Early molecular response and female sex strongly predict stable undetectable BCR-ABL1, the criteria for imatinib discontinuation in patients with CML. *Blood.* 2013;121(19):3818-3824.
- Jain P, Kantarjian H, Nazha A, et al. Early responses predict better outcomes in patients with newly diagnosed chronic myeloid leukemia: results with four tyrosine kinase inhibitor modalities. *Blood.* 2013;121(24):4867-4874.
- Hughes TP, Saglio G, Kantarjian HM, et al. Early molecular response predicts outcomes in patients with chronic myeloid leukemia in chronic phase treated with frontline nilotinib or imatinib. *Blood.* 2014;123(9):1353-1360.
- Hehlmann R, Muller MC, Lauseker M, et al. Deep molecular response is reached by the majority of patients treated with imatinib, predicts survival, and is achieved more quickly by optimized high-dose imatinib: results from the randomized CML-study IV. *J Clin Oncol.* 2014;32(5):415-423.
- Hochhaus A, Saglio G, Hughes TP, et al. Long-term benefits and risks of frontline nilotinib vs imatinib for chronic myeloid leukemia in chronic phase: 5-year update of the randomized ENESTnd trial. *Leukemia.* 2016;30(5):1044-1054.
- Cortes JE, Saglio G, Kantarjian HM, et al. Final 5-Year Study Results of DASISION: The Dasatinib Versus Imatinib Study in Treatment-Naive Chronic Myeloid Leukemia Patients Trial. *J Clin Oncol.* 2016;34(20):2333-2340.
- Hehlmann R, Lauseker M, Saussele S, et al. Assessment of imatinib as first-line treatment of chronic myeloid leukemia: 10-year survival results of the randomized CML study IV and impact of non-CML determinants. *Leukemia.* 2017;31(11):2398-2406.
- Hughes TP, Branford S. Monitoring disease response to tyrosine kinase inhibitor therapy in CML. *Hematology Am Soc Hematol Educ Program.* 2009:477-487.
- Press RD, Love Z, Tronnes AA, et al. BCR-ABL mRNA levels at and after the time of a complete cytogenetic response (CCR) predict the duration of CCR in imatinib mesylate-treated patients with CML. *Blood.* 2006;107(11):4250-4256.
- Press RD, Galderisi C, Yang R, et al. A half-log increase in BCR-ABL RNA predicts a higher risk of relapse in patients with chronic myeloid leukemia with an imatinib-induced complete cytogenetic response. *Clin Cancer Res.* 2007;13(20):6136-6143.

17. Iacobucci I, Saglio G, Rosti G, et al. Achieving a major molecular response at the time of a complete cytogenetic response (CCgR) predicts a better duration of CCgR in imatinib-treated chronic myeloid leukemia patients. *Clin Cancer Res.* 2006;12(10):3037-3042.
18. Palandri F, Iacobucci I, Soverini S, et al. Treatment of Philadelphia-positive chronic myeloid leukemia with imatinib: importance of a stable molecular response. *Clin Cancer Res.* 2009;15(3):1059-1063.
19. Kantarjian HM, Shan J, Jones D, et al. Significance of increasing levels of minimal residual disease in patients with Philadelphia chromosome-positive chronic myelogenous leukemia in complete cytogenetic response. *J Clin Oncol.* 2009;27(22):3659-3663.
20. Foroni L, Wilson G, Gerrard G, et al. Guidelines for the measurement of BCR-ABL1 transcripts in chronic myeloid leukaemia. *Br J Haematol.* 2011;153(2):179-190.
21. Branford S. Chronic myeloid leukemia: molecular monitoring in clinical practice. *Hematology Am Soc Hematol Educ Program.* 2007:376-383.
22. Carrera PM, Kantarjian HM, Blinder VS. The financial burden and distress of patients with cancer: Understanding and stepping-up action on the financial toxicity of cancer treatment. *CA Cancer J Clin.* 2018;68(2):153-165.
23. Clark RE, Polydoros F, Apperley JF, et al. De-escalation of tyrosine kinase inhibitor dose in patients with chronic myeloid leukaemia with stable major molecular response (DE-TINY): an interim analysis of a non-randomised, phase 2 trial. *Lancet Haematol.* 2017;4(7):e310-e316.
24. Marin D, Bazeos A, Mahon FX, et al. Adherence is the critical factor for achieving molecular responses in patients with chronic myeloid leukemia who achieve complete cytogenetic responses on imatinib. *J Clin Oncol.* 2010;28(14):2381-2388.
25. Druker BJ, Guilhot F, O'Brien SG, et al. Five-year follow-up of patients receiving imatinib for chronic myeloid leukemia. *N Engl J Med.* 2006;355(23):2408-2417.
26. Kantarjian H, O'Brien S, Shan J, et al. Cytogenetic and molecular responses and outcome in chronic myelogenous leukemia: need for new response definitions? *Cancer.* 2008;112(4):837-845.
27. Marin D, Milojkovic D, Olavarria E, et al. European LeukemiaNet criteria for failure or suboptimal response reliably identify patients with CML in early chronic phase treated with imatinib whose eventual outcome is poor. *Blood.* 2008;112(12):4437-4444.
28. Saussele S, Richter J, Guilhot J, et al. Discontinuation of tyrosine kinase inhibitor therapy in chronic myeloid leukaemia (EURO-SKI): a prespecified interim analysis of a prospective, multicentre, non-randomised, trial. *Lancet Oncol.* 2018;19(6):747-757.
29. Claudiani S, Apperley JF, Gale RP, et al. E14a2 BCR-ABL1 transcript is associated with a higher rate of treatment-free remission in individuals with chronic myeloid leukemia after stopping tyrosine kinase inhibitor therapy. *Haematologica.* 2017;102(8):e297-e299.
30. Etienne G, Guilhot J, Rea D, et al. Long-Term Follow-Up of the French Stop Imatinib (STIM1) Study in Patients With Chronic Myeloid Leukemia. *J Clin Oncol.* 2017;35(3):298-305.
31. Rea D, Nicolini FE, Tulliez M, et al. Discontinuation of dasatinib or nilotinib in chronic myeloid leukemia: interim analysis of the STOP 2G-TKI study. *Blood.* 2017;129(7):846-854.

# Cell-intrinsic depletion of Aml1-ETO-expressing pre-leukemic hematopoietic stem cells by K-Ras activating mutation

Cristina Di Genua,<sup>1</sup> Ruggiero Norfo,<sup>1</sup> Alba Rodriguez-Meira,<sup>1</sup> Wei Xiong Wen,<sup>1,2</sup> Roy Drissen,<sup>1</sup> Christopher A.G. Booth,<sup>1</sup> Benjamin Povinelli,<sup>1</sup> Emmanouela Repapi,<sup>3</sup> Nicki Gray,<sup>3</sup> Joana Carrelha,<sup>1</sup> Laura M. Kettle,<sup>1</sup> Lauren Jamieson,<sup>1</sup> Wen Hao Neo,<sup>1</sup> Supat Thongjuea,<sup>1,2</sup> Claus Nerlov,<sup>1</sup> and Adam J. Mead<sup>1</sup>

<sup>1</sup>MRC Molecular Haematology Unit; <sup>2</sup>WIMM Centre for Computational Biology and

<sup>3</sup>Computational Biology Research Group, MRC Weatherall Institute of Molecular Medicine, University of Oxford, Oxford, UK

CN and AJM contributed equally to this work.



Haematologica 2019  
Volume 104(11):2215-2224

## ABSTRACT

Somatic mutations in acute myeloid leukemia are acquired sequentially and hierarchically. First, pre-leukemic mutations, such as t(8;21) that encodes AML1-ETO, are acquired within the hematopoietic stem cell (HSC) compartment, while signaling pathway mutations, including KRAS activating mutations, are late events acquired during transformation of leukemic progenitor cells and are rarely detectable in HSC. This raises the possibility that signaling pathway mutations are detrimental to clonal expansion of pre-leukemic HSC. To address this hypothesis, we used conditional genetics to introduce Aml1-ETO and K-RasG12D into murine HSC, either individually or in combination. In the absence of activated Ras, Aml1-ETO-expressing HSC conferred a competitive advantage. However, activated K-Ras had a marked detrimental effect on Aml1-ETO-expressing HSC, leading to loss of both phenotypic and functional HSC. Cell cycle analysis revealed a loss of quiescence in HSC co-expressing Aml1-ETO and K-RasG12D, accompanied by an enrichment in E2F and Myc target gene expression and depletion of HSC self-renewal-associated gene expression. These findings provide a mechanistic basis for the observed absence of KRAS signaling mutations in the pre-malignant HSC compartment.

## Introduction

Acute myeloid leukemia (AML) is a poor prognosis hematopoietic malignancy caused by the uncontrolled proliferation of differentiation-arrested myeloid cells.<sup>1,2</sup> Genome sequencing studies have comprehensively characterized the mutational landscape of AML, identifying many somatically acquired recurrent driver mutations.<sup>3</sup> Whilst AML is a genetically complex disease, a number of general principles underlie the clonal evolution in AML. Genes mutated in AML can be classified into distinct categories such as chromatin modifiers, transcription factor fusions, and signal transduction genes,<sup>3</sup> with most patients showing co-mutation of genes within at least two of these functional groups. Genomic data from sequencing studies, together with mechanistic studies using mouse models,<sup>4,6</sup> support the concept that certain classes of mutation frequently co-occur during leukemia development, whereas mutations of the same functional group are often mutually exclusive.<sup>7</sup>

Acute myeloid leukemia has long been recognized as a hierarchically organized, stem cell-propagated disease.<sup>8</sup> However, more recently, analysis of purified hematopoietic stem cells (HSC) and progenitor populations from AML patients have revealed that leukemia-initiating mutations, which include balanced translocations and mutations in epigenetic regulators, are frequently acquired within the HSC compartment as early events in disease evolution, generating so called “pre-leukemic” stem cells.<sup>9-12</sup> In particular, the t(8;21) translocation, which generates the fusion protein AML1-ETO (also known as RUNX1-RUNX1T1 and AML1-MTG8) occurs in approximately 7% of adult AML patients.<sup>13</sup> Several lines of evidence sug-

## Correspondence:

ADAM J. MEAD  
adam.mead@imm.ox.ac.uk

CLAUS NERLOV  
claus.nerlov@imm.ox.ac.uk

Received: September 19, 2018.

Accepted: April 9, 2019.

Pre-published: May 10, 2019.

doi:10.3324/haematol.2018.205351

Check the online version for the most updated information on this article, online supplements, and information on authorship & disclosures: [www.haematologica.org/content/104/11/2215](http://www.haematologica.org/content/104/11/2215)

©2019 Ferrata Storti Foundation

Material published in *Haematologica* is covered by copyright. All rights are reserved to the Ferrata Storti Foundation. Use of published material is allowed under the following terms and conditions:

<https://creativecommons.org/licenses/by-nc/4.0/legalcode>. Copies of published material are allowed for personal or internal use. Sharing published material for non-commercial purposes is subject to the following conditions: <https://creativecommons.org/licenses/by-nc/4.0/legalcode>, sect. 3. Reproducing and sharing published material for commercial purposes is not allowed without permission in writing from the publisher.



gest that *AML1-ETO* is acquired in pre-leukemic HSC. First, *AML1-ETO* mRNA could still be detected in AML patients who had been in clinical remission for up to 150 months.<sup>14</sup> Secondly, *AML1-ETO* remains stable in patients who relapse, while additional mutations were highly dynamic with mutations both gained and lost at relapse.<sup>15</sup> Finally, evidence from mouse models support the concept that pre-leukemic mutations confer a competitive advantage to cells within the phenotypic HSC compartment, without causing transformation of downstream progenitor cells.<sup>16,17</sup> In particular, *Aml1-ETO* knock-in mice did not develop leukemia, but *Aml1-ETO*-expressing cells had an enhanced *in vitro* replating ability, indicating greater self-renewal capacity.<sup>16</sup>

In contrast, signaling transduction mutations of genes such as *FLT3*, *KIT* or *KRAS* occur as late events that are detected in the transformed leukemic progenitors but rarely detected in the pre-leukemic HSC compartment.<sup>11,12</sup> *RAS* mutations also frequently co-occur with t(8;21) (*NRAS* = 12.9%, *KRAS* = 4.3%).<sup>15</sup> In AML patients who achieve remission, *RAS* mutations are unstable and often lost at subsequent relapse, with gain of a novel signaling transduction mutation (e.g. *FLT3-ITD*), while the initiating translocation remains. This is consistent with *RAS* mutations occurring as a late event during leukemic transformation.<sup>15</sup> Finally, the *Kras<sup>G12D/+</sup>;Mx1-Cre<sup>tg/+</sup>* mouse model develops a fatal myeloproliferative neoplasm (MPN); however, these mice do not develop AML.<sup>18,19</sup> Collectively, these studies provide evidence that *RAS* mutations are secondary events in AML development and are not present within pre-leukemic HSC. Mouse models in which activating signaling pathway mutations were introduced into wild-type (WT) HSC have revealed both cell-intrinsic and cell-extrinsic effects on the HSC compartment, usually resulting in a depletion of HSC.<sup>20-24</sup> However, the impact of signaling transduction mutations on pre-leukemic HSC remains unclear. This is of considerable importance for understanding why signaling mutations are absent from the pre-leukemic HSC compartment.

We hypothesized that the absence of signaling mutations in the HSC may reflect a detrimental impact of such mutations on pre-leukemic HSC. To address this question, we used conditional mouse genetics to introduce *Aml1-ETO* and *K-RasG12D* separately or in combination, both expressed from their endogenous loci, into WT HSC, to determine the effect of *K-Ras* activation on a well-defined pre-leukemic HSC population. While *Aml1-ETO* expression enhanced the long-term repopulating ability of HSC, expression of *K-RasG12D* in *Aml1-ETO*-expressing HSC led to loss of quiescence and self-renewal-associated gene expression, and was detrimental to their function. Such functional impairment would limit clonal expansion of pre-malignant HSC co-expressing *AML1-ETO* and activated *RAS*, providing a molecular and cellular basis for the observed absence of activating *RAS* mutations in pre-leukemic HSC.

## Methods

### Animals

All mouse lines were maintained on a C57Bl/6J genetic background. Conditional knock-in mice expressing *Aml1-ETO* (*Aml1<sup>ETO/+</sup>*)<sup>16</sup> and *K-Ras* (*Kras<sup>G12D/+</sup>*),<sup>25</sup> either individually or combined (*Aml1<sup>ETO/+</sup>;Kras<sup>G12D/+</sup>*), were crossed to the *Mx1-Cre* mouse

line.<sup>26</sup> All mice were bred and maintained in accordance with UK Home Office regulations. Experiments were conducted following approval by the University of Oxford Animal Welfare and Ethical Review Body (project license n. 30/3103).

### Competitive transplantation

Competitive transplants were performed as previously described.<sup>27</sup> See *Online Supplementary Appendix* for further details.

Serial transplantations were performed by co-transplanting  $1.25 \times 10^5$  CD45.2 fetal liver (FL) cells with  $5 \times 10^6$  CD45.1 WT bone marrow (BM) competitor cells into lethally irradiated recipients ( $2 \times 500$  rads). Bulk secondary and tertiary transplants were performed by transplanting  $3 \times 10^6$  BM cells from primary and secondary recipients respectively into lethally irradiated recipients at eight weeks post-poly(I:C) for secondary transplants or 12 weeks post-transplantation for tertiary transplants. Tertiary transplanted mice were analyzed 12 weeks post-transplantation.

### Flow cytometry and fluorescence-activated cell sorting

Details of antibodies and viability dyes are shown in *Online Supplementary Table S1*. All antibodies were used at pre-determined optimal concentrations. Hematopoietic stem and progenitor cells were analyzed as previously described.<sup>28</sup> Cell acquisition and analysis were performed on a BD LSRFortessa (BD Biosciences, San Jose, CA, USA) using BD FACSDiva™ software (BD Biosciences). Cell sorting was performed on a BD FACSAriaII cell sorter (BD Biosciences). Cells used in cell sorting experiments were c-Kit-enriched (MACS Miltenyi Biotec, Bergisch Gladbach, Germany) and were stained with specific antibodies following initial Fc-block incubation. Gates were set using a combination of fluorescence minus one controls and populations known to be negative for the antigen.

For HSC cell cycle staining, BM cells were c-Kit-enriched and stained following initial Fc-block incubation. Stained cells were then fixed and permeabilized using BD cytofix/cytoperm fixation and permeabilization solution (BD Biosciences). Cells were then stained with Ki-67 PE (BD Biosciences) overnight. Cells were then stained with 4',6-diamidino-2-phenylindole (DAPI) (0.5 μg/mL) (ThermoFisher Scientific, Waltham, MA, USA) for one hour before analysis.

### In vitro serial replating assay

Serial replating was performed as previously described.<sup>5</sup> Briefly,  $100$  CD45.2 Lineage<sup>-</sup>Sca1<sup>+</sup>cKit<sup>+</sup> (LSK) BM cells were sorted from mice transplanted with  $2.5 \times 10^5$  FL cells and  $1 \times 10^6$  CD45.1 WT BM competitor cells eight weeks post-poly(I:C). Cells were seeded into 1 mL of methylcellulose medium (Methocult, M3434, STEMCELL Technologies, Vancouver, BC, Canada) and incubated in 37°C, in 5% CO<sub>2</sub>, with ≥95% humidity. Colonies (≥30 cells) were counted after eight days. Cells were re-suspended and re-plated at  $1 \times 10^4$  cells per 1 mL of methylcellulose medium. Cells were then counted and re-plated after 6-7 days.

### RNA-sequencing

Fifty cells per biological replicate were sorted into 4 μL of lysis buffer containing; 0.2% Triton X-100 (Sigma-Aldrich, St Louis, MO, US), 2.5 μM OligodT (Biomers, Ulm, Germany), 2.5 mM dNTPs (ThermoFisher Scientific), RNase Inhibitor 20 U (Takara Bio USA Inc., Mountain View, CA, USA) and ERCC spike-in  $1.4 \times 10^6$  (ThermoFisher Scientific). For details on cDNA synthesis, library preparation and data analysis see *Online Supplementary Appendix*.

### Statistical analysis

Unless otherwise indicated, statistical significance of differences

between samples was determined using an analysis of variance (ANOVA) for multiple comparisons following Tukey's multiple comparisons test.

## Results

### Aml1-ETO ameliorates key features of the myeloproliferative neoplasm phenotype caused by K-RasG12D

To study the effect of combining Aml1-ETO with mutant K-Ras, whilst avoiding the previously described spontaneous recombination in primary *Kras*<sup>G12D/+</sup>;*Mx1-Cre*<sup>tg/+</sup> mice,<sup>19,20</sup> we generated E14.5 FL cells with the necessary genotypes: *Aml1*<sup>ETO/+</sup>;*Mx1-Cre*<sup>tg/+</sup> (AM genotype); *Kras*<sup>G12D/+</sup>;*Mx1-Cre*<sup>tg/+</sup> (KM genotype); *Aml1*<sup>ETO/+</sup>;*Kras*<sup>G12D/+</sup>;*Mx1-Cre*<sup>tg/+</sup> (AKM genotype); and *Mx1-Cre*<sup>tg/+</sup> controls (CON genotype); all CD45.2 allotype. FL cells were used as these have been previously shown to have either no or minor spontaneous recombination using *Mx1-Cre*.<sup>29</sup> To create a scenario where competitive advantage and disadvantage of mutant HSC could be observed, mice were generated where the hematopoietic system was partially repopulated by experimental cells and par-

tially by WT competitor cells (CD45.1 allotype). This was done by competitively transplanting  $2.5 \times 10^5$  FL cells (CD45.2) and  $1 \times 10^6$  WT BM competitor cells (CD45.1) into lethally irradiated CD45.1 recipients, as previously described.<sup>27</sup> Recombination was induced four weeks post-transplantation by subcutaneous injection of poly(I:C), with all groups of mice treated, including controls. Long-term monitoring of primary transplanted mice was not possible as both KM and AKM developed a T-cell leukemia (*data not shown*), as previously reported for KM.<sup>20</sup> Therefore, the hematopoietic phenotype was analyzed eight weeks post-poly(I:C) before T-cell leukemia development occurred (Figure 1A).

AM-transplanted recipients displayed mild leukopenia compared to CON-transplanted mice (Figure 1B), due to a decrease in B and T cells in the peripheral blood (PB) (Online Supplementary Figure S1A and B), whereas no difference in hemoglobin levels, BM cellularity, *Mac1*<sup>+</sup>*Gr1*<sup>lo</sup> myeloid cells in the PB or spleen, or spleen weight was observed (Figure 1C-H). However, AM showed a 27% decrease in platelet count compared to CON (Figure 1I). These results suggest Aml1-ETO affects B and T cell, as well as platelet development, in line with known functions of AML1 (also known as RUNX1).<sup>30,31</sup>

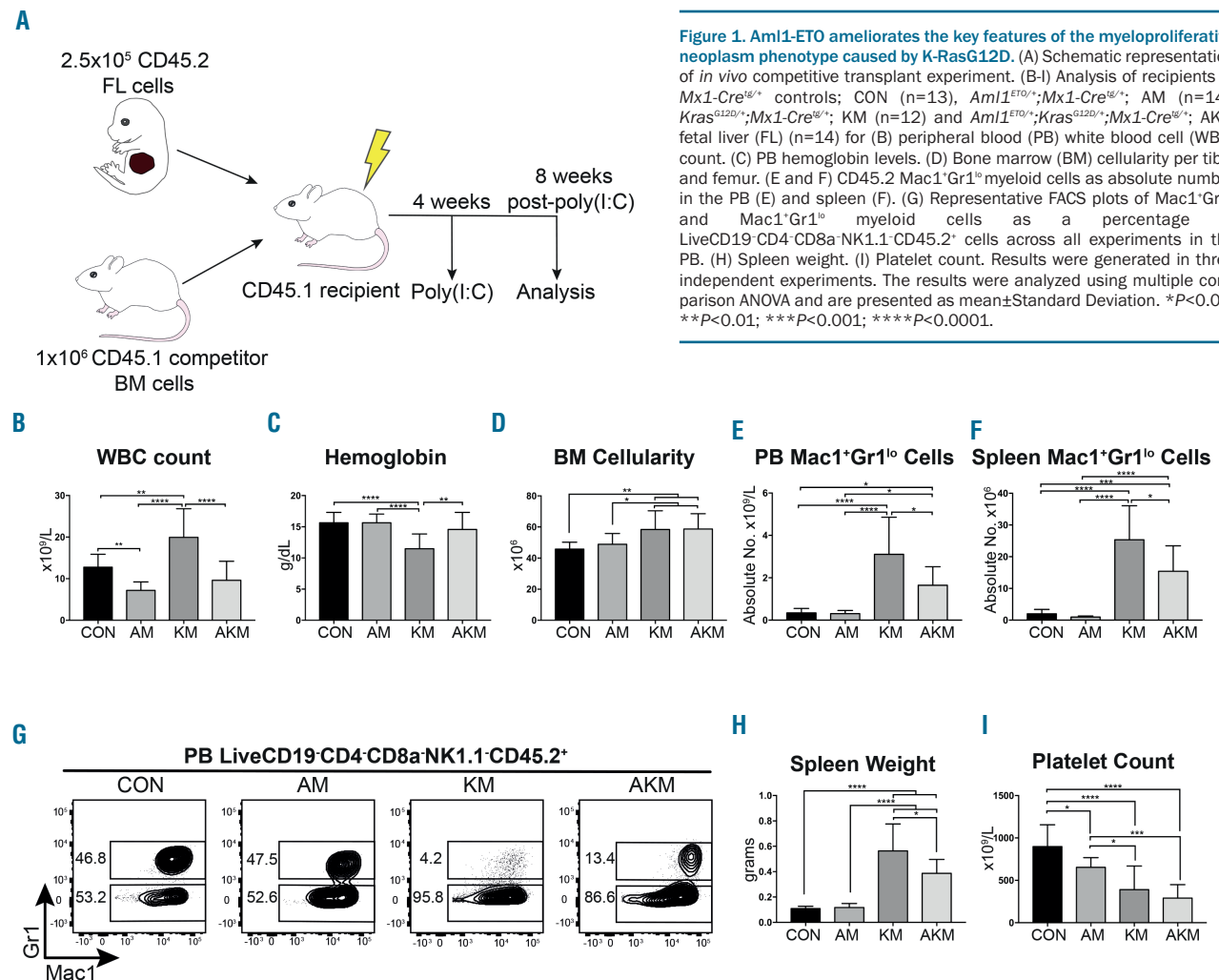


**Figure 1. Aml1-ETO ameliorates the key features of the myeloproliferative neoplasm phenotype caused by K-RasG12D.** (A) Schematic representation of *in vivo* competitive transplant experiment. (B-I) Analysis of recipients of *Mx1-Cre*<sup>tg/+</sup> controls; CON (n=13), *Aml1*<sup>ETO/+</sup>;*Mx1-Cre*<sup>tg/+</sup>; AM (n=14), *Kras*<sup>G12D/+</sup>;*Mx1-Cre*<sup>tg/+</sup>; KM (n=12) and *Aml1*<sup>ETO/+</sup>;*Kras*<sup>G12D/+</sup>;*Mx1-Cre*<sup>tg/+</sup>; AKM fetal liver (FL) (n=14) for (B) peripheral blood (PB) white blood cell (WBC) count. (C) PB hemoglobin levels. (D) Bone marrow (BM) cellularity per tibia and femur. (E and F) CD45.2 *Mac1*<sup>+</sup>*Gr1*<sup>lo</sup> myeloid cells as absolute number in the PB (E) and spleen (F). (G) Representative FACS plots of *Mac1*<sup>+</sup>*Gr1*<sup>+</sup> and *Mac1*<sup>+</sup>*Gr1*<sup>lo</sup> myeloid cells as a percentage of LiveCD19<sup>-</sup>CD4<sup>-</sup>CD8a<sup>-</sup>NK1.1<sup>-</sup>CD45.2<sup>+</sup> cells across all experiments in the PB. (H) Spleen weight. (I) Platelet count. Results were generated in three independent experiments. The results were analyzed using multiple comparison ANOVA and are presented as mean±Standard Deviation. \**P*<0.05; \*\**P*<0.01; \*\*\**P*<0.001; \*\*\*\**P*<0.0001.

In line with previous reports,<sup>18,19</sup> expression of K-RasG12D (KM genotype) caused a myeloproliferative phenotype, consisting of leukocytosis, anemia, increased BM cellularity, increase in the Mac1<sup>+</sup>Gr1<sup>lo</sup> myeloid cells in the PB and spleen, splenomegaly, and thrombocytopenia (Figure 1B-I and *Online Supplementary Table S2*).

Strikingly, co-expression of Aml1-ETO and K-RasG12D did not result in a more aggressive disease, but ameliorated key features of the phenotype associated with K-RasG12D expression, including restoration of white blood cell (WBC) count and hemoglobin levels (Figure 1B and C), reduction in the Mac1<sup>+</sup>Gr1<sup>lo</sup> myeloid cells in the PB and spleen, and reduced spleen weight (Figures 1E-H). Platelet count was, however, further reduced compared to CON (Figure 1I) and mice still showed an increase in BM cellularity (Figure 1D).

Myelo-erythroid progenitors were analyzed by flow cytometry (Figure 2 and *Online Supplementary Figure S2*). We found both Aml1-ETO (2-fold,  $P=0.0093$ ) and K-RasG12D (8-fold,  $P<0.0001$ ) expression decreased the number of megakaryocyte progenitors (MkP), and when

co-expressed resulted in a further reduction (15-fold,  $P<0.0001$ ) in the BM compared to CON (Figure 2A). This paralleled the decrease in platelet counts found in the PB (Figure 1I). Aml1-ETO also increased in the number of MkP in the spleen compared to CON (2-fold,  $P=0.005$ ) (Figure 2B). BM colony forming unit – erythrocytes (CFU-E) were not affected in any genotypes compared to controls (Figure 2C). However, K-RasG12D caused an increase in CFU-E in the spleen compared to CON (36-fold increase,  $P=0.0004$ ) (Figure 2D), indicating stress erythropoiesis, which was reversed in AKM mice. BM pre-granulocyte/macrophage progenitors (pre-GM) were unperturbed in all three genotypes compared to CON (Figure 2E). However, K-RasG12D expression caused an increase in pre-GM in the spleen compared to CON (9-fold increase,  $P<0.0001$ ) (Figure 2F). The increase in pre-GM was reversed when K-RasG12D was co-expressed with Aml1-ETO (3-fold decrease,  $P<0.0001$ ) (Figure 2F). There was no difference in BM lymphoid-primed multipotent progenitor (LMPP) across all genotypes; however, there was an increase in the number of spleen LMPP in

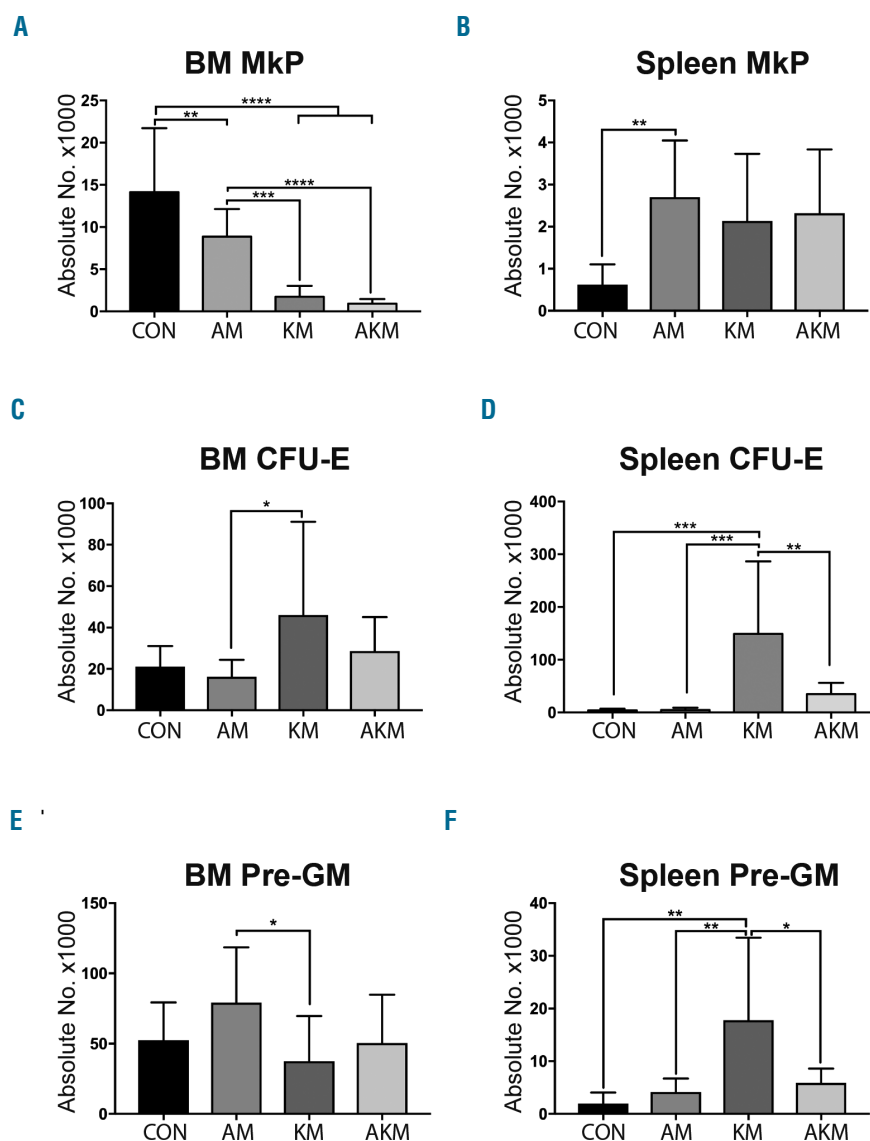


**Figure 2. Aml1-ETO reverses some of the myelo-erythroid progenitor cell phenotypes caused by K-RasG12D.** (A, C, E) Absolute number of CD45.2 megakaryocyte progenitor (MkP) (A), CFU-E (C) and Pre-GM (E) in the bone marrow (BM) from recipients of CON (n=12), AM (n=14), KM (n=12) and AKM FL (n=14). Results were generated in three independent experiments. (B, D, F) Absolute numbers of CD45.2 MkP (B), colony forming unit-erythrocyte (CFU-E) (D) and pre-granulocyte-monocyte (Pre-GM). (F) in the spleen from recipients of CON (n=8), AM (n=10), KM (n=8) and AKM FL (n=10). Results were generated in two independent experiments. The results were analyzed using multiple comparison ANOVA and are presented as the mean±Standard Deviation. \* $P<0.05$ ; \*\* $P<0.01$ ; \*\*\* $P<0.001$ ; \*\*\*\* $P<0.0001$ .

KM mice compared to CON, likely reflecting increased mobilization associated with myeloproliferation. The increase in LMPP was reversed in AKM mice (*Online Supplementary Figure S3*). Together, these data demonstrate that when Aml1-ETO is co-expressed with K-RasG12D the myeloproliferative phenotype caused by K-RasG12D is ameliorated rather than enhanced.

### K-RasG12D reverses the hematopoietic stem cell expansion associated with Aml1-ETO

As the co-expression of Aml1-ETO and K-RasG12D was insufficient to induce acute leukemic transformation, this provided an ideal model to study the impact of these mutations on pre-leukemic HSC. Here, expression of the mutations from their endogenous loci (rather than through viral transduction) is crucial in order to ensure faithful expression level of the mutations within the hematopoietic hierarchy, including the HSC compartment. We reasoned that the myeloproliferative phenotype may have been ameliorated when Aml1-ETO and K-RasG12D were co-expressed due to loss of disease propagating HSC. We therefore analyzed LSKCD150<sup>+</sup>Flt3<sup>-</sup> phenotypic HSC eight weeks post-poly(I:C). The SLAM marker CD48 was not used as it was previously reported that CD48 expression is dysregulated in Aml1 deficient HSC.<sup>32</sup>

We observed an expansion of HSC expressing Aml1-ETO compared to CON (5-fold increase,  $P < 0.0001$ ) (Figure 3A and B). There was no significant difference in HSC number expressing K-RasG12D compared to CON. However, when K-RasG12D was co-expressed with Aml1-ETO the HSC expansion caused by Aml1-ETO was reversed (3-fold decrease,  $P < 0.0001$ ) (Figure 3A and B).

To determine if K-RasG12D is detrimental to the function of Aml1-ETO-expressing HSC we performed serial transplantations. In secondary recipients, Aml1-ETO-expressing cells showed an increase in myeloid reconstitution over time and a 10-fold increase in phenotypic HSC number compared to CON (Figure 3C and D), indicating a competitive advantage, possibly due to an enhanced self-renewal capacity. In contrast, secondary transplant with K-RasG12D-expressing cells, or in combination with Aml1-ETO, showed markedly decreased myeloid reconstitution and HSC number (Figure 3C and D). The lack of engraftment following bulk BM transplantation from AKM mice also supports the concept that AKM progenitor cells (which would be included in bulk BM transplants) do not acquire aberrant self-renewal capacity. Furthermore, Aml1-ETO-expressing LSK cells showed increased replating potential *in vitro* (Figure 3E), in keeping with previous reports.<sup>16</sup> In contrast, the additional expression of K-RasG12D abrogated this enhanced replating potential (Figure 3E). Collectively, these results support the concept that Aml1-ETO expression is associated with increased self-renewal of HSC. But in the additional presence of K-RasG12D, HSC are at a competitive disadvantage, consistent with functional impairment of AKM HSC.

### K-RasG12D expression induces loss of quiescence in Aml1-ETO-expressing hematopoietic stem cells

To gain molecular insight into the functional impairment of HSC expressing K-RasG12D, we carried out RNA sequencing of AM, KM, AKM and CON CD45.2 LSKCD150<sup>+</sup>Flt3<sup>-</sup> cells from competitively transplanted recipients eight weeks post-poly(I:C) ( $n=5$  replicates per

genotype). Gene set enrichment analysis (GSEA) revealed a marked enrichment in E2F, Myc, and G2M checkpoint associated gene expression in AKM compared to AM, likely indicating higher levels of cell cycle activity. In keeping with the observed functional impairment of HSC (Figure 4A-C). Cell cycle activation was confirmed by flow cytometry, showing a 4-fold decrease in quiescent (G0) AKM, compared to AM, HSC (Figure 4D and E). This was accompanied by loss of HSC self-renewal-associated gene expression and an acquisition of gene expression associated with granulocyte-macrophage progenitors (GMP) that lack Gata1 expression that give rise to neutrophils and monocytes (Figure 4F-H).<sup>35</sup> This is consistent with phenotypic HSC from AKM mice showing transcriptional signatures of myeloid progenitor cells rather than HSC.

To identify genes that may be involved in the loss of quiescence and HSC function, we performed differential gene expression analysis. Aml1-ETO expression caused an up-regulation of 52 genes and down-regulation of 36 genes in phenotypic HSC compared to CON (Figure 5A-C). Among the down-regulated genes were *Gja1* and *Gzmb* (Figure 5D and E). K-RasG12D caused more extensive disruption of gene expression, with up-regulation of 389 genes and down-regulation of 526 genes compared to CON (Figure 5A and B). Among the up-regulated genes were MAPK pathway genes such as *Eiv4* and *Ccnd1* (Figure 5F and G). Genes that were down-regulated by KRAS activation were down-regulated in KM versus CON and AKM versus CON HSC (*Online Supplementary Figure S4A and B*), in keeping with activation of this signaling pathway by activated K-RasG12D in both Aml1-ETO positive and negative cells.<sup>34</sup>

Hematopoietic stem cells co-expressing Aml1-ETO and K-RasG12D showed up-regulation of 319 genes and down-regulation of 482 genes compared to CON (Figure 5A and B). Many of the up- and down-regulated genes in AKM HSC overlapped with KM HSC (Figure 5A and B), indicating that KRAS confers some of the same transcriptional changes in both Aml1-ETO positive and negative HSC. This was confirmed in a principal component analysis (PCA) and hierarchical clustering of the HSC from all four genotypes which demonstrated that AKM HSC clustered closely with KM HSC indicating that K-RasG12D is driving the separation in gene expression in AKM HSC from CON and AM HSC (*Online Supplementary Figure S4C-F*). However, the majority of these genes were only dysregulated in the presence of both mutations (Figure 5A and B), indicating that the two mutations together collaborated to induce a distinct pattern of gene expression that only partially overlapped with K-RasG12D or Aml1-ETO regulated genes (Figure 5A-C). *Gja1* and *Gzmb* were up-regulated in HSC co-expressing Aml1-ETO and K-RasG12D when compared to Aml1-ETO (Figure 5C-E).

Gene set enrichment analysis showed an enrichment of oxidative phosphorylation and loss of genes associated with hypoxia in AKM HSC compared to AM (Figure 5H and I and *Online Supplementary Table S3*). Interestingly, *Gzmb* causes reactive oxygen species (ROS) production,<sup>35,36</sup> which can lead to apoptosis and cell death of HSC, suggesting *Gzmb* expression may lead to increased levels of ROS and apoptosis in AKM HSC. Genes associated with the p53 pathway were also down-regulated in AKM HSC compared to AM (Figure 5J). Loss of *Gja1* has been shown to increase p53 levels;<sup>37</sup> therefore, increased

expression of *Gja1* in AKM HSC may lead to loss of p53. Analysis of biological GO terms showed a number of metabolic processes up-regulated in AKM versus AM HSC (Online Supplementary Table S4) indicating metabolic dysregulation could also be involved in loss of quiescence in AKM HSC.<sup>39</sup>

Finally, in order to determine relevance of the genes/pathways described for human AML1-ETO, we studied genes that are up-regulated in human HSC transduced with AML1-ETO.<sup>39</sup> There was an enrichment of these genes in AM HSC compared to AKM, suggest a correlation between human and mouse AML1-ETO target genes (Figure 5K).

Collectively, these results demonstrate that K-RasG12D is detrimental to HSC harboring Aml1-ETO, causing a loss

of functional HSC, associated with down-regulation of HSC-associated gene expression and loss of quiescence.

## Discussion

We have here tested the hypothesis that the observed absence of mutations in signaling pathway genes, such as *KRAS*, in pre-leukemic HSC from AML patients<sup>11,12</sup> is due to such mutations being detrimental not only to normal HSC, but also to pre-leukemic HSC. While Aml1-ETO improved the repopulating capacity of HSC, K-RasG12D had a markedly detrimental effect on Aml1-ETO-expressing pre-leukemic HSC, leading to their eventual depletion, likely due to loss of quiescence and HSC-associated gene expres-

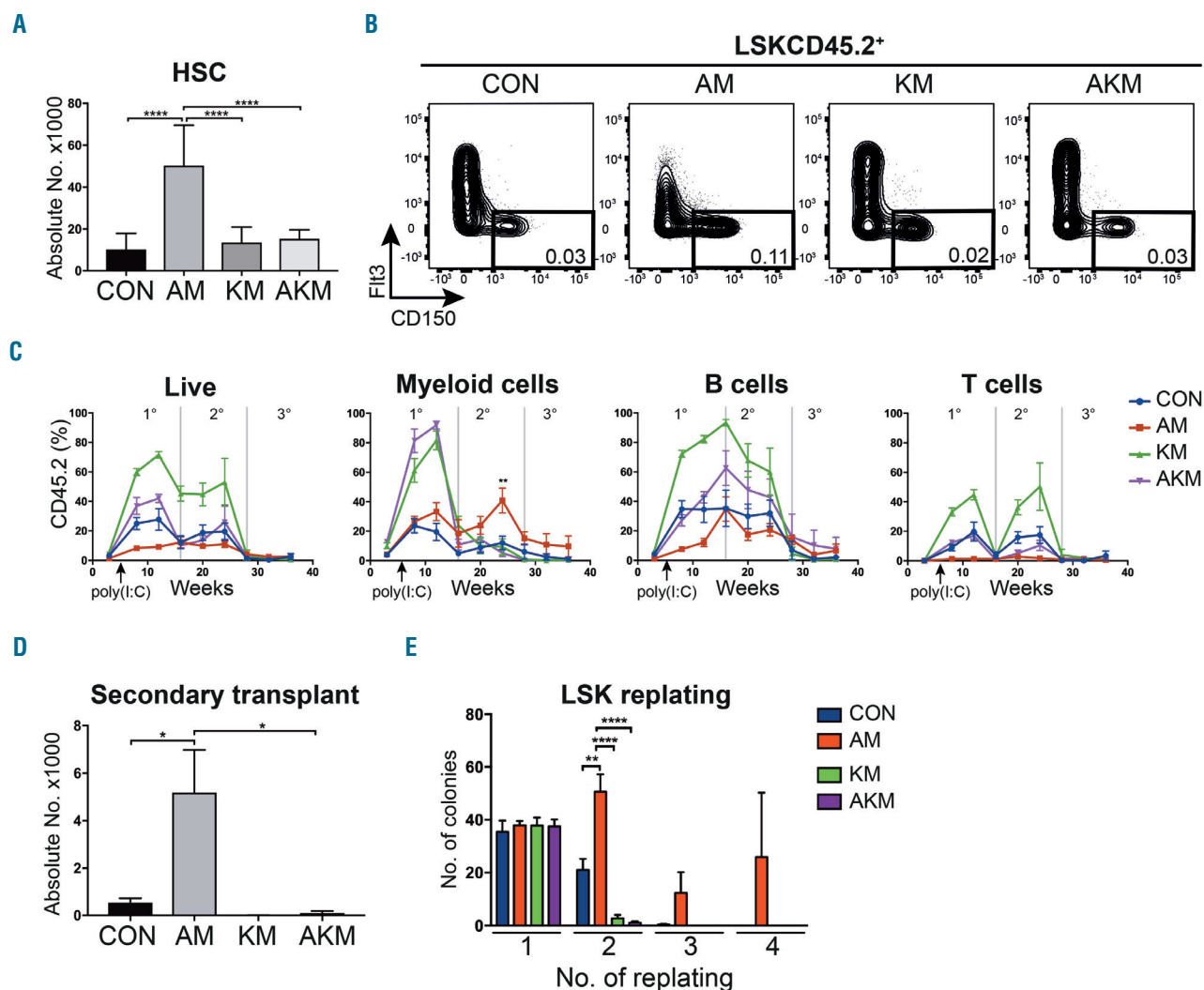


**Figure 3. Hematopoietic stem cell (HSC) expansion caused by Aml1-ETO is reversed by K-RasG12D.** (A) Absolute number of CD45.2 HSC in the bone marrow (BM) from recipients of CON (n=11), AM (n=14), KM (n=13) and AKM fetal liver (FL) cells (n=14). Results were generated in three independent experiments; (B) Representative FACS plots showing gating used to quantify HSC as a percentage of the BM mononuclear cells across all experiments. (C) Percentage reconstitution of total CD45.2 cells, CD45.2 myeloid (LiveCD19-CD4-CD8a-NK1.1<sup>-</sup>), CD45.2 B cells (LiveNK1.1-Mac1-CD19<sup>+</sup>) and CD45.2 T cell (LiveNK1.1-Mac1-CD4-CD8a<sup>+</sup>) compartments in primary, secondary and tertiary transplantations. (D) Absolute number of CD45.2 HSC in secondary recipients of CON (n=9 recipient mice in 2 independent experiments), AM (n=10 recipient mice in 3 independent experiments), KM (n=4 recipient mice in 2 independent experiments), and AKM FL cells (n=7 recipient mice in 2 independent experiments). (E) Replating efficiency of CD45.2 LSK BM cells. Average number of colonies is shown for 5-6 biological replicates per genotype in two independent experiments. The results were analyzed using multiple comparison ANOVA. The results are presented as the mean±Standard Error of Mean. \**P*<0.05; \*\**P*<0.01; \*\*\**P*<0.001; \*\*\*\**P*<0.0001.

sion. The loss of disease-propagating HSC also likely underlies the amelioration of the K-RasG12D-induced myeloproliferative phenotype when the mutations were combined.

Signaling mutations are thought to have a negative cell-intrinsic impact on HSC as enhanced proliferation tends to reduce competitiveness and self-renewal potential. Previous studies have shown N-RasG12D increases cell division and reduces the self-renewal in a subset of HSC. However, this negative impact is counteracted as N-RasG12D also increases the self-renewal potential and reduces division in another subset of HSC. This bimodal

effect allows NRasG12D-expressing HSC to outcompete WT HSC, in contrast to our observations with K-RasG12D.<sup>23</sup> Recently, signaling mutations have also been shown to have a negative cell-extrinsic impact on HSC by disrupting HSC-supporting BM stromal cells and increasing inflammation-associated gene expression.<sup>24</sup> Sabnis *et al.* have shown that K-RasG12D expression cell-intrinsically drives HSC into cycle and reduces HSC frequency; however, long-term fitness of K-RasG12D-expressing HSC was not analyzed due to lethality caused by K-RasG12D-induced myeloproliferation.<sup>20</sup>

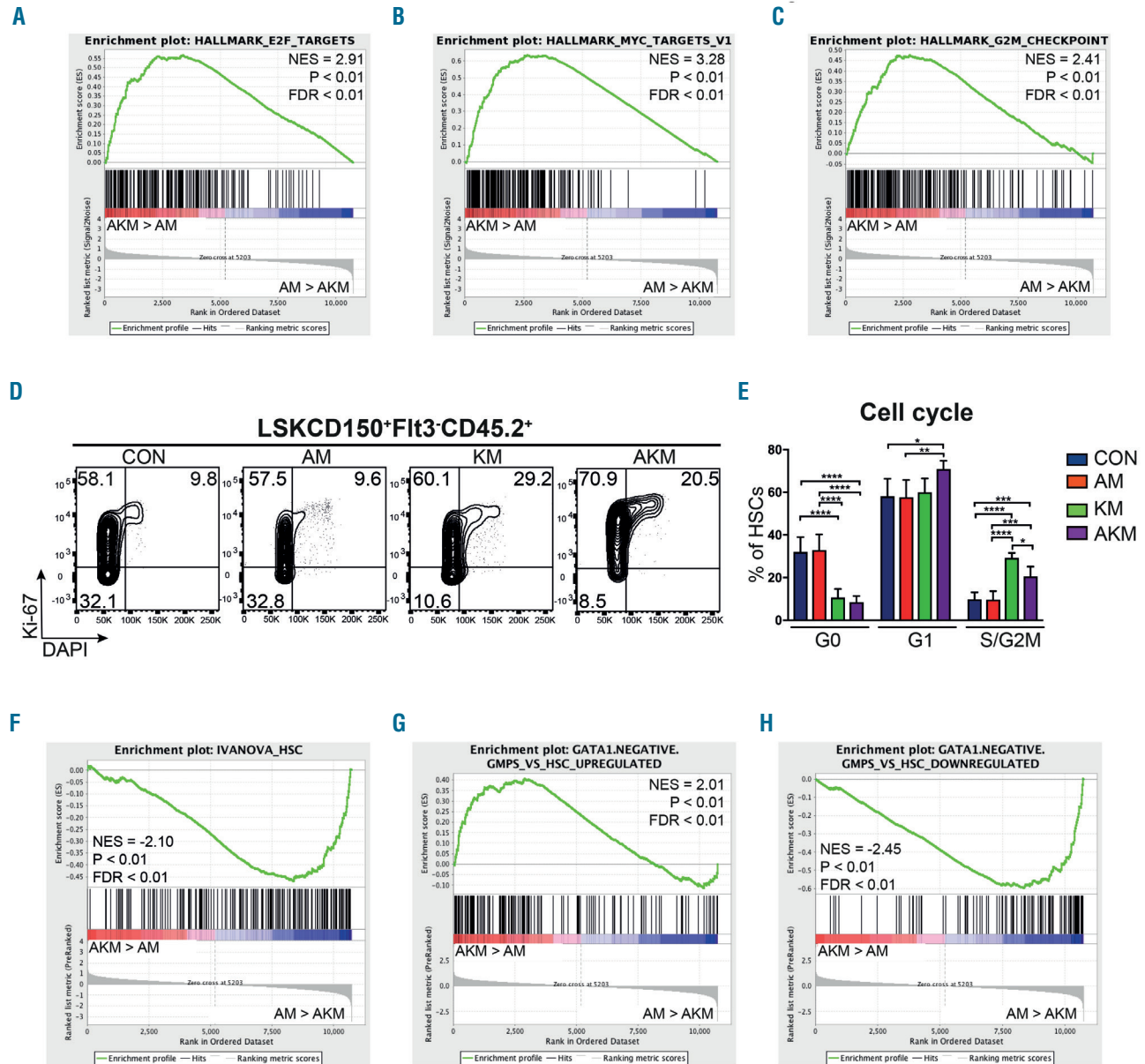


**Figure 4. Hematopoietic stem cells (HSC) co-expressing Aml1-ETO and K-RasG12D are characterized by loss of quiescence and HSC-associated gene expression.** (A-C) Bulk CD45.2 LSKCD150<sup>+</sup>Fit3<sup>-</sup> cells were subjected to RNA sequencing (5-6 biological replicates per genotype in two independent experiments). Gene set enrichment analysis (GSEA) of AKM versus AM HSC for E2F targets (A), Myc targets (B), and genes associated with G2M checkpoint (C). (D) Representative FACS plots showing cell cycle analysis of CD45.2 LSKCD150<sup>+</sup>Fit3<sup>-</sup> phenotypic HSC from the bone marrow (BM) of recipients of CON (n=6 recipient mice in 2 independent experiments), AM (n=9 recipient mice in 3 independent experiments), KM (n=4 recipient mice in 2 independent experiments), and AKM FL (n=6 recipient mice in 3 independent experiments). (E) Percentage of BM CD45.2 LSKCD150<sup>+</sup>Fit3<sup>-</sup> cells at each cell cycle stage. The results were analyzed using multiple comparison ANOVA. The results are presented as mean±Standard Deviation. \*P<0.05; \*\*P<0.01; \*\*\*P<0.001. (F-H) GSEA analysis of AKM versus AM HSC for HSC gene signature (F), genes up-regulated in granulocyte-monocyte progenitor (GMP) that lack Gata1 expression compared to HSC (G), and genes down-regulated in GMP that lack Gata1 expression compared to HSC (H). NES: normalized enrichment score; FDR: false discovery rate.

Experimental approaches investigating collaboration between Aml1-ETO and activated Ras have mainly used retroviral expression of oncogenes, showing that such mutations collaborate to cause an acute leukemia.<sup>40,41</sup> However, retroviral transduction can lead to expression at non-physiological levels as well as ectopic expression within the cellular hierarchy.<sup>4</sup> This method, therefore, may not accurately address the effect of the mutant proteins on HSC function or the ability of mutations expressed at relevant levels to induce transformation of progenitor cells. Consistent with this, in our model system, knock-in of Am1-ETO and K-RasG12D was insuffi-

cient to cause transformation of myeloid progenitors. Other approaches using conditional knock-in mutations or gene knock-out to study the collaboration between pre-leukemic mutations, such as the bi-allelic *Cebpa* mutations, *Tet2* and *Dnmt3a* knock-out, in combination with the signaling mutation *Flt3-ITD* have resulted in leukemic transformation.<sup>4-6</sup> However, *Flt3* is not expressed at detectable levels in repopulating mouse HSC.<sup>42</sup> Therefore, such modeling cannot measure the intrinsic effect of a signaling mutation on pre-leukemic HSC, whereas cell-extrinsic effects of *FLT3-ITD* would be likely to play a role.<sup>24</sup> Indeed, in order to study pre-

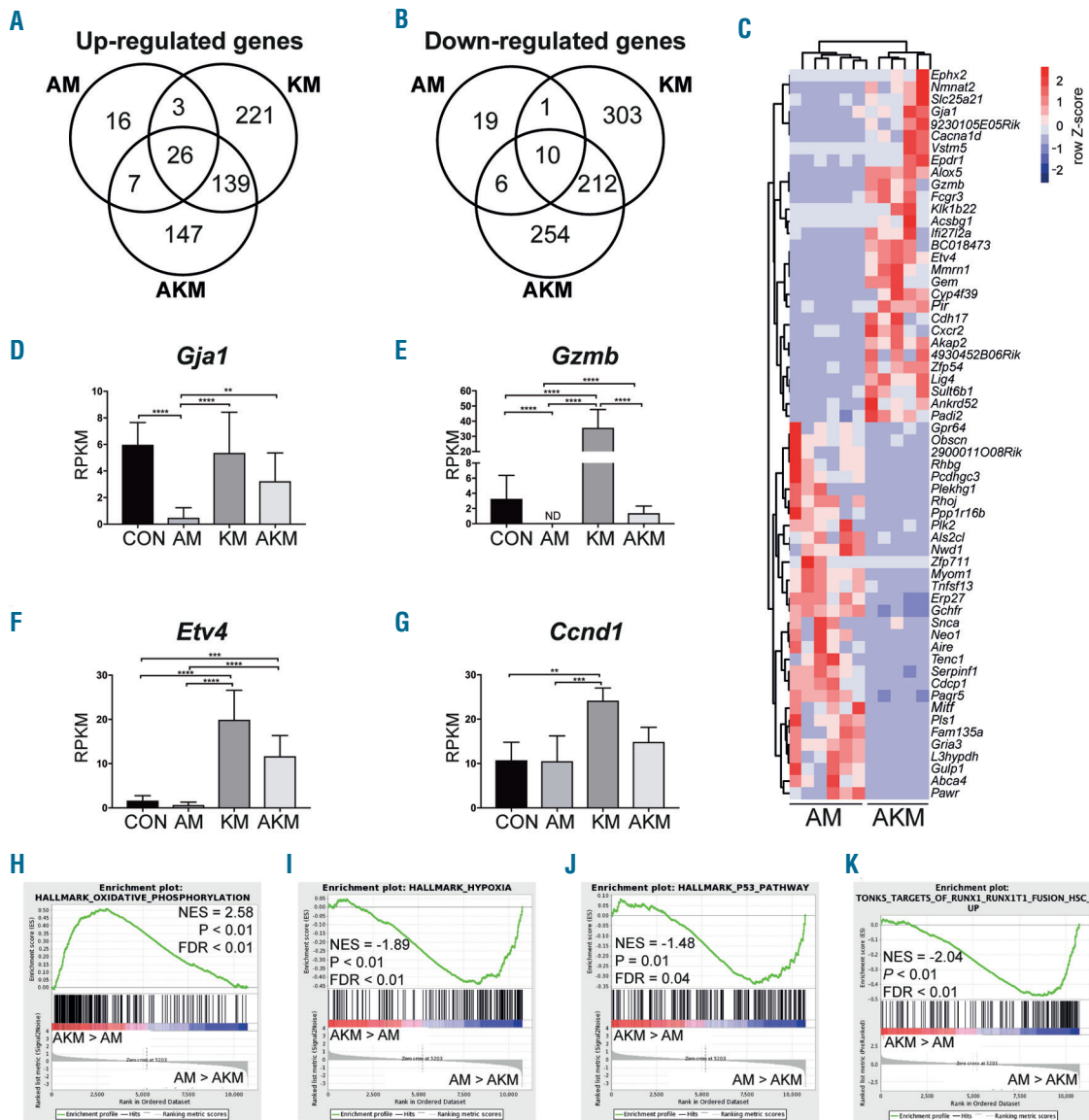


**Figure 5. RNA sequencing reveals distinct molecular signatures of hematopoietic stem cells (HSC) co-expressing Aml1-ETO and K-RasG12D.** (A and B) Venn-diagram of significantly up-regulated (A) and down-regulated genes (B) in HSC identified by RNA sequencing. (C) Heatmap depicting the read per kilobase of transcript per million (RPKM) values of the top 30 significantly up-regulated and down-regulated genes in AKM HSC versus AM [false discovery rate (FDR) < 0.05]. (D-G) RPKM of selected genes identified from RNA sequencing, *Gja1* (D), *Gzmb* (E), *Etv4* (F), and *Ccnd1* (G). RPKM and FDR were generated using edgeR package. The results are presented as mean±Standard Deviation. \**P*<0.05; \*\**P*<0.01; \*\*\**P*<0.001; \*\*\*\**P*<0.0001. (H-K) Gene set enrichment analysis (GSEA) of AKM versus AM HSC for oxidative phosphorylation (H), hypoxia (I), p53 pathway (J), and genes up-regulated in human HSC transduced with AML1-ETO (K). NES: normalized enrichment score.

leukemic HSC, it is preferable that the model used retains a relatively unperturbed hematopoietic hierarchy without overt leukemia or other malignancy. In addition, the use of “knock-in” models of oncogenes that are expressed from their own promoter at their original loci is important to retain faithful expression patterns within the hematopoietic hierarchy. Both these conditions are fulfilled by the *Aml1*<sup>ETO/+</sup>; *Kras*<sup>G12D/+</sup>; *Mx1-Cre*<sup>tg/+</sup> model used here.

The results from this study differs to other models that demonstrate that Ras mutations collaborate with pre-leukemic mutations to develop an AML, such as *Dnmt3a*<sup>-/-</sup>; *Kras*<sup>G12D/+</sup> and *Cbfb*<sup>MYH11/+</sup>; *Nras*<sup>G12D/+</sup>, where both models develop a more aggressive disease when combined.<sup>43,44</sup> Both models lead to transformation of myeloid progenitors, in contrast to the lack of transformation seen in AKM mice, even after serial transplantation. Both *Dnmt3a*<sup>-/-</sup>; *Kras*<sup>G12D/+</sup> and *Cbfb*<sup>MYH11/+</sup>; *Nras*<sup>G12D/+</sup> models do, however, result in a loss of LT-HSC which is consistent with our results. The lack of transformation of myeloid progenitors in AKM mice gave us a unique opportunity to study pre-leukemic stem cells functionally in the absence of progenitor cell transformation as seen in the other models.

RNA sequencing revealed genes that may underlie the observed HSC phenotype of AM and AKM mice. *Gzmb* is a serine protease that has recently been reported to be important in HSC function.<sup>35</sup> Knock-out of *Gzmb* confers enhanced self-renewal to HSC in a cell-intrinsic manner.

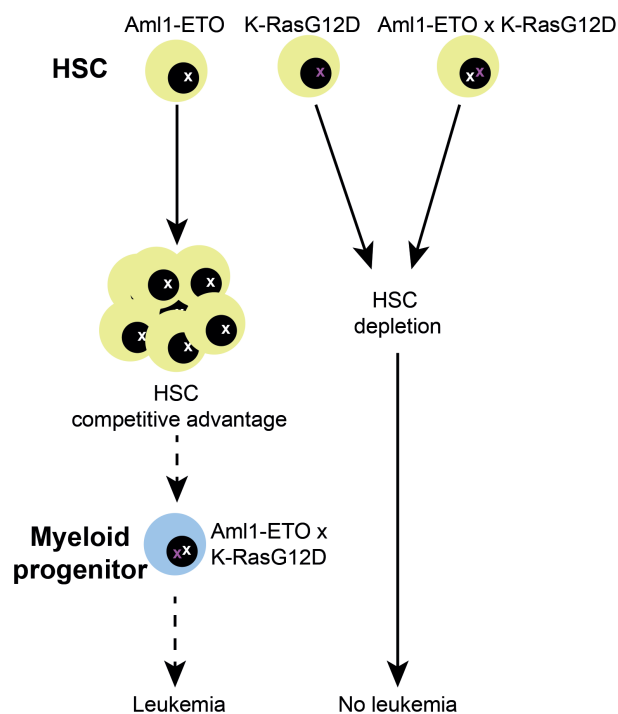


**Figure 6. Schematic summarizing the effect of K-RasG12D on pre-leukemic hematopoietic stem cells (HSC).** HSC that acquire Aml1-ETO gain a competitive advantage, leading to an expansion in HSC number. Acquisition of K-RasG12D and Aml1-ETO concurrently leads to HSC depletion. It remains to be determined whether sequential acquisition of Aml1-ETO followed by K-RasG12D might support development of leukemia. As this was not tested in the current study, this is depicted as a dotted arrow.

*Gzmb* deficient mice also had a better survival rate after administering 5-FU.<sup>35</sup> *Gja1* encodes gap junction channel protein connexin 43 found on HSC. *Gja1* deficient HSC were shown to be more quiescent after 5-FU treatment. *Gja1* deficient HSC also developed an accumulation of ROS.<sup>37</sup> ROS levels in HSC have been shown to play an important role in hematopoietic reconstitution;<sup>45</sup> however, oxidative phosphorylation gene expression was not enriched in AM HSC versus CON suggesting down-regulation of *Gja1* in AM HSC did not lead to an increase in ROS. *GJA1* has lower expression on CD34<sup>+</sup> BM cells from AML patients with AML1-ETO compared to WT CD34<sup>+</sup> BM cells.<sup>46</sup> Down-regulation of *GZMB* and *Gja1* have also both been identified in human and murine leukemic stem cells, respectively.<sup>47-49</sup> Together, down-regulation of *GZMB* and *GJA1* may contribute to the AML1-ETO-associated competitive advantage of HSC that we observed, and could potentially be important for pre-leukemic HSC persistence after chemotherapy. Importantly, expression of both *Gzmb* and *Gja1* were increased in the presence of K-RasG12D, indicating that re-expression of these genes may have contributed to the loss of HSC function and self-renewal. However, as we identified disruption of multiple genes and pathways in AKM HSC, it seems likely that the underlying mechanistic basis for loss of functional Aml1-ETO expressing HSC associated with K-RasG12D is complex, and is unlikely to be attributable to one single target gene and more likely to involve an interplay of many genes and pathways.

Mutations are acquired in a stepwise manner in AML, and the consequence of the type and order of the mutations acquired will make the HSC more or less likely to facilitate subsequent evolution to leukemia.<sup>50</sup> Our findings help to provide a cellular and molecular basis for the observed patterns of clonal evolution during AML development. HSC that acquire Aml1-ETO gain a competitive advantage, leading to an expansion in HSC number, increasing the pool of cells available to acquire additional mutation that could eventually promote leukemia development. HSC that acquire a *Kras* mutation, either alone or in combination with Aml1-ETO, are depleted. A potential limitation of our study is that the mutations are introduced simultaneously rather than sequentially. New model systems that allow knock-in mutations to be introduced sequentially, and potentially also in specific cellular compartments, warrant further investigation (Figure 6).

In summary, our findings help to explain why signaling mutations such as *KRAS* are not observed within pre-leukemic HSC in AML patients and usually occur as a late event in leukemogenesis. The distinct molecular signatures associated with pre-leukemic mutations in HSC suggest that approaches to target leukemic versus pre-leukemic stem cell expansion are likely to be different.

#### Acknowledgments

A.J.M received funding from a Medical Research Council Senior Clinical Fellowship (MR/L006340/1). This work was supported by the Medical Research Council (MC\_UU\_12009, and G0701761, G0900892 and MC\_UU\_12009/7 to CN). The authors acknowledge the contributions of the WIMM Flow Cytometry Facility, supported by the MRC HIU; MRC MHU (MC\_UU\_12009); NIHR Oxford BRC and John Fell Fund (131/030 and 101/517), the EPA fund (CF182 and CF170) and by the WIMM Strategic Alliance awards G0902418 and MC\_UU\_12025.

## References

- Sykes SM, Kokkaliaris KD, Milsom MD, Levine RL, Majeti R. Clonal Evolution of Preleukemic Hematopoietic Stem Cells in Acute Myeloid Leukemia. *Exp Hematol*. 2015; 43(12):989-992.
- Estey E, Dohner H. Acute myeloid leukaemia. *Lancet*. 2006;368(9550):1894-1907.
- Cancer Genome Atlas Research N. Genomic and epigenomic landscapes of adult de novo acute myeloid leukemia. *N Engl J Med*. 2013; 368(22):2059-2074.
- Reckzeh K, Bereshchenko O, Mead A, et al. Molecular and cellular effects of oncogene cooperation in a genetically accurate AML mouse model. *Leukemia*. 2012;26(7):1527-1536.
- Shih AH, Jiang Y, Meydan C, et al. Mutational cooperativity linked to combinatorial epigenetic gain of function in acute myeloid leukemia. *Cancer Cell*. 2015; 27(4):502-515.
- Yang L, Rodriguez B, Mayle A, et al. DNMT3A Loss Drives Enhancer Hypomethylation in FLT3-ITD-Associated Leukemias. *Cancer Cell*. 2016;29(6):922-934.
- Papaemmanuil E, Gerstung M, Bullinger L, et al. Genomic Classification and Prognosis in Acute Myeloid Leukemia. *N Engl J Med*. 2016;374(23):2209-2221.
- Bonnet D, Dick JE. Human acute myeloid leukemia is organized as a hierarchy that originates from a primitive hematopoietic cell. *Nat Med*. 1997;3(7):730-737.
- Miyamoto T, Weissman IL, Akashi K. AML1/ETO-expressing nonleukemic stem cells in acute myelogenous leukemia with 8;21 chromosomal translocation. *Proc Natl Acad Sci U S A*. 2000;97(13):7521-7526.
- Jan M, Snyder TM, Corces-Zimmerman MR, et al. Clonal evolution of preleukemic hematopoietic stem cells precedes human acute myeloid leukemia. *Sci Transl Med*. 2012;4(149):149ra118.
- Shlush LI, Zandi S, Mitchell A, et al. Identification of pre-leukaemic haematopoietic stem cells in acute leukaemia. *Nature*. 2014;506(7488):328-333.
- Corces-Zimmerman MR, Hong WJ, Weissman IL, Medeiros BC, Majeti R. Preleukemic mutations in human acute myeloid leukemia affect epigenetic regulators and persist in remission. *Proc Natl Acad Sci U S A*. 2014;111(7):2548-2553.
- Dohner H, Estey E, Grimwade D, et al. Diagnosis and management of AML in adults: 2017 ELN recommendations from an international expert panel. *Blood*. 2017;129(4):424-447.
- Miyamoto T, Nagafuji K, Akashi K, et al. Persistence of multipotent progenitors expressing AML1/ETO transcripts in long-term remission patients with t(8;21) acute myelogenous leukemia. *Blood*. 1996;87(11):4789-4796.
- Krauth MT, Eder C, Alpermann T, et al. High number of additional genetic lesions in acute myeloid leukemia with t(8;21)/RUNX1-RUNX1T1: frequency and impact on clinical outcome. *Leukemia*. 2014;28(7):1449-1458.
- Higuchi M, O'Brien D, Kumaravelu P, Lenny N, Yeoh EJ, Downing JR. Expression of a conditional AML1-ETO oncogene bypasses embryonic lethality and establishes a murine model of human t(8;21) acute myeloid leukemia. *Cancer Cell*. 2002;1(1):63-74.
- Guryanova OA, Shank K, Spitzer B, et al. DNMT3A mutations promote anthracycline resistance in acute myeloid leukemia via impaired nucleosome remodeling. *Nat Med*. 2016;22(12):1488-1495.
- Braun BS, Tuveson DA, Kong N, et al. Somatic activation of oncogenic Kras in hematopoietic cells initiates a rapidly fatal myeloproliferative disorder. *Proc Natl Acad Sci U S A*. 2004;101(2):597-602.
- Chan IT, Kutok JL, Williams IR, et al. Conditional expression of oncogenic K-ras from its endogenous promoter induces a myeloproliferative disease. *J Clin Invest*. 2004;113(4):528-538.
- Sabnis AJ, Cheung LS, Dail M, et al. Oncogenic Kras initiates leukemia in hematopoietic stem cells. *PLoS Biol*. 2009;7(3):e59.
- Chu SH, Heiser D, Li L, et al. FLT3-ITD knockin impairs hematopoietic stem cell quiescence/homeostasis, leading to myeloproliferative neoplasm. *Cell Stem Cell*. 2012;11(3):346-358.
- Chan G, Kalaitzidis D, Usenko T, et al. Leukemogenic Ptpn11 causes fatal myeloproliferative disorder via cell-autonomous effects on multiple stages of hematopoiesis. *Blood*. 2009;113(18):4414-4424.
- Li Q, Bohin N, Wen T, et al. Oncogenic Nras has bimodal effects on stem cells that sustainably increase competitiveness. *Nature*. 2013;504(7478):143-147.
- Mead AJ, Neo WH, Barkas N, et al. Niche-mediated depletion of the normal hematopoietic stem cell reservoir by Flt3-ITD-induced myeloproliferation. *J Exp Med*. 2017;214(7):2005-2021.
- Jackson EL, Willis N, Mercer K, et al. Analysis of lung tumor initiation and progression using conditional expression of oncogenic K-ras. *Genes Dev*. 2001;15(24):3243-3248.
- Kuhn R, Schwenk F, Aguet M, Rajewsky K. Inducible gene targeting in mice. *Science*. 1995;269(5229):1427-1429.
- Bereshchenko O, Mancini E, Moore S, et al. Hematopoietic stem cell expansion precedes the generation of committed myeloid leukemia-initiating cells in C/EBPalpha mutant AML. *Cancer Cell*. 2009;16(5):390-400.
- Pronk CJ, Rossi DJ, Mansson R, et al. Elucidation of the phenotypic, functional, and molecular topography of a myeloerythroid progenitor cell hierarchy. *Cell Stem Cell*. 2007;1(4):428-442.
- Velasco-Hernandez T, Sawen P, Bryder D, Cammenga J. Potential pitfalls of the Mx1-Cre system: implications for experimental modeling of normal and malignant hematopoiesis. *Stem Cell Reports*. 2016; 7(1):11-18.
- Ichikawa M, Asai T, Saito T, et al. AML-1 is required for megakaryocytic maturation and lymphocytic differentiation, but not for maintenance of hematopoietic stem cells in adult hematopoiesis. *Nat Med*. 2004; 10(3):299-304.
- Growney JD, Shigematsu H, Li Z, et al. Loss of Runx1 perturbs adult hematopoiesis and is associated with a myeloproliferative phenotype. *Blood*. 2005;106(2):494-504.
- Cai X, Gaudet JJ, Mangan JK, et al. Runx1 loss minimally impacts long-term hematopoietic stem cells. *PLoS One*. 2011;6(12):e28430.
- Drissen R, Buza-Vidas N, Woll P, et al. Distinct myeloid progenitor-differentiation pathways identified through single-cell RNA sequencing. *Nat Immunol*. 2016;17(6):666-676.
- Pratiles CA, Taylor BS, Ye Q, et al. (V600E)BRAF is associated with disabled feedback inhibition of RAF-MEK signaling and elevated transcriptional output of the pathway. *Proc Natl Acad Sci U S A*. 2009; 106(11):4519-4524.
- Camevalli LS, Scognamiglio R, Cabezas-Wallscheid N, et al. Improved HSC reconstitution and protection from inflammatory stress and chemotherapy in mice lacking granzyme B. *J Exp Med*. 2014;211(5):769-779.
- Aguilo JI, Anel A, Catalan E, et al. Granzyme B of cytotoxic T cells induces extramitochondrial reactive oxygen species production via caspase-dependent NADPH oxidase activation. *Immunol Cell Biol*. 2010;88(5):545-554.
- Taniguchi Ishikawa E, Gonzalez-Nieto D, Ghiaur G, et al. Connexin-43 prevents hematopoietic stem cell senescence through transfer of reactive oxygen species to bone marrow stromal cells. *Proc Natl Acad Sci U S A*. 2012;109(23):9071-9076.
- Ito K, Ito K. Hematopoietic stem cell fate through metabolic control. *Exp Hematol*. 2018;64:1-11.
- Tonks A, Pearn L, Musson M, et al. Transcriptional dysregulation mediated by RUNX1-RUNX1T1 in normal human progenitor cells and in acute myeloid leukaemia. *Leukemia*. 2007;21(12):2495-2505.
- Zhao S, Zhang Y, Sha K, et al. KRAS (G12D) cooperates with AML1/ETO to initiate a mouse model mimicking human acute myeloid leukemia. *Cell Physiol Biochem*. 2014;33(1):78-87.
- Chou FS, Wunderlich M, Griesinger A, Mulloy JC. N-Ras(G12D) induces features of stepwise transformation in preleukemic human umbilical cord blood cultures expressing the AML1-ETO fusion gene. *Blood*. 2011;117(7):2237-2240.
- Adolfsson J, Borge OJ, Bryder D, et al. Upregulation of Flt3 expression within the bone marrow Lin(-)Sca1(+)-c-kit(+) stem cell compartment is accompanied by loss of self-renewal capacity. *Immunity*. 2001;15(4):659-669.
- Chang YI, You X, Kong G, et al. Loss of Dnmt3a and endogenous Kras(G12D/+) cooperate to regulate hematopoietic stem and progenitor cell functions in leukemogenesis. *Leukemia*. 2015;29(9):1847-1856.
- Xue L, Pulikkan JA, Valk PJ, Castilla LH. NrasG12D oncoprotein inhibits apoptosis of preleukemic cells expressing Cbfbeta-SMMHC via activation of MEK/ERK axis. *Blood*. 2014;124(3):426-436.
- Lewandowski D, Barroca V, Duconge F, et al. In vivo cellular imaging pinpoints the role of reactive oxygen species in the early steps of adult hematopoietic reconstitution. *Blood*. 2010;115(3):443-452.
- El-Hadya SBM, Almasryc E, ElHefeyb AM. Detection of Cx43 and P27 in acute myeloid leukemia patients with t(8;21). *Egypt J Haematol*. 2012;37(2):1110-1067.
- Ng SW, Mitchell A, Kennedy JA, et al. A 17-gene stemness score for rapid determination of risk in acute leukaemia. *Nature*. 2016;540(7633):433-437.
- Krivtsov AV, Twomey D, Feng Z, et al. Transformation from committed progenitor to leukaemia stem cell initiated by MLL-AF9. *Nature*. 2006;442(7104):818-822.
- Kirstetter P, Schuster MB, Bereshchenko O, et al. Modeling of C/EBPalpha mutant acute myeloid leukemia reveals a common expression signature of committed myeloid leukemia-initiating cells. *Cancer Cell*. 2008;13(4):299-310.
- Grove CS, Vassiliou GS. Acute myeloid leukaemia: a paradigm for the clonal evolution of cancer? *Dis Model Mech*. 2014;7(8):941-951.

# Antileukemic activity and mechanism of action of the novel PI3K and histone deacetylase dual inhibitor CUDC-907 in acute myeloid leukemia

Xinyu Li,<sup>1#</sup> Yongwei Su,<sup>1#</sup> Gerard Madlambayan,<sup>2</sup> Holly Edwards,<sup>3,4</sup> Lisa Polin,<sup>3,4</sup> Juiwanna Kushner,<sup>3,4</sup> Sijana H. Dzinic,<sup>3,4</sup> Kathryn White,<sup>3,4</sup> Jun Ma,<sup>1</sup> Tristan Knight,<sup>5,6</sup> Guan Wang,<sup>1</sup> Yue Wang,<sup>7</sup> Jay Yang,<sup>3</sup> Jeffrey W. Taub,<sup>5,6</sup> Hai Lin,<sup>8</sup> and Yubin Ge<sup>3,4,6</sup>

<sup>1</sup>National Engineering Laboratory for AIDS Vaccine, Key Laboratory for Molecular Enzymology and Engineering, the Ministry of Education, School of Life Sciences, Jilin University, Changchun, P.R. China; <sup>2</sup>Department of Biological Sciences, Oakland University, Rochester, MI, USA; <sup>3</sup>Department of Oncology, Wayne State University School of Medicine, Detroit, MI, USA; <sup>4</sup>Molecular Therapeutics Program, Barbara Ann Karmanos Cancer Institute, Wayne State University School of Medicine, Detroit, MI, USA; <sup>5</sup>Division of Pediatric Hematology/Oncology, Children's Hospital of Michigan, Detroit, MI, USA; <sup>6</sup>Department of Pediatrics, Wayne State University School of Medicine, Detroit, MI, USA; <sup>7</sup>Department of Pediatric Hematology and Oncology, The First Hospital of Jilin University, Changchun, P.R. China and <sup>8</sup>Department of Hematology and Oncology, The First Hospital of Jilin University, Changchun, P.R. China

<sup>#</sup>XL and YS contributed equally to this work.

## ABSTRACT

Induction therapy for patients with acute myeloid leukemia (AML) has remained largely unchanged for over 40 years, while overall survival rates remain unacceptably low, highlighting the need for new therapies. The PI3K/Akt pathway is constitutively active in the majority of patients with AML. Given that histone deacetylase inhibitors have been shown to synergize with PI3K inhibitors in preclinical AML models, we investigated the novel dual-acting PI3K and histone deacetylase inhibitor CUDC-907 in AML cells both *in vitro* and *in vivo*. We demonstrated that CUDC-907 induces apoptosis in AML cell lines and primary AML samples and shows *in vivo* efficacy in an AML cell line-derived xenograft mouse model. CUDC-907-induced apoptosis was partially dependent on Mcl-1, Bim, and c-Myc. CUDC-907 induced DNA damage in AML cells while sparing normal hematopoietic cells. Downregulation of CHK1, Wee1, and RRM1, and induction of DNA damage also contributed to CUDC-907-induced apoptosis of AML cells. In addition, CUDC-907 treatment decreased leukemia progenitor cells in primary AML samples *ex vivo*, while also sparing normal hematopoietic progenitor cells. These findings support the clinical development of CUDC-907 for the treatment of AML.

## Introduction

Acute myeloid leukemia (AML) is a myeloid malignancy characterized by increased self-renewal, limited differentiation, and deregulated proliferation of myeloid blasts.<sup>1</sup> Little has changed in the treatment of AML over the past 40 years. Despite low overall 5-year survival rates (~25% for adults and ~65% for children),<sup>2</sup> standard induction therapy for AML patients continues to consist of cytarabine and an anthracycline (e.g., daunorubicin) backbone. The major contributor to such low overall survival rates is resistance to chemotherapy. Leukemia-initiating cells are one population thought to be responsible for relapse. Due to the quiescent nature of leukemia-initiating cells, current chemotherapy is often incapable of fully eradicating all these cells.<sup>3</sup> Therefore, new therapies that not only eliminate bulk leukemia cells but also eradicate leukemia-initiating cells are urgently needed to improve the overall survival rates of people with this deadly disease.



Haematologica 2019  
Volume 104(11):2225-2240

## Correspondence:

YUBIN GE  
gey@karmanos.org

HAI LIN  
maillinhai@sina.com

Received: July 5, 2018.

Accepted: February 28, 2019.

Pre-published: February 28, 2019.

doi:10.3324/haematol.2018.201343

Check the online version for the most updated information on this article, online supplements, and information on authorship & disclosures: [www.haematologica.org/content/104/11/2225](http://www.haematologica.org/content/104/11/2225)

©2019 Ferrata Storti Foundation

Material published in *Haematologica* is covered by copyright. All rights are reserved to the Ferrata Storti Foundation. Use of published material is allowed under the following terms and conditions:

<https://creativecommons.org/licenses/by-nc/4.0/legalcode>. Copies of published material are allowed for personal or internal use. Sharing published material for non-commercial purposes is subject to the following conditions: <https://creativecommons.org/licenses/by-nc/4.0/legalcode>, sect. 3. Reproducing and sharing published material for commercial purposes is not allowed without permission in writing from the publisher.



The phosphoinositide 3-kinase (PI3K)/mammalian target of rapamycin (mTOR) pathway is involved in cellular proliferation, differentiation, and survival. It has been reported that 50-80% of AML patients have a constitutively active PI3K/mTOR pathway, which correlates with very poor prognosis.<sup>4,5</sup> In addition, aberrant activation of the PI3K pathway is a feature of leukemia-initiating cells.<sup>6,7</sup> Although PI3K inhibitors have been shown to target AML cells, including leukemia-initiating cells, clinical results have been disappointing, likely due to compensatory activation of other survival pathways.<sup>8-10</sup> Thus, PI3K inhibitors must be used in combination to prevent compensation by other survival pathways and ensure successful eradication of AML cells.

Preclinical testing has revealed promising anti-cancer activity for the combination of PI3K inhibitors with histone deacetylase (HDAC) inhibitors.<sup>11-15</sup> This prompted the design and synthesis of the dual PI3K and HDAC inhibitor CUDC-907 (fimepinostat).<sup>14</sup> CUDC-907 has shown encouraging preclinical activity against multiple types of cancers and the drug is currently being tested in phase I and II clinical trials for the treatment of lymphoma, multiple myeloma, and advanced/relapsed solid tumors ([www.clinicaltrials.gov](http://www.clinicaltrials.gov)).<sup>15-17</sup> It has shown such promising clinical efficacy that the US Food and Drug Administration recently granted Fast Track designation to CUDC-907 for the treatment of adults with relapsed or refractory diffuse large B-cell lymphoma (<http://www.curis.com/>). In this study, we investigated CUDC-907 in AML cell lines, primary AML samples, and a cell line-derived xenograft AML model. We showed that CUDC-907 induces apoptosis in AML cell lines and primary AML samples and this effect is, at least partially, mediated by Mcl-1, Bim, and c-Myc. Additionally, CUDC-907 treatment down-regulates CHK1, Wee1, and ribonucleotide reductase (RR) catalytic subunit M1 (RRM1) and induces DNA replication stress and damage. *In vivo* results show that CUDC-907 has potential for the treatment of AML.

## Methods

A detailed description of the methods is given in the *Online Supplementary Material*.

### Cell culture

The characteristics of the cell lines are presented in *Online Supplementary Table S1*.

### Clinical samples

Diagnostic AML blast samples were obtained from patients at the First Hospital of Jilin University (Changchun, China). Written informed consent was provided according to the Declaration of Helsinki. The Human Ethics Committee of the First Hospital of Jilin University approved this study. Clinical samples were screened for gene mutations by polymerase chain reaction (PCR) amplification and automated DNA sequencing, and fusion genes by real-time reverse transcriptase PCR, as described previously.<sup>18,19</sup> The patients' characteristics are presented in *Online Supplementary Table S2*. Samples were chosen based on availability of adequate material at the time the assay was performed.

### Annexin V/propidium iodide staining

Apoptosis was determined using an Annexin V-Fluorescein Isothiocyanate (FITC)/Propidium Iodide (PI) Apoptosis Kit (Beckman Coulter; Brea, CA, USA), as described elsewhere.<sup>20,21</sup> The

mean percentage ( $\pm$  standard error of mean) of annexinV<sup>+</sup>/PI<sup>-</sup> (early apoptotic) and annexin V<sup>+</sup>/PI<sup>+</sup> (late apoptotic and/or dead) cells from one representative experiment is shown.

### Colony formation assay

Cells were treated with CUDC-907 for 24 h, washed with phosphate-buffered saline, plated in triplicate in MethoCult (Stem Cell Technologies, Cambridge, MA, USA) and incubated for 10-14 days, according to the manufacturer's instructions. Colony-forming units were visualized using an inverted microscope and colonies containing >50 cells were enumerated.

### Leukemia xenograft model

Immunocompromised triple transgenic NSG-SGM3 female mice at 8 weeks of age [NSGS, JAX#103062; non-obese diabetic scid gamma (NOD.Cg-Prkdc<sup>scid</sup> Il2r<sup>tm1Wjl</sup> Tg(CMV-IL3, CSF2, KITLG)1Eav/MloySzj; Jackson Laboratory, Bar Harbor ME, USA] were injected with MV4-11 cells ( $1 \times 10^6$  cells/mouse; 0.2 mL/injection) intravenously (day 0). Mice were randomly divided into three groups (5 mice/group; day 3): one group was the no treatment control group, the other two groups were given 100 or 150 mg/kg CUDC-907 [3% ethanol (200 proof), 1% Tween-80 (polyoxyethylene 20 sorbitan monooleate) and sterile water; all USP grade; v/v]. Mice were treated daily for 8 days followed by 4 days off treatment, and then treated for a further 6 days. Body weights were recorded daily and condition assessed (at least twice daily) for the duration of the study. Mice were humanely euthanized when they presented with: >20% weight loss, decreased mobility limiting access to food and water, lymph node metastases, progressive anemia, or lateral recumbency. The percentage increase in lifespan (%ILS) was calculated: % ILS =  $[(T-C)/C] \times 100$  where "T" is the median day of death of treated mice and "C" is the median day of death of control animals. *In vivo* experiments were approved by the Institutional Animal Care and Use Committee at Wayne State University.

For the pharmacodynamics study, NSG mice were injected with MV4-11 cells ( $1 \times 10^7$  cells/mouse) intravenously. Twenty-one days later, mice were randomized (5 mice/group) and injected once with vehicle control, 100 or 150 mg/kg CUDC-907. The mice were sacrificed 24 h later and bone marrow cells were collected. Human cells were enriched using the EasySep Mouse/Human Chimera Isolation Kit (Stem Cell Technologies).

### Statistical analysis

Differences were compared using the pair-wise two-sample *t*-test (comparisons of apoptosis, colony-forming units, and %DNA in the tail) or the Mann-Whitney two-sample U test [comparison of CUDC-907 half maximal inhibitory concentration (IC<sub>50</sub>)]. The overall survival probability was estimated using the Kaplan-Meier method and the statistical analysis was performed using the log-rank test. The statistical computations were conducted using GraphPad Prism 5.0. The level of statistical significance was set at  $P < 0.05$ .

## Results

### CUDC-907 decreases viable cells and induces apoptosis in acute myeloid leukemia cell lines, and shows promise against a MV4-11-derived xenograft model *in vivo*

CUDC-907 IC<sub>50</sub> for seven AML cell lines, as measured by MTT assays, ranged from 12.4 nM (for MOLM-13) to 73.7 nM (for CTS) (Figure 1A). Annexin V/PI staining and flow cytometry analysis revealed that treatment with

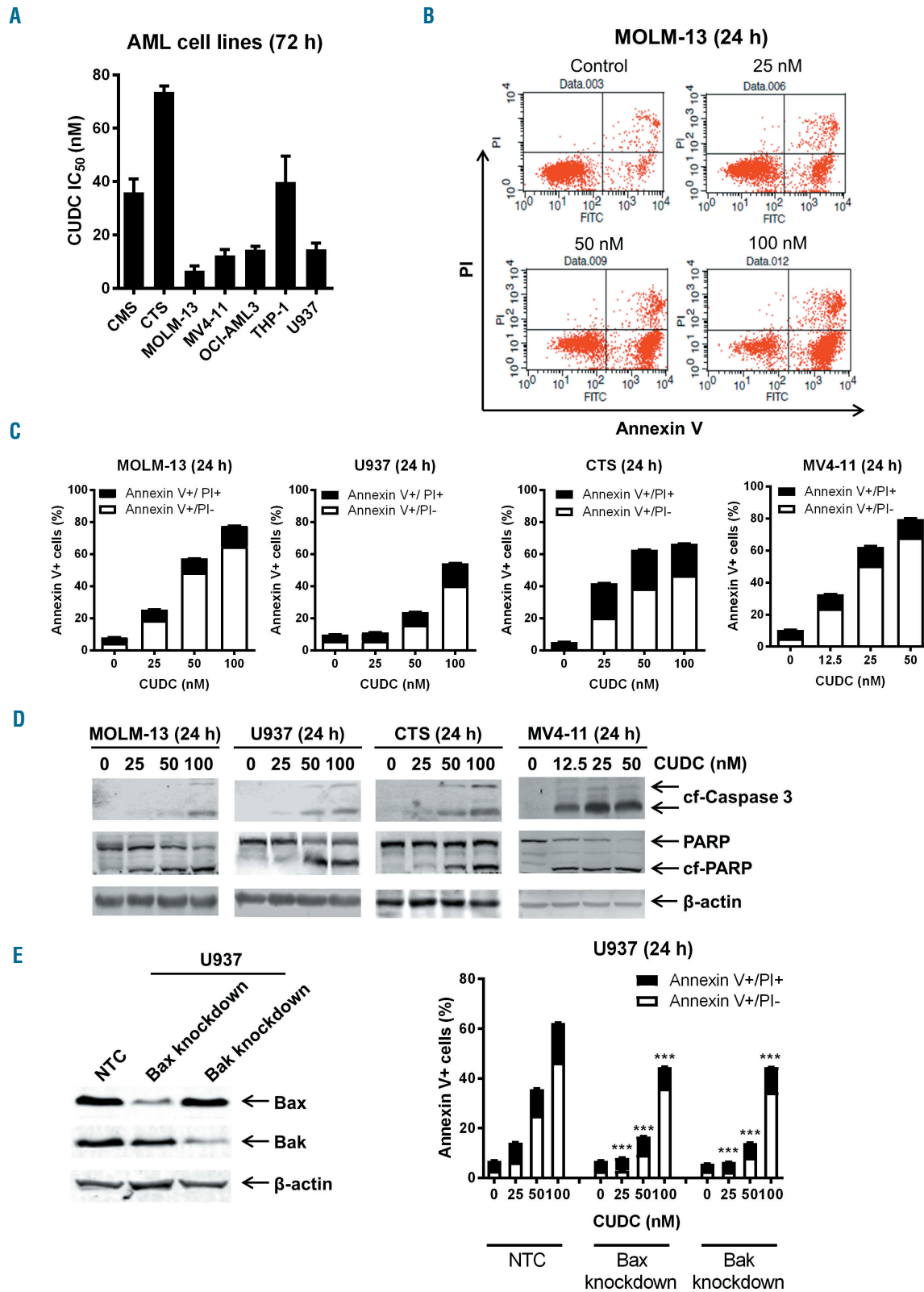


**Figure 1. CUDC-907 treatment decreases viable cells and induces apoptosis in acute myeloid leukemia cell lines and shows promise in an acute myeloid leukemia cell line-derived mouse model.** (A) Acute myeloid leukemia cell lines were treated with variable concentrations of CUDC-907 for 72 h and viable cells were determined using MTT reagent. Data are shown as mean  $\pm$  standard error of mean (SEM). (B, C) MOLM-13, U937, CTS, and MV4-11 cells were treated with CUDC-907 for 24 h and then subjected to annexin V-FITC/propidium iodide (PI) staining and flow cytometry analyses. Representative dot plots are shown in panel (B). Mean percent annexin V<sup>+</sup> cells  $\pm$  SEM are shown in panel (C). (D) MOLM-13, U937, CTS, and MV4-11 cells were treated with CUDC-907 for 24 h. Whole cell lysates were subjected to western blotting. (E) U937 cells were infected with NTC-, Bax-, or Bak-shRNA lentivirus particles overnight, then washed and incubated for 48 h prior to the addition of puromycin to the culture medium. Whole cell lysates of puromycin-resistant cells were subjected to western blotting (left panel). U937 NTC, Bax knockdown, and Bak knockdown cells were treated with CUDC-907 for 24 h and then subjected to annexin V/PI staining and flow cytometry analysis (right panel). \*\*\* $P$ <0.001. (continued on the next page).

CUDC-907 for 24 h caused an increase in annexin V<sup>+</sup> cells, which was accompanied by increased cleaved caspase 3 and PARP (Figure 1B-D), demonstrating that the cells underwent apoptosis. Short hairpin (sh)RNA knockdown of Bax and Bak partially rescued U937 cells from CUDC-907-induced apoptosis (Figure 1E). Furthermore, overexpression of Bcl-xL abolished CUDC-907-induced apoptosis demonstrating that CUDC-907 induces apoptosis through the intrinsic apoptosis pathway (Figure 1F). The potential *in vivo* efficacy of CUDC-907 was evaluated in an early stage MV4-11-derived xenograft mouse model. Mice were treated with CUDC-907 daily for 8 days, given 4 days off treatment, and then treated daily for another 6 days (Figure 1G). All mice were given a 4-day break due to the 3% body weight loss in the mice treated with 150 mg/kg CUDC-907 after the initial eight doses (Figure 1H).

This body weight loss was completely reversible within 4 days. The median survival following CUDC-907 treatment was 44 days for the animals given the 100 mg/kg dose and 47 days for those given the 150 mg/kg, which are 11 and 14 days longer (or 33.3% and 42.2% increases in lifespan), respectively, than the median survival of the mice given the vehicle control (33 days;  $P=0.002$ ) (Figure 1I). These results suggest that CUDC-907 treatment possesses modest antileukemic activity *in vivo*.

### CUDC-907 treatment decreases viable cells and induces apoptosis in primary acute myeloid leukemia samples from patients

CUDC-907 IC<sub>50</sub> ranged from 8.1 to 1,831 nM (*Online Supplementary Table S2*) in primary AML patient samples. Interestingly, samples from patients positive for *FLT3*-

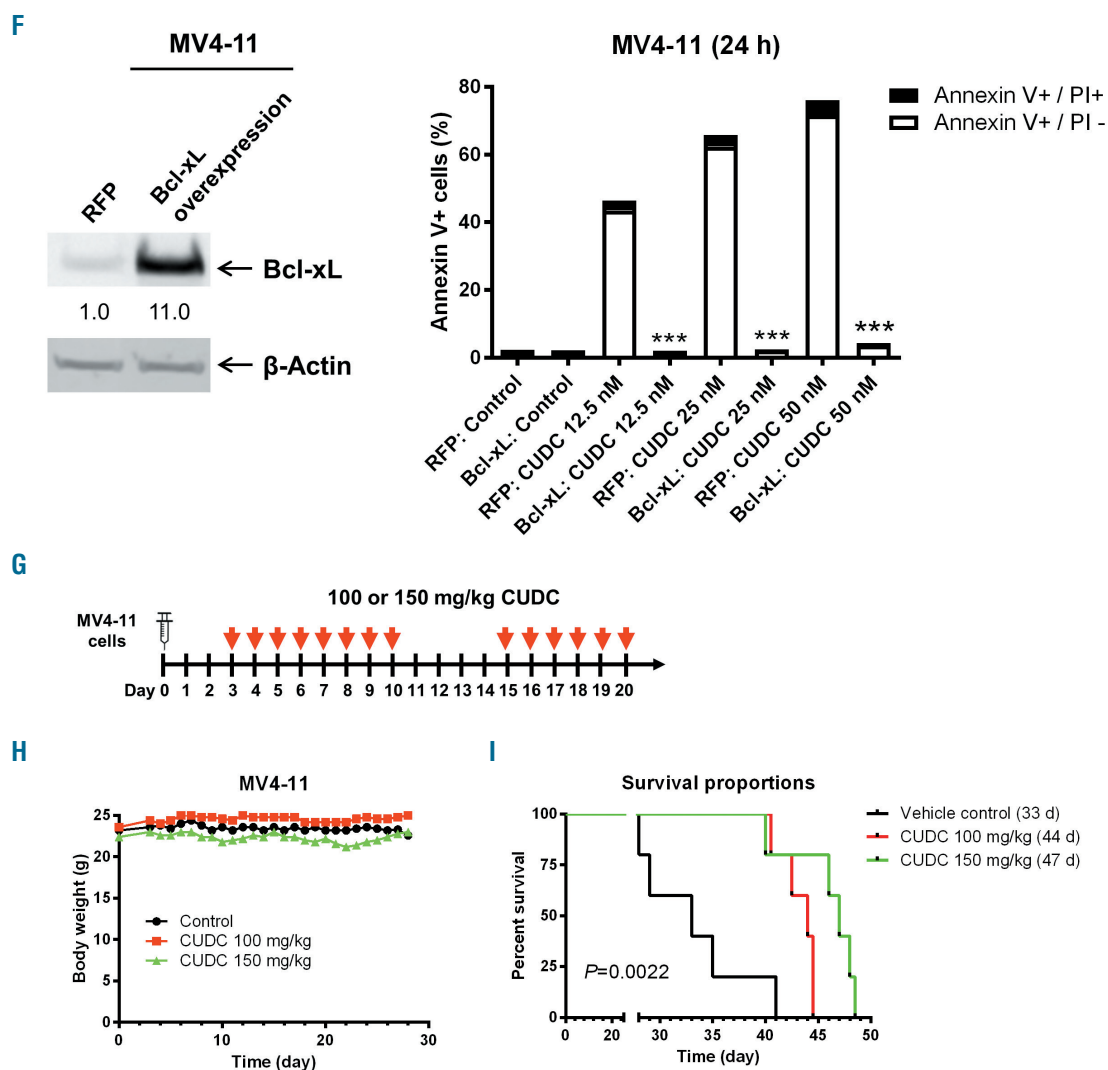


**Figure 1. CUDC-907 treatment decreases viable cells and induces apoptosis in acute myeloid leukemia cell lines and shows promise in an acute myeloid leukemia cell line-derived mouse model.** (continued from the previous page) (F) MV4-11 cells were infected with Precision LentiORF Bcl-xL and RFP control overexpression lentivirus particles overnight, then washed and incubated for 48 h prior to addition of blasticidin to the culture medium. Whole cell lysates were subjected to western blotting. The fold changes for the Bcl-xL densitometry measurements, normalized to  $\beta$ -actin and then compared to no drug treatment control, are indicated (left panel). The cells were treated with CUDC-907 for 24 h and then subjected to annexin V/PI staining and flow cytometry analysis. \*\*\* $P<0.001$  (right panel). (G-I) MV4-11 cells ( $1 \times 10^6$  cells/mouse) were injected through the tail vein of immunocompromised NSGS mice. Three days after cell injection the mice were randomized (5 mice/group) and treated with vehicle control (3% 200 proof ethanol, 1% polyoxyethylene 20 sorbitan monooleate, and USP water), 100 mg/kg CUDC-907, or 150 mg/kg CUDC-907 for 8 consecutive days followed by 4 days off treatment, and then an additional 6 days of treatment. (H) Body weights were measured on a daily basis and are shown as mean  $\pm$  SEM. (I) Overall survival probability, estimated with the Kaplan-Meier method. AML: acute myeloid leukemia; CUDC: CUDC-907; NTC: non-treated control; RFP: red fluorescent protein; cf-Caspase 3: cleaved caspase 3; cf-PARP: cleaved PARP.

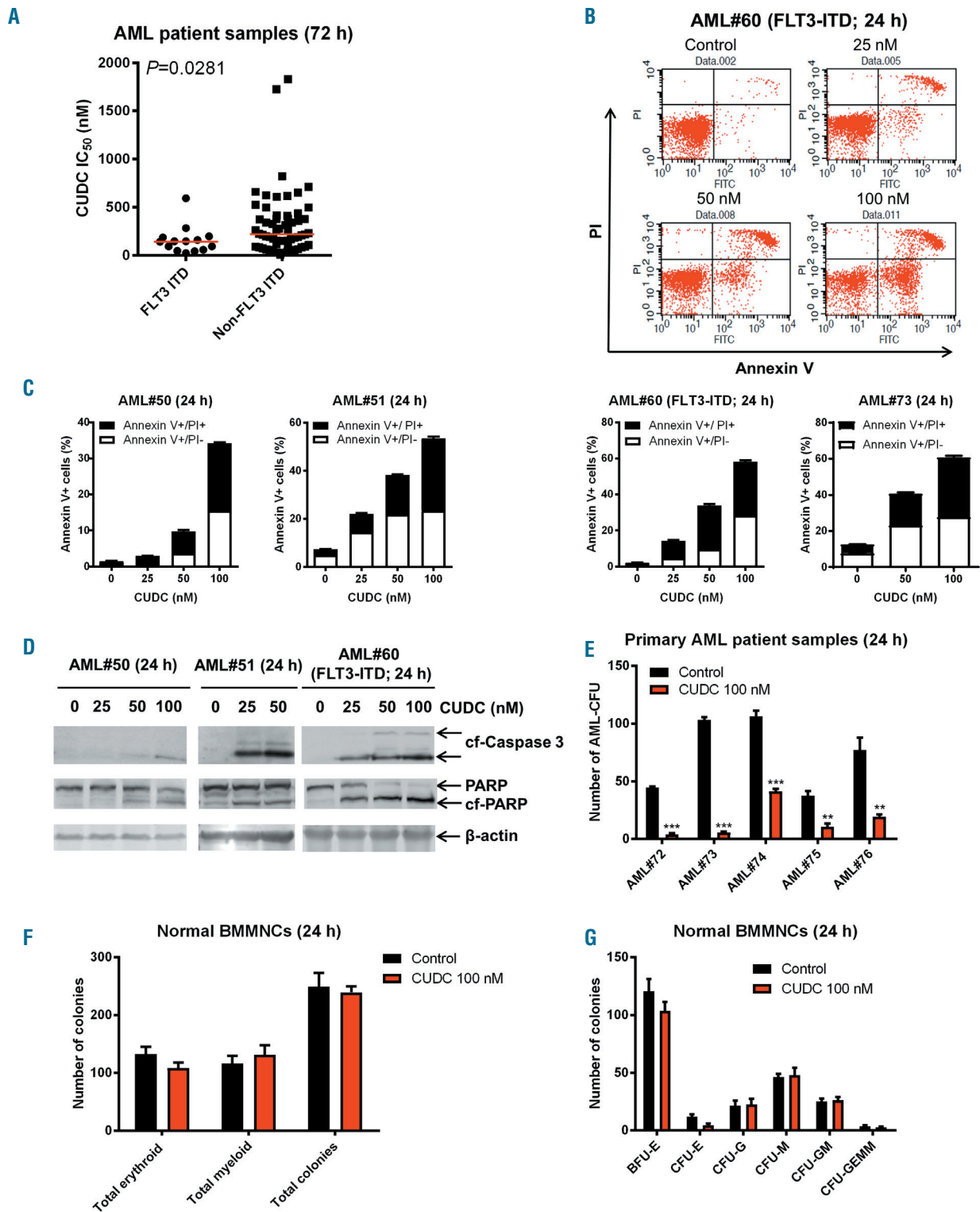


**Figure 2. CUDC-907 treatment induces apoptosis and inhibits colony formation in primary acute myeloid leukemia cells, but spares normal human bone marrow mononuclear cells.** (A) Primary samples from patients with *FLT3*-ITD-positive and *FLT3*-ITD-negative acute myeloid leukemia (AML) (n=14 and n=61, respectively) were treated with variable concentrations of CUDC-907 in 96-well plates for 72 h and then viable cells were determined using MTT reagent. The IC<sub>50</sub> values are means of duplicates from one experiment due to limited samples. The horizontal lines indicate the median. (B, C) Primary AML patient samples were treated with CUDC-907 for 24 h and then subjected to annexin V-FITC/propidium iodide (PI) staining and flow cytometry analyses. Representative dot plots are shown (B). Mean percent of annexin V<sup>+</sup> cells ± standard error of mean (SEM) are shown (panel C). (D) Primary AML patient samples were treated with CUDC-907 for 24 h. Whole cell lysates were subjected to western blotting. (E) Primary AML patient samples were cultured with vehicle control or 100 nM CUDC-907 for 24 h and then plated in methylcellulose. After incubation for 2 weeks, the number of surviving AML cells capable of generating leukemia colonies (AML-CFU) were enumerated. Data are presented as mean ± SEM. \*\*P<0.01, \*\*\*P<0.001. (F) Normal human bone marrow mononuclear cells from a single donor were cultured with vehicle control or 100 nM CUDC-907 for 24 h and then plated in methylcellulose. After incubation for 2 weeks, the number of surviving hematopoietic cells capable of generating colonies was counted. Total erythroid and myeloid colonies are presented as mean ± SEM. (G) The numbers of BFU-E, CFU-E, CFU-G, CFU-M, CFU-GM, and CFU-GEMM colonies are presented as mean ± SEM. AML: acute myeloid leukemia; CUDC: CUDC-907; cf-Caspase 3: cleaved caspase 3; cf-PARP: cleaved PARP; BMMNC: bone marrow mononuclear cells; BFU-E: burst-forming unit - erythroid; CFU-E: colony-forming unit - erythroid; CFU-G: colony-forming unit - granulocyte; CFU-M: colony-forming unit - monocyte; CFU-GM: colony-forming unit - granulocyte, macrophage; CFU-GEMM: colony-forming unit - granulocyte, erythroid, macrophage megaryocyte.

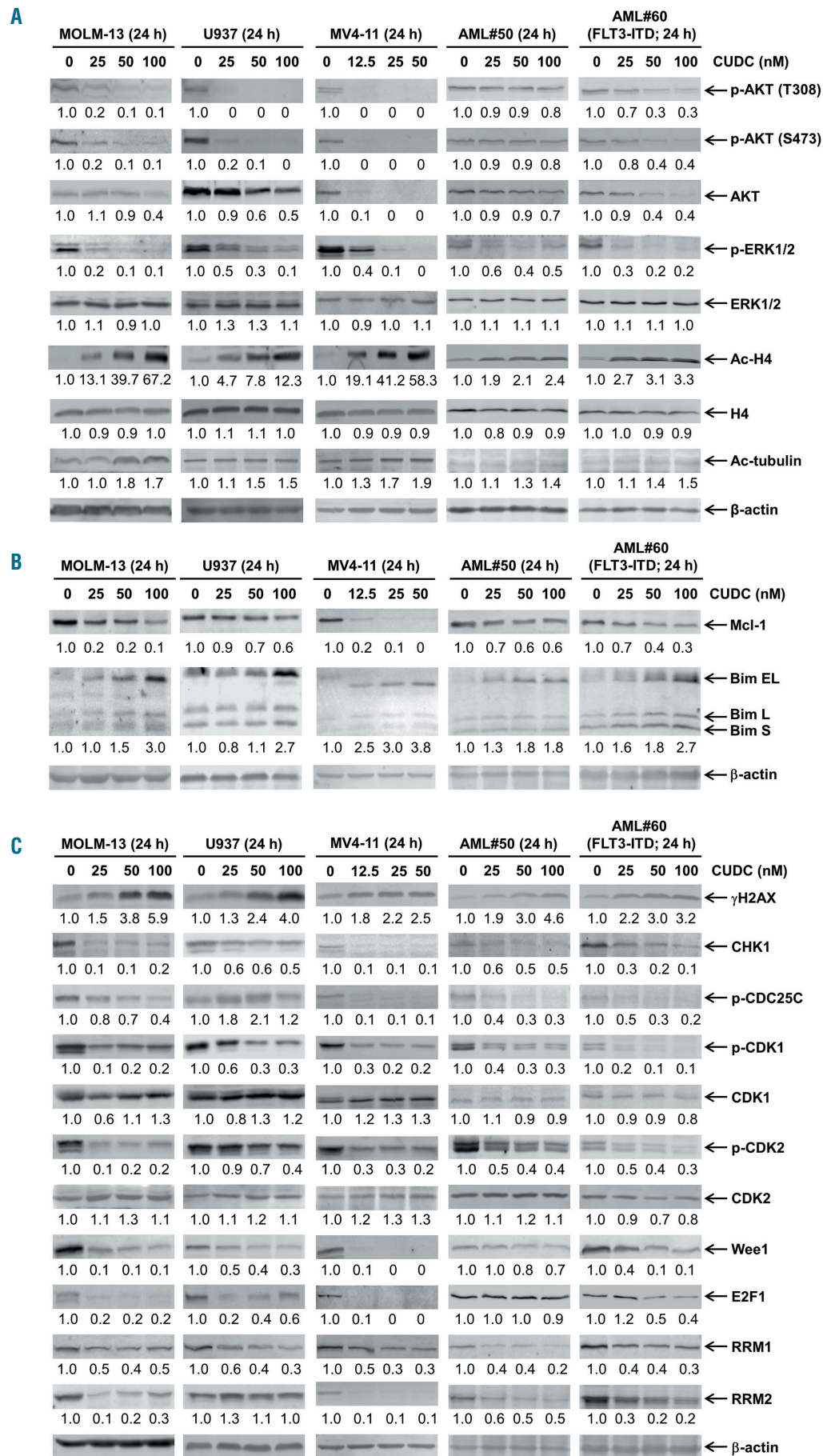


**Figure 3. CUDC-907 treatment inactivates PI3K and ERK and causes downregulation of Mcl-1, CHK1, Wee1, and RRM1, and upregulation of Bim and γH2AX.** (A-C) Acute myeloid leukemia (AML) cell lines and primary AML samples were treated with CUDC-907 for 24 h. Whole cell lysates were subjected to western blotting. The fold changes for the densitometry measurements, normalized to β-actin and then compared to no drug control, are indicated below the corresponding blot. Bim S, L, and EL indicate Bim short, long, and extra-long isoforms, respectively. (continued on the next page).

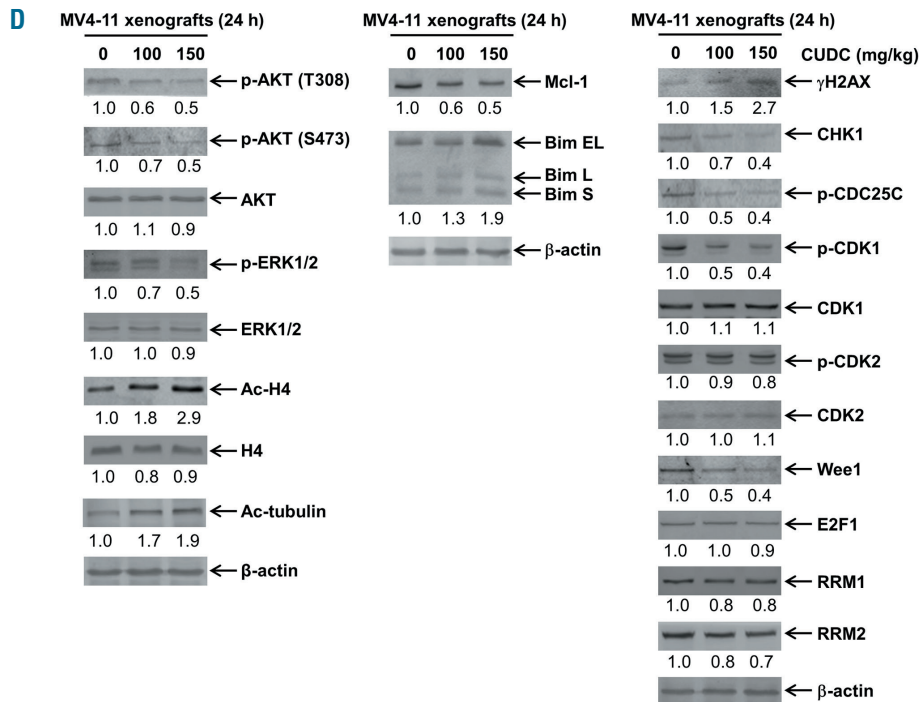


**Figure 3. CUDC-907 treatment inactivates PI3K and ERK and causes downregulation of Mcl-1, CHK1, Wee1, and RRM1, and upregulation of Bim and γH2AX.** (continued from the previous page) (D) NSG mice were injected with MV4-11 cells (1x10<sup>7</sup> cells/mouse). After 21 days, the mice were randomized into three groups and treated with the vehicle control or a single dose of CUDC-907. 24 h after treatment, the mice were sacrificed and bone marrow cells were harvested. Human cells were enriched as described in the Methods section. Whole cell lysates were subjected to western blotting. Normalized densitometry measurements are shown below the corresponding blot. CUDC: CUDC-907.

internal tandem duplication (ITD) (n=14, median IC<sub>50</sub> 143.3 nM) were significantly more sensitive to CUDC-907 than those from patients without *FLT3*-ITD (n=61, median IC<sub>50</sub> 217.6 nM; *P*=0.0281) (Figure 2A). CUDC-907 treatment induced a concentration-dependent increase of annexin V<sup>+</sup> cells accompanied by increased cleaved caspase 3 and PARP (Figure 2B-D), demonstrating that CUDC-907 treatment induced apoptosis in primary AML samples *ex vivo*. Next, we treated five primary AML samples with or without 100 nM CUDC-907 for 24 h and then plated the cells in methylcellulose. After 2 weeks, the number of surviving AML cells capable of generating leukemia colonies (AML-CFU) were enumerated. CUDC-907 treatment significantly reduced the number of AML-CFU in all samples tested, indicating that CUDC-907 treatment decreased leukemia progenitor cells (Figure 2E). In contrast, CUDC-907 treatment did not have a significant effect on colony formation of normal bone marrow mononuclear cells (Figure 2F, G), suggesting that CUDC-907 treatment spares normal hematopoietic progenitor cells.

**CUDC-907 downregulates Mcl-1, CHK1, Wee1, and RRM1, and upregulates Bim in acute myeloid leukemia cells**

As previously reported,<sup>15</sup> CUDC-907 treatment decreased the levels of p-AKT (both T308 and S473) in three AML cell lines and two primary AML samples (Figure 3A). CUDC-907 treatment also decreased p-ERK1/2 levels, while total ERK levels remained relatively unchanged. p-AKT changes were detected as early as 3 h after CUDC-907 treatment in the cell lines (*Online Supplementary Figure S1*). These results confirm that CUDC-907 inactivated the PI3K/AKT and MEK/ERK pathways at these concentrations. Total AKT levels were decreased after 24 h of CUDC-907 treatment, although 3 h of treatment caused a decrease of p-AKT in the absence

of changes in total AKT (*Online Supplementary Figure S1*). Increased acetylation of histone H4 and tubulin (deacetylated by HDAC6) was detected in the AML cell lines, confirming inhibition of HDAC at these concentrations as early as 3 h after treatment (Figure 3A and *Online Supplementary Figure S1*). Substantially increased acetylation of histone H4 was also detected in both primary AML samples, while the acetylation of tubulin was increased to a much lesser extent. Inhibition of the PI3K pathway and HDAC have been shown to cause downregulation of Mcl-1 and upregulation of Bim, respectively.<sup>22,25</sup> Accordingly, CUDC-907 treatment caused a reduction of Mcl-1 and an increase of Bim (Figure 3B), while Bcl-2, Bcl-xL, Bax, and Bak protein levels remained unchanged (*Online Supplementary Figure S2*). Based on the reports that HDAC inhibitors can downregulate DNA damage response proteins,<sup>23-26</sup> we looked at γH2AX (a potential biomarker of DNA double-strand breaks), DNA damage response proteins CHK1, Wee1, and related downstream proteins. CUDC-907 treatment caused an increase of γH2AX and decreases of CHK1, p-CDK1, p-CDK2, Wee1, and RRM1 in AML cell lines and primary AML samples (Figure 3C). Total CDK1 and CDK2 levels were largely unaffected. p-CDC25C and RRM2 decreased, except in U937 cells. E2F1 levels decreased in the cell lines and in one primary AML samples. These results suggest that CUDC-907 may induce DNA damage, which causes death of AML cells. The above results were further confirmed in the MV4-11 xenograft mouse model following administration of a single dose of CUDC-907 (Figure 3D). Downregulation of CHK1, Wee1, and RRM1 by CUDC-907 treatment was not affected by the pan-caspase inhibitor Z-VAD-FMK (*Online Supplementary Figure S3*). In contrast, Z-VAD-FMK treatment itself caused an increase in Mcl-1 protein levels, suggesting that caspases are involved in the regulation of Mcl-1 protein. Surprisingly, co-treatment of AML cells with CUDC-907 and Z-VAD-FMK resulted in substantial-

ly increased Mcl-1 protein levels compared to Z-VAD-FMK alone (*Online Supplementary Figure S3*). Using the parental compounds of CUDC-907, SAHA (a pan-HDAC inhibitor) and GDC-0941 (a PI3K inhibitor), alone or combined (at a 1:1 ratio) at inhibitory concentrations, we found that SAHA and GDC-0941 synergistically induced apoptosis (*Online Supplementary Figure S4A, C*). The half maximal effective concentrations ( $EC_{50}$ ) were much higher for the combination of SAHA plus GDC-0941 than for CUDC-907, suggesting that while they do synergize, the hybrid is more potent than the parental compounds.

Western blotting analysis of whole cell lysates from MOLM-13 cells treated with CUDC-907 for up to 24 h, revealed decreased Mcl-1 and increased Bim, cleaved caspase 3, and cleaved PARP at the 12 h time-point (Figure 4A). Decreased RRM1 and CHK1, and increased  $\gamma$ H2AX were also detected at the 12 h time-point, while decreased Wee1 was detected as early as 4 h after CUDC-907 treatment (Figure 4B). Similar protein level changes were detected 16 h after treatment in U937 cells (*Online Supplementary Figure S5*). Annexin V/PI staining revealed a significant increase in annexin V<sup>+</sup> cells, indicating that

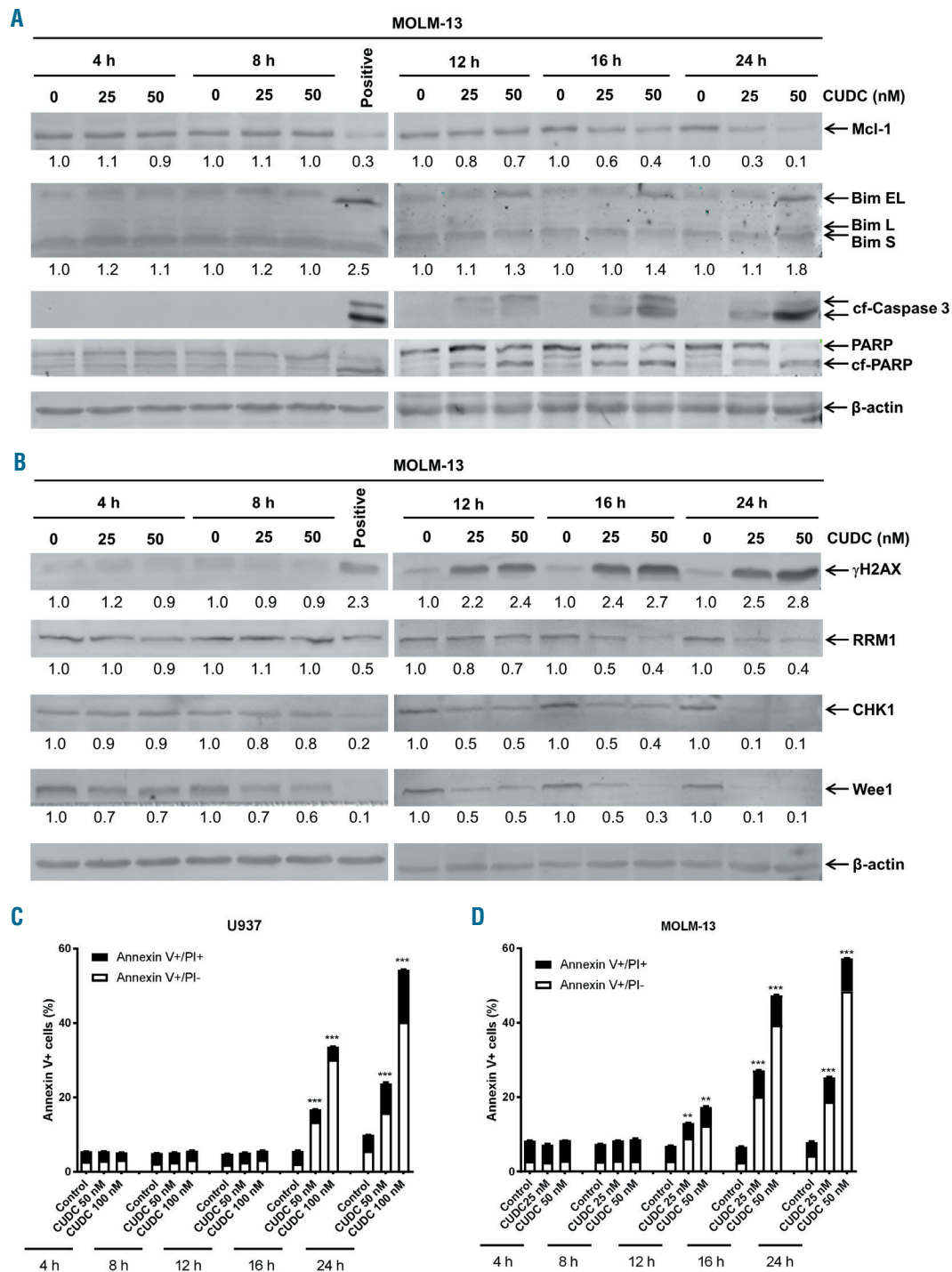


**Figure 4. Upregulation of Bim and downregulation of Mcl-1, CHK1, Wee1, and RRM1 coincide with induction of apoptosis.** (A, B) MOLM-13 cells were treated with CUDC-907 for up to 24 h. Whole cell lysates were subjected to western blotting and probed with the indicated antibodies. The fold changes for the densitometry measurements, normalized to  $\beta$ -actin and then compared to no drug control, are indicated below the corresponding blot. Cells treated with 50 nM CUDC-907 for 24 h were used as a positive control for  $\gamma$ H2AX and cleaved caspase 3. (C, D) U937 (C) and MOLM-13 (D) cells were treated with CUDC-907 for up to 24 h and then subjected to annexin V-FITC/propidium iodide (PI) staining and flow cytometry analyses. Mean percent annexin V<sup>+</sup> cells  $\pm$  standard error of mean are shown. \*\* $P < 0.01$ , \*\*\* $P < 0.001$ . Bim S, L, and EL indicate Bim short, long, and extra-long isoforms, respectively. CUDC: CUDC-907; cf-Caspase 3: cleaved caspase 3; cf-PARP: cleaved PARP.

induction of apoptosis begins at 12 h for MOLM-13 cells and 16 h for U937 cells (Figure 4C, D). Taken together, these results suggest that these changes in protein levels coincide with the induction of apoptosis.

**Mcl-1 and Bim play important roles in CUDC-907-induced apoptosis**

To confirm the roles of Mcl-1 and Bim in CUDC-907-induced apoptosis, Mcl-1 overexpression and Bim shRNA knockdown were performed in U937 cells. Western blot analysis confirmed overexpression of Mcl-1 and knock-

down of Bim (Figure 5A, B; left panels). Annexin V/PI staining and flow cytometry analysis revealed that Mcl-1 overexpression and Bim knockdown partially prevented CUDC-907-induced apoptosis (Figure 5A, B; right panels), providing evidence that Mcl-1 and Bim play roles in CUDC-907-induced apoptosis. Real-time reverse transcriptase PCR results showed that CUDC-907 treatment caused a concentration-dependent and significant increase of Bim transcripts, while Mcl-1 transcript levels remained largely unchanged in both AML cell lines and two primary patient samples (Figure 5C, D). Similar results were

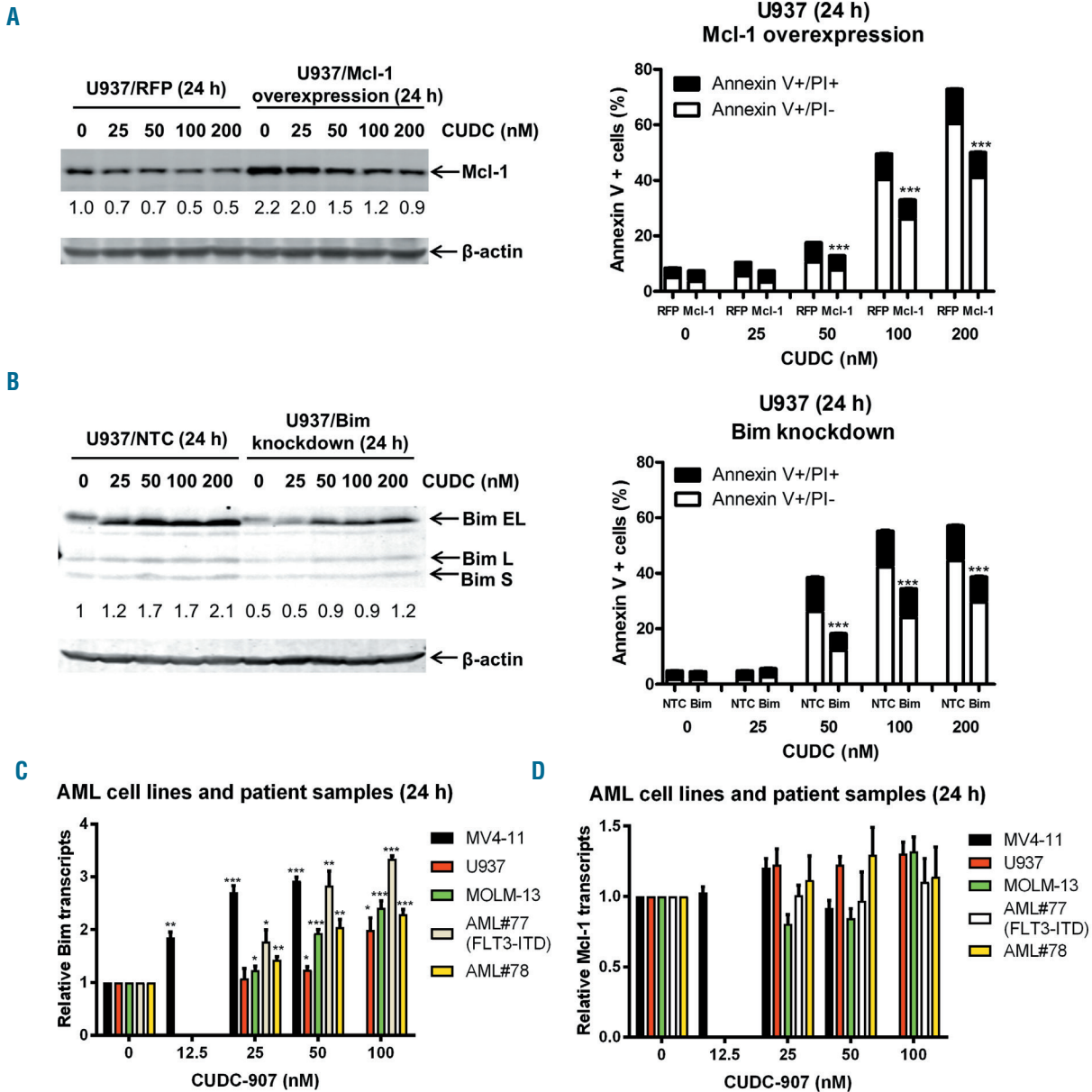


**Figure 5. Mcl-1 and Bim play important roles in CUDC-907-induced apoptosis in acute myeloid leukemia cells.** (A, B) U937 cells were infected with Precision LentiORF Mcl-1 (U937/Mcl-1) and RFP control (U937/RFP) (A) or NTC (U937/NTC) and Bim-shRNA (U937/Bim) (B) lentivirus particles overnight, then washed and incubated for 48 h prior to the addition of blasticidin or puromycin, respectively, to the culture medium. The antibiotic-resistant cells were treated with CUDC-907 for 24 h. Whole cell lysates were subjected to western blotting. The fold changes for the Mcl-1 or Bim densitometry measurements, normalized to β-actin and then compared to no drug treatment control, are indicated (left panel). The cells were treated with CUDC-907 for 24 h and then subjected to annexin V/propidium iodide staining and flow cytometry analysis. \*\*\**P*<0.001 (right panel). Bim S, L, and EL indicate Bim short, long, and extra-long isoforms, respectively. (C, D) MV4-11, U937 and MOLM-13 AML cell lines and two primary AML patient samples were treated with 0-100 nM CUDC-907 for 24 h. Total RNA was isolated and Bim (C) and Mcl-1 (D) transcripts were determined by real-time reverse transcriptase polymerase chain reaction (RT-PCR). \**P*<0.05, \*\**P*<0.01, and \*\*\**P*<0.001. (continued on the next page)

obtained in MV4-11 xenograft samples following a single dose of CUDC-907 (Figure 5E). A Mcl-1 protein stability assay using cycloheximide (10  $\mu\text{g}/\text{mL}$ ) revealed that Mcl-1 levels decreased faster in CUDC-907-treated cells than in vehicle-treated cells, resulting in a significantly shorter half-life (MOLM-13: 58 vs. 83 min,  $P=0.0266$ ; U937: 79 vs. 94 min,  $P=0.0211$ ) (Figure 5F, G). These results demonstrate that CUDC-907 downregulates Mcl-1 expression by decreasing the stability of Mcl-1 protein.

Phosphorylation of Mcl-1 at T163 has been shown to stabilize Mcl-1 by prolonging its half-life<sup>27</sup> and phosphorylation at S159 enhances ubiquitylation and degradation.<sup>28</sup> In MOLM-13 and U937 cells, CUDC-907 treatment caused downregulation of p-Mcl-1 (T163), while p-Mcl-1

(S159) levels remained unchanged (Figure 5H; upper panel). Treatment with the proteasome inhibitor MG-132, prevented downregulation of Mcl-1 by CUDC-907 (Figure 5H; lower panel). Since ERK has been reported to phosphorylate Mcl-1 at T163<sup>27</sup> and CUDC-907 treatment inactivates ERK, we treated MOLM-13 cells with the ERK inhibitor SCH-772984 and found that treatment did indeed downregulate p-Mcl-1 (T163), while having little to no effect on p-Mcl-1 (S159) levels (*Online Supplementary Figure S6A*). MG-132 treatment prevented downregulation of Mcl-1 following SCH-772984 treatment (*Online Supplementary Figure S6B*). Taken together, these results suggest that CUDC-907 inactivates ERK, resulting in decreased Mcl-1 stability and Mcl-1 protein levels.

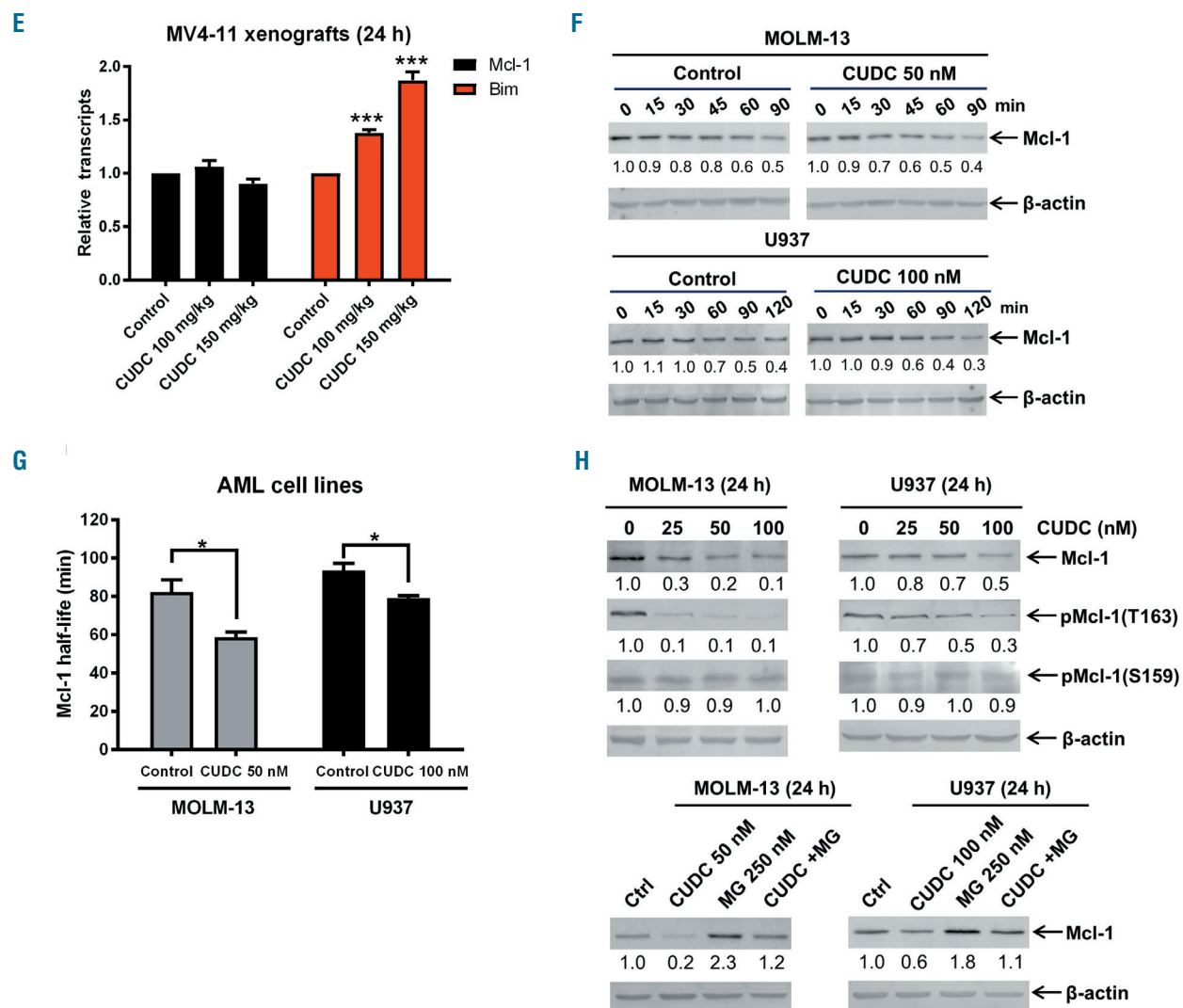


**Figure 5.** (continued from the previous page) (E) Cells obtained from the MV4-11 xenografts, which were treated with a single dose of CUDC-907, were enriched for human cells. Then total RNA was isolated and real-time RT-PCR performed to determine Mcl-1 and Bim transcripts. \*\*\* $P<0.001$ . (F, G) MOLM-13 and U937 cells were treated with vehicle control, 50 nM CUDC-907 or 100 nM CUDC-907 for 12 h, washed and then treated with cycloheximide (CHX) for up to 2 h. Whole cell lysates were subjected to western blotting and probed with anti-Mcl-1 or anti- $\beta$ -actin antibody. The fold changes for the Mcl-1 densitometry measurements, normalized to  $\beta$ -actin and then compared with no drug treatment control, are shown as mean  $\pm$  standard error of mean. \* $P<0.05$ . (H) MOLM-13 and U937 cells were treated with CUDC-907, MG-132, or MG-132 plus CUDC-907 for 24 h. Western blot analyses of whole cell lysates are shown. The fold changes for the densitometry measurements, normalized to  $\beta$ -actin and then compared to no drug treatment control, are indicated. RFP: red fluorescent protein; CUDC: CUDC-907; NTC: non-treated control; AML: acute myeloid leukemia; MG: MG-132, a proteasome inhibitor.

**CUDC-907 treatment induces DNA damage in acute myeloid leukemia cells but spares normal human bone marrow mononuclear cells**

Western blot analysis revealed that CUDC-907 treatment substantially increased chromatin-bound RPA32 and  $\gamma$ H2AX levels, indicating that CUDC-907 treatment induced DNA replication stress and damage (Figure 6A, B). Furthermore, alkaline comet assay results showed that

CUDC-907 induced significant increases in DNA strand breaks, as indicated by increased %DNA in the tail (greater %DNA in the tail corresponds to increased DNA strand breaks), for both AML cell lines (Figure 6C, D). The pan-caspase inhibitor Z-VAD-FMK did not have an effect on the %DNA in the tail following CUDC-907 treatment, demonstrating that the increased DNA damage was not a reflection of caspase-dependent cell death (*Online*

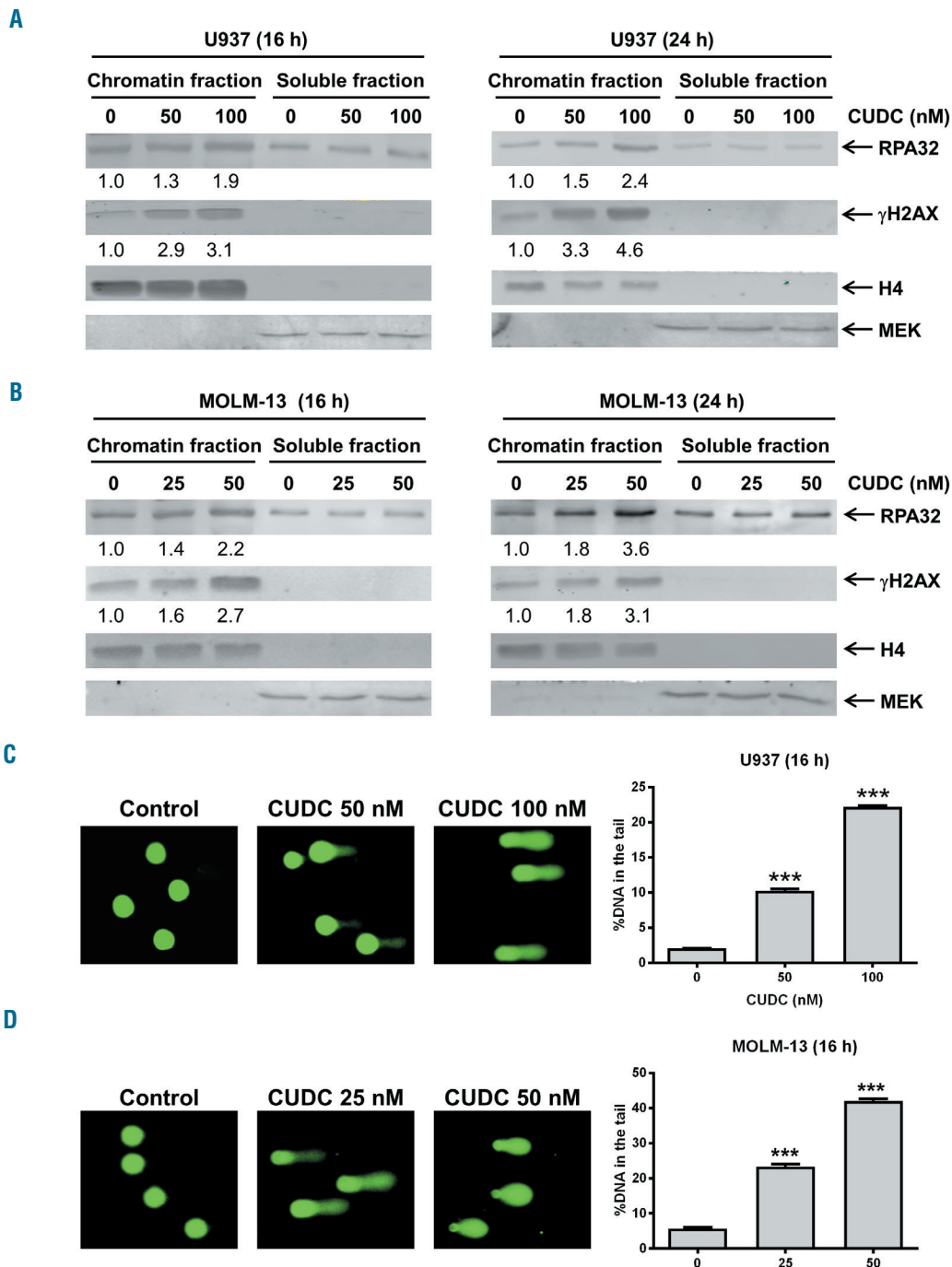


**Figure 6. CUDC-907 treatment induces DNA replication stress and damage in acute myeloid leukemia cells but not in normal human bone marrow mononuclear cells.** (A, B) U937 (A) and MOLM-13 (B) cells were treated with CUDC-907 for 16 or 24 h. Chromatin-bound and soluble RPA32 and  $\gamma$ H2AX were analyzed by western blotting and probed with the indicated antibodies. Densitometry measurements, normalized to histone H4 and then compared to the control, are indicated. (C, D) U937 (C) and MOLM-13 (D) cells were treated with CUDC-907 for 16 h and then subjected to alkaline comet assay analysis. Representative images are shown. Data are presented as mean percent DNA in the tail from three replicate gels  $\pm$  the standard error of mean (SEM). \*\*\* $P$ <0.001. (continued on the next page)

E

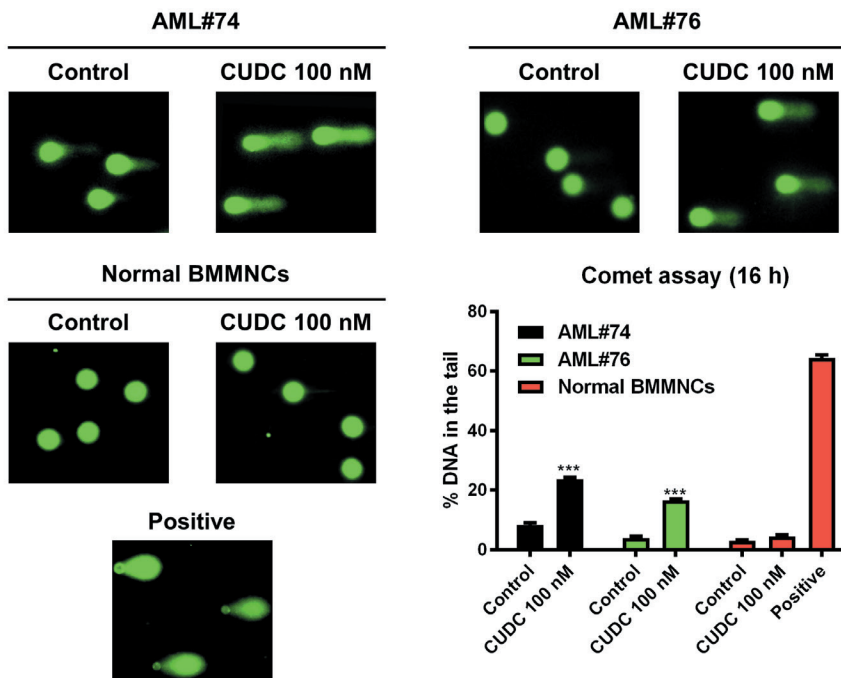
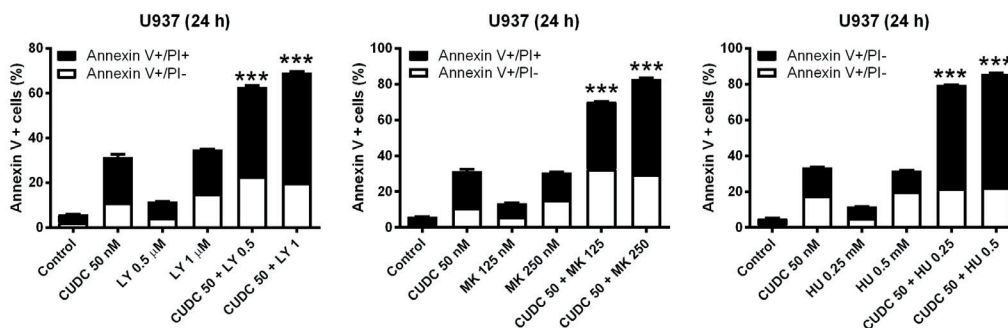
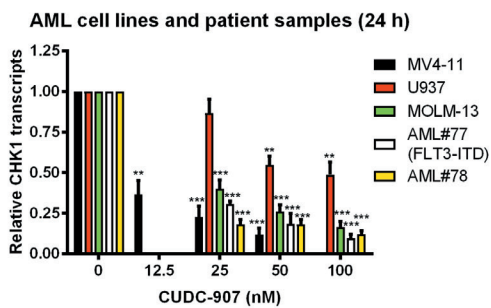


**Figure 6.** (continued from the previous page) (E) Primary cells from patients with acute myeloid leukemia (AML) and normal human bone marrow mononuclear cells (BMMNC) from a single donor were treated with CUDC-907 for 16 h and then subjected to alkaline comet assay analysis. Cells treated with 20 μM daunorubicin (DNR) for 4 h were used as a positive control. Representative images are shown. Data are presented as mean percent DNA in the tail from three replicate gels ± SEM. \*\*\**P*<0.001. (F) U937 cells were treated with CUDC-907 in the presence or absence of LY2603618 (LY), MK-1775 (MK), or hydroxyurea (HU) for 24 h and then subjected to annexin V/propidium iodide (PI) staining and flow cytometry analyses. \*\*\**P*<0.001. (G-I) MV4-11, U937 and MOLM-13 AML cell lines and two primary AML patients samples were treated with 0-100 nM CUDC-907 for 24 h. Total RNA was isolated and CHK1 (G), RRM1 (H), and Wee1 (I) transcripts were determined by real-time reverse transcriptase polymerase chain reaction (RT-PCR). \**P*<0.05, \*\**P*<0.01, and \*\*\**P*<0.001. (J) Cells obtained from the MV4-11 xenografts, which were treated with a single dose of CUDC-907, were enriched for human cells. Then total RNA was isolated and real-time RT-PCR performed to determine CHK1, RRM1, and Wee1 transcripts. \**P*<0.05, \*\**P*<0.01, and \*\*\**P*<0.001.

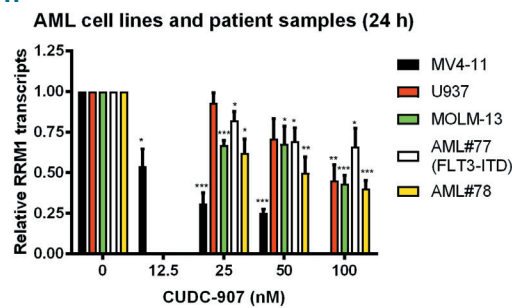
F



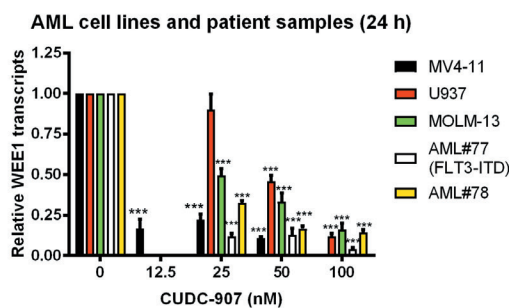
G



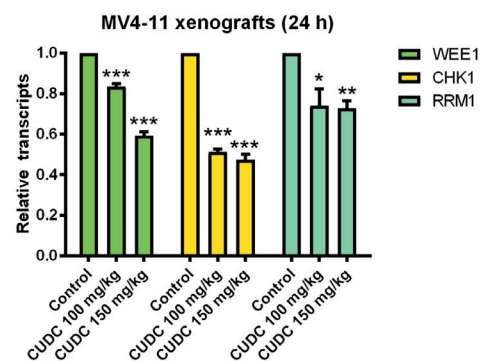
H



I



J



Supplementary Figure S7). DNA strand breaks induced by CUDC-907 were also detected in two primary AML patient samples but not in normal human bone marrow mononuclear cells (Figure 6E), suggesting that CUDC-907 does not induce DNA damage in normal hematopoietic cells. To determine the functional role of CHK1, Wee1, and RRM1 in apoptosis induced by CUDC-907, U937 cells were treated with CUDC-907 alone or in combination with the CHK1 inhibitor LY2603618, Wee1 inhibitor MK-1775, or the RR inhibitor hydroxyurea for 24 h. Annexin V/PI staining and flow cytometry revealed that each inhibitor significantly enhanced CUDC-907-induced apoptosis (Figure 6F), which suggests that CHK1, Wee1, and RRM1 also play important roles in CUDC-907-induced apoptosis in the cells. Real-time reverse transcriptase PCR results showed that CUDC-907 treatment caused significant decreases of CHK1, Wee1, and RRM1 transcripts in the AML cells both *in vitro* and *in vivo* (Figure 6G-J), suggesting that CUDC-907 downregulates CHK1, Wee1, and RRM1 expression in the cells through transcriptional regulation. While it has been reported that non-isofom selective PI3K inhibitors also inhibit DNA-PK, inhibition of DNA-PK is not likely to have contributed to the increased DNA damage-induced by CUDC-907 since its effect on DNA-PK activity was minimal (Online Supplementary Figure S8).

**CUDC-907 downregulates c-Myc in acute myeloid leukemia cells**

CUDC-907 treatment was shown to downregulate c-Myc protein in diffuse large B-cell lymphoma cells.<sup>16</sup> Since c-Myc is an oncoprotein that is frequently activated in AML cells and plays a role in leukemogenesis,<sup>29,30</sup> we next determined the role of c-Myc in CUDC-907-induced apoptosis in AML cells. Indeed, CUDC-907 treatment decreased expression of c-Myc in AML cell lines and a primary AML sample (Figure 7A). In addition, decreased expression was detected in our MV4-11 xenograft mouse model following a single dose of CUDC-907 (Figure 7B). The pan-caspase inhibitor Z-VAD-FMK did not have an effect on downregulation of c-Myc by CUDC-907 (Online Supplementary Figure S9A). Furthermore, treatment with SAHA, GDC-0941, and SAHA plus GDC-0941 did not reduce c-Myc protein levels, again suggesting that the hybrid is more potent than the parental compounds (Online Supplementary Figure S9B). In both MOLM-13 and U937 cells, downregulation of c-Myc was detected as early as 4 h after CUDC-907 treatment (Figure 7C). c-Myc transcript levels were decreased in AML cell lines, two primary AML patient samples (Figure 7D) and in the MV4-11 xenograft mouse model following a single dose of CUDC-907 (Figure 7E). Overexpression of c-Myc resulted in partial inhibition of CUDC-907-induced apoptosis (Figure

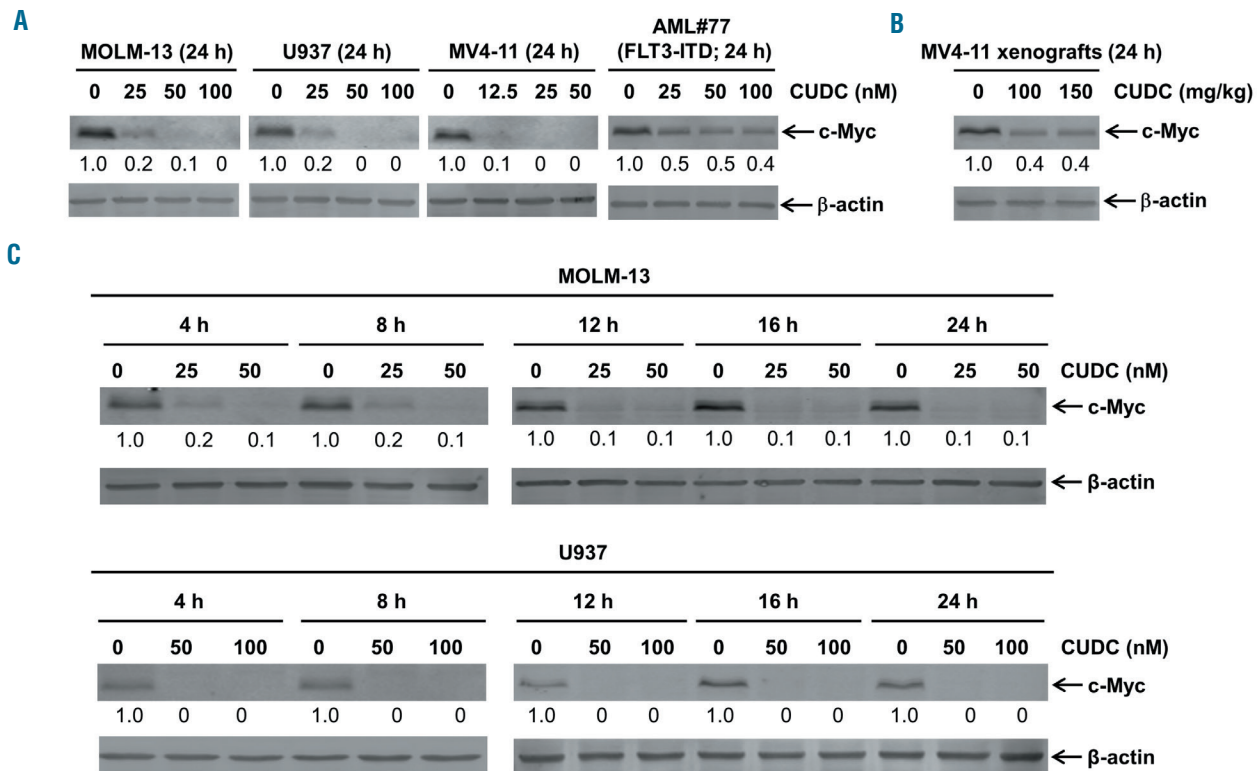


**Figure 7. CUDC-907 treatment downregulates c-Myc in acute myeloid leukemia cells.** (A) Acute myeloid leukemia (AML) cell lines and primary AML patient sample AML#77 were treated with CUDC-907 for 24 h. Whole cell lysates were subjected to western blotting. Normalized densitometry measurements are shown. (B) The MV4-11 xenograft model was treated with a single dose of CUDC-907 21 days after cell injection. Bone marrow cells were harvested 24 h after treatment. Human cells were enriched and then whole cell lysates were subjected to western blotting. (C) MOLM-13 and U937 cells were treated with CUDC-907 for up to 24 h. Whole cell lysates were subjected to western blotting. (continued on the next page)

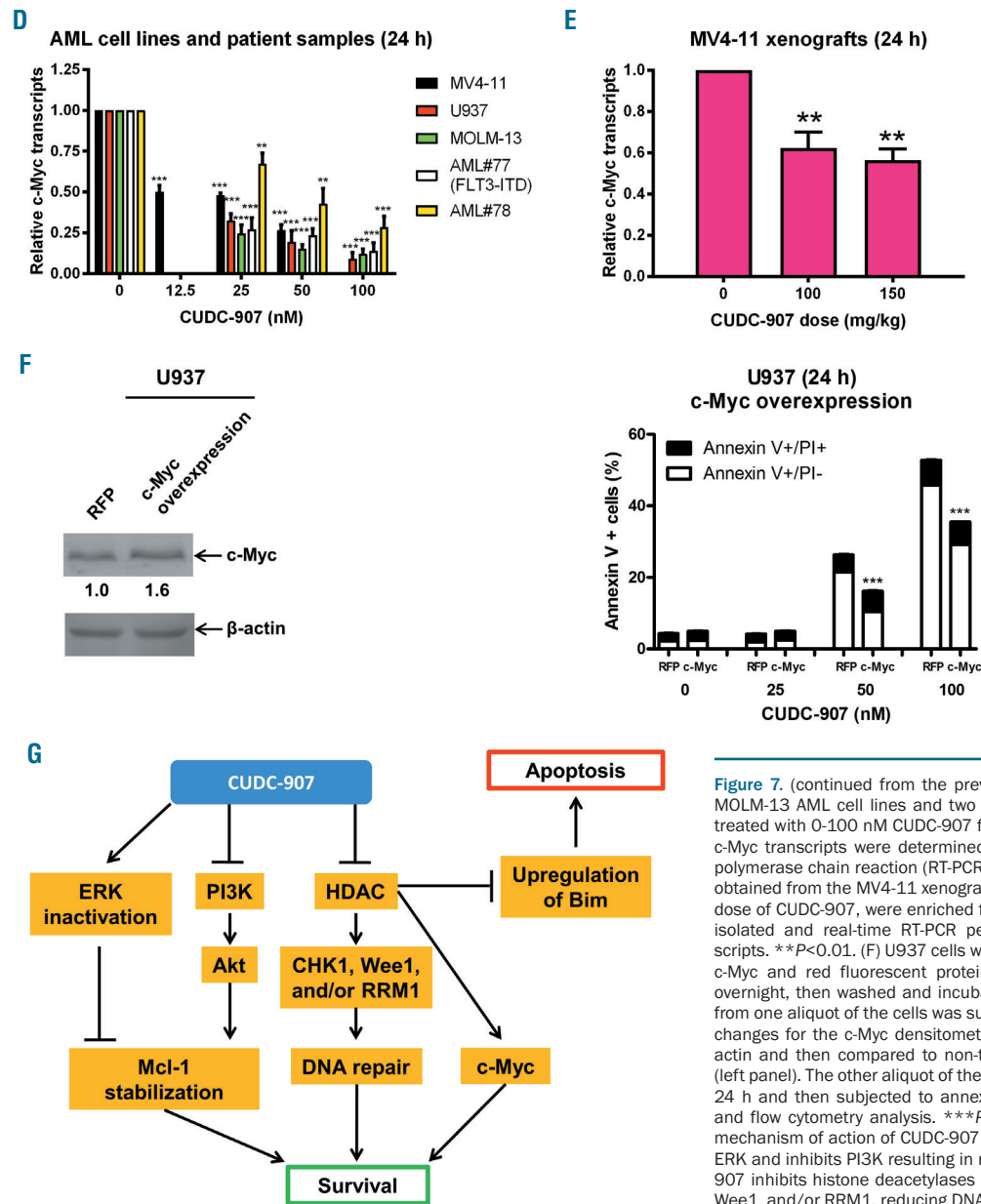


**Figure 7.** (continued from the previous page) (D) MV4-11, U937 and MOLM-13 AML cell lines and two primary AML patient samples were treated with 0-100 nM CUDC-907 for 24 h. Total RNA was isolated and c-Myc transcripts were determined by real-time reverse transcriptase polymerase chain reaction (RT-PCR). \*\* $P < 0.01$ , \*\*\* $P < 0.001$ . (E) Cells obtained from the MV4-11 xenografts, which were treated with a single dose of CUDC-907, were enriched for human cells. Then total RNA was isolated and real-time RT-PCR performed to determine c-Myc transcripts. \*\* $P < 0.01$ . (F) U937 cells were infected with Precision LentiORF c-Myc and red fluorescent protein (RFP) control lentivirus particles overnight, then washed and incubated for 24 h. The whole cell lysate from one aliquot of the cells was subjected to western blotting. The fold changes for the c-Myc densitometry measurements, normalized to  $\beta$ -actin and then compared to non-treated control (NTC), are indicated (left panel). The other aliquot of the cells was treated with CUDC-907 for 24 h and then subjected to annexin V/propidium iodide (PI) staining and flow cytometry analysis. \*\*\* $P < 0.001$  (right panel). (G) Proposed mechanism of action of CUDC-907 treatment: (i) CUDC-907 inactivates ERK and inhibits PI3K resulting in reduced Mcl-1 expression; (ii) CUDC-907 inhibits histone deacetylases (HDAC) which downregulates CHK1, Wee1, and/or RRM1, reducing DNA repair; (iii) CUDC-907 inhibits HDAC decreasing c-Myc; and (iv) CUDC-907 inhibits HDAC which upregulates Bim. The foregoing molecular changes lead to apoptosis.

7F), demonstrating that c-Myc plays a role in CUDC-907-induced apoptosis in AML cells.

**Discussion**

A major hurdle in the successful treatment of AML is resistance to standard therapies, which warrants the development of novel strategies. Here, we showed that CUDC-907 has promising antileukemic activity against AML cell lines, both *in vitro* and *in vivo*, and against leukemia progenitor cells from primary AML patient samples. CUDC-907 treatment decreased expression of the anti-apoptotic protein Mcl-1 and increased expression of the pro-apoptotic protein Bim. Ectopic overexpression of

Mcl-1 and shRNA knockdown of Bim demonstrated that both proteins play important roles in CUDC-907-induced apoptosis in AML cells (Figure 5A, B). Our results are consistent with the known effects of PI3K and HDAC inhibition, which have been shown to decrease the anti-apoptotic protein Mcl-1 and upregulate the pro-apoptotic protein Bim.<sup>22-25</sup> In addition, they are in agreement with the findings of Rahmani *et al.* who demonstrated that Bim and Mcl-1 play a role in HDAC and PI3K inhibitor lethality in non-Hodgkin lymphoma.<sup>12</sup> Our data show that CUDC-907 treatment decreases the stability of Mcl-1, at least partially through its ability to inactivate ERK (Figure 5D-H). Based on the reported transcriptional regulation of Bim following HDAC inhibitor treatment<sup>31,32</sup> and the increase in Bim transcripts following CUDC-907 treatment (Figure

5C), the upregulation of Bim (Figure 3B) was likely due to transcriptional regulation mediated by the HDAC inhibitor moiety of CUDC-907. However, given the evidence that the ERK pathway regulates Bim degradation,<sup>33,34</sup> post-transcriptional mechanisms cannot be ruled out. Additionally, inactivation of AKT and ERK may also contribute to the antileukemic activity of CUDC-907 through other downstream targets.<sup>12,14</sup>

HDAC inhibitors have been shown to induce differentiation, cell cycle arrest, DNA damage, and apoptosis in AML cells.<sup>20,26,35-37</sup> One mechanism through which HDAC inhibitors exert their anticancer activity is through downregulation of DNA damage response proteins, such as CHK1 and Wee1, as we and others have reported.<sup>23-26</sup> In agreement, we detected downregulation of CHK1 and Wee1 protein and transcript levels (Figures 3C and 6G, I, and J). HDAC inhibitor-induced downregulation of CHK1 and Wee1 has been shown to be mediated through downregulation of E2F1.<sup>37,38</sup> However, the decrease of E2F1 was not consistent in the AML cell lines and primary AML patient sample. CUDC-907 treatment caused decreases of E2F1, CHK1, and Wee1 in three AML cell lines and one primary AML patient's sample. However, in the other primary AML patient sample, CUDC-907 treatment did not result in a decrease of E2F1 protein but did decrease both CHK1 and Wee1 protein levels. These results suggest that downregulation of CHK1 and Wee1 was probably mediated through transcript regulation, though it may not have been entirely mediated through downregulation of E2F1.

CUDC-907 treatment also decreased RRM1 protein and transcript levels (Figures 3C and 6H, J), suggesting that downregulation of this gene was probably mediated by a transcriptional mechanism. Based on our results using hydroxyurea, RRM1 likely played an important role in CUDC-907-induced DNA damage. Inhibition of RR decreases dNTP pools, resulting in DNA replication fork stalling, impaired DNA repair, and DNA damage.<sup>39</sup> In agreement with Sun *et al.*,<sup>16</sup> we found that CUDC-907 treatment reduced expression of c-Myc protein prior to induction of apoptosis (Figures 4C, D and 7C). Given its role in cell growth, proliferation, and survival, the early downregulation of c-Myc may play a more prominent role in CUDC-907-induced apoptosis since changes in CHK1, Wee1, RRM1, Bim, and Mcl-1 levels occur after c-Myc downregulation.

*FLT3*-ITD AML has been shown to be associated with increased DNA damage and misrepair,<sup>40</sup> potentially making such leukemias more sensitive to DNA replication fork stalling, impaired DNA repair, and DNA damage. Interestingly, we found that primary AML samples from patients with *FLT3*-ITD were significantly more sensitive to CUDC-907 *ex vivo* (Figure 2A). *FLT3*-ITD has also been shown to constitutively activate downstream PI3K and ERK pathways, conferring resistance to PI3K and ERK inhibitors. However, HDAC inhibitors have been shown to upregulate ubiquitin conjugase<sup>41</sup> and inhibit HSP90 resulting in proteasomal degradation of *FLT3*.<sup>42,43</sup> Consistent with those reports, CUDC-907 treatment did indeed decrease *FLT3* protein levels in the *FLT3*-ITD AML cell line MOLM-13 (Online Supplementary Figure S10). Thus, the HDAC inhibitor moiety of CUDC-907 reduces *FLT3* levels, relieving constitutive activation of the PI3K and ERK pathways, and allowing the PI3K inhibitor function of

CUDC-907 to induce AML cell death. This may explain the superior response of *FLT3*-ITD AML cells to CUDC-907 (Figure 2A), although the effects of CUDC-907 on AML cell apoptosis, colony-formation capacity, and *FLT3* protein levels need to be further elucidated in additional primary samples from patients with *FLT3*-ITD AML.

Results of the first phase I trial of CUDC-907 were recently published, outlining the safety, tolerability, and preliminary activity in patients with lymphoma or multiple myeloma.<sup>17</sup> In that study, the recommended dosing for further clinical studies was identified to be 60 mg administered orally, once daily for 5 days, followed by 2 days off treatment, as there were no dose-limiting toxicities at this dosing and schedule. In addition, side effects were consistent with the known profile of HDAC or PI3K inhibitors and deemed manageable. Our data show promising *in vivo* efficacy against an AML cell line-derived xenograft mouse model, supporting further clinical development of CUDC-907 as an AML-focused therapy. While modest weight loss was seen after CUDC-907 treatment (nadir: -5.4% on day 22, 2 days after last treatment), it was completely reversible within 4 days. This fact coupled with the observed modest survival benefit produced from the interrupted treatment schedule indicate that either or both the dosing and schedule can be further optimized (i.e. in hindsight, the drug was so well tolerated that the 4-day interruption of treatment may not have been necessary). Furthermore, the tolerability of CUDC-907 suggests that it may be used in combination with other therapies. Conventional chemotherapy drugs, such as cytarabine or daunorubicin, may synergize with CUDC-907 as these drugs induce DNA damage and would likely add further insult to the stressed DNA repair system following CUDC-907 treatment.

In summary, our study demonstrates that CUDC-907 induces DNA damage and apoptosis in AML cell lines and primary patients' samples, and targets AML progenitor cells while sparing normal hematopoietic cells *in vitro*. In addition, our initial *in vivo* study generated a promising increase in survival following CUDC-907 monotherapy. As a dual inhibitor, CUDC-907 lends itself to the possibility of combination therapies to further eliminate AML and prevent disease relapse. Our findings provide new insights into the mechanism of action of CUDC-907 in AML cells (Figure 7G) and support its clinical development for the treatment of AML.

#### Acknowledgments

This study was supported by Jilin University, Changchun, China, the Barbara Ann Karmanos Cancer Institute, Wayne State University School of Medicine, and by grants from the National Natural Science Foundation of China, NSFC 31671438 and NSFC 31471295, Hyundai Hope on Wheels, LaFontaine Family/U Can-Cer Vive Foundation, Kids Without Cancer, Children's Hospital of Michigan Foundation, Decerchio/Guisewite Family, Justin's Gift, Elana Fund, Ginopolis/Karmanos Endowment and the Ring Screw Textron Endowed Chair for Pediatric Cancer Research. The Animal Models and Therapeutics Evaluation Core is supported, in part, by NIH Center grant P30 CA022453 to the Karmanos Cancer Institute at Wayne State University. The funders had no role in study design, data collection, analysis and interpretation of data, decision to publish, or preparation of the manuscript.

## References

- Marcucci G, Haferlach T, Dohner H. Molecular genetics of adult acute myeloid leukemia: prognostic and therapeutic implications. *J Clin Oncol*. 2011;29(5):475-486.
- Rubnitz JE, Inaba H, Dahl G, et al. Minimal residual disease-directed therapy for childhood acute myeloid leukaemia: results of the AML02 multicentre trial. *Lancet Oncol*. 2010;11(6):543-552.
- Doan PL, Chute JP. The vascular niche: home for normal and malignant hematopoietic stem cells. *Leukemia*. 2012;26(1):54-62.
- Min YH, Eom JI, Cheong JW, et al. Constitutive phosphorylation of Akt/PKB protein in acute myeloid leukemia: its significance as a prognostic variable. *Leukemia*. 2003;17(5):995-997.
- Gallay N, Dos Santos C, Cuzin L, et al. The level of AKT phosphorylation on threonine 308 but not on serine 473 is associated with high-risk cytogenetics and predicts poor overall survival in acute myeloid leukaemia. *Leukemia*. 2009;23(6):1029-1038.
- Guo W, Schubert S, Chen JY, et al. Suppression of leukemia development caused by PTEN loss. *Proc Natl Acad Sci U S A*. 2011;108(4):1409-1414.
- Xu Q, Simpson SE, Scialla TJ, Bagg A, Carroll M. Survival of acute myeloid leukemia cells requires PI3 kinase activation. *Blood*. 2003;102(3):972-980.
- Fransecky L, Mochmann LH, Baldus CD. Outlook on PI3K/AKT/mTOR inhibition in acute leukemia. *Mol Cell Ther*. 2015;3:2.
- Rozenfurt E, Soares HP, Sinnet-Smith J. Suppression of feedback loops mediated by PI3K/mTOR induces multiple overactivation of compensatory pathways: an unintended consequence leading to drug resistance. *Mol Cancer Ther*. 2014;13(11):2477-2488.
- Mendoza MC, Er EE, Blenis J. The Ras-ERK and PI3K-mTOR pathways: cross-talk and compensation. *Trends Biochem Sci*. 2011;36(6):320-328.
- Rahmani M, Yu C, Reese E, et al. Inhibition of PI-3 kinase sensitizes human leukemic cells to histone deacetylase inhibitor-mediated apoptosis through p44/42 MAP kinase inactivation and abrogation of p21(CIP1/WAF1) induction rather than AKT inhibition. *Oncogene*. 2003;22(40):6231-6242.
- Rahmani M, Aust MM, Benson EC, Wallace L, Friedberg J, Grant S. PI3K/mTOR inhibition markedly potentiates HDAC inhibitor activity in NHL cells through BIM- and MCL-1-dependent mechanisms in vitro and in vivo. *Clin Cancer Res*. 2014;20(18):4849-4860.
- Gupta M, Ansell SM, Novak AJ, Kumar S, Kaufmann SH, Witzig TE. Inhibition of histone deacetylase overcomes rapamycin-mediated resistance in diffuse large B-cell lymphoma by inhibiting Akt signaling through mTORC2. *Blood*. 2009;114(14):2926-2935.
- Qian C, Lai CJ, Bao R, et al. Cancer network disruption by a single molecule inhibitor targeting both histone deacetylase activity and phosphatidylinositol 3-kinase signaling. *Clin Cancer Res*. 2012;18(15):4104-4113.
- Kotian S, Zhang L, Boufraqueh M, et al. Dual inhibition of HDAC and tyrosine kinase signaling pathways with CUDC-907 inhibits thyroid cancer growth and metastases. *Clin Cancer Res*. 2017;23(17):5044-5054.
- Sun K, Atoyian R, Borek MA, et al. Dual HDAC and PI3K inhibitor CUDC-907 Downregulates MYC and suppresses growth of MYC-dependent cancers. *Mol Cancer Ther*. 2017;16(2):285-299.
- Younes A, Berdeja JG, Patel MR, et al. Safety, tolerability, and preliminary activity of CUDC-907, a first-in-class, oral, dual inhibitor of HDAC and PI3K, in patients with relapsed or refractory lymphoma or multiple myeloma: an open-label, dose-escalation, phase 1 trial. *Lancet Oncol*. 2016;17(5):622-631.
- Niu X, Wang G, Wang Y, et al. Acute myeloid leukemia cells harboring MLL fusion genes or with the acute promyelocytic leukemia phenotype are sensitive to the Bcl-2-selective inhibitor ABT-199. *Leukemia*. 2014;28(7):1557-1560.
- Ma J, Li X, Su Y, et al. Mechanisms responsible for the synergistic antileukemic interactions between ATR inhibition and cytarabine in acute myeloid leukemia cells. *Sci Rep*. 2017;7:41950.
- Xie C, Edwards H, Xu X, et al. Mechanisms of synergistic antileukemic interactions between valproic acid and cytarabine in pediatric acute myeloid leukemia. *Clin Cancer Res*. 2010;16(22):5499-5510.
- Edwards H, Xie C, LaFiura KM, et al. RUNX1 regulates phosphoinositide 3-kinase/AKT pathway: role in chemotherapy sensitivity in acute megakaryocytic leukemia. *Blood*. 2009;114(13):2744-2752.
- Martelli AM, Evangelisti C, Chappell W, et al. Targeting the translational apparatus to improve leukemia therapy: roles of the PI3K/PTEN/Akt/mTOR pathway. *Leukemia*. 2011;25(7):1064-1079.
- Inoue S, Riley J, Gant TW, Dyer MJ, Cohen GM. Apoptosis induced by histone deacetylase inhibitors in leukemic cells is mediated by Bim and Noxa. *Leukemia*. 2007;21(8):1773-1782.
- Chen S, Dai Y, Pei XY, Grant S. Bim upregulation by histone deacetylase inhibitors mediates interactions with the Bcl-2 antagonist ABT-737: evidence for distinct roles for Bcl-2, Bcl-xL, and Mcl-1. *Mol Cell Biol*. 2009;29(23):6149-6169.
- Fiskus W, Sharma S, Saha S, et al. Pre-clinical efficacy of combined therapy with novel beta-catenin antagonist BC2059 and histone deacetylase inhibitor against AML cells. *Leukemia*. 2015;29(6):1267-1278.
- Qi W, Zhang W, Edwards H, et al. Synergistic anti-leukemic interactions between panobinostat and MK-1775 in acute myeloid leukemia ex vivo. *Cancer Biol Ther*. 2015;16(12):1784-1793.
- Domina AM, Vrana JA, Gregory MA, Hann SR, Craig RW. MCL1 is phosphorylated in the PEST region and stabilized upon ERK activation in viable cells, and at additional sites with cytotoxic okadaic acid or taxol. *Oncogene*. 2004;23(31):5301-5315.
- Maurer U, Charvet C, Wagman AS, Dejardin E, Green DR. Glycogen synthase kinase-3 regulates mitochondrial outer membrane permeabilization and apoptosis by destabilization of MCL-1. *Mol Cell*. 2006;21(6):749-760.
- Hoffman B, Amanullah A, Shafarenko M, Liebermann DA. The proto-oncogene c-myc in hematopoietic development and leukemogenesis. *Oncogene*. 2002;21(21):3414-3421.
- Renneville A, Roumier C, Biggio V, et al. Cooperating gene mutations in acute myeloid leukemia: a review of the literature. *Leukemia*. 2008;22(5):915-931.
- Xargay-Torrent S, Lopez-Guerra M, Saborit-Villarroya I, et al. Vorinostat-induced apoptosis in mantle cell lymphoma is mediated by acetylation of proapoptotic BH3-only gene promoters. *Clin Cancer Res*. 2011;17(12):3956-3968.
- Yang Y, Zhao Y, Liao W, et al. Acetylation of FoxO1 activates Bim expression to induce apoptosis in response to histone deacetylase inhibitor depsipeptide treatment. *Neoplasia*. 2009;11(4):313-324.
- Ley R, Balmanno K, Hadfield K, Weston C, Cook SJ. Activation of the ERK1/2 signaling pathway promotes phosphorylation and proteasome-dependent degradation of the BH3-only protein, Bim. *J Biol Chem*. 2003;278(21):18811-18816.
- Luciano F, Jacquelin A, Colosetti P, et al. Phosphorylation of Bim-EL by Erk1/2 on serine 69 promotes its degradation via the proteasome pathway and regulates its proapoptotic function. *Oncogene*. 2003;22(43):6785-6793.
- Quintas-Cardama A, Santos FP, Garcia-Manero G. Histone deacetylase inhibitors for the treatment of myelodysplastic syndrome and acute myeloid leukemia. *Leukemia*. 2011;25(2):226-235.
- Minucci S, Pelicci PG. Histone deacetylase inhibitors and the promise of epigenetic (and more) treatments for cancer. *Nat Rev Cancer*. 2006;6(1):38-51.
- Xie C, Drenberg C, Edwards H, et al. Panobinostat enhances cytarabine and daunorubicin sensitivities in AML cells through suppressing the expression of BRCA1, CHK1, and Rad51. *PLoS One*. 2013;8(11):e79106.
- Carrassa L, Broggin M, Vikhanskaya F, Damia G. Characterization of the 5' flanking region of the human Chk1 gene: identification of E2F1 functional sites. *Cell Cycle*. 2003;2(6):604-609.
- Aye Y, Li M, Long MJ, Weiss RS. Ribonucleotide reductase and cancer: biological mechanisms and targeted therapies. *Oncogene*. 2015;34(16):2011-2021.
- Sallmyr A, Fan J, Datta K, et al. Internal tandem duplication of FLT3 (FLT3/ITD) induces increased ROS production, DNA damage, and misrepair: implications for poor prognosis in AML. *Blood*. 2008;111(6):3173-3182.
- Buchwald M, Pietschmann K, Muller JP, Bohmer FD, Heinzel T, Kramer OH. Ubiquitin conjugase UBC8 targets active FMS-like tyrosine kinase 3 for proteasomal degradation. *Leukemia*. 2010;24(8):1412-1421.
- Bali P, George P, Cohen P, et al. Superior activity of the combination of histone deacetylase inhibitor LAQ824 and the FLT-3 kinase inhibitor PKC412 against human acute myelogenous leukemia cells with mutant FLT-3. *Clin Cancer Res*. 2004;10(15):4991-4997.
- Nishioka C, Ikezoe T, Yang J, Takeuchi S, Koeffler HP, Yokoyama A. MS-275, a novel histone deacetylase inhibitor with selectivity against HDAC1, induces degradation of FLT3 via inhibition of chaperone function of heat shock protein 90 in AML cells. *Leuk Res*. 2008;32(9):1382-1392.

# Prolonged survival in the absence of disease-recurrence in advanced-stage follicular lymphoma following chemo-immunotherapy: 13-year update of the prospective, multicenter randomized GITMO-III trial

Riccardo Bruna,<sup>1,5</sup> Fabio Benedetti,<sup>2</sup> Carola Boccomini,<sup>3</sup> Caterina Patti,<sup>4</sup> Anna Maria Barbui,<sup>5</sup> Alessandro Pulsoni,<sup>6</sup> Maurizio Musso,<sup>7</sup> Anna Marina Liberati,<sup>8</sup> Guido Gini,<sup>9</sup> Claudia Castellino,<sup>10</sup> Fausto Rossini,<sup>11</sup> Fabio Ciceri,<sup>12</sup> Delia Rota-Scalabrini,<sup>13</sup> Caterina Stelitano,<sup>14</sup> Francesco Di Raimondo,<sup>15</sup> Alessandra Tucci,<sup>16</sup> Liliana Devizzi,<sup>17</sup> Valerio Zoli,<sup>18</sup> Francesco Zallio,<sup>19</sup> Franco Narni,<sup>20</sup> Alessandra Dondi,<sup>21</sup> Guido Parvis,<sup>22</sup> Gianpietro Semenzato,<sup>23</sup> Francesco Lanza,<sup>24</sup> Tommasina Perrone,<sup>25</sup> Francesco Angrilli,<sup>26</sup> Atto Billio,<sup>27</sup> Angela Gueli,<sup>1</sup> Barbara Mantoan,<sup>28</sup> Alessandro Rambaldi,<sup>5,29</sup> Alessandro Massimo Gianni,<sup>1</sup> Paolo Corradini,<sup>17,29</sup> Roberto Passera,<sup>30</sup> Marco Ladetto,<sup>19</sup> Corrado Tarella<sup>\*1,31</sup>

<sup>1</sup>Onco-Hematology Division, IEO, European Institute of Oncology IRCCS, Milano; <sup>2</sup>Hematology University Division, Verona; <sup>3</sup>Hematology Division, Città della Salute Hospital, Torino; <sup>4</sup>Hematology Division, Azienda Villa Sofia-Cervello, Palermo; <sup>5</sup>Hematology Division, Papa Giovanni XXIII Hospital, Bergamo; <sup>6</sup>Department of Cellular Biotechnologies and Hematology, La Sapienza University, Roma; <sup>7</sup>Hematology Unit, La Maddalena Hospital, Palermo; <sup>8</sup>SC Oncoematologia, Università degli Studi di Perugia; <sup>9</sup>Hematology University Division, Ancona; <sup>10</sup>Department of Hematology, S. Croce e Carle Hospital, Cuneo; <sup>11</sup>Hematology University Division, Monza; <sup>12</sup>Hematology Unit HSR, Milano; <sup>13</sup>Oncologia Medica, Cancer Institute FPO, IRCCS, Candiolo; <sup>14</sup>Hematology Division, Reggio Calabria; <sup>15</sup>Hematology University Division, Catania; <sup>16</sup>Division of Hematology, Brescia; <sup>17</sup>University Division of Hematology, Fondazione IRCCS Istituto Nazionale dei Tumori, Milano; <sup>18</sup>Hematology Division, S. Camillo Hospital, Roma; <sup>19</sup>SC Ematologia AO SS Antonio e Biagio e Cesare Arrigo, Alessandria; <sup>20</sup>Hematology University Division, Modena; <sup>21</sup>Division of Oncology, Modena; <sup>22</sup>Division of Internal Medicine, S. Luigi Hospital, Orbassano; <sup>23</sup>Hematology University Division, Padova; <sup>24</sup>Hematology Unit, Cremona; <sup>25</sup>Hematology University Division, Bari; <sup>26</sup>Hematology Division, Pescara; <sup>27</sup>Hematology Division, Bolzano; <sup>28</sup>Hematology University Division, Città della Salute Hospital, Torino; <sup>29</sup>Department of Oncology and Onco-Hematology, University of Milan, Milano; <sup>30</sup>Nuclear Medicine Division, Città della Salute Hospital, Torino and <sup>31</sup>Department of Health Sciences, University of Milan, Milano, Italy

Present address: <sup>5</sup>Division of Hematology, Ospedale Maggiore della Carità, Novara, <sup>\*</sup>University Hematology Division, Mauriziano Hospital, Torino <sup>^</sup>Hematology and SCT Unit, Ospedale di Ravenna

## ABSTRACT

A prospective trial conducted in the period 2000-2005 showed no survival advantage for high-dose chemotherapy with rituximab and autograft (R-HDS) *versus* conventional chemotherapy with rituximab (CHOP-R) as first-line therapy in 134 high-risk follicular lymphoma patients aged <60 years. The study has been updated at the 13-year median follow up. As of February 2017, 88 (66%) patients were alive, with overall survival of 66.4% at 13 years, without a significant difference between R-HDS (64.5%) and CHOP-R (68.5%). To date, 46 patients have died, mainly because of disease progression (47.8% of all deaths), secondary malignancies (3 solid tumor, 9 myelodysplasia/acute leukemia; 26.1% of all deaths), and other toxicities (21.7% of all deaths). Complete remission was documented in 98 (73.1%) patients and associated with overall survival, with 13-year estimates of 77.0% and 36.8% for complete remission *versus* no-complete remission, respectively. Molecular remission was documented in 39 (65%) out of 60 evaluable patients and associated with improved survival. In multivariate analysis, complete remission achievement had the strongest effect on survival ( $P<0.001$ ), along with younger age ( $P=0.002$ ) and female sex ( $P=0.013$ ). Overall, 50 patients (37.3%) survived with no disease recurrence (18 CHOP-R, 32 R-HDS). This follow up is the longest reported on follicular lymphoma treated upfront with rituximab-chemotherapy and demonstrates an unprecedented improvement in survival compared to the pre-rituximab era, regardless of the use of intensified or conventional treatment. Complete remission was the most important factor for prolonged survival and a high proportion of patients had prolonged survival in their first remission, raising the issue of curability in follicular lymphoma. (Registered at clinicaltrials.gov identifier: 00435955)



Ferrata Storti Foundation

Haematologica 2019  
Volume 104(11):2241-2248

## Correspondence:

CORRADO TARELLA  
corrado.tarella@unimi.it

Received: October 22, 2018.

Accepted: April 10, 2019.

Pre-published: April 11, 2019.

doi:10.3324/haematol.2018.209932

Check the online version for the most updated information on this article, online supplements, and information on authorship & disclosures: [www.haematologica.org/content/104/11/2241](http://www.haematologica.org/content/104/11/2241)

©2019 Ferrata Storti Foundation

Material published in *Haematologica* is covered by copyright. All rights are reserved to the Ferrata Storti Foundation. Use of published material is allowed under the following terms and conditions:

<https://creativecommons.org/licenses/by-nc/4.0/legalcode>. Copies of published material are allowed for personal or internal use. Sharing published material for non-commercial purposes is subject to the following conditions: <https://creativecommons.org/licenses/by-nc/4.0/legalcode>, sect. 3. Reproducing and sharing published material for commercial purposes is not allowed without permission in writing from the publisher.



## Introduction

The current first-line treatment strategy for symptomatic and advanced follicular lymphoma (FL) is chemo-immunotherapy, with rituximab in combination with various chemotherapy regimens.<sup>1,2</sup> For a long time now, the upfront use of intensified chemotherapy with autograft has been proposed as an effective treatment option for patients presenting with high-risk disease.<sup>3-8</sup> We previously conducted a prospective randomized trial of these regimens in Italy, including patients <60 years of age who were affected by high-risk FL. The results showed no survival advantage from high-dose sequential chemotherapy with rituximab and autograft (R-HDS) compared to conventional cyclophosphamide, doxorubicin, vincristine, and prednisone supplemented with rituximab (CHOP-R).<sup>9</sup> Despite the limited median follow up of four years, this observation has discouraged the upfront use of intensive chemo-immunotherapy with autograft in FL, including in patients with high-risk disease presentation.

Follicular lymphoma patients now have prolonged life expectancy, with a median survival of ten years. This survival rate is possible because of the availability of rituximab along with improvements in the supportive care instruments.<sup>10-15</sup> The increase in patient survival warrants a long-term update of clinical trials to evaluate the real benefit of any treatment. For this purpose, our previous results of the randomized R-HDS *versus* CHOP-R have been updated by extending the period of analysis to 2017 with a median follow up of 13 years. The prolonged observation of this prospective cohort of patients offers the opportunity to define the following in advanced-stage, high-risk FL patients: (i) the long-term survival following conventional *versus* intensified chemotherapy with autograft, both delivered with rituximab; (ii) the main causes of death; (iii) the main factors affecting long-term outcome; and (iv) the rate of patients with prolonged survival in the absence of disease recurrence.

## Methods

### Patients' characteristics

Between March 2000 and May 2005, a total of 136 patients were enrolled in the multicenter randomized study, launched in Italy among centers affiliated with Gruppo Italiano Trapianto Midollo Osseo (GITMO) and/or to the Italian Lymphoma Intergroup (IIL).<sup>9</sup> The institutional review boards of all the participating centers approved the study. The study was designed for the first-line treatment of patients aged 16-60 years with a histologically proven diagnosis of FL.<sup>14</sup> Patients were eligible if they had Ann Arbor stage III or IV and a high-risk prognostic presentation, according to the prognostic risk scores in use at the time the protocol was designed, i.e. the age-adjusted International Prognostic Index (IPI) score >2 and the IIL score >3 for FL.<sup>15,16</sup> The CONSORT Diagram in the *Online Supplementary Appendix* gives details about treatment outcome of the 136 enrolled patients. Table 1 describes the main features of the 134 evaluable patients and the main clinical features of patients who are presently alive *versus* those who have died since protocol entry.

### Study design, treatment schedule and end points

The aim of the study was to assess the superiority of an intensive chemo-immunotherapy strategy including autologous hematopoietic stem cell transplantation (auto-HSCT) compared to

conventional chemo-immunotherapy. A centralized computer generated a simple randomization sequence and patients were randomly assigned either to the intensified or conventional arm.

Both conventional CHOP-R and intensified R-HDS treatments have already been described.<sup>9,17-20</sup> Details of the treatment schedules along with study end points and molecular analysis performed are reported in the *Online Supplementary Appendix*.<sup>9,19,21</sup>

### Long-term follow up and statistical analysis

The update was made by taking information from 28 out of 29 participating centers regarding the clinical status of each patient entered in the prospective trial: (i) status alive or dead or lost to follow up, with the date of death or last follow up alive; (ii) cause of death, i.e. lymphoma progression, secondary neoplasm, non-neoplastic late fatal complications, or other causes; (iii) occurrence of secondary hematopoietic or non-hematopoietic neoplasm; or (iv) disease status at last follow up alive, i.e. continuous first, second or more complete remission (CR).

In the present update, alive patients were censored at the date of last contact (February 2nd, 2017), providing a median event-free survival (EFS) and overall survival (OS) follow-up time of 13.01 years [range: 0.5-16.6, interquartile range (IQR); 11.8-14.7]. All analyses were carried out on an intention-to-treat basis.

Survival curves were estimated by the Kaplan-Meier method according to the revised response criteria published in 2007, and compared using the log-rank test.<sup>22-24</sup> EFS, OS, progression-free survival (PFS), and disease-free survival (DFS) were analyzed by the Cox proportional hazards model, comparing the two treatment arms (R-CHOP *vs.* R-HDS) by the Wald test and calculating 95% Confidence Intervals (CI).<sup>25</sup>

The CI of secondary myeloid dysplastic syndrome (sMDS) / acute myeloid leukemia (AML) and solid malignancies in the whole cohort and stratified by the treatment arm were estimated at 5, 10, and 13 years from diagnosis and were assessed by the Gray test.<sup>26</sup> All reported *P*-values were two-sided, at the conventional 5% significance level. Data were analyzed as of January 2018 using R 3.4.3.<sup>27</sup>

## Results

### Overall survival and causes of death

As of February 2017, 88 (66%) patients were alive at their last follow up. Overall, median survival had not yet been reached at the 13-year median follow up, with a 13-year OS estimate of 66.4% for the whole patient cohort. Similar OS values were observed in the two treatment arms, with 13-year OS estimates of 68.5% and 64.5% for patients in the CHOP-R and R-HDS arms, respectively (Figure 1).

At the latest follow up, 46 patients had died. The main causes of deaths were disease progression for 22 patients (16.4% of the whole series, 47.8% of all deaths), secondary malignancies (3 solid tumor, 9 sMDS/AML) for 12 patients (8.9% of the whole series, 26.1% of all deaths), 12 patients died of various causes, including six fatal cardiovascular events, three documented infections, one graft failure following autograft, one anaphylactic shock following intravenous immunoglobulin (Ig i.v.) infusion, and one late sudden death. Among patients in the CHOP-R arm, 13 of 20 (65%) died from disease-related causes, whereas lymphoma progression was the cause of death for 9 of 26 (35%) patients in the R-HDS arm. Main causes of death per each treatment arm are summarized in Figure 2.

**Table 1.** Main patient features at presentation according to last survival status

	All patients	Patients alive <sup>†</sup>	Patients dead <sup>†</sup>	P
All	134	88	46	
M/F	78/56	45/43	33/13	0.022
Age (y), median (range)	51 (22-59)	50 (22-59)	53 (35-59)	0.297
Histologic grade I-II, n. (%)	98 (73)	65 (73)	33 (71)	0.792
age-adjusted IPI 2 or more, n. (%)	120 (89)	75 (85)	45 (98)	0.024
FLIPI 3 or more, n. (%)	78 (58)	52 (59)	26 (56)	0.775
Ann Arbor stage IV, n (%)	118 (88)	77 (86)	41 (89)	0.648
B symptoms, n. (%)	63 (47)	40 (46)	23 (50)	0.617
ECOG PS 2 or more, n. (%)	80 (60)	49 (56)	31 (67)	0.189
Bulky disease, n. (%)	75 (56)	51 (58)	24 (52)	0.522
Spleen involvement, n. (%)	50 (37)	28 (32)	22 (48)	0.061
Bone marrow involvement, n (%)	113 (84)	72 (82)	41 (89)	0.269
Extranodal involvement, n. (%)	42 (31)	29 (33)	13 (28)	0.578
Abnormal LDH, n. (%)	65 (59)	38 (43)	22 (48)	0.608
Treatment arm (CHOP-R/R-HDS), n.	66/68	46/42	20/26	0.371

IPI: International Prognostic Index; FLIPI: follicular lymphoma IPI; n: number; M: male; F: female; ECOG: Eastern Cooperative Oncology Group; LDH: lactate dehydrogenase. <sup>†</sup>Status after 13 years of median follow up.

### Complete remission and molecular response: achievement and durability

Complete remission was documented in 98 (73.1%) patients: 39 (59.1%) of 66 undergoing CHOP-R treatment and 59 (86.7%) of 68 R-HDS-treated patients. CR achievement had a significantly favorable impact on survival, with 13-year OS estimates of 77.0% and 36.8%, for CR *versus* no-CR achievement, respectively (Figure 3A). Moreover, a durable CR was associated with prolonged survival. Overall, of 79 patients in CR at two years since treatment initiation, 65 (82.3%) were alive at 13 years compared to 21 (58.3%) among 36 patients with early relapse ( $P=0.003$ ).

Molecular response was documented in 39 (65%) out of 60 evaluable patients: 11 (44%) of 25 undergoing CHOP-R treatment and 28 (80%) out of 35 R-HDS-treated patients ( $P<0.001$ ).<sup>9</sup> Again, MR achievement was associated with a superior OS compared to patients not in MR following treatment (13-year OS estimates of 82.1% and 51.9%, for MR *vs.* no-MR achievement, respectively) (Figure 3B).

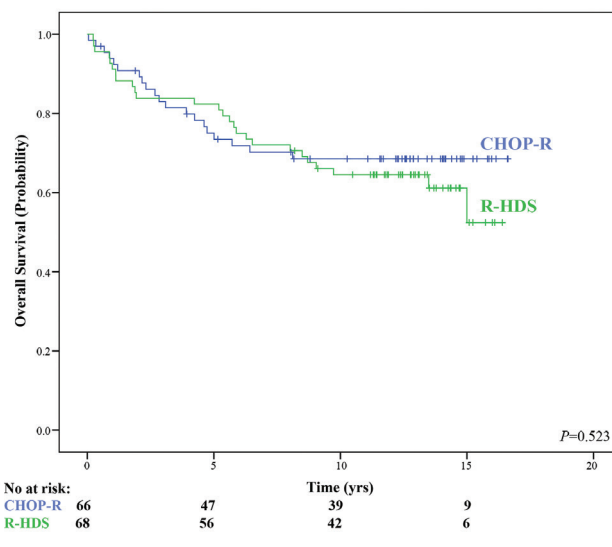


**Figure 1.** Updated overall survival (OS) according to treatment arms. Intensive chemo-immunotherapy with autograft (R-HDS) versus conventional chemoimmunotherapy (CHOP-R). Median follow-up: 13 years. No: number; yrs: years.

Overall, 50 patients (37.3% of the whole series) were alive at this follow up without any disease recurrence (18 in the CHOP-R and 32 in the R-HDS arms) since their first CR achievement. Among 98 patients obtaining CR, 39 had disease recurrence (39.8%). In the CHOP-R and R-HDS arms, the last disease recurrence respectively was recorded at ten years and at seven years from CR achievement. In addition, there were nine late toxic events (1 in CHOP-R and 9 in R-HDS) in patients in their first continuous CR.

For patients reaching CR, the DFS estimate was 57.9% at 13 years. The 13-year DFS estimate was 47.1% for the 39 patients in CR following CHOP-R and 65.3% for the 59 patients in CR following R-HDS (Figure 4).

A subgroup of patients was further monitored for their molecular disease at long-term. After a median of four years of molecular monitoring since treatment completion, of the 24 patients alive in their first CR and evaluable for molecular disease, 20 (83%) patients were still in their first MR.

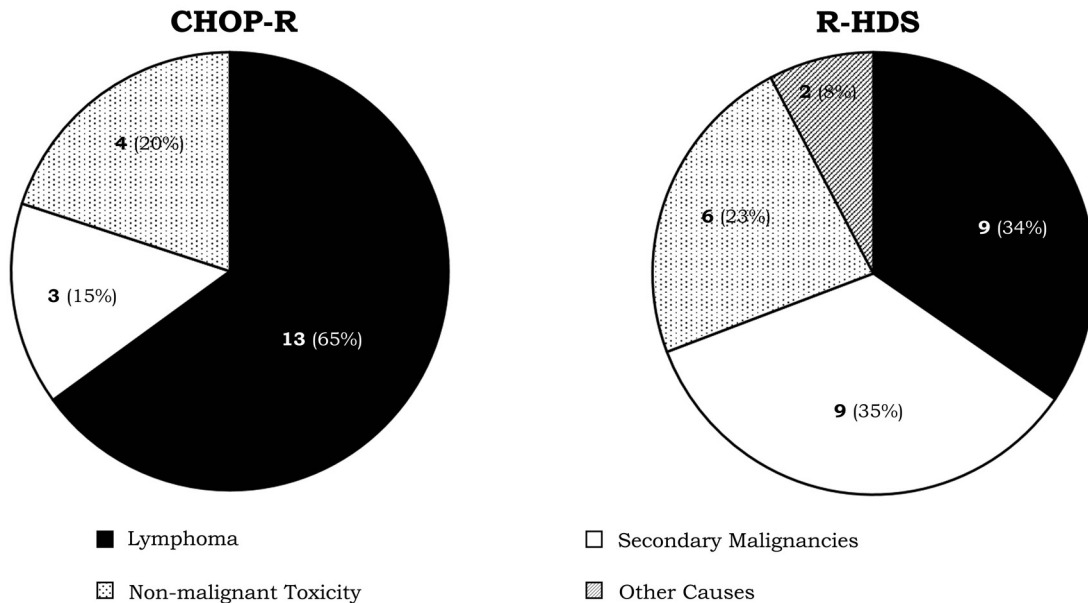


**Figure 2. Main causes of death in the two treatment arms.** Main causes of death include deaths due to: lymphoma, secondary malignancies (3 solid tumor, 9 secondary myeloid dysplastic syndrome (sMDS) / acute myeloid leukemia (AML)), non-malignant fatal events (6 fatal cardiovascular complications, 3 documented infections, 1 graft failure following autograft) and other causes (not clearly related to treatment).

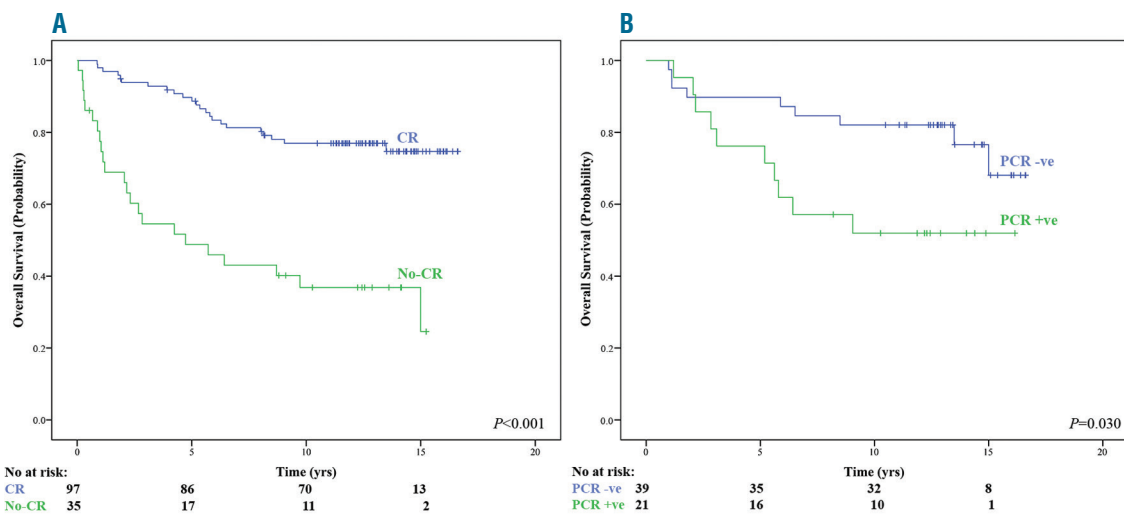


**Figure 3. Updated overall survival according to end of treatment clinical status.** (A) Complete remission (CR) achievement. (B) Molecular remission [polymerase chain reaction negative (PCR)] achievement. No: number; yrs: years.

The 13-year estimates for EFS and PFS were 37.3% and 46.3% among all patients, respectively. Both EFS and PFS curves remained significantly superior in the R-HDS compared to CHOP-R arm. For CHOP-R and R-HDS, 13-year EFS estimates were respectively 26.6% (median EFS: 1.6 years) and 48.5% (median EFS: 7.4 years) (Figure 5A). The 13-year PFS estimates were 28.8% (median PFS: 1.9%) and 59.1% (median PFS: not reached), for the CHOP-R and R-HDS arms, respectively (Figure 5B).

### Rescue of patients with refractory and relapsed disease

Overall, 72 patients (53.7%) had disease progression (45 CHOP-R and 27 R-HDS), following partial response (PR) or refractory disease after induction (33 patients) or recurrence after CR achievement (39 patients). Five patients had progression with documented histological transformation and four with central nervous system involvement. As of the last follow up, 38 (52.8%) out of 72 progressing patients were long-term survivors following salvage therapies after disease recurrence. Among rescued patients, 28 patients were in the CHOP-R and ten in the R-HDS arms. At the last follow up, besides the 50 patients alive in their first CR, 20 patients were long-term survivors in their second CR (14 CHOP-R and 6 R-HDS) and 18 were surviving beyond a second CR (14 CHOP-R and 4 R-HDS).

High-dose therapy and autograft were employed as salvage therapy in 28 patients with disease progression following initial CHOP-R. Nineteen of them at this follow up were long-term survivors, with a median PFS-2 of 6.2 years. Nine patients eventually died because of lymphoma (7 patients) or secondary malignancy (2 patients).

Allogeneic stem cell transplant was employed as the ultimate rescue approach in five patients; two of them were long-term survivors at this follow up, while three died (one from graft-versus-host disease, one from lymphoma progression, and one from a secondary tumor).

### Factors affecting long-term survival

In univariate analysis, the main features at disease presentation and treatment end that significantly favored long-term survival were female sex, age <50 years, treatment completion, MR and CR achievement (see Table 2). When these factors were evaluated in multivariate analysis, CR still showed a strong impact along with a borderline value for female sex (Table 2). When PCR status (assay performed on 60 patients only) was excluded from the multivariate analysis, CR was still the strongest factor favorably affecting survival. In addition, younger age had a strong significant impact along with female sex (Table 2).

### Secondary tumor occurrence

The respective cumulative incidences of sMDS/AL at 5, 10, and 13 years were 5.9%, 8.9% and 10.5% for the R-HDS arm and 0.0%, 10.7%, and 10.7%, respectively, for the CHOP-R arm ( $P=0.832$ ). The respective cumulative incidences of secondary non-MDS/AL neoplasms at 5, 10, and 13 years were 5.9%, 10.4%, and 11.9% for the R-HDS arm and 0%, 4.9%, and 8.8% for the CHOP-R arm ( $P=0.792$ ). Secondary neoplasms in the R-CHOP arm were carcinomas (five total: two laryngeal, two urothelial, one pancreatic), Hodgkin's lymphomas (two), MDS (two total, one of which evolved in AML), AML (one), and ALL Ph<sup>+</sup> (one). In the R-HDS arm, we observed five carcinoma cases (three head-and-neck, one mammary, one gastric), one non-melanoma skin cancer, one plasma cell dyscrasia, four MDS cases, and four AMLs.

**Table 2.** Univariate and multivariate proportional hazard models for overall survival.

	Univariate		Multivariate (with PCR)		Multivariate (without PCR) <sup>1</sup>	
	HR (95% CI)	P	HR (95% CI)	P	HR (95% CI)	P
Sex (F vs. M)	0.46 (0.24-0.88)	0.019	0.38 (0.14-1.04)	0.06	0.43 (0.22-0.84)	0.013
Age (> 50 y vs. < 50 y)	2.21 (1.18-4.15)	0.013	2.11 (0.79-5.66)	0.137	2.76 (1.45-5.23)	0.002
Spleen involvement (Yes vs. No)	1.62 (0.9-2.9)	0.109	NA	–	NA	–
MRD (Pos vs. neg)	2.26 (1.07-6.65)	0.036	0.94 (0.28-3.2)	0.919	–	–
Treatment completed (Yes vs. No)	0.39 (0.22-0.70)	0.002	0.49 (0.15-1.64)	0.248	0.56 (0.26-1.22)	0.139
Response (no CR vs. CR)	6.61 (2.53-17.25)	<0.001	6.79 (2.66-17.32)	<0.001	3.82 (2.12-6.89)	<0.001
Arm (R-HDS vs. CHOP-R)	1.21 (0.68-2.17)	0.524	NA	–	NA	–

HR: Hazard Ratio; CI: Confidence Interval; MRD: minimal residual disease; F: female; M: male; y: years; Pos.: positive; neg.: negative; CR: complete remission; R-HDS: high-dose chemotherapy with rituximab and autograft; CHOP-R: conventional chemotherapy with rituximab. <sup>1</sup>Polymerase chain reaction (PCR) data are available for a subgroups of 60 patients. NA: not included in the analysis.

### Discussion

The present study reports outcomes after a median 13 years of follow up of a multicenter prospective trial comparing high-dose chemotherapy and autograft *versus* CHOP chemotherapy, both delivered with rituximab (R-HDS *vs.* CHOP-R), as upfront therapy in high-risk FL patients. To our knowledge, this follow up is the longest ever reported for first-line treatment of FL with rituximab-supplemented chemotherapy. The prolonged observation shows an extraordinary improvement in OS compared to the pre-rituximab era.<sup>15,16</sup> The survival was similar in both treatment arms, confirming over the long-term our preliminary observation that R-HDS does not add survival advantages compared to CHOP-R in the upfront therapy of high-risk FL.<sup>9</sup> CR achievement was the most important factor for prolonged survival. The importance of disease response is further emphasized by the first-time observation that MR achievement is associated with survival duration and a high proportion of patients had prolonged survival in the absence of disease recurrence.

The GITMO-III trial was designed for patients with high-risk FL, histologically diagnosed according to the Revised European-American Classification of Lymphoid Neoplasms (REAL)/World Health Organization (WHO) lymphoma classification.<sup>14</sup> The FL diagnosis was confirmed by the high rate of *BCL-2* gene translocation detected in patients with molecular assessment. The high-risk presentation was proved using the clinical prognostic scores available when the protocol was designed.<sup>15-16</sup> The subsequently developed FLIPI score employs other clinical parameters, and a proportion of our patients were not true “high risk” according to FLIPI.<sup>28</sup> Nevertheless, all study patients clearly belonged to a severely ill population, with a 5-year survival expectancies of 43.6% (age-adjusted IPI score) and 38% (Italian Lymphoma Intergroup score), according to treatment available at the time the trial was conceived.<sup>15,16</sup> The 13-year survival of 66.4% recorded in our series represents a marked improvement in life expectancy compared to survival reported in the pre-rituximab era for similar high-risk FL patients. This result is especially notable because only

four rituximab doses were applied to the majority of patients, and the treatment schedule was not that most frequently delivered in present times.

Recently, two other prospective trials performed in advanced-stage FL with rituximab-based upfront regimens have been updated: the Italian FOLL05 study comparing R-CVP, R-CHOP, and R-FM and the SWOG study comparing R-CHOP *versus* CHOP followed by radioimmunotherapy.<sup>29,30</sup> Both the FOLL05 study, with 8-year OS of 83%, and the SWOG study, with 10-year OS of 78%, showed extended life expectancies in the absence of rituximab maintenance. These values are in line with our 13-year OS of 66% obtained in a selected group of high-risk FL. The results strengthen the observations from several retrospective studies showing prolonged survival in FL following immunochemotherapy.<sup>10-13</sup> Moreover, results from all of these studies indicate that the CHOP schedule delivered

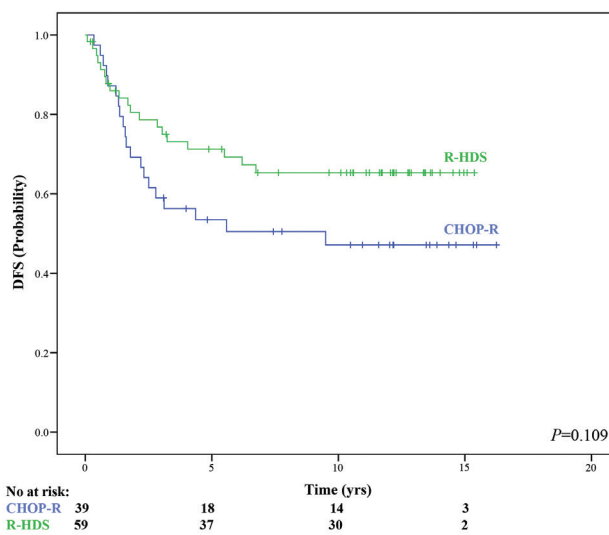


Figure 4. Updated disease-free survival (DFS) according to treatment arms. Intensive chemo-immunotherapy with autograft (R-HDS) *vs.* conventional chemoimmunotherapy (CHOP-R). No: number; yrs: years.

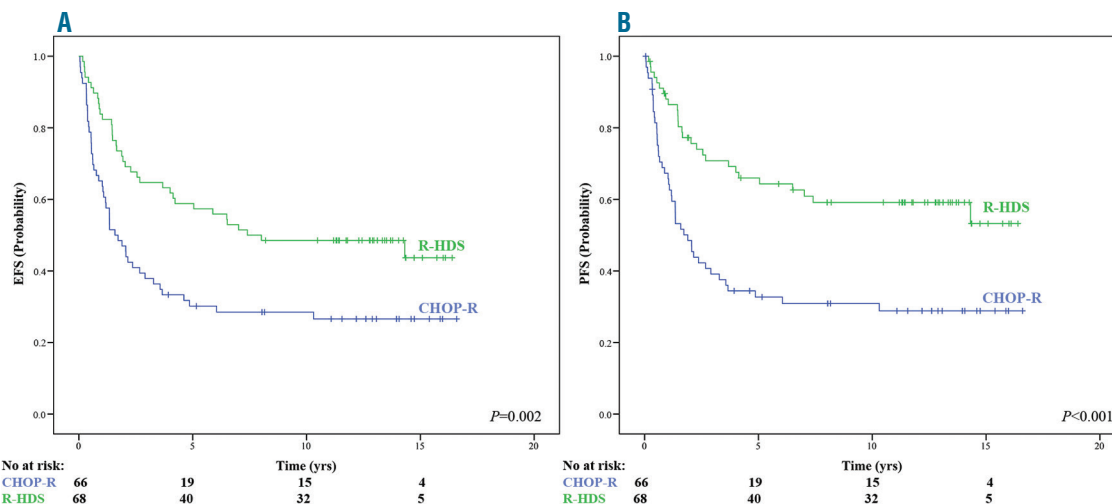


Figure 5. Updated event-free survival (EFS) and progression-free survival (PFS) according to treatment arms. Intensive chemoimmunotherapy with autograft (R-HDS) *versus* conventional chemoimmunotherapy (CHOP-R). (A) EFS. (B) PFS. No: number; yrs: years.

with rituximab is currently the first choice for the upfront treatment of advanced stage FL, ensuring prolonged survival, with adequate information about possible late side effects.

In our whole series, lymphoma progression remained the most frequent cause of failure, accounting for 47.8% of all causes of death. This is in line with several previous observations, including a recent report on a large series of FL.<sup>31</sup> Indeed, lymphoma progression was much more often responsible for fatal outcome among patients allocated to the CHOP-R arm, with 65% of all deaths, compared to the R-HDS arm with only 35% of all deaths. On the other hand, early and late toxicities were the most frequent cause of failure for patients in the R-HDS arm, which counterbalanced the increased anti-lymphoma activity of R-HDS compared to CHOP-R, resulting in analogous overall survival for the two treatment arms. Rituximab maintenance is now used with the aim of reducing disease recurrence risk.<sup>32</sup> In addition, both bendamustine and the novel anti-CD20 obinutuzumab antibody have been proposed as more effective first-line treatments compared to R-CHOP.<sup>33,34</sup> In particular, bendamustine is now frequently used as first-line treatment in place of the CHOP schedule. However, no evidence is currently available to suggest that these novel treatment strategies will substantially reduce the risk for disease-related deaths without affecting the treatment safety profile in the long term. Indeed, our update reinforces the need for prolonged observation to define the true survival advantage of any novel treatment for FL. Novel treatments for FL should combine potent anti-lymphoma activity along with low risk of both early and late toxicities.

Most late toxicities were secondary malignancies associated with the use of high-dose therapy with autograft delivered either upfront in the R-HDS arm or as salvage therapy in a good proportion of patients failing after upfront CHOP-R. This finding is in line with previous reports, including a retrospective study from the Gruppo Italiano Terapie Innovative nei Linfomi (GITIL) group indicating increased risk for secondary MDS/AL in lymphoma patients receiving high-dose therapy and autograft.<sup>35</sup> A recent surveillance study by the Spanish Lymphoma Group (GELTAMO) group has further stressed the risk of secondary MDS/AL in FL patients undergoing autograft.<sup>36</sup> Moreover, both the GITIL and GELTAMO studies indicated a trend for increased risk for secondary solid tumors when autograft is delivered along with rituximab.<sup>35,36</sup> Thus, the risk for late occurrence of secondary malignancy is a main issue in the long-term management of FL patients. This concern must be kept in mind in the long-term assessment of the efficacy

of novel drugs and drug combinations.<sup>33,34,37-39</sup>

The present study allows identification of the factors favoring the long-term survival of high-risk FL patients treated with rituximab-containing chemotherapy. Somewhat unexpectedly, CR achievement proved to be the strongest prerequisite for long-term survival. Several recent observations indicate that response to initial treatment along with the achievement of a strong and durable response may favorably affect long-term outcome.<sup>31,40-44</sup> The present update clearly demonstrates in a prospective study that CR achievement shows the strongest association with prolonged survival. The importance of the response depth for long-term survival is confirmed by our molecular monitoring of measurable residual disease (MRD) performed in a subset of patients. Most studies have shown a remarkable prognostic value of MRD assessment in terms of PFS and response duration.<sup>9,17,20,45,46</sup> Nevertheless, the impact on OS could not be fully addressed in most studies, usually because of inadequate follow up.<sup>47,48</sup> Here, it was possible to demonstrate for the first time that MRD assessment is predictive for both PFS and OS, and that MR was associated with a prolonged survival.

The association of response depth with long-term survival in our FL series is further substantiated by the observation that a good proportion of patients (approx. 37% of the whole series) could survive in their first CR at long term. The DFS curves were definitely promising, with a 13-year estimate as high as 65% in R-HDS-treated patients. Moreover, most patients achieving MR following induction treatment maintained their MR during long-term molecular monitoring. Taken together, these results indicate that an extensive disease response in FL may translate into both prolonged survival and in the long-term persistence of CR; a state that has been described as functional cure in other clinical settings. This in turn raises the issue of the curability of FL, at least in patients with a high-risk clinical presentation such as those selected in the present study.

### Funding

*This work was supported in part by the Ministero Italiano Università e Ricerca (MIUR), Rome, Italy (grant PRIN 2010-2011, pr. N.: 2010B5B2NL), and by Banca del Piemonte (Torino, Italy). The initial clinical trial (March 2000 - May 2005) was made possible by Compagnia di San Paolo (Torino, Italy), Regione Piemonte (Torino, Italy), and by Roche (Milan, Italy), which provided free rituximab for all patients. We are indebted to GITMO (Gruppo Italiano Trapianto Midollo Osseo) and to ILL, now merged into FIL (Fondazione Italiana Linfomi) for their fundamental participation in the development and completion of the study.*

### References

- National Comprehensive Cancer Network. NCCN clinical practice guidelines in oncology. B-cell lymphomas. Version 7.2017 — December 5, 2017. [https://www.nccn.org/professionals/physician\\_gls/pdf/b-cell.pdf](https://www.nccn.org/professionals/physician_gls/pdf/b-cell.pdf). Accessed January 10, 2018.
- Dreyling M, Ghielmini M, Rule S, et al, on behalf of the ESMO. Guidelines Committee. Newly diagnosed and relapsed follicular lymphoma: ESMO Clinical Practice Guidelines for diagnosis, treatment and follow-up. *Ann Oncol.* 2016; 27(Supplement 5):v83–v90.
- Corradini P, Ladetto M, Zallio F, et al. Long-term follow-up of indolent lymphoma patients treated with high-dose sequential chemotherapy and autografting: evidence that durable molecular and clinical remission frequently can be attained only in follicular subtypes. *J Clin Oncol.* 2004;22(8):1460-1468.
- Lenz G, Dreyling M, Schiegnitz E, et al. Myeloablative radiochemotherapy followed by autologous stem cell transplantation in first remission prolongs progression-free survival in follicular lymphoma: results of a prospective, randomized trial of the German Low-Grade Lymphoma Study Group. *Blood.* 2004;104(9):2667-2674.
- Deconinck E, Foussard C, Milpied N, et al. High-dose therapy followed by autologous purged stem-cell transplantation and doxorubicin-based chemotherapy in patients with advanced follicular lymphoma: a randomized multicenter study by GOELAMS. *Blood.* 2005;105(10):3817-3823.
- Hiddemann W, Buske C, Dreyling M, et al. Treatment strategies in follicular lymphomas: current status and future perspectives. *J Clin Oncol.* 2005;23(26):6394-6399.
- Sebban C, Mounier N, Brousse N, et al.

- Standard chemotherapy with interferon compared with CHOP followed by high-dose therapy with autologous stem cell transplantation in untreated patients with advanced follicular lymphoma: the GELF-94 randomized study from the Groupe d'Etude des Lymphomes de l'Adulte (GELA) *Blood*. 2006;108(8):2540-2544.
8. Brown JR, Feng Y, Gribben JG, et al. Long-term survival after autologous bone marrow transplantation for follicular lymphoma in first remission. *Biol Blood Marrow Transplant*. 2007;13(9):1057-1065.
  9. Ladetto M, De Marco F, Benedetti F, et al. Prospective, multicenter randomized GITMO/IL trial comparing intensive (R-HDS) versus conventional (CHOP-R) chemoimmunotherapy in high-risk follicular lymphoma at diagnosis: the superior disease control of R-HDS does not translate into an overall survival advantage. *Blood*. 2008;111(8):4004-4013.
  10. Liu Q, Fayad L, Cabanillas F, et al. Improvement of overall and failure-free survival in stage IV follicular lymphoma: 25 years of treatment experience at The University of Texas M.D. Anderson Cancer Center. *J Clin Oncol*. 2006;24(10):1582-1589.
  11. Schulz H, Bohlius JF, Trelle S, et al. Immunochemotherapy with rituximab and overall survival in patients with indolent or mantle cell lymphoma: A systematic review and meta-analysis. *J Natl Cancer Inst*. 2007;99(9):706-714.
  12. Tan D, Homing SJ, Hoppe RT, et al. Improvements in observed and relative survival in follicular grade 1-2 lymphoma during 4 decades: the Stanford University experience. *Blood*. 2013;122(6):981-987.
  13. Nabhan C, Aschebrook-Kilfoy B, Chiu BC, Kruczek K, Smith SM, Evens AM. The impact of race, age, and sex in follicular lymphoma: a comprehensive SEER analysis across consecutive treatment eras. *Am J Hematol*. 2014;89(6):633-638.
  14. Harris NL, Jaffe ES, Stein H, et al. A revised European-American classification of lymphoid neoplasms: a proposal from the International Lymphoma Study Group. *Blood*. 1994;84(5):1361-1392.
  15. López-Guillermo A, Montserrat E, Bosch F, Terol MJ, Campo E, Rozman C. Applicability of the International Index for aggressive lymphomas to patients with low-grade lymphoma. *J Clin Oncol*. 1994;12(7):1343-1348.
  16. Federico M, Vitolo U, Zinzani PL, et al. Prognosis of follicular lymphoma: a predictive model based on a retrospective analysis of 987 cases *Blood*. 2000;95(3):783-789.
  17. Rambaldi A, Lazzari M, Manzoni C, et al. Monitoring of minimal residual disease after CHOP and rituximab in previously untreated patients with follicular lymphoma. *Blood*. 2002;99(3):856-862.
  18. Tarella C, Caracciolo D, Corradini P, et al. Long-term follow-up of advanced-stage low-grade lymphoma patients treated upfront with high-dose sequential chemotherapy and autograft. *Leukemia*. 2000;14(4):740-747.
  19. Ladetto M, Corradini P, Vallet S, et al. High rate of clinical and molecular remissions in follicular lymphoma patients receiving high-dose sequential chemotherapy and autografting at diagnosis: a multicenter, prospective study by the Gruppo Italiano Trapianto Midollo Osseo (GITMO). *Blood*. 2002;100(5):1559-1565.
  20. Cheson BD, Homing SJ, Coiffier B, et al. Report of an international workshop to standardize re-sponse criteria for non-Hodgkin's lymphomas: NCI Sponsored International Working Group. *J Clin Oncol*. 1999;17(4):1244-1253.
  21. Corradini P, Astolfi M, Cherasco C, et al. Molecular monitoring of minimal residual disease in follicular and mantle cell non-Hodgkin's lymphomas treated with high-dose chemotherapy and peripheral blood progenitor cell autografting. *Blood*. 1997;89(2):724-731.
  22. Kaplan EL, Meier P. Non parametric estimation from incomplete observations. *J Am Stat Assoc*. 1958;53(282):457-481.
  23. Cheson BD, Pfistner B, Juweid ME, et al. International Harmonization Project on Lymphoma. Revised response criteria for malignant lymphoma. *J Clin Oncol*. 2007;25(5):579-86.
  24. Mantel H, Haenzel W. Statistical aspects of the analysis of data from retrospective studies of disease. *J Natl Cancer Inst*. 1959;22(4):719-748.
  25. Cox DR. Regression models and life tables. *J Royal Stat Soc Series B*. 1972;34:187-220.
  26. Gray RS. A class of K-sample tests for comparing the cumulative incidence of a competing risk. *Ann Stat*. 1988;16(3):1141-1154.
  27. R Foundation for Statistical Computing, Vienna-A, <http://www.R-project.org>
  28. Solal-Celigny, P. Roy, P. Colombat, et al. Follicular lymphoma international prognostic index. *Blood*. 2004;104(5):1258-1265.
  29. Luminari S, Ferrari A, Manni M, et al. Long-term results of the FOLL05 trial comparing R-CVP versus R-CHOP versus R-FM for the initial treatment of patients with advanced-stage symptomatic follicular lymphoma. *J Clin Oncol*. 2017;36(7):689-696.
  30. Shadman M, Li H, Rimsza L, et al. continued excellent outcomes in previously untreated patients with follicular lymphoma after treatment with CHOP plus rituximab or CHOP plus 131I-Tositumomab: long-term follow-up of Phase III randomized study SWOG-S0016. *J Clin Oncol*. 2018;36(7):697-703.
  31. Sarkozy C, Maurer MJ, Link BK, et al. Cause of death in follicular lymphoma in the first decade of the rituximab era: a pooled analysis of French and US cohorts. *J Clin Oncol*. 2019;37(2):144-152.
  32. Salles G, Seymour JF, Offner F, et al. Rituximab maintenance for 2 years in patients with high tumour burden follicular lymphoma responding to rituximab plus chemotherapy (PRIMA): A phase 3, randomised controlled trial. *Lancet*. 2011;377(9759):42-51.
  33. Rummel MJ, Niederle N, Maschmeyer G, et al. Bendamustine plus rituximab versus CHOP plus rituximab as first-line treatment for patients with indolent and mantle-cell lymphomas: An open-label, multicentre, randomised, phase 3 non-inferiority trial. *Lancet*. 2013;381(9873):1203-1210.
  34. Marcus R, Davies A, Ando K, et al. Obinutuzumab for the First-Line Treatment of Follicular Lymphoma. *N Engl J Med*. 2017;377(14):1331-1344.
  35. Tarella C, Passera R, Magni M, et al. Risk Factors for the Development of Secondary Malignancy After High-Dose Chemotherapy and Autograft, With or Without Rituximab: A 20-Year Retrospective Follow-Up Study in 1,347 Patients With Lymphoma. *J Clin Oncol*. 2011;29(7):814-824.
  36. Jiménez-Ubieto A, Grande C, Caballero D, et al., on behalf of GELTAMO (Grupo Español de Linfomas y Trasplantes de Médula Ósea) Cooperative Study Group. Secondary malignancies and survival outcomes after autologous stem cell transplantation for follicular lymphoma in the pre-rituximab and rituximab eras: a long-term follow-up analysis from the Spanish GELTAMO registry. *Bone Marrow Transplant*. 2018;53(6):780-783.
  37. Smith SM, Pitcher BN, Jung SH, et al. Safety and tolerability of idelalisib, lenalidomide, and rituximab in relapsed and refractory lymphoma: The Alliance for Clinical Trials in Oncology A051201 and A051202 phase 1 trials. *Lancet Haematol*. 2017;4(4):e176-e182.
  38. Leonard JP, Jung SH, Johnson J, et al. Randomized trial of lenalidomide alone versus lenalidomide plus rituximab in patients with recurrent follicular lymphoma: CALGB 50401 (Alliance). *J Clin Oncol*. 2015;33(31):3635-3640.
  39. Davids MS, Roberts AW, Seymour JF, et al. Phase I first-in-human study of venetoclax in patients with relapsed or refractory non-Hodgkin lymphoma. *J Clin Oncol*. 2017;35(8):826-833.
  40. Tarella C, Gueli A, Delaini F, et al. Rate of Primary Refractory Disease in B and T-Cell Non-Hodgkin's Lymphoma: Correlation with Long-Term Survival. *PLoS One*. 2014;9(9):e106745.
  41. Casulo C, Byrtek M, Dawson KL, et al. Early relapse of follicular lymphoma after rituximab plus cyclophosphamide, doxorubicin, vincristine, and prednisone defines patients at high risk for death: an analysis from the National LymphoCare Study. *J Clin Oncol*. 2015;33(23):2516-2522.
  42. Shi Q, Flowers CR, Hiddemann W, et al. Thirty-month complete response as a surrogate end point in first-line follicular lymphoma Therapy: an individual patient-level analysis of multiple randomized trials. *J Clin Oncol*. 2017;35(5):552-560.
  43. Sorigue M, Mercadal S, Alonso S, et al. Refractoriness to immunochemotherapy in follicular lymphoma: predictive factors and outcome. *Hematol Oncol*. 2017;35(4):520-527.
  44. Provencio M, Royuela A, Torrente M, et al, on behalf of the Spanish Lymphoma Oncology Group. Prognostic value of event-free survival at 12 and 24 months and long-term mortality for non-Hodgkin follicular lymphoma patients: A study report from the Spanish Lymphoma Oncology Group. *Cancer*. 2017;123(19):3709-3716.
  45. Gribben JG, Freedman AS, Neuberg D, et al. Immunologic purging of marrow assessed by PCR before autologous bone marrow transplantation for B-cell lymphoma. *N Engl J Med*. 1991;325(22):1525-1533.
  46. Ladetto M, Lobetti-Bodoni C, Mantoan B, et al, on behalf of Fondazione Italiana Linfomi. Persistence of minimal residual disease in bone marrow predicts outcome in follicular lymphomas treated with a rituximab-intensive program. *Blood*. 2013;122(23):3759-3766.
  47. Gritti G, Pavoni C, Rambaldi A. Is There a Role for Minimal Residual Disease Monitoring in Follicular Lymphoma in the Chemo-Immunotherapy Era? *Mediterr J Hematol Infect Dis*. 2017;9(1):e2017010.
  48. Casulo C, Nastoupil L, Fowler NH, Friedberg JW, Flowers CR. Unmet needs in the first-line treatment of follicular lymphoma. *Ann Oncol*. 2017;28(9):2094-2106.

# High prognostic value of measurable residual disease detection by flow cytometry in chronic lymphocytic leukemia patients treated with front-line fludarabine, cyclophosphamide, and rituximab, followed by three years of rituximab maintenance

José A. García-Marco,<sup>1</sup> Javier López Jiménez,<sup>2</sup> Valle Recasens,<sup>3</sup> Miguel Fernández Zazoso,<sup>4</sup> Eva González-Barca,<sup>5</sup> Nieves Somolinos De Marcos,<sup>6</sup> M. Jose Ramírez,<sup>7</sup> Francisco Javier Peñalver Parraga,<sup>8</sup> Lucrecia Yañez,<sup>9</sup> Javier De La Serna Torroba,<sup>10</sup> Maria Dolores Garcia Malo,<sup>11</sup> Guillermo Deben Ariznavarreta,<sup>12</sup> Ernesto Perez Persona,<sup>13</sup> M. Angeles Ruiz Guinaldo,<sup>14</sup> Raquel De Paz Arias,<sup>15</sup> Elena Bañas Llanos,<sup>16</sup> Isidro Jarque,<sup>17</sup> M. del Carmen Fernandez Valle,<sup>18</sup> Ana Carral Tatay,<sup>19</sup> Jaime Perez De Oteyza,<sup>20</sup> Eva Maria Donato Martin,<sup>21</sup> Inmaculada Perez Fernández,<sup>22</sup> Rafael Martinez Martinez,<sup>23</sup> M. Angeles Andreu Costa,<sup>24</sup> Diana Champ,<sup>25</sup> Julio García Suarez,<sup>26</sup> Marcos González Díaz,<sup>27</sup> Secundino Ferrer,<sup>4</sup> Félix Carbonell<sup>28</sup> and José A. García-Vela<sup>29</sup> on behalf of the GELLC Study Group

<sup>1</sup>Hematology, Hospital Universitario Puerta de Hierro-Majadahonda, Madrid; <sup>2</sup>Hematology, Hospital Ramon y Cajal, Madrid; <sup>3</sup>Hematology, Hospital Miguel Servet, Zaragoza; <sup>4</sup>Hematology, Hospital Universitario Dr Peset, Valencia; <sup>5</sup>Hematology, Institut Català d'Oncologia, L'Hospitalet de Llobregat, Barcelona; <sup>6</sup>Hematology, Hospital Universitario de Getafe, Madrid; <sup>7</sup>Hematology, Hospital de Jerez de la Frontera, Jerez; <sup>8</sup>Fundación Hospital de Alcorcón, Madrid; <sup>9</sup>Hospital Universitario Marqués de Valdecilla, Servicio de Hematología, Santander; <sup>10</sup>Department of Hematology, Hospital Doce de Octubre, Madrid; <sup>11</sup>Hematology, Hospital Morales Meseguer, Murcia; <sup>12</sup>Hematology, CHU Juan Canalejo, A Coruña; <sup>13</sup>Hematology, Hospital Txagorritxu, Vitoria; <sup>14</sup>Hematology, Hospital Francesc Borja, Valencia; <sup>15</sup>Hematology, Hospital La Paz, Madrid; <sup>16</sup>Hematology, Hospital San Pedro de Alcantara, Cáceres; <sup>17</sup>Hematology, Hospital Universitario La Fe, Valencia; <sup>18</sup>Hematology, Hospital Universitario Puerta del Mar, Cadiz; <sup>19</sup>Hematology, Hospital de Sagunto, Valencia; <sup>20</sup>Hematology, Hospital Madrid Norte Sanchinarro, Madrid; <sup>21</sup>Hematology, Hospital General Castellon, Castellon; <sup>22</sup>Hematology, Hospital Regional Universitario de Málaga, Málaga; <sup>23</sup>Hematology, Hospital Clínico Universitario San Carlos, Madrid; <sup>24</sup>Hematology, Hospital General de Móstoles, Madrid; <sup>25</sup>Roche Farma, S.A., Madrid; <sup>26</sup>Hematology, Hospital Universitario Príncipe Asturias, Madrid; <sup>27</sup>Hematology, University Hospital of Salamanca-IBSAL, CIBERONC, USAL-CSIC, CIC-IBMCC, Salamanca; <sup>28</sup>Hematology, Consorcio Hospital General Universitario, Valencia and <sup>29</sup>Hematology, Hospital Universitario de Getafe, Madrid, Spain

## ABSTRACT

It has been postulated that monitoring measurable residual disease (MRD) could be used as a surrogate marker of progression-free survival (PFS) in chronic lymphocytic leukemia (CLL) patients after treatment with immunochemotherapy regimens. In this study, we analyzed the outcome of 84 patients at 3 years of follow-up after first-line treatment with fludarabine, cyclophosphamide and rituximab (FCR) induction followed by 36 months of rituximab maintenance therapy. MRD was assessed by a quantitative four-color flow cytometry panel with a sensitivity level of  $10^{-4}$ . Eighty out of 84 evaluable patients (95.2%) achieved at least a partial response or better at the end of induction. After clinical evaluation, 74 patients went into rituximab maintenance and the primary endpoint was assessed in the final analysis at 3 years of follow-up. Bone marrow (BM) MRD analysis was performed after the last planned induction course and every 6 months in cases with detectable residual disease during the 36 months of maintenance therapy. Thirty-seven patients (44%) did not have detectable residual disease in the BM prior to maintenance therapy. Interestingly, 29 patients with detectable residual disease in the BM after



Haematologica 2019  
Volume 104(11):2249-2257

## Correspondence:

JOSÉ GARCÍA-MARCO  
jagarciam@aehh.org

Received: August 20, 2018.

Accepted: March 18, 2019.

Pre-published: March 19, 2019.

doi:10.3324/haematol.2018.204891

Check the online version for the most updated information on this article, online supplements, and information on authorship & disclosures: [www.haematologica.org/content/104/11/2249](http://www.haematologica.org/content/104/11/2249)

©2019 Ferrata Storti Foundation

Material published in Haematologica is covered by copyright. All rights are reserved to the Ferrata Storti Foundation. Use of published material is allowed under the following terms and conditions:

<https://creativecommons.org/licenses/by-nc/4.0/legalcode>. Copies of published material are allowed for personal or internal use. Sharing published material for non-commercial purposes is subject to the following conditions: <https://creativecommons.org/licenses/by-nc/4.0/legalcode>, sect. 3. Reproducing and sharing published material for commercial purposes is not allowed without permission in writing from the publisher.



induction no longer had detectable disease in the BM following maintenance therapy. After a median follow-up of 6.30 years, the median overall survival (OS) and PFS had not been reached in patients with either undetectable or detectable residual disease in the BM, who had achieved a complete response at the time of starting maintenance therapy. Interestingly, univariate analysis showed that after rituximab maintenance OS was not affected by IGHV status (mutated *vs.* unmutated OS: 85.7% alive at 7.2 years *vs.* 79.6% alive at 7.3 years, respectively). As per protocol, 15 patients (17.8%), who achieved a complete response and undetectable peripheral blood and BM residual disease after four courses of induction, were allowed to stop fludarabine and cyclophosphamide and complete two additional courses of rituximab and continue with maintenance therapy for 18 cycles. Surprisingly, the outcome in this population was similar to that observed in patients who received the full six cycles of the induction regimen. These data show that, compared to historic controls, patients treated with FCR followed by rituximab maintenance have high-quality responses with fewer relapses and improved OS. The tolerability of this regime is favorable. Furthermore, attaining an early undetectable residual disease status could shorten the duration of chemoimmunotherapy, reducing toxicities and preventing long-term side effects. The analysis of BM MRD after fludarabine-based induction could be a powerful predictor of post-maintenance outcomes in patients with CLL undergoing rituximab maintenance and could be a valuable tool to identify patients at high risk of relapse, influencing further treatment strategies. This trial is registered with EudraCT n. 2007-002733-36 and ClinicalTrials.gov Identifier: NCT00545714.

## Introduction

Chronic lymphocytic leukemia (CLL) is a mature B-cell neoplasm characterized by a clonal proliferation and compartmentalized accumulation of neoplastic B cells within the blood, bone marrow and secondary lymphatic organs. The neoplastic B cells typically co-express CD5, and CD19, CD20, and CD23; compared with normal B cells, the levels of CD20 and CD79b on CLL cells are usually diminished.<sup>1,4</sup> Mutations of immunoglobulin heavy variable chain (IGHV) genes and chromosomal abnormalities are the most important predictors of disease course.

For physically fit patients requiring treatment according to the International Workshop on CLL criteria, the combination of fludarabine, cyclophosphamide and the chimeric anti-CD20 antibody rituximab (FCR) is the standard of care for first-line treatment, based on the improvement of progression-free survival (PFS) and overall survival (OS) of patients treated with this combination compared with those treated with combination chemotherapy alone.<sup>5</sup> Following the introduction of purine analogs as a treatment option, higher response rates and a higher proportion of complete remissions were observed, and even better outcomes have been reported in patients carrying mutated IGHV genes (excluding 11q or 17p deletions); patients treated with combination therapies such as FCR may achieve a life expectancy close to that observed in the matched normal general population.<sup>6,8</sup>

Achieving higher CR rates with chemoimmunotherapy has translated into a documented increase in PFS and seems to lead to an OS benefit, as shown in the CLL8 trial, which reported a 33% reduced risk of death ( $P=0.01$ ) with the FCR regimen when compared to fludarabine plus cyclophosphamide as first-line therapy. However, while attainment of a CR has historically been considered the gold-standard for treatment response, many of these patients have persistent disease that cannot be easily identified by routine testing approaches.<sup>9</sup> This, coupled with the development of extremely sensitive testing technologies, has led to the emergence of measurable residual disease (MRD) as an important endpoint in the treatment of

CLL, especially in the era of chemoimmunotherapy. Indeed, achieving undetectable MRD after chemoimmunotherapy is a desirable goal, as MRD below a threshold of  $10^{-4}$  (0.01%) results in improvement of PFS and OS.<sup>8</sup> We hypothesized that using MRD as a surrogate of treatment effectiveness would allow determination of the efficacy of new treatments without the need for prolonged observation.

Several studies have shown that sequential use of induction/maintenance treatment can improve the quality of response achieved with induction. Abrisqueta *et al.* recently reported an analysis of whether maintenance therapy can improve the response achieved with induction chemotherapy.<sup>10</sup> Sixty-seven patients responding to induction therapy with FCR plus mitoxantrone (R-FCM) received rituximab maintenance therapy (375 mg/m<sup>2</sup>) every 3 months for 2 years. Approximately 40.6% of patients achieved a CR with undetectable MRD at the end of the maintenance treatment. It is important to note that 21% of the patients who had detectable MRD at the end of R-FCM induction had an improved response after rituximab maintenance therapy. Another study showed that after responding to a fludarabine induction, patients who had detectable MRD and were consolidated with four monthly cycles of rituximab followed by a maintenance regimen of 12 monthly rituximab doses had significantly longer responses, compared to those who did not receive consolidation (5-year OS: 87% *vs.* 32%;  $P<0.001$ ). The estimated 5-year PFS after induction was 73%.<sup>11</sup>

However, despite the improvements achieved with rituximab maintenance therapy, there are some biological features which confer a poor response to consolidation plus maintenance therapy. Dal Bo *et al.* showed that patients harboring the NOTCH1 mutation had a significantly shorter OS compared with those with unmutated NOTCH1. The independent prognostic impact of NOTCH1 mutation on OS was confirmed in multivariate analysis.<sup>12</sup>

In the light of these observations, we conducted a multicenter, non-randomized phase II clinical trial that aimed to evaluate the efficacy, in terms of CR rate, of FCR as

first-line treatment for CLL, and to investigate the impact of rituximab maintenance therapy on the response rate and PFS following FCR. A key secondary objective was to analyze MRD status after chemoimmunotherapy and rituximab maintenance.

## Methods

Physically fit patients between 18 and 70 years old with active CD20<sup>+</sup> CLL according to the World Health Organization classification, with an Eastern Cooperative Oncology Group Performance Status  $\leq 2$ , were recruited into the REM (rituximab in maintenance) trial and received treatment with fludarabine (25 mg/m<sup>2</sup> iv on days 1-3), cyclophosphamide (250 mg/m<sup>2</sup> iv on days 1-3) and rituximab (375 mg/m<sup>2</sup> iv cycle 1 and 500 mg/m<sup>2</sup> iv cycles 2-6) every 28 days, for up to six cycles. Major exclusion criteria were prior treatment for CLL, severe cardiac, pulmonary, neurological, psychiatric, or metabolic disease, continuous systemic corticosteroids, active autoimmune hemolytic anemia or thrombocytopenia, active severe infection, creatinine clearance <50 mL/min, or transformation to an aggressive B-cell malignancy. All cases were CD20<sup>+</sup> as analyzed by flow cytometry, with a mean fluorescence intensity lower than the expression found in normal mature B lymphocytes in peripheral blood and bone marrow (BM).

At the 3-month post-induction clinical response evaluation, patients achieving a CR, partial response (PR) or nodular PR (nPR), based on International Workshop on CLL guidelines, were treated with rituximab 375 mg/m<sup>2</sup> iv every 2 months for 3 years (18 cycles). Anti-microbial prophylaxis included trimethoprim-sulfamethoxazole and acyclovir during treatment and until the level of CD4<sup>+</sup> lymphocytes reached  $0.3 \times 10^9/L$ . Patients achieving a CR and undetectable MRD in both peripheral blood and BM after four courses of FCR were allowed to stop fludarabine plus cyclophosphamide and complete two courses of rituximab and continue with rituximab maintenance therapy.

The primary endpoint was the CR rate after FCR treatment. Secondary endpoints included PFS, OS, correlation of response with the level of MRD after FCR and rituximab maintenance therapy, adverse events, and the prognostic impact of the biological markers CD38 and ZAP70, IGHV mutational status, cytogenetic abnormalities and BM-MRD on the course of the disease. Fluorescence *in situ* hybridization and IGHV analysis were performed locally in accredited laboratories using standardized procedures.

The study protocol was approved by the institutional review board of each participating institution and complied with the Declaration of Helsinki, and existing Good Clinical Practice guidelines, laws and regulations. All participants provided written informed consent before enrollment.

### Flow cytometry and measurable residual disease analysis

Samples were stained and lysed using a direct immunofluorescence technique as previously described.<sup>13</sup> The following antibody combinations were used: (i) CD22/CD23/CD19/CD5; (ii) FMC7/CD43/CD19/CD5; (iii) CD103/CD25/CD19/CD5; (iv) CD10/CD11c/CD19/CD5; (v) CD20/CD38/CD19/CD5; (vi) CD81/CD22/CD19/CD5; (vii) CD20/CD49d/CD19/CD5; (viii) sIgk/sIgl/CD19/CD5, and (ix) ZAP70/CD3+CD56/CD19/CD5. All monoclonal antibodies except ZAP70 were provided by Becton Dickinson (San José, CA, USA). ZAP70 was purchased from Immunotech (Marseille, France). Samples were acquired in a FACSCalibur flow cytometer (Becton Dickinson) and analyzed using Paint-A-Gate PRO software (Becton Dickinson). At least 20,000 events were acquired. B-lymphocytes were identified

according to their SSC/CD19<sup>+</sup> distribution and the total percentage of pathological CD38 and CD49d B cells was reported. ZAP70 was quantified using a cut-off of  $\geq 20\%$  to define the ZAP70<sup>+</sup> subset of B cells.<sup>14</sup>

MRD was analyzed in samples from peripheral blood and BM after induction and from BM during rituximab maintenance therapy, with a combination of monoclonal antibodies slightly modified from that in the European Research Initiative on CLL (ERIC) protocol: (i) CD20/CD38/CD19/CD5; (ii) CD81/CD22/CD19/CD5; (iii) sIgL/sIgK/CD19/CD5; and (iv) CD22/CD79b/CD19/CD5. CD43 was not included in the analysis: we included the last combination instead of CD43/CD79b/CD19/CD5 based on our previous experience with that combination in the analysis of MRD in CLL.<sup>13</sup> The minimum number of pathological B cells acquired was that in the ERIC recommendations.<sup>15</sup> To achieve a limit of detection of 0.01%, at least 200,000 events were acquired if the minimum population size was 20 and 500,000 events if the minimum population size was 50. We prepared the necessary number of tubes for each combination to acquire at least 200,000 events. The complete gating strategy is described in the *Online Supplement*.

### Statistical analysis

This was a two-staged, Simon optimal phase II clinical trial. Based on a CR rate observed in previous trials of first-line therapy ranging around 30%, the inactivity cut-off was chosen to equal 30% and the activity cut-off at least 50%. Hence, the hypotheses of interest were  $H_0: r \leq 0.3$  against  $H_1: r \geq 0.5\%$ , where  $r$  is the CR rate. Using a type I error rate ( $\alpha$ , probability of accepting an insufficiently active treatment, a false positive outcome) set at 0.05, and a type II error rate ( $\beta$ , probability of rejecting an active treatment, a false negative outcome) set at 0.20, we estimated that 90 patients should be enrolled into this trial, assuming a 10% loss.

A descriptive analysis of continuous and qualitative variables was performed. PFS, OS and duration of response were summarized descriptively and graphically using the Kaplan and Meier method in the overall population and separately by biological factors, genetic profiles and MRD status. The log-rank test was used for comparisons of PFS and OS curves. The  $\chi^2$  test was used to assess the frequencies and differences of biological and cytogenetic abnormalities. The relationship between these abnormalities and MRD level was analyzed using logistic regression models. Safety data were summarized for all treated patients during induction, maintenance and combined. All hypothesis tests were two-sided and a  $P$ -value <0.05 was considered statistically significant. All statistical computations were carried out with SPSS version 14.0 or subsequent versions.

## Results

We present the results of an end-of-study analysis at 3 years of follow-up after 36 months of rituximab maintenance therapy following FCR induction. Between October 2007 and December 2012, 90 patients were assessed for eligibility in 29 center across Spain, and 84 were assigned to FCR (6 patients did not meet the eligibility criteria, of whom 2 after 1 treatment infusion) and were evaluable for response in an intent-to-treat analysis (Figure 1). Overall, 79.8% (n=67) of the enrolled patients were aged 64 years or younger, 67.9% (n=57) were male and 83.3% (n=70) had Binet stage B or C disease. The median age of trial participants was 59.5 years (range, 37-70), and 70.5% (n=55) of participants were in a good state of health with an Eastern Cooperative Oncology Group Performance Status

of 0-1. Overall, 53.7% (n=45) of the trial population had B symptoms.

Table 1 summarizes the biological and genetic abnormalities assessed at baseline that were considered to be prognostic for outcome. Overall, 57.14% (n=48) of patients had unmutated IGHV, 47.6% (n=39) were CD38<sup>+</sup> and 57.3% (n=43) were ZAP70<sup>+</sup>. Forty-two (50.0%) patients had a 13q14 deletion, 22 (26.1%) had a 11q22-q23 deletion, 13 (15.4%) harbored trisomy 12, four (4.7%) patients had a 17p deletion, and three (3.5%) had a 6q deletion.

Overall, 12 patients (14%) ended treatment induction prematurely. The reasons for discontinuation included toxicity (n=6), progressive disease (n=1), ineligibility (n=2), and investigators' decision (n=3: 1 patient with ischemic cerebrovascular disease, 1 patient with concomitant idiopathic thrombocytopenic purpura and 1 patient with a karyotype with chromosomal random losses). The median number of FCR cycles was six, and complete treatment was administered to 80% of the patients.

## Response and treatment outcomes

### Induction

Of 84 evaluable patients in an intent-to-treat analysis of the effects of FCR induction treatment, 80 patients had a CR/CR with incomplete hematologic recovery (CRi), PR or nPR for an overall response rate of 95.2% (75.0% CR/CRi(2), n=63; 7.1% nPR, n=6; 13.1% PR, n=11) while four patients failed to respond to FCR. Of the 80 patients evaluable for BM-MRD status, 44.1% (n=37) had undetectable MRD at 3 months after induction, of whom 35 (41.7%) had a CR and two (2.4%) had a PR, while 43 had detectable MRD, of whom 28 (35.0%) had a CR, eight (10.0%) had a nPR, and seven (8.8%) had a PR.

### Rituximab maintenance

Of the 80 patients with CR or PR after FCR induction, 74 entered the maintenance study. At the end of the maintenance phase, 52 patients had a CR and seven had a PR (2 nPR; 5 PR). At cycle 12 of treatment, 29 patients had a CR and four patients had attained a PR. At cycle 9, 42 patients had a CR and five had a PR. Reasons for discon-

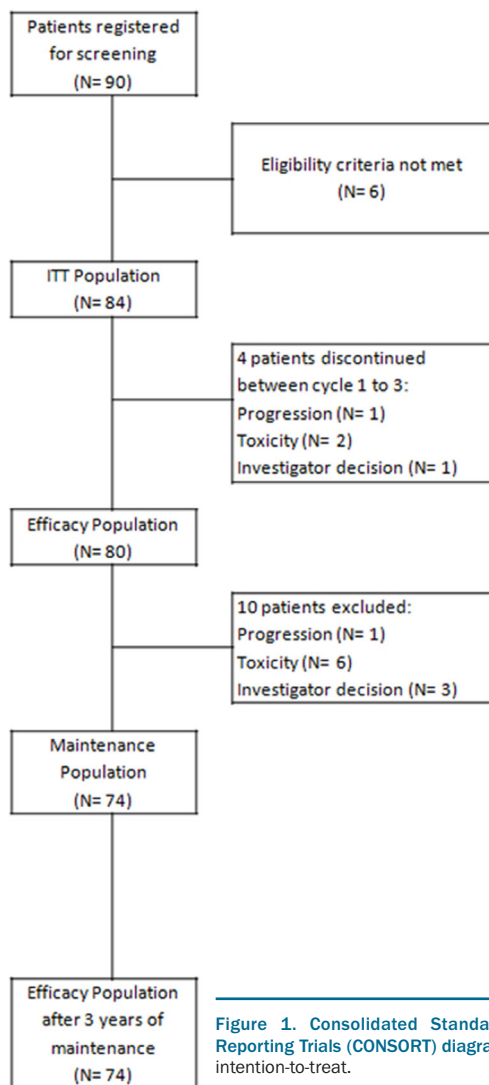


Figure 1. Consolidated Standards of Reporting Trials (CONSORT) diagram. ITT: intention-to-treat.

Table 1. Patients' baseline characteristics.

Patients' characteristics	
Median age (range)	59.5 years (37,1-70,9)
Sex (n; %)	
Men	57 (67.9)
Women	27 (32.1)
ECOG performance status (n; %)	
PS-0	55 (70.5)
PS ≥1	23 (29.4)
Binet stage (n; %)	
A	14 (16.7)
B	53 (63.1)
C	17 (20.2)
FISH cytogenetic status (n; %)	
del(13q)	42 (50.0)
del(11q)	22 (26.1)
trisomy 12	13 (15.4)
del(17p)	4 (4.7)
del(6q)	3 (3.5)
IGHV status (n; %)	
unmutated	48 (57.1)
IGHV 3-21	3 (3.6)
mutated	27 (32.1)
inconclusive	6 (7.1)
Immunophenotyping (n; %).	
>10% CD38 positive	53 (64.6)
>30% CD38 positive	39 (47.6)
>20% ZAP70 positive	43 (57.3)
>20% CD49d positive	30 (37.0)
Response (n; %)	
Complete response	63 (75.0)
Partial response	11 (13.1)
Nodular partial response	6 (7.1)
Undetectable MRD status post-induction	
Peripheral blood	60 (71.4)
Bone marrow	37 (44.0)

ECOG: Eastern Cooperative Oncology Group; PS: Performance Status; FISH: fluorescence *in-situ* hybridization; MRD: measurable residual disease.

tinuation were myelotoxicity (n=14; 18.9%), clinical progression (n=8; 10.8%), consent withdrawal (n=3; 4.0%) investigator's decision (n=1; 1.3%), protocol violation (n=1; 1.3%), infection (n=3; 4.0%) and death (n=2; 2.7%). During the follow-up period, all patients who were analyzed maintained CR or PR.

At the end of maintenance therapy, MRD assessed at cycles 9, 12, 15 and 18 was negative in 44 of the 72 patients (61.1%) evaluable for response. Interestingly, 29 patients who had detectable BM-MRD immediately after induction converted to an undetectable BM-MRD status following rituximab maintenance therapy. In detail, after nine cycles, 13 patients with detectable BM-MRD converted to having undetectable BM-MRD and two with undetectable BM-MRD became MRD-positive. After 18 cycles, 16 patients with detectable BM-MRD converted to being MRD-negative and five with undetectable BM-MRD became BM-MRD-positive (2 CR relapsed after 18 months, 1 CR interrupted treatment at 12 months because of toxicity, 1 PR progressed after 13 months and 1 CR relapsed after 4 months) (Table 2).

### Survival

At the end of the study, with a median follow-up of 6.3 years, the estimated proportions of patients who were alive and progression-free were 0.76 and 0.61, respectively. Analyzed according to their MRD status, patients with a CR and either undetectable or detectable MRD did not reach the median PFS and OS, while for patients with

detectable MRD and a PR the median PFS was 2.04 years (95% CI: 0-4.3 years) and the median OS was 4.60 years (95% CI: 3.0-6.1 years). Regarding response duration, a total of 56 patients (71.2%) maintained their response throughout the whole study: the median response duration was 6.4 years (95%CI: 6.08-6.68). Univariate Cox regression analysis showed that IGHV status affected PFS: the PFS rate at 7.3 years in patients with mutated IGHV was 0.85, whereas it was 0.39 in those with unmutated IGHV. However, the median OS for patients with either mutated or unmutated IGHV was not reached (Figure 1). No correlations were identified between the other clinical, biological or molecular factors and the achievement of undetectable MRD.

When MRD values were categorized into low (<0.01%, i.e. less than 1 CLL cell per 10,000 leukocytes), intermediate (0.01% to 1%) and high (>1%), the median PFS and OS were not reached in patients with low and intermediate MRD levels and were 2.0 years (95% CI: 0-4.3) and 4.6 years (95% CI: 4.2-4.9), respectively, in patients with high MRD levels (Figure 2, and Table 3A and 3B).

### Safety

As per protocol, 86 patients were evaluated for safety after FCR induction. The most common adverse events were grade 1-2 rituximab infusion reactions (65.1%), grade 3-4 myelosuppression (29 patients, 33.7%) and infections (grade 1-2: 30 patients, 34.9%; grade 3-4: 3 patients, 3.5%). In addition, there were 11 (12.8%) grade

Table 2. Measurable residual disease assessment.

MRD status	Induction (n=74)	6 Rm cycles (1 year) (n= 56)	12 Rm cycles (2 years) (n= 35)	18 Rm cycles (3 years) (n= 42)
Negative	33	36	23	31
Positive	41	20	12	11

MRD: measurable residual disease; Rm: rituximab maintenance therapy.

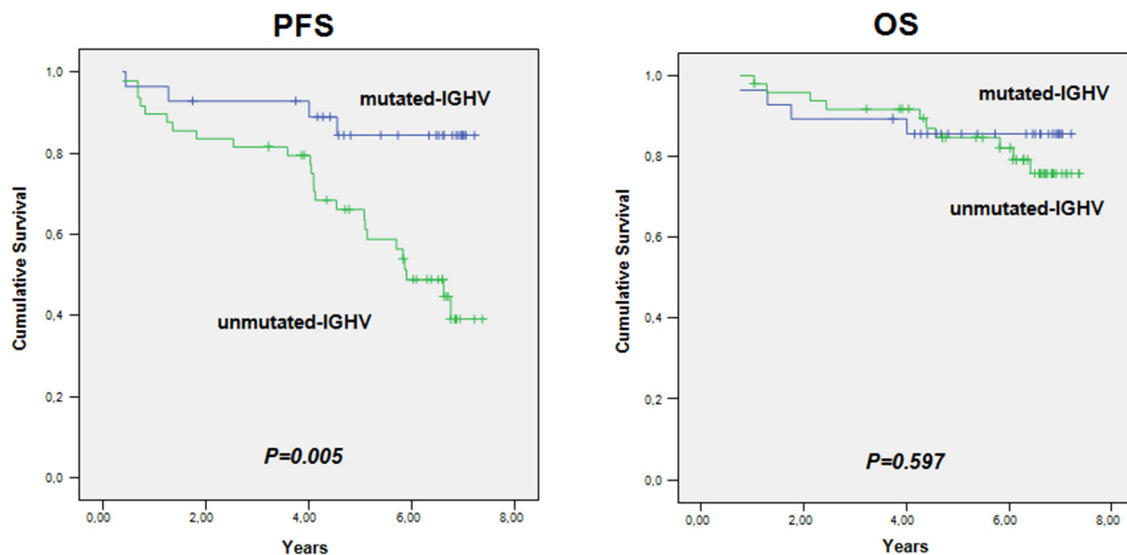


Figure 2. Progression-free survival and overall survival according to IGHV mutational status. PFS: progression-free survival; OS: overall survival.

3-4 non-hematologic serious adverse events.

The most common adverse event during rituximab maintenance therapy was grade 3-4 myelosuppression, which occurred in 28 patients (37.8%). In more detail, neutropenia between cycles and anemia were observed in 27 patients (36.5%) and one patient (1.4%), respectively. Grade 1-2 infections were detected in 43 patients (58.1%), while grade 3-4 infections were documented in ten patients (13.5%) and were pneumonia (n=5), respiratory tract infections (n=2), meningitis (n=1), viral myocarditis (n=1), and gastroenteritis (n=1). Febrile neutropenia was observed in five patients (6.8%).

**Discussion**

Despite the improved efficacy of currently approved chemoimmunotherapy in CLL patients, the majority of patients, including those who achieve CR, eventually relapse as a consequence of residual malignant cells still present after therapy. The high CR rate recorded in this study indicates that FCR induction followed by rituximab maintenance therapy produces a high overall response rate in patients considered fit for fludarabine-based therapy. By increasing the quality of clinical responses through obtaining a high undetectable MRD CR rate, the PFS of patients with a clinical response is prolonged. Ultimately, this confirms the role and value of undetectable MRD status in CLL.

In our study, MRD in BM was undetectable at the 10<sup>-4</sup> level in 44% of the 80 patients evaluated after the induction treatment and in 68% of 59 patients at the end of maintenance therapy. Furthermore, rituximab maintenance therapy significantly increased the number of patients with undetectable MRD in BM. Indeed, 40 patients with detectable BM-MRD converted to an undetectable BM-MRD status from cycle 9 and subsequent

cycles. Additionally, although small numbers limited our subgroup analysis, it is remarkable that 41%, 58% and 60% of patients with undetectable MRD following rituximab maintenance therapy (n=40) harbored factors well-known to be associated with lower response and poor long-term outcomes.<sup>16-18</sup> Our data suggest a PFS benefit from rituximab maintenance therapy in IGHV-mutated vs. unmutated patients (PFS at 7.2 year: 84.5% vs. 39.1%, respectively). Overall, clinical outcomes were encouraging in this study as the median OS and PFS were not reached. The estimated 7-year PFS and OS rates were 56.2% and 78.0%, respectively. Of note, the median OS and PFS for patients with a CR and either undetectable BM-MRD or detectable BM-MRD were not reached. However, despite these data suggesting a benefit on time-to-event curves, it is important to note that this was not a randomized study. Nevertheless, although direct comparisons between trials

**Table 3A.** Progression-free and overall survival according to measurable residual disease group assessment at the staging following treatment with fludarabine, cyclophosphamide, and rituximab.

MRD Group	Low (<0.01%)	Intermediate (0.01%-1%)	High (>1%)
PFS	NR	NR	2.0 years (95% CI: 0-4.3)
OS	NR	NR	4.6 years (95% CI: 0-4.3)

MRD: measurable residual disease; PFS: progression-free survival; OS: overall survival; NR: not reached; 95% CI: 95% confidence interval.

**Table 3B.** Seven-year progression-free and overall survival rates after 36 months of maintenance therapy according to measurable residual disease group.

MRD Group	Low (<0.01%)	Intermediate (0.01%-1%)	High (>1%)
PFS	93.2%	25.0%	28.6%
OS	100%	100%	68.6%

MRD: measurable residual disease; PFS: progression-free survival; OS: overall survival.

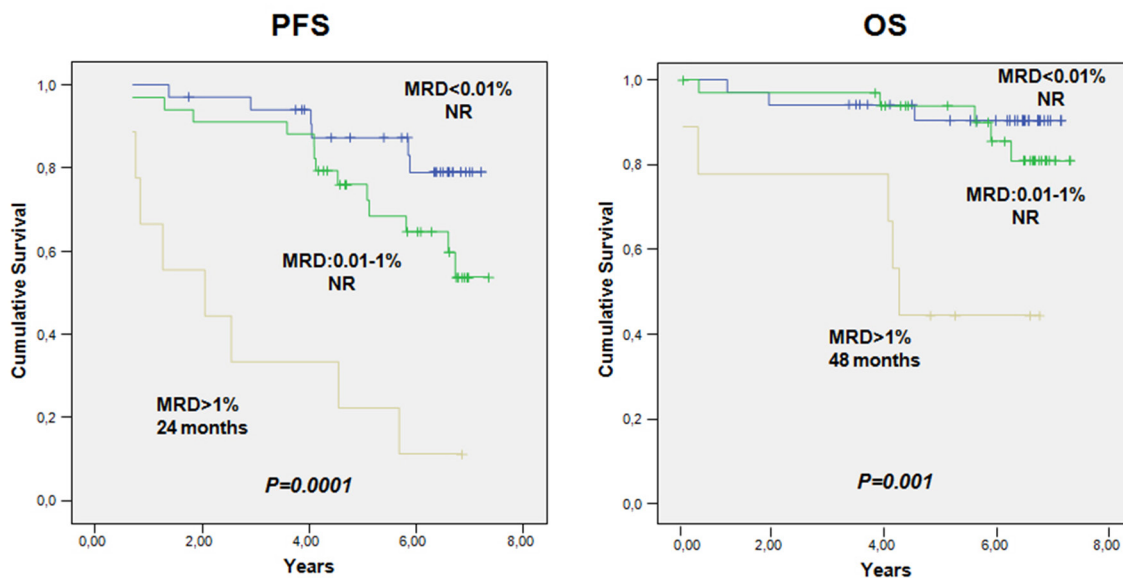


**Figure 3.** Progression-free survival and overall survival according to measurable residual disease status. PFS: progression-free survival; OS: overall survival; MRD: measurable residual disease; NR: not reached.

is not recommended, these results (along with published data), suggest that maintenance treatment with a chemotherapy-free approach would improve long-term outcomes with acceptable toxicity. Furthermore, when MRD values were categorized into low (<0.01%), intermediate (0.01% to 1%) and high (>1%), low and intermediate MRD levels were associated with longer PFS and OS following rituximab maintenance therapy (OS:  $P < 0.0001$ ) compared with higher MRD levels which were associated with significantly shorter PFS and OS (2.0 and 4.6 years, respectively), suggesting a favorable prognostic effect of MRD level for patients given rituximab maintenance therapy.

The relationship between undetectable MRD following frontline therapy and long-term outcomes, namely PFS and OS, has been investigated extensively in recent years. Nevertheless, to our knowledge, our study has one of the longest maintenance phases given to CLL patients in first remission. The German CLL Study Group (GCLLSG) updated the CLL8 trial which compared FCR to fludarabine plus cyclophosphamide in untreated CLL patients. With a median follow-up of 5.9 years, the median PFS for the patients treated with FCR was 56.8 months, and the median OS was not reached in the FCR group.<sup>5,6</sup> Furthermore, patients achieving undetectable MRD had a significantly longer PFS (64.0 months) while the median OS was not reached. The rituximab-containing arm produced twice the number of patients achieving undetectable MRD.

In our study, median PFS and OS were not reached for patients with undetectable BM-MRD. We hypothesized that this difference was probably due to the source of samples. These data suggest that higher response rates and longer response durations could be expected by intensifying therapy through prolonged maintenance treatment with anti-CD20 immunotherapy.<sup>19</sup> In addition, a combined analysis of the CLL8 and CLL10 trials showed that PFS was significantly longer in patients with undetectable MRD than in those with detectable MRD, despite being unaffected by the residual tumor load, thus supporting the prognostic significance of undetectable MRD in CLL patients.<sup>20</sup> In another study Greil *et al.* enrolled patients who had achieved a CR, CRi or PR after first- or second-line rituximab-based chemoimmunotherapy.<sup>21</sup> PFS was significantly longer in the rituximab maintenance arm (47.0 vs. 35.5 months, HR 0.50, 95% CI: 0.38-0.66;  $P < 0.0001$ ), suggesting that remission maintenance is an effective and safe option for CLL patients. In that study, MRD progression was documented more frequently in patients on observation than in those on rituximab maintenance therapy ( $P < 0.0001$ ) and, interestingly, conversion to undetectable MRD status occurred more frequently in the rituximab maintenance arm (12 patients vs. 1 patient;  $P = 0.003$ ). Based on these data, it seems that maintenance therapy may improve the quality of remission in CLL subjects and prolong PFS.

Although firm conclusions are limited by the number of subjects in our trial, patients who discontinued chemoimmunotherapy after achieving undetectable BM-MRD CR at cycle 4 and continued with the maintenance phase had similar PFS and OS rates to those of patients who achieved undetectable MRD but continued treatment for all six cycles: 93.3% and 76.5% were alive at 7 years, while 80.0% and 60.6% were free of disease at 7 years, respectively. In the light of these data, it might be useful to eval-

uate the efficacy and efficiency of a strategy that adapts the duration of treatment to achieve undetectable MRD. Although a high rate of falsely negative MRD in peripheral blood up to 12 months has been reported with rituximab-containing regimens (20-30%), our hypothesis was based on the predictive model published by Dimier *et al.*, testing the effect of treatment on PFS using MRD as a surrogate endpoint.<sup>22</sup> Thus, we only stopped FCR after four cycles when MRD was undetectable in both peripheral blood and BM. Although MRD-tailored therapy has not been validated prospectively, Strati *et al.* showed that patients who discontinued frontline FCR after achieving undetectable MRD after three cycles of treatment had similar PFS and OS to those who achieved undetectable MRD but continued treatment for all six cycles.<sup>23</sup> Furthermore, PFS in the subgroup of patients who discontinued frontline FCR after three cycles of treatment because they had achieved undetectable MRD was better than the PFS of patients who remained with detectable MRD at the end of the course of six cycles, despite the shorter duration of treatment in the former group. In addition, Thompson *et al.* recently reported that undetectable MRD after course 3 of FCR predicted a greater likelihood of undetectable MRD at the end of therapy.<sup>24</sup>

Although the study was designed before the ERIC recommended diagnostic markers were published, with a median number of BM leukocytes of around 410,000 (range, 150,000-610,000) and a sensitivity of MRD detection of  $\geq 10^{-4}$ , the immunophenotypic CLL analysis performed in this study was robust. The methodology for assessing MRD was similar to the flow cytometry methodology established by the ERIC consortium, as three of the tubes were similar to the subsequently published ERIC recommendations.<sup>15,25,26</sup> The potential limitation of the flow cytometry assay is the need for at least  $10^6$  cells per tube and a total of four tubes, which may be an issue to keep in mind when small samples are available. In addition, selection of the sample source remains a challenge, as a significant discrepancy between MRD status determined in peripheral blood and BM has been reported.<sup>27</sup> A paired analysis of peripheral blood and BM samples in our study revealed that 60 patients did not have detectable MRD in peripheral blood, while only 37 achieved undetectable MRD in the BM. This discrepancy is partially a result of the compartmental nature of CLL, with disease reservoirs in the BM, blood, lymph nodes, liver, and spleen. As rituximab targets CD20 on mature, malignant and benign B cells, rituximab-based therapy will achieve undetectable MRD much more rapidly in peripheral blood than in BM. Indeed, in the REM trial we decided to use the CD20 marker in two of our MRD tubes for two reasons, (i) CD20 as a single marker provides the most powerful separation of CLL cells from normal B cells, and (ii) in patients treated with rituximab-containing regimens, the correlation between real-time quantitative polymerase chain reaction findings and the results of assays with combinations including the CD20 marker was not weaker than that with combinations not including the CD20 marker.<sup>28</sup>

Based on the results described above, it appears that 3 years of rituximab maintenance therapy was beneficial for enrolled patients, improving the quality of remissions and prolonging survival. The reason for the high response rates, undetectable MRD and favorable PFS and OS rates compared to those from clinical trials with similar entry

criteria is probably multifactorial, but may include the age and Performance Status of the patients: their median age was 59.5 years and up to 70.5% patients had an Eastern Cooperative Oncology Group Performance Status of 0. Additionally, the protocol-defined anti-microbial prophylaxis scheduled for this trial allowed a treatment compliance of around 80%. Furthermore, the secondary endpoint of undetectable MRD is strongly associated with outcome: at the post-maintenance assessment, 68% of assessed patients had undetectable MRD. Finally, the median follow-up of 75.6 months is long enough to allow solid interpretation of both PFS and OS.

A weakness of this trial is that, since its design, new drugs targeting signaling pathways, and newer monoclonal antibodies have become available, and the interest in chemoimmunotherapy, such as FCR, has weakened. Additionally, since OS findings have been inconsistent and one could argue that prolonged maintenance use of certain molecules could expose CLL patients to increased toxicity and ultimately reduce their quality of life, the debate should be whether to use rituximab for maintenance or to watch and wait and give these therapies when the patients relapse. Upon closer examination of our results, patients with unfavorable cytogenetics, unmutated somatic IGHV genes, and CD38 and ZAP70 expression benefited from rituximab maintenance therapy. Further research is now needed to identify subgroups of patients who may benefit while on maintenance therapy.

Of the 957 treatment-emergent adverse events, 54% occurred during induction treatment; most were classed as neutropenia or lymphopenia, and almost half (47.4%) were suspected to be related to rituximab. However, the same adverse events could be related to more than one of

the drugs administered. The most frequent of the 440 treatment-emergent adverse events recorded during the maintenance period was neutropenia, which was recorded in 43.3% of the patients. Of the total of 957 treatment-emergent adverse events, 26.6% were assessed as grade  $\geq 3$  and the majority were associated with disorders in the blood and lymphatic systems. Sixteen out of 20 deaths reported in the study occurred during the maintenance period. There was only one treatment-related death, which happened during the maintenance period. Overall, the safety profile of rituximab in the maintenance setting was consistent with its expected safety profile and no new unexpected adverse events were reported.

In summary, this study provides the first insights into the potential clinical use of FCR treatment followed by a 3-year period of rituximab maintenance as a treatment strategy. Our study suggests that maintenance therapy with rituximab further prolongs responses in CLL patients with detectable MRD (when judged against historical outcomes after FCR treatment), with significantly improved PFS and OS for patients who achieved at least a PR after FCR induction. Based on these results, undetectable MRD is confirmed as a predictive biomarker associated with treatment response following rituximab maintenance therapy. Prospective studies aimed at evaluating long-term outcomes following early treatment discontinuation and the potential benefit in terms of reducing acute and delayed toxicity are necessary before MRD testing can be used to guide treatment decisions in clinical practice.

#### Funding

*This work was funded by Roche Farma, S.A., Madrid, Spain.*

## References

- Müller-Hermelink HK, Montserrat E, Catovsky D, et al. Chronic lymphocytic leukaemia/small lymphocytic lymphoma. In: Swerdlow SH, Campo E, Harris NL, et al., editors. WHO Classification of Tumours of Haematopoietic and Lymphoid Tissues. Lyon, France: IARC Press; 2008. pp.180-182.
- Ginaldi L, De Martinis M, Matutes E, Farahat N, Morilla R, Catovsky D. Levels of expression of CD19 and CD20 in chronic B cell leukaemias. *J Clin Pathol.* 1998;51(5):364-369.
- Moreau EJ, Matutes E, A'Hern RP, et al. Improvement of the chronic lymphocytic leukemia scoring system with the monoclonal antibody SN8 (CD79b). *Am J Clin Pathol.* 1997;108(4):378-382.
- Hallek M, Cheson BD, Catovsky D, et al. Guidelines for the diagnosis and treatment of chronic lymphocytic leukemia: a report from the International Workshop on Chronic Lymphocytic Leukemia updating the National Cancer Institute-Working Group 1996 guidelines. *Blood.* 2008;111(12):5446-5456.
- Hallek M, Fischer K, Fingerle-Rowson G, et al. Addition of rituximab to fludarabine and cyclophosphamide in patients with chronic lymphocytic leukaemia: a randomised, open-label, phase 3 trial. *Lancet.* 2010;376(9747):1164-1174.
- Rossi D, Terzi-di-Bergamo L, De Paoli L, et al. Molecular prediction of durable remission after first-line fludarabine-cyclophosphamide-rituximab in chronic lymphocytic leukemia. *Blood.* 2015;126(16):1921-1924.
- Fischer K, Bahlo J, Fink AM, et al. Long-term remissions after FCR chemoimmunotherapy in previously untreated patients with CLL: updated results of the CLL8 trial. *Blood.* 2016;127(2):208-215.
- Thompson PA, Tam CS, O'Brien SM, et al. Fludarabine, cyclophosphamide, and rituximab treatment achieves long-term disease-free survival in IGHV-mutated chronic lymphocytic leukemia. *Blood.* 2016;127(3):303-309.
- Thompson PA, Wierda WG. Eliminating minimal residual disease as a therapeutic end point: working toward cure for patients with CLL. *Blood.* 2016;127(3):279-286.
- Abrisqueta P, Villamor N, Terol MJ, et al. Rituximab maintenance after first-line therapy with rituximab, fludarabine, cyclophosphamide, and mitoxantrone (R-FCM) for chronic lymphocytic leukemia. *Blood.* 2013;122(24):3951-3959.
- Del Poeta G, Del Principe MI, Buccisano F, et al. Consolidation and maintenance immunotherapy with rituximab improve clinical outcome in patients with B-cell chronic lymphocytic leukemia. *Cancer.* 2008;112(1):119-128.
- Bo MD, Del Principe MI, Pozzo F, et al. NOTCH1 mutations identify a chronic lymphocytic leukemia patient subset with worse prognosis in the setting of a rituximab-based induction and consolidation treatment. *Ann Hematol.* 2014;93(10):1765-1774.
- García Vela JA, Delgado I, Benito L, et al. CD79b expression in B cell chronic lymphocytic leukemia: its implication for minimal residual disease detection. *Leukemia.* 1999;13(10):1501-1505.
- Wang YH, Fan L, Xu W, Li JY. Detection methods of ZAP70 in chronic lymphocytic leukemia. *Clin Exp Med.* 2012;12(2):69-77.
- Rawstron AC, Fazi C, Agathangelidis A, et al. A complementary role of multiparameter flow cytometry and high-throughput sequencing for minimal residual disease detection in chronic lymphocytic leukemia: an European Research Initiative on CLL study. *Leukemia.* 2016;30(4):929-936.
- Hamblin TJ, Davis Z, Gardiner A, Oscier DG, Stevenson FK. Unmutated Ig V(H) genes are associated with a more aggressive form of chronic lymphocytic leukemia. *Blood.* 1999;94(6):1848-1854.
- Hamblin TJ, Orchard JA, Ibbotson RE, et al. CD38 expression and immunoglobulin variable region mutations are independent prognostic variables in chronic lymphocytic leukemia, but CD38 expression may vary during the course of the disease. *Blood.* 2002;99(3):1023-1029.
- Dürig J, Nuckel H, Cremer M, et al. ZAP-70

- expression is a prognostic factor in chronic lymphocytic leukemia. *Leukemia*. 2003;17(12):2426-2434.
19. Böttcher S, Ritgen M, Fischer K, et al. Minimal residual disease quantification is an independent predictor of progression-free and overall survival in chronic lymphocytic leukemia: a multivariate analysis from the randomized GCLLSG CLL8 trial. *J Clin Oncol*. 2012;30(9):980-988.
  20. Kovacs G, Robrecht S, Fink AM, et al. Minimal residual disease assessment improves prediction of outcome in patients with chronic lymphocytic leukemia (CLL) who achieve partial response: comprehensive analysis of two phase III studies of the German CLL Study Group. *J Clin Oncol*. 2016;34(31):3758-2765.
  21. Greil R, Obrtlíková P, Smolej L, et al. Rituximab maintenance versus observation alone in patients with chronic lymphocytic leukaemia who respond to first-line or second-line rituximab-containing chemotherapy: final results of the AGMT CLL-8a Maintenance randomised trial. *Lancet Haematol*. 2016;3(7):e317-e329.
  22. Dimier N, Delmar P, Ward C, et al. A model for predicting effect of treatment on progression-free survival using MRD as a surrogate end point in CLL. *Blood*. 2018;131(9):955-962.
  23. Strati P, Keating MJ, O'Brien SM, et al. Eradication of bone marrow minimal residual disease may prompt early treatment discontinuation in CLL. *Blood*. 2014;123(24):3727-3732.
  24. Thompson PA, Peterson CB, Strati P, et al. Serial minimal residual disease (MRD) monitoring during first-line FCR treatment for CLL may direct individualized therapeutic strategies. *Leukemia*. 2018;32(11):2388-2398.
  25. Rawstron AC, Kreuzer KA, Soosapilla A, et al. Reproducible diagnosis of chronic lymphocytic leukemia by flow cytometry: an European Research Initiative on CLL (ERIC) & European Society for Clinical Cell Analysis (ESCCA) harmonisation project. *Cytometry B Clin Cytom*. 2018;94(1):121-128.
  26. Rawstron AC, Villamor N, Ritgen M, et al. International standardized approach for flow cytometric residual disease monitoring in chronic lymphocytic leukaemia. *Leukemia*. 2007;21(5):956-964.
  27. Rawstron A, Cohen D, de Tute R, et al. Bone marrow is more sensitive than peripheral blood for detection of MRD in CLL and provides a more reliable prediction of outcome across different treatments. *Haematologica*. 2015;100(Suppl 1):Abstract S794.
  28. Rawstron AC, Böttcher S, Letestu R, et al. Improving efficiency and sensitivity: European Research Initiative in CLL (ERIC) update on the international harmonised approach for flow cytometric residual disease monitoring in CLL. *Leukemia*. 2013;27(1):142-149.



Ferrata Storti Foundation

# Utility of positron emission tomography-computed tomography in patients with chronic lymphocytic leukemia following B-cell receptor pathway inhibitor therapy

Anthony R. Mato,<sup>1</sup> William G. Wierda,<sup>2</sup> Matthew S. Davids,<sup>3</sup> Bruce D. Cheson,<sup>4</sup> Steven E. Coutre,<sup>5</sup> Michael Choi,<sup>6</sup> Richard R. Furman,<sup>7</sup> Leonard Heffner,<sup>8</sup> Paul M. Barr,<sup>9</sup> Herbert Eradat,<sup>10</sup> Sharanya M. Ford,<sup>11</sup> Lang Zhou,<sup>11</sup> Maria Verdugo,<sup>11</sup> Rod A. Humerickhouse,<sup>11</sup> Jalaja Potluri<sup>11</sup> and John C. Byrd<sup>12</sup>

Haematologica 2019  
Volume 104(11):2258-2264

<sup>1</sup>CLL Program, Leukemia Service, Division of Hematologic Oncology, Memorial Sloan Kettering Cancer Center, New York, NY; <sup>2</sup>University of Texas MD Anderson Cancer Center, Houston, TX; <sup>3</sup>Dana-Farber Cancer Institute, Boston, MA; <sup>4</sup>Georgetown University Hospital, Washington, DC; <sup>5</sup>Stanford Cancer Center, Stanford University School of Medicine, Stanford, CA; <sup>6</sup>UCSD Moores Cancer Center, San Diego, CA; <sup>7</sup>Weill Cornell Medicine, New York, NY; <sup>8</sup>Emory University School of Medicine, Atlanta, GA; <sup>9</sup>Wilmot Cancer Institute, University of Rochester Medical Center, Rochester, NY; <sup>10</sup>University of California Los Angeles, Los Angeles, CA; <sup>11</sup>AbbVie Inc. North Chicago, IL and <sup>12</sup>The Ohio State University, Columbus, OH, USA

## ABSTRACT

The utility of positron emission tomography-computed tomography (PET-CT) in distinguishing Richter's transformation *versus* chronic lymphocytic leukemia (CLL) progression after ibrutinib and/or idelalisib was assessed in a *post hoc* analysis of a phase II study of venetoclax. Patients underwent PET-CT at screening and were not enrolled/treated if Richter's transformation was confirmed pathologically. Of 167 patients screened, 57 met criteria for biopsy after PET-CT. Of 35 patients who underwent biopsy, eight had Richter's transformation, two had another malignancy, and 25 had CLL. A PET-CT maximum standardized uptake value (SUVmax)  $\geq 10$  had 71% sensitivity and 50% specificity for detecting Richter's transformation [Odds Ratio (OR): 2.5, 95%CI: 0.4-15;  $P=0.318$ ]. Response rate to venetoclax was similar for screening SUVmax  $< 10$  *versus*  $\geq 10$  (65% *vs.* 62%) ( $n=127$  enrolled), though median progression-free survival was longer at  $< 10$  months (24.7 *vs.* 15.4 months;  $P=0.0335$ ). Six patients developed Richter's transformation on venetoclax, of whom two had screening biopsy demonstrating CLL (others did not have a biopsy) and five had screening SUVmax  $< 10$ . We have defined the test characteristics for PET-CT to distinguish progression of CLL as compared to Richter's transformation when biopsied in patients treated with B-cell receptor signaling pathway inhibitors. Overall diminished sensitivity and specificity as compared to prior reports of patients treated with chemotherapy/chemoimmunotherapy suggest it has diminished ability to discriminate these two diagnoses using a SUVmax  $\geq 10$  cutoff. This cutoff did not identify venetoclax-treated patients with an inferior response but may be predictive of inferior progression-free survival. (Registered at *clinicaltrials.gov* identifier: 02141282)

## Correspondence:

ANTHONY R. MATO  
matoa@mskcc.org

Received: September 28, 2018.

Accepted: March 20, 2019.

Pre-published: March 28, 2019.

doi:10.3324/haematol.2018.207068

Check the online version for the most updated information on this article, online supplements, and information on authorship & disclosures: [www.haematologica.org/content/104/11/2258](http://www.haematologica.org/content/104/11/2258)

©2019 Ferrata Storti Foundation

Material published in Haematologica is covered by copyright. All rights are reserved to the Ferrata Storti Foundation. Use of published material is allowed under the following terms and conditions:

<https://creativecommons.org/licenses/by-nc/4.0/legalcode>.

Copies of published material are allowed for personal or internal use. Sharing published material for non-commercial purposes is subject to the following conditions:

<https://creativecommons.org/licenses/by-nc/4.0/legalcode>,

sect. 3. Reproducing and sharing published material for commercial purposes is not allowed without permission in writing from the publisher.



## Introduction

Chronic lymphocytic leukemia (CLL) is an indolent, low-grade B-cell lymphoproliferative disorder, which can undergo Richter's transformation (RT) to a diffuse large B-cell lymphoma (DLBCL)<sup>1</sup> or Hodgkin lymphoma. The prognosis of RT is extremely poor, with a median survival of about eight months.<sup>2-5</sup> Clinical signs and symptoms associated with RT are non-specific and include rapid clinical deterioration.<sup>6</sup> Potential factors that may predict RT include mutational status, such as *TP53*

dysfunction (including 17p deletion and/or *TP53* mutation), advanced stage disease, disease burden, and therapeutic regimen.<sup>1,6,7</sup>

Chronic lymphocytic leukemia generally exhibits low levels of 18-F-fluorodeoxyglucose (FDG) uptake on positron emission tomography-computed tomography (PET-CT), compared to aggressive lymphomas and transformed lymphomas.<sup>8,9</sup> This difference suggests that PET-CT would be a useful tool for distinguishing aggressive *versus* indolent lymphomas and for selection of nodes for transformation confirmation biopsy. Various studies examining CLL and RT provide a considerable amount of data to inform the use of PET-CT imaging as a tool for distinguishing RT from CLL after chemoimmunotherapy, including standardized uptake value (SUVmax) cutoff thresholds.<sup>3,9,10</sup> Recent studies have emphasized the unfavorable prognosis for patients with RT following treatment with targeted agents, such as the B-cell receptor signaling pathway inhibitors (BCRi) ibrutinib or idelalisib.<sup>11,12</sup> Patients who progress after BCRi therapy often demonstrate highly proliferative CLL, even in the absence of a RT, possibly relating to biological differences required for rapid disease progression after BCRi, and thus requiring re-evaluation of PET-CT SUVmax cutoffs for distinguishing RT from CLL.

Venetoclax is a selective, orally bioavailable small-molecule BCL-2 inhibitor that has been approved for patients with previously-treated CLL del(17)(p13.1) and for those without del(17)(p13.1) or *TP53* mutation who have not responded to chemoimmunotherapy and BCR-inhibitor therapy.<sup>13,14</sup> Given the promising efficacy of venetoclax across a broad range of patients with relapsed/refractory CLL,<sup>15,16</sup> an open-label, phase II study was conducted to evaluate venetoclax monotherapy in patients with CLL refractory to or progressed after discontinuation of ibrutinib or idelalisib. Per protocol, all consenting patients were required to undergo PET-CT imaging at screening, with FDG-avid lymph node biopsy in patients with a suspicion of RT. Here we describe a *post hoc* analysis to determine if PET-CT and/or patient characteristics were able to differentiate RT *versus* CLL progression for patients who discontinued BCRi. We also report on the incidence of RT on venetoclax in these patients and how pre-venetoclax PET-CT SUVmax may predict clinical outcomes.

## Methods

### Study design and overview

Data from a phase II, open-label, multicenter trial ([clinicaltrials.gov](https://clinicaltrials.gov/ct2/show/study?term=02141282) identifier: 02141282) of venetoclax monotherapy enrolled patients with CLL relapsed/refractory following ibrutinib or idelalisib were analyzed *post hoc*.<sup>17</sup> At each participating site, the institutional review board approved the study protocol and amendments. Study activities were conducted in accordance with ethical principles established in the Declaration of Helsinki and the International Conference on Harmonization Guideline for Good Clinical Practice. All patients provided written informed consent.

### Patients

Adults with CLL refractory to or progressed after discontinuation of ibrutinib or idelalisib who required therapy according to 2008 International Workshop on Chronic Lymphocytic Leukemia (iwCLL) criteria<sup>18</sup> were eligible. Included patients had Eastern

Cooperative Oncology Group performance score of  $\leq 2$ , adequate bone marrow function (absolute neutrophil count  $\geq 1 \times 10^9/L$ , platelet count  $\geq 30 \times 10^9/L$ , hemoglobin  $\geq 8$  g/dL), and creatinine clearance  $\geq 50$  mL/minute. Patients were excluded if RT was confirmed on biopsy (see details below), and if they had active and uncontrolled autoimmune cytopenias, unresolved toxicities from prior therapy, or allogeneic stem cell transplantation within one year of study entry.<sup>17</sup>

### Venetoclax treatment

Venetoclax was administered orally once daily beginning no sooner than three days after the last prior therapy. Patients received 20 mg daily for one week, followed by a weekly dose increase to reach the final dose of 400 mg daily by week 5.<sup>17</sup>

### Assessments

**Screening** - patients who signed informed consent, had at least one screening assessment; in case of failed screening they did not proceed on the study. PET-CT imaging within 28 days prior to venetoclax administration was performed on all patients; results were locally reviewed and the node with highest SUV that met protocol criteria was chosen to have either excisional or core biopsy. Based on published literature,<sup>3,9,19</sup> and as per the study protocol, biopsy of the suspicious area was mandatory if FDG uptake on PET-CT scan was above SUVmax  $\geq 10$ , or for patients with CD38 positive, ZAP-70 positive, *TP53* disrupted or IGHV unmutated CLL with SUVmax 4-10 with at least one of the following: B-symptoms, lymph node  $>5$  cm, and/or lactate dehydrogenase (LDH) elevation. Additional screening procedures and on-study assessments are described in the *Online Supplementary Appendix*.

### Statistical analysis

Using June 30<sup>th</sup> 2017 as the data cutoff, this *post hoc* analysis was conducted to evaluate PET-CT characteristics (lymph node SUVmax  $\geq 5$  and SUVmax  $\geq 10$ ) and patients' clinical features that may differentiate RT from CLL progression for patients who were screening for this study following discontinuation of prior BCRi therapy.<sup>3,9</sup> Descriptive statistics were used to describe PET-CT test characteristics and patients' clinical features. Logistic regression analyses were performed to evaluate if biopsy following PET-CT could differentiate RT post-BCRi therapy during screening. Additional available data on clinical/laboratory parameters for CD38, ZAP70, *TP53* and IGHV mutation status, LDH, beta-2 ( $\beta$ 2)-microglobulin, and tumor size by logistic regression were also evaluated to determine if any of these patient features may distinguish RT from CLL in this patient population. Based on statistical experience, the small sample size, and uniform direction for all analyses for clinical applicability, sensitivity, specificity, positive predictive value (PPV), negative predictive value (NPV), and area under the receiver operator characteristic (ROC) curve were calculated. The following definitions were used.

Sensitivity: number of patients with true positive divided by observed positive;

Specificity: number of patients with true negative divided by observed negative;

PPV: number of patients with true positive divided by estimated positive;

NPV: number of patients with true negative divided by estimated negative.

Statistical analyses were evaluated for all patients who enrolled and received at least one dose of venetoclax. Overall response rate (ORR) was calculated with a 95% confidence interval based on binomial distribution. Kaplan-Meier methods were used for time-to-event analyses. Differences in outcomes on venetoclax were stratified based on screening SUVmax cutoff of 10. SAS software

**Table 1. Positron emission tomography-computed tomography findings and baseline characteristics for screened patients.**

	Screened patients N=167
PET-CT findings at screening	
Number of FDG-avid nodes,* median (range)	5 (1 – 12)
SUVmax, median (range)	5 (0 – 73)
SUVmax $\geq 10$	25 (15)
Baseline patient characteristics	
Age, median (range), years	67 (28 – 85)
N. of prior therapies, median (range)	4 (1 – 15)
Ibrutinib, n (%)	104 (62)
Idelalisib, n (%)	55 (33)
Ibrutinib and idelalisib, n (%)	37 (22)
Purine analogs, n (%)	104 (62)
Rituximab/other monoclonal antibodies, n (%)	146 (87) / 56 (34)
Bendamustine/other alkylating agents, n (%)	75 (45) / 124 (74)
Bulky nodes $\geq 5$ cm, n (%)	69 (41)
Bulky nodes $\geq 10$ cm, n (%)	17 (10)
$\beta$ -2 microglobulin,* median (range), mg/L	3.4 (0 – 59.6)
Lactate dehydrogenase above the upper limit of normal,† n/N (%)	111/164 (68)
Prognostic factors,‡ n/N (%)	
Unmutated IGHV	93/118 (79)
del(17p)	69/166 (42)
del(11q)	56/165 (34)
TP53 mutation	48/161 (30)
CD38 positive	70/155 (45)
ZAP-70 positive	45/125 (36)

PEFCT: positron emission tomography-computed tomography; FDG: 18-F-fluorodeoxyglucose, SUVmax: maximum standardized uptake value of FDG. \*PEFavid defined as SUV  $> 3$  per nuclear medicine ranges provided by participating institutions. †Site reported data; presented for all patients with available data. N/n: number.

(SAS Institute Inc., Cary, NC) was used to generate all statistical summaries. Unless otherwise stated, statistical analyses were 2-sided with  $P \leq 0.05$  considered significant.

## Results

### Patients' characteristics

A total of 167 BCRi-failure patients were screened for this study (*Online Supplementary Figure S1*). There were 40 patients who were screened but did not proceed in the study.<sup>20</sup> 27 failed to meet inclusion criteria per study protocol [most commonly due to inadequate liver or renal function (n=9), biopsy confirmed RT (n=7), and inadequate bone marrow function (n=5)], nine withdrew consent (for different reasons), and four did not participate for other reasons [investigator decision, second primary malignancy discovered on screening (not RT), spleen biopsy required to assess for RT but not recommended by investigator, congestive heart failure (n=1 each)]. Demographics and baseline characteristics for all screened patients are presented in Table 1. Patients had received a median of four prior therapies (range: 1-15), 42% of patients with available data had chromosome 17p deletion (del[17p]), 30% had TP53 mutation, and 79% had unmutated IGHV.

### Positron emission tomography-computed tomography imaging and biopsy at screening

Of the 167 screened patients, 84 (50%) had a lymph node with SUVmax  $\geq 5$  and 25 (15%) patients had SUVmax  $\geq 10$  (Table 1).<sup>3,9</sup> Following PET-CT imaging, 57 patients met protocol criteria for the required core biopsy of the FDG-avid lymph node to evaluate for RT, of whom 22 failed screening for other reasons and did not have a biopsy. (Other reasons for screen failure were heterogeneous and have been previously reported<sup>20</sup>) (*Online Supplementary Figure S1*). Of the remaining 35 patients who underwent biopsy, 19 had SUVmax  $\geq 10$  and 16 had SUVmax  $< 10$  with other high risk clinical/laboratory features that mandated biopsy. Additionally, one patient had an abnormal CT result prior to study-related procedures which led to biopsy of a node during screening (patient did not have PET-CT at screening). Eight patients had RT: 22% of all patients who were biopsied (n=36) and 4.8% of all 167 patients progressing after BCRi screened for this clinical trial (all DLBCL). These eight patients were not enrolled on the clinical trial (Table 2), three failed screening due to other reasons including other malignancies (metastatic anal cancer and neuroendocrine tumor), and 25 patients had a biopsy demonstrating CLL without transformation and were subsequently enrolled on study. Of the eight patients with biopsy-confirmed RT, five had

Table 2. Characteristics of patients with biopsy-confirmed Richter's transformation at screening.

	Patients								Summary
	1	2	3	4	5	6	7	8	
Age, † years	54	81	63	76	84	81	72	68	74 (54–84)
Sex‡	Female	Male	7 (88)						
Time from diagnosis, † years	6.7	6.6	3.1	3.3	6.2	14.2	16	N/A	6.6 (3.2–16)
Prior therapies, † n	3	8	2	3	3	12	9	3	3 (2–12)
del(17p)/TP53 mutation‡	Yes	No	Yes	Yes	Yes	No	Yes	Yes	5 (63)
Screening PET-CT SUVmax†	12	19	12	11	22	2	0.5	N/A*	12 (0.5–22)
Largest node at baseline, † cm	3	8	3	7	N/A	N/A	N/A	4	4 (3–8)
β2 microglobulin, † mg/L	n/A	3.7	1.6	5.9	3.5	N/A	N/A	N/A	3.6 (1.6–5.9)
ALC, x10 <sup>9</sup> /L‡	1.5	30.9	21.4	1.3	30.4	1.1	3.5	160	12.4 (1.1–160)

del(17p): chromosome 17p deletion; PET-CT: positron emission tomography-computed tomography; SUVmax: maximum standardized uptake value of 18-F-fluorodeoxyglucose; ALC: absolute lymphocyte count; N/A: data not available. †Summary column describes the median (range) across the eight patients. ‡Summary column describes the number (n) (%) across the eight patients. \*Patient had an abnormal CT SCAN prior to screening for study, which led to a biopsy to confirm Richter's transformation. PETCT was not performed but the patient was excluded based on biopsy findings.

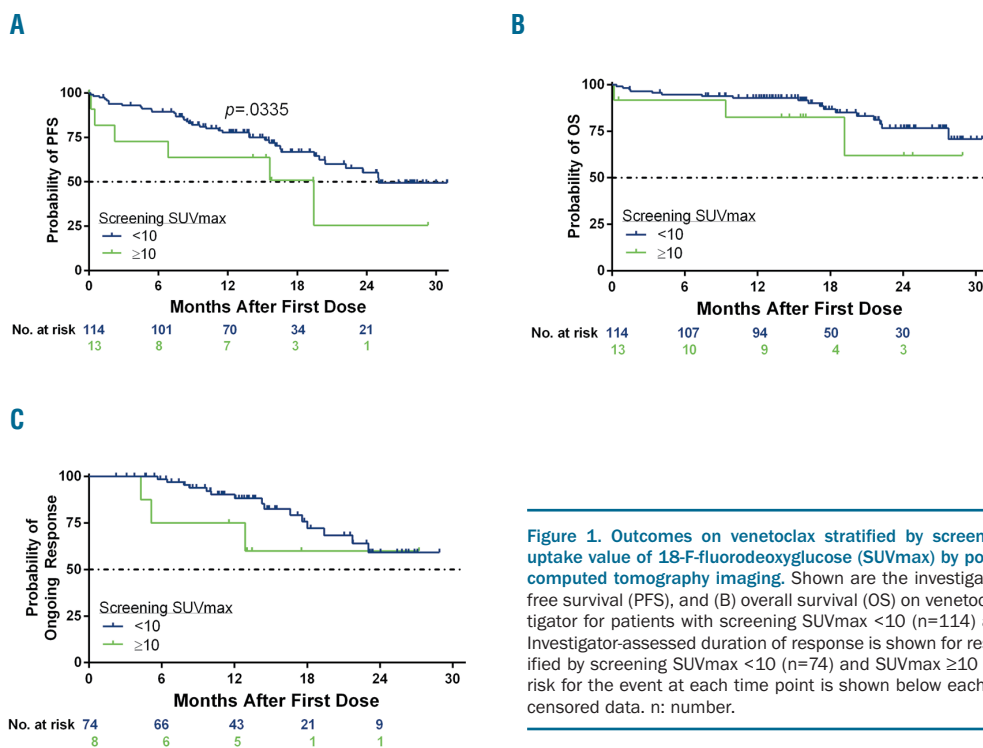


Figure 1. Outcomes on venetoclax stratified by screening maximum standardized uptake value of 18-F-fluorodeoxyglucose (SUVmax) by positron emission tomography-computed tomography imaging. Shown are the investigator-assessed (A) progression-free survival (PFS), and (B) overall survival (OS) on venetoclax as assessed by the investigator for patients with screening SUVmax <10 (n=114) and SUVmax ≥10 (n=13). (C) Investigator-assessed duration of response is shown for responders on venetoclax stratified by screening SUVmax <10 (n=74) and SUVmax ≥10 (n=8). Number of patients at risk for the event at each time point is shown below each curve. Tick marks represent censored data. n: number.

SUVmax ≥10, two had SUVmax <10 with other factors that required biopsy per protocol, and one did not have PET-CT at screening and thus was not included in the following sensitivity/specificity analysis. Fourteen patients with SUVmax ≥10 had biopsy demonstrating CLL without evidence of RT. Of the 14 patients with SUVmax ≥10 with biopsy demonstrating CLL, nine patients were off BCRi [7 off ibrutinib and 2 off idelalisib with median time off therapy of 0.8 months (range: 0.1-18)] at the time of PET-CT, and five patients were on a BCRi at the time of PET-CT (3 on ibrutinib, 2 on idelalisib). There was no difference between the median SUVmax in patients on or off BCRi at time of PET-CT [5 (range: 0.5-28) vs. 5 (range: 0-73), respectively].

In a prior analysis, Michallet *et al.* showed that SUVmax >10 was the most effective cutoff value to identify RT in

patients largely treated with chemotherapy or chemoimmunotherapy.<sup>10</sup> Given this, we also evaluated this cutoff in the post-BCRi setting. In the current analysis, screening SUVmax ≥10 had 71% sensitivity, 50% specificity, 26% PPV, and 88% NPV for detection of biopsy-confirmed RT *versus* CLL progression in patients post-BCRi therapy [odds ratio: 2.5 (0.4-15);  $P=0.318$ ] (Table 3). The ROC area for SUVmax ≥10 was 61%. Other reports have shown that SUVmax ≥5 provided high sensitivity and specificity to distinguish RT in patients treated with chemotherapy or chemoimmunotherapy.<sup>3,9</sup> In BCRi-exposed patients, we observed no difference in sensitivity with SUVmax ≥5 (71%), with decreased specificity for identifying RT (4%) *versus* what we report for SUVmax ≥10. SUVmax cutoff points of ≥11 and ≥12 were also evaluated, although the sensitivity remained the same or decreased compared

**Table 3.** Detection of biopsy-confirmed Richter's transformation (RT) versus chronic lymphocytic leukemia (CLL) progression based on positron emission tomography-computed tomography and clinical factors.

	Sensitivity	Specificity	Logistic regression analyses			Odds ratio [95% CI], logistic P
			PPV	NPV	ROC area	
PET-CT SUVmax <10/≥10	71%	50%	26%	88%	61%	2.5 [0.4–15], P=0.318
PET-CT SUVmax <5/≥5	71%	4%	16%	33%	63%	0.09 [0.01–1.2], P=0.071
PET-CT SUVmax <11/≥11	71%	61%	31%	89%	66%	3.8 [0.6–24], P=0.143
PET-CT SUVmax <12/≥12	57%	68%	31%	86%	63%	2.8 [0.5–15], P=0.231
Lactate dehydrogenase ≤/≥ULN	83%	29%	20%	89%	56%	2 [0.2–20], P=0.554
SPD at baseline	67%	48%	24%	86%	59%	1 [1–1], P=0.244
TP53* mutated/unmutated	60%	63%	25%	88%	61%	2.5 [0.35–18], P=0.362
IGHV* mutated/unmutated	25%	86%	25%	86%	56%	2.1 [0.16–28], P=0.569
CD-38* positive/negative	25%	40%	6%	77%	68%	0.22 [0.02–2.5], P=0.220
ZAP-70* positive/negative	50%	23%	9%	75%	64%	0.3 [0.01–6.4], P=0.440
β2 microglobulin * </≥3 mg/L	75%	25%	20%	80%	50%	1 [0.08–13], P=1.0

PPV: positive predictive value; NPV: negative predictive value; ROC: Receiver Operator Characteristic; PET-CT: positron emission tomography-computed tomography; SUVmax: maximum standardized uptake value of 18-F-fluorodeoxyglucose; ULN: upper limit of the normal range; SPD: sum products of the greatest transverse diameters (tumor size). \*Site-reported data. The logistic regression analyses only included patients with available data.

with SUVmax ≥10. Other baseline clinical/prognostic features were evaluated, including above normal LDH and β2-microglobulin levels (Table 3).

### Outcomes on venetoclax

At the time of analysis, patients enrolled on study had been on venetoclax for a median of 10.3 months (range: 0.1–26 months). Falchi *et al.* had previously reported that patients with SUVmax ≥10 had an inferior survival on chemotherapy/chemoimmunotherapy;<sup>3</sup> therefore, we evaluated outcomes of venetoclax using this cutoff of screening SUVmax. The ORR on venetoclax was 65% (82 of 127) for all enrolled patients, and was similar when stratified by screening PET-CT SUVmax <10 (65%, 74 of 114) versus ≥10 (62%, 8 of 13) ( $P=0.81$ ). Median progression-free survival (PFS) was longer for venetoclax-treated patients with screening PET-CT SUVmax <10 versus ≥10 [24.7 months (95%CI: 20.1, -) vs. 15.4 months [95% CI: 0.4, -];  $P=0.0335$ ], with Kaplan-Meier estimates at 12 months of 79% (95%CI: 69%, 85%) and 58% (95%CI: 27%, 80%), respectively (Figure 1A). The median time on study, including follow up, was 13.8 months (range: 0.03–31 months). Median overall survival had not been reached at the time of analysis, though 12-month estimates for patients with SUVmax <10 versus ≥10 were 94% (95%CI: 87%, 97%) and 76% (95%CI: 43, 92%), respectively ( $P=0.061$ ) (Figure 1B). For patients who responded to venetoclax, the median duration of response had not been reached at the time of analysis, and 12-month estimates for patients with SUVmax <10 versus ≥10 were 90% (95%CI: 80%, 96%) and 75% (95% CI: 32%, 93%), respectively ( $P=0.17$ ) (Figure 1C). In an intent-to-treat analysis, 29% (33 of 114) of patients with screening SUVmax <10 achieved minimal residual disease (MRD) negativity in peripheral blood, with 19 of these patients achieving this outcome by week 24. For patients with screening SUVmax ≥10, 23% (3 of 13) achieved MRD negativity in peripheral blood, with one who had this outcome by week 24. Of three patients with screening SUVmax ≥10 who achieved MRD negativity on veneto-

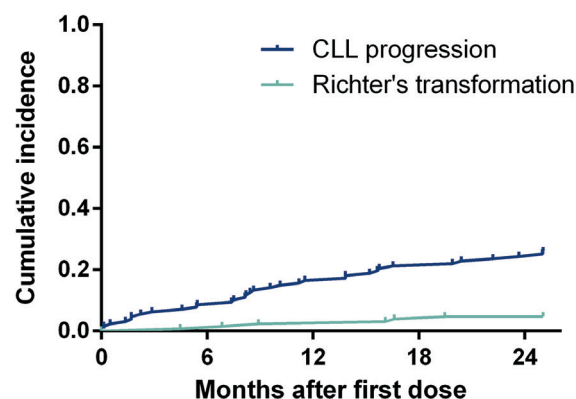


**Figure 2.** Time to chronic lymphocytic leukemia (CLL) progression or Richter's transformation (RT) on venetoclax. Shown is the cumulative incidence of CLL progression or Richter's transformation on venetoclax. Thirty-three patients discontinued venetoclax due to CLL progression and six due to biopsy-confirmed RT following both imaging and clinical changes. Median time to CLL progression was 8.5 months (range: 0.1–28 months) and to RT was 12.8 months (range: 4.4–19.7 months). Tick marks represent patients with events.

clax, two are still on study and receiving treatment, and one patient discontinued venetoclax and later died due to squamous cell carcinoma of head and neck. There was no statistical difference in the rate of MRD-negativity in blood based on screening SUVmax ≥10 versus <10 ( $P=0.83$ ).

Sixty-two (49%) patients discontinued venetoclax (*Online Supplementary Figure S1*), with a median time to discontinuation for any reason of 8.6 months (range: 0.1–28). Thirty-three patients (26%) discontinued venetoclax due to CLL progression and six (4.7%) due to biopsy-confirmed RT following clinical findings and radiographic changes (Table 4). The median time to CLL progression was 8.5 months (range: 0.1–28 months) and to RT was 12.8 months (range: 4.4–19.7 months) (Figure 2). Of six

**Table 4.** Characteristics of patients who underwent Richter's transformation on venetoclax.

	Patients						Summary
	1	2	3	4	5	6	
Age, <sup>†</sup> years	56	65	58	63	65	66	64 (56 – 66)
Sex <sup>‡</sup>	Male	Female	Female	Male	Female	Male	3 (50)
Time from diagnosis, <sup>†</sup> years	12	12	9	6	18	20	12 (6 – 20)
Prior therapies, <sup>†</sup> n	5	9	9	2	6	5	5.5 (2 – 9)
del(17p)/TP53 mutation <sup>‡</sup>	Yes	Yes	Yes	No	No	Yes	4 (67)
Screening PET-CT SUVmax <sup>†</sup>	11	8	5	<3	6	<3	7 (<3 – 11)
Largest node at baseline, <sup>†</sup> cm	4.8	10.8	2.5	7.2	3.1	8.6	4.8 (2.5 – 10.8)
β-2 microglobulin, <sup>†</sup> mg/L	2.5	5.7	2.8	6.8	N/A	2.8	2.8 (2.5 – 6.8)
ALC, x10 <sup>9</sup> /L <sup>†</sup>	20	2	71	6	406	.9	13 (0.9 – 406)
Best response on venetoclax	PR	SD	PR	PR	CR*	PR	83% ORR
Time to RT, <sup>†</sup> weeks	30	19	87	68	72	71	69.5 (19 – 87)

del(17p): chromosome 17p deletion; PET-CT: positron emission tomography-computed tomography; SUVmax: maximum standardized uptake value of 18-F-fluorodeoxyglucose; N/A: data not available; ALC: absolute lymphocyte count; PR: partial remission; SD: stable disease; CR: complete remission; ORR: overall response rate (CR+PR); RT: Richter's transformation. \*Patient had PR at weeks 8 and 24 and then CR at week 60. †Summary column describes the median (range) across the six patients. ‡Summary column describes the number (n) (%) across the six patients.

patients who discontinued venetoclax due to a relapse with RT, two met criteria for biopsy and underwent biopsy at screening. Both biopsies were negative for RT, though one patient had prior RT and the other had prior DLBCL both more than two years prior to enrollment. Five of the six patients who developed RT on venetoclax had screening SUVmax on PET <10 and screening SUVmax for all six patients with RT was not statistically different from other enrolled patients ( $P=0.24$ ).

## Discussion

The diagnosis and management of RT remain challenging due to rapid progression and refractoriness to chemotherapy and targeted therapies.<sup>3</sup> Evaluation of patients following chemotherapy or chemoimmunotherapy showed that PET-CT imaging is helpful to detect RT and identify sites to target for biopsy,<sup>3,9,10</sup> with SUVmax of  $\geq 10$  identified as an optimal threshold for distinguishing RT *versus* CLL progression,<sup>10</sup> and associated with poor survival, independently of RT diagnosis.<sup>3</sup>

Newer treatments, including BCRI or BCL-2 inhibitors, are highly active for patients with relapsed/refractory CLL<sup>15,16,21,22</sup> and have begun to supplant the use of chemotherapy. Data reported here represent the largest series of prospective PET-CT scans performed based on predetermined criteria in patients following discontinuation of either ibrutinib or idelalisib. Of 167 patients who were screened for this phase II study, 57 met protocol criteria for a biopsy to evaluate for RT following PET-CT imaging, and RT was confirmed for 4.8% of all screened patients. Five of these patients had SUVmax  $\geq 10$  while the other two had SUVmax <10 with other factors associated with RT (e.g. LDH elevation or B symptoms). Based on this analysis, we report the test characteristics for PET-CT with SUVmax  $\geq 10$ . We observed a lower sensitivity (71%) and specificity (50%) for SUVmax  $\geq 10$  in patients who have been exposed to BCRI therapy as compared to prior reports in patients not progressing on BCRI.<sup>10</sup> We emphasize the importance of biopsy to confirm clinical or radiographic suspicion of RT or a secondary malignancy. PET-CT should not be used without biopsy to diagnose RT.

Our data suggest that CLL progression following BCRI exposure may be more metabolically active compared to progression following chemoimmunotherapy. In addition, these data suggest no difference in FDG avidity in patients with CLL regardless of whether they were on their BCRI at the time of imaging or not. Only LDH above the upper limit of normal and  $\beta$ -2 microglobulin  $\geq 3$  mg/L had high sensitivity for detection of RT from CLL progression. Limitations of our study are the small sample size in each group of patients on or off BCRI at the time of PET-CT and the fact that other patient features (such as cytogenetics) were not available for all patients, so statistical analyses for those factors only include subsets of the patients with available data. Another limitation of the analysis was that PET-CT was not centrally reviewed and there may be differences in imaging methodologies, number of lymph nodes assessed per study, and interpretations of imaging studies. Though pathology results were also not centrally reviewed, all biopsies were reviewed by hematopathology experts at the study sites, which were major academic institutions. Although there was a relatively small number of patients with RT events included in these analyses, to our knowledge, this dataset is the largest of BCRI-treated patients who had PET-CT and were prospectively evaluated.

For 127 patients who enrolled in the study, no difference was seen in the response rate with venetoclax monotherapy when stratified by screening SUVmax of 10 in whom a biopsy ruled out RT, suggesting that PET-CT performed prior to venetoclax initiation may identify patients with an inferior PFS. We have identified a population of high-risk CLL patients previously treated with BCRI for whom venetoclax monotherapy may result in inferior PFS and in whom venetoclax-based combination regimens should be studied.

Whereas in prior ibrutinib studies, the development of RT appeared to be a relatively early event (median approx. 6 months),<sup>23</sup> in this study, the development of RT on venetoclax for six patients occurred later (median 12.8 months). This may reflect differences in how individual therapies (BCRI *vs.* BCL2 inhibitor) affect the CLL clone and/or the patient populations. More likely, the later

occurrence of RT in the current study suggests that most patients with RT were prospectively identified and excluded from participating in this study utilizing the pre-specified criteria for biopsy based on PET-CT imaging and other clinical features. It is also possible that there was a treatment effect of venetoclax, which would be consistent with the results for the DLBCL patients with RT in a previous Phase I study across non-Hodgkin lymphomas.<sup>24</sup> Venetoclax is currently being studied in CLL patients with RT (*clinicaltrials.gov* identifier: 03054896).

The primary role of PET-CT in patients with CLL is to identify the most appropriate target for biopsy to assess for the presence of RT or other malignancy. Overall, our data suggest that CLL progression may be more metabolically active on PET-CT following BCRi failure as compared to chemoimmunotherapy. PET-CT SUVmax cutoff of 10 was able to distinguish suspected RT from CLL progression at screening with a sensitivity of 71% and specificity of 50%, test characteristics which are modest compared to those reported in prior studies with chemotherapy or CIT-treated patients.<sup>10</sup> SUVmax cutoff of 10 at baseline also did not predict the development of RT in patients on venetoclax. Clinical features, including elevated  $\beta$ -2 microglobulin and LDH may provide additional information when considering biopsy to confirm RT. Future analyses including assessment of additional genetic fac-

tors, BCR stereotypes, or gene expression could be tested as predictors for the risk of RT following BCRi exposure.

### Acknowledgments

*Special thanks to the patients and their families, study coordinators, and support staff.*

### Funding

*AbbVie and Genentech provided financial support for the study. AbbVie is committed to responsible data sharing regarding the clinical trials we sponsor. This includes access to anonymized, individual and trial-level data (analysis data sets), as well as other information (e.g. protocols and Clinical Study Reports), as long as the trials are not part of an ongoing or planned regulatory submission. This includes requests for clinical trial data for unlicensed products and indications. This clinical trial data can be requested by any qualified researchers who engage in rigorous, independent scientific research, and will be provided following review and approval of a research proposal and Statistical Analysis Plan and execution of a Data Sharing Agreement. Data requests can be submitted at any time and the data will be accessible for 12 months, with possible extensions considered. For more information on the process, or to submit a request, visit the following link: <https://www.abbvie.com/our-science/clinical-trials/clinical-trials-data-and-information-sharing/data-and-information-sharing-with-qualified-researchers.html>.*

## References

- Rossi D, Cerri M, Capello D, et al. Biological and clinical risk factors of chronic lymphocytic leukaemia transformation to Richter syndrome. *Br J Haematol.* 2008;142(2):202-215.
- Molica S. A systematic review on Richter syndrome: what is the published evidence? *Leuk Lymphoma.* 2010;51(3):415-421.
- Falchi L, Keating MJ, Marom EM, et al. Correlation between FDG/PET, histology, characteristics, and survival in 332 patients with chronic lymphoid leukemia. *Blood.* 2014;123(18):2783-2790.
- Tsimberidou AM, Kantarjian HM, Cortes J, et al. Fractionated cyclophosphamide, vincristine, liposomal daunorubicin, and dexamethasone plus rituximab and granulocyte-macrophage-colony stimulating factor (GM-CSF) alternating with methotrexate and cytarabine plus rituximab and GM-CSF in patients with Richter syndrome or fludarabine-refractory chronic lymphocytic leukemia. *Cancer.* 2003;97(7):1711-1720.
- Tsimberidou AM, O'Brien SM, Cortes JE, et al. Phase II study of fludarabine, cytarabine (Ara-C), cyclophosphamide, cisplatin and GM-CSF (FACPGM) in patients with Richter's syndrome or refractory lymphoproliferative disorders. *Leuk Lymphoma.* 2002;43(4):767-772.
- Rossi D, Gaidano G. Richter syndrome: pathogenesis and management. *Semin Oncol.* 2016;43(2):311-319.
- Parikh SA, Rabe KG, Call TG, et al. Diffuse large B-cell lymphoma (Richter syndrome) in patients with chronic lymphocytic leukaemia (CLL): a cohort study of newly diagnosed patients. *Br J Haematol.* 2013;162(6):774-782.
- Shaikh F, Janjua A, Van Gestel F, Ahmad A. Richter Transformation of Chronic Lymphocytic Leukemia: A Review of Fluorodeoxyglucose Positron Emission Tomography-Computed Tomography and Molecular Diagnostics. *Cureus.* 2017; 9(1):e968.
- Bruzzi JF, Macapinlac H, Tsimberidou AM, et al. Detection of Richter's transformation of chronic lymphocytic leukemia by PET/CT. *J Nucl Med.* 2006;47(8):1267-1273.
- Michallet AS, Sesques P, Rabe KG, et al. An 18F-FDG-PET maximum standardized uptake value > 10 represents a novel valid marker for discerning Richter's Syndrome. *Leuk Lymphoma.* 2016;57(6):1474-1477.
- Jain P, Keating M, Wierda W, et al. Outcomes of patients with chronic lymphocytic leukemia after discontinuing ibrutinib. *Blood.* 2015;125(13):2062-2067.
- Maddocks KJ, Ruppert AS, Lozanski G, et al. Etiology of Ibrutinib Therapy Discontinuation and Outcomes in Patients With Chronic Lymphocytic Leukemia. *JAMA Oncol.* 2015;1(1):80-87.
- VENCLEXTA [Prescribing Information]. AbbVie Inc., North Chicago, IL, USA. Genentech USA Inc., South San Francisco, CA, USA., 2016.
- VENCLYXTO [Summary of Product Characteristics]. AbbVie Ltd., Maidenhead, United Kingdom., 2016.
- Roberts AW, Davids MS, Pagel JM, et al. Targeting BCL2 with Venetoclax in Relapsed Chronic Lymphocytic Leukemia. *N Engl J Med.* 2016;374(4):311-322.
- Stigenbauer S, Eichhorst B, Schetelig J, et al. Venetoclax in relapsed/refractory chronic lymphocytic leukemia with 17p deletion: a phase 2, open label, multicenter study. *Lancet Oncol.* 2016;17(6):768-778.
- Jones JA, Mato AR, Wierda WG, et al. Venetoclax for chronic lymphocytic leukaemia progressing after ibrutinib: an interim analysis of a multicentre, open-label, phase 2 trial. *Lancet Oncol.* 2017;19(1):65-75.
- Hallek M, Cheson BD, Catovsky D, et al. Guidelines for the diagnosis and treatment of chronic lymphocytic leukemia: a report from the International Workshop on Chronic Lymphocytic Leukemia updating the National Cancer Institute-Working Group 1996 guidelines. *Blood.* 2008; 111(12):5446-5456.
- Bodet-Milin C, Kraeber-Bodere F, Moreau P, et al. Investigation of FDG-PET/CT imaging to guide biopsies in the detection of histological transformation of indolent lymphoma. *Haematologica.* 2008;93(3):471-472.
- Jones JA, Mato AR, Wierda WG, et al. Venetoclax for chronic lymphocytic leukaemia progressing after ibrutinib: an interim analysis of a multicentre, open-label, phase 2 trial. *Lancet Oncol.* 2018;19(1):65-75.
- Byrd JC, Furman RR, Coutre SE, et al. Targeting BTK with ibrutinib in relapsed chronic lymphocytic leukemia. *N Engl J Med.* 2013;369(1):32-42.
- Furman RR, Sharman JP, Coutre SE, et al. Idelalisib and rituximab in relapsed chronic lymphocytic leukemia. *N Engl J Med.* 2014;370(11):997-1007.
- O'Brien S, Jones JA, Coutre SE, et al. Ibrutinib for patients with relapsed or refractory chronic lymphocytic leukaemia with 17p deletion (RESONATE-17): a phase 2, open-label, multicentre study. *Lancet Oncol.* 2016;17(10):1409-1418.
- Davids MS, Roberts AW, Seymour JF, et al. Phase I First-in-Human Study of Venetoclax in Patients With Relapsed or Refractory Non-Hodgkin Lymphoma. *J Clin Oncol.* 2017;35(8):826-833.

# Phase II study of carfilzomib, thalidomide, and low-dose dexamethasone as induction and consolidation in newly diagnosed, transplant eligible patients with multiple myeloma; the Carthadex trial



Haematologica 2019  
Volume 104(11):2265-2273

Ruth Wester,<sup>1</sup> Bronno van der Holt,<sup>2</sup> Emelie Asselbergs,<sup>1</sup> Sonja Zweegman,<sup>3</sup> Marie Jose Kersten,<sup>2</sup> Edo Vellenga,<sup>4</sup> Marinus van Marwijk Kooy,<sup>5</sup> Okke de Weerd,<sup>6</sup> Monique Minnema,<sup>7</sup> Sarah Lonergan,<sup>1</sup> Antonio Palumbo,<sup>8</sup> Henk Lokhorst,<sup>3</sup> Annemiek Broijl<sup>1</sup> and Pieter Sonneveld<sup>1</sup>

<sup>1</sup>Department of Hematology, Erasmus MC Cancer Institute, Rotterdam, the Netherlands; <sup>2</sup>HOVON Data Center, Department of Hematology, Erasmus MC Cancer Institute, Rotterdam, the Netherlands; <sup>3</sup>Department of Hematology, Amsterdam UMC, Amsterdam, the Netherlands; <sup>4</sup>Department of Hematology, University Medical Center Groningen, University of Groningen, the Netherlands; <sup>5</sup>Department of Hematology, Isala Clinics, Zwolle, the Netherlands; <sup>6</sup>Department of Internal Medicine, St. Antonius Hospital, Nieuwegein, the Netherlands; <sup>7</sup>Department of Hematology, UMC Utrecht Cancer Center, Utrecht, the Netherlands and <sup>8</sup>Department of Hematology, University of Torino, Torino, Italy

## ABSTRACT

This is a phase II dose escalation trial of carfilzomib in combination with thalidomide and dexamethasone for induction and consolidation in transplant-eligible patients with newly diagnosed multiple myeloma (NDMM). The results of four dose levels are reported. Induction therapy consisted of four cycles of carfilzomib 20/27 mg/m<sup>2</sup> (n=50), 20/36 mg/m<sup>2</sup> (n=20), 20/45 mg/m<sup>2</sup> (n=21), and 20/56 mg/m<sup>2</sup> (n=20) on days 1, 2, 8, 9, 15, 16 of a 28-day cycle; thalidomide 200 mg on day 1 through 28 and dexamethasone 40 mg weekly. Induction therapy was followed by high-dose melphalan and autologous stem cell transplantation and consolidation therapy with four cycles of carfilzomib, thalidomide and dexamethasone in the same schedule except a lower dose of thalidomide (50 mg). Very good partial response rate or better and complete response rate or better after induction therapy were 65% and 18%, respectively, increasing to 86% and 63%, respectively, after consolidation therapy. In all cohorts combined, after a median follow up of 58.7 months, median progression-free survival was 58 months (95%CI: 45-67 months). Median overall survival was 83 months (95%CI: 83 months-not reached). Grade 3/4 adverse events consisted mainly of infections, respiratory disorders, skin and vascular disorders in 11%, 8%, 9%, and 9%, respectively. Grade 3 polyneuropathy was only reported in one patient. Cardiac events were limited: grade 3/4 in 5% of patients. Carfilzomib, thalidomide and dexamethasone as induction and consolidation treatment after high-dose melphalan and autologous stem cell transplantation is highly efficacious and safe in transplant-eligible patients with NDMM. This study was registered as #NTR2422 at <http://www.trialregister.nl>

## Introduction

Survival rates in patients with multiple myeloma (MM) have significantly improved during the last decades. However, eventually the majority of patients progress and the need for new therapeutic approaches remains. In transplant-eligible patients with newly diagnosed multiple myeloma (NDMM), depth of

## Correspondence:

RUTH WESTER  
[r.wester@erasmusmc.nl](mailto:r.wester@erasmusmc.nl)

Received: September 2, 2018.

Accepted: March 28, 2019.

Pre-published: April 4, 2019.

doi:10.3324/haematol.2018.205476

Check the online version for the most updated information on this article, online supplements, and information on authorship & disclosures: [www.haematologica.org/content/104/11/2265](http://www.haematologica.org/content/104/11/2265)

©2019 Ferrata Storti Foundation

Material published in Haematologica is covered by copyright. All rights are reserved to the Ferrata Storti Foundation. Use of published material is allowed under the following terms and conditions:

<https://creativecommons.org/licenses/by-nc/4.0/legalcode>. Copies of published material are allowed for personal or internal use. Sharing published material for non-commercial purposes is subject to the following conditions: <https://creativecommons.org/licenses/by-nc/4.0/legalcode>, sect. 3. Reproducing and sharing published material for commercial purposes is not allowed without permission in writing from the publisher.



response before and after high-dose melphalan/autologous stem cell transplantation (HDM/ASCT) is associated with improvement in progression-free survival (PFS) and overall survival (OS).<sup>1-5</sup> Therefore, it is important to select the appropriate induction and consolidation therapy in order to achieve a maximum response after ASCT and to maintain or even increase this response during consolidation therapy and thereafter.

Standard induction treatment consists of triple therapy including a proteasome inhibitor, and/or an immunomodulatory drug and dexamethasone. The combination of bortezomib, thalidomide and dexamethasone (VTD) has been extensively investigated in transplant-eligible patients with NDMM.<sup>6-8</sup> However, treatment with bortezomib is associated with higher rates of polyneuropathy (PN) and a consequent discontinuation of treatment.<sup>7,8</sup> It is important to use a regimen that is highly effective and safe in patients with NDMM. This could improve treatment adherence and subsequently outcome after induction and consolidation therapy.

Carfilzomib is a selective proteasome inhibitor with irreversible binding to the constitutive proteasome and immunoproteasome. It is approved in the United States and in Europe as a single-agent for the treatment of patients with relapsed and/or refractory MM (RRMM). Carfilzomib is approved at a dose of 27 mg/m<sup>2</sup> in combination with lenalidomide and dexamethasone in RRMM based on the data from the ASPIRE trial showing a superior PFS of median 26.3 months *versus* 17.4 months when patients were treated with lenalidomide/dexamethasone.<sup>9</sup> Carfilzomib is also approved at a dose of 56 mg/m<sup>2</sup> in combination with dexamethasone, based on data from the ENDEAVOR trial showing a superior PFS over bortezomib/dexamethasone of median 18.7 months *versus* 9.4 months ( $P < 0.0001$ ).<sup>10</sup> Previous trials showed that the incidence of PN with carfilzomib is lower compared to bortezomib.<sup>9-11</sup>

Carfilzomib has not yet been approved for treatment in NDMM in Europe. Recent trials in patients with NDMM, using different treatment regimens, showed high response rates.<sup>12-15</sup> A phase I/II trial of patients with NDMM treated with carfilzomib at a maximum dose of 36 mg/m<sup>2</sup> combined with lenalidomide and low-dose dexamethasone showed a very good partial response (VGPR) rate of 81%. PFS at 24 months was 92%.<sup>12</sup>

We previously initiated a Phase II dose-escalation trial of carfilzomib combined with thalidomide and dexamethasone. The combination of a proteasome inhibitor and an immunomodulating agent has a proven synergistic effect.<sup>6</sup> Moreover, thalidomide is an effective and affordable drug available in many countries.

In NDMM, there is no consensus as to the optimum dose level of carfilzomib, implicating the need for dose-finding trials. The goal of this trial was to investigate the efficacy of this combination at various dose levels of carfilzomib in NDMM. Results of the first three cohorts of this Carthadex trial were published in 2015.<sup>11</sup> Overall response rate (ORR) after induction therapy was 90% with a VGPR rate of 68%. PFS at 36 months was 72%. The combination of carfilzomib, thalidomide and dexamethasone (KTd) was well tolerated.<sup>11</sup> Four different dose levels were included in this trial based on the hypothesis that a higher dose level induces a higher response rate.<sup>12,16</sup> We report herein the results of our dose escalation cohorts with a long follow up. This is the first study using

KTd for both induction and consolidation therapy and comparing different dose levels.

## Methods

### Patients

Transplant-eligible patients with NDMM, aged 18-65 years, were eligible for enrollment. Patients were required to have a World Health Organization (WHO) performance status of 0-3; WHO 3 was allowed only when caused by MM and not by co-morbid conditions.

Patients were ineligible if they had grade 3/4 polyneuropathy (PN) or grade 2 painful PN, severe cardiac dysfunction (New York Heart Association class II-IV), known intolerance of thalidomide, systemic amyloid light-chain amyloidosis, non-secretory MM, Waldenström macroglobulinemia or IgM MM, creatinine clearance <15 mL/min, absolute neutrophil count <1.0×10<sup>9</sup>/L, platelets <75×10<sup>9</sup>/L, hemoglobin <4.9 mmol/L, active malignancy during the past five years with the exception of basal carcinoma of the skin or stage 0 cervical carcinoma.

This independent investigator-initiated multi-institutional study was conducted in accordance with the Declaration of Helsinki, the International Conference on Harmonization Guidelines for Good Clinical Practice, and the European Clinical Trial Directive as implemented under Dutch law. The protocol was approved by institutional review boards and ethics committees. All patients gave informed consent.

### Study design and treatment

This single-arm, open-label, phase II trial was conducted at eight hematology centers. Patients were treated with four cycles KTd of a 28-day cycle for induction therapy. Carfilzomib was administered in a 30-minute infusion. The dose in the first dosing cohort was 20 mg/m<sup>2</sup> on days 1 and 2 and was escalated to a dose of 27 mg/m<sup>2</sup> on days 8, 9, 15 and 16 of cycle 1 and on days 1, 2, 8, 9, 15 and 16 of cycles 2-4. Thalidomide 200 mg was given orally on days 1 through 28 and dexamethasone 40 mg was given orally on days 1, 8, 15 and 22. Induction therapy was followed by stem cell harvest after cyclophosphamide priming (2-4 mg/m<sup>2</sup> i.v.) and daily 10 µg/kg granulocyte colony-stimulating factor. Hereafter, patients received high-dose melphalan (HDM, 200 mg/m<sup>2</sup>) and ASCT followed by consolidation treatment with four cycles of KTd in the same schedule and dose as induction treatment except that the dose of thalidomide was 50 mg instead of 200 mg. The dose of carfilzomib was escalated to 20/36 mg/m<sup>2</sup>, 20/45 mg/m<sup>2</sup> and 20/56 mg/m<sup>2</sup> in cohorts 2, 3 and 4, respectively. Under the study protocol, patients were required to maintain adequate hydration. In addition, patients were treated prophylactically with antibiotics (ciprofloxacin or another fluoroquinolone) and with antiviral medication (acyclovir or a similar anti varicella agent). All patients received antithrombotic prophylaxis with aspirin in case of low thrombotic risk or with low-molecular-weight heparin in patients with pre-existing thrombotic risk factors.<sup>17</sup>

The primary end point of the study was response after induction therapy and overall response, specifically complete response (CR) and VGPR. Secondary end points were efficacy and safety, maximum tolerated dose (MTD), dose limiting toxicities (DLT), PFS and overall survival (OS). PFS was defined as time from registration to progression or death, whichever came first. OS was calculated from registration to death from any cause; patients still alive at last contact were censored.

This study was registered as #NTR2422 at <http://www.trialregister.nl>.

## Assessments

Treatment responses and disease progression were assessed by study investigators and were classified according to International Myeloma Working Group (IMWG) Uniform Response Criteria, with categories for CR, VGPR, and partial response (PR).<sup>18</sup> Toxicity was assessed according to the National Cancer Institute Common Terminology Criteria of Adverse Events version 4.0.<sup>19</sup> Bone marrow analysis was performed at diagnosis to quantify myeloma cell involvement. Molecular, cytogenetic and fluorescence *in situ* hybridization (FISH) studies were performed on these samples. CD138<sup>+</sup> purified MM cells were used to determine the presence of the following cytogenetic abnormalities: t(4;14)(p16;q32), t(14;16)(q32;q32), del(13q), del(17p), 1p/q abnormalities, numerical abnormalities of chromosome 9 or 11, and complex cytogenetic abnormalities.<sup>11</sup>

## Statistical analysis

This study was designed to investigate whether induction treatment with KTD warrants further investigation in future trials. The intention-to-treat principle was used for all analyses, restricted to eligible patients. A CR + VGPR rate lower than 25% after induction treatment, was considered too low to warrant further investigation in future trials; however, if the CR + VGPR rate was higher than 45%, therapeutic activity was considered sufficiently high to support further investigation. To reject the null hypothesis in favor of the alternative hypothesis with power  $1 - \beta = 0.80$  (two-sided significance level  $\alpha = 0.05$ ), a minimum of 41 patients should be included. A 95% confidence interval (CI) was constructed around the CR + VGPR rate after induction treatment and the null hypothesis was rejected if the lower boundary was larger than 25%.

Predefined subgroup analyses were performed to investigate the effect of risk status, using cytogenetic/FISH criteria, International Staging System (ISS) stage and revised (R)-ISS stage, on response and survival. In this trial, patients were considered to be high-risk if they had t(4;14) and/or del(17p) and/or add(1q) and/or ISS stage III.

Continuous and categorical data were summarized with descriptive statistics. Survival end points were estimated using the Kaplan-Meier method, and 95%CI were constructed. The log-rank was used to evaluate differences in PFS and OS between subgroups. Statistical analysis was performed using Stata v15.1 software (StataCorp, College Station, TX, USA).

## Results

### Patients and treatment

One hundred and eleven patients were enrolled between September 16<sup>th</sup>, 2010 and December 30<sup>th</sup>, 2013. The analysis was based on data available as of February 27<sup>th</sup>, 2018 with a median follow up of 58.7 months (range: 25.1-88.0 months). Four different dose levels were investigated (27 mg/m<sup>2</sup>, n=50; 36 mg/m<sup>2</sup>, n=20; 45 mg/m<sup>2</sup>, n=21; 56 mg/m<sup>2</sup>, n=20). Baseline demographics and disease characteristics are shown in Table 1. Median age was 58 years (range: 29-66 years) and the male/female distribution 61%/39%. Nine percent of patients had an R-ISS stage 3 and in 9% of patients R-ISS stage was unknown, mainly due to missing cytogenetics. A total of 39% of patients were classified as high-risk based on cytogenetics and ISS stage; 41% of patients were classified as standard risk. In 20% of patients, risk status was unknown, mainly due to missing cytogenetics. Seven patients had a history of grade 1/2 PN and two patients a grade 3 PN at diagnosis; in nine patients, baseline assessment of PN was missing at enrollment. A total of 5% of patients had renal insufficiency with a creatinine  $\geq 177$

$\mu\text{mol/L}$  at diagnosis.

All 111 patients started induction therapy with KTD (Figure 1). Six patients discontinued treatment because of the following adverse events (AE): grade 3 rash (carfilzomib 27 mg/m<sup>2</sup>), grade 2 fever with sepsis (carfilzomib 27 mg/m<sup>2</sup>), grade 1 hyponatremia (carfilzomib 27 mg/m<sup>2</sup>), grade 2 exanthema (carfilzomib 27 mg/m<sup>2</sup>), grade 3 congestive heart failure (carfilzomib 27 mg/m<sup>2</sup>), grade 3 pneumonia (carfilzomib 36 mg/m<sup>2</sup>), grade 3 drug reaction with eosinophilia and systemic symptoms (Dress syndrome) (carfilzomib 56 mg/m<sup>2</sup>). One patient appeared not eligible for further treatment and two patients discontinued treatment due to progressive disease. Out of 111 patients, 102 (92%) continued treatment with high-dose cyclophosphamide and stem cell collection. Stem cell collection was successful in 100 of 102 patients with a median CD34<sup>+</sup> yield of  $5.5 \times 10^3$ . A total of 98 patients (88%) continued treatment with a single HDM (200 mg/m<sup>2</sup>) and ASCT. Four patients were not eligible for HDM: one because of insufficient CD34<sup>+</sup> yield and three because of progression of disease after stem cell collection. After treatment with HDM and ASCT, 94 patients (85%) initiated consolidation therapy. Four patients were not eligible for consolidation treatment because of progression of disease (n=1), a delayed hematologic recovery after ASCT (n=1), non-related disease (n=1), and uncontrolled pain after ASCT (n=1). Nine patients discontinued consolidation treatment because of progressive disease (n=2), thrombotic thrombocytopenic purpura (TTP) (n=1), a TTP-like syndrome (n=1), overall worsening of condition (n=1), grade 3 fatigue (n=1), refusal of further treatment (n=2), and persisting PN (n=1). A total of 83 patients (75%) completed all four consolidation cycles.

### Efficacy

Table 2 shows response to induction, HDM/ASCT and consolidation therapy. Response according to risk group and R-ISS is shown in Table 3. Overall response after induction therapy in all 111 patients was 93% with a CR rate of 18%. The  $\geq$  VGPR rate after induction therapy was 65% (95%CI: 55-74%) leading to rejection of the null hypothesis, as the 95%CI is above 25%. The  $\geq$  VGPR rate increased to 77% after HDM/ASCT and to 86% after consolidation therapy. ORR increased to 94% after consolidation therapy. CR rate after induction therapy between the four different dose levels was comparable and increased after consolidation therapy. At the three highest dose levels, CR rate after consolidation therapy was higher in comparison to the lowest dose level (75%, 67% and 65% vs. 56%, respectively); however, this was not statistically significant (test for trend,  $P=0.39$ ;  $\chi^2$  test, 27 mg/m<sup>2</sup> vs. 36-56 mg/m<sup>2</sup>,  $P=0.16$ ). Response after consolidation treatment between standard risk patients and high-risk patients (defined by ISS stage and cytogenetics) was similar with CR rates of 67% versus 58%. Response after consolidation therapy according to R-ISS stage (I, II and III) was comparable with CR rates of 73%, 57% and 60%, respectively.

Median PFS in all 111 patients was 58 months (95%CI: 45-67 months). Dose level was not associated with PFS. Median PFS in high-risk patients was worse compared to standard risk patients (42 vs. 60 months;  $P=0.006$ ), while a higher R-ISS stage was also associated with a worse PFS ( $P=0.04$ ) (Figure 2).

Median OS was 83 months and 5-year OS was 76% (95%CI: 66-83%) (Figure 3). Dose level and risk status were not associated with OS.

**Safety**

Any grade hematologic toxicity occurred in 15% of patients. Grade 3/4 hematologic toxicity occurred in 10% of patients. At dose level 27 mg/m<sup>2</sup>, 36 mg/m<sup>2</sup>, 45 mg/m<sup>2</sup> and 56 mg/m<sup>2</sup>, grade 3/4 hematologic toxicity occurred in

12%, 10%, 10% and 10%, respectively. Main grade 3/4 non-hematologic toxicity consisted of infections, respiratory disorders, skin and vascular disorders in 11%, 8%, 9%, and 9%, respectively. There was a gradual increase in grade 3/4 infections from lower to higher doses of carfil-

**Table 1. Baseline characteristics.**

Characteristic	20/27 mg/m <sup>2</sup>	20/36 mg/m <sup>2</sup>	20/45 mg/m <sup>2</sup>	20/56 mg/m <sup>2</sup>	All patients
Patients, n	50	20	21	20	111
Male, n (%)	34 (68)	11 (55)	16 (76)	7 (35)	68 (61)
Age, median (range), years	58 (29-66)	58 (47-64)	56 (33-65)	58 (37-65)	58 (29-66)
ISS stage, n (%)					
1	18 (36)	5 (25)	14 (67)	9 (45)	46 (41)
2	20 (40)	7 (35)	4 (19)	7 (35)	38 (34)
3	12 (24)	8 (40)	2 (10)	4 (20)	26 (23)
Unknown	0 (0)	0 (0)	1 (5)	0 (0)	1 (1)
R-ISS stage, n (%)					
1	7 (14)	3 (15)	10 (48)	6 (30)	26 (23)
2	37 (74)	10 (50)	7 (33)	11 (55)	65 (59)
3	2 (4)	5 (25)	0 (0)	3 (15)	10 (9)
Unknown	4 (8)	2 (10)	4 (19)	0 (0)	10 (9)
WHO performance status, n (%)					
0	24 (48)	7 (35)	11 (52)	12 (60)	54 (49)
1	20 (40)	10 (50)	7 (33)	8 (40)	45 (41)
2	2 (4)	1 (5)	1 (5)	0 (0)	4 (4)
3	0 (0)	0 (0)	2 (10)	0 (0)	2 (2)
Unknown	4 (8)	2 (10)	0 (0)	0 (0)	6 (5)
M-protein isotype, n (%)					
IgA	11 (22)	5 (25)	4 (19)	4 (20)	24 (22)
IgG	30 (60)	8 (40)	10 (48)	11 (55)	59 (53)
IgD	1 (2)	1 (5)	1 (5)	0 (0)	3 (3)
Light-chain disease	7 (14)	4 (20)	6 (29)	5 (25)	22 (20)
Unknown	1 (2)	2 (10)	0 (0)	0 (0)	3 (3)
Genetic abnormalities, n (%) <sup>*</sup>					
add 1q					
Yes	5 (10)	4 (20)	2 (10)	7 (35)	18 (16)
No	35 (70)	12 (60)	15 (71)	10 (50)	72 (65)
Unknown	10 (20)	4 (20)	4 (19)	3 (15)	21 (19)
t(4;14)(p16;32)					
Yes	2 (4)	2 (10)	0 (0)	3 (15)	7 (6)
No	39 (78)	14 (70)	19 (90)	13 (65)	85 (77)
Unknown	9 (18)	4 (20)	2 (10)	4 (20)	19 (17)
del(17p13)					
Yes	3 (6)	2 (10)	1 (5)	1 (5)	7 (6)
No	38 (76)	14 (70)	18 (86)	16 (80)	86 (77)
Unknown	9 (18)	4 (20)	2 (10)	3 (15)	18 (16)
t(11;14)(q13;q32)					
Yes	5 (10)	1 (5)	2 (10)	1 (5)	9 (8)
No	36 (72)	15 (75)	17 (81)	15 (75)	83 (75)
Unknown	9 (18)	4 (20)	2 (10)	4 (20)	19 (17)
t(14;16)(q32;q23)					
Yes	3 (6)	1 (5)	0 (0)	0 (0)	4 (4)
No	38 (76)	15 (75)	19 (90)	16 (80)	88 (79)
Unknown	9 (18)	4 (20)	2 (10)	4 (20)	19 (17)
Risk status, n (%) <sup>†</sup>					
High	19 (38)	10 (50)	4 (19)	10 (50)	43 (39)
Standard	21 (42)	6 (30)	12 (57)	7 (35)	46 (41)
Unknown	10 (20)	4 (20)	5 (24)	3 (15)	22 (20)
Grade 1/2 PN, n (%) <sup>‡</sup>	3 (6)	2 (10)	0 (0)	2 (10)	7 (7)

PN: polyneuropathy. <sup>\*</sup>A total of 93 patients were evaluable. The table shows the presence of the genetic abnormality in all four dose levels together and in each dose level separately. <sup>†</sup>High-risk: t(4;14) and/or 17p- and/or add1q cytogenetic abnormalities and/or ISS stage 3 disease. Standard risk: the remaining patients with available cytogenetics and ISS stage. <sup>‡</sup>Not recorded in 9 patients. Ktd: carfilzomib, thalidomide and dexamethasone; n: number; HDM + ASCT: high-dose melphalan + autologous stem cell transplantation. n: number; ISS: International Staging System; R-ISS: Revised International Staging System; WHO: World Health Organisation; PN: polyneuropathy.

zomib (0%, 5%, 10%, and 15%, respectively) and consisting mainly of pneumonia (*Online Supplementary Table S1*).

Table 4 summarizes cardiac AE. Any grade cardiac AE were reported in 12% of patients after induction therapy (14% in carfilzomib 27mg/m<sup>2</sup>, 15% in carfilzomib 36 mg/m<sup>2</sup>, 19% in carfilzomib 45 mg/m<sup>2</sup>, and 5% in carfilzomib 56 mg/m<sup>2</sup>). These cardiac events consisted mainly of grade 1/2 toxicity (11 of 15 events). Five (5%) grade 3 cardiac AE were reported: three at dose level 27 mg/m<sup>2</sup>, one at dose level 45 mg/m<sup>2</sup>, and one at dose level 56 mg/m<sup>2</sup>.

Any grade cardiac AE increased to 18% after consolidation therapy with no reports of grade 4 AE at all four dose levels, (18% in carfilzomib 27 mg/m<sup>2</sup>, 15% in carfilzomib 36 mg/m<sup>2</sup>, 19% in carfilzomib 45 mg/m<sup>2</sup>, and 15% in carfilzomib 56 mg/m<sup>2</sup>). These cardiac events consisted mainly of grade 1/2 toxicity (14 of 19 events). Five (5%) grade 3 cardiac AE were reported.

Nine patients (8%) developed hypertension during treatment (carfilzomib 27 mg/m<sup>2</sup>, n=3; carfilzomib 36 mg/m<sup>2</sup>, n=3; carfilzomib 45 mg/m<sup>2</sup>, n=2; carfilzomib 56 mg/m<sup>2</sup>, n=1); four (4%) of them had grade 3 toxicity. Five (5%) patients needed antihypertensive treatment.

Seven patients (6%) had pre-existing PN grade 1/2 and two patients (2%) had pre-existing grade 3 PN. During induction and consolidation therapy, 52 patients (47%) developed PN. Grade ≥ 2 PN events occurred in 23 patients (20%) independently from carfilzomib dose; these events were clinically manageable (carfilzomib 27 mg/m<sup>2</sup>, n=11; carfilzomib 36 mg/m<sup>2</sup>, n=3; carfilzomib 45 mg/m<sup>2</sup>, n=6; carfilzomib 56 mg/m<sup>2</sup>, n=3). Only one patient (1%) reported grade 3 PN (carfilzomib 27 mg/m<sup>2</sup>).

At least one serious AE (SAE) was reported in 43% of patients. In cohort 1, an SAE was reported in 21 (42%) patients, in cohort 2 in 8 (40%) patients, in cohort 3 in 7 (33%) patients, and in cohort 4 in 12 (60%) patients.

As reported above, nine patients (8%) discontinued treatment due to excessive toxicity: six patients during induction therapy, and three patients during consolidation therapy. In cohort 1, four (8%) patients went off protocol due to AE: one (5%) patient in cohort 2 and four (20%) patients in cohort 4. Table 5 shows an analysis of treat-

ment adherence to protocol. During consolidation treatment, normal completion rate for carfilzomib and dexamethasone was similar to induction treatment whereas this was higher for thalidomide, probably due to the lower dose of thalidomide during consolidation treatment. A higher percentage of patients prematurely discontinued treatment at the highest dose level of carfilzomib (5 patients, 30%). Four patients (20%) had excessive toxicity

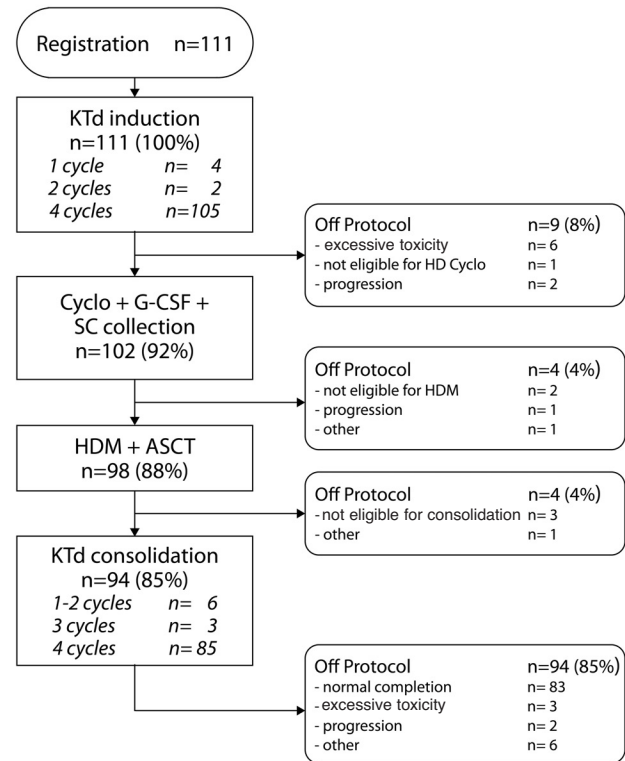


**Figure 1. Consort diagram.** Cyclo: cyclophosphamide; G-CSF: granulocyte colony-stimulating factor; HD: high dose; SC: stem cell. Ktd: carfilzomib, thalidomide and dexamethasone; n: number; HDM + ASCT: high-dose melphalan + autologous stem cell transplantation.

**Table 2. Response after induction, after high-dose melphalan (HDM) and after consolidation therapy.**

Dosing level carfilzomib	20/27 mg/m <sup>2</sup>	20/36 mg/m <sup>2</sup>	20/45 mg/m <sup>2</sup>	20/56 mg/m <sup>2</sup>	All patients
Patients, n	50	20	21	20	111
Response after induction, n (%)					
sCR	4 (8)	1 (5)	0 (0)	1 (5)	6 (5)
≥ CR	8 (16)	5 (25)	3 (14)	4 (20)	20 (18)
≥ VGPR	27 (54)	16 (80)	13 (62)	16 (80)	72 (65)
≥ PR	45 (90)	20 (100)	20 (95)	18 (90)	103 (93)
Response after HDM, n (%)					
sCR	5 (10)	2 (10)	3 (14)	1 (5)	11 (10)
≥ CR	12 (24)	7 (35)	9 (43)	6 (30)	34 (31)
≥ VGPR	32 (64)	17 (85)	19 (90)	18 (90)	86 (77)
≥ PR	46 (92)	20 (100)	20 (95)	18 (90)	104 (94)
Response after consolidation, n (%)					
sCR	17 (34)	4 (20)	8 (38)	4 (20)	33 (30)
≥ CR	28 (56)	15 (75)	14 (67)	13 (65)	70 (63)
≥ VGPR	40 (80)	18 (90)	20 (95)	18 (90)	96 (86)
≥ PR	46 (92)	20 (100)	20 (95)	18 (90)	104 (94)

n: number; sCR: stringent complete remission; CR: complete remission; VGPR: very good partial response; PR: partial response.

and two patients (10%) asked to discontinue treatment (Online Supplementary Table S2).

**Discussion**

Results of the first three dose levels of this phase II trial have been published before.<sup>11</sup> In this paper, we discuss the results of four dose levels of carfilzomib. As reported above, treatment with KTD for induction and consolidation in transplant eligible patients with NDMM is safe, tolerable and effective. We included the additional cohort with the highest dose level of 56 mg/m<sup>2</sup>, based on the hypothesis that a higher dose level induces a higher response rate.<sup>12,16</sup> Response after induction was high, with 65% of patients reaching at least VGPR, increasing to 86%

after consolidation therapy. CR rate after consolidation was high at 63%. Response (i.e. >CR) after consolidation at the three higher dose levels (20/36, 20/45, 20/56) was better than at the lowest dose level (20/27); however, the small sample size and the non-randomized design of the study preclude firm conclusions about superiority of the highest dose levels. In the ARROW trial, 478 patients with RRMM were randomized between treatment with carfilzomib twice a week 27 mg/m<sup>2</sup> or once weekly 70 mg/m<sup>2</sup>. PFS was higher with once weekly 70 mg/m<sup>2</sup> than with twice weekly 27 mg/m<sup>2</sup> (11.2 months vs. 7.6 months).<sup>20</sup> These data and our data (based on response) suggest that a dose of at least 36 mg/m<sup>2</sup> twice weekly (which equals 70 mg/m<sup>2</sup> once weekly) would be the preferred dose.

An important remaining question relates to the efficacy of this regimen in high-risk patients. In this trial with lim-

**Table 3.** Response after consolidation therapy according to risk status and R-ISS.

	Standard risk*	High-risk*	R-ISS 1	R-ISS 2	R-ISS 3	Total
Patients, n	46	43	26	65	10	111
sCR, n (%)	16 (35)	9 (21)	10 (38)	19 (29)	0 (0)	33 (30)
≥ CR, n (%)	31 (67)	25 (58)	19 (73)	37 (57)	6 (60)	70 (63)
≥ VGPR, n (%)	40 (87)	36 (84)	24 (92)	54 (83)	9 (90)	96 (86)
≥ PR, n (%)	44 (96)	38 (88)	26 (100)	58 (91)	10 (100)	104 (94)

\*High-risk: t(4;14) and/or 17p- and/or add1q cytogenetic abnormalities and/or ISS stage 3 disease. Standard risk: the remaining patients with available cytogenetics and ISS stage. n: number; ISS: International Staging System; R-ISS: Revised International Staging System; sCR: stringent complete remission; CR: complete remission; VGPR: very good partial response; PR: partial response.

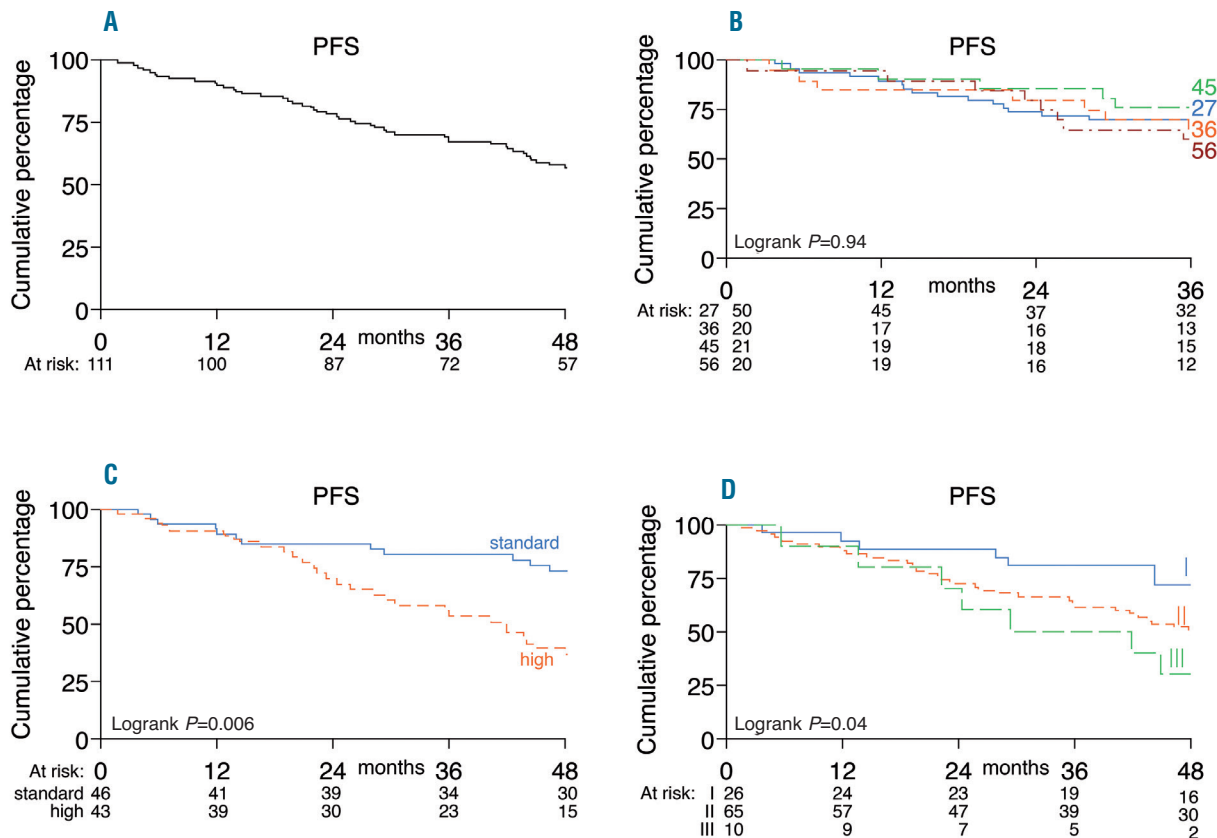


**Figure 2.** Kaplan-Meier curves of progression-free survival (PFS). (A) PFS in all 111 patients. (B) PFS per dose level. (C) PFS according to risk status. (D) PFS according to Revised-International Staging System.

ited numbers, the negative impact of high-risk cytogenetics was not abrogated by carfilzomib.<sup>21</sup> At the same time, overall risk status, based on cytogenetics and ISS stage, was not significantly associated with response. However, high-risk patients and patients with a higher R-ISS score had a significantly worse PFS. Median PFS and OS for all patients were 58 months and 83 months, respectively. These data show that treatment with KTD is effective as front-line treatment of transplant eligible patients with NDMM. Also, this regimen had no effect on stem cell mobilization and collection, with the exception of two patients in whom stem cell collection failed. Several phase

II trials have investigated treatment with carfilzomib in NDMM using different regimens.<sup>12-15</sup> For example, in the CYKLONE trial, cyclophosphamide was added to the KTD regimen; this showed a comparable ORR of 91% and a PFS at 24 months of 76%. In this study, MTD was 20/36 mg/m<sup>2</sup>.<sup>15</sup> In comparison, in the Carthadex trial, dose levels of 45 mg/m<sup>2</sup> and 56 mg/m<sup>2</sup> were well tolerated without additional toxicity compared to dose levels 27 mg/m<sup>2</sup> and 36 mg/m<sup>2</sup>. The number of patients going off treatment due to excessive toxicity was low: 9 out of 111 patients (8%). Our data show that efficacy and safety are comparable at dose levels 36 mg/m<sup>2</sup> and upward. Main grade 3/4 non-

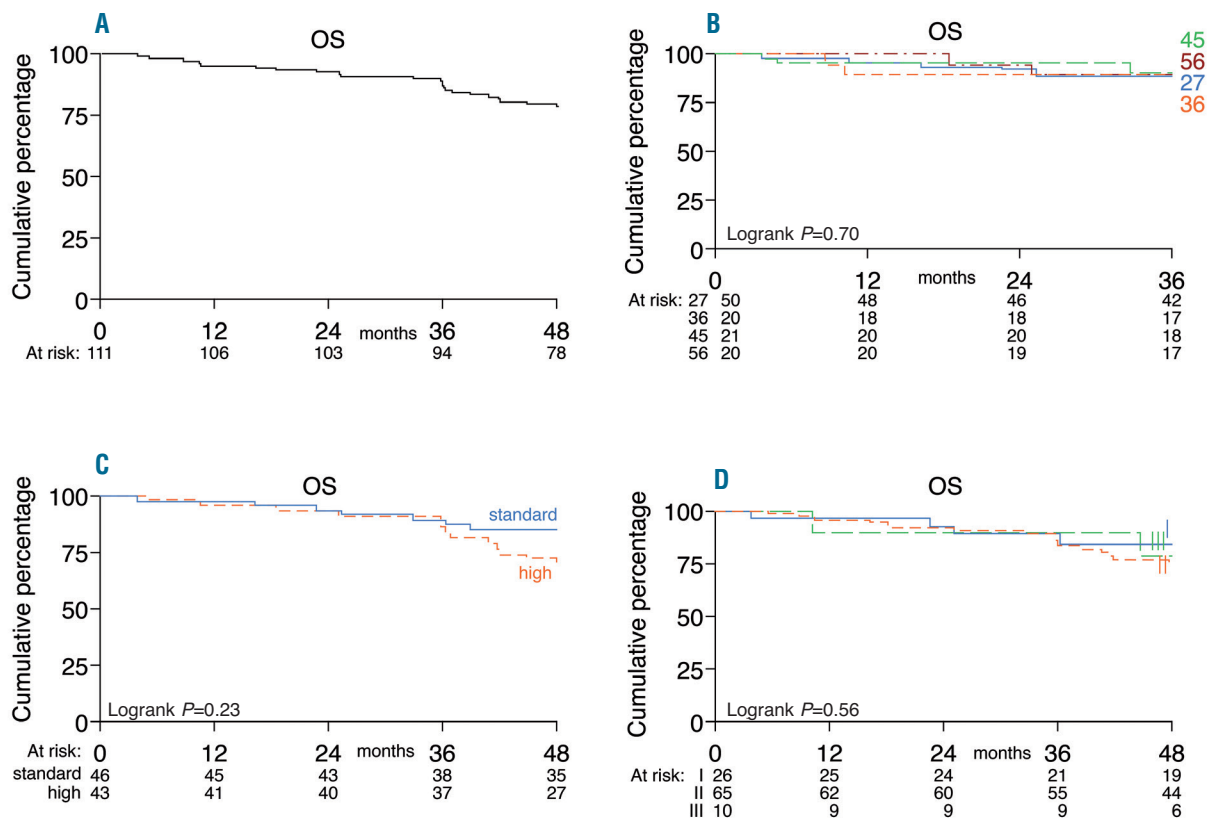


**Figure 3. Kaplan-Meier curves overall survival (OS).** (A) OS in all 111 patients. (B) OS per dose level. (C) OS according to risk status. (D) OS according to Revised-International Staging System.

**Table 4. Cardiac adverse events between dose levels.**

Cardiac toxicity, n (%)	20/27 mg/m <sup>2</sup> , n=50		20/36 mg/m <sup>2</sup> , n=20		20/45 mg/m <sup>2</sup> , n=21		20/56 mg/m <sup>2</sup> , n=20	
	Grade 1/2	Grade 3/4						
Acute coronary syndrome	0 (0)	0 (0)	1 (5)	0 (0)	0 (0)	0 (0)	0 (0)	0 (0)
Atrial flutter	1 (2)	0 (0)	0 (0)	0 (0)	0 (0)	0 (0)	0 (0)	0 (0)
Atrial fibrillation	1 (2)	0 (0)	0 (0)	0 (0)	0 (0)	0 (0)	0 (0)	0 (0)
Angina pectoris	3 (6)	0 (0)	1 (5)	0 (0)	2 (10)	1 (5)	1 (5)	0 (0)
Congestive heart failure	1 (2)	2 (4)	1 (5)	0 (0)	0 (0)	0 (0)	0 (0)	1 (5)
Dyspnea	0 (0)	1 (2)	0 (0)	0 (0)	0 (0)	0 (0)	0 (0)	0 (0)
Palpitations	1 (2)	0 (0)	1 (5)	0 (0)	1 (5)	0 (0)	0 (0)	0 (0)
Pericardial fluid	0 (0)	0 (0)	0 (0)	0 (0)	0 (0)	0 (0)	1 (5)	0 (0)
Total of cardiac events	7 (14)	3 (6)	4 (20)	0 (0)	3 (14)	(5)	1 (5)	1 (5)

n: number.

**Table 5.** Adherence to treatment protocol during induction and consolidation.

Kolom1	Induction (N=111)	Consolidation (N=94)
<b>Carfilzomib</b>		
Normal completion	68 (61)	61 (55)
Dose delay, reduction and/or interruption	37 (33)	24 (22)
Premature stop	6 (5)	9 (10)
<b>Thalidomide</b>		
Normal completion	54 (49)	63 (67)
Dose delay, reduction and/or interruption	42 (38)	8 (9)
Premature stop	15 (14) <sup>a</sup>	23 (24) <sup>b</sup>
<b>Dexamethasone</b>		
Normal completion	85 (77)	66 (70)
Dose delay, reduction and/or interruption	20 (18)	18 (19)
Premature stop	6 (5)	10 (11)

<sup>a</sup>Including 9 patients who received no thalidomide during induction cycle 4. <sup>b</sup>Including 14 patients who received no thalidomide during consolidation cycle 4. n: number.

hematologic toxicity consisted of infections, respiratory, skin, and vascular disorders. The rate of cardiac AE was low in this trial. Five patients (5%) experienced grade 3 cardiac AE, including congestive heart failure, dyspnea and chest pain. This is comparable to other trials investigating carfilzomib in NDMM.<sup>12-14</sup> The rate of grade 3/4 cardiac toxicity is slightly higher in RRMM, most likely because patients are older and due to previous treatment.<sup>9,10</sup> However, the limited number of patients preclude firm conclusions about safety regarding cardiac events between the different dose levels. Jakubowiak *et al.* performed a phase I/II trial of carfilzomib combined with lenalidomide and dexamethasone (CRd). In this trial, patients not proceeding to ASCT continued treatment with CRd beyond eight cycles with a median of 12 cycles. PFS at 24 months was 92%.<sup>12</sup> However, thalidomide remains a valuable treatment option in many countries,

due to its availability and low costs, and offers an excellent alternative to treatment with lenalidomide.

Recently, several trials have been performed in patients with NDMM, using alternative schedules for induction and consolidation. The Intergroupe Francophone du Myélome (IFM) performed a phase II trial of lenalidomide combined with bortezomib and dexamethasone (RVD) for induction and consolidation. PFS at three years was 77% and CR was 58%. Most common toxicities were grade 1/2 PN in 55%.<sup>22</sup> In the EMN02 trial, VCD for induction was followed by VRD for consolidation treatment. CR rate was 55% and PFS not reached at 60 months.<sup>23</sup> Although it should be taken into account that this is a cross comparison between trials, the Carthadex trial efficacy data are similar with median PFS of 58 months and CR rate of 63%, and acceptable toxicity. Moreover, the combination of carfilzomib, thalidomide and dexamethasone is an affordable treatment regimen. These data suggest that KTD is an effective and safe induction and consolidation regimen in newly diagnosed MM.

In conclusion, the combination of carfilzomib, thalidomide and low-dose dexamethasone appears highly efficacious and safe in transplant-eligible patients with NDMM across all dose levels with manageable toxicities. Consolidation therapy after ASCT results in a major improvement in response. In addition, we observed that higher dose levels of carfilzomib (36-56 mg/m<sup>2</sup>) result in better response rates after consolidation therapy. Current studies in newly diagnosed MM patients are performed using 36 mg/m<sup>2</sup> twice weekly. The preferred dose to be used in practice would be 36 mg/m<sup>2</sup> twice weekly (or 70 mg/m<sup>2</sup> once weekly), which we would recommend based on our carthadex response data. Results of cohort 5, in which patients were treated with eight instead of four induction cycles, will follow in the near future.

Further randomized, prospective studies are needed to confirm these data and determine the place for carfilzomib in the treatment of patients with NDMM.

#### Acknowledgments

This trial was supported by funding from Onyx Pharmaceuticals, Inc., an Amgen subsidiary.

#### References

- Lahuerta JJ, Mateos MV, Martinez-Lopez J, et al. Influence of pre- and post-transplantation responses on outcome of patients with multiple myeloma: sequential improvement of response and achievement of complete response are associated with longer survival. *J Clin Oncol.* 2008;26(35):5775-5782.
- Cavo M, Brioli A, Tacchetti P, et al. Role of consolidation therapy in transplant eligible multiple myeloma patients. *Semin Oncol.* 2013;40(5):610-617.
- Niesvizky R, Richardson PG, Rajkumar SV, et al. The relationship between quality of response and clinical benefit for patients treated on the bortezomib arm of the international, randomized, phase 3 APEX trial in relapsed multiple myeloma. *Br J Haematol.* 2008;143(1):46-53.
- Harousseau JL, Dimopoulos MA, Wang M, et al. Better quality of response to lenalidomide plus dexamethasone is associated with improved clinical outcomes in patients with relapsed or refractory multiple myeloma. *Haematologica.* 2010;95(10):1738-1744.
- van de Velde HJ, Liu X, Chen G, et al. Complete response correlates with long-term survival and progression-free survival in high-dose therapy in multiple myeloma. *Haematologica.* 2007;92(10):1399-1406.
- Cavo M, Tacchetti P, Patriarca F, et al. Bortezomib with thalidomide plus dexamethasone compared with thalidomide plus dexamethasone as induction therapy after, double autologous stem-cell transplantation in newly diagnosed multiple myeloma: a randomised phase 3 study. *Lancet.* 2010;376(9758):2075-2085.
- Rosinol L, Oriol A, Teruel AI, et al. Superiority of bortezomib, thalidomide, and dexamethasone (VTD) as induction pretransplantation therapy in multiple myeloma: a randomized phase 3 PETHEMA/GEM study. *Blood.* 2012;120(8):1589-1596.
- Moreau P, Hulin C, Macro M, et al. VTD is superior to VCD prior to intensive therapy in multiple myeloma: results of the prospective IFM2013-04 trial. *Blood.* 2016;127(21):2569-2574.
- Stewart AK, Rajkumar SV, Dimopoulos MA, et al. Carfilzomib, lenalidomide, and dexamethasone for relapsed multiple myeloma. *N Engl J Med.* 2015;372(2):142-152.
- Dimopoulos MA, Moreau P, Palumbo A, et al. Carfilzomib and dexamethasone versus bortezomib and dexamethasone for patients with relapsed or refractory multiple myeloma (ENDEAVOR): a randomised, phase 3, open-label, multicentre study.

- Lancet Oncol. 2016;17(1):27-38.
11. Sonneveld P, Asselbergs E, Zweegman S, et al. Phase 2 study of carfilzomib, thalidomide, and dexamethasone as induction/consolidation therapy for newly diagnosed multiple myeloma. *Blood*. 2015; 125(3):449-456.
  12. Jakubowiak AJ, Dytfeld D, Griffith KA, et al. A phase 1/2 study of carfilzomib in combination with lenalidomide and low-dose dexamethasone as a frontline treatment for multiple myeloma. *Blood*. 2012;120(9): 1801-1809.
  13. Mikhael JR, Reeder CB, Libby EN, et al. Phase Ib/II trial of CYKLONE (cyclophosphamide, carfilzomib, thalidomide and dexamethasone) for newly diagnosed myeloma. *Br J Haematol*. 2015;169(2):219-227.
  14. Bringhen S, Petrucci MT, Larocca A, et al. Carfilzomib, cyclophosphamide, and dexamethasone in patients with newly diagnosed multiple myeloma: a multicenter, phase 2 study. *Blood*. 2014;124(1):63-69.
  15. Moreau P, Kolb B, Attal M, et al. Phase 1/2 study of carfilzomib plus melphalan and prednisone in patients aged over 65 years with newly diagnosed multiple myeloma. *Blood*. 2015;125(20):3100-3104.
  16. Papadopoulos KP, Siegel DS, Vesole DH, et al. Phase I study of 30-minute infusion of carfilzomib as single agent or in combination with low-dose dexamethasone in patients with relapsed and/or refractory multiple myeloma. *J Clin Oncol*. 2015; 33(7):732-739.
  17. Larocca A, Cavallo F, Bringhen S, et al. Aspirin or enoxaparin thromboprophylaxis for patients with newly diagnosed multiple myeloma treated with lenalidomide. *Blood*. 2012;119(4):933-939
  18. Kumar S, Paiva B, Anderson KC, et al. International Myeloma Working Group consensus criteria for response and minimal residual disease assessment in multiple myeloma. *Lancet Oncol*. 2016;17(8):e328-e346.
  19. Dueck AC, Mendoza TR, Mitchell SA, et al. Validity and Reliability of the US National Cancer Institute's Patient-Reported Outcomes Version of the Common Terminology Criteria for Adverse Events (PRO-CTCAE). *JAMA Oncol*. 2015; 1(8):1051-1059.
  20. Moreau P, Mateos MV, Berenson JR, et al. Once weekly versus twice weekly carfilzomib dosing in patients with relapsed and refractory multiple myeloma (A.R.R.O.W.): interim analysis results of a randomised, phase 3 study. *Lancet Oncol*. 2018; 19(7):953-964.
  21. Goldschmidt H, Lokhorst HM, Mai EK, et al. Bortezomib before and after high-dose therapy in myeloma: long-term results from the phase III HOVON-65/GMMG-HD4 trial. *Leukemia*. 2018;32(2):383-390.
  22. Roussel M, Lauwers-Cances V, Robillard N, et al. Front-line transplantation program with lenalidomide, bortezomib, and dexamethasone combination as induction and consolidation followed by lenalidomide maintenance in patients with multiple myeloma: a phase II study by the Intergroupe Francophone du Myelome. *J Clin Oncol*. 2014;32(25):2712-2717.
  23. Sonneveld P, Juni 2018. Consolidation followed by maintenance vs. maintenance alone in newly diagnosed, transplant eligible multiple myeloma: a randomized phase 3 study of the European Myeloma Network (EMN02/HO95 MM TRIAL). Abstract presented at the EHA meeting, Stockholm, Sweden. Abstract retrieved from <https://learningcenter.ehaweb.org/eha/2018/stockholm/214488/pieter.sonneveld.consolidation.followed.by.maintenance.vs.maintenance.alone.in.html>. Abstract # S108.



## Bortezomib-based induction followed by stem cell transplantation in light chain amyloidosis: results of the multicenter HOVON 104 trial

Monique C. Minnema,<sup>1</sup> Kazem Nasserinejad,<sup>2</sup> Bouke Hazenberg,<sup>3</sup> Ute Hegenbart,<sup>4</sup> Philip Vlummens,<sup>5</sup> Paula F. Ypma,<sup>6</sup> Nicolaus Kröger,<sup>7</sup> Ka Lung Wu,<sup>8</sup> Marie Jose Kersten,<sup>9</sup> M. Ron Schaafsma,<sup>10</sup> Sandra Croockewit,<sup>11</sup> Esther de Waal,<sup>12</sup> Sonja Zweegman,<sup>13</sup> Lidwien Tick,<sup>14</sup> Annemieke Broijl,<sup>15</sup> Harry Koene,<sup>16</sup> Gerard Bos,<sup>17</sup> Pieter Sonneveld<sup>15</sup> and Stefan Schönland<sup>4</sup>

Haematologica 2019  
Volume 104(11):2274-2282

<sup>1</sup>Department of Hematology, UMC Utrecht Cancer Center, Utrecht, the Netherlands; <sup>2</sup>HOVON Data Center, Department of Hematology, Erasmus MC Cancer Institute, Rotterdam, the Netherlands; <sup>3</sup>Department of Rheumatology & Clinical Immunology, University of Groningen Medical Center, Groningen, the Netherlands; <sup>4</sup>Department of Hematology, Oncology and Rheumatology, Heidelberg University, Amyloidosis Center, Heidelberg, Germany; <sup>5</sup>Department of Haematology, Ghent University, Gent, Belgium; <sup>6</sup>Department of Hematology, HagaZiekenhuis, Den Haag, the Netherlands; <sup>7</sup>Department of Stem Cell Transplantation, University Medical Center Hamburg-Eppendorf, Hamburg, Germany; <sup>8</sup>Department of Hematology, ZNA Stuivenberg, Antwerp, Belgium; <sup>9</sup>Department of Hematology, Academic Medical Center, Lymphoma and Myeloma Center, Amsterdam, the Netherlands; <sup>10</sup>Department of Hematology, Medisch Spectrum Twente, Enschede, the Netherlands; <sup>11</sup>Department of Hematology, Radboud University Medical Center, Nijmegen, the Netherlands; <sup>12</sup>Department of Hematology, University of Groningen, Medical Center, Groningen, the Netherlands; <sup>13</sup>Department of Hematology, VU University Medical Center, Amsterdam Cancer Center, Amsterdam, the Netherlands; <sup>14</sup>Department of Internal Medicine, Maxima Medisch Centrum, Eindhoven, the Netherlands; <sup>15</sup>Department of Hematology, Erasmus MC Cancer Institute, Rotterdam, the Netherlands; <sup>16</sup>Department of Hematology, St. Antonius Hospital, Nieuwegein, the Netherlands and <sup>17</sup>Department of Hematology, Maastricht University Medical Center, Maastricht, the Netherlands

### Correspondence:

MONIQUE C. MINNEMA  
m.c.minnema@umcutrecht.nl

Received: December 6, 2018.

Accepted: March 18, 2019.

Pre-published: March 28, 2019.

doi:10.3324/haematol.2018.213900

Check the online version for the most updated information on this article, online supplements, and information on authorship & disclosures: [www.haematologica.org/content/104/11/2274](http://www.haematologica.org/content/104/11/2274)

©2019 Ferrata Storti Foundation

Material published in Haematologica is covered by copyright. All rights are reserved to the Ferrata Storti Foundation. Use of published material is allowed under the following terms and conditions:

<https://creativecommons.org/licenses/by-nc/4.0/legalcode>. Copies of published material are allowed for personal or internal use. Sharing published material for non-commercial purposes is subject to the following conditions: <https://creativecommons.org/licenses/by-nc/4.0/legalcode>, sect. 3. Reproducing and sharing published material for commercial purposes is not allowed without permission in writing from the publisher.



### ABSTRACT

This prospective, multicenter, phase II study investigated the use of four cycles of bortezomib-dexamethasone induction treatment, followed by high-dose melphalan and autologous stem cell transplantation (SCT) in patients with newly diagnosed light chain amyloidosis. The aim of the study was to improve the hematologic complete remission (CR) rate 6 months after SCT from 30% to 50%. Fifty patients were enrolled and 72% had two or more organs involved. The overall hematologic response rate after induction treatment was 80% including 20% CR and 38% very good partial remissions (VGPR). Fifteen patients did not proceed to SCT for various reasons but mostly treatment-related toxicity and disease-related organ damage and death (2 patients). Thirty-one patients received melphalan 200 mg/m<sup>2</sup> and four patients a reduced dose because of renal function impairment. There were no deaths related to the transplantation procedure. Hematologic responses improved at 6 months after SCT to 86% with 46% CR and 26% VGPR. However, due to the high treatment discontinuation rate before transplantation the primary endpoint of the study was not met and the CR rate in the intention-to-treat analysis was 32%. Organ responses continued to improve after SCT. We confirm the high efficacy of bortezomib-dexamethasone treatment in patients with AL amyloidosis. However, because of both treatment-related toxicity and disease characteristics, 30% of the patients could not proceed to SCT after induction treatment. (Trial registered at Dutch Trial Register identifier NTR3220).

## Introduction

Light chain (AL) amyloidosis is a potentially fatal disorder caused by a small monoclonal population of plasma cells in the bone marrow, which synthesize monoclonal light chains. The light chains are considered toxic and aggregate into amyloid fibrils. These fibrils form extracellular deposits in one or more vital organs, most frequently in the kidneys, heart and liver as well as in the peripheral and autonomic nervous systems.<sup>1</sup>

The main goal of treatment is to reduce the supply of the amyloidogenic monoclonal light chains rapidly and to achieve a very good partial response (VGPR) or a complete hematologic response (CR).<sup>2</sup> Achieving a hematologic response is closely related with survival. This has been demonstrated following both high-dose and standard-dose chemotherapy.<sup>2,3</sup> Organ responses are also induced in patients with prolonged hematologic responses.

High-dose melphalan (HDM) followed by autologous SCT (auto-SCT) is considered the most effective treatment for selected patients with AL amyloidosis.<sup>4</sup> However, this treatment is only feasible in around 20% or fewer of newly diagnosed patients. Due to more strict selection criteria for eligibility for transplantation, the treatment-related mortality of auto-SCT has decreased to below 5% and transplanted patients have an excellent survival after their transplant.<sup>5,7</sup>

In the previous HOVON (Haemato-Oncology Foundation for Adults in the Netherlands) 41 study we examined a two-step approach consisting of non-intensive induction therapy followed by HDM and auto-SCT.<sup>8</sup> Although the vincristine-adriamycin-dexamethasone (VAD) induction treatment was considered too toxic, the survival of patients was good with a median survival of 8 years from registration and, for the transplanted patients, a median survival of 10 years from the date of transplantation. Other retrospective single-center studies have also examined the value of various induction regimens before HDM and auto-SCT and concluded that induction therapy is associated with a better overall survival (OS), with possibly the greatest benefit for patients with >10% bone marrow plasma cell infiltration.<sup>9,10</sup>

Bortezomib (Velcade®), a proteasome inhibitor frequently used in first-line and relapse treatment in patients with multiple myeloma (MM), has been given to newly diagnosed and relapsed AL amyloidosis patients in mostly retrospective and only one prospective multicenter study. The hematologic response rate to bortezomib was excellent, ranging from 50% to 80% with a CR rate from 25% to 47%; furthermore, the CR occurred rapidly, especially when the drug was administered bi-weekly.<sup>11-15</sup> Common toxicities included thrombocytopenia, peripheral sensory neuropathy, neuropathic pain, hypotension and peripheral edema.

Considering the potent effect of bortezomib in relapsed AL amyloidosis patients and the improvement in response rates achieved when used as first-line treatment in MM patients, we hypothesized that the use of this drug, in combination with auto-SCT, could also improve the response rates of AL amyloidosis patients. Because the CR rate, in particular, is closely related to progression-free survival (PFS), OS and organ responses, the current trial investigated the efficacy of induction treatment consisting of bortezomib and dexamethasone followed by HDM and auto-SCT to improve the CR rate after auto-SCT.

## Methods

The HOVON 104 study was conducted in 15 centers in the Netherlands, Germany, and Belgium. The trial started with a randomized, phase III design but due to slow accrual the dexamethasone arm closed after including seven patients and the trial continued as a single-arm, phase II study.

Patients with biopsy-proven, systemic, AL amyloidosis, aged between 18-70 years, with detectable M-protein and/or involved free light chains (FLC) >50 mg/L, World Health Organization (WHO) Performance Status 0-2, and New York Heart Association (NYHA) stage 1-2 were included. Eligibility criteria at inclusion corresponded to eligibility criteria for auto-SCT with the exception of measurement of cardiac ejection fraction. Major exclusion criteria were concurrent MM defined as Salmon-Durie stage II or III, previous treatment of plasma cell dyscrasia, symptomatic orthostatic hypotension, symptomatic effusions, a N-terminal pro-brain natriuretic peptide (NT-proBNP) level >5,000 pg/mL, troponin T >0.06 µg/L or troponin I >2 x upper limit of normal, estimated glomerular filtration rate (eGFR) <30 mL/min/1.73 m<sup>2</sup>, National Cancer Institute Common Terminology Criteria for Adverse Events (NCI CTCAE) sensory peripheral neuropathy > grade 2 or > grade 1 with pain and motor peripheral neuropathy > grade 2 (see the *Online Supplement* for the complete list). Inclusion and exclusion criteria were also established for stem cell mobilization. Inclusion criteria comprised a WHO Performance Status 0-2, NYHA stage 1-2, and ejection fraction >45%. The exclusion criteria are listed in the *Online Supplement*. The study was approved by the ethics committee of all participating hospitals and the University Medical Center Utrecht (Institutional Review Board n. 10-426). All procedures were conducted in compliance with the Declaration of Helsinki. Written informed consent to participation in the study was provided by all patients (*EudraCT number 2010-021445-42*).

### Treatment design

Four 21-day cycles of induction treatment were given. The cycles consisted of bortezomib subcutaneously (sc) 1.3 mg/m<sup>2</sup> on days 1, 4, 8, and 11 and dexamethasone 20 mg orally on each day of bortezomib administration and the following day. Dose adjustments are described in the *Online Supplement*. Stem cell mobilization began within 4-6 weeks after the start of the last induction cycle using granulocyte colony-stimulating factor 10 µg/kg divided in two doses, given for 5 days. The melphalan dosage was 200 mg/m<sup>2</sup> given in 2 days. Patients with an eGFR <40 mL/min/1.73 m<sup>2</sup> were given 100 mg/m<sup>2</sup> melphalan. Hematologic response was measured after each induction cycle and it was planned that all patients would receive HDM. Patients not responding to induction treatment could proceed directly to stem cell mobilization and auto-SCT if eligibility criteria were met.

### Hematologic and organ response criteria

Organ involvement and hematologic and organ responses were evaluated according to the consensus criteria of the International Society of Amyloidosis published in 2005 with some modifications such as the addition of a VGPR category and addition of NT-proBNP for cardiac response<sup>14,15</sup> (see the *Online Supplement*).

Both hematologic and organ responses were measured after

each induction cycle, after stem cell mobilization and before auto-SCT, and thereafter every 3 months for 5 years after registration. In addition, patients could participate in a side study with measurement of minimal residual disease by flow cytometry when a CR was reached or 6 months after auto-SCT. Flow cytometry was performed centrally with a sensitivity level of  $10^{-5}$ . Details are provided in the *Online Supplement*.

### Statistical design and endpoints

The primary endpoint was the efficacy of bortezomib-dexamethasone induction treatment followed by HDM and auto-SCT,

measured as the proportion of patients with a CR at 6 months after auto-SCT. The secondary endpoints and analysis of the effect of baseline characteristics on auto-SCT, OS and PFS are described in the *Online Supplement*.

## Results

### Patients' characteristics

Between March 2012 and April 2016, 50 patients were enrolled in the phase II part of the trial. Table 1 summa-

**Table 1.** Baseline characteristics of 50 patients, separated for groups that did or did not proceed to autologous stem cell transplantation.

Characteristic	Patients who proceeded to auto-SCT (N = 35)	Patients who did not proceed to auto-SCT (N = 15)	All patients (N = 50)
Age (years), median (IQR)	59 (50-63)	60 (53-63)	59 (51-63)
Sex (female), n (%)	14 (40%)	6 (40%)	20 (40%)
WHO performance status, n (%)			
0	17 (49%)	6 (40%)	23 (46%)
1	16 (46%)	5 (33%)	21 (42%)
2	1 (3%)	4 (27%)	5 (10%)
Clonal disease, n (%)			
Lambda	27 (77%)	13 (87%)	40 (80%)
Kappa	8 (23%)	2 (13%)	10 (20%)
Involved FLC level, median (IQR)	167 (63-341)	205 (64-493)	181 (73-35)
dFLC, median (IQR)	214 (103-342)	212 (68-461)	213 (80-397)
Number of patients with dFLC $\geq$ 180 mg/L, median (IQR)	17 (49%)	8 (53%)	25 (50%)
% plasma cells in bone marrow, median (IQR)	6 (4-11)	5 (2-8)	6 (0-33)
Number of patients with $\geq$ 10% plasma cells, median (IQR)	12 (34%)	2 (13%)	14 (28%)
Median number of organs involved, n (%)	2 (1-3)	2 (1-3)	2 (1-3)
Number of organs involved			
$\geq$ 2	26 (74%)	10 (67%)	36 (72%)
$\geq$ 3	12 (34%)	7 (47%)	19 (38%)
Organ involvement, n (%)			
Kidney	29 (83%)	12 (80%)	41 (82%)
Heart	23 (66%)	10 (67%)	33 (66%)
Nervous system	4 (11%)	3 (20%)	7 (14%)
Gastrointestinal system	4 (11%)	0 (0%)	4 (8%)
Liver	8 (23%)	5 (33%)	13 (26%)
Soft tissues	5 (14%)	3 (20%)	8 (16%)
Mayo classification, n (%)			
I	12 (34%)	4 (27%)	16 (32%)
II	10 (29%)	6 (40%)	16 (32%)
III	12 (34%)	5 (33%)	17 (34%)
NYHA stage, n (%)			
I	22 (63%)	6 (40%)	28 (56%)
II	12 (34%)	9 (60%)	21 (42%)
NT-proBNP level (ng/L), median (IQR)	675 (166-1638)	1110 (264-2292)	832 (204-1638)
Echo cardiography, median (IQR)			
Mean left ventricular wall thickness	12 mm (11-15)	13 mm (12-14)	13 mm (11-15)
Ejection fraction	63% (55-71)	58% (53-66)	60% (55-68)
Diastolic dysfunction	60% present	60% present	60% present
eGFR (mL/min/1.73 m <sup>2</sup> ), median (IQR)	68 (58-87)	90 (60-95)	72 (59-90)
Renal stage			
I	12 (34%)	8 (53%)	20 (40%)
II	19 (54%)	6 (40%)	25 (50%)
III	4 (11%)	1 (7%)	5 (10%)

Auto-SCT: autologous stem cell transplantation; WHO: World Health Organization; FLC: free light chain; dFLC: difference between involved and uninvolved free light chains; NYHA: New York Heart Association; NT-proBNP: N-terminal pro-brain natriuretic peptide; eGFR: estimated glomerular filtration rate.

rized the patients' characteristics separately for those who proceeded to auto-SCT and those who did not. The median age of all the patients included was 59 years [interquartile range (IQR), 51-63]. The median number of organs involved was two (range, 1 to 5). Two or more organs were involved in 36 patients (72%) and three or more in 19 (18%). The kidney was the organ most frequently involved, with renal disease in 82% of patients, followed by the heart (in 66% of patients) and liver (in 26% of patients). The median eGFR at inclusion was 72 mL/min/1.73 m<sup>2</sup> (IQR, 59-90) and 20, 25 and 5 patients had renal stage I, II or III, respectively.<sup>16</sup> Mayo cardiac stage was I, II and III for 16, 16 and 17 patients, respectively (data unavailable for 1 patient).<sup>17</sup> The initial median NT-proBNP level was 832 pg/mL (IQR, 204-1638). Echocardiography data were available for 47 patients.

Fourteen patients (28%) had a plasma cell infiltration of  $\geq 10\%$  in the bone marrow. Most patients presented with  $\lambda$  light chains (80%). The median concentration of involved FLC was 180 mg/L (IQR, 73-352) for  $\lambda$  light chains and 169 mg/L (IQR, 61-879) for  $\kappa$  light chains. The median difference between involved and uninvolved FLC (dFLC) was 213 mg/L (IQR, 80-397) and 50% of patients had a dFLC  $\geq 180$  mg/L. Of note, seven patients were included without an M-protein or dFLC value that could qualify them for the PR or VGPR category and three of these patients also did not have a urine protein electrophoresis  $>0.1$  g/day.

In the group of seven patients enrolled in the dexamethasone arm of the closed, phase III part of the trial one patient was not eligible. The median age of the other six patients was 57 years and these patients' other baseline characteristics were also comparable to those of the 50 patients in the phase II part (*data not shown*). Three patients underwent auto-SCT and the estimated 3-year PFS was 83%. These six patients are not included in this final analysis.

### Treatment characteristics

All patients started with induction treatment. Most patients (88%) received four cycles of bortezomib-dexamethasone, two patients received three cycles, two patients received only two cycles and two patients had to discontinue induction treatment after the first cycle. Half of the patients had dose modifications in the administered cycles as prescribed per protocol: in 50% of patients the bortezomib dose was modified and in 44% the dexamethasone dose was modified. The reasons for dose modifications for bortezomib were mostly neurotoxicity, both sensory and autonomic neuropathy (9 patients) and infection (3 patients) and for dexamethasone heart failure (4 patients), edema (3 patients), infection (3 patients) and myopathy (2 patients).

Eleven patients did not have their stem cells collected after induction therapy. Five patients did not fulfill the eligibility criteria, including two patients who stopped induction due to progressive heart failure and kidney failure. Two patients died, one during the first cycle of induction, three patients experienced bortezomib-related toxicity and were taken off the trial during induction treatment (1 patient with bronchial hyperreactivity, 1 patient with gastrointestinal necrosis and 1 patient with NCI CTCAE grade 4 sensory neuropathy) and one patient refused stem cell collection.

The median number of stem cells collected was  $6.3 \times 10^6$

CD34/kg (IQR, 4.6-9.3). Ten patients needed 2 days of apheresis and cyclophosphamide was given to nine patients according to local policy. After stem cell collection, four patients did not proceed to HDM and stem cell reinfusion. All four had clinical deterioration: two patients developed symptomatic pleural effusions, one patient started dialysis and one patient had several toxicities, a worsening clinical condition and was taken off the trial by decision of the treating physician.

In total 35 patients (70%) received HDM and stem cell reinfusion as an inpatient procedure. Thirty-one patients were given a full dose of HDM, per protocol; in four patients the melphalan dose was reduced to 100 mg/m<sup>2</sup> because their eGFR was  $<40$  mL/min/1.73 m<sup>2</sup>. All patients engrafted without granulocyte colony-stimulating factor support in a median time of 13 days for white blood cells and 16 days for platelets. A CONSORT diagram summarizes the treatment course of all 50 patients (Figure 1).

Based on a univariate logistic regression model we could not identify a prognostic baseline characteristic such as NYHA stage, NT-proBNP, Mayo stage,  $\geq 10\%$  plasma cells, dFLC  $\geq 180$  mg/L, or number of involved organs that was related to proceeding to auto-SCT after induction therapy. As shown in Table 1 the baseline Mayo stage was not statistically different between the groups of patients who did or did not proceed to auto-SCT ( $P=0.80$ ). In the 35 patients who underwent auto-SCT, 22 received full-dose bortezomib and 23 full-dose dexamethasone. In contrast, in the 15 patients who did not proceed to auto-SCT only three received full-dose bortezomib and five full-dose dexamethasone. Because troponin levels were only measured at baseline, a Mayo stage assessment could not be calculated after induction treatment or before auto-SCT.

### Hematologic responses

Hematologic responses are summarized in Table 2. The overall response rate (ORR) after induction treatment was 80%, which included the 38% of patients with a VGPR and 20% with a CR. The median time to first response was 28 days (IQR, 21-43) and the median time to best response was 67 days (IQR, 28-240). Eighty percent of the responses were detected within the first 3 months after starting treatment (Figure 2). Ten patients (20%) had a CR after induction treatment and eight of them proceeded to auto-SCT. Responses assessed 6 months after auto-SCT, which was the primary endpoint of the study, improved but were assessed in 35 patients only, since 15 patients did not proceed to auto-SCT. In these 35 patients, the CR rate doubled from 23% after induction treatment to 46% at 6 months after auto-SCT. The ORR increased to 86% at 6 months after auto-SCT. In the intention-to-treat analysis the CR rate at 6 months after auto-SCT was 32% and therefore the primary endpoint of the study was not met. In the group of 15 patients who did not proceed to auto-SCT, ten (67%) had a hematologic response. In univariate logistic regression analyses a dFLC  $\geq 180$  mg/L and bone marrow plasma cell infiltration  $\geq 10\%$  at diagnosis were not related to the depth of the hematologic response.

### Flow cytometry

Samples for flow cytometry were available at diagnosis for 26 patients. Of this group, 20 patients proceeded to auto-SCT. The median percentage of clonal plasma cells

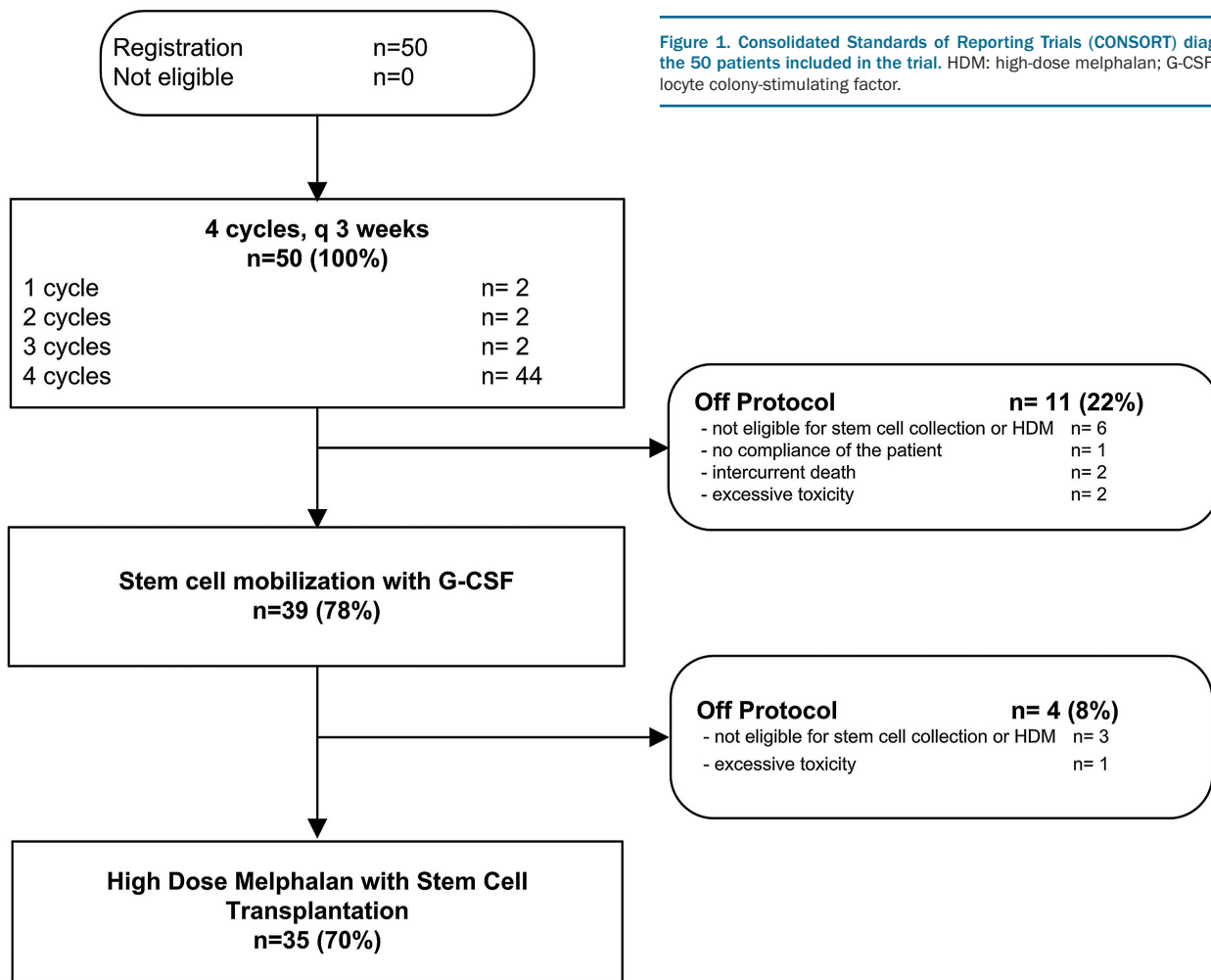


Figure 1. Consolidated Standards of Reporting Trials (CONSORT) diagram of the 50 patients included in the trial. HDM: high-dose melphalan; G-CSF: granulocyte colony-stimulating factor.

Table 2. Hematologic response rates during the different treatment phases.

	After induction therapy	+6 months after auto-SCT (n=35)	+12 months after auto-SCT (n=34)	+24 months after auto-SCT (n=33)
Hematologic response (intention to treat)				
≥PR (ORR)	83% (80%)	86% (60%)	89% (60%)	91% (60%)
≥VGPR	66% (58%)	72% (50%)	77% (52%)	76% (50%)
CR	23% (20%)	46% (32%)	56% (38%)	58% (38%)
Median time to first response	28 days			
Median time to best response	67 days			

\*The first percentage concerns patients who underwent autologous stem cell transplantation (35 in total), the second percentage between brackets is the response rate assessed in an intention-to-treat analysis. Auto-SCT: autologous stem cell transplantation; PR: partial response; ORR: overall response rate; VGPR: very good partial response; CR: complete response.

detected at baseline was 1.4% (range, 0.17-4.9). At 6 months after auto-SCT, samples were collected from seven patients. Six of these patients had a CR and were also negative for minimal residual disease. Additional analyses were performed, such as those previously reported by Perez-Persona *et al.* who described that a ratio of clonal plasma cells within the total bone marrow plasma cells (aPC/BMPC) ≥95% had prognostic value for progression to MM in patients with monoclonal gammopathy of unknown significance and smoldering MM.<sup>18</sup> In the current study patients with aPC/BMPC ≥95% at

baseline had a shorter PFS (hazard ratio 8.44, 95% confidence interval: 1.05-67.96) and a lower probability of proceeding to auto-SCT; however, given the small sample size this was not statistically significant (odds ratio 0.16, 95% confidence interval: 0.02-1.67).

### Organ responses

Organ responses were already seen after induction treatment and improved after HDM plus auto-SCT and are summarized in Figure 3 for both patients who proceeded to auto-SCT and those who did not. The rate of

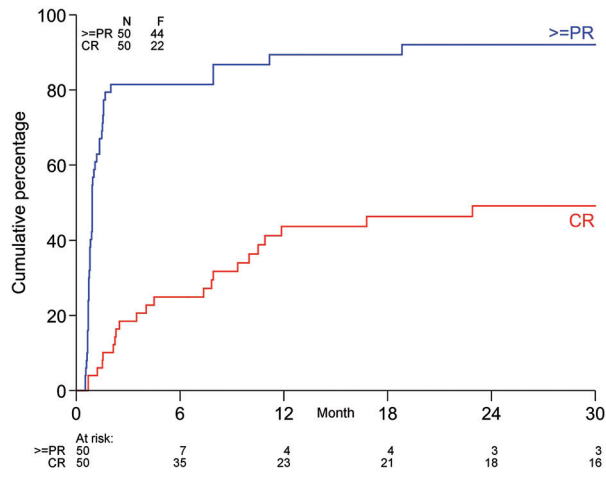


**Figure 2. Response rates following the initiation of treatment.** The upper line represents the time to first response, defined as partial response or better, while the lower line represents the time to first complete response. PR: partial response; CR: complete response.

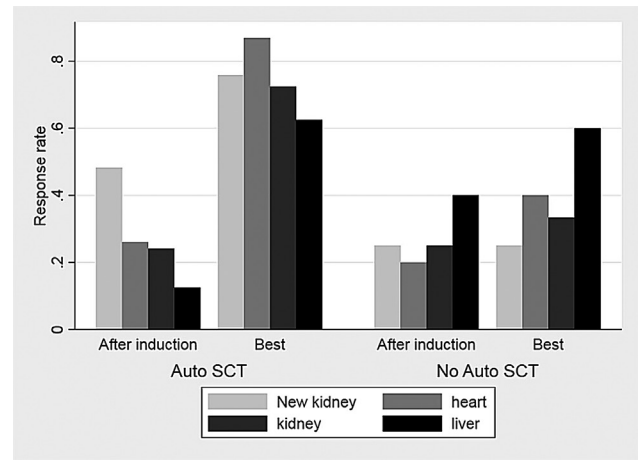


**Figure 3. Organ responses depicted separately for patients who proceeded to autologous stem cell transplantation or not.** Organ responses were assessed according to consensus criteria after induction and as best responses achieved during study treatment and follow-up. Auto-SCT: autologous stem cell transplantation.

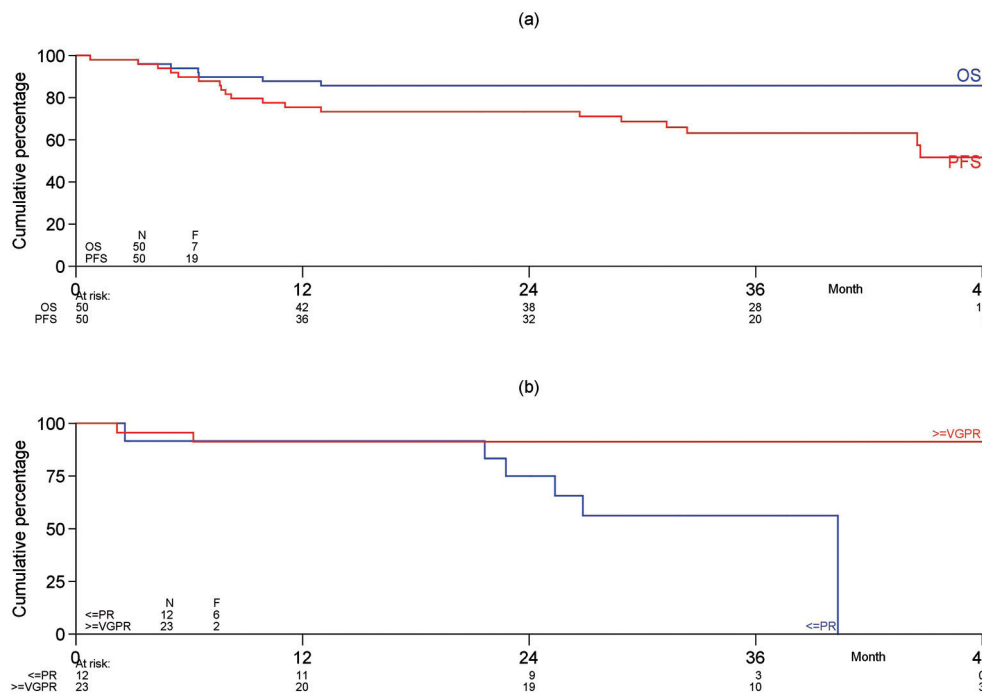


**Figure 4. Overall and progression-free survival of the total cohort of patients and the 35 patients who underwent autologous stem cell transplantation.** (A) Progression-free and overall survival from date of registration in the trial for the 50 patients included. (B) Progression-free survival from autologous stem cell transplantation of the 35 transplanted patients according to response achieved after induction therapy. PFS: progression-free survival; OS: overall survival; PR: partial remission; VGPR: very good partial remission.

kidney responses improved from 24% to 69% at 2 years after auto-SCT and that of cardiac responses from 24% to 78%. In intention-to-treat analysis 61% of patients achieved a renal response, 72% a cardiac response and 62% a liver response. During the HDM and auto-SCT procedure two patients had a deterioration of their renal function, defined as a decrease of 25% in eGFR, which persisted during the follow-up. The median time to first organ response was 222 days for the heart (IQR, 125-395) and 318 days (IQR 91-615) for the kidney. Organ progression was seen in six of 33 patients with cardiac involve-

ment, 13 out of 41 patients with kidney involvement, and three of 13 patients with liver involvement.

During the study new renal response criteria were developed ( $\geq 30\%$  decrease in proteinuria or drop of proteinuria  $< 0.5$  g/day in the absence of renal progression, defined as a  $\geq 25\%$  decrease in eGFR). According to these criteria 14 patients (48%) who proceeded to auto-SCT had a renal response after induction treatment and this increased to 22 patients (76%) after auto-SCT (Figure 3).

Patients with a deep hematologic response (CR/VGPR) at 6 months after auto-SCT and at subsequent time-

points had a higher renal response rate (72% vs. 28%,  $P=0.03$ ). Although more patients in this group also had a higher cardiac response rate (65% vs. 35%), the difference was not statistically significant for cardiac response at any time-point after auto-SCT.

### Overall survival and progression-free survival

The median follow-up of the 43 patients still alive is 38.3 months (IQR, 34-46) while that of all 50 patients is 36.9 months (IQR, 29-46). Five patients died during the follow-up, in most cases due to amyloid-related organ failure. None of the transplanted patients has died. Kaplan-Meier PFS curves for all 50 patients and the 35 transplanted patients are shown in Figure 4. The median OS and PFS were not reached. The 3-year estimated OS and PFS rates are 86% and 63%, respectively. In total seven patients had progression of their plasma cell dyscrasia after auto-SCT, including one patient with a previous CR, three with a VGPR, two with a PR and one patient who did not have any response. None of the eight patients with a CR before auto-SCT has progressed, whereas eight of the patients who had not achieved a CR prior to auto-SCT have done so ( $P=0.13$ ). Using univariate Cox regression prognostic baseline characteristics, such as type of hospital (high vs. low number of included patients), eGFR ( $>30$  and  $<50$  vs.  $\geq 50$  mL/min/1.73 m<sup>2</sup>, NYHA class (I vs. II), NT-proBNP (as a continuous variable), plasma cell infiltration ( $<10\%$  vs.  $\geq 10\%$ ), dFLC  $<180$  mg/L vs.  $\geq 180$  mg/L, number of organs involved ( $\leq 2$  vs.  $>2$ ), Mayo stage, nervous system involvement and cardiac involvement were tested but none of these variables was statistically related to OS.

### Adverse events and mortality

Adverse events were commonly seen during induction treatment in all patients. The most frequent adverse events seen during induction treatment are summarized in Table 3. The most commonly experienced adverse events were neurotoxicity, gastrointestinal symptoms, infections and cardiac disorders. Although dizziness, orthostatic hypotension and syncope may also have cardiac origins, all these events were grouped together as autonomic neuropathic events if no cardiac cause, such as arrhythmias or deterioration in ejection fraction, was detected. In total, 10% of patients experienced autonomic neuropathy and 34% had sensory neuropathy related

to bortezomib. Interestingly, patients with nervous system involvement at the start of therapy did not require more dose adjustments for bortezomib compared to patients without nervous system involvement. No engraftment syndrome was seen after auto-SCT.

Overall, 47 serious adverse events were reported in 29 patients, 34 during induction treatment, three during stem cell mobilization and ten following 30 days after HDM and auto-SCT. The serious adverse events were mostly due to hospitalization (81%) and 28 were considered related to the treatment. Twenty-nine serious adverse events resolved completely, the others were ongoing. Two patients died during the study treatment phase. One patient had a sudden cardiac death during the first induction cycle, probably related to the cardiac amyloidosis, and one patient died due to hepato-renal syndrome after receiving four cycles of induction treatment. There were no cases of transplant-related mortality.

### Discussion

The aim of the current prospective, multicenter study was to investigate whether a more effective induction regimen before HDM and auto-SCT could lead to better outcomes in newly diagnosed AL amyloidosis patients. Bortezomib is considered the first drug of choice both because of the high response rates that it induces and the fact that the responses tend to occur rapidly.<sup>19</sup> We therefore hypothesized that using a two-step approach with effective induction, starting immediately after diagnosing and staging the AL amyloidosis, would not only improve response rates after auto-SCT but would also rescue more patients from amyloidosis-related organ damage.

The ORR of 80%, with 20% CR, 38% VGPR and 22% PR rates achieved after induction treatment, is indeed comparable to that reported previously by Reece *et al.* in relapsed AL amyloidosis patients (ORR 66.7%).<sup>13</sup> In their study a median of six cycles of bi-weekly bortezomib was given compared to the four cycles of bi-weekly bortezomib in the current study. In retrospective analyses high response rates up to 80% have been reported in both relapsed and newly diagnosed patients.<sup>11,12</sup> We confirm a rapid time to response with median times to first response of 28 days and to best response of 67 days.

Because of these fast and deep responses we expected

**Table 3.** Percentages of the most common treatment-related adverse events of bortezomib-dexamethasone induction treatment.

Adverse event	Grade 1	Grade 2	Grade 3	Grade 4	Grade 5	Total
Nervous system, total	12	24	12	2	-	50
- sensory PNP	12	14	6	2	-	34
- autonomic (syncope, dizziness, orthostatic hypotension)	-	6	4	-	-	10
- motor	-	-	2	-	-	4
- neuropathic pain	-	4	-	-	-	4
Gastrointestinal (constipation, diarrhea, nausea, vomiting)	na	30	10	4	-	44
Infections	na	20	10	-	-	30
Cardiac	na	12	12	2	2	28
Metabolic/nutrition	na	18	6	-	-	24
Fatigue	na	10	2	-	-	12

PNP: polyneuropathy, na: not assessed.

that a higher proportion of patients would be able to proceed to HDM and auto-SCT. However, the discontinuation rate of 30% in the current study was similar to the 33% observed in the previous HOVON 41 study in which VAD induction therapy was given.<sup>8</sup> The discontinuation rate was substantially higher than those in two other prospective, single-center studies in which bortezomib-dexamethasone induction was given prior to HDM and auto-SCT (0% and 14%).<sup>20,21</sup> These differences could be explained by different treatment designs; for example, in the studies by Sanchorawala *et al.* and Huang *et al.*, only two cycles of bortezomib and dexamethasone induction were given, instead of four. Perhaps more importantly, these were single-center studies in large, experienced hospitals, while the HOVON 104 trial was performed in 16 hospitals, which enrolled between one and eight patients per site which may impair the quality of care. We therefore think that our prospective data may better represent the real-life outcome of patients following first-line AL amyloidosis treatment. Although the discontinuation rate could not be assessed in other retrospective studies because only transplanted patients were included, these studies do suggest that induction regimens can be beneficial in patients by inducing deeper hematologic responses and better OS.<sup>9,10</sup>

The reasons for 15 patients not proceeding to HDM and auto-SCT were mostly non-eligibility according to protocol, generally caused by symptomatic effusions and poor Performance Status. Some patients had bortezomib-related toxicity and in four patients the physician decided that the patient should not proceed to auto-SCT because of organ progression. The other toxicities seen during induction treatment are summarized in Table 2. These toxicities are comparable to those reported by Reece *et al.*, and most involved the gastrointestinal tract, heart, and nervous system or were infections.<sup>13</sup> Although 78% of patients received four cycles of bortezomib-dexamethasone, half of the patients needed dose reductions of bortezomib and 44% needed reductions of dexamethasone. Due to the multiple organ dysfunctions typically seen in AL amyloidosis, these patients do not tolerate the same chemotherapy schedules as MM patients do. This also seems to hold true for the “fittest” patients who appeared to be eligible for auto-SCT at diagnosis. Encouraging data from retrospective analyses illustrate that other bortezomib-based regimens with reduced doses of bortezomib to 1.0 m/m<sup>2</sup> bi-weekly or 1.5 mg/m<sup>2</sup> once weekly, combined with dexamethasone and cyclophosphamide once weekly, could maintain the high response rates but data on toxicity are limited.<sup>22,23</sup> Once weekly dosing of bortezomib could therefore be the preferred schedule in AL amyloidosis patients.

Using flow cytometry analysis at diagnosis we identified a negative association between aPC/BMPC  $\geq 95\%$  and PFS. In addition, we found that patients with aPC/BMPC  $\geq 95\%$  had a lower probability of proceeding to auto-SCT; however, due to our small sample size of 26 patients this was not statistically significant. A high ratio of clonal plasma cells may reflect a more aggressive plasma cell clone in the bone marrow and its prognostic value has been determined in patients with monoclonal gammopathy of undetermined significance and smoldering MM.<sup>18</sup> In patients with AL amyloidosis it has been demonstrated that the persistence of 5% or more normal plasma cells at diagnosis was related to OS, but due to the

shorter follow-up and excellent survival in the current study, this association could not be confirmed.<sup>24</sup> The small sample size of the current study could perhaps be the reason that we could not confirm that other baseline characteristics, such as  $\geq 10\%$  plasma cells or a dFLC  $\geq 180$  mg/L, were negatively associated with survival.

There was no transplant-related mortality among the 35 patients who did receive HDM and auto-SCT and the patients had an excellent outcome. This is remarkable, because a previous prospective, multicenter study performed by Jaccard *et al.* reported a high mortality rate of 24% related to the auto-SCT procedure. This study, like ours, was also conducted in less experienced centers.<sup>25</sup> It could be speculated that the induction treatment before HDM and auto-SCT functions as a selection mechanism because only patients who are able to tolerate chemotherapy proceed to high-dose treatment. Indeed, more patients who received the full doses of the induction regimen without dose adjustments proceeded to auto-SCT. A randomized trial is needed to investigate the role of induction therapy before auto-SCT. Interestingly, our study demonstrates that HDM with auto-SCT is also possible for some patients with the highest cardiac Mayo risk score of III, which was present in 34% of our study population. These patients did not experience more toxicity than the other risk groups. However since the start of this study new prognostic cardiac scoring systems have been published which may improve the selection of patients suitable for HDM and auto-SCT.<sup>26,27</sup>

The hematologic responses improved to 86% at 6 months after auto-SCT. In particular, the CR rate increased steadily after auto-SCT. Since the quality of response in AL amyloidosis patients is closely related to survival this is a very important observation. The hematologic responses after auto-SCT are less than those reported in the two other prospective, single-center trials but are better than those reported in larger retrospective cohorts.<sup>7,20,21,28,29</sup> However, due to the high discontinuation rate before auto-SCT the primary endpoint of the study, an improvement, in intention-to-treat analysis, of the CR rate from 30% to 50% was not achieved.

Organ responses were already detected after induction therapy and the rates were 24%, 24% and 23% for the kidney, heart and liver, respectively. The new renal response criteria set was also prospectively evaluated and was 27% after induction treatment.<sup>16</sup> In total, six patients developed kidney failure, defined as an eGFR  $< 30$  mL/min/1.73 m<sup>2</sup>: two of them had renal stage I at diagnosis, two had stage II and two had stage III. After auto-SCT organ response rates continued to improve to 60%-80% (Figure 3) which are comparable to those after auto-SCT in previous reports.<sup>29</sup>

In conclusion, although the primary endpoint of the study was not met, in this first, multicenter, prospective trial with twice-weekly bortezomib, combined with dexamethasone treatment, we documented a high hematologic response rate of 80% in patients with newly diagnosed AL amyloidosis. However, these responses cannot prevent amyloidosis-related organ failure and the treatment-induced NCI-CTCAE grade 2 and higher gastrointestinal, cardiac, metabolic and neurotoxicity in more than 70% of patients, leading to a high discontinuation rate of 30% before auto-SCT. Possibly due to the unintended selection of induction treatment prior to HDM and auto-SCT, the transplants were performed without

any mortality and improved the CR rate from 20% to 46% at 6 months after auto-SCT.

### Acknowledgments

The authors would like to thank all participating patients and study centers. The authors also thank the local data managers

for study coordination and collecting patients' data, in particular the study team at the HOVON Data Center, Klaartje Nijssen and Marianne Gawlik. This investigator-sponsored trial was financially supported by the Dutch Cancer Society (KWF UU-2010-4884) and Janssen Cilag which provided the drug bortezomib, free of charge.

### References

- Wechalekar AD, Gillmore JD, Hawkins PN. Systemic amyloidosis. *Lancet*. 2016;387(10038):2641-2654.
- Palladini G, Dispenzieri A, Gertz MA, et al. New criteria for response to treatment in immunoglobulin light chain amyloidosis based on free light chain measurement and cardiac biomarkers: impact on survival outcomes. *J Clin Oncol*. 2012;30(36):4541-4549.
- Gertz MA, Lacy MQ, Dispenzieri A, et al. Effect of hematologic response on outcome of patients undergoing transplantation for primary amyloidosis: importance of achieving a complete response. *Haematologica*. 2007;92(10):1415-1418.
- Merlini G, Wechalekar AD, Palladini G. Systemic light chain amyloidosis: an update for treating physicians. *Blood*. 2013;121(26):5124-5130.
- Gertz MA, Lacy MQ, Dispenzieri A, et al. Refinement in patient selection to reduce treatment-related mortality from autologous stem cell transplantation in amyloidosis. *Bone Marrow Transplant*. 2013;48(4):557-561.
- Sanchorawala V, Sun F, Quillen K, Sloan JM, Berk JL, Seldin DC. Long-term outcome of patients with AL amyloidosis treated with high-dose melphalan and stem cell transplantation: 20-year experience. *Blood*. 2015;126(20):2345-2347.
- D'Souza A, Dispenzieri A, Wirk B, et al. Improved outcomes after autologous hematopoietic cell transplantation for light chain amyloidosis: a center for international blood and marrow transplant research study. *J Clin Oncol*. 2015;33(32):3741-3749.
- Hazenbergh BP, Croockewit A, van der Holt B, et al. Extended follow up of high-dose melphalan and autologous stem cell transplantation after vincristine, doxorubicin, dexamethasone induction in amyloid light chain amyloidosis of the prospective phase II HOVON-41 study by the Dutch-Belgian Co-operative Trial Group for Hematology Oncology. *Haematologica*. 2015;100(5):677-682.
- Hwa YL, Kumar SK, Gertz MA, et al. Induction therapy pre-autologous stem cell transplantation in immunoglobulin light chain amyloidosis: a retrospective evaluation. *Am J Hematol*. 2016;91(10):984-988.
- Afrough A, Saliba RM, Hamdi A, et al. Impact of induction therapy on the outcome of immunoglobulin light chain amyloidosis after autologous hematopoietic stem cell transplantation. *Biol Blood Marrow Transplant*. 2018;24(11):2197-2203.
- Wechalekar AD, Lachmann HJ, Offer M, Hawkins PN, Gillmore JD. Efficacy of bortezomib in systemic AL amyloidosis with relapsed/refractory clonal disease. *Haematologica*. 2008;93(2):295-298.
- Kastritis E, Wechalekar AD, Dimopoulos MA, et al. Bortezomib with or without dexamethasone in primary systemic (light chain) amyloidosis. *J Clin Oncol*. 2010;28(6):1031-1037.
- Reece DE, Hegenbart U, Sanchorawala V, et al. Efficacy and safety of once-weekly and twice-weekly bortezomib in patients with relapsed systemic AL amyloidosis: results of a phase 1/2 study. *Blood*. 2011;118(4):865-873.
- Gertz MA, Comenzo R, Falk RH, et al. Definition of organ involvement and treatment response in immunoglobulin light chain amyloidosis (AL): a consensus opinion from the 10th International Symposium on Amyloid and Amyloidosis, Tours, France, 18-22 April 2004. *Am J Hematol*. 2005;79(4):319-328.
- Comenzo RL, Reece D, Palladini G, et al. Consensus guidelines for the conduct and reporting of clinical trials in systemic light-chain amyloidosis. *Leukemia*. 2012;26(11):2317-2325.
- Palladini G, Hegenbart U, Milani P, et al. A staging system for renal outcome and early markers of renal response to chemotherapy in AL amyloidosis. *Blood*. 2014;124(15):2325-2332.
- Dispenzieri A, Gertz MA, Kyle RA, et al. Prognostication of survival using cardiac troponins and N-terminal pro-brain natriuretic peptide in patients with primary systemic amyloidosis undergoing peripheral blood stem cell transplantation. *Blood*. 2004;104(6):1881-1887.
- Perez-Persona E, Vidriales MB, Mateo G, et al. New criteria to identify risk of progression in monoclonal gammopathy of uncertain significance and smoldering multiple myeloma based on multiparameter flow cytometry analysis of bone marrow plasma cells. *Blood*. 2007;110(7):2586-2592.
- Palladini G, Merlini G. What is new in diagnosis and management of light chain amyloidosis? *Blood*. 2016;128(2):159-168.
- Huang X, Wang Q, Chen W, et al. Induction therapy with bortezomib and dexamethasone followed by autologous stem cell transplantation versus autologous stem cell transplantation alone in the treatment of renal AL amyloidosis: a randomized controlled trial. *BMC Med*. 2014;12:2.
- Sanchorawala V, Brauneis D, Shelton AC, et al. Induction therapy with bortezomib followed by bortezomib-high dose melphalan and stem cell transplantation for light chain amyloidosis: results of a prospective clinical trial. *Biol Blood Marrow Transplant*. 2015;21(8):1445-1451.
- Mikhael JR, Schuster SR, Jimenez-Zepeda VH, et al. Cyclophosphamide-bortezomib-dexamethasone (CyBorD) produces rapid and complete hematologic response in patients with AL amyloidosis. *Blood*. 2012;119(19):4391-4394.
- Venner CP, Lane T, Foard D, et al. Cyclophosphamide, bortezomib, and dexamethasone therapy in AL amyloidosis is associated with high clonal response rates and prolonged progression-free survival. *Blood*. 2012;119(19):4387-4390.
- Paiva B, Vidriales MB, Perez JJ, et al. The clinical utility and prognostic value of multiparameter flow cytometry immunophenotyping in light-chain amyloidosis. *Blood*. 2011;117(13):3613-3616.
- Jaccard A, Moreau P, Leblond V, et al. High-dose melphalan versus melphalan plus dexamethasone for AL amyloidosis. *N Engl J Med*. 2007;357(11):1083-1093.
- Kumar S, Dispenzieri A, Lacy MQ, et al. Revised prognostic staging system for light chain amyloidosis incorporating cardiac biomarkers and serum free light chain measurements. *J Clin Oncol*. 2012;30(9):989-995.
- Wechalekar AD, Schonland SO, Kastritis E, et al. A European collaborative study of treatment outcomes in 346 patients with cardiac stage III AL amyloidosis. *Blood*. 2013;121(17):3420-3427.
- Madan S, Kumar SK, Dispenzieri A, et al. High-dose melphalan and peripheral blood stem cell transplantation for light-chain amyloidosis with cardiac involvement. *Blood*. 2012;119(5):1117-1122.
- Cibeira MT, Sanchorawala V, Seldin DC, et al. Outcome of AL amyloidosis after high-dose melphalan and autologous stem cell transplantation: long-term results in a series of 421 patients. *Blood*. 2011;118(16):4346-4352.

# Long-term treatment with romiplostim and treatment-free platelet responses in children with chronic immune thrombocytopenia



Michael D. Tarantino,<sup>1</sup> James B. Bussel,<sup>2</sup> Victor S. Blanchette,<sup>3</sup> Donald Beam,<sup>4</sup> John Roy,<sup>5</sup> Jenny Despotovic,<sup>6</sup> Ashok Raj,<sup>7</sup> Nancy Carpenter,<sup>8</sup> Bhakti Mehta,<sup>9</sup> and Melissa Eisen<sup>9</sup>

<sup>1</sup>The Bleeding and Clotting Disorders Institute, University of Illinois College of Medicine-Peoria, Peoria, IL, USA; <sup>2</sup>Department of Pediatrics, Division of Hematology, Weill Cornell Medicine, New York, NY, USA; <sup>3</sup>Department of Pediatrics, University of Toronto, Division of Hematology/Oncology, The Hospital for Sick Children, Toronto, Ontario, Canada; <sup>4</sup>Cook Children's Medical Center, Fort Worth, TX, USA; <sup>5</sup>Children's Health Queensland and Pathology Queensland, South Brisbane, Queensland, Australia and The University of Queensland, Saint Lucia, Queensland, Australia; <sup>6</sup>Texas Children's Hematology Center, Houston, TX, USA; <sup>7</sup>Pediatric Cancer and Blood Disorders Clinic, Louisville, KY, USA; <sup>8</sup>Amgen Ltd., Uxbridge, Middlesex, UK and <sup>9</sup>Amgen Inc., Thousand Oaks, CA, USA

**Haematologica** 2019  
Volume 104(11):2283-2291

## ABSTRACT

Children with immune thrombocytopenia for  $\geq 6$  months completing a romiplostim study received weekly subcutaneous romiplostim (1-10  $\mu\text{g}/\text{kg}$  targeting platelet counts of 50-200 $\times 10^9/\text{L}$ ) in this extension to examine romiplostim's long-term safety and efficacy. Sixty-five children received romiplostim for a median of 2.6 years (range: 0.1-7.0 years). Median baseline age was 11 years (range: 3-18 years) and platelet count was 28 $\times 10^9/\text{L}$  (range: 2-458 $\times 10^9/\text{L}$ ). No patient discontinued treatment for an adverse event. Median average weekly dose was 4.8  $\mu\text{g}/\text{kg}$  (range: 0.1-10  $\mu\text{g}/\text{kg}$ ); median platelet counts remained  $>50\times 10^9/\text{L}$ , starting at week 2. Nearly all patients (94%) had  $\geq 1$  platelet response ( $\geq 50\times 10^9/\text{L}$ , no rescue medication in the previous 4 weeks), 72% had responded at  $\geq 75\%$  of visits, and 58% had responded at  $\geq 90\%$  of visits. Treatment-free response (platelets  $\geq 50\times 10^9/\text{L}$   $\geq 24$  weeks without immune thrombocytopenia treatment) was seen in 15 of 65 patients while withholding romiplostim doses. At onset of treatment-free response, the nine girls and six boys had a median immune thrombocytopenia duration of four years (range: 1-12 years) and had received romiplostim for two years (range: 1-6 years). At last observation, treatment-free responses lasted for a median of one year (range: 0.4-2.1 years), with 14 of 15 patients still in treatment-free response. Younger age at first dose and platelet count  $>200\times 10^9/\text{L}$  in the first four weeks were associated with treatment-free responses. In this 7-year open-label extension, three-quarters of the patients responded  $\geq 75\%$  of the time, and romiplostim was well tolerated, with no substantial treatment-related adverse events. Importantly, 23% of children maintained treatment-free platelet responses while withholding romiplostim and all other immune thrombocytopenia medications for  $\geq 6$  months. (Registered at *clinicaltrials.gov* identifier: 01071954)

## Introduction

Chronic immune thrombocytopenia (ITP) in children is an autoimmune disorder characterized by increased platelet destruction and suboptimal platelet production.<sup>1</sup> Newly diagnosed and persistent ITP in children have high rates of spontaneous remission; only a small minority develop clinically severe chronic disease.<sup>2</sup> However, these children often have very low platelet counts that are very difficult to treat, have an ongoing risk of intracranial hemorrhage and other bleeding, and have an impaired quality of life.<sup>3,4</sup> There are few data on long-term improvement

## Correspondence:

MICHAEL D. TARANTINO  
mtarantino@ilbcdi.org

Received: July 20, 2018.

Accepted: March 6, 2019.

Pre-published: March 7, 2019.

doi:10.3324/haematol.2018.202283

Check the online version for the most updated information on this article, online supplements, and information on authorship & disclosures: [www.haematologica.org/content/104/11/2283](http://www.haematologica.org/content/104/11/2283)

©2019 Ferrata Storti Foundation

Material published in *Haematologica* is covered by copyright. All rights are reserved to the Ferrata Storti Foundation. Use of published material is allowed under the following terms and conditions:

<https://creativecommons.org/licenses/by-nc/4.0/legalcode>. Copies of published material are allowed for personal or internal use. Sharing published material for non-commercial purposes is subject to the following conditions: <https://creativecommons.org/licenses/by-nc/4.0/legalcode>, sect. 3. Reproducing and sharing published material for commercial purposes is not allowed without permission in writing from the publisher.



beyond two years of disease,<sup>5,6</sup> and all major centers are familiar with patients with very long-term (i.e. of many years' duration) refractory chronic ITP for whom they have no good treatment options.

Thrombopoietin (TPO) receptor agonists are an important second-line option in children with chronic ITP. The overall efficacy, safety, and tolerability profile compares favorably to other treatment options, with the major concern being that treatment may need to be continued indefinitely. While there are two large randomized, placebo-controlled trials of eltrombopag in children with chronic ITP,<sup>7,8</sup> there are no long-term safety and efficacy data of eltrombopag in children with ITP. In phase I/II and III placebo-controlled studies in children with ITP for  $\geq 6$  months, the TPO receptor agonist romiplostim increased and maintained platelet counts in most patients.<sup>9,10</sup> Children completing the placebo-controlled romiplostim studies could enroll in the open-label long-term extension study reported here. An interim report described data for 22 patients in the phase I/II study, including 12 who entered this extension study.<sup>11</sup> This report includes final data from all 66 patients in the extension study, including 12 patients from the phase I/II study and 54 patients from the phase III study.

The objectives of this study were to describe the safety and efficacy of long-term use of romiplostim in children with ITP. End points included the occurrence of adverse events (AE), platelet responses, bleeding, reduced use of concurrent ITP medications, and a *post hoc* end point of treatment-free response, defined as maintaining platelet counts  $\geq 50 \times 10^9/L$  for at least six months with no ITP medications, including romiplostim. As this was not a predicted occurrence, there were no prospective immunological studies to explore markers of treatment-free response.

## Methods

Patients were recruited from 28 sites in the US, Canada, Spain, and Australia. The study ran from 30<sup>th</sup> December 2009 (first patient enrolled) to 12<sup>th</sup> January 2017 (last visit). Study guidelines for romiplostim dosing and possible reasons for withholding romiplostim doses are summarized in *Online Supplementary Figure S1*. Romiplostim was administered weekly, starting at 1  $\mu g/kg$  or continuing at the last dose from the previous study. The dose of romiplostim was adjusted to a maximum of 10  $\mu g/kg$  based on platelet count. If, in the opinion of the investigator, the patient maintained acceptable platelet counts without weekly dosing, romiplostim could be withheld until the platelet count fell to  $< 50 \times 10^9/L$ . Dose reduction by 1  $\mu g/kg$  was required for two consecutive weekly platelet counts  $> 200$  and  $< 400 \times 10^9/L$ . If any platelet count was  $\geq 400 \times 10^9/L$ , romiplostim was withheld until the platelet count was  $< 200 \times 10^9/L$ , then decreased by 1  $\mu g/kg$ . If the current dose was 1  $\mu g/kg$  and a dose reduction was required for elevated platelet counts, then romiplostim was withheld until platelet counts fell to  $< 50 \times 10^9/L$ , when it was restarted at a dose of 1  $\mu g/kg$ . Patients could receive other ITP medications at a stable dose and schedule, which could be reduced or withheld for platelet counts  $\geq 50 \times 10^9/L$ . Patients could receive rescue medications [intravenous immunoglobulin (IVIg), anti-D, platelet transfusions, corticosteroids, or antifibrinolytics] for platelet counts  $< 10 \times 10^9/L$ , for bleeding/wet purpura, or per investigator (e.g. pre-procedure).

Eligible patients had completed a placebo-controlled romiplostim ITP study,<sup>9,10</sup> had ITP for  $\geq 6$  months (before initial study),

and were  $\leq 18$  years of age; those turning 18 after enrollment were allowed to stay on study. The studies were conducted in compliance with all regulatory obligations and institutional review board and informed consent regulations at each investigational site and the Declaration of Helsinki. All patients/legal representatives provided written informed consent/assent.

Assessments included platelet count, blood smear, and review of AE (including bleeding) every four weeks; and physical examination, vital signs, complete blood count, and serum chemistries every 12 weeks. Samples for binding antibodies against romiplostim and TPO were tested yearly and at study end; positive samples were tested for neutralizing antibodies. Bone marrow aspirates/biopsies were not required but could be performed at the investigator's discretion.

Efficacy outcomes included platelet counts and platelet response ( $\geq 50 \times 10^9/L$ , no rescue medication use in the previous 4 weeks). Missing data for platelet counts were imputed using the average of neighboring values within  $\pm 1$  week. Treatment-free response was defined *post hoc* as platelet counts  $\geq 50 \times 10^9/L$  in the absence of all ITP medications including romiplostim for  $\geq 24$  weeks.

Statistical analyses were descriptive. Categorical end points were summarized by the number and percentage of patients in each category. Continuous end points were summarized by number of patients, mean, standard deviation, median, and 25<sup>th</sup> percentile and 75<sup>th</sup> percentile, with minimum and maximum values. AE were also summarized as the number of events and rate per 100 patient-years of exposure. Proportional hazards models were used to evaluate factors correlating with time to treatment-free response; patients without treatment-free response were censored at their final platelet count. For the univariate model, each potential factor was considered alone (analogous to a log-rank test). If the assumption of proportional hazards was violated, non-parametric tests (Fisher exact test for categorical variables and Kruskal-Wallis test for continuous variables) were used. For multivariate models, a forward stepwise selection criterion was used with significance levels for entry and exit set at 0.05.

## Results

### Demographics and disposition

Sixty-six patients gave consent for this extension study; one withdrew before treatment and 65 received romiplostim. Fifteen patients had received placebo previously and this study was their first exposure to romiplostim; patients already receiving romiplostim could enroll without interruption of dosing. At baseline, patient median age was 11 years (range: 3-18 years), 56% (37 of 66) were female, and median platelet count was  $28 \times 10^9/L$  (range:  $2-458 \times 10^9/L$ ) (Table 1). Median ITP duration was 3.0 years (range: 1-13 years), past ITP treatments included IVIg, anti-D, corticosteroids, and rituximab, and 9% (6 of 66) had prior splenectomy (Table 2). There were no notable differences at baseline for patients achieving treatment-free response.

Investigators reported that 37 of 66 patients (56%) completed romiplostim treatment (Figure 1). Reasons for discontinuation of romiplostim treatment (28 of 66, 42%) included consent withdrawn (n=10), required other therapy (n=5), non-compliance (n=4), per protocol (n=3), administrative decision (n=2), AE (n=2), and other (n=2). AE were asthenia, headache, dehydration, and vomiting in one patient and anxiety in the other; investigators did not consider these AE to be treatment-related.

### Romiplostim exposure

Median romiplostim treatment duration was 2.6 years (range: 0.1-7.0 years) and total exposure to romiplostim was 182 patient-years. Median average weekly romiplostim dose (i.e. cumulative romiplostim dose divided by duration of treatment) was 4.8 µg/kg (range: 0.1-10 µg/kg). The mean maximum weekly romiplostim dose was 6.9 µg/kg and the median maximum weekly dose was 8.0 µg/kg. Twenty patients started on 1 µg/kg of romiplostim, including the 15 patients who previously received placebo and five patients with >24 weeks since the last dose of romiplostim. The median weekly dose was typically between 4 and 5 µg/kg during the first two years (Figure 2A). The smaller number of patients continuing romiplostim treatment for more than four years complicated median dose calculations at later visits. In a *post hoc* analysis, all 65 patients received their doses per protocol >90% of the time; 21 patients missed ≥1 dose as a result of non-compliance a total of 65 times.

### Safety

The most common AE were headache and contusion (Table 3). Fifty-four serious AE occurred in 19 patients (Online Supplementary Table S1). One patient had treatment-related concurrent serious AE of grade 4 thrombocytopenia, grade 3 epistaxis, and grade 2 anemia, using investigator-reported severity ratings from the Common Terminology Criteria for Adverse Events (CTCAE) version 3.0. Five patients with serious AE of low platelet counts had fluctuating platelet counts (Online Supplementary Figure S2). Bleeding AE occurred in 57 patients; only three of these AE were deemed treatment-related (injection site hemorrhage, injection site bruising, and epistaxis). The most frequent bleeding AE were contusion (51%, 33 of 65), epistaxis (49%, 32 of 65), and petechiae (31%, 20 of 65). There were no cases of intracranial hemorrhage; specific bleeding events included menorrhagia (3 of 65, 5%), hematuria (3 of 65, 5%), rectal hemorrhage (3 of 65, 5%), hematochezia (2 of 65, 3%), hemoptysis (2 of 65, 3%), anal hemorrhage (1 of 65, 2%), and hematemesis (1 of 65, 2%) (Figure 2B). There were seven patients with serious or

grade 3 AE of bleeding (Online Supplementary Table S2). For one patient, the investigator considered the serious AE of worsening epistaxis (and serious AE of anemia and thrombocytopenia) to be treatment-related; tests for the patient's anti-drug binding antibodies were all negative. No arterial or venous thromboembolic AE were reported. Of note, the contusion rate dropped from 239 to 92 per 100 patient-years when one patient who had 499 AE was excluded from the analysis (Table 3). That patient, a 7-year old boy at baseline, was in the study for 3.4 years and had several serious AE: six of decreased platelet count, and one each of headache, head injury, vomiting, leukopenia, hematoma, pharyngitis streptococcal, and gastroenteritis. His platelet counts ranged from 10 to 872x10<sup>9</sup>/L and his dose was increased to 7-10 µg/kg. Seventy percent of his reported AE were non-serious AE of contusion (271 events) or petechiae (78 events). Per the treating investigator, he was a very active child who played multiple sports.

Post-dosing antibodies were assayed annually in 60 patients; data covered >200 patient-years of exposure (including parent studies). One girl had anti-romiplostim neutralizing antibody detected upon leaving the study to receive other therapy; the neutralizing antibody was absent on retesting three and six months later. She received multiple additional therapies and was stable on mycophenolate mofetil. No patients developed anti-TPO neutralizing antibody.

Bone marrow biopsies were performed in two patients with additional cytopenias; both were found to have iron-deficiency anemia and no abnormal cellularity, fibrosis, or malignancy. The first was a 17-year old girl who underwent a bone marrow biopsy after two years on study to evaluate her persistent anemia. With regular supplemental iron intake and lighter menstrual bleeding, her anemia improved. The second bone marrow biopsy, performed after six weeks on study, was in an 11-year old girl who developed neutropenia and anemia; she received iron for

Table 1. Baseline demographics.

	All patients enrolled N=66	Patients with treatment-free response N=15
Female, n (%)	37 (56)	9 (60)
Race/ethnicity, n (%)		
White	40 (61)	10 (67)
African American	9 (14)	3 (20)
Hispanic/Latino	9 (14)	1 (7)
Asian	6 (9)	1 (7)
Other	2 (3)	0 (0)
Age, years, median (range)	11 (3-18)	8 (4-18)
Age group, years, n (%)		
≥1 to <6	12 (18)	2 (13)
≥6 to <12	25 (38)	8 (53)
≥12	29 (44)	5 (33)
Baseline platelet count, x10 <sup>9</sup> /L, median (range)	28 (2-458)*	14 (1-44)†

\*For extension study described in this paper (i.e. not parent studies); 19 of 21 patients with baseline platelet count >50x10<sup>9</sup>/L had previous romiplostim treatment; only one had rescue medication use right before baseline. †At start of parent study.

Table 2. Patient immune thrombocytopenia (ITP) medication history.

	All patients enrolled N=66 n (%)	Patients with treatment-free response N=15 n (%)
ITP duration, median (range), years	3.0 (1-13)	4 (1-12)
Number of prior ITP treatments		
1	7 (11)	2 (13)
2	17 (26)	4 (27)
3	15 (23)	3 (20)
>3	26 (39)	6 (40)
Prior splenectomy	6 (9)	0 (0)
Received specific therapies in the past		
IVIg	60 (91)	15 (100)
Corticosteroid	54 (82)	12 (80)
Anti-D antibody	24 (36)	5 (33)
Rituximab	24 (36)	5 (33)
Vincristine/vinblastine	4 (6)	0 (0)
Danazol	4 (6)	1 (7)
Azathioprine	4 (6)	0 (0)
Other*	26 (39)	5 (33)

IVIg: intravenous immunoglobulin. \*Other includes aminocaproic acid, cyclosporine, dapsone, mercaptopurine, mycophenolate mofetil, platelets, sirolimus, and tranexamic acid. Designation of platelet transfusion as a rescue medication was per investigator.

the anemia and had pre-existing intermittent neutropenia, which eventually resolved.

### Efficacy

Median platelet counts remained  $>50 \times 10^9/L$  from week 2 on and  $>100 \times 10^9/L$  from weeks 24 to 260 (Figure 2C). Nearly all patients (94%) had  $\geq 1$  platelet response (platelet counts  $\geq 50 \times 10^9/L$ , excluding counts  $\leq 4$  weeks after rescue medication). Most patients (72%) had a platelet response  $\geq 75\%$  of the time and over half (58%) had a platelet response  $\geq 90\%$  of the time. Fifty-nine patients (91%) or their caregivers self-administered romiplostim at least once (i.e. administered at home, not at the clinic). In a *post hoc* analysis, self-administration started at a median study week of 7 (1-162) for a total duration of 112 weeks (range: 3-362 weeks). After patients started self-administration, they remained on self-administration (i.e. they did not interrupt it to receive romiplostim in the clinic for  $\geq 4$  weeks) for a median of 92% (range: 8-100%) of the time. Most subjects (45 of 59, 76%) remained on self-administration to the last non-zero dose of romiplostim. Twenty-three of 65 patients (35%) received rescue medications (Online Supplementary Table S3); usage was highest in the first few months of the study (Online Supplementary Figure S3A). At baseline, five patients were taking other ITP medications: aminocaproic acid, prednisolone, prednisone, and tranexamic acid. The rate of ITP medication use decreased during the study (Online Supplementary Figure S3B).

### Treatment-free responses

Per the study dosing guidelines (Online Supplementary Figure S4), romiplostim doses were withheld if consecutive platelet counts were  $>200 \times 10^9/L$  but  $<400 \times 10^9/L$  and the current dose was  $1 \mu\text{g}/\text{kg}/\text{week}$ ; if the platelet count was  $\geq 400 \times 10^9/L$  at any dose of romiplostim; or if, in the investigator's opinion, the patient could maintain acceptable platelet counts of  $\geq 50 \times 10^9/L$  without weekly romiplostim treatment. Fifteen patients (23%) achieved a treatment-free response when romiplostim was withheld, and maintained platelet counts  $\geq 50 \times 10^9/L$  with no ITP medications for  $\geq 24$  weeks (Table 4). All 15 patients also maintained platelet counts  $>100 \times 10^9/L$  for  $\geq 24$  weeks and the median time having platelet counts  $>100 \times 10^9/L$  was 46 weeks (range: 25-109 weeks).

Platelet counts and romiplostim doses are shown in Online Supplementary Figure S4 for each patient with a treatment-free response. Among these patients, median platelet counts were  $14 (1-44) \times 10^9/L$  at baseline and  $299 \times 10^9/L$  (range:  $217-730 \times 10^9/L$ ) in the last few months before romiplostim was first withheld.

At the onset of treatment-free response (i.e. when romiplostim was first withheld), these nine girls and six boys had had ITP for a median of 4 years (range: 1-12 years) and had received romiplostim for two years (range: 1-6 years) (Figure 3A). Three were from the phase I/II study and 12 were from the phase III study. Eleven received romiplostim throughout and four received placebo in the phase III parent study. No patient with a treatment-free response

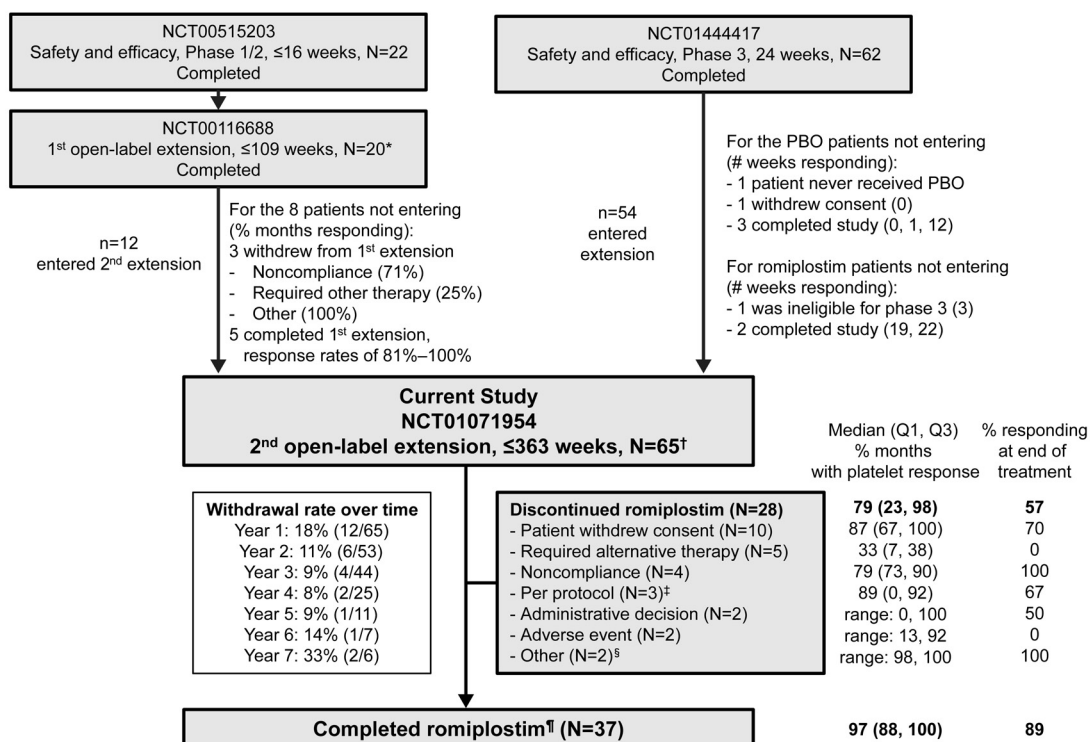


**Figure 1. Study flow and patient disposition.** Reasons for discontinuing romiplostim are provided. \*Of the 21 patients who entered the first extension, one withdrew consent before treatment. †Of the 66 patients who enrolled on the second extension, one withdrew consent before treatment. ‡Of these three patients, two had treatment-free response and one had platelet counts  $<30 \times 10^9/L$  despite ten weeks on  $10 \mu\text{g}/\text{kg}$ . §Other reasons were that the study ended and treatment-free response. ¶Received romiplostim until study end January 2017 (12 months after the last patient enrolled). #: number of; PBO: placebo; Q1, Q3: 25<sup>th</sup> and 75<sup>th</sup> percentiles.

had prior splenectomy; of those without treatment-free response, six had prior splenectomy (Table 2).

Treatment-free responses lasted for a median of one year (range: 0.4-2.1 year). Fourteen patients maintained a treatment-free response without restarting romiplostim by study end. The 15<sup>th</sup> patient, a 4-year old boy, achieved

a treatment-free response while withholding romiplostim in weeks 36 to 67; he received romiplostim again in weeks 68 to 96, then was off all ITP treatments again in weeks 97 to 99 per the dosing rules (he had consecutive platelet counts of  $397 \times 10^9/L$  and  $343 \times 10^9/L$ ).

In *post hoc* analyses, baseline characteristics and out-

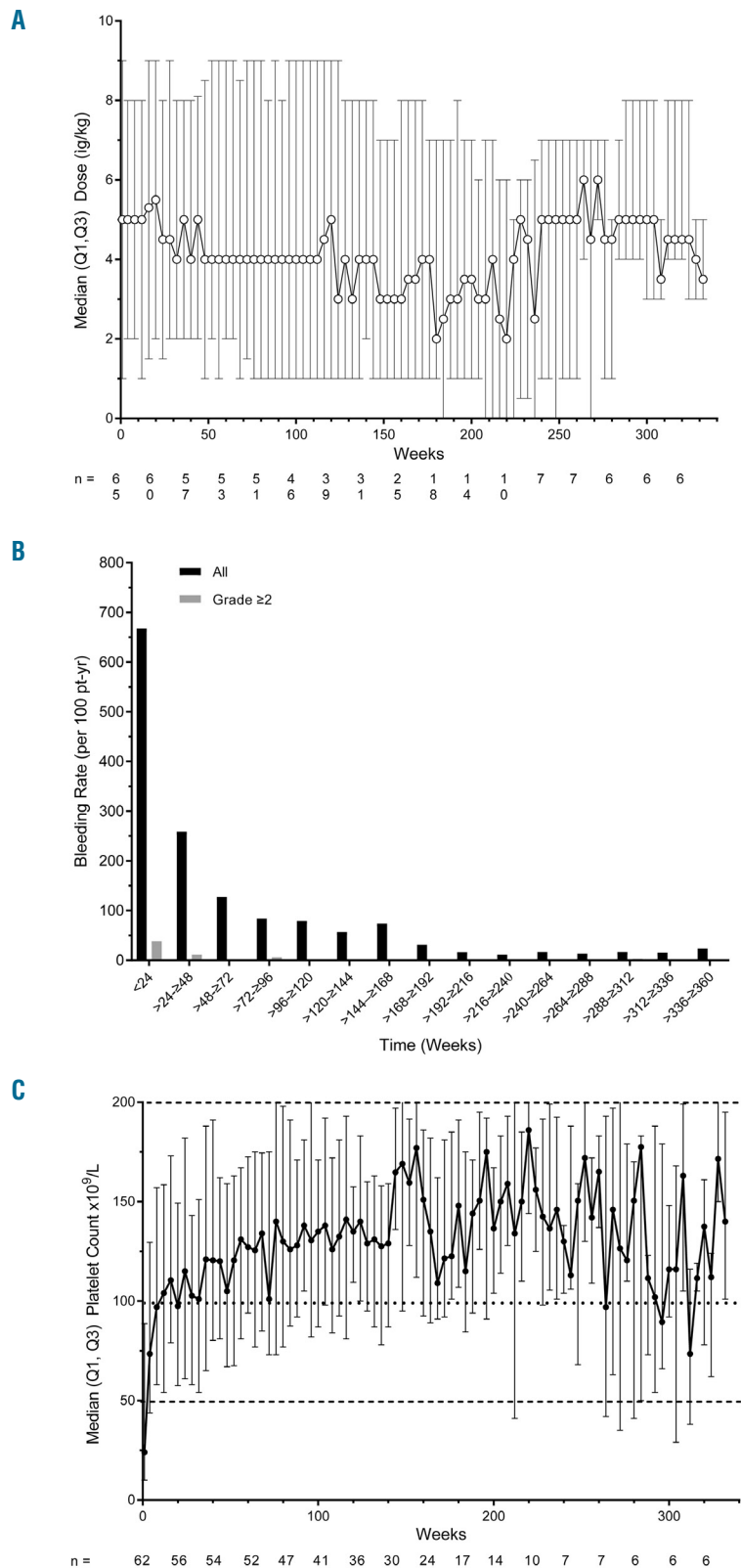


**Figure 2. Dose, bleeding adverse events, and platelet counts over time.** Shown are median dose (A), rate of bleeding adverse events per 100 patient-year (all and grade  $\geq 2$ ) (B), and median platelet counts (C) over time. (C) The area marked by the dotted lines indicates the target platelet count of  $50-200 \times 10^9/L$ . Patients received weekly subcutaneous romiplostim, starting with the same dose as the final dose in the parent study or  $1 \mu g/kg$  [if previously on placebo ( $n=15$ ) or  $>24$  weeks since the last dose ( $n=5$ )]. The dose was adjusted weekly by  $1 \mu g/kg$  from  $1-10 \mu g/kg$  to target platelet counts of  $50-200 \times 10^9/L$ . Bleeding was assessed per Common Terminology Criteria for Adverse Events version 3.0 grading of adverse events: 1, mild; 2, moderate; 3, severe; 4, life-threatening; 5, fatal. pt-yr: patient-years; Q1, Q3: 25<sup>th</sup> and 75<sup>th</sup> percentiles.

comes such as ITP duration, past ITP treatments, and platelet counts in the first four weeks on study were evaluated for their ability to predict treatment-free response. In the univariate model, younger age at diagnosis, younger age at first dose, platelets  $>200 \times 10^9/L$  in the first four weeks, and higher mean platelet count in the first four weeks were each associated with developing a treatment-free response (Table 5). In the multivariate model, age at first dose ( $P=0.0012$ ) and platelet counts  $>200 \times 10^9/L$  in the first four weeks ( $P=0.0035$ ) continued to correlate with treatment-free response (Figure 3B).

## Discussion

The data from up to seven years of treatment in this open-label extension study in children with ITP demonstrated that romiplostim was well tolerated and generally maintained its efficacy. There were no complications of thrombotic events, fatalities, or new safety concerns, despite 182 patient-years of exposure to romiplostim ( $>200$  patient-years including parent studies) in 65 patients, half of whom were 11 years of age or less at study baseline. Approximately one-third of patients had serious AE in this trial in which patients were on study for a median of 2.6 years, but only one patient had an episode of concurrent treatment-related serious AE: thrombocytopenia, epistaxis, and anemia. One patient developed neutralizing anti-romiplostim antibodies, discovered when she discontinued the study due to needing other treatments, but neither she nor any other patient developed neutralizing antibody to TPO. This finding in 1 of 60 children is consistent with data from adults treated with romiplostim for ITP. In an integrated database of romiplostim ITP trials, anti-romiplostim neutralizing antibodies were found in 4 of 1,046 adult patients with a total exposure of 1,832 patient-years.<sup>12</sup>

The most common reasons for discontinuation of study

treatment were withdrawal of consent ( $n=10$ ) and required alternative therapy ( $n=5$ ). Over 90% of patients had a peak platelet count of  $>50 \times 10^9/L$  without rescue medication at least once and approximately three-quarters of patients had  $\geq 75\%$  of their platelet counts  $>50 \times 10^9/L$ , suggesting a very high rate of efficacy of romiplostim in these children with chronic ITP with a median ITP duration of three years at the start of therapy. Furthermore, median platelet counts were maintained in the desired range ( $50\text{--}200 \times 10^9/L$ ) from week 2 on and at  $>100 \times 10^9/L$  from weeks 24 to 260 despite a median dose of 4–5  $\mu\text{g}/\text{kg}$ , the same median dose as in the phase III study.<sup>10</sup>

Overall, 15 of 65 children (23%) achieved a treatment-free response, which was defined as platelet counts of  $\geq 50 \times 10^9/L$  for at least 24 weeks while withholding romi-

**Table 3.** Adverse events.

Category AE	Patient incidence All treated patients N=65 n (%)	Duration-adjusted events per 100 pt-yr	
		All treated patients 182 pt-yr # (rate)	Excluding 1 patient with 499 AE* 178 pt-yr # (rate)
<b>Most common AE</b>			
Headache	38 (59)	151 (83)	126 (71)
Contusion	33 (51)	435 (239)	164 (92)
Epistaxis	32 (49)	103 (57)	98 (55)
Upper respiratory tract infection	32 (49)	101 (56)	101 (57)
<b>Most common serious AE<sup>†</sup></b>			
Any	19 (29)	54 (30)	41 (23)
Thrombocytopenia	4 (6)	6 (3)	6 (3)
Pyrexia	3 (5)	3 (2)	3 (2)
Epistaxis	2 (3)	2 (1)	2 (1)
Headache	2 (3)	2 (1)	1 (0.6)
Vomiting	2 (3)	2 (1)	1 (0.6)

AE: adverse event; pt-yr: patient-years. \*See text for a description of the AE in this patient. †A full list of serious AE is provided in *Online Supplementary Table S1*.

**Table 4.** Patients achieving treatment-free response (defined as a treatment-free period of  $\geq 24$  weeks with platelet counts  $\geq 50 \times 10^9/L$ ).

Parent study	Phase I/II			Phase III														
	1	2	3	4	5	6	7	8	9	10	11	12	13	14	15			
Patient number	1	2	3	4	5	6	7	8	9	10	11	12	13	14	15			
Age at treatment-free response start, y	16	6	10	8	6	12	18	7	6	9	4	5	6	16	14			
Sex	F	M	M	F	F	F	F	M	M	F	M	F	F	M	F			
Race/ethnicity	W	B	W	W	W	W	W	W	B	A	W	B	H	W	W			
Parent study treatment	Rom	Rom	Rom	Rom	Rom	Rom	Pbo	Rom	Rom	Pbo	Pbo	Pbo	Rom	Rom	Rom			
Baseline platelet count, $\times 10^9/L^*$	12	5	9	18	7	44	15	26	28	28	25	1	11	4	14			
Number of past ITP therapies*	3	6	4	2	2	3	4	5	2	1	2	1	4	3	4			
ITP duration, years <sup>†</sup>	7	6	5	1	4	11	12	3	1	2	3	4	3	3	5			
Rituximab use, years <sup>†</sup>	4	5	5	–	–	–	–	–	–	–	–	–	2	–	5			
Romiplostim use, years <sup>†</sup>	7	6	5	2	3	5	4	3	3	2	2	2	3	1	3			
Maximum romiplostim dose, $\mu\text{g}/\text{kg}$	10	8	9	5	10	2	2	1	3	1	2	1	9	10	4			
ITP treatment-free response, year	1.1	2.1	1.1	1.6	1.0	0.8	0.9	1.7	2.1	1.1	0.6 <sup>‡</sup>	0.6	0.8	0.4 <sup>§</sup>	0.6			

Data are integrated over parent study and extension study. –: no rituximab use; A: Asian; B: black; F: female; H: Hispanic/Latino; ITP: immune thrombocytopenia; M: male; Pbo: placebo; Rom: romiplostim; W: white. \*At start of parent study. †Before treatment-free response. ‡Treatment-free response ended before study end. §This patient met treatment-free response criteria for 0.4 years on study and  $\geq 0.5$  years post-study.

plostim and all other ITP treatments. There were two parent studies for this long-term extension.<sup>9,10</sup> Treatment-free response rates were similar for children from the earlier phase I/II study (3 of 12, 25%) and the phase III study (12 of 54, 22%). The three patients entering treatment-free response from the earlier study had received romiplostim longer (5-7 years vs. 1-5 years), but their age, ITP duration, number of past ITP therapies, and other characteristics were not particularly different from the patients from the phase III study.

Which children were more likely to enter treatment-free response? In a *post hoc* multivariate analysis of this study, younger age at first dose and platelet count increasing to  $\geq 200 \times 10^9/L$  in the first four weeks were both independently associated with developing treatment-free response. However, this dataset may not have been large enough to detect additional factors that may also play a role in treatment-free response. Factors found in other studies to be predictive of spontaneous treatment-free response in children with ITP include higher platelet count at diagnosis ( $>60 \times 10^9/L$ ),<sup>6</sup> younger age,<sup>15-18</sup> recent onset ( $<2$  weeks) of bleeding symptoms,<sup>17,18</sup> decreased bleeding in the first six months,<sup>19</sup> higher bleeding grade at diagnosis,<sup>14</sup> and treatment with IVIg and corticosteroids at diagnosis.<sup>14</sup> Of note, these studies generally considered children with relatively newly diagnosed, persistent, and chronic ITP all together (as definitions changed over time),<sup>20</sup> whereas the treatment-free response in this study occurred in children who had chronic ITP for a median of three years.

The ongoing development of treatment-free response in children with chronic, difficult-to-treat ITP with continuing romiplostim treatment could be explained either by patients improving spontaneously years after their diagnosis of ITP, or by a sustained effect of romiplostim on ITP in certain patients. The correlation of treatment-free response with early very good response in the first four

weeks of romiplostim treatment suggests either that these patients were uniquely sensitive to romiplostim or possibly that they just had milder disease. Arguing against the latter hypothesis was the absence of other clinical factors related to treatment-free response (e.g. relatively few previous treatments, short duration of ITP). There is remarkably little published data describing children such as these (i.e. with chronic ITP and median ITP duration of 3 years). Further studies will be needed to distinguish between the long-term effects of romiplostim and the natural history of chronic ITP in childhood.

Definitions of response, remission, and sustained response can vary considerably. Here, we chose platelet counts  $\geq 50 \times 10^9/L$  for response and platelet counts  $\geq 50 \times 10^9/L$  for  $\geq 6$  months with no ITP medications for treatment-free response. Other studies have used different platelet thresholds for response and treatment-free periods, such as response per the International Working Group criteria,<sup>20</sup> in which thresholds of  $30 \times 10^9/L$  and  $100 \times 10^9/L$  were used for response and complete response, both in the absence of bleeding, or treatment-free periods of at least a year, as in a long-term rituximab study.<sup>21</sup> Nonetheless, six months of no treatment in this study, with treatment-free response in 15 patients and platelet counts mostly over  $100 \times 10^9/L$ , clearly defines a substantial change between the pre-romiplostim experience and on-study experience of these children.

Several studies have suggested pathways by which romiplostim could affect disease progression. These include, but are not limited to, induction of T-regulatory cells and alteration of FcγRs in favor of FcγRIIb, the inhibitory FcγR.<sup>22-26</sup> Overall, the lack of toxicity despite long-term treatment indicates that romiplostim does not overly impair patients' immunity to an extent that there is a predisposition to infections. To our knowledge, other than a few cases in a retrospective case review,<sup>27</sup> this is the

**Table 5. Univariate model for predictors of treatment-free response.**

Characteristic	Patients with treatment free response N=15	Patients without treatment free response N=50	HR	95% CI	P
Sex, female, n (%)	9 (60)	27 (54)	1.19	0.42, 3.41	0.74
Race, white, n (%)	10 (67)	30 (60)	1.05	0.36, 3.09	0.93
Age at first dose*	6.5 (4.0)	10.6 (4.0)	0.81	0.71, 0.93	0.0019
Age at ITP diagnosis*	4.8 (3.6)	7.5 (3.4)	0.83	0.70, 0.98	0.031
Baseline ITP duration	2.3 (2.4)	3.6 (2.7)	0.79	0.61, 1.03	0.080
Baseline platelet count†	16.5 (11.8)	15.9 (9.5)	1.09	0.66, 1.80	0.74
# Prior therapies	3.1 (1.4)	3.3 (1.9)	0.77	0.56, 1.07	0.12
Prior rituximab, n (%)	5 (33)	19 (38)	NA	NA	1.0
Splenectomized, n (%)	0 (0)	6 (12)	NA	NA	0.32
Dose at first response, μg/kg	3.1 (2.9)	4.1 (3.0)	0.87	0.71, 1.07	0.19
Platelet count $>200 \times 10^9/L$ in first 4 weeks, n (%)	4 (27)	3 (6)	5.48	1.63, 18.42	0.0059
Platelet counts in first 4 weeks†	128 (149)	57.5 (42.9)	1.09	1.04, 1.13	$<0.0001$
Grade $\geq 2$ bleeding in first 6 months, n (%)	4 (27)	8 (16)	1.44	0.46, 4.53	0.53
Rescue meds in first 6 months	4 (27)	20 (40)	0.65	0.21, 2.04	0.46

Data are mean (standard deviation) unless indicated otherwise. NA for HR and 95% CI when proportional hazards assumption in model was violated and model results are not reliable. P-value calculated using Fisher exact test (categorical variables) or Kruskal-Wallis test (continuous variables). #: number of; CI: confidence interval; HR: hazard ratio; ITP: immune thrombocytopenia; meds: medications; NA: not applicable. \*Per year of age. †Indicates per  $1 \times 10^9/L$ .

first such report of children entering treatment-free response after treatment with a TPO receptor agonist, although this has been observed in adults.<sup>28-30</sup>

Only 2 of 66 patients discontinued romiplostim due to AE. However, investigators reported that 42% (28 of 66) of patients stopped romiplostim treatment early. It is unknown how many of these patients changed to commercially available romiplostim to avoid the constraints of protocol-required study visits. The withdrawal rate is comparable to the romiplostim ITP extension study in adults (31% withdrawal rate in a 7-year study)<sup>31</sup> and the eltrombopag ITP extension study in adults (55% in an 8-year study).<sup>32</sup>

The lack of a control group in this study limits the interpretation of the results. However, even without a control group, the low number of treatment-related serious AE, lack of new types of AE, and the absence of bone marrow or thromboembolic findings are reassuring. The international nature of this study may have increased the degree of patient and previous treatment heterogeneity but at the

same time increased generalizability of the results. The requirement for regular clinic visits and platelet count measurements/dose modifications could have presented a deterrent both for patients to enter and to continue the study; dose modifications required weekly visits again for a short period. A number of children left the study without obvious explanation, suggesting that even when self-administration is an option, a few patients will discontinue treatment despite responding, and are not leaving due to AE or loss of treatment effect. There were no quality-of-life assessments, which could also have indicated how increased platelet counts and decreased use of other ITP medications, and also the requirements of the study itself, affected quality of life.

In conclusion, romiplostim was a highly successful maintenance therapy even in children with ITP  $\geq 6$  months' duration not responsive to other therapies, a majority of whom (62%) had received three or more past ITP treatments. Romiplostim treatment demonstrated consistent safety and efficacy over the course of this long-term study. Patients staying on study were able to

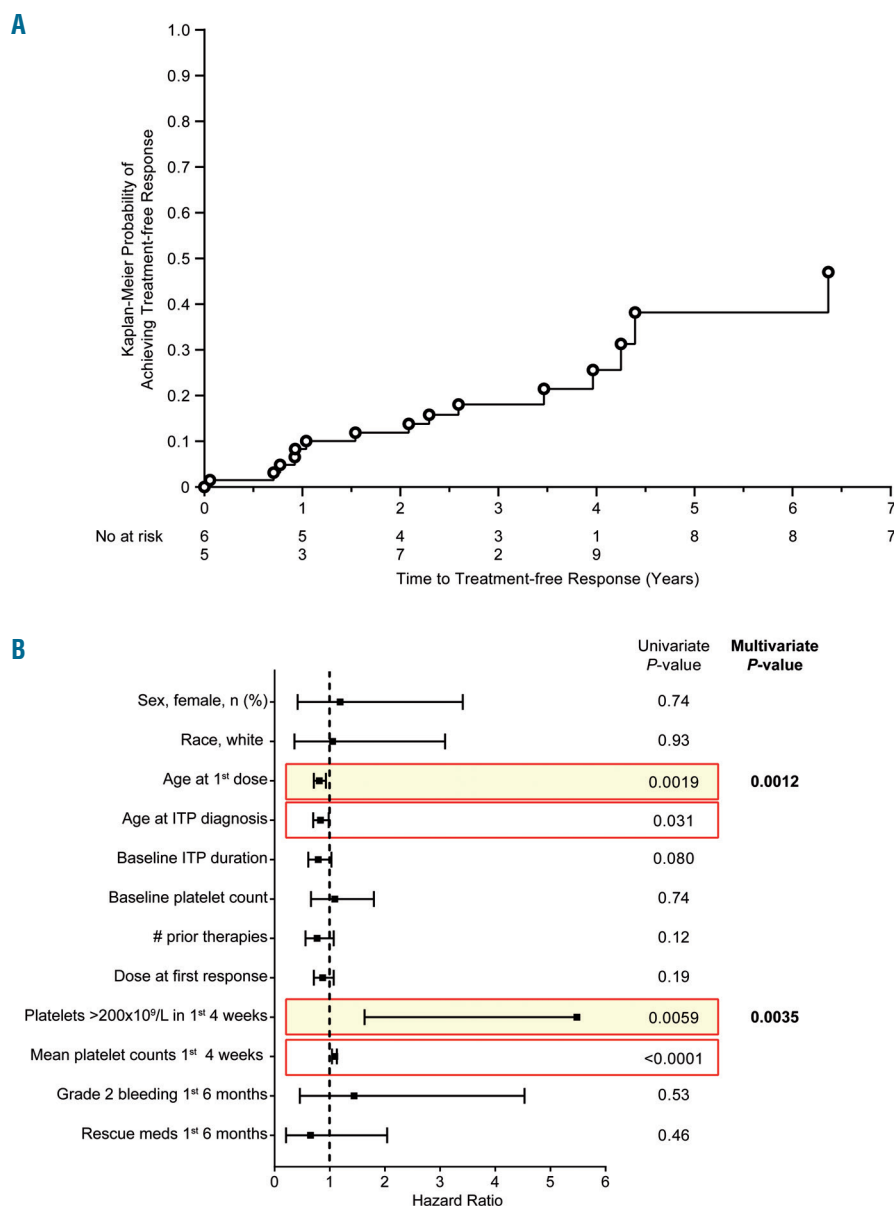


**Figure 3. Treatment-free response for at least six months.** Shown are time to onset (A) and modeling of characteristics associated with treatment-free response (B). If, in the opinion of the investigator, the patient maintained acceptable platelet counts without weekly dosing, romiplostim could be withheld until the platelet count fell to  $<50 \times 10^9/L$ . If the platelet count was  $>200$  to  $<400 \times 10^9/L$  for two consecutive weeks, the dose was reduced by  $1 \mu g/kg$  at the next scheduled dose. If the platelet count was  $\geq 400 \times 10^9/L$ , the dose was withheld and reduced on the next scheduled day of dosing when the platelet count was  $<200 \times 10^9/L$ . Red boxes indicate factors significant in the univariate analyses; yellow highlighting indicates those significant in the multivariate analyses. Hazard ratios for age at first dose and age at immune thrombocytopenia (ITP) diagnosis are per year of age, the hazard ratio for baseline platelet count is per  $1 \times 10^9/L$ , and the hazard ratio for mean platelet count in the first four weeks is per  $10 \times 10^9/L$ . Hazard ratios greater than 1 indicate an increased likelihood of developing treatment-free response. Note: the univariate models for prior rituximab use ( $P=1.0$ ) and prior splenectomy ( $P=0.32$ ) had non-proportional hazards, hence neither factor has a hazard ratio. #: number of; meds: medications.

maintain platelet counts in a hemostatic range, with median platelets  $>50\text{-}100 \times 10^9/\text{L}$ ; very few patients left the study because of AE or treatment failure. Development of treatment-free response in almost one-quarter of patients suggests that maintenance with romiplostim in children will not always be a “life-long treatment.” The continued, steady development of treatment-free response in patients treated for three or more years is encouraging as well. Additional studies in larger numbers of patients may further clarify some of the issues discussed in this study.

### Acknowledgments

*Susanna Mac, a medical writer from Amgen Inc., assisted the authors with drafting the manuscript and revised the manuscript based on extensive guidance from the authors. We would also like to thank all of the investigators, study staff, and patients who were part of this study. A full list of investigators is in Online Supplementary Table S4.*

### Funding

*This study (NCT01071954; Amgen #20090340) and all analyses were funded by Amgen Inc.*

## References

- Nugent D, McMillan R, Nichol JL, Slichter SJ. Pathogenesis of chronic immune thrombocytopenia: increased platelet destruction and/or decreased platelet production. *Br J Haematol.* 2009;146(6):585-596.
- Cooper N. A review of the management of childhood immune thrombocytopenia: how can we provide an evidence-based approach? *Br J Haematol.* 2014;165(6):756-767.
- George JN, Woolf SH, Raskob GE, et al. Idiopathic thrombocytopenic purpura: a practice guideline developed by explicit methods for the American Society of Hematology. *Blood.* 1996;88(1):3-40.
- Psaila B, Petrovic A, Page LK, Menell J, Schonholz M, Bussel JB. Intracranial hemorrhage (ICH) in children with immune thrombocytopenia (ITP): study of 40 cases. *Blood.* 2009;114(23):4777-4783.
- Schifferli A, Holbro A, Chitlur M, et al. A comparative prospective observational study of children and adults with immune thrombocytopenia: 2-year follow-up. *Am J Hematol.* 2018;93(6):751-759.
- Chotsampancharoen T, Sripornsawan P, Duangchoo S, Wongchanchailert M, McNeil E. Clinical outcome of childhood chronic immune thrombocytopenia: A 38-year experience from a single tertiary center in Thailand. *Pediatr Blood Cancer.* 2017;64(11):e26598.
- Bussel JB, de Miguel PG, Despotovic JM, et al. Eltrombopag for the treatment of children with persistent and chronic immune thrombocytopenia (PETIT): a randomised, multicentre, placebo-controlled study. *Lancet Haematol.* 2015;2(8):e315-325.
- Grainger JD, Locatelli F, Chotsampancharoen T, et al. Eltrombopag for children with chronic immune thrombocytopenia (PETIT2): a randomised, multicentre, placebo-controlled trial. *Lancet.* 2015;386(10004):1649-1658.
- Bussel JB, Buchanan GR, Nugent DJ, et al. A randomized, double-blind study of romiplostim to determine its safety and efficacy in children with immune thrombocytopenia. *Blood.* 2011;118(1):28-36.
- Tarantino MD, Bussel JB, Blanchette VS, et al. Romiplostim in children with immune thrombocytopenia: a phase 3, randomised, double-blind, placebo-controlled study. *Lancet.* 2016;388(10039):45-54.
- Bussel JB, Hsieh L, Buchanan GR, et al. Long-term use of the thrombopoietin-mimetic romiplostim in children with severe chronic immune thrombocytopenia (ITP). *Pediatr Blood Cancer.* 2015;62(2):208-213.
- Cines DB, Wasser J, Rodeghiero F, et al. Safety and efficacy of romiplostim in splenectomized and nonsplenectomized patients with primary immune thrombocytopenia. *Haematologica.* 2017;102(8):1342-1351.
- Bansal D, Bhamare TA, Trehan A, Ahluwalia J, Varma N, Marwaha RK. Outcome of chronic idiopathic thrombocytopenic purpura in children. *Pediatr Blood Cancer.* 2010;54(3):403-407.
- Bennett CM, Neunert C, Grace RF, et al. Predictors of remission in children with newly diagnosed immune thrombocytopenia: Data from the Intercontinental Cooperative ITP Study Group Registry II participants. *Pediatr Blood Cancer.* 2018;65(1):e26818.
- Evim MS, Baytan B, Gunes AM. Childhood immune thrombocytopenia: Long-term follow-up data evaluated by the criteria of the international working group on immune thrombocytopenic purpura. *Turk J Haematol.* 2014;31(1):32-39.
- Kim CY, Lee EH, Yoon HS. High remission rate of chronic immune thrombocytopenia in children: Result of 20-year follow-up. *Yonsei Med J.* 2016;57(1):127-131.
- Revel-Vilk S, Yacobovich J, Frank S, et al. Age and duration of bleeding symptoms at diagnosis best predict resolution of childhood immune thrombocytopenia at 3, 6, and 12 months. *J Pediatr.* 2013;163(5):1335-1339 e1331-1332.
- Rosthøj S, Rajantie J, Treutiger I, et al. Duration and morbidity of chronic immune thrombocytopenic purpura in children: five-year follow-up of a Nordic cohort. *Acta Paediatr.* 2012;101(7):761-766.
- Imbach P, Kühne T, Müller D, et al. Childhood ITP: 12 months follow-up data from the prospective registry I of the Intercontinental Childhood ITP Study Group (ICIS). *Pediatr Blood Cancer.* 2006;46(3):351-356.
- Rodeghiero F, Stasi R, Gernsheimer T, et al. Standardization of terminology, definitions and outcome criteria in immune thrombocytopenic purpura of adults and children: report from an international working group. *Blood.* 2009;113(11):2386-2393.
- Patel VL, Mahevas M, Lee SY, et al. Outcomes 5 years after response to rituximab therapy in children and adults with immune thrombocytopenia. *Blood.* 2012;119(25):5989-5995.
- Bao W, Bussel JB, Heck S, et al. Improved regulatory T-cell activity in patients with chronic immune thrombocytopenia treated with thrombopoietic agents. *Blood.* 2010;116(22):4639-4645.
- Chong BH. ITP: Tregs come to the rescue. *Blood.* 2010;116(22):4388-4390.
- Johansson U, Macey MG, Kenny D, Provan AB, Newland AC. The role of natural killer T (NKT) cells in immune thrombocytopenia: is strong in vitro NKT cell activity related to the development of remission? *Br J Haematol.* 2005;129(4):564-565.
- Li X, Zhong H, Bao W, et al. Defective regulatory B-cell compartment in patients with immune thrombocytopenia. *Blood.* 2012;120(16):3318-3325.
- Liu XG, Liu S, Feng Q, et al. Thrombopoietin receptor agonists shift the balance of Fcγ receptors toward inhibitory receptor IIb on monocytes in ITP. *Blood.* 2016;128(6):852-861.
- Grainger JD, Routledge DJM, Kruse A, et al. Thrombopoietin receptor agonists in paediatric ITP patients: Long term follow up data in 34 patients [abstract]. *Blood.* 2014;124(21):4206.
- Bussel JB, Wang X, Lopez A, Eisen M. Case study of remission in adults with immune thrombocytopenia following cessation of treatment with the thrombopoietin mimetic romiplostim. *Hematology.* 2016;21(4):257-262.
- Mahevas M, Fain O, Ebbro M, et al. The temporary use of thrombopoietin-receptor agonists may induce a prolonged remission in adult chronic immune thrombocytopenia. Results of a French observational study. *Br J Haematol.* 2014;165(6):865-869.
- Newland A, Godeau B, Priego V, et al. Remission and platelet responses with romiplostim in primary immune thrombocytopenia: final results from a phase 2 study. *Br J Haematol.* 2016;172(2):262-273.
- Kuter DJ, Bussel JB, Newland A, et al. Long-term treatment with romiplostim in patients with chronic immune thrombocytopenia: safety and efficacy. *Br J Haematol.* 2013;161(3):411-423.
- Wong RSM, Saleh MN, Khelif A, et al. Safety and efficacy of long-term treatment of chronic/persistent ITP with eltrombopag: final results of the EXTEND study. *Blood.* 2017;130(23):2527-2536.



## Differences and similarities in the effects of ibrutinib and acalabrutinib on platelet functions

Jennifer Series,<sup>1,2</sup> Cédric Garcia,<sup>2</sup> Marie Levade,<sup>1,2</sup> Julien Viaud,<sup>1</sup> Pierre Sié,<sup>1,2</sup> Loïc Ysebaert<sup>3,§</sup> and Bernard Payrastra<sup>1,2,§</sup>

<sup>1</sup>Inserm, U1048 and Université Toulouse 3, Toulouse Cedex 04; <sup>2</sup>Laboratoire d'Hématologie, CHU de Toulouse, Toulouse Cedex 04; <sup>3</sup>Service d'Hématologie IUCT-Oncopôle, Toulouse Cedex 09, France

<sup>§</sup>These authors share senior authorship.

Haematologica 2019  
Volume 104(11):2292-2299

### ABSTRACT

While efficient at treating B-cell malignancies, Bruton tyrosine kinase (BTK) inhibitors are consistently reported to increase the risk of bleeding. Analyzing platelet aggregation response to collagen in platelet-rich plasma allowed us to identify two groups in the healthy population characterized by low or high sensitivity to ibrutinib *in vitro*. Inhibition of drug efflux pumps induced a shift from ibrutinib low-sensitive platelets to high-sensitive ones. At a clinically relevant dose, acalabrutinib, a second-generation BTK inhibitor, did not affect maximal collagen-induced platelet aggregation in the ibrutinib low-sensitive group but did inhibit aggregation in a small fraction of the ibrutinib high-sensitive group. Consistently, acalabrutinib delayed aggregation, particularly in the ibrutinib high-sensitive group. In chronic lymphocytic leukemia patients, acalabrutinib inhibited maximal platelet aggregation only in the ibrutinib high-sensitive group. Acalabrutinib inhibited collagen-induced tyrosine-753 phosphorylation of phospholipase C $\gamma$ 2 in both groups, but, in contrast to ibrutinib, did not affect Src-family kinases. Acalabrutinib affected thrombus growth under flow only in the ibrutinib high-sensitive group and potentiated the effect of cyclooxygenase and P2Y<sub>12</sub> receptor blockers in both groups. Since the better profile of acalabrutinib was observed mainly in the ibrutinib low-sensitive group, replacement therapy in patients may not systematically reduce the risk of bleeding.

### Correspondence:

BERNARD PAYRASTRE  
bernard.payrastra@inserm.fr

LOIC YSEBAERT  
ysebaert.loic@iuct-oncopole.fr

Received: October 1, 2018.

Accepted: February 28, 2019.

Pre-published: February 28, 2019.

doi:10.3324/haematol.2018.207183

Check the online version for the most updated information on this article, online supplements, and information on authorship & disclosures: [www.haematologica.org/content/104/11/2292](http://www.haematologica.org/content/104/11/2292)

©2019 Ferrata Storti Foundation

Material published in *Haematologica* is covered by copyright. All rights are reserved to the Ferrata Storti Foundation. Use of published material is allowed under the following terms and conditions:

<https://creativecommons.org/licenses/by-nc/4.0/legalcode>.

Copies of published material are allowed for personal or internal use. Sharing published material for non-commercial purposes is subject to the following conditions:

<https://creativecommons.org/licenses/by-nc/4.0/legalcode>, sect. 3. Reproducing and sharing published material for commercial purposes is not allowed without permission in writing from the publisher.



### Introduction

Bruton tyrosine kinase (Btk) inhibitors are efficient therapeutic agents for the treatment of chronic lymphocytic leukemia (CLL), mantle-cell lymphoma and Waldenström macroglobulinemia.<sup>1-3</sup> However, these drugs are recognized to increase the rate of bleeding in up to 50% of treated patients.<sup>4,5</sup> Most bleeding events are of grade 1-2, and include spontaneous bruising, petechiae and hematomas, but, in 5% of patients, they are of grade 3 or higher.<sup>6,9</sup> Such an incidence of bleeding warrants concerns, particularly during invasive procedures or surgery or when Btk inhibitors are associated with antithrombotic therapy.<sup>4,5</sup>

Several studies have now clearly shown that the first-in-class Btk inhibitor, ibrutinib, causes platelet dysfunction in a significant proportion of treated patients. *In vitro*, in normal platelets, the drug has been shown to affect activation mechanisms downstream of the collagen receptor GPVI, GPIb and  $\alpha$ IIB $\beta$ 3 integrin.<sup>10-13</sup> Btk and Tec are two members of the same family of tyrosine kinases involved in platelet activation, at least via their contribution to phospholipase C $\gamma$ 2 (PLC $\gamma$ 2) phosphorylation.<sup>14,15</sup> Experimental mouse models of Btk inactivation have shown that Btk is involved in collagen/GPVI and von Willebrand factor/GPIb-IX-V-induced platelet activation.<sup>14,16</sup> However, patients with X-linked agammaglobulinemia do not have a bleeding phenotype and their Btk-deficient platelets exhibit only a weak defect, suggesting compensation of Btk by Tec.<sup>14,17,18</sup> Accordingly, inactivation of both Btk and Tec in mice was required to impair platelet responses evoked by GPVI agonists.<sup>15</sup>

Like ibrutinib, the second-generation Btk inhibitor, acalabrutinib, inhibits Btk by covalent modification of the cysteine residue C481 in the ATP binding domain. While ibrutinib is known to irreversibly inhibit both Btk and Tec, acalabrutinib exhibits a higher specificity towards Btk and less activity on Tec,<sup>9,19,20</sup> although a recent study suggests that its selectivity for Btk over Tec is not substantial.<sup>21</sup> At the highest clinically achievable doses, ibrutinib has also been shown to inhibit Src-kinases in washed human platelets.<sup>10-13</sup> Src-kinases are essential for platelet activation and act upstream of Btk and Tec in the GPVI signaling pathway.<sup>22</sup> Their inhibition has been shown to induce bleeding *in vivo*.<sup>23</sup> Of note, acalabrutinib seems to have less inhibitory potential than ibrutinib on Src-kinases.<sup>19,24</sup> A clinical trial that enrolled 61 relapsed CLL patients demonstrated the efficacy of acalabrutinib and did not document any major bleeding although a significant incidence of low-grade bleeding including petechiae (16%) and contusions (18%) was observed.<sup>9</sup> Using an elegant experimental mouse model of arterial thrombosis and platelets from acalabrutinib-treated patients, it was also shown in this study that this second-generation Btk inhibitor has fewer anti-platelet effects than ibrutinib. Another recent study in a small cohort of patients also documented significant low-grade bleeding in acalabrutinib-treated patients and less platelet dysfunction in these patients than in ibrutinib-treated patients.<sup>24</sup> Of note, a very recent report suggests that ibrutinib and the second generation Btk inhibitors, acalabrutinib and tirabrutinib (ONO/GS-4059), have the capacity to prevent platelet thrombus formation on human atherosclerotic plaque homogenate.<sup>25</sup>

There are only limited available data on the effects of second-generation Btk inhibitors to guide physicians who switch from ibrutinib to another kinase inhibitor (e.g. in the case of bleeding, or co-medication with antithrombotic drugs). Therefore, we evaluated in this study whether acalabrutinib could represent a safer option. We first identified two groups of healthy donors based on their sensitivity to collagen-induced platelet aggregation inhibition by ibrutinib *in vitro*. We then characterized the differences and similarities in the effects of acalabrutinib and ibrutinib in the two groups and analyzed the impact of an association of acalabrutinib with antiplatelet drugs. Our data suggest that switching Btk therapy may not be a systematically good option for patients who bleed under ibrutinib treatment, and that the association of any of these Btk inhibitors with antiplatelet drugs significantly potentiates the inhibition of collagen-induced platelet aggregation.

## Methods

### Reagents

The sources of the reagents used in this study are provided in the *Online Supplement*.

### Preparation of human platelets

Human platelets from adult healthy volunteers who had not taken aspirin or any anti-platelet or anti-inflammatory drugs in the preceding 10 days or CLL patients were isolated from blood collected under citrate. All experiments were performed within 1 h after blood sample collection for healthy donors and within 2 h after blood sample collection for CLL patients. Platelet-rich plasma (PRP) and washed platelets were prepared as indicated in the *Online Supplement* and elsewhere.<sup>23</sup>

### Light transmission aggregometry

Platelet aggregation was monitored in siliconized glass cuvettes under continuous stirring (1000 rpm) at 37°C using a turbidimetric method in a multi-channel aggregometer (SD Medical, France). Platelet aggregation was monitored for 10 min and the extent of platelet aggregation and area under curve (AUC) were analyzed using Thrombosoft 1.6 software (SD Medical, France).

### Ex vivo model of thrombosis under flow conditions

Glass microcapillaries (Cellix System, New York, NY, USA) were coated with 50 µg/mL type I collagen from equine tendon overnight at 4°C and saturated with a solution of 1% bovine serum albumin (fatty acid-free) in phosphate-buffered saline for 30 min. Heparin-anticoagulated whole blood from healthy human donors was pre-treated with ibrutinib, acalabrutinib or vehicle (dimethylsulfoxide) for 60 min at 37°C and platelets were labeled with DiOC<sub>6</sub> (2 µM, 10 min at 37°C). Blood was then perfused through the microfluidic system for the indicated times at an arterial shear rate of 1500 s<sup>-1</sup> as previously described.<sup>26</sup> Platelet adhesion and thrombus formation were measured in real time with an epifluorescence microscope (Axiovert 200; Zeiss) with a 40X oil immersion objective (Plan-Apo 40x/1.3 Oil DIC UVVIS-IR) and a Colibri LED System light source (Zeiss, Jena, Germany). The results were recorded in real time (acquisition rate: 1 frame every 30 s) using a high resolution CCD cooled camera (Orca-R2, Hamamatsu, Hamamatsu City, Japan). Image sequences of the time-lapse recording and surface coverage were analyzed using Image J software.

### Statistical analysis

Data are presented as mean ± standard error of the mean (SEM). Statistical analyses were performed using one-way analysis of variance (ANOVA) with the Bonferroni post-test (GraphPad PRISM software, San Diego, CA, USA). *P*-values <0.05 were considered statistically significant. Two-way ANOVA with the Bonferroni post-test was used for statistical analysis of the surface coverage in the thrombus formation assay and a one sample *t*-test was applied to analyze thrombus volume at 180 s.

### Ethical approval

Ethical approval for collecting blood from patients and healthy volunteers was granted by the *Hémopathies Inserm Midi-Pyrénées* (HIMIP) collection declared to the French Ministry of Higher Education and Research (DC 2008-307 collection 1) and a transfer agreement (AC 2008-129) was obtained after approval from the ethical committee *Comité de Protection des Personnes Sud-Ouest et Outremer II* and the Toulouse Hospital Bio-Resources biobank, declared to the Ministry of Higher Education and Research (DC 2016-2804). In accordance with French law, clinical and biological annotations of patients' samples were declared to the *Comité National Informatique et Libertés* (CNIL), the French data protection authority.

## Results

### Effect of ibrutinib and acalabrutinib on collagen-induced platelet aggregation in healthy donors

It is important to note that only a subset of ibrutinib-treated patients develop spontaneous bleeding and have a defect in collagen-induced platelet aggregation.<sup>3,10,11</sup> Moreover, we consistently observed great heterogeneity in the intensity of the *in vitro* effect of ibrutinib on collagen-induced platelet aggregation in PRP from healthy donors (*unpublished observation*). We therefore first tested the effect

of ibrutinib at the clinically achievable dose of 0.5  $\mu\text{M}$  on collagen-induced platelet aggregation in PRP from 70 healthy volunteers. Ibrutinib inhibited collagen-induced platelet aggregation (maximal platelet aggregation <50%) in 56% of healthy donors while it had no or little effect (maximal platelet aggregation >50%) in the remaining 44% (Figure 1A). Interestingly, when we performed this aggregometry assay again 6 months later in 29 out of the 70 donors, the response profile was comparable. Indeed, the same donors were either sensitive or resistant to ibrutinib (Figure 1A). Figure 1B highlights the important difference in the dose-dependent effect of ibrutinib in the two groups. This effect was probably not related to an apparent difference of collagen sensitivity among the healthy donor population since the maximal platelet aggregation in response to a low dose of collagen (3.3  $\mu\text{g}/\text{mL}$ ) was not significantly different in the two groups. Moreover, increasing the collagen

concentration from 3.3  $\mu\text{g}/\text{mL}$  to 6  $\mu\text{g}/\text{mL}$  reduced but did not overcome the inhibitory effect of ibrutinib in the high sensitivity group (Online Supplementary Figure S1). These two groups will hereafter be referred to as ibrutinib “high sensitive” (HS) and “low sensitive” (LS) donors. To further characterize this marked difference, similar experiments were performed in the presence of drug efflux pump inhibitors, reserpine and verapamil, in LS donors (Online Supplementary Figure S2). While these two drugs alone or in combination had no effect on collagen-induced platelet aggregation, each drug significantly increased ibrutinib sensitivity. In combination, they induced high ibrutinib sensitivity in LS donors. Since it was recently shown that the effects of ibrutinib are incubation time-dependent,<sup>27</sup> we also performed a time-course analysis of the effects of ibrutinib treatment (Online Supplementary Figure S2C). We found that incubation with ibrutinib for 1 h caused the maximal inhi-

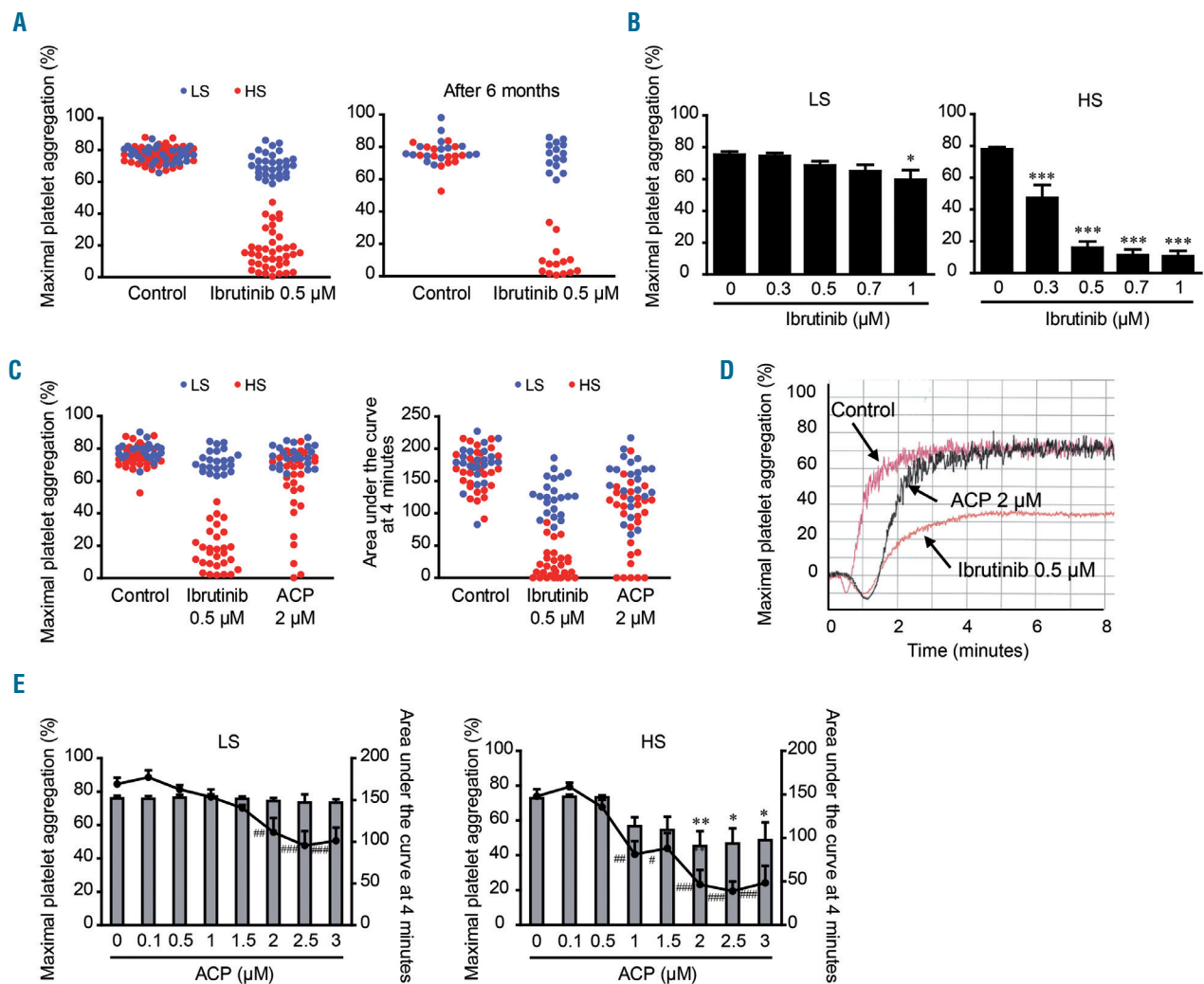


**Figure 1.** Effect of ibrutinib and acalabrutinib on collagen-induced platelet aggregation *in vitro*, in healthy donors. Platelet-rich plasma (PRP) from healthy volunteers was treated or not with ibrutinib (A-D) or acalabrutinib (ACP) (C-E) at the indicated concentrations for 1 h at 37 °C and stimulated with collagen 3.3  $\mu\text{g}/\text{mL}$ . Platelet aggregation was assessed by turbidimetry during 10 min and results, expressed as percentage of maximal platelet aggregation and area under the curve, are mean  $\pm$  standard error of mean. A maximal platelet aggregation response below 50% indicated ibrutinib high-sensitive donors (HS, in red, n=39) while a maximal aggregation response above 50% indicated ibrutinib low-sensitive donors (LS, in blue, n=31). The same analysis was performed 6 months later (After 6 months) in 29 out of the 70 healthy donors (A). Platelet aggregation curves showing representative platelet responses to ACP and ibrutinib on PRP from ibrutinib HS healthy donors are shown (D). The numbers of donors analyzed in each experiment were: (A) n=70, after 6 months: n=29; (B) LS: n=15, HS: n=7; (C) n=52; (E) LS: n=10, HS: n=12. \* $P$ <0.05, \*\* $P$ <0.01, \*\*\* $P$ <0.001, # $P$ <0.05, ## $P$ <0.01, ### $P$ <0.001 according to one-way analysis of variance.

bition and that the effect of the efflux pump inhibitors was visible at 30 min and maximal at 1 h in the LS group. These data are in agreement with those from Nicolson *et al.*<sup>27</sup> and suggest that the intra-platelet concentration of the drug correlates with the aggregation defect.

Thus, with regard to collagen-induced platelet aggregation in the normal population, two groups of individuals were distinguished based on their *in vitro* sensitivity to ibrutinib, as previously found in CLL patients treated with this drug.<sup>10,11</sup>

Since acalabrutinib could be an option for patients requiring a switch from ibrutinib therapy, we analyzed its effect at the clinically relevant dose of 2  $\mu\text{M}$  in the two groups. Acalabrutinib was less efficient than ibrutinib on maximal platelet aggregation induced by collagen (Figure 1C, D). The ibrutinib LS donors were not affected by acalabrutinib and a large proportion of ibrutinib HS donors were not or only weakly affected. In a small percentage of donors (10%) both drugs strongly inhibited collagen-induced platelet aggregation. Dose-dependent curves illustrate the lack of effect of acalabrutinib in the LS group and its relatively weak effect in the HS group (Figure 1E). However, while acalabrutinib was less efficient than ibrutinib on maximal platelet aggregation, it consistently delayed the aggregation response (Figure 1D). This is illustrated by a decrease in the area under the aggregation curve (Figure 1C, D). This effect was dose-dependent and more pronounced in the ibrutinib HS group (Figure 1E). It is noteworthy that acalabrutinib had no impact on platelet aggregation induced by thrombin receptor activating peptide (TRAP), the thromboxane A2 analog U46619 or ADP but did affect to some extent platelet aggregation induced by the GPVI agonist, collagen-related peptide, particularly in the HS group (*Online Supplementary Figure S3*). Of note, the drug efflux pump inhibitors alone or in combination did not significantly amplify the effect of acalabrutinib on maximal platelet aggregation but tended to increase its impact on the delay of aggregation in response to collagen (3.3  $\mu\text{g}/\text{mL}$ ) in the LS group (*data not shown*).

The effect of acalabrutinib on collagen-induced platelet aggregation was also tested *in vitro* in PRP from 16 Btk inhibitor-naïve CLL patients. The maximal platelet aggregation evoked by collagen was reduced compared to that of healthy donors but two groups, ibrutinib LS (n=4) and ibrutinib HS (n=12), were again identified (Figure 2A). While acalabrutinib had no significant effect in ibrutinib LS CLL patients, it significantly decreased the maximal platelet aggregation in ibrutinib HS CLL patients (Figure 2B). In the ibrutinib HS group, only one patient was not sensitive to acalabrutinib.

#### Acalabrutinib is less efficient than ibrutinib at inhibiting signaling events downstream of GPVI

We then compared the impact of acalabrutinib and ibrutinib on tyrosine phosphorylation events downstream of GPVI using washed platelets. Compared with PRP, in which plasma proteins are known to bind and sequester the drug, acalabrutinib was more efficient at inhibiting collagen-induced aggregation of washed platelets. In ibrutinib LS donors the half maximal inhibitory concentration ( $\text{IC}_{50}$ ) was  $1.07 \pm 0.35 \mu\text{M}$ , while it was  $0.69 \pm 0.44 \mu\text{M}$  in HS donors (Figure 3A). Both ibrutinib and acalabrutinib strongly inhibited Btk autophosphorylation in ibrutinib LS and HS groups (Figure 3B). Ibrutinib was very efficient at blocking PLC $\gamma$ 2 phosphorylation on the Btk-dependent phosphory-

lation site Tyr753 in both groups. Acalabrutinib at 1 or 2  $\mu\text{M}$  significantly inhibited PLC $\gamma$ 2 Tyr753 phosphorylation in both groups (Figure 3B). The observed stronger effect of ibrutinib on PLC $\gamma$ 2 phosphorylation would be consistent with an off-target effect of this drug on Tec and possibly Src kinases. Indeed, consistent with previous reports,<sup>10,24</sup> ibrutinib significantly affected Src activation as assessed by the intensity of its tyrosine 418 phosphorylation. The effect of ibrutinib was more pronounced in the ibrutinib HS group ( $44 \pm 6\%$  inhibition in the HS group vs.  $15 \pm 5\%$  in the LS group,  $P < 0.01$ , n=7 for HS and n=10 for LS). Interestingly, while ibrutinib inhibited Src particularly in the HS group, acalabrutinib had no or very little effect on Src activation in both groups. The improved profile of acalabrutinib over ibrutinib on global tyrosine phosphorylation events was confirmed by western blot analysis of the pan-tyrosine phosphorylation pattern in response to collagen stimulation (*Online Supplementary Figure S4*).

#### Weak impact of acalabrutinib on thrombus formation on collagen under flow

Ibrutinib has been shown to affect thrombus formation and stability on a collagen matrix under flow<sup>12,24</sup> and firm platelet adhesion on von Willebrand factor.<sup>10</sup> Given the difference of effects of acalabrutinib observed in the two groups of healthy donors, we performed platelet adhesion and thrombus formation assays under an arterial shear rate to mimic the *in vivo* situation. Whole blood, treated or not

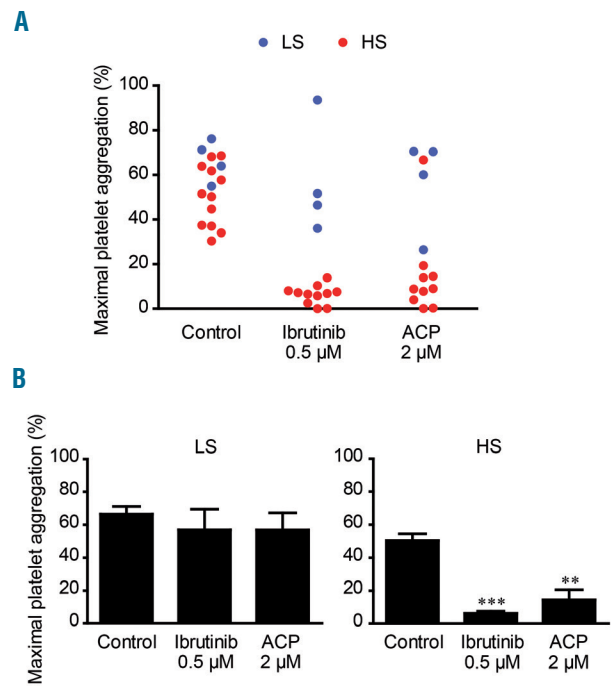


**Figure 2. Effect of ibrutinib and acalabrutinib on collagen-induced platelet aggregation *in vitro* in patients with chronic lymphocytic leukemia.** Platelet-rich plasma from 16 Bruton kinase inhibitor-naïve patients with chronic lymphocytic leukemia was treated or not with ibrutinib or acalabrutinib (ACP) for 1 h at 37 °C and stimulated with collagen 3.3  $\mu\text{g}/\text{mL}$ . Platelet aggregation was assessed by turbidimetry during 10 min. (A) Four patients were identified as having low sensitivity (LS) to ibrutinib (reduction of maximal platelet aggregation <50%, blue) and 12 as having high sensitivity (HS) to ibrutinib (reduction of maximal platelet aggregation >50%, red). (B) Results, expressed as percentage of maximal platelet aggregation in the two groups, are mean  $\pm$  standard error of mean. \*\* $P < 0.01$ , \*\*\* $P < 0.001$  according to one-way analysis of variance.

with 0.5  $\mu\text{M}$  ibrutinib or 2  $\mu\text{M}$  acalabrutinib for 1 h, was perfused over a collagen matrix and platelet adhesion and thrombus formation were monitored by real-time imaging. Acalabrutinib had no effect on platelet surface coverage in both groups, indicating that platelet adhesion was spared (Figure 4A, B). However, while this drug had no impact on the thrombus volume in the ibrutinib LS group of healthy donors, it significantly decreased thrombus volume in the HS group (Figure 4A, B). As expected, in similar conditions, ibrutinib significantly decreased surface coverage and thrombus volume in the ibrutinib HS group and tended to decrease thrombus volume in the LS group.

### Effect of associations of antiplatelet drugs and ibrutinib or acalabrutinib

The management of bleeding risk in patients with cardiovascular disease under dual antiplatelet therapy for primary or secondary prevention treated with Btk inhibitors is of concern in clinical practice.<sup>4,5,28</sup> There is currently little information to guide clinicians in making decisions about antiplatelet therapy concurrently with Btk inhibitors. We therefore tested the effect of combinations of ibrutinib or acalabrutinib with indomethacin (an aspirin-like drug) or cangrelor (ARC69931MX), an antagonist of the P2Y<sub>12</sub> ADP receptor, on platelet aggregation evoked by collagen in PRP from the two groups of healthy donors (Figure 5). In both

groups, platelet aggregation was significantly inhibited by indomethacin and to a lesser extent by cangrelor. Importantly, the combination of indomethacin or cangrelor with ibrutinib at a clinically relevant dose amplified the inhibition of platelet aggregation in the ibrutinib HS group. In the ibrutinib LS group, ibrutinib at 0.5  $\mu\text{M}$  did not have a significant effect on the maximal platelet aggregation induced by collagen but increased the effect of indomethacin or cangrelor (in accordance with the 6-8% grade 3-4 bleeding events reported in clinical trials). Interestingly, acalabrutinib, at a clinically relevant dose which had no impact on maximal platelet aggregation induced by collagen, also strongly potentiated, in a dose-dependent manner, the effect of indomethacin and cangrelor in both groups (Figure 5A, B). These data indicate that these two Btk inhibitors potentiated the effect of cyclooxygenase inhibition and P2Y<sub>12</sub> antagonism, even in the ibrutinib LS group (Figure 5).

### Discussion

The first-generation Btk inhibitor ibrutinib has revolutionized the therapy of CLL and mantle cell lymphoma but the drug can cause some side effects such as atrial fibrillation and bleeding.<sup>1-3,28</sup> The occurrence of side effects is the

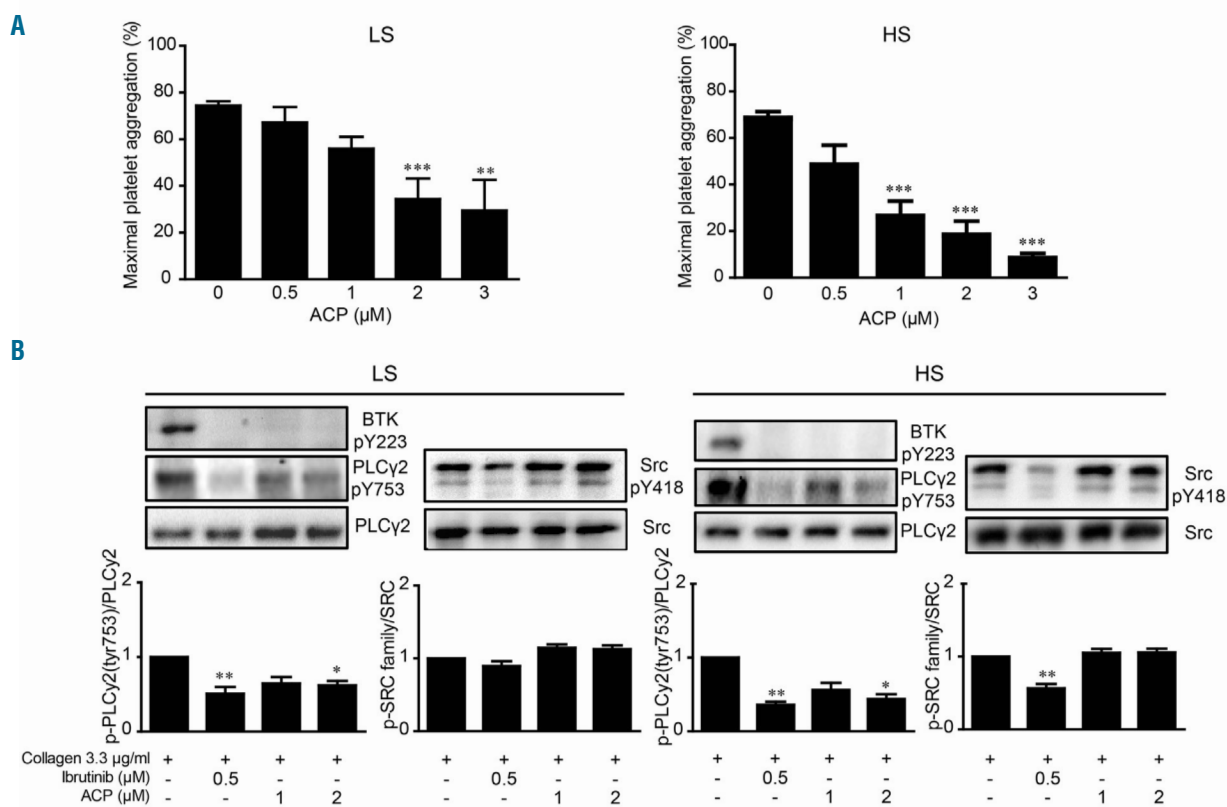


**Figure 3. Effect of ibrutinib and acalabrutinib on tyrosine phosphorylation events.** (A) Washed platelets from healthy donors were treated or not with increasing doses of acalabrutinib (ACP) for 1 h at 37 °C and stimulated with collagen 3.3  $\mu\text{g/ml}$ . Platelet aggregation was assessed by turbidimetry during 10 min and results, expressed as percentage of maximal aggregation, are mean  $\pm$  standard error of mean (SEM). Ten donors with low sensitivity (LS) and eight with high sensitivity (HS) to ibrutinib were analyzed. \*\* $P < 0.01$ , according to one-way analysis of variance (ANOVA). Half maximal inhibitory concentrations ( $\text{IC}_{50}$ ) were determined using GraphPad Prism software. (B) In parallel to aggregation, the effect of ibrutinib and acalabrutinib on platelet tyrosine phosphorylation events (PLC $\gamma$ 2 phosphorylation on Tyr-753 and Src phosphorylation on Tyr-418) in response to 1 min stimulation with collagen 3.3  $\mu\text{g/ml}$  was assessed by western blotting. The results of the western blot quantification by densitometric analysis are shown as means  $\pm$  SEM from ten independent experiments for LS and seven independent experiments for HS. \* $P < 0.05$ , \*\* $P < 0.01$ , according to one-way ANOVA. Representative western blots are shown for each group.

major reason for discontinuing ibrutinib during the first year of treatment, with this translating into shorter progression-free and overall survivals.<sup>29</sup> Management of bleeding is therefore of paramount importance, especially in the 10–12% of cases who develop atrial fibrillation and require anticoagulation (which increases the risk of grade 3–4 bleeding). The second-generation irreversible Btk inhibitor, acalabrutinib, with less off-target kinase inhibition, is expected

to improve the safety profile, including bleeding, of Btk inhibition.<sup>9,19,24</sup> In this study we characterized the effects of acalabrutinib on platelet functions *in vitro* and *ex vivo* and compared these effects with those of ibrutinib.

We performed a series of assays on two populations of healthy donors characterized by high or low sensitivity to ibrutinib, based on the degree of inhibition of collagen-induced platelet aggregation in PRP achieved by the drug.

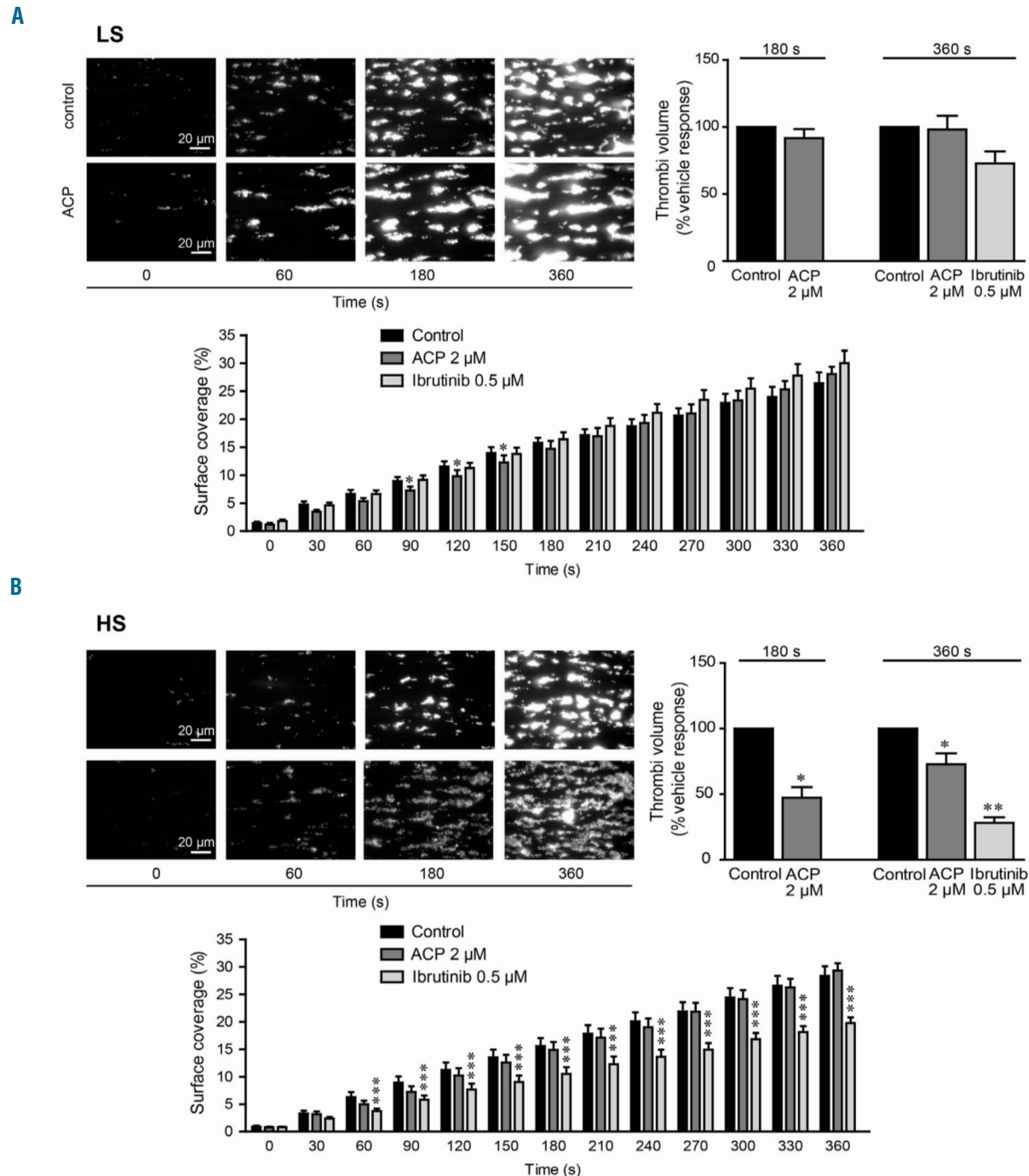


**Figure 4. Effect of acalabrutinib on platelet thrombus formation *ex vivo* on collagen under arterial flow.** (A, B) DIOC<sub>6</sub>-labeled platelets from healthy donors with (A) low sensitivity (LS) or (B) high sensitivity (HS) to ibrutinib (determined on the basis of their aggregation response as in Figure 1) pre-incubated with acalabrutinib (ACP) 2 μM, ibrutinib 0.5 μM or dimethylsulfoxide (control) for 1 h at 37 °C were perfused through a collagen-coated microcapillary at a physiological arterial shear rate of 1500 s<sup>-1</sup> for 180 or 360 s. Surface coverage (%) and thrombi volume (% of vehicle response) were analyzed using ImageJ software. Results are presented as mean ± standard error of mean of three or four independent experiments. \*P<0.05, \*\*P<0.01, \*\*\*P<0.001 according to two-way analysis of variance (ANOVA) for surface coverage, one-way ANOVA for thrombi volume at 360 s and a one sample t-test for thrombi volume at 180 s.

We provide evidence that one factor contributing to predispose platelets to ibrutinib sensitivity *in vitro* is the drug efflux pump system. Indeed, inhibition of drug efflux pumps was sufficient to induce ibrutinib sensitivity in the LS group of healthy donors. This suggests that the actual dose of ibrutinib reaching intracellular targets is critical and will determine the extent of inhibition of Btk and Tec and possibly other undesired targets such as Src-kinases. These data are in line with those of a very recent study suggesting that the ibrutinib-mediated increase of bleeding is due to off-targets effects of the drug occurring because of unfavorable pharmacodynamics.<sup>27</sup> The authors propose that the bleeding side effect of ibrutinib may be avoided by reduction of the dose. Our data suggest that an efficient platelet drug efflux pump system may limit the multifactorial antiplatelet effects of ibrutinib. This is important new information to take into consideration when interpreting the results of *in vitro* experiments with ibrutinib. Moreover, it could be interesting to analyze a potential link between polymorphisms of drug efflux pumps and the risk of bleeding in patients treated with ibrutinib. These data may also stimulate pharmacists to look for intake of P-glycoprotein inhibitors among co-medications in patients with prolonged bleeding under ibrutinib. Since verapamil increases the plasma concentrations of amiodarone and likely the intra-platelet concentration of ibrutinib, cardiologists may favor the use of  $\beta$ -blockers when prescribing drugs to lower the heart rate. Evaluating the sensitivity of a patient's platelets to ibrutinib before starting therapy could also help clinicians to establish a personalized therapeutic strategy.

Our standard *in vitro* aggregation tests indicated that acalabrutinib had no effect on the maximal platelet aggregation response in the ibrutinib LS group of healthy donors. In the

ibrutinib HS group of healthy donors, acalabrutinib affected maximal platelet aggregation only in a few cases. However, acalabrutinib consistently delayed platelet aggregation in both groups. As expected, acalabrutinib had no effect on platelet aggregation induced by TRAP, U46619 or ADP. These data point to a better profile of acalabrutinib on platelets from healthy donors compared to that of ibrutinib.

Importantly, when acalabrutinib was tested on PRP from CLL patients, it had no effect on the maximal platelet aggregation response in the ibrutinib LS group, but significantly inhibited platelet aggregation in the ibrutinib HS group of patients. These data suggest that a switch from ibrutinib to acalabrutinib therapy may not be systematically appropriate to prevent bleeding in CLL patients.<sup>5</sup> The results from clinical trials show that, although no grade 3 bleeding was observed in relapsed CLL patients treated with acalabrutinib, low-grade hemorrhages occurred in a significant proportion of patients, comparable with those observed with ibrutinib.<sup>4,9,24</sup>

Ibrutinib has been shown to reduce the stability of platelet thrombus on collagen<sup>24</sup> and firm platelet adhesion on the von Willebrand factor matrix.<sup>10</sup> Consistent with the data reported by Bye *et al.*,<sup>24</sup> we found here that acalabrutinib had no effect on thrombus formation on collagen in the ibrutinib LS group of healthy donors. However, in the ibrutinib HS group, while acalabrutinib did not affect platelet adhesion it was able to significantly reduce thrombus volume. Again these data show a better profile of acalabrutinib, although with some significant impact in the ibrutinib HS group.

The effects of ibrutinib and acalabrutinib on the Btk-mediated tyrosine phosphorylation of PLC $\gamma$ 2 on Tyr-753 and on the Src autophosphorylation site Tyr-418 (activated

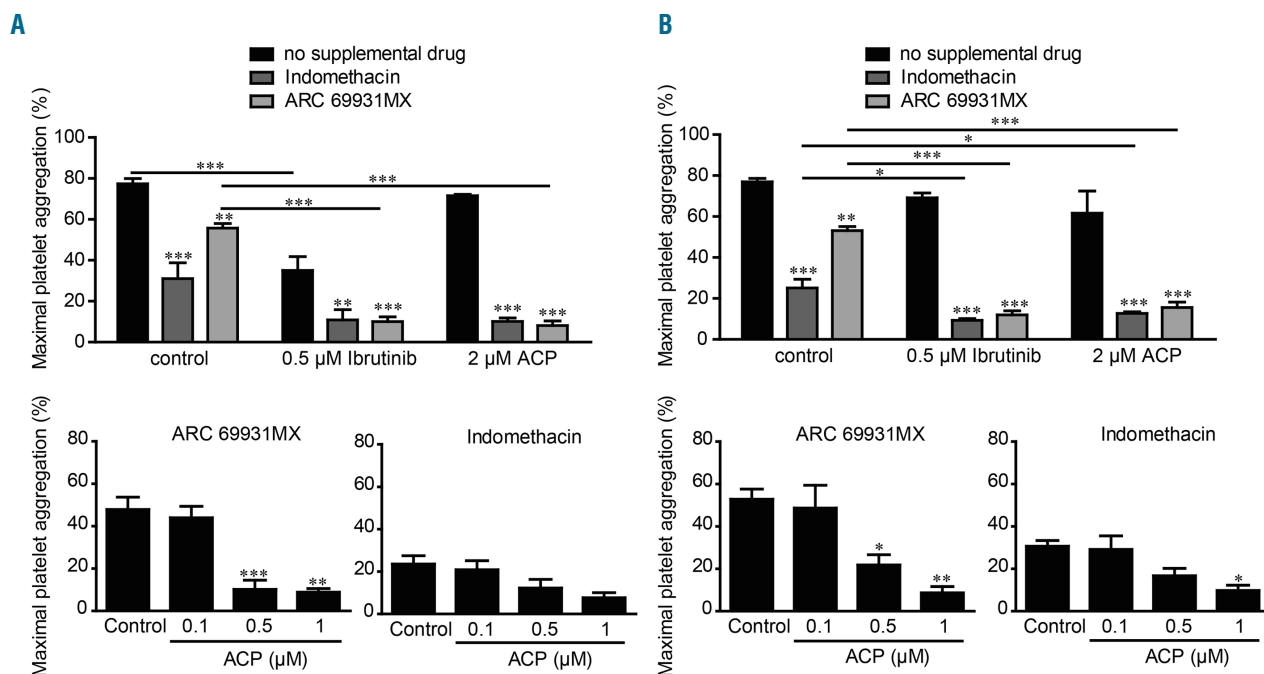


**Figure 5. Effect of ibrutinib and acalabrutinib in association with anti-platelet drugs.** (A, B) Platelet-rich plasma from healthy donors with (A) high sensitivity (HS) or (B) low sensitivity (LS) to ibrutinib was pre-treated or not with the indicated doses of acalabrutinib (ACP) or ibrutinib for 1 h at 37 °C and anti-platelets drugs (10  $\mu$ M indomethacin and/or 10  $\mu$ M ARC69931MX) were added 10 min before stimulation with collagen 3.3  $\mu$ g/mL. Platelet aggregation was assessed by turbidimetry during 10 min and results, expressed as percentage of maximal aggregation, are the mean  $\pm$  standard error of mean of three to five independent experiments. \* $P$ <0.05, \*\* $P$ <0.01, \*\*\* $P$ <0.001 according to one-way and two-way analyses of variance.

form of Src-kinases) were investigated in washed platelets from the two groups of healthy donors. Ibrutinib, at the clinically relevant dose of 0.5  $\mu\text{M}$ , inhibited phosphorylation at both sites, with a significantly more intense effect in the ibrutinib HS group. The strong inhibition of phosphorylation observed in the ibrutinib HS group correlated with the inhibition of platelet aggregation. The weaker inhibition of phosphorylation in the ibrutinib LS group was accompanied by a weaker decrease of aggregation. Acalabrutinib efficiently inhibited Btk phosphorylation, significantly decreased PLC $\gamma$ 2 Tyr-753 but had no effect on Src phosphorylation in either group, even at a dose of 2  $\mu\text{M}$  which is above the 1.3  $\mu\text{M}$  mean peak of free plasma drug concentrations measured in patients.<sup>9</sup> These data are consistent with the better selectivity of acalabrutinib on Btk, also shown by the whole tyrosine phosphorylation profile of collagen-stimulated platelets. However, it is worth noting that while a dose of 2  $\mu\text{M}$  acalabrutinib had no effect on Src activation it did decrease platelet aggregation significantly in the ibrutinib HS group.

A relevant clinical scenario is the association of Btk inhibitors with dual antiplatelet therapy in patients with cardiovascular diseases, particularly after percutaneous

coronary intervention with stent placement. The current dual antiplatelet therapy is based on aspirin and a P2Y<sub>12</sub> ADP receptor antagonist such as clopidogrel, prasugrel, ticagrelor or cangrelor. Our data are consistent with those of a previous study showing that ibrutinib amplifies the effect of cangrelor on platelets<sup>12</sup> and also demonstrate that acalabrutinib strongly potentiated the effect of indomethacin or cangrelor on platelet aggregation induced by collagen both in the ibrutinib HS and LS groups of healthy donors. This is important information for guiding therapeutic strategies in patients under antiplatelet therapy at high risk of bleeding.

In conclusion, this study provides new insights into the impact of the first- and second-generation Btk inhibitors, ibrutinib and acalabrutinib, on platelets and contributes to the improvement of evidence-based recommendations for a safer use of these targeted therapies.

### Acknowledgments

*This work was supported by grants from Inserm, Fondation pour la Recherche Médicale (DEQ20170336737) and Janssen. We thank the Genotoul imaging facility of I2MC (Inserm U1048). BP is a scholar of the Institut Universitaire de France.*

### References

1. Thompson PA, Burger JA. Bruton's tyrosine kinase inhibitors: first and second generation agents for patients with chronic lymphocytic leukemia (CLL). *Expert Opin Investig Drugs*. 2018;27(1):31-42.
2. Seiler T, Dreyling M. Bruton's tyrosine kinase inhibitors in B-cell lymphoma: current experience and future perspectives. *Expert Opin Investig Drugs*. 2017;26(8):909-915.
3. Chakraborty R, Kapoor P, Ansell SM, Gertz MA. Ibrutinib for the treatment of Waldenström macroglobulinemia. *Expert Rev Hematol*. 2015;8(5):569-579.
4. Shatzel JJ, Olson SR, Tao DL, McCarty OJT, Danilov AV, Deloughery TG. Ibrutinib-associated bleeding: pathogenesis, management and risk reduction strategies. *J Thromb Haemost*. 2017;15(5):835-847.
5. Caron F, Leong DP, Hillis C, Fraser G, Siegal D. Current understanding of bleeding with ibrutinib use: a systematic review and meta-analysis. *Blood Adv*. 2017;1(12):772-778.
6. Rushworth SA, MacEwan DJ, Bowles KM. Ibrutinib in relapsed chronic lymphocytic leukemia. *N Engl J Med*. 2013;369(13):1277-1278.
7. Byrd JC, Fruman RR, Coutre SE, et al. Targeting BTK with ibrutinib in relapsed chronic lymphocytic leukemia. *N Engl J Med*. 2013;369(1):32-42.
8. Wang ML, Rule S, Martin P, Goy A, et al. Targeting BTK with ibrutinib in relapsed or refractory mantle-cell lymphoma. *N Engl J Med*. 2013;369(6):507-516.
9. Byrd JC, Harrington B, O'Brien S, et al. Acalabrutinib (ACP-196) in relapsed chronic lymphocytic leukemia. *N Engl J Med*. 2016;374(4):323-332.
10. Levade M, David E, Garcia C, et al. Ibrutinib treatment affects collagen and von Willebrand factor-dependent platelet functions. *Blood*. 2014;124(26):3991-3995.
11. Kamel S, Horton L, Ysebaert L, et al. Ibrutinib inhibits collagen-mediated but not ADP-mediated platelet aggregation. *Leukemia*. 2015;29(4):783-787.
12. Bye AP, Unsworth AJ, Vaiyapuri S, Stainer AR, Fry MJ, Gibbins JM. Ibrutinib inhibits platelet integrin  $\alpha\text{IIb}\beta$ 3 outside-in signaling and thrombus stability but not adhesion to collagen. *Arterioscler Thromb Vasc Biol*. 2015;35(11):2326-2335.
13. Rigg RA, Aslan JE, Healy LD, et al. Oral administration of Bruton's tyrosine kinase inhibitors impairs GPVI-mediated platelet function. *Am J Physiol Cell Physiol*. 2016;310(5):C373-380.
14. Quek LS, Bolen J, Watson SP. A role for Bruton's tyrosine kinase (Btk) in platelet activation by collagen. *Cur Biol*. 1998;8(20):1137-1140.
15. Atkinson BT, Ellmeier W, Watson SP. Tec regulates platelet activation by GPVI in the absence of Btk. *Blood*. 2003;102(10):3592-3599.
16. Liu J, Fitzgerald ME, Berndt MC, Jackson CW, Gartner TK. Bruton tyrosine kinase is essential for botrocetin/VWF-induced signaling and GPIIb-dependent thrombus formation in vivo. *Blood*. 2006;108(8):2596-2603.
17. Futatani T, Watanabe C, Baba Y, Tsukada S, Ochs HD. Bruton's tyrosine kinase is present in normal platelets and its absence identifies patients X-linked agammaglobulinemia and carrier females. *Br J Haematol*. 2001;114(1):141-149.
18. Winkelstein JA, Marino MC, Lederman HM, et al. X-linked agammaglobulinemia: report on a United States registry of 201 patients. *Medicine*. 2006;85(4):193-202.
19. Wu J, Zhang M, Liu D. Acalabrutinib (ACP-196): a selective second-generation BTK inhibitor. *J Hematol Oncol*. 2016;9:21.
20. Barf T, Covey T, Izumi R, et al. Acalabrutinib (ACP-196): a covalent bruton tyrosine kinase inhibitor with a differentiated selectivity and in vivo potency profile. *J Pharmacol Exp Ther*. 2017;363(2):240-252.
21. Chen J, Kinoshita T, Gururaja T, et al. The effect of Bruton's tyrosine kinase (BTK) inhibitors on collagen-induced platelet aggregation, BTK, and tyrosine kinase expressed in hepatocellular carcinoma (TEC). *Eur J Haematol*. 2018 Jun 20. [Epub ahead of print]
22. Senis YA, Mazharian A, Mori J. Src family kinases: at the forefront of platelet activation. *Blood*. 2014;124(13):2013-2024.
23. Gratacap MP, Martin V, Valéra MC, et al. The new tyrosine-kinase inhibitor and anticancer drug dasatinib reversibly affects platelet activation in vitro and in vivo. *Blood*. 2009;114(9):1884-1892.
24. Bye AP, Unsworth AJ, Desborough MJ, et al. Severe platelet dysfunction in NHL patients receiving ibrutinib is absent in patients receiving acalabrutinib. *Blood Adv*. 2017;1(26):2610-2623.
25. Busygina K, Jamasbi J, Seiler T, et al. Oral Bruton tyrosine kinase inhibitors selectively block atherosclerotic plaque-triggered thrombus formation. *Blood*. 2018;131(24):2605-2616.
26. Laurent PA, Séverin S, Hechler B, et al. Platelet PI3kbeta and GSK3 regulate thrombus stability at a high shear rate. *Blood*. 2015;125(5):881-888.
27. Nicolson PLR, Hughes CE, Watson S, et al. Inhibition of Btk-specific concentrations of ibrutinib and acalabrutinib delays but does not block platelet aggregation to GPVI. *Haematologica*. 2018;103(12):2097-2108.
28. Aguilar C. Ibrutinib-related bleeding: pathogenesis, clinical implications and management. *Blood Coagul Fibrinolysis*. 2018;29(6):481-487.
29. Mato AR, Nabhan C, Thompson MC, et al. Toxicities and outcomes of 616 ibrutinib-treated patients in the united states: a real-world analysis. *Haematologica*. 2018;103(5):874-879.



## Dynamic prediction of bleeding risk in thrombocytopenic preterm neonates

Susanna F. Fustolo-Gunnink,<sup>1,2</sup> Karin Fijnvandraat,<sup>2,3</sup> Hein Putter,<sup>4</sup> Isabelle M. Ree,<sup>5</sup> Camila Caram-Deelder,<sup>1</sup> Peter Andriessen,<sup>6</sup> Esther J. d'Haens,<sup>7</sup> Christian V. Hulzebos,<sup>8</sup> Wes Onland,<sup>9</sup> André A. Kroon,<sup>10</sup> Daniël C. Vijlbrief,<sup>11</sup> Enrico Lopriore<sup>5</sup> and Johanna G. van der Bom<sup>1-12</sup>

<sup>1</sup>Sanquin/LUMC, Center for Clinical Transfusion Research, Leiden; <sup>2</sup>Amsterdam University Medical Center, Emma Children's Hospital, Department of Pediatric Hematology, Amsterdam-Zuidoost; <sup>3</sup>Sanquin Blood Supply Foundation, Department of Plasma Proteins, Sanquin Research, Amsterdam; <sup>4</sup>Leiden University Medical Center, Department of Medical Statistics, Leiden; <sup>5</sup>Leiden University Medical Center, Willem Alexander Children's Hospital, Department of Neonatology, Leiden; <sup>6</sup>Máxima Medical Center, Department of Neonatology, Veldhoven; <sup>7</sup>Isala Zwolle, Amalia Children's Center, Department of Neonatology, Zwolle; <sup>8</sup>University Medical Center Groningen, Beatrix Children's Hospital, Department of Neonatology, Groningen; <sup>9</sup>Amsterdam University Medical Center, Emma Children's Hospital, Department of Neonatology, Amsterdam-Zuidoost; <sup>10</sup>Erasmus Medical Center, Sophia Children's Hospital, Department of Neonatology, Rotterdam; <sup>11</sup>University Medical Center Utrecht, Utrecht University, Wilhelmina Children's Hospital, Department of Neonatology, Utrecht and <sup>12</sup>Leiden University Medical Center, Department of Clinical Epidemiology, Leiden, the Netherlands.

Haematologica 2019  
Volume 104(11):2300-2306

### ABSTRACT

Over 75% of severely thrombocytopenic neonates receive platelet transfusions, though little evidence supports this practice, and only 10% develop major bleeding. In a recent randomized trial, giving platelet transfusions at a threshold platelet count of  $50 \times 10^9/L$  compared to a threshold of  $25 \times 10^9/L$  was associated with an increased risk of major bleeding or mortality. This finding highlights the need for improved and individualized guidelines on neonatal platelet transfusion, which require accurate prediction of bleeding risk. Therefore, the objective of this study was to develop a dynamic prediction model for major bleeding in thrombocytopenic preterm neonates. This model allows for calculation of bleeding risk at any time-point during the first week after the onset of severe thrombocytopenia. In this multicenter cohort study, we included neonates with a gestational age <34 weeks, admitted to a neonatal intensive care unit, who developed severe thrombocytopenia (platelet count  $<50 \times 10^9/L$ ). The study endpoint was major bleeding. We obtained predictions of bleeding risk using a proportional baselines landmark supermodel. Of 640 included neonates, 71 (11%) had a major bleed. We included the variables gestational age, postnatal age, intrauterine growth retardation, necrotizing enterocolitis, sepsis, platelet count and mechanical ventilation in the model. The median cross-validated c-index was 0.74 (interquartile range, 0.69-0.82). This is a promising dynamic prediction model for bleeding in this population that should be explored further in clinical studies as a potential instrument for supporting clinical decisions. The study was registered at [www.clinicaltrials.gov](http://www.clinicaltrials.gov) (NCT03110887).

### Correspondence:

J.G. VAN DER BOM  
[j.g.vanderbom@lumc.nl](mailto:j.g.vanderbom@lumc.nl)

Received: October 9, 2018.

Accepted: February 27, 2019.

Pre-published: February 28, 2019.

doi:10.3324/haematol.2018.208595

Check the online version for the most updated information on this article, online supplements, and information on authorship & disclosures: [www.haematologica.org/content/104/11/2300](http://www.haematologica.org/content/104/11/2300)

©2019 Ferrata Storti Foundation

Material published in *Haematologica* is covered by copyright. All rights are reserved to the Ferrata Storti Foundation. Use of published material is allowed under the following terms and conditions:

<https://creativecommons.org/licenses/by-nc/4.0/legalcode>.

Copies of published material are allowed for personal or internal use. Sharing published material for non-commercial purposes is subject to the following conditions:

<https://creativecommons.org/licenses/by-nc/4.0/legalcode>,

sect. 3. Reproducing and sharing published material for commercial purposes is not allowed without permission in writing from the publisher.



### Introduction

Neonatal major bleeding occurs in approximately 5-15% of preterm neonates admitted to a neonatal intensive care unit and can lead to lifelong disabilities and death. The most common type of bleeding is intraventricular hemorrhage.<sup>1,2</sup>

Since platelets are required for primary hemostasis, preterm neonates with severe thrombocytopenia are thought to be particularly at risk of major bleeding. However, the associations between thrombocytopenia, platelet transfusions and bleeding in preterm neonates are not clear. In a recently published systematic review, only six studies could be included. These provided insufficient evidence to

assess whether platelet counts are causally related to major bleeding, or whether platelet transfusions reduce bleeding risk in thrombocytopenic preterm neonates.<sup>3</sup> Despite this lack of evidence, platelet transfusions are given to approximately 75% of thrombocytopenic preterm neonates.<sup>4,5</sup>

Recently, the results of the first randomized trial assessing currently used platelet count thresholds in preterm infants was published. The trial showed that giving prophylactic transfusions of platelets at a platelet count threshold of  $50 \times 10^9/L$  was associated with an increased risk of bleeding and mortality compared to a lower threshold of  $25 \times 10^9/L$ , within 28 days after randomization.<sup>6</sup> These results highlight the need for improved and individualized guidelines on platelet transfusion in neonates.

In addition to lack of evidence regarding transfusion thresholds and identification of platelet transfusion-related harm, indications for platelet transfusions are based primarily on platelet count. However, two neonates with similar platelet counts but different clinical conditions may have very different risks of bleeding, and benefit differently from platelet transfusions.<sup>7</sup> We need to be able to predict which neonates will develop major bleeding and quantify this bleeding risk, using a model that includes not only platelet count but also a set of relevant clinical variables. Such a prediction model could be used to define indications for transfusion in future studies, which is a first step towards individualized platelet transfusion therapy.

Some prediction models for bleeding in neonates have already been developed, but these models were not derived specifically for neonates with thrombocytopenia, and only allow for a risk assessment at baseline.<sup>8-15</sup> The disadvantage of baseline prediction models is that they do not take into account the clinical course of the neonate, which can change substantially over time, and may have a profound impact on bleeding risk. In dynamic predictions, the clinical course can be incorporated into the model. The objective of this study was, therefore, to develop a dynamic prediction model for major bleeding in thrombocytopenic preterm neonates.

## Methods

The study protocol was published online at [www.clinicaltrials.gov](http://www.clinicaltrials.gov) (NCT03110887). The institutional review board of the Academic Medical Center Amsterdam approved the study and waived the need for informed consent. The study was conducted in accordance with the Declaration of Helsinki and reported according to The Transparent Reporting of a Multivariable Prediction Model for Individual Prognosis or Diagnosis (TRIPOD) guidelines.<sup>16</sup> An extended methods section is available in the *Online Supplementary Materials*, including the procedure for predictor selection, outcome definitions, a list of participating centers with an overview of their clinical practice, description of the data acquisition process, sample size calculations, details on statistical methods and the role of the funding source.

## Population

We performed a cohort study among consecutive preterm neonates with thrombocytopenia admitted to any one of seven participating neonatal intensive care units in the Netherlands between January 2010 and January 2015. The cohort comprised all neonates with a gestational age at birth <34 weeks and at least one platelet count  $<50 \times 10^9/L$ . We excluded patients: (i) with severe

congenital malformations; (ii) for whom there was a high suspicion of spurious platelet count (e.g. clots in the sample, or spontaneous platelet count recovery within 6 h, or a platelet count labeled as spurious in the medical file); (iii) with thrombocytopenia occurring exclusively in the context of exchange transfusion; (iv) with a prior admission to another neonatal intensive care unit or readmission; and (v) who had major bleeding prior to severe thrombocytopenia. Neonates with major bleeding after the end of the follow-up were not excluded, but registered as not having experienced major bleeding during the study.

## Model development and statistics

The core research team drafted and approved a statistical analysis plan prior to the data analysis. We developed a proportional baseline landmark supermodel, with bleeding within the subsequent 3 days as the outcome.<sup>17</sup> Variables included in the model were gestational age, intrauterine growth retardation (IUGR), mechanical ventilation, platelet count, platelet transfusion, postnatal age at inclusion, and necrotizing enterocolitis (NEC) and/or sepsis (combined).

## Model validation

We validated the model by internal calibration using the heuristic shrinkage factor described by van Houwelingen *et al.*<sup>18</sup> We evaluated the model's accuracy in correctly discriminating between patients with and without major bleeding using the dynamic cross-validated c-index. A c-index of 1.0 indicates perfect discrimination, while a c-index of 0.5 is obtained when the model performs as well as chance. We calculated a c-index at each 2 h time-point, and reported this series of c-indices as a graph. Analyses were carried out using SPSS (version 24.0), Stata (version 14.1) and R (version 3.4.2).

## Clinical applicability of the model

Our study is a first, basic prediction model for major bleeding in preterm neonates with severe thrombocytopenia. Due to the dynamic nature of the model, it cannot be fully summarized in one table, but once validation studies have been performed, we will develop an online calculator. We have chosen not to publish the calculator along with this paper, in order to prevent inappropriate premature use of the model in clinical practice. The model is available upon request for researchers looking to perform model validation and impact studies.

## Results

### Baseline characteristics

Of 9,333 neonates with a gestational age <34 weeks, 927 had at least one platelet count  $<50 \times 10^9/L$ . Of these, 67 were excluded due to spurious platelet counts and 29 because thrombocytopenia occurred only during a readmission. Of the remaining 831 neonates, 191 were excluded based on major bleeding prior to thrombocytopenia (n=55), previous admission to another neonatal intensive care unit (n=51), congenital malformations (n=47), missing medical files (n=35) and because thrombocytopenia occurred exclusively during exchange transfusion (n=3). The remaining 640 neonates (7%) were included in the study (Figure 1). The median gestational age at birth was 28.1 weeks, the median birth weight was 900 grams (Table 1 and *Online Supplementary Figures S1* and *S2*) and 73% of the neonates received at least one platelet transfusion. No cases of fetal and neonatal alloimmune thrombocytopenia were identified. The lowest platelet counts dur-

ing study for neonates with and without major bleeding are reported in *Online Supplementary Figure S3*.

### Major bleeds

A total of 71 (11%) major bleeds occurred, of which 55 were intraventricular hemorrhages and other intracerebral hemorrhages, 12 were pulmonary hemorrhages and four were gastrointestinal hemorrhages (Table 2). The major bleeds occurred at a median of 1 day (interquartile range, 1-4) after the onset of severe thrombocytopenia. At the end of the 10-day follow-up period, 73 patients (11%) had died, 63 (10%) had developed major bleeding and 93 (15%) had been discharged or transferred (Figure 2). Of the 93 discharged neonates, 76 (82%) were discharged to a stepdown unit. Ninety-one percent of the neonates underwent at least one ultrasound scan, with a mean of two scans during the 10-day follow-up period. In four neonates, major intracranial hemorrhage was already diagnosed on the first ultrasound scan after birth, on the first day of life.

### Model development

The model contained 12 variables: all seven selected variables, plus the interaction term between platelet count and transfusion, plus interactions between time and IUGR and time and platelet count (both linear and quadratic). Platelet count was converted to a log-scale. The number of major bleeds included in the model was 63, because eight bleeds occurred more than 10 days after  $T_0$  (Table 2).

### Final model

The median c-index of the final model was 0.74 (interquartile range, 0.69 - 0.82) (Figure 3). This indicates good predictive performance. An example of a risk-estimation by the model is shown in Figure 4, a plot of bleeding risk of two neonates with distinct risk profiles. During study days 1-3, the predicted risk of major bleeding within the subsequent 3 days in child A is substantially higher than that in child B, indicating that the use of this prediction model during that time-period would have correctly identified child A as being at high risk of bleeding. This image also illustrates that bleeding risk can increase or decrease rapidly. Table 3 shows the details of the model. A hazard ratio  $>1$  indicates that the increase of a risk fac-

tor is associated with a higher risk of bleeding, and a hazard ratio  $<1$  indicates that the increase of a risk factor is associated with a lower risk of bleeding. The effects of platelet count and IUGR varied over time, while the effects of all other variables were constant over time. Table 4 shows predicted risks of bleeding for different clinical scenarios.

### Sensitivity analyses

None of the sensitivity analyses resulted in substantial changes in hazard ratios for the individual covariates, indicating that our model is robust (*Online Supplementary Table S3*).

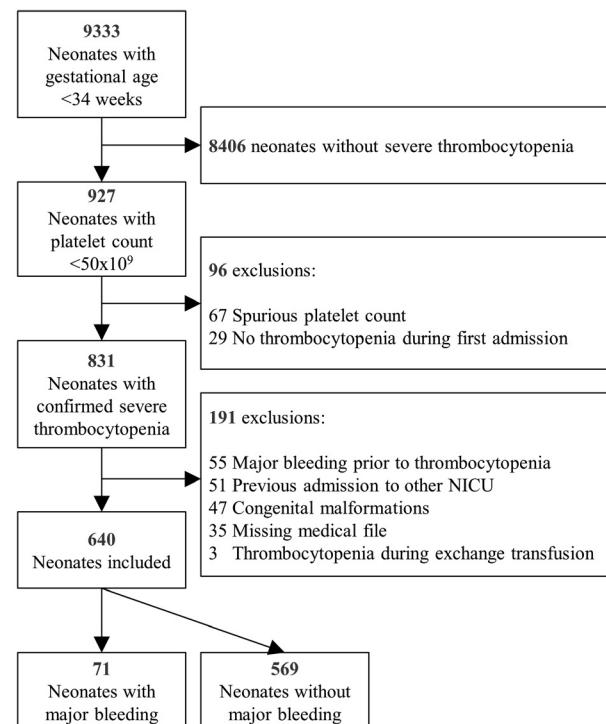


**Figure 1. CONSORT flow chart.** CONSORT: consolidated standards of reporting trials; NICU: neonatal intensive care unit.

**Table 1. Baseline characteristics of the study cohort (n=640).**

	Total cohort (n=640)		Major bleed (n=71)		No major bleed (n=569)	
<i>At birth</i>						
Gestational age in weeks: median (IQR) <sup>1</sup>	28.1	(26.4-30.4)	27.7	(26.1-29.1)	28.1	(26.4-30.6)
Birth weight in grams: median (IQR)	900	(710-1180)	945	(760-1200)	900	(705-1178)
Intrauterine growth retardation, n (%)	206	(32)	14	(20)	192	(34)
<i>At onset of severe thrombocytopenia</i>						
Postnatal age in days: median (IQR)	3.9	(1.6-9.25)	2.6	(1.0-6.8)	4.1	(1.8-9.8)
Platelet count x10 <sup>9</sup> /L, median (IQR)	38	(29-45)	39	(31-44)	38	(28-45)
Mechanical ventilation, n (%)	329	(51)	49	(69)	280	(49)
Necrotizing enterocolitis/sepsis, n (%)	330	(52)	39	(55)	291	(51)
Sepsis, n (%)	293	(46)	37	(52)	256	(45)
Necrotizing enterocolitis, n (%)	73	(11)	5	(7)	68	(12)

IQR: interquartile range. <sup>1</sup>In five cases the exact gestational age could not be determined due to uncontrolled pregnancies. It was estimated in full weeks.

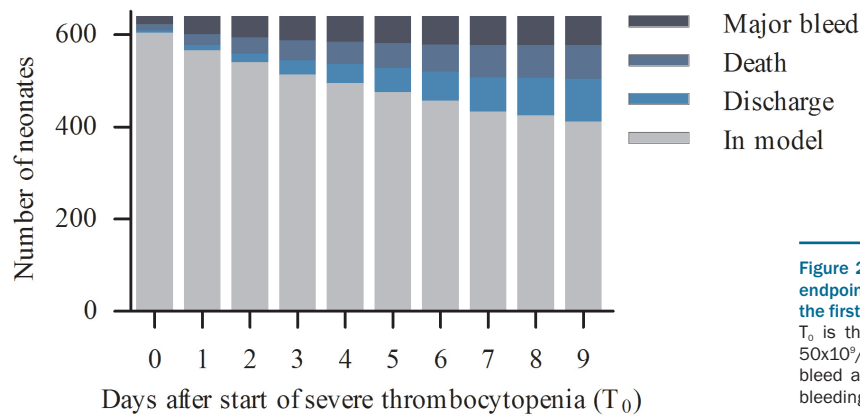


**Figure 2.** Number of neonates reaching the different study endpoints (major bleeding, death or discharge/transfer) in the first 10 days after the onset of severe thrombocytopenia. T<sub>0</sub> is the day on which the platelet count dropped below 50x10<sup>9</sup>/L for the first time. Neonates who developed a major bleed and then died were only registered as having major bleeding (no overlap between major bleeding and mortality).

**Discussion**

In this study, we developed a dynamic prediction model for major bleeding in thrombocytopenic preterm neonates. The model has a good predictive performance with a median c-index of 0.74. To our knowledge, this is the first dynamic prediction model for bleeding in preterm neonates.

The importance of using a dynamic model is illustrated by a recent survey assessing at which thresholds clinicians would administer a platelet transfusion to a preterm neonate with a gestational age of 27 weeks at birth.<sup>19</sup> The study showed that if this neonate was 2 days old and in a stable condition, most (European) clinicians would transfuse at a threshold platelet count of 30x10<sup>9</sup>/L. However, if the same neonate was septic, mechanically ventilated and receiving vasopressors, most clinicians would transfuse at a threshold of 50x10<sup>9</sup>/L. This illustrates that although neonates may have a comparable clinical status at baseline (gestational age 27 weeks), their clinical course in the following days is perceived as an important determinant of bleeding risk. We have developed a model that allows clinicians to quantify bleeding risk and adjust it as the clinical situation of the neonate changes.

Future validation studies should externally validate and preferably expand the model, to improve its predictive accuracy. Once a larger, externally validated model has been developed, it can be used to study the effect of platelet transfusion indications based on predicted risk of bleeding in an impact study. Ultimately, this is a first step towards individualized platelet transfusion guidelines. Individualized guidelines are important because several studies have shown that there is a large discrepancy between the number of thrombocytopenic neonates receiving platelet transfusions (75%) and the number of neonates who develop major bleeding (9%).<sup>5,20</sup> These numbers are comparable to our results: 70% of neonates received transfusions and 11% developed major bleeding. In addition, results of a recent randomized trial indicate platelet transfusion-related harm when using a platelet count threshold of 50x10<sup>9</sup>/L compared to 25x10<sup>9</sup>/L. Although the overall results of this study showed benefit associated with the low threshold, not all neonates in the high threshold group developed major bleeding or died. Moreover, 19% of neonates in the low threshold group died or developed major bleeding. This indicates that a

**Table 2.** Types of bleeding.

Major bleeds, n (%)	71	(11)
Type of major bleeding, n (%)	32	(45)
Uni-/bilateral IVH grade 3 with or without parenchymal involvement		
IVH grade 1 or 2 (uni- or bilateral) with parenchymal involvement	4	(6)
Solitary (non-cerebellar) parenchymal hemorrhage	4	(6)
Cerebellar parenchymal hemorrhage	11	(15)
Subdural hemorrhage	4	(6)
Pulmonary hemorrhage	12	(17)
Gastrointestinal hemorrhage	4	(6)

Eight bleeds (of 71) were excluded from the model because they occurred more than 10 days after T<sub>0</sub>: one cerebellar, one IVH grade 1 plus basal ganglia infarction, one IVH grade 1 and grade 2 plus basal ganglia infarction, one gastrointestinal bleed, one pulmonary bleed, one bilateral IVH grade 3, one frontal-parietal bleed and one subdural hemorrhage. IVH: intraventricular hemorrhage.

platelet count-based transfusion threshold does not accurately separate neonates whose bleeding or death will be prevented by a platelet transfusion. A threshold that includes clinical variables, such as one based on our dynamic prediction model, might perform better and thereby improve outcomes.

It is important to note that individual covariates in the model should not be interpreted as causal associations, because the associations may be confounded in multiple ways. For example, IUGR was associated with lower predicted bleeding risk in our model, but we cannot conclude that IUGR protects against bleeding. Firstly, because IUGR is also a risk factor for thrombocytopenia, and we restricted our population to neonates with thrombocytopenia. It is possible that other causes of thrombocytopenia, for example viral infections, are associated with a higher risk of bleeding than that of IUGR. A neonate with thrombocytopenia as a result of IUGR is therefore not protected by IUGR, but has a lower bleeding risk because the thrombocytopenia was not caused by a viral infection. This is an epidemiological concept called collider stratification bias.<sup>21</sup> Secondly, perhaps neonates with IUGR received more treatments intended to decrease the risk of bleeding as compared to neonates without IUGR, as neonatologists perceived them to be at higher risk of bleeding (confounding by indication). And lastly, because the number of events in our study was limited, we were not able to cor-

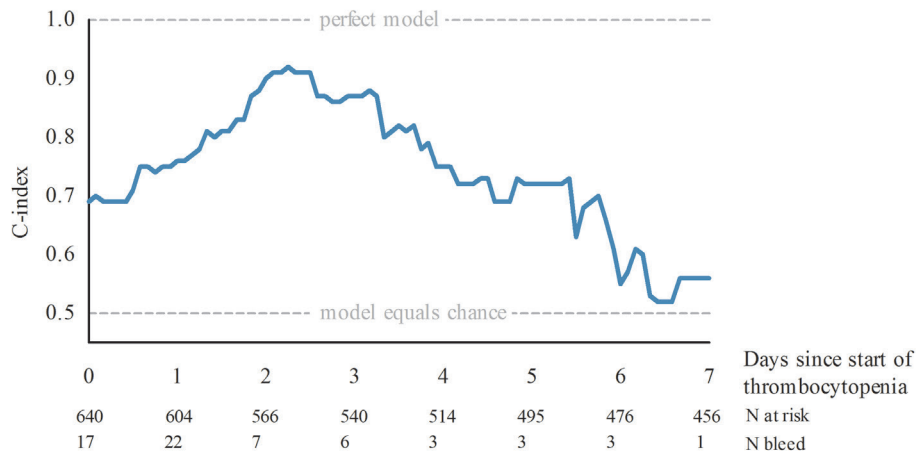


**Figure 3. Dynamic, cross-validated c-index.** This graph represents the dynamic, cross-validated c-index of the main model. A c-index of 1 resembles a model that discriminates perfectly between patients with and without major bleeding, while a c-index of 0.5 indicates that the prediction is as good as chance. For each time-point, the number at risk at the beginning of that day has been reported, as well as the total number of major bleeds that occurred during those 24 hours. For example, at the start of day 1, the number of patients still at risk was 604, and during this day 22 neonates developed a major bleed.

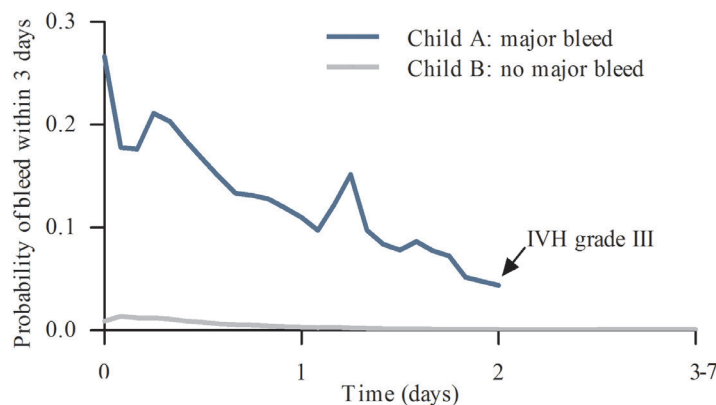


**Figure 4. Change in probability of having a major bleed within 3 days for two example patients.** Day 0 is the day of onset of severe thrombocytopenia ( $T_0$ ). Characteristics of child A: gestational age (weeks+days) 27+2, birthweight 1100 grams, 2 days old at  $T_0$ , sepsis, mechanical ventilation, two platelet transfusions, platelet counts ( $\times 10^9/L$ ): 41, 104, 47, and 88. Bilateral grade III intraventricular hemorrhage on day 2. Characteristics of child B: gestational age (weeks+days) 32+3, birth weight 1175 grams, 5 days old at  $T_0$ , sepsis, no mechanical ventilation, no platelet transfusions, platelet counts ( $\times 10^9/L$ ) 4, 53, 49, 63, 195 and 376. No major bleed. Days 3-7 not shown because no substantial change in bleeding risk occurred. During study days 1-3, the predicted risk of major bleeding within the subsequent 3 days is substantially higher in child A than in child B, indicating that the use of this prediction model during that time-period would have correctly identified child A as being at a high risk of bleeding.

rect for all possible confounders. In short, the association between IUGR and bleeding is complex, our model only indicates that it is a good predictor for bleeding, but we cannot draw any causal conclusion based on this information. This applies to all individual covariates in the model.

Various possible limitations of our study need to be discussed. Firstly, we could not externally validate our model because a similar database is currently not available. Secondly, identification of prognostic variables could possibly have been improved with a prior systematic review assessing all potential predictors. However, despite this limitation, our model contains variables generally considered best candidates for predicting major bleeding, as many of them were included in various existing baseline models. Some variables, such as mean platelet volume and immature platelet count, could not be included in our model because they were not routinely measured. Thirdly, the time a major bleed occurs is not similar to the time it is diagnosed on an ultrasound scan, because major intracranial bleeds in neonates are often asymptomatic, and detected during routine screening. To address this issue, we performed two additional sensitivity analyses, one in which we corrected time of bleeding based on whether or not minor bleeding was visible on prior ultrasound scans, and one in which we removed events for which we could not determine whether they occurred prior to or after the bleeding. Results of these analyses

showed only minor changes in hazard ratios of individual coefficients, suggesting that this problem does not substantially affect the predictive power of our model (*Online Supplementary Table S3*). Fourthly, after day 6, the c-index drops below 0.60, possibly due to a lower event rate, therefore the model should be applied with caution after day 6. We hypothesize that the variation in predictive accuracy over time, depicted in Figure 2, may be caused by a balance between having enough clinical information to predict (difficult on days 1 and 2), and enough events to fit a good model (difficult after day 4). Fifthly, the risk of bleeding in neonates in our population may have been affected by treatment with platelet transfusions. Therefore, the risks calculated using our model may be an underestimation of the 'true' risk (without transfusion). However, there are no cohorts available in which platelet transfusions were not administered and various studies, including the previously described randomized controlled trial, suggest that the effect of platelet transfusions on bleeding risk may be limited.<sup>6,22-24</sup> We therefore estimate that our model's predictions are accurate. Finally, four neonates had a gestational age at birth of less than 24 weeks. In addition, local policies differed with respect to active support for neonates born at a gestational age between 24+0 and 25+6 weeks. Therefore, the neonates with a gestational age less than 26 weeks in our population might be a selection of neonates for whom good out-

**Table 3. The dynamic prediction model.**

	Hazard ratio	95% CI
<i>Covariates with time-constant effects</i>		
Gestational age (days)	1.00	0.98 – 1.02
Postnatal age (days)	0.88	0.83 – 0.94*
Mechanical ventilation	5.08	2.03 – 10.65*
NEC/sepsis	0.85	0.43 – 1.58
Platelet transfusion	1.06	0.38 – 2.95
Interaction term log <sub>10</sub> platelet count and platelet transfusion	1.23	0.63 – 2.38
<i>Covariates with time-varying effects</i>		
LM (2-hour intervals)	2.30	0.89 – 5.94
LM2 (2-hour intervals)	0.85	0.74 – 0.98*
IUGR constant	0.51	0.17 – 1.59
IUGR time-varying: LM	0.31	0.09 – 1.14
IUGR time-varying: LM <sup>2</sup>	1.22	1.04 – 1.44*
Log <sub>10</sub> platelet count constant	1.74	0.72 – 4.24
Log <sub>10</sub> platelet count time-varying LM	0.35	0.19 – 0.63*
Log <sub>10</sub> platelet count time-varying: LM <sup>2</sup>	1.12	1.03 – 1.21*

A hazard ratio >1 indicates that an increase of the risk factor is associated with a higher risk of bleeding. For example, a mechanically ventilated neonate has a 5.08 times higher risk of bleeding than a neonate who is not mechanically ventilated. If both boundaries of the confidence interval are either higher than 1 or lower than 1, the variable is a statistically significant predictor, indicated by \*. LM: landmark time, linear interaction. LM2: landmark time, quadratic interaction. LM or landmark time refers to time since onset of severe thrombocytopenia (time-dependent variable), in 2-hour time intervals. Postnatal age refers to the postnatal age at the onset of severe thrombocytopenia (baseline variables). Time-varying covariates should not be confused with time-dependent covariates, such as platelet count or platelet transfusion, for which the value of the variable is not fixed (it is not a baseline variable) but can change over time. In time-varying covariates, the effect of the covariate can change over time, for example, the strength and direction of a potential association of intrauterine growth retardation with bleeding could be different immediately after the onset of thrombocytopenia compared to a few days after the onset of thrombocytopenia, due to interactions with other risk factors and changes in the clinical situation of the neonate. NEC: necrotizing enterocolitis; IUGR: intrauterine growth retardation. 95% CI: 95% confidence interval.

comes were expected. The model should thus be applied with caution in neonates with a gestational age of less than 26 weeks.

Strengths of our study are the size of the cohort and the fact that we selected the predictors prior to data analysis rather than performing a stepwise selection. In addition, our data collection was meticulous and we performed multiple additional sensitivity analyses to confirm the robustness of our model. Our model is easy to apply,

**References**

- Baer VL, Lambert DK, Henry E, Christensen RD. Severe thrombocytopenia in the NICU. *Pediatrics*. 2009;124(6):e1095-100.
- von Lindern JS, van den Bruele T, Lopriore E, Walther FJ. Thrombocytopenia in neonates and the risk of intraventricular hemorrhage: a retrospective cohort study. *BMC Pediatr*. 2011;11(1):16.
- Fustolo-Gunnink SF, Huijssen-Huisman EJ, van der Bom JG, et al. Are thrombocytopenia and platelet transfusions associated with major bleeding in preterm neonates? A sys-

- tematic review. *Blood Rev*. 2019;36:1-9.
- Stanworth SJ, Clarke P, Watts T, et al. Prospective, observational study of outcomes in neonates with severe thrombocytopenia. *Pediatrics*. 2009;124(5):e826-34.
- von Lindern JS, van den Bruele T, Lopriore E, Walther FJ. Thrombocytopenia in neonates and the risk of intraventricular hemorrhage: a retrospective cohort study. *BMC Pediatr*. 2011;11(1):16.
- Curley A, Stanworth SJ, Willoughby K, et al. Randomized trial of platelet-transfusion thresholds in neonates. *N Engl J Med*. 2018;380(3):242-251.
- New H V., Berryman J, Bolton-Maggs PHB,

- et al. Guidelines on transfusion for fetuses, neonates and older children. *Br J Haematol*. 2016;175(5):784-828.
- Luque MJ, Tapia JL, Villarreal L, et al. A risk prediction model for severe intraventricular hemorrhage in very low birth weight infants and the effect of prophylactic indomethacin. *J Perinatol*. 2014;34(1):43-48.
- van de Bor M, Verloove-Vanhorick SF, Brand R, Keirse MJ, Ruys JH. Incidence and prediction of periventricular-intraventricular hemorrhage in very preterm infants. *J Perinat Med*. 1987;15(4):333-339.
- Heuchan AM, Evans N, Henderson Smart DJ, Simpson JM. Perinatal risk factors for

**Table 4. Risk predictions for different clinical scenarios.**

Patient’s characteristics: GA 28 weeks, platelet count 10x10<sup>9</sup>/L at day 3 of life (first time <50x10<sup>9</sup>/L), no transfusion.

	Ventilation	No ventilation
NEC/sepsis; IUGR	8%	2%
No NEC/sepsis No; IUGR	17%	3%
NEC/sepsis No; IUGR	14%	3%
No NEC/sepsis; IUGR	9%	2%

Patient’s characteristics: GA 28 weeks, platelet count 50x10<sup>9</sup>/L at day 3 of life (first time <50x10<sup>9</sup>/L) , no transfusion.

	Ventilation	No ventilation
NEC/sepsis; IUGR	11%	2%
No NEC/sepsis No; IUGR	24%	5%
NEC/sepsis No; IUGR	20%	4%
No NEC/sepsis; IUGR	13%	3%

GA: gestational age; NEC: necrotizing enterocolitis. IUGR: intrauterine growth retardation.

because we have used clear and simple definitions of the covariates. Once the model has been externally validated, we will develop an online calculator, with which it should only take a few minutes to enter the variables and calculate absolute risk of bleeding.

In short, this dynamic prediction model allows clinicians to quantify bleeding risk and adjust it as the clinical situation of the neonate changes. Risk can be predicted at any time-point during the first week after the onset of severe thrombocytopenia. This is a promising model that should be explored in future studies, as it is a first step towards individualized platelet transfusion guidelines.

**Acknowledgments**

*This research was supported by grant PPOC-12-012027 from Sanquin Research, Amsterdam, the Netherlands. The sponsor of this study is a nonprofit organization that supports science in general. It had no role in gathering, analyzing, or interpreting the data. SFFG is a PhD candidate at the University of Amsterdam. This work has been submitted in partial fulfillment of the requirement for the PhD. We thank Sahile Makineli and Nick van Hijum, both medical students at the time of this study, for their contribution to data collection and data analysis. We also thank Yavanna Oostveen, data manager, for her contribution to the data management.*

- major intraventricular haemorrhage in the Australian and New Zealand Neonatal Network, 1995-97. *Arch Dis Child Fetal Neonatal Ed.* 2002;86(2):F86-90.
11. Singh R, Visintainer P. Predictive models for severe intraventricular hemorrhage in preterm infants. *J Perinatol.* 2014;34(10):802-802.
  12. Vogtmann C, Koch R, Gmyrek D, Kaiser A, Friedrich A. Risk-adjusted intraventricular hemorrhage rates in very premature infants. *Dtsch Arztebl Int.* 2012;109(31-32):527-533.
  13. Gleißner M, Jorch G, Avenarius S, Kinderheilkunde Z, Magdeburg OU. Risk factors for intraventricular hemorrhage in a birth cohort of 3721 premature infants. *J Perinat Med.* 2000;28(2):104-110.
  14. Horbar JD, Pasnick M, McAuliffe TL, Lucey JF. Obstetric events and risk of periventricular hemorrhage in premature infants. *Am J Dis Child.* 1983;137(7):678-681.
  15. Koch R, Gmyrek D, Vogtmann C. Risicoadjustierte Qualitätsbeurteilung in Perinatalzentren ausgehend von der Perinatal- und Neonatallerhebung in Sachsen. *Z Geburtsh Neonatol.* 2005;209(6):210-218.
  16. Collins GS, Reitsma JB, Altman DG, Moons KGM. Transparent reporting of a multivariable prediction model for individual prognosis or diagnosis (TRIPOD): the TRIPOD statement. *BMJ.* 2014;350:g7594.
  17. Fontein DBY, Klinten Grand M, Nortier JWR, et al. Dynamic prediction in breast cancer: proving feasibility in clinical practice using the TEAM trial. *Ann Oncol.* 2015;26(6):1254-1262.
  18. van Houwelingen J, Le Cessie S. Predictive value of statistical models. *Stat Med.* 1990;9(11):1303-1325.
  19. Cremer M, Sola-Visner M, Roll S, et al. Platelet transfusions in neonates: practices in the United States vary significantly from those in Austria, Germany, and Switzerland. *Transfusion.* 2011;51(12):2634-2641.
  20. Stanworth SJ, Clarke P, Watts T, et al. Prospective, observational study of outcomes in neonates with severe thrombocytopenia. *Pediatrics.* 2009;124(5):e826-834.
  21. Whitcomb B, Schisterman E, Perkins N, Platt R. Quantification of collider-stratification bias and the birthweight paradox. *Paediatr Perinat Epidemiol.* 2009;23(5):394-402.
  22. Usemann J, Garten L, Bühner C, Dame C, Cremer M. Fresh frozen plasma transfusion - a risk factor for pulmonary hemorrhage in extremely low birth weight infants? *J Perinat Med.* 2017;45(5):627-633.
  23. Sparger KA, Assmann SF, Granger S, et al. Platelet transfusion practices among very-low-birth-weight infants. *JAMA Pediatr.* 2016;170(7):687-694.
  24. Andrew M, Vegh F, Caco C, et al. A randomized, controlled trial of platelet transfusions in thrombocytopenic premature infants. *J Pediatr.* 1993;123(2):285-291.

# Christmas disease in a Hovawart family resembling human hemophilia B Leyden is caused by a single nucleotide deletion in a highly conserved transcription factor binding site of the *F9* gene promoter

Bertram Brenig,<sup>1\*</sup> Lilith Steingraber<sup>1\*</sup>, Shuwen Shan,<sup>1</sup> Fangzheng Xu,<sup>1</sup> Marc Hirschfeld,<sup>1,2</sup> Reiner Andag,<sup>3</sup> Mirjam Spengeler,<sup>4</sup> Elisabeth Dietschi,<sup>4</sup> Reinhard Mischke<sup>5</sup> and Tosso Leeb<sup>4</sup>

<sup>1</sup>University of Göttingen, Institute of Veterinary Medicine, Göttingen, Germany;

<sup>2</sup>Department of Obstetrics and Gynecology, Freiburg University Medical Center, Freiburg, Germany; <sup>3</sup>University Medical Center Göttingen, Institute for Clinical Chemistry, Göttingen, Germany; <sup>4</sup>Institute of Genetics, University of Bern, Bern, Switzerland and

<sup>5</sup>Small Animal Clinic, University of Veterinary Medicine Hannover Foundation, Hannover, Germany

\*BB and LS contributed equally to this work.



Ferrata Storti Foundation

Haematologica 2019

Volume 104(11):2307-2313

## ABSTRACT

Hemophilia B is a classical monogenic, X-chromosomal, recessively transmitted bleeding disorder caused by genetic variants within the coagulation factor IX gene (*F9*). Although hemophilia B has been described in dogs, it has not yet been reported in the Hovawart breed. Here we describe the identification of a Hovawart family transmitting typical signs of an X-linked bleeding disorder. Five males were reported to suffer from recurrent hemorrhagic episodes. A blood sample from one of these males with only 2% of the normal concentration of plasma factor IX together with samples from seven relatives were provided. Next-generation sequencing of the mother and grandmother revealed a single nucleotide deletion in the *F9* promoter. Genotyping of the deletion in 1,298 dog specimens including 720 Hovawarts revealed that the mutant allele was only present in the aforementioned Hovawart family. The deletion is located 73 bp upstream of the *F9* start codon in the conserved overlapping DNA binding sites of hepatocyte nuclear factor 4 $\alpha$  (HNF-4 $\alpha$ ) and androgen receptor (AR). The deletion only abolished binding of HNF-4 $\alpha$ , while AR binding was unaffected as demonstrated by electrophoretic mobility shift assay using human HNF-4 $\alpha$  and AR with double-stranded DNA probes encompassing the mutant promoter region. Luciferase reporter assays using wild-type and mutated promoter fragment constructs transfected into Hep G2 cells showed a significant reduction in expression from the mutant promoter. The data provide evidence that the deletion in the Hovawart family caused a rare type of hemophilia B resembling human hemophilia B Leyden.

## Introduction

Hemophilia B (Christmas disease) is a recessive, X-linked bleeding disorder caused by genetic variants within the clotting factor IX gene (*F9*) resulting in the absence or insufficient levels of factor IX (FIX) in the blood.<sup>1</sup> In humans hemophilia B is also known as the “royal disease” as it was transmitted into several European royal dynasties by Queen Victoria.<sup>2,3</sup> As of present, 1,113 unique *F9* variants have been described in humans.<sup>4</sup> The majority of the pathogenic variants are located within exons (n=923) and intronic regions (n=137) of *F9*. Only 33 variants (2.96%) have been described in the 5'-UTR (n=28) and 3'-UTR (n=5) accounting for 2.52% and 0.45% of human pathogenic hemophilia B variants, respectively.<sup>4</sup>

Although the first reports about canine hemophilia B date back to the early 1960s

## Correspondence:

BERTRAM BRENING  
bbrenig@gwdg.de

Received: December 26, 2018

Accepted: March 6, 2019.

Pre-published: March 7, 2019.

doi:10.3324/haematol.2018.215426

Check the online version for the most updated information on this article, online supplements, and information on authorship & disclosures: [www.haematologica.org/content/104/11/2307](http://www.haematologica.org/content/104/11/2307)

©2019 Ferrata Storti Foundation

Material published in *Haematologica* is covered by copyright. All rights are reserved to the Ferrata Storti Foundation. Use of published material is allowed under the following terms and conditions:

<https://creativecommons.org/licenses/by-nc/4.0/legalcode>.

Copies of published material are allowed for personal or internal use. Sharing published material for non-commercial purposes is subject to the following conditions:

<https://creativecommons.org/licenses/by-nc/4.0/legalcode>, sect. 3. Reproducing and sharing published material for commercial purposes is not allowed without permission in writing from the publisher.



and this was the first disorder in dogs characterized on the DNA level, data on hemophilia B cases in dogs remain rather scarce compared to data from humans.<sup>5-8</sup> For instance, in the Cairn Terrier colony of the Francis Owen Blood Research Laboratory (University of North Carolina, Chapel Hill, NC, USA) a G>A transition (NC\_006621.3:g.109,532,018G>A) in exon 8 causing an amino acid exchange (NP\_001003323.1:p.Gly418Glu) that resulted in a complete lack of circulating FIX was detected in affected dogs.<sup>9</sup> Due to a complete deletion of *F9* in a Labrador Retriever, FIX inhibitors were produced after transfusion of canine blood products.<sup>10</sup> In a study of Pit Bull Terrier mixed breed dogs and Airedale Terrier dogs a large deletion of the entire 5' region of *F9* extending to exon 6 was found in the former and a 5 kb insertion disrupting exon 8 was described in the latter.<sup>11</sup> As in the Labrador Retriever with hemophilia B, FIX inhibitors were produced in both breeds. A mild form of hemophilia B in German Wirehaired Pointers was caused by a 1.5 kb Line-1 insertion in intron 5 of *F9* at position NC\_006621.3:g.109,521,130.<sup>12</sup> Until today, hemophilia B has been described in four mixed-breed dogs and nine dog breeds, i.e. German Shepherd, Lhasa Apso, Labrador Retriever, Rhodesian Ridgeback, Airedale Terrier, Cairn Terrier, Maltese, Mongrel and German Wirehaired Pointer.<sup>9-17</sup>

In the canine cases analyzed so far on the DNA level, mutations have been observed only in exons and introns of *F9*, whereas alterations of the *F9* promoter have not yet been reported. In humans promoter variants have been detected and result in the so-called hemophilia B Leyden characterized by low levels of FIX until puberty, whereas after puberty FIX concentrations rise to almost normal levels.<sup>18-20</sup> Since its first description, the genetic background of human hemophilia B Leyden was elucidated by various studies identifying variants in different transcription factor binding sites in the *F9* promoter including the androgen-responsive element (ARE), hepatocyte nuclear factor 4 $\alpha$  (HNF4 $\alpha$ ), one cut homeobox (ONECUT1/2) and CCAAT/enhancing-binding protein  $\alpha$  (C/EBP $\alpha$ ) binding sites.<sup>21,22</sup> HNF4 $\alpha$  is a liver-enriched member of the nuclear receptor superfamily of ligand-dependent transcription factors and has been associated with several disorders, including diabetes, atherosclerosis, hepatitis, cancer, and hemophilia.<sup>23</sup> Promoter analyses have identified at least 140 genes with HNF4 $\alpha$  binding sites. A recent, more detailed analysis using protein binding microarrays identified an additional 1,400 potential binding sites.<sup>24,25</sup> Hence, HNF4 $\alpha$  plays an important role in the regulation of numerous genes especially in the maintenance of many liver-specific functions. Liver-specific HNF4 $\alpha$ -null mice have been used to study the involvement of hepatic HNF4 $\alpha$  in blood coagulation. In the murine model it was shown that expression of factors V, XI, XII, and XIII B depends directly on hepatic HNF4 $\alpha$  and FIX expression was decreased with significantly prolonged activated partial thromboplastin time (aPTT).<sup>26</sup> Ten of the so far identified 28 5'-UTR variants (35.7%) are located within the overlapping binding sites of the androgen receptor (AR) and HNF4 $\alpha$  in the human *F9* promoter.<sup>4,21</sup> Four variants at positions -21, -20 and -19 only affect HNF4 $\alpha$  binding and all of them have been shown to cause hemophilia B Leyden.<sup>19,27-30</sup> The remaining six variants at positions -26, -24 and -23, located in the overlapping region, cause the so-called hemophilia B

Brandenburg.<sup>31,32</sup> Unlike the classical hemophilia B Leyden, FIX levels in patients with these variants cannot be restored by testosterone-driven AR activity and remain low after puberty with no clinical recovery.<sup>21,32</sup>

## Methods

### Animals and genomic DNA isolation

Canine blood and/or hair samples were collected by local veterinarians. The collection of samples was approved by the Lower Saxony State Office for Consumer Protection and Food Safety (33.19-42502-05-15A506) according to §8a Abs. 1 Nr. 2 of the German Animal Protection Law (TierSchG). Blood collected into EDTA and/or hair samples were provided by different Hovawart and dog breeders with written consent from the dogs' owners. DNA was extracted from 30-50 hair roots using the QIAamp DNA Mini Kit (Qiagen, Hilden, Germany) according to the manufacturer's instructions.<sup>33</sup> A salting out procedure was used to obtain DNA from the EDTA blood samples.<sup>34</sup> Additional DNA samples deposited with the Institute of Veterinary Medicine were used as controls. All samples were pseudonymized using internal identities.

### Next-generation sequencing and genotyping

DNA from animals #4 and #6 was used for next-generation sequencing on an Illumina HiSeq2500. The quality of the fastq-files was analyzed using FastQC 0.11.7.<sup>35</sup> Total reads of 1,029,601,630 (#4; sequencing depth 51x) and 1,000,503,256 (#6; sequencing depth 50x) were obtained and mapped to the reference canine *F9* gene (NC\_006621.3, region 109,501,341 to 109,533,798; CanFam3.1) using DNASTAR Lasergene Genomics Suite SeqMan NGen 15.2.0 (130).<sup>36-40</sup>

Targeted genotyping of the promoter deletion was done by polymerase chain reaction (PCR) amplification with primers *cfa\_F9\_Ex1\_F* (5'-CCACTGAGGGAGATGGACAC-3') and *cfa\_F9\_Ex1\_R* (5'-CCCACATGCTGACGACTAGA-3') resulting in a fragment of 328 bp (wildtype) or 327 bp (deletion) spanning the variant position. The resulting PCR products were either directly sequenced on an ABI 3730 Genetic Analyzer (Thermo Fisher Scientific, Basel, Switzerland) or genotypes were determined by restriction fragment length polymorphism analysis after cleavage with *RsaI*. The wildtype allele generated two fragments of 52 bp and 276 bp while the allele with the deletion remained uncut.

### Electrophoretic mobility shift assay

For the electrophoretic mobility shift assay, biotin-labeled, double-stranded wildtype (*cfa\_F9n\_wt\_Biotin*: 5'-CAGAAGTAAAT-ACAGCTCAACTTGTACTTTGGAACAACTGGTCAACC-3') and mutated (*cfa\_F9n\_mut\_Biotin*: 5'-CCAGAAGTAAAT-ACAGCTCAACTTGTATTTGGAACAACTGGTCAACC-3') oligonucleotides were synthesized (Integrated DNA Technologies IDT, Leuven, Belgium) harboring the overlapping HNF4 $\alpha$  and AR binding sites (underlined). The position of the deleted C-nucleotide is indicated in bold and italics. Recombinant human HNF4 $\alpha$  and human AR overexpression lysate were purchased from Origene Technologies Inc. (Rockville, MD, USA).

DNA was detected using the Chemiluminescent Nucleic Acid Detection Module Kit (Thermo Scientific, USA) with minor modifications, i.e. membranes were incubated for 1 min in the substrate working solution.

### Luciferase assay

pGL3 Luciferase Reporter Vectors (pGL3-Basic, pGL3-Control)

were used for the luciferase assay (Promega, Mannheim, Germany). The wildtype *F9* promoter fragment (971 bp wildtype) was generated by PCR using primers *cfa9\_HindIII\_F\_neu* (5'-CGTAGACTTAGCACTGTTCAAAGCTTTCACACACACAGTTCTTAAAT-3') and *cfa9\_HindIII\_R\_neu* (5'-ATGGCTAGCAACCGTCTAAGAAGCTTAATTGTGCAAGGAGCAAGG-3'). The mutated *F9* promoter fragment (970 bp) was generated by PCR using primers *cfa9\_HindIII\_F* (5'-ATCGTCAAGCTTTCACACACACAGTTCTTAAAT-3') and *cfa9\_HindIII\_R* (5'-CGTACGAAGCTTAATTGTGCAAGGAGCAAGG-3'). For cloning into the *HindIII* restriction site of pGL3, primers were designed with an unspecific random 5'-tag (italics) followed by a *HindIII* restriction site (underlined) (*Online Supplementary Figure S1*). DNA from female carrier #6 served as a template for amplification. Low expression levels of C/EBP in Hep G2 cells were complemented by co-transfection of a C/EBP $\alpha$  expression vector.<sup>22</sup> Data are presented as relative response ratios.<sup>41</sup> A Mann-Whitney U test was used to determine statistical significance. Values were considered statistically significant when  $P < 0.05$  (weakly significant),  $P < 0.01$  (medium-strength significance) and  $P < 0.001$  (strongly significant).

**Other methods**

Further details of the study methods are given in the *Online Supplementary Appendix*.

**Results**

Hemophilias are rare diseases in dogs and hence it was rather coincidental that a case in a Hovawart (#3, Figure 1) was reported to us. With the reconstruction of the pedigree using the online dog breed database and pedigree data of individual dogs provided by the owners it was possible to trace the disease back to the female carrier #39 (Figure 1, *Online Supplementary Figure S2*).<sup>42</sup> In the studied family the hemophilia was transmitted to animals #19, #4 and #6. Bitch #19 had one litter with three hemophilic males (#48, #51, #53). Bitches #4 and #6 had litters with one affected male each, #60 and #3, respectively. Although DNA samples from animals #48, #51, #53 and #60 were not available, blood parameters and medical reports about recurrent hemorrhagic episodes were provided (*Online*

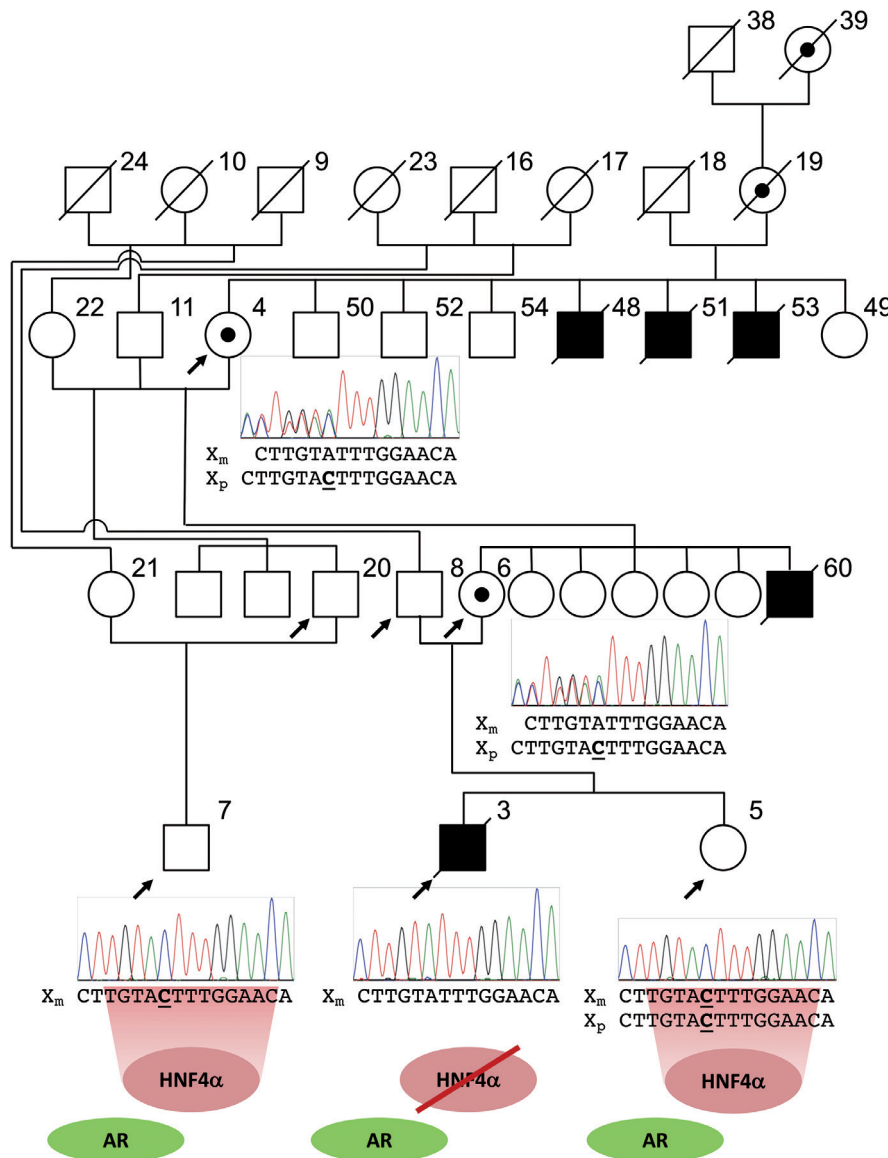


**Figure 1.** Pedigree section of the hemophilia B Leyden Hovawart family and DNA sequence comparison of the mutant hepatocyte nuclear factor 4 $\alpha$ /androgen receptor binding site in the promoter of canine *F9* in the hemophilic male (#3) and relatives (#4 grandmother, #5 sister, #6 mother, #7 cousin). Pedigree symbols are according to the standardized human pedigree nomenclature.<sup>61</sup> Individuals are pseudonymized using internal identities. DNA samples were available from individuals indicated with an arrow. DNA sequences of heterozygous bitches #4 and #6 (female carriers) show overlapping peaks with similar heights 5' of the deletion position. For males #48, #51, #53 and #60, signs of hemophilia (*Online Supplementary Table S1*) were reported and the dogs had to be euthanized after recurrent hemorrhages. X<sub>m</sub>: maternal X chromosome; X<sub>p</sub>: paternal X chromosome; HNF4 $\alpha$ : hepatocyte nuclear factor 4 $\alpha$  binding site (consensus sequence: 5'-TGNACTTTG-3');<sup>21,48</sup> AR: 3'-part of the androgen receptor binding site (consensus sequence: 5'-AGNACANNNTGNTCT-3').<sup>21,48</sup>

Supplementary Table S1). These males had increased aPTT ratios of 2.93 (#53) to 4.76 (#51) indicative of defects in the intrinsic coagulation pathway and also reduced FIX concentrations in the blood as is normally the case in hemophilia B. The affected dog #3 presented only 2% of the standard FIX concentration. The female carriers #4 and #6 showed aPTT ratios within the reference range. FIX concentrations, however, were slightly below the reference range (#6). This was not surprising as it has been shown that minute reductions in FIX concentrations might not always be reflected in an aPTT increase because of the sensitivity of commercial reagents.<sup>43</sup> The clinical signs together with the blood coagulation parameters and X-linked transmission supported the diagnosis of hemophilia B. The definite clinical diagnosis prompted us to search for the molecular cause initially on the DNA level. The canine *F9* gene is located on chromosome X (CFAX) between positions 109,501,341 (transcription start site) and 109,533,798 and has a length of 32,458 bp (NC\_006621.3, CanFam3.1). The canine *F9* gene, similarly to that of other mammals, has eight exons with an open reading frame of 1,356 bp coding for 452 amino acids.<sup>44</sup> DNA of female carriers #4 and #6 was subjected to whole genome sequencing and aligned to the canine reference *F9* gene sequence. Surprisingly, only six sequence variants outside the coding regions of *F9* were identified (Table 1). Five variants were located in introns and were excluded as the cause of the hemophilia B in the Hovawarts because these variants were also detected in unaffected controls. The remaining variant (deletion) was located in the promoter of *F9* 73 bp upstream of the start codon (Online Supplementary Figures S1 and S3). As this deletion was located within a putative transcription factor binding site of HNF4 $\alpha$  and AR, which had been shown in humans to be important for *F9* expression and mutated in hemophilia B Leyden and Brandenburg,<sup>31,32</sup> this position was analyzed in more detail.

Figure 1 shows the segregation of the nucleotide deletion in the affected Hovawart family. The female carriers #4 and #6 were heterozygous, as evidenced by the overlap-

ping peaks with similar heights 5' of the deletion position. The affected male #3 was hemizygous for the deleted allele whereas his sister #5 and cousin #7 were homozygous wildtype. Genotyping of 1,298 dogs (including 83 different breeds, 720 unrelated Hovawarts, and 12 Hovawart family members) demonstrated the occurrence of the deletion only among members of the affected Hovawart family (Table 2, Online Supplementary Table S2). To provide proof that the deletion represented the causative genetic variant and resulted in the low expression of *F9*, functional analyses using electrophoretic mobility shift and luciferase reporter assays were performed.

As shown in Figure 2, no binding of recombinant HNF4 $\alpha$  to the mutated promoter region was detected. On the other hand, the AR lysate clearly showed binding to both fragments and hence the deletion seems not to influence AR binding to the androgen-responsive element in the canine *F9* promoter. To analyze the effect of the promoter variant on *F9* expression, wildtype and mutated promoter fragment luciferase constructs were transfected into Hep G2 cells. As shown in Figure 3 the mutated promoter fragment resulted in a statistically highly significant ( $P=2.2 \times 10^{-9}$ ) reduction of the relative response ratio to approximately 34.6% of the wildtype promoter in the presence of C/EBP (+ C/EBP). C/EBP is clearly also an important transcription factor in the regulation of the canine *F9* promoter as shown when C/EBP was not co-transfected (- C/EBP). In the absence of C/EBP the relative response ratio of the wildtype promoter was 29.8%. On the other hand there were no significant differences between the mutated promoter fragment (+/- C/EBP) and the wildtype promoter fragment (- C/EBP). As for variants of the HNF4 $\alpha$  site, disruption of the C/EBP binding site has also been shown to be causative for hemophilia B in humans.<sup>45,46</sup>

## Discussion

As in humans, hemophilia A and B are also rare diseases in dogs caused by sequence variants in the coagulation

**Table 1.** DNA sequence variants in the canine *F9* gene determined by next-generation sequencing of DNA of animals #4 and #6.

Position	Ref/Alt <sup>a</sup>	Gene region	HGVS <sup>b</sup> g.
X:109501492	C/-	5'-flanking region	NC_006621.3:g.109501492delC
X:109504229	C/-	intron 1	NC_006621.3:g.109504229delC
X:109505462	-/AG	intron 1	NC_006621.3:109505462_109505463insAG
X:109507446	-/A	intron 2	NC_006621.3:109507446_109507446insA
X:109510986	G/A	intron 3	NC_006621.3:g.109510986G>A
X:109524055	A/G	intron 6	NC_006621.3:g.109524055A>G

<sup>a</sup>Ref/Alt: reference nucleotide/alternate nucleotide; <sup>b</sup>HGVS: Human Genome Variation Society (<http://www.hgvs.org>).

**Table 2.** *F9* genotype frequencies

Genotype	HB <sup>a</sup> affected (n=1)	Hovawart		Control, unknown relationship (n= 720)	Other breeds <sup>b</sup> Controls (n= 567)
		HB carrier (n=2)	Control, related (n=12)		
C/C			12	720	567
C/-		2			
-/-	1				

<sup>a</sup>HB: hemophilia B; <sup>b</sup>dog breeds used as controls are listed in Online Supplementary Table S2.

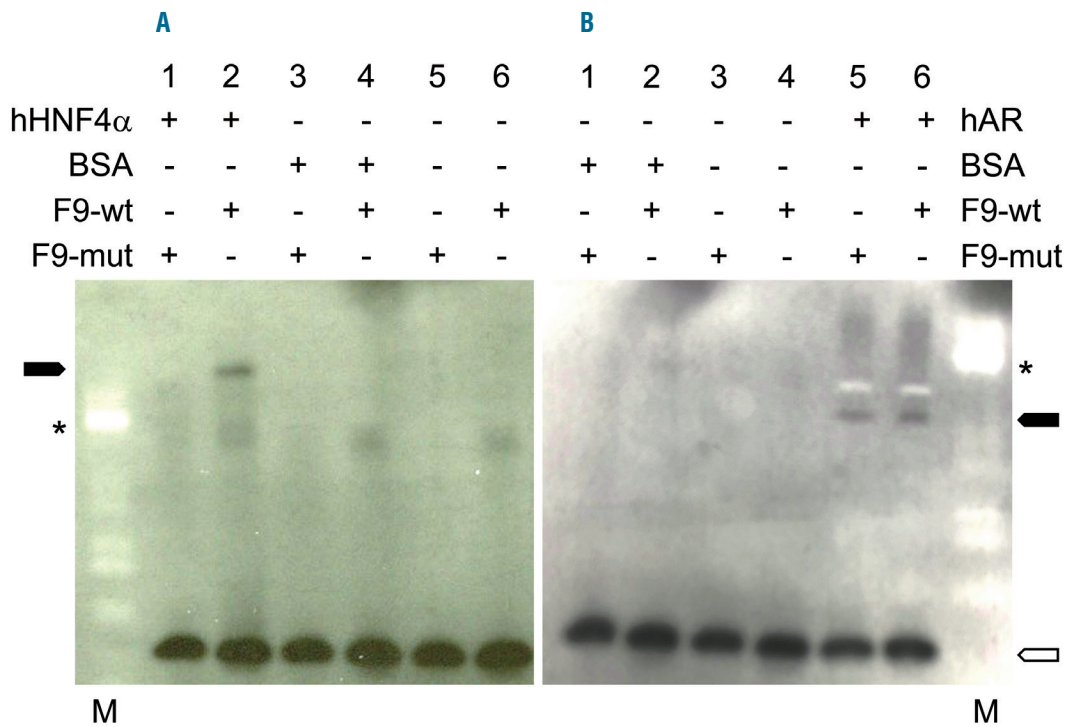


**Figure 2. Analysis of hepatocyte nuclear factor 4α and androgen receptor binding of wildtype and mutated F9 promoter regions using an electrophoretic mobility shift assay.** (A, B) Human hepatocyte nuclear factor 4α (HNF4α) and (B) androgen receptor (AR) were used to bind biotin-labeled wildtype and mutated F9 promoter fragments (F9-wt, F9-mut). Specific shifted bands (solid arrowheads) are detected in lane 2 (A) for HNF4α and lanes 5 and 6 (B) for AR. To test specificity, binding reactions were also performed using bovine serum albumin [BSA; lanes 3 and 4 (A), lanes 1 and 2 (B)]. In lanes 5 and 6 (A) and lanes 3 and 4 (B) no protein was added. Binding reactions were separated on 12% Tris-Glycine gels. X-ray films were cropped using GIMP 2.8.22. The 70 kDa protein marker band (PageRuler Prestained Protein Ladder, Fermentas) is indicated with an asterisk (lane M). The open arrowhead indicates unbound, free DNA.

factor VIII (*F8*) and IX (*F9*) gene, respectively.<sup>47</sup> Since the 1960s cases of canine hemophilia B have been reported and in 1989 the first description of the molecular cause in a Cairn Terrier population at the Francis Owen Blood Research Laboratory was published.<sup>5,8,9,44</sup>

Since then only six further types of variants, all of them affecting the coding region of the *F9* gene, *i.e.* deletions, insertions, missense variants, have been described as causative for canine hemophilia B.<sup>10-12,15,16</sup> The identification of a causative promoter variant in the Hovawart dogs described here is therefore unique in two respects: it is the first regulatory variant described in dogs and secondly this variant resembles a specific subtype of hemophilia B, known as hemophilia B Leyden, in humans.<sup>21</sup> Hitherto, 21 distinct variants in the human *F9* promoter have been determined in families affected by hemophilia B Leyden.<sup>48</sup> These variants cluster in the so-called Leyden-specific region (LSR) and interfere with the binding of different transcription factors, *e.g.* AR, HNF4α, ONECUT, and C/EBPα.<sup>49</sup> The deletion identified in the Hovawart dogs was located 73 bp upstream of the start codon of the canine *F9* gene corresponding to position -23 in the third human promoter cluster harboring the overlapping binding sites of AR and HNF4α.<sup>48</sup> Similar to analyses in humans, it was possible to show by electrophoretic mobility shift assay that the deletion in the canine promoter abolished HNF4α binding because it affects the highly conserved core sequence of the HNF4α binding motif.<sup>24</sup> On the other hand, binding of AR was not affected. This might be due to the fact that AR DNA-binding

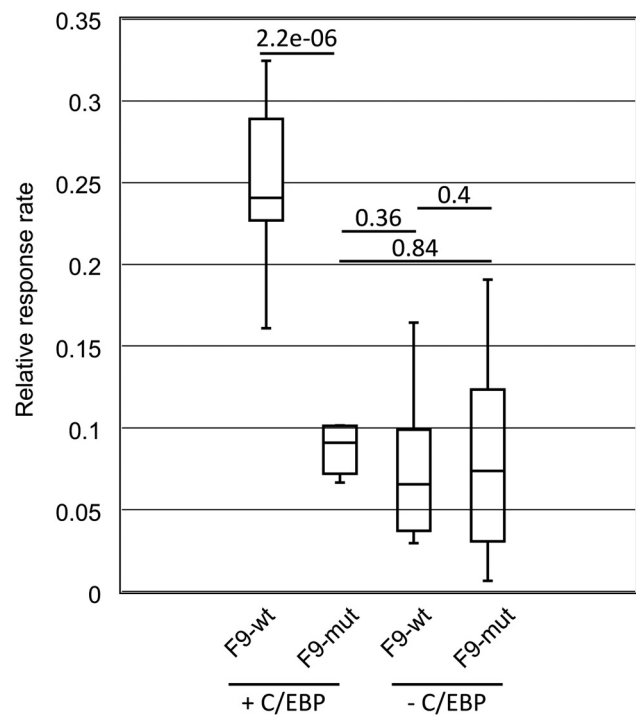


**Figure 3. Dual-luciferase reporter analysis of F9 promoter activities in Hep G2 cells.** Box and whisker plot showing the change of relative response ratios (RRR) between the wildtype (F9-wt) and mutant promoter (F9-mut) gene constructs. The lines in the boxes represent the medians. Whiskers indicate minimum and maximum RRR values. Values were normalized as described in the Online Supplementary Methods. P-values are indicated.

sites display an exceptional amount of sequence variation.<sup>50</sup> Although the C-deletion is located in the consensus TGTNCT-motif of class I AR-binding sites several alternative motifs, e.g. TGT TTC in the stomatin-like protein 3 gene or TGTATC in the prostate-specific antigen gene enhancer III region, have been reported.<sup>50-52</sup> Therefore, it can be assumed that the affected males would have recovered from hemophilia during puberty. To what extent a sex- or possibly also age-dependent amelioration of the hemophilia B Leyden, as described in humans and also a mouse model, might be present in the affected Hovawarts remains to be determined.<sup>49,53</sup> In this respect the Hovawart family could also be of interest as a model in the comparative analysis of age-dependent normalization of *F9* expression in symptomatic carriers of hemophilia B Leyden in humans.

To analyze whether the deletion not only affected HNF4 $\alpha$  binding but also resulted in a downregulation of *F9* expression, we performed luciferase assays. Although relative response ratios do not directly reflect *F9* mRNA or FIX levels *in vivo*, silencing of the promoter activity due to the deletion was obvious from these experiments. Similar findings have been made using HNF4 $\alpha$ -null mice.<sup>26</sup> In the murine model it was shown that expression of factors V, XI, XII, and XIII B directly depends on hepatic HNF4 $\alpha$ . Northern blot analysis also demonstrated that *F9* expression was decreased with a significantly prolonged aPTT in the HNF4 $\alpha$ -null mice.<sup>26</sup> The finding that *F9* expression was not completely dependent on HNF4 $\alpha$  is in agreement with the observation that control of *F9* transcription in mice and humans is complex and depends on a plethora of factors.<sup>26</sup> For instance, in earlier studies it was shown, using DNaseI footprinting, that there are further binding

sites of HNF4 $\alpha$  and other factors, e.g. ARP1, COUP/Ear3, in the human *F9* promoter influencing *F9* expression.<sup>54</sup> However, the classical HNF4 $\alpha$  binding site at position -26 to -19 only binds HNF4 $\alpha$ . When analyzing the canine *F9* promoter using transcription factor binding site prediction algorithms, further potential binding motifs for HNF4 $\alpha$  and other transcription factors were predicted (*data not shown*).<sup>55-57</sup> As ectopic expression of *F9* *in vivo* can be excluded or at least ignored according to recent RNA-sequencing analyses,<sup>58</sup> a remaining reduced hepatic activity of the mutated promoter is in agreement with the clinical findings of residual FIX activity in the affected males (*Online Supplementary Table S1*) and the results of the electrophoretic mobility shift assay showing binding of AR in androgen-dependent promoter activation.

In summary, we have identified and elucidated the causative genetic variant for hemophilia B Leyden in Hovawarts. This is the first report on a single nucleotide deletion within the binding sites of HNF4 $\alpha$  and AR in the *F9* promoter causing hemophilia B Leyden in dogs. As the deletion only abolishes the binding of HNF4 $\alpha$ , it can be assumed that male dogs will most likely recover during puberty, as reported in humans.<sup>30,59,60</sup> However, to prevent any risk of a further propagation of the disorder, genotyping of females is recommended in further breeding.

#### Acknowledgments

The authors are grateful to S. Pach for expert technical assistance and L. Binder for support. The owners of Hovawarts who have provided blood samples are thanked for their generous help. A. Leutz and E. Kowenz-Leutz are thanked for providing the C/EBP $\alpha$  expression vector. S. Shan and F. Xu are supported by a fellowship from the Chinese Scholarship Council (CSC).

#### References

- Dolan G, Benson G, Duffy A, et al. Haemophilia B: where are we now and what does the future hold? *Blood Rev*. 2018;32(1):52-60.
- Green P. The 'royal disease'. *J Thromb Haemost*. 2010;8(10):2214-2215.
- Rogaev EI, Grigorenko AP, Faskhutdinova G, Kittler EL, Moliaka YK. Genotype analysis identifies the cause of the "royal disease". *Science*. 2009;326(5954):817.
- Rallapalli PM, Kemball-Cook G, Tuddenham EG, Gomez K, Perkins SJ. An interactive mutation database for human coagulation factor IX provides novel insights into the phenotypes and genetics of hemophilia B. *J Thromb Haemost*. 2013;11(7):1329-1340.
- Mustard JF, Rowsell HC, Robinson GA, Hoeksema TD, Downie HG. Canine haemophilia B (Christmas disease). *Br J Haematol*. 1960;6:259-266.
- Mustard JF, Basser W, Hedgard G, Secord D, Rowsell HC, Downie HG. A comparison of the effect of serum and plasma transfusions on the clotting defect in canine haemophilia B. *Br J Haematol*. 1962;8:36-42.
- Parks BJ, Brinkhous KM, Harris PF, Penick GD. Laboratory detection of female carriers of canine hemophilia. *Thromb Diath Haemorrh*. 1964;12:368-376.
- Rowsell HC, Downie HG, Mustard JF, Leeson JE, Archibald JA. A disorder resembling hemophilia B (Christmas disease) in dogs. *J Am Vet Med Assoc*. 1960;137:247-250.
- Evans JP, Brinkhous KM, Brayer GD, Reisner HM, High KA. Canine hemophilia B resulting from a point mutation with unusual consequences. *Proc Natl Acad Sci U S A*. 1989;86(24):10095-10099.
- Brooks MB, Gu W, Ray K. Complete deletion of factor IX gene and inhibition of factor IX activity in a Labrador retriever with hemophilia B. *J Am Vet Med Assoc*. 1997;211(11):1418-1421.
- Gu W, Brooks M, Catalfamo J, Ray J, Ray K. Two distinct mutations cause severe hemophilia B in two unrelated canine pedigrees. *Thromb Haemost*. 1999;82(4):1270-1275.
- Brooks MB, Gu W, Barnas JL, Ray J, Ray K. A Line 1 insertion in the factor IX gene segregates with mild hemophilia B in dogs. *Mamm Genome*. 2003;14(11):788-795.
- Feldman DG, Brooks MB, Dodds WJ. Hemophilia B (factor IX deficiency) in a family of German shepherd dogs. *J Am Vet Med Assoc*. 1995;206(12):1901-1905.
- Kooistra HS, Slappendel RJ. [A young male mongrel with hemophilia-B (Christmas disease)]. *Tijdschr Diergeneesk*. 1991;116(6):281-285.
- Mauser AE, Whitlark J, Whitney KM, Lothrop CD Jr. A deletion mutation causes hemophilia B in Lhasa Apso dogs. *Blood*. 1996;88(9):3451-3455.
- Mischke R, Kuhnlein P, Kehl A, et al. G244E in the canine factor IX gene leads to severe haemophilia B in Rhodesian Ridgebacks. *Vet J*. 2011;187(1):113-118.
- Nakata M, Sakai M, Sakai T. Hemophilia B in a crossbred Maltese dog. *J Vet Med Sci*. 2006;68(11):1223-1224.
- Reitsma PH, Mandalaki T, Kasper CK, Bertina RM, Briet E. Two novel point mutations correlate with an altered developmental expression of blood coagulation factor IX (hemophilia B Leyden phenotype). *Blood*. 1989;73(3):743-746.
- Reitsma PH, Bertina RM, Ploos van Amstel JK, Riemens A, Briet E. The putative factor IX gene promoter in hemophilia B Leyden. *Blood*. 1988;72(3):1074-1076.
- Veltkamp JJ, Meilof J, Remmelts HG, van der Vlerk D, Loeliger EA. Another genetic variant of haemophilia B: haemophilia B Leyden. *Scand J Haematol*. 1970;7(2):82-90.
- Funnell AP, Crossley M. Hemophilia B Leyden and once mysterious cis-regulatory mutations. *Trends Genet*. 2014;30(1):18-23.
- Picketts DJ, Lillicrap DP, Mueller CR. Synergy between transcription factors DBP and C/EBP $\alpha$  compensates for a haemophilia B Leyden factor IX mutation. *Nat Genet*. 1993;3(2):175-179.
- Yuan X, Ta TC, Lin M, et al. Identification of an endogenous ligand bound to a native orphan nuclear receptor. *PLoS One*. 2009;4(5):e5609.
- Bolotin E, Liao H, Ta TC, et al. Integrated approach for the identification of human hepatocyte nuclear factor 4 $\alpha$  target genes using protein binding microarrays.

- Hepatology. 2010;51(2):642-653.
25. Weltmeier F, Borlak J. A high resolution genome-wide scan of HNF4alpha recognition sites infers a regulatory gene network in colon cancer. *PLoS One*. 2011;6(7):e21667.
  26. Inoue Y, Peters LL, Yim SH, Inoue J, Gonzalez FJ. Role of hepatocyte nuclear factor 4alpha in control of blood coagulation factor gene expression. *J Mol Med (Berl)*. 2006;84(4):334-344.
  27. Belvini D, Salviato R, Radossi P, et al. Molecular genotyping of the Italian cohort of patients with hemophilia B. *Haematologica*. 2005;90(5):635-642.
  28. Ghanem N, Costes B, Martin J, et al. Twenty-four novel hemophilia B mutations revealed by rapid scanning of the whole factor IX gene in a French population sample. *Eur J Hum Genet*. 1993;1(2):144-155.
  29. Ketterling RP, Liu JZ, Liao D, et al. Two novel factor IX promoter mutations: incremental progress towards 'saturation in vivo mutagenesis' of a human promoter region. *Hum Mol Genet*. 1995;4(4):769-770.
  30. Reijnen MJ, Peerlinck K, Maasdam D, Bertina RM, Reitsma PH. Hemophilia B Leyden: substitution of thymine for guanine at position -21 results in a disruption of a hepatocyte nuclear factor 4 binding site in the factor IX promoter. *Blood*. 1993;82(1):151-158.
  31. Heit JA, Ketterling RP, Zapata RE, Ordonez SM, Kasper CK, Sommer SS. Hemophilia B Brandenburg-type promoter mutation. *Haemophilia*. 1999;5(1):73-75.
  32. Crossley M, Ludwig M, Stowell KM, De Vos P, Olek K, Brownlee GG. Recovery from hemophilia B Leyden: an androgen-responsive element in the factor IX promoter. *Science*. 1992;257(5068):377-379.
  33. Pfeiffer I, Volkel I, Taubert H, Brenig B. Forensic DNA-typing of dog hair: DNA-extraction and PCR amplification. *Forensic Sci Int*. 2004;141(2-3):149-151.
  34. Miller SA, Dykes DD, Polesky HF. A simple salting out procedure for extracting DNA from human nucleated cells. *Nucleic Acids Res*. 1988;16(3):1215.
  35. Brown J, Pirrung M, McCue LA. FQC Dashboard: integrates FastQC results into a web-based, interactive, and extensible FASTQ quality control tool. *Bioinformatics*. 2017 Jun 9. [Epub ahead of print]
  36. Lindblad-Toh K, Wade CM, Mikkelsen TS, et al. Genome sequence, comparative analysis and haplotype structure of the domestic dog. *Nature*. 2005;438(7069):803-819.
  37. Burland TG. DNASTAR's Lasergene sequence analysis software. *Methods Mol Biol*. 2000;132:71-91.
  38. Clewley JP. Macintosh sequence analysis software. *DNASTAR's LaserGene*. *Mol Biotechnol*. 1995;3(3):221-224.
  39. Jiang M, Li H, Zhang Y, et al. Transitional basal cells at the squamous-columnar junction generate Barrett's oesophagus. *Nature*. 2017;550(7677):529-533.
  40. Lawson B, Robinson RA, Fernandez JR, et al. Spatio-temporal dynamics and aetiology of proliferative leg skin lesions in wild British finches. *Sci Rep*. 2018;8(1):14670.
  41. Eggers C, Hook B, Lewis S, Strayer C, Landreman A. Designing a bioluminescent reporter assay: normalization. 2016 [cited 14.11.2018]; Available from: <http://www.promega.de/resources/pub-hub/designing-a-bioluminescent-reporter-assay-normalization/>
  42. Dögel M. Working Dog. 2019 [cited 01.02.2019]; Available from: <https://en.working-dog.com>
  43. Mischke R. [Comparison of factor VIII:C and factor IX sensitivity of different commercial APTT reagents for canine plasma]. *Berl Munch Tierarztl Wochenschr*. 1999;112(10-11):394-399.
  44. Evans JP, Watzke HH, Ware JL, Stafford DW, High KA. Molecular cloning of a cDNA encoding canine factor IX. *Blood*. 1989;74(1):207-212.
  45. Bentley AK, Rees DJ, Rizza C, Brownlee GG. Defective propeptide processing of blood clotting factor IX caused by mutation of arginine to glutamine at position -4. *Cell*. 1986;45(3):343-348.
  46. Crossley M, Brownlee GG. Disruption of a C/EBP binding site in the factor IX promoter is associated with haemophilia B. *Nature*. 1990;345(6274):444-446.
  47. Mischke R. [Haemophilia A and B in dogs]. *Tierarztl Prax Ausg K Kleintiere Heimtiere*. 2012;40(1):44-53; quiz 54.
  48. Funnell AP, Wilson MD, Ballester B, et al. A CpG mutational hotspot in a ONECUT binding site accounts for the prevalent variant of hemophilia B Leyden. *Am J Hum Genet*. 2013;92(3):460-467.
  49. Kurachi S, Huo JS, Ameri A, Zhang K, Yoshizawa AC, Kurachi K. An age-related homeostasis mechanism is essential for spontaneous amelioration of hemophilia B Leyden. *Proc Natl Acad Sci U S A*. 2009;106(19):7921-7926.
  50. Reid KJ, Hendy SC, Saito J, Sorensen P, Nelson CC. Two classes of androgen receptor elements mediate cooperativity through allosteric interactions. *J Biol Chem*. 2001;276(4):2943-2952.
  51. Wilson S, Qi J, Filipp FV. Refinement of the androgen response element based on ChIP-Seq in androgen-insensitive and androgen-responsive prostate cancer cell lines. *Sci Rep*. 2016;6:32611.
  52. Schuur ER, Henderson GA, Kmetec LA, Miller JD, Lamparski HG, Henderson DR. Prostate-specific antigen expression is regulated by an upstream enhancer. *J Biol Chem*. 1996;271(12):7043-7051.
  53. Hildyard C, Keeling D. Effect of age on factor IX levels in symptomatic carriers of haemophilia B Leyden. *Br J Haematol*. 2015;169(3):448-449.
  54. Naka H, Brownlee GG. Transcriptional regulation of the human factor IX promoter by the orphan receptor superfamily factor, HNF4, ARP1 and COUP/Ear3. *Br J Haematol*. 1996;92(1):231-240.
  55. Fang B, Mane-Padros D, Bolotin E, Jiang T, Sladek FM. Identification of a binding motif specific to HNF4 by comparative analysis of multiple nuclear receptors. *Nucleic Acids Res*. 2012;40(12):5343-5356.
  56. Farre D, Roset R, Huerta M, et al. Identification of patterns in biological sequences at the ALGGEN server: PROMO and MALGEN. *Nucleic Acids Res*. 2003;31(13):3651-3653.
  57. Messeguer X, Escudero R, Farre D, Nunez O, Martinez J, Alba MM. PROMO: detection of known transcription regulatory elements using species-tailored searches. *Bioinformatics*. 2002;18(2):333-334.
  58. Fagerberg L, Hallstrom BM, Oksvold P, et al. Analysis of the human tissue-specific expression by genome-wide integration of transcriptomics and antibody-based proteomics. *Mol Cell Proteomics*. 2014;13(2):397-406.
  59. Reijnen MJ, Sladek FM, Bertina RM, Reitsma PH. Disruption of a binding site for hepatocyte nuclear factor 4 results in hemophilia B Leyden. *Proc Natl Acad Sci U S A*. 1992;89(14):6300-6303.
  60. Morgan GE, Rowley G, Green PM, Chisholm M, Giannelli F, Brownlee GG. Further evidence for the importance of an androgen response element in the factor IX promoter. *Br J Haematol*. 1997;98(1):79-85.
  61. Bennett RL, French KS, Resta RG, Doyle DL. Standardized human pedigree nomenclature: update and assessment of the recommendations of the National Society of Genetic Counselors. *J Genet Couns*. 2008;17(5):424-433.



Ferrata Storti Foundation

# Role of interferon- $\gamma$ in immune-mediated graft failure after allogeneic hematopoietic stem cell transplantation

Pietro Merli,<sup>1</sup> Ignazio Caruana,<sup>1</sup> Rita De Vito,<sup>2</sup> Luisa Strocchio,<sup>1</sup> Gerrit Weber,<sup>1</sup> Francesca Del Bufalo,<sup>1</sup> Vanessa Buatois,<sup>3</sup> Paolo Montanari,<sup>3</sup> Maria Giuseppina Cefalo,<sup>1</sup> Angela Pitisci,<sup>1</sup> Mattia Algeri,<sup>1</sup> Federica Galaverna,<sup>1</sup> Concetta Quintarelli,<sup>1</sup> Valentina Cirillo,<sup>1</sup> Daria Pagliara,<sup>1</sup> Walter Ferlin,<sup>3</sup> Maria Ballabio,<sup>3</sup> Cristina De Min<sup>3</sup> and Franco Locatelli<sup>1,4</sup>

Haematologica 2019  
Volume 104(11):2314-2323

<sup>1</sup>Bambino Gesù Children's Hospital, Department of Pediatric Hematology/Oncology, Cellular and Gene Therapy, Rome, Italy; <sup>2</sup>Bambino Gesù Children's Hospital, Department of Laboratories, Pathology Unit, Rome, Italy; <sup>3</sup>Novimmune SA, Geneva, Switzerland and <sup>4</sup>Department of Pediatrics, Sapienza, University of Rome, Rome, Italy

## ABSTRACT

Pathophysiology of graft failure (GF) occurring after allogeneic hematopoietic stem cell transplantation (HSCT) still remains elusive. We measured serum levels of several different cytokines/chemokines in 15 children experiencing GF, comparing their values with those of 15 controls who had sustained donor cell engraftment. Already at day +3 after transplantation, patients developing GF had serum levels of interferon (IFN)- $\gamma$  and CXCL9 (a chemokine specifically induced by IFN $\gamma$ ) significantly higher than those of controls ( $8859 \pm 7502$  vs.  $0$  pg/mL,  $P=0.03$ , and  $1514.0 \pm 773$  vs.  $233.6 \pm 50.1$  pg/mL,  $P=0.0006$ , respectively). The role played by IFN $\gamma$  in HSCT-related GF was further supported by the observation that a rat anti-mouse IFN $\gamma$ -neutralizing monoclonal antibody promotes donor cell engraftment in *Ifngr1<sup>-/-</sup>* mice receiving an allograft. In comparison to controls, analysis of bone marrow-infiltrating T lymphocytes in patients experiencing GF documented a predominance of effector memory CD8<sup>+</sup> cells, which showed markers of activation (overexpression of CD95 and downregulation of CD127) and exhaustion (CD57, CD279, CD223 and CD366). Finally, we obtained successful donor engraftment in 2 out of 3 children with primary hemophagocytic lymphohistiocytosis who, after experiencing GF, were re-transplanted from the same HLA-haploidentical donor under the compassionate use coverage of emapalumab, an anti-IFN $\gamma$  monoclonal antibody recently approved by the US Food and Drug Administration for treatment of patients with primary hemophagocytic lymphohistiocytosis. Altogether, these results suggest that the IFN $\gamma$  pathway plays a major role in GF occurring after HSCT. Increased serum levels of IFN $\gamma$  and CXCL9 represent potential biomarkers useful for early diagnosis of GF and provide the rationale for exploring the therapeutic/preventive role of targeted neutralization of IFN $\gamma$ .

## Correspondence:

PIETRO MERLI  
pietro.merli@opbg.net

Received: January 7, 2019.

Accepted: February 18, 2019.

Pre-published: February 21, 2019.

doi:10.3324/haematol.2019.216101

Check the online version for the most updated information on this article, online supplements, and information on authorship & disclosures: [www.haematologica.org/content/104/11/2314](http://www.haematologica.org/content/104/11/2314)

©2019 Ferrata Storti Foundation

Material published in Haematologica is covered by copyright. All rights are reserved to the Ferrata Storti Foundation. Use of published material is allowed under the following terms and conditions:

<https://creativecommons.org/licenses/by-nc/4.0/legalcode>.

Copies of published material are allowed for personal or internal use. Sharing published material for non-commercial purposes is subject to the following conditions:

<https://creativecommons.org/licenses/by-nc/4.0/legalcode>,

sect. 3. Reproducing and sharing published material for commercial purposes is not allowed without permission in writing from the publisher.



## Introduction

Graft failure (GF), estimated to occur in 1-5% of cases after myeloablative conditioning and in up to 30% of cases after reduced-intensity conditioning (RIC),<sup>1</sup> still remains a relevant cause of morbidity and mortality after allogeneic hematopoietic stem cell transplantation (HSCT).<sup>2</sup> Despite a slight reduction of its incidence over the last decade, mortality after GF remains as high as 11%.<sup>3</sup> To date, in the absence of effective treatment options, re-transplantation, from either the same, or whenever possible, a different donor is considered the treatment of choice.<sup>2</sup> Currently identified risk factors for GF include: i) human leukocyte antigen (HLA)-disparity and sex mismatch in the donor/recipient pair; ii) presence of

donor-specific antibodies (DSA) in the recipient; iii) T-cell depletion (TCD) of the graft; iv) ABO-blood group mismatch; v) use of RIC; vi) a diagnosis of non-malignant disorders (in particular thalassemia, severe aplastic anemia, SAA, and hemophagocytic lymphohistiocytosis, HLH); vii) viral infections; viii) low nucleated cell dose in the graft; and ix) the use of myelotoxic drugs in the post-transplant period.<sup>1-4</sup>

In the last two decades, several groups have investigated immune-mediated GF. In particular, it has been shown that immune-mediated GF is mainly caused by host T and natural killer (NK) cells surviving the conditioning regimen, through a classical alloreactive immune response against non-shared, major (in case of HLA-partially-matched HSCT) or minor (in case of fully HLA-matched HSCT) histocompatibility antigens.<sup>2,5,6</sup> However, to date the molecular pathways involved in immune-mediated GF have not yet been completely clarified. Indeed, since the inhibition of different pathways (including perforin-, FasL-, TNFR-1-, and TRAIL-dependent cytotoxicity) did not prove to be efficient in preventing GF, the pathophysiological mechanisms responsible for GF seem to be multiple and likely to be redundant.<sup>7</sup> Nonetheless, consistently over the years, different groups have suggested a pivotal pathogenic role of IFN $\gamma$  in GF pathophysiology,<sup>8-14</sup> through both direct [e.g. inhibition of hematopoietic stem cell (HSC) self-renewal, proliferative capacity, and multilineage differentiation]<sup>10,11</sup> and indirect (e.g. induction of FAS expression on HSC, with increased apoptosis in the presence of activated cytotoxic T cells)<sup>8,12</sup> effects.

Despite these experimental data, there has still not been any *in vivo* characterization of GF in humans. Indeed, although the expansion of host CD8<sup>+</sup> T cells in patients experiencing GF has been previously demonstrated *in vivo*,<sup>15,16</sup> a more detailed characterization of this cell population is lacking. Thus, we started a prospective study aimed at better characterizing the pathophysiology of GF, focusing on the identification of biological markers that: (i) could predict early the occurrence of GF in the clinical setting; and (ii) could be used as a therapeutic target with clinically available biological agents. For this purpose, we broadly investigated cytokine and chemokine levels in peripheral blood (PB), as well as the cellular features in bone marrow (BM) biopsies of patients experiencing this complication. After confirming *in vivo* a role of IFN $\gamma$ -pathway in the development of GF, we also investigated in an animal model of GF whether the sole inhibition of IFN $\gamma$  would be able to prevent/treat GF. Finally, in view of these findings and the similarity between immune-mediated GF and HLH, we treated, in compassionate use (CU), with emapalumab, an anti-IFN $\gamma$  monoclonal antibody recently approved for the treatment of HLH,<sup>17</sup> three patients with primary HLH, who, after having experienced GF, underwent a second HSCT.

## Methods

### Patients

Patients aged from 0.3 to 21 years, who received an allograft from any type of donor/stem cell source between January 1<sup>st</sup> 2016 and August 31<sup>st</sup> 2017 at the IRCCS Bambino Gesù Children's Hospital in Rome, Italy, were considered eligible for the study. All patients or legal guardians provided written informed consent, and the entire research was conducted under

institutional review board approved protocols and in accordance with the Declaration of Helsinki. The Bambino Gesù Children's Hospital Institutional Review Board approved the study.

### Cytokine profile

In order to identify a cytokine/chemokine profile predictive of GF, PB samples were collected at different time points after HSCT: day 0, +3 $\pm$ 2, +7 $\pm$ 2, +10 $\pm$ 2, +14 $\pm$ 2, +30 $\pm$ 2 after transplantation. Validated MesoScale Discovery (MSD, Rockville, MD, USA) platform-based immunoassay was used for the quantification of IFN $\gamma$ , sIL2R $\alpha$ , CXCL9, CXCL10, TNF $\alpha$ , IL6, IL10, and sCD163 serum levels.

### Bone marrow biopsy: histopathology analysis and immunofluorescence

Bone marrow biopsies were obtained when GF was suspected. (Since BM characterization was a secondary end point of this study and BM aspiration is not routinely performed in this condition, parents/legal guardians could refuse the procedure.) Details on BM specimen preparation, histopathology analysis and immunofluorescence are reported in the *Online Supplementary Appendix*.

### Immune-phenotypic analysis

The following monoclonal antibodies (mAbs) were used: anti-CD3, CD4, CD8, CD25, CD27, CD28, CD45RA, CD45RO, CD56, CD57, CD62L, CD95, CD127, CD137, CD197, CD223 (Lag3), CD279 (PD1), and CD366 (TIM3) (BD Biosciences, NJ, Biologend, CA and Affymetrix, CA, USA).

### *In vivo* murine model of hematopoietic stem cell transplantation rejection

C57BL/6 Ifngr1<sup>-/-</sup> mice were used as recipient, while C57BL/6 Ifngr1<sup>+/+</sup> were used as donor. All animal experiments were performed in accordance with the Swiss animal protection law. Details on experiments are reported in the *Online Supplementary Appendix*.

### Emapalumab administration in compassionate use to hemophagocytic lymphohistiocytosis patients experiencing graft failure

Emapalumab (previously known as NI-0501), a fully human anti-IFN $\gamma$  monoclonal antibody, was administered on a CU basis (after local ethical committee approval) to three patients affected by HLH who experienced GF after a first TCD HSCT from a partially-matched family donor (PMFD) with the aim of preventing flares of HLH and a second GF. The drug was administered by 1-hour intravenous infusion twice a week until sustained donor engraftment or GF. The dose varied between 1 and 6 mg/kg, based on pharmacokinetic data.

Additional methods are presented in the *Online Supplementary Appendix*.

### Statistical analysis

Unless otherwise specified, quantitative variables were reported as Mean $\pm$ Standard Error of Mean (SEM); categorical variables were expressed as absolute value and percentage. Clinical characteristics of patients were compared using the  $\chi^2$  test or Fisher exact test for categorical variables, while the Mann-Whitney rank sum test or the Student *t*-test (two-sided) was used for continuous variables, as appropriate. For multiple comparison analyses, statistical significance was evaluated by a repeated measure ANOVA test, followed by a Log-rank (Mantel-Cox) test for multiple comparisons.

## Results

### Patients' characteristics

During the study period, 15 consecutive patients who experienced GF were eligible for the study. Most of them were affected by non-malignant disorders characterized by a high risk of GF (e.g. SAA and HLH) and received a TCD allograft from a PMFD. Fifteen children, matched for transplant characteristics, who had sustained donor engraftment during the same period were used as controls. Patients' and control characteristics are detailed in Table 1. Main transplant characteristics (i.e. conditioning regimen, type of donor, graft manipulation) were comparable between the two groups (except for a trend for a lower age in the GF group). Of the 15 patients experiencing GF, ten were tested for anti-HLA antibodies, which were detected in five patients (50%). Those who had a mean fluorescence intensity (MFI) of anti-HLA antibodies >5000 received rituximab and underwent plasma-exchange to lower the value below the threshold of 5000 MFI;<sup>18</sup> this treatment successfully reduced the MFI value in all cases.

Signs and symptoms of patients who either did or did not experience GF are detailed in Table 2. The most frequent sign associated with GF was fever, occurring at a median time of six days from the infusion of the graft (range 1-16 days). Moreover, both lactate dehydrogenase (LDH) and ferritin increased in many patients (80% and 46.7%, respectively); these laboratory findings appeared late after HSCT (at a median of 11 and 10 days, respectively). All patients received steroids in an attempt to avoid GF, without benefit. Chimerism analysis performed on PB showed only recipient cells in all GF cases, while in all controls but one, who showed mixed chimerism, only donor-origin cells were found.

### Cytokine/chemokine profile

Kinetics of IFN $\gamma$ , CXCL9, IL10 and IL2R $\alpha$  serum levels are shown in Figure 1A-D, while serum levels of TNF $\alpha$ , CXCL10, sCD163 and IL6 are shown in Figure 2A-D. Serum levels of these cytokines/chemokines differed between patients experiencing GF and controls, starting from the first days after the infusion of the graft. Notably, for IFN $\gamma$ , CXCL9, IL10 and TNF $\alpha$ , this difference became

**Table 1.** Characteristics of patients who either did or did not experience graft failure (GF).

	GF patients (%)	Controls (%)	P
Total	15 (100)	15 (100)	
Gender			0.27
Female	9 (60)	10 (66.5)	
Male	6 (40)	5 (33.5)	
Age at transplant, years (median and range)	2.6 (0.3-16.3)	8.1 (0.9-18)	0.1
Disease			0.38
SAA	4 (27)	4 (27)	
HLH	3 (20)	0	
AML	1 (6.5)	2 (13.5)	
ALL	1 (6.5)	3 (20)	
Erythroid disorders <sup>§</sup>	1 (6.5)	4 (27)	
CAMT	1 (6.5)	0	
Metabolic disorders <sup>*</sup>	2 (13.5)	1 (6.5)	
Osteopetrosis	1 (6.5)	0	
PID <sup>¶</sup>	1 (6.5)	1 (6.5)	
Type of transplant			0.13
TCD haploidentical	13 (87)	10 (66.5)	
MUD	1 (6.5)	5 (33.5)	
UCBT	1 (6.5)	0	
Source of stem cells			0.22
PBSC	13 (87)	11 (73)	
BM	1 (6.5)	4 (27)	
Cord blood	1 (6.5)	0	
Conditioning regimen			0.23
TBI-based	0	2 (13.5)	
Busulfan-based	8 (53)	10 (66.5)	
Treoosulfan-based	3 (20)	2 (13.5)	
Other regimens	4 (27)	1 (6.5)	
Donor/recipient pair sex mismatch			0.14
Yes	4 (27)	9 (60)	
No	11 (73)	6 (40)	

SAA: severe aplastic anemia; HLH: hemophagocytic lymphohistiocytosis; AML: acute myeloid leukemia; ALL: acute lymphoblastic leukemia; CAMT: congenital amegakaryocytic thrombocytopenia; PID: primary immunodeficiency; TCD: Tcell depleted; MUD: matched unrelated donor; UCBT: unrelated cord blood transplant; PBSC: peripheral blood stem cells; BM: bone marrow; TBI: total-body irradiation; MLD: metachromatic leukodystrophy; MPS: mucopolysaccharidosis; ALD: adrenoleukodystrophy; DBA: Diamond-Blackfan anemia; \*1 case each of MLD and MPS-1 in GF group; 1 case of ALD among controls; <sup>§</sup>1 case of Thalassemia in GF group; 2 cases of Thalassemia and 2 of DBA among controls; <sup>¶</sup>1 case of combined immunodeficiency in GF group; 1 case of autosomal recessive hyper-IgE syndrome among controls. SAA: severe aplastic anemia.

**Table 2.** Signs and symptoms of patients who experienced graft failure (GF).

Signs/symptoms	GF patients (total=15)	Percentage	Median day of onset	Range	Controls (total=15)	Percentage	P
Fever	13	86.7	6	1-16	7	46.7	0.02
Increase of ferritin serum levels <sup>*</sup>	12	80.0	11	4-20	2	13.3	0.0007
Hemophagocytosis <sup>^</sup>	5 <sup>^</sup>	71.4 <sup>^</sup>			0 <sup>§</sup>	0	0.02
Hypertriglyceridemia/hypofibrinogenemia	7	46.7	12	4-16	2	13.3	N.S.
Increase of LDH serum levels	7	46.7	10	8-17	1	6.7	0.03
Splenomegaly	5	33.3	11	8-13	0	0	0.04
Skin rash	3	20.0	10	10-19	2	13.3	N.S.
Other							
Bradycardia	1	6.7	9	NA	0	0	N.S.

LDH: lactate dehydrogenase; N.S.: not significant. <sup>°</sup> >3000 ng/mL. <sup>^</sup> Seven patients out of 15 were evaluated. <sup>§</sup> Five patients out of 15 were evaluated.

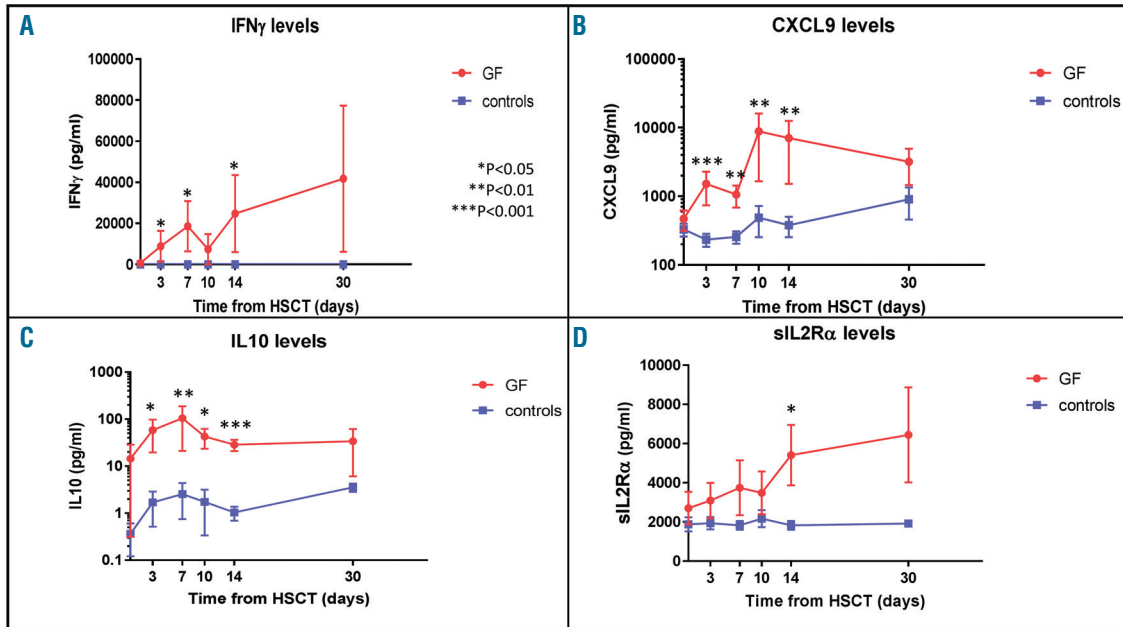


**Figure 1. Cytokine/chemokine profile.** Serum levels of interferon (IFN)- $\gamma$  (A), CXCL9 (B), CXCL10 (C), and sIL2R $\alpha$  (D) in patients who either did (red line) or did not (blue line) experience graft failure (GF). All graphs represent Mean and Standard Error of Mean for each variable. HSCT: hematopoietic stem cell transplantation.

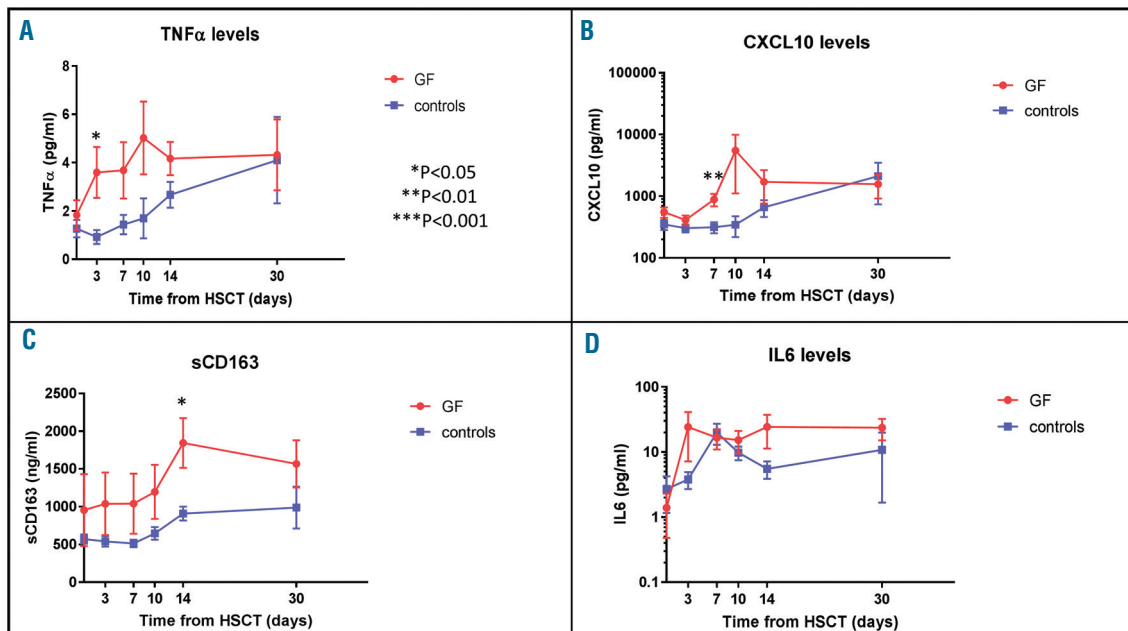


**Figure 2. Cytokine/chemokine profile.** Serum levels of TNF $\alpha$  (A), CXCL10 (B), sCD163 (C), IL6 (panel D). Red line: patients who experience graft failure (GF); blue line: controls. All graphs represent Mean and Standard Error of Mean for each variable. HSCT: hematopoietic stem cell transplantation.

statistically significant already at day +3 after HSCT. In particular, mean IFN $\gamma$  levels at day +3 were 8859 $\pm$ 7502 pg/mL in GF patients versus 0 pg/mL in controls ( $P=0.03$ ); CXCL9 levels were 1514.0 $\pm$ 773 pg/ml versus 233.6 $\pm$ 50.1 pg/mL ( $P=0.0006$ ); IL10 levels were 58.8 $\pm$ 39.1 pg/mL versus 1.7 $\pm$ 1.1 pg/mL ( $P=0.01$ ); TNF $\alpha$  levels were 3.5 $\pm$ 1.0 pg/mL versus 0.9 $\pm$ 0.2 pg/mL ( $P=0.02$ ). In this cohort, receiver operating characteristics (ROC) analysis on CXCL9 levels at day +3 showed an area under the curve (AUC) of 0.905 [95% Confidence Interval (CI) 0.709-0.987;  $P<0.0001$ ] (*Online Supplementary Figure S1*); a cut-off value of 274.5 pg/mL had a sensitivity of 88.89% and a specificity of 78.57%. The ROC analysis of other markers, which were significantly increased at day +3 showed an AUC of 0.802 for TNF $\alpha$  (95%CI: 0.566-0.944;  $P=0.006$ ), of 0.756 for IL10 (95%CI: 0.529-0.912;  $P=0.011$ ) and of 0.682 for IFN $\gamma$  (95%CI: 0.471-0.849;  $P=0.017$ ).

Since primary HLH patients commonly present increased IFN $\gamma$  and its related chemokines serum levels during disease reactivation/flare (that is frequent after failure of HSCT<sup>19</sup>), we performed additional analyses excluding this subset of patients in order to validate the data in disorders other than HLH. Even after excluding HLH patients, CXCL9 and IL10 serum levels remained significantly higher in patients experiencing GF in comparison with controls (*Online Supplementary Figure S2*).

#### Activation of macrophages and T lymphocytes characterizes graft failure in allogeneic hematopoietic stem cell transplantation

Bone marrow biopsies were obtained at time of GF in seven patients and were compared to those of five controls (obtained in a similar time period, i.e. between 2 and 3 weeks after HSCT). In all GF patients, evaluation of BM morphology showed different stages of GF with reduced cellularity (*Figure 3A* and *Online Supplementary Figure S3A*

and *B*) as compared to patients with sustained donor engraftment (*Online Supplementary Figure S4A*). In GF patients, the percentage of myelocytes and erythroid precursors was reduced compared to controls (*Figure 3B*). Erythroid colonies were markedly smaller, with a higher percentage of premature erythroid cells. The megakaryocytic lineage was well represented in all GF cases, but with irregular distribution (*Figure 3C*). In several areas of the specimens, a remarkable number of apoptotic cells partially grouped in clusters was observed (*Figure 3D*). All biopsies showed stromal damage resulting in edema (*Figure 3E*). While the total number of CD68<sup>+</sup> macrophages was comparable between GF patients and controls (*Figure 4A*), significantly higher percentages of CD68<sup>+</sup> and CD163<sup>+</sup> macrophages, with cellular fragments, erythrocytes and lipid vacuoles in their cytoplasm, (indicating activation and phagocytic activity) (*Figure 3F* and *G* and *Online Supplementary Figure S3C* and *D*), were observed in comparison to controls [median 80% (range 30-100%) vs. 0% (range 0-5%);  $P<0.0001$ ] (*Figure 4B* and *Online Supplementary Figure S4B* and *C*). In all analyzed samples from GF patients, a significant increase in T lymphocytes (*Figures 3H* and *4A* and *Online Supplementary Figure S3G*), with a predominance of CD8<sup>+</sup> cytotoxic T cells, expressing perforin, Granzyme B and TIA-1 (*Figures 3I* and *J* and *4A* and *Online Supplementary Figure S5*) was observed. The *Online Supplementary Appendix* provides further details.

#### Polyclonal T-cell pattern with predominant CD8 effector memory phenotype effector memory phenotype

In order to better characterize the role of T lymphocytes in GF, the TCR repertoire was initially analyzed in the CD3<sup>+</sup> population, showing a polyclonal distribution of the V $\beta$  chains (*Online Supplementary Figure S6*). Then, we

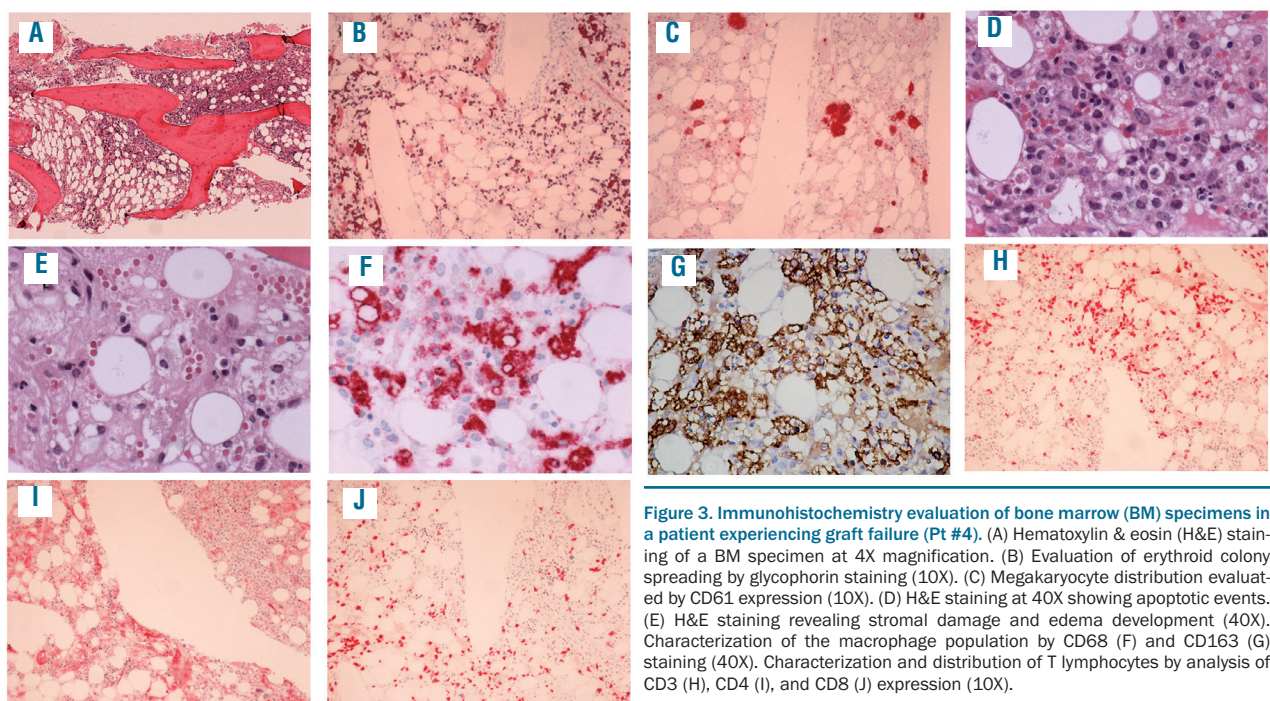


**Figure 3. Immunohistochemistry evaluation of bone marrow (BM) specimens in a patient experiencing graft failure (Pt #4).** (A) Hematoxylin & eosin (H&E) staining of a BM specimen at 4X magnification. (B) Evaluation of erythroid colony spreading by glycophorin staining (10X). (C) Megakaryocyte distribution evaluated by CD61 expression (10X). (D) H&E staining at 40X showing apoptotic events. (E) H&E staining revealing stromal damage and edema development (40X). Characterization of the macrophage population by CD68 (F) and CD163 (G) staining (40X). Characterization and distribution of T lymphocytes by analysis of CD3 (H), CD4 (I), and CD8 (J) expression (10X).

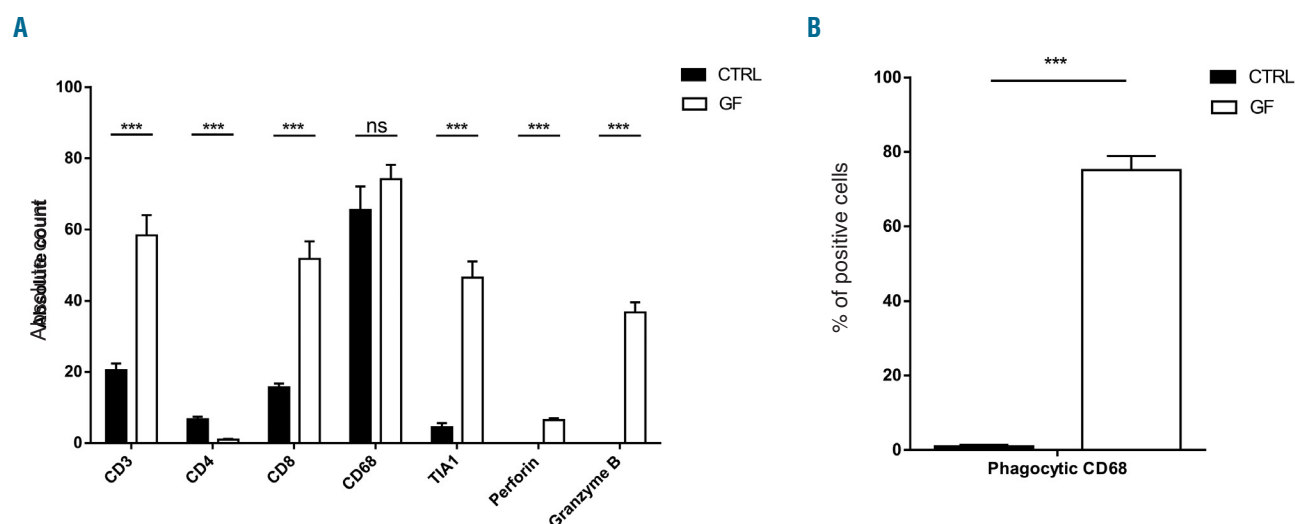


**Figure 4. Immunohistochemistry characterization of bone marrow (BM) in patients who either did or did not experience graft failure (GF).** (A) Comparison of absolute number of CD3<sup>+</sup>, CD4<sup>+</sup>, CD8<sup>+</sup>, CD68<sup>+</sup>, TIA-1<sup>+</sup>, perforin<sup>+</sup> and granzyme<sup>+</sup> cells in BM of GF patients and controls (CTRL). The total number of positive cell for each marker was counted in five fields per sample under 20-fold magnification and reported as Mean±Standard Deviation. (B) Percentages of CD68<sup>+</sup> cells with hemophagocytic activity (i.e. showing cellular fragments, erythrocytes and lipid vacuoles in their cytoplasm) in BM of GF patients and CTRL. \* $P < 0.05$ ; \*\* $P < 0.01$ ; \*\*\* $P < 0.001$ .

extended our analysis on BM-infiltrating lymphocytes through flow-cytometry in both controls and GF patients. Regarding NK (CD56<sup>+</sup>/CD3<sup>-</sup>) and  $\gamma\delta$  T cells (CD3<sup>+</sup>/CD4<sup>-</sup>/CD8<sup>-</sup>) no difference was observed between the two patient groups (*data not shown*). By contrast, in the  $\alpha\beta$  T-cell subset, the analysis revealed a significant difference in both CD4 (58.9%±13.4% vs. 7.6%±7.3%, controls vs. GF patients) and CD8 (25.9%±6.1% vs. 66.5%±18.2%, controls vs. GF patients) subsets ( $P < 0.0001$  and  $P = 0.0018$ , respectively) (Figure 5A). We further characterized both CD4<sup>+</sup> and CD8<sup>+</sup> populations for the expression of memory markers. While no significant difference was detected in the CD4<sup>+</sup> subpopulation, the CD8<sup>+</sup> subset displayed a significant enrichment of effector memory T cells (Efm) (CD45RO<sup>+</sup>/CCR7<sup>-</sup>) (40.3±24.6% vs. 20.7%±7.3%, GF patients vs. CTRL patients;  $P = 0.034$ ) (Figure 5B and C) and a significant reduction of the naïve subset (CD45RA<sup>+</sup>/CCR7<sup>+</sup>) (18.6%±16.6% vs. 28.6%±12.1%, GF patients vs. controls;  $P = 0.014$ ). See *Online Supplementary Appendix* for further details.

#### Increasing expression of activation and exhaustion markers on T cells during graft failure

We evaluated the expression of several activation and exhaustion markers on infiltrating cells. As expected, in patients experiencing GF, both CD4<sup>+</sup> and CD8<sup>+</sup> cells displayed a significant activation profile, as demonstrated by the overexpression of CD95 (69.2%±23.0% vs. 93.9%±6.9% and 57.9%±27.2% vs. 98.35%±2.0%, controls vs. GF patients, respectively;  $P = 0.021$  and  $P = 0.002$ ) (Figure 5D) and downregulation of CD127 (recently shown to be associated with prolonged T-cell receptor stimulation<sup>20</sup>) on the proliferating CD8<sup>+</sup> cells (69.3%±16.9% vs. 37.9%±18.8%, controls vs. GF patients, respectively;  $P = 0.014$ ) (Figure 5E). The expression of several exhaustion and senescence markers confirmed the status of prolonged activation of T lymphocytes located in the BM of GF patients, such as the upregulation of CD57 (CD57<sup>+</sup>:

10.2%±10.5% vs. 37.4%±12.4% and 34.7%±17.3% vs. 68.0%±18.8% controls vs. GF patients in CD4 and CD8 respectively;  $P = 0.003$  and  $P = 0.011$ ) (Figure 5F). See *Online Supplementary Appendix* for further details.

#### Interferon- $\gamma$ drives rejection of donor cells in *Ifngr1*<sup>-/-</sup> mice

In order to understand if the sole IFN $\gamma$ -inhibition would be sufficient to prevent GF, we used an established mouse model of GF.<sup>13</sup> As previously reported by Rottman *et al.*,<sup>13</sup> the infection of *Ifngr1*<sup>-/-</sup> mice with *Bacillus Calmette-Guérin* (BCG) resulted in a rapid increase of circulating IFN $\gamma$  levels reaching a concentration of 11,000 pg/mL on day 20 post-infection (Figure 6A). HSCT performed at day 21, i.e. at the peak of IFN $\gamma$  levels, resulted in poor chimerism as only 5% of the *Ifngr1*<sup>+/+</sup> donor cells engrafted in the BCG-infected *Ifngr1*<sup>-/-</sup> recipient mice. After day 21 post-BCG infection, serum IFN $\gamma$  levels gradually decreased to a steady state level of approximately 100 pg/mL. This decrease in IFN $\gamma$  serum levels correlated with an increase in chimerism as the *Ifngr1*<sup>-/-</sup> recipient mice exhibited 19% HSC engraftment of donor cells at day 84 (Figure 6A). For further assessing the role played by IFN $\gamma$  in GF, BCG-infected *Ifngr1*<sup>-/-</sup> recipient mice were given a neutralizing IFN $\gamma$  mAb, XMG1.2, pre- and post-HSCT. Neutralization of IFN $\gamma$  improved engraftment in BCG-infected *Ifngr1*<sup>-/-</sup> recipient mice because, at three months after the allograft, 45% of the lymphocytes were of donor origin (i.e. Ly5.1 positive), as compared to 19% in isotype control-treated mice (Figure 6B). In order to assess IFN $\gamma$  activity and ensure neutralization by XMG1.2, the IFN $\gamma$ -dependent chemokine CXCL9 was measured. A decrease in CXCL9 serum levels during the XMG1.2 treatment was observed, confirming IFN $\gamma$  neutralization in contrast to isotype control-treated mice (Figure 6C). Once XMG1.2 treatment was interrupted, at day 42 post-BCG infection, a gradual increase in CXCL9 serum levels was observed, indicating restoration of IFN $\gamma$  activity.

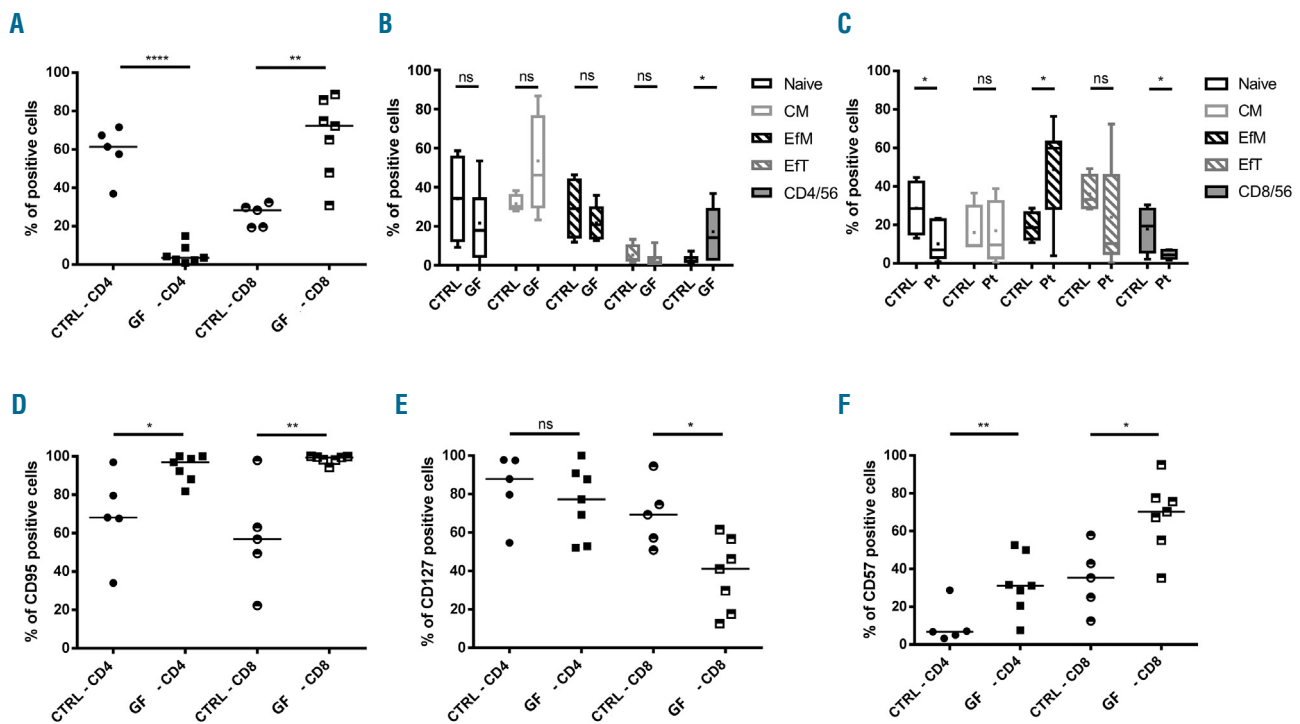


**Figure 5. Immunological characterization of the T lymphocytes present in bone marrow aspirates of patients who either did or did not experience graft failure (GF).** (A) Flow cytometry analysis of CD4<sup>+</sup> and CD8<sup>+</sup> population in patients with GF and controls (CTRL). Distribution of naïve (CD45RA<sup>+</sup>/CCR7<sup>+</sup>), central memory (CD45RO<sup>+</sup>/CCR7<sup>+</sup>), effector memory (CD45RO<sup>+</sup>/CCR7<sup>-</sup>), effector terminal (CD45RA<sup>+</sup>/CCR7<sup>-</sup>), and NK-T (CD3<sup>+</sup>/CD56<sup>+</sup>) subsets in CD4<sup>+</sup> (B) or CD8<sup>+</sup> (C) T cells. Activation and exhaustion profile in both the CD4<sup>+</sup> and CD8<sup>+</sup> population by the analysis of CD95 (D), CD127 (E), and CD57 (F). (A, D, E, and F) Each patient or CTRL is represented by a symbol and a horizontal line marks the median. (B and C) The average (+) and Median±Standard Deviation are shown. \*P<0.05; \*\*P<0.01; \*\*\*P<0.001; \*\*\*\*P<0.0001.

### Emapalumab administration to patients after hematopoietic stem cell transplantation failure

Three patients with primary HLH who experienced GF together with disease reactivation after a first TCD HSCT from a PMFD were treated with emapalumab both before and after the second HSCT (details are reported in *Online Supplementary Table S1*). For all these patients, the use of the other parent as a donor was not possible because of non-eligibility due to viral hepatitis. The CU of emapalumab was requested and obtained with the objective of controlling, without the use of myelosuppressive drugs other than those used in the conditioning regimen, HLH reactivation before and after a second HSCT. Emapalumab was administered at doses of 1-6 mg/kg every three days. Drug infusions were well tolerated and no significant safety event occurred. Two patients engrafted, while one rejected also the second HSCT without, however, experiencing a new HLH flare. This patient was successfully rescued with a third HSCT employing an unrelated cord blood (UCB) unit (notably, she received emapalumab until 3 days before UCB infusion). Remarkably, the two patients who engrafted upon treatment with emapalumab had very low levels of CXCL9 (i.e. below 102 pg/mL), indicating IFN $\gamma$  neutralization, while this was not the case for the third patient at the time of the second transplant rejection. All these three patients are currently alive and disease-free, with a follow up of 24, 23 and 21 months, respectively.

### Discussion

Diagnosis and treatment of GF in HSCT recipients remain challenging. Indeed, sign and symptoms (e.g. fever, increase in LDH or ferritin serum levels) associated with this transplant complication are non-specific; moreover, re-transplantation, although associated with relevant risk of tissue-toxicity and infections, represents the treatment of choice, since steroids and other immunosuppressive drugs are usually ineffective for rescuing these patients.<sup>2</sup> In this study, we investigated humoral and cellular features of GF occurring after allogeneic HSCT in children, documenting a pivotal role played by IFN $\gamma$  in the pathophysiology of this complication. Apart from the indirect evidence provided by the observation of very high rates of primary and secondary rejection after HLA-identical HSCT in patients with IFN $\gamma$ -receptor 1 deficiency,<sup>21</sup> currently available clinical data about the role of IFN $\gamma$  in GF in humans remain limited. Interestingly, we found that GF is characterized by the same clinical (including high-grade fever, hepato/splenomegaly, hemophagocytosis in BM)<sup>22,23</sup> and laboratory (i.e. increased ferritin, IFN $\gamma$ , CXCL9, CXCL10, sCD163 and sIL-2R $\alpha$  levels)<sup>24,26</sup> features found in patients with HLH, where a central role of IFN $\gamma$  has been shown.<sup>29</sup>

Our data indicate that IFN $\gamma$  levels, and even more CXCL9 levels measured in PB, can predict GF with high sensitivity and specificity already at day +3 after graft

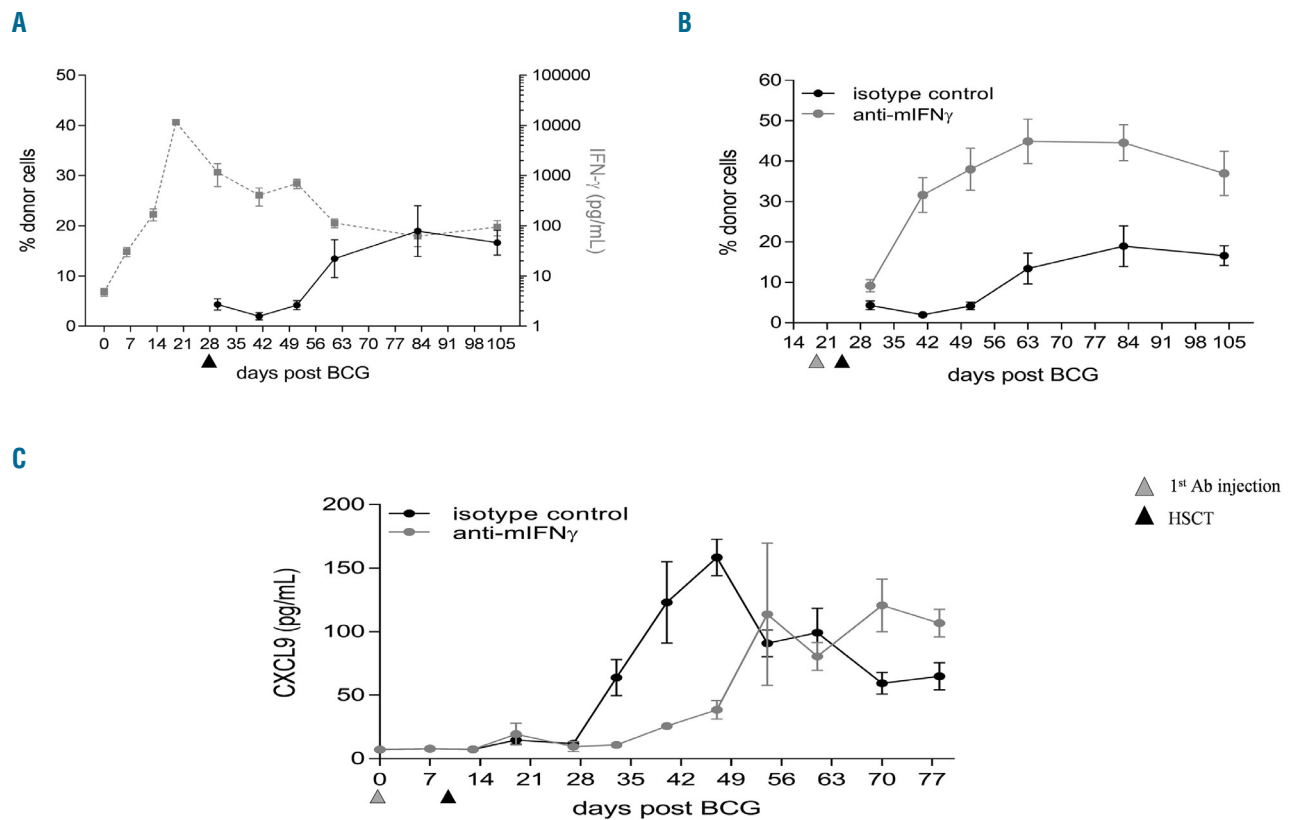


**Figure 6. Successful hematopoietic stem cell transplantation (HSCT) chimerism in interferon (IFN) $\gamma$ R1 $^{-/-}$  mice correlates with low IFN $\gamma$  activity; circulating CXCL9 levels is a biomarker of *in vivo* IFN $\gamma$  activity.** Ifng $1^{-/-}$  mice (expressing the Ly5.2 congenic marker) were intravenously (i.v.) infected with 1,106 CFU of *Bacillus Calmette–Guérin* (BCG) (strain Pasteur 1173P2). After 14, 20, 28, 35 and 42 days mice were treated i.v. with 100 mg/kg of an isotype control (n=5) or the anti-mIFN $\gamma$ , XMG1.2 (n=5). At day 21, mice were infused with bone marrow from Ifng $1^{+/+}$  mice, expressing the Ly5.1 marker, after mild irradiation (550 rads). Chimerism, assessed by determining the surface expression of Ly5.1 and Ly5.2 on lymphocytes, was analyzed by flow cytometry at different time points after HSCT treatment. IFN $\gamma$  levels were quantified at different time points by ELISA using the Luminex technology. (A) Graph represents the super-imposition of the chimerism (black straight line) and the IFN $\gamma$  levels (gray dotted line) in the isotype control treated mice. (B) Graph represents the chimerism determined in mice treated with the isotype control (black straight line) or with the XMG1.2 (gray straight line) mAbs. (C) Ifng $1^{-/-}$  mice were i.v. infected with 1,106 CFU of BCG (strain Pasteur 1173P2). After 14, 20, 28, 35 and 42 days mice were treated i.v. with 100 mg/kg of an isotype control (black straight line; n=5) or the anti-mIFN $\gamma$ , XMG1.2 (gray straight line; n=5). At day 21, mice were transplanted with bone marrow from Ifng $1^{+/+}$  mice, expressing the Ly5.1 marker, after mild irradiation (550 rads). At different time points post-BCG infection, circulating CXCL9 levels were quantified by ELISA using the Luminex technology. Ab: antibody.

infusion, while signs and symptoms of GF appear only later (see Table 2). Indeed, the current proposed risk score for GF determined on day +21 after HSCT, based on eight patient and transplant variables, showed good specificity, but low sensitivity.<sup>1</sup> The high accuracy of CXCL9 in predicting GF, as indicated by the AUC of 0.905, renders this chemokine an ideal “candidate biomarker”, as stated by the 2014 National Institutes of Health consensus on biomarkers.<sup>30,31</sup> CXCL9, also known as monokine induced by  $\gamma$ -interferon (MIG), is a chemokine specifically induced by IFN $\gamma$ ,<sup>32</sup> and represent the most sensitive and specific of the soluble factors we analyzed. It binds to the chemokine receptor CXCL3 expressed on naïve T cells, Th1 CD4 $^{+}$  T cells, effector CD8 $^{+}$  T cells, as well as on NK and NKT cells, driving Th1 inflammation. Circulating CXCL9 levels have been shown to reflect the amount of IFN $\gamma$  produced in organs, such as liver and spleen,<sup>25</sup> which are the typical target of inflammation. This strong correlation with IFN $\gamma$  produced in organs rather than in blood provides an explanation why, despite high CXCL9 serum levels, serum levels of IFN $\gamma$  were found to be low or even undetectable in a few of our GF patients. Furthermore, elevated levels of

CXCL9 have been related to graft rejection in solid organ transplantation (such as heart, kidney and lung transplantation),<sup>33,35</sup> but, to the best of our knowledge, this is the first report demonstrating that the hyperproduction of IFN $\gamma$  in GF occurring after HSCT results in increased CXCL9 serum levels. Among other cytokines/chemokines, we also observed increased levels of IL10, an important Th2 cytokine with anti-inflammatory properties, this finding being in agreement with the hyperproduction of this molecule recorded in patients with HLH.<sup>36</sup>

Our results are not only relevant for diagnostic purposes, but also suggest that IFN $\gamma$  is a potential therapeutic target in GF. Indeed, independently of the mechanism of IFN $\gamma$ -mediated GF (i.e. direct effect on HSC or HLH-like effect), our results support the investigation of IFN $\gamma$  neutralization for prevention and/or treatment of GF in patients undergoing HSCT. The encouraging efficacy and safety data reported from the ongoing study in primary HLH with emapalumab (NI-0501), an anti-IFN $\gamma$  monoclonal antibody,<sup>17,37</sup> provides additional support for the rationale for using this drug.<sup>38</sup> The data we generated in the murine model of GF confirm and extend the role played by IFN $\gamma$

previously demonstrated by Rottman *et al.*<sup>13</sup> Moreover, we also show that the sole neutralization of IFN $\gamma$ , without the administration of anti-IL12 (employed in the experiments reported by Rottman *et al.*),<sup>13</sup> is able to improve engraftment. The observation that decreased CXCL9 production correlates with improved HSCT chimerism provides further support to a therapeutic intervention aimed at neutralizing IFN $\gamma$ -pathway signaling. Finally, the data obtained in the three patients treated on a CU basis indicate that the use of an anti-IFN $\gamma$  monoclonal antibody is safe also in a very fragile population, namely infants with a previous GF undergoing a second HSCT.

Four out of the seven patients we studied who underwent BM aspirate and biopsy showed evidence of hemophagocytosis. Indeed, it has been shown that an increased number of hemophagocytic macrophages in the BM obtained 14 $\pm$ 7 days after HSCT is associated with higher risk of death due to GF.<sup>39</sup> Moreover, in a cohort of adult patients receiving cord blood transplantation, GF was strictly related to the occurrence of HLH manifestations.<sup>23</sup> Recently, in a retrospective study on peri-engraftment BM samples from 32 adult patients, Kawashima *et al.* proposed two histological measures, namely macrophage ratio and CD8<sup>+</sup> ratio (defined as the ratio between the macrophage or CD8<sup>+</sup> lymphocyte number on the total nucleated cell number), as predictors of GF at day +14.<sup>15</sup>

Despite some preliminary studies characterizing host T cell expansion in patients with GF,<sup>15,16</sup> no information is available regarding the phenotype of these cells. Our data indicate an active role of T lymphocytes in mediating GF. As previously reported,<sup>15</sup> in these patients, the mononuclear infiltrate is mainly constituted by cytotoxic CD8<sup>+</sup> lymphocytes with a predominant effector memory phenotype. This population was demonstrated to be activated, proliferating and cytotoxic, expressing specific molecules, such as Granzyme B, Perforin and TIA-1, involved in target-killing, as well as various activation and proliferation markers. Interestingly, we observed that CD8<sup>+</sup> lymphocyte expansion is predominantly polyclonal, suggesting that the immune response is directed towards several antigens and not against few immunodominant epitopes. However, a significant enrichment of certain  $\beta$  clones was found. The cytopathic effect was clearly demonstrated by apoptotic cells surrounding proliferating T cells, which are long-term activated, as demonstrated by the expression of several exhaustion markers.<sup>40,41</sup> Furthermore, the remaining  $\gamma\delta$  and CD4<sup>+</sup> T-cell populations are similarly expressing exhaustion markers, underlying an over-stimulated environment. Notably, a particular behavior was observed

in the NKT-cell population with a significant reduction of CD8<sup>+</sup> NKT, probably due to their activation and a significant increase of CD4<sup>+</sup> NKT. The role of these cells is yet to be fully elucidated, although they were shown to be able to prevent pancreatic islet transplant rejection, but also to sustain CD8<sup>+</sup> T-cell expansion.<sup>42,43</sup> Given these data, a treatment able to interrupt the overproduction of molecules responsible for inflammation,<sup>33</sup> such as an anti-IFN $\gamma$ , could be beneficial in this setting.

Fifty percent of tested patients had anti-HLA antibodies: all those with positivity >5,000 MFI received a desensitization therapy in order to lower the antibody titer with the aim of reducing the risk of GF. Although we cannot exclude a role of anti-HLA antibodies in causing GF in our patients, all five positive patients showed increased values of IFN $\gamma$  and/or related cytokines after HSCT. Thus, we can hypothesize that there may be a common final pathway and/or combined action (like that reported in solid organ transplantation)<sup>44</sup> between humoral and cellular mechanisms sustaining GF.

Limitations of this study are the lack of a validation cohort and the relatively small number of patients included in the study. Another important limitation is that most patients experiencing GF that we report were transplanted from a PMFD after a TCD procedure (both being well-known risk factors for GF);<sup>2,3</sup> thus, our results should be further validated in other transplant settings, especially when post-transplant pharmacological graft-versus-host disease prophylaxis is used. Indeed, the use of calcineurin inhibitors or other immunosuppressive agents can modify IFN $\gamma$  (and related cytokines) secretion kinetics.<sup>45</sup>

Overall, our data suggest that immune-mediated GF may share clinical and laboratory characteristics with HLH. Besides providing evidence for further investigating the use of markers to allow a non-invasive, prompt identification of patients at high risk of developing this severe complication of HSCT, the increased serum levels of IFN $\gamma$  and CXCL9 found in GF patients provide a rationale for investigating a targeted therapy (i.e. anti-IFN $\gamma$  therapy) in this complication. We are currently designing a clinical trial on the use of emapalumab for prevention and/or treatment of GF in patients at high risk of developing this complication.

### Funding

This work was supported by "Ricerca corrente" (Ministero della Salute) (PM), Investigator Grant 2015 Id. 17200 by Associazione Italiana per la Ricerca sul Cancro (AIRC) (FL) and by Novimmune SA, Switzerland.

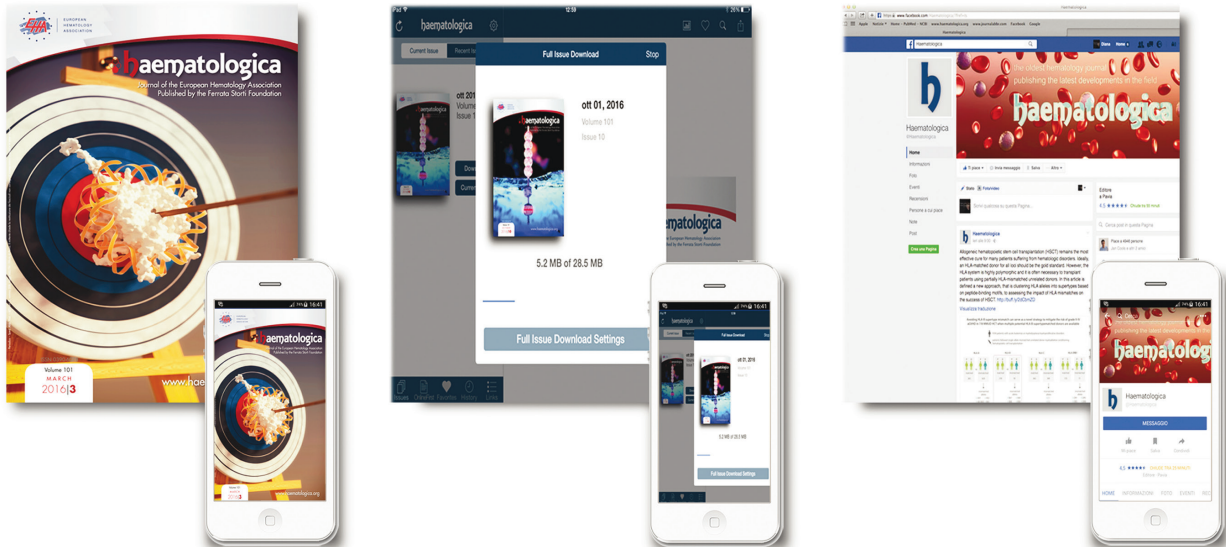
### References

- Olsson RF, Logan BR, Chaudhury S, et al. Primary graft failure after myeloablative allogeneic hematopoietic cell transplantation for hematologic malignancies. *Leukemia*. 2015;29(8):1754-1762.
- Locatelli F, Lucarelli B, Merli P. Current and future approaches to treat graft failure after allogeneic hematopoietic stem cell transplantation. *Expert Opin Pharmacother*. 2014;15(1):23-36.
- Olsson R, Remberger M, Schaffer M, et al. Graft failure in the modern era of allogeneic hematopoietic SCT. *Bone Marrow Transplant*. 2013;48(4):537-543.
- Cluzeau T, Lambert J, Raus N, et al. Risk factors and outcome of graft failure after HLA matched and mismatched unrelated donor hematopoietic stem cell transplantation: a study on behalf of SFGM-TC and SFHI. *Bone Marrow Transplant*. 2016;51(5):687-691.
- Masouridi-Levrat S, Simonetta F, Chalandon Y. Immunological Basis of Bone Marrow Failure after Allogeneic Hematopoietic Stem Cell Transplantation. *Front Immunol*. 2016;7:362.
- Murphy WJ, Kumar V, Bennett M. Acute rejection of murine bone marrow allografts by natural killer cells and T cells. Differences in kinetics and target antigens recognized. *J Exp Med*. 1987;166(5):1499-1509.
- Komatsu M, Mammolenti M, Jones M, Jurecic R, Sayers TJ, Levy RB. Antigen-primed CD8<sup>+</sup> T cells can mediate resistance, preventing allogeneic marrow engraftment in the simultaneous absence of perforin-, CD95L-, TNFR1-, and TRAIL-dependent killing. *Blood*. 2003;101(10):3991-3999.
- Chen J, Feng X, Desierto MJ, Keyvanfar K, Young NS. IFN- $\gamma$ -mediated hematopoietic cell destruction in murine models of immune-mediated bone marrow failure. *Blood*. 2015;126(24):2621-2631.

9. Chen J, Lipovsky K, Ellison FM, Calado RT, Young NS. Bystander destruction of hematopoietic progenitor and stem cells in a mouse model of infusion-induced bone marrow failure. *Blood*. 2004;104(6):1671-1678.
10. de Bruin AM, Demirel O, Hooibrink B, Brandts CH, Nolte MA. Interferon- $\gamma$  impairs proliferation of hematopoietic stem cells in mice. *Blood*. 2013;121(18):3578-3585.
11. Lin FC, Karwan M, Saleh B, et al. IFN- $\gamma$  causes aplastic anemia by altering hematopoietic stem/progenitor cell composition and disrupting lineage differentiation. *Blood*. 2014;124(25):3699-3708.
12. Maciejewski J, Selleri C, Anderson S, Young NS. Fas antigen expression on CD34+ human marrow cells is induced by interferon  $\gamma$  and tumor necrosis factor  $\alpha$  and potentiates cytokine-mediated hematopoietic suppression in vitro. *Blood*. 1995;85(11):3183-3190.
13. Rottman M, Soudais C, Vogt G, et al. IFN- $\gamma$  mediates the rejection of haematopoietic stem cells in IFN- $\gamma$ R1-deficient hosts. *PLoS Med*. 2008;5(1):e26.
14. Selleri C, Maciejewski JP, Sato T, Young NS. Interferon- $\gamma$  constitutively expressed in the stromal microenvironment of human marrow cultures mediates potent hematopoietic inhibition. *Blood*. 1996; 87(10):4149-4157.
15. Kawashima N, Terakura S, Nishiwaki S, et al. Increase of bone marrow macrophages and CD8+ T lymphocytes predict graft failure after allogeneic bone marrow or cord blood transplantation. *Bone Marrow Transplant*. 2017;52(8):1164-1170.
16. Koyama M, Hashimoto D, Nagafuji K, et al. Expansion of donor-reactive host T cells in primary graft failure after allogeneic hematopoietic SCT following reduced-intensity conditioning. *Bone Marrow Transplant*. 2014;49(1):110-115.
17. Jordan M, Locatelli F, Allen C, et al. A Novel Targeted Approach to the Treatment of Hemophagocytic Lymphohistiocytosis (HLH) with an Anti-Interferon  $\gamma$  (IFN  $\gamma$ ) Monoclonal Antibody (mAb), NI-0501: First Results from a Pilot Phase 2 Study in Children with Primary HLH. *Blood*. 2015; 126(23):3.
18. Ciurea SO, Thall PF, Milton DR, et al. Complement-Binding Donor-Specific Anti-HLA Antibodies and Risk of Primary Graft Failure in Hematopoietic Stem Cell Transplantation. *Biol Blood Marrow Transplant*. 2015;21(8):1392-1398.
19. Messina C, Zecca M, Fagioli F, et al. Outcomes of Children with Hemophagocytic Lymphohistiocytosis Given Allogeneic Hematopoietic Stem Cell Transplantation in Italy. *Biol Blood Marrow Transplant*. 2018;24(6):1223-1231.
20. Utschneider DT, Alfei F, Roelli P, et al. High antigen levels induce an exhausted phenotype in a chronic infection without impairing T cell expansion and survival. *J Exp Med*. 2016;213(9):1819-1834.
21. Roesler J, Horwitz ME, Picard C, et al. Hematopoietic stem cell transplantation for complete IFN- $\gamma$  receptor 1 deficiency: a multi-institutional survey. *J Pediatr*. 2004; 145(6):806-812.
22. Abe Y, Choi I, Hara K, et al. Hemophagocytic syndrome: a rare complication of allogeneic nonmyeloablative hematopoietic stem cell transplantation. *Bone Marrow Transplant*. 2002;29(9):799-801.
23. Takagi S, Masuoka K, Uchida N, et al. High incidence of haemophagocytic syndrome following umbilical cord blood transplantation for adults. *Br J Haematol*. 2009; 147(4):543-553.
24. Bracaglia C, de Graaf K, Pires Marafon D, et al. Elevated circulating levels of interferon- $\gamma$  and interferon- $\gamma$ -induced chemokines characterize patients with macrophage activation syndrome complicating systemic juvenile idiopathic arthritis. *Ann Rheum Dis*. 2017;76(1):166-172.
25. Buatois V, Chatel L, Cons L, et al. Use of a mouse model to identify a blood biomarker for IFN $\gamma$  activity in pediatric secondary hemophagocytic lymphohistiocytosis. *Transl Res*. 2017;180:37-52.e2.
26. Henter JI, Elinder G, Soder O, Hansson M, Andersson B, Andersson U. Hypercytokinemia in familial hemophagocytic lymphohistiocytosis. *Blood*. 1991; 78(11):2918-2922.
27. Xu XJ, Tang YM, Song H, et al. Diagnostic accuracy of a specific cytokine pattern in hemophagocytic lymphohistiocytosis in children. *J Pediatr*. 2012;160(6):984-990.e1.
28. Yang SL, Xu XJ, Tang YM, et al. Associations between inflammatory cytokines and organ damage in pediatric patients with hemophagocytic lymphohistiocytosis. *Cytokine*. 2016;85:14-17.
29. Jordan MB, Hildeman D, Kappler J, Marrack P. An animal model of hemophagocytic lymphohistiocytosis (HLH): CD8+ T cells and interferon  $\gamma$  are essential for the disorder. *Blood*. 2004;104(3):735-743.
30. Paczesny S. Biomarkers for posttransplantation outcomes. *Blood*. 2018;131(20):2193-2204.
31. Paczesny S, Hakim FT, Pidala J, et al. National Institutes of Health Consensus Development Project on Criteria for Clinical Trials in Chronic Graft-versus-Host Disease: III. The 2014 Biomarker Working Group Report. *Biol Blood Marrow Transplant*. 2015;21(5):780-792.
32. Groom JR, Luster AD. CXCR3 ligands: redundant, collaborative and antagonistic functions. *Immunol Cell Biol*. 2011;89(2):207-215.
33. Fahmy NM, Yamani MH, Starling RC, et al. Chemokine and chemokine receptor gene expression indicates acute rejection of human cardiac transplants. *Transplantation*. 2003;75(1):72-78.
34. Gupta A, Broin PO, Bao Y, et al. Clinical and molecular significance of microvascular inflammation in transplant kidney biopsies. *Kidney Int*. 2016;89(1):217-225.
35. Medoff BD, Wain JC, Seung E, et al. CXCR3 and its ligands in a murine model of obliterative bronchiolitis: regulation and function. *J Immunol*. 2006;176(11):7087-7095.
36. An Q, Hu SY, Xuan CM, Jin MW, Ji Q, Wang Y. Interferon  $\gamma$  and interleukin 10 polymorphisms in Chinese children with hemophagocytic lymphohistiocytosis. *Pediatr Blood Cancer*. 2017;64(9).
37. Locatelli F, Jordan M, Allen C, et al. Safety and efficacy of emapalumab in pediatric patients with primary hemophagocytic lymphohistiocytosis. *Blood*. 2018;132(Suppl 1):LBA-6.
38. Prencipe G, Caiello I, Pascarella A, et al. Neutralization of interferon- $\gamma$  reverts clinical and laboratory features in a mouse model of macrophage activation syndrome. *J Allergy Clin Immunol*. 2018; 141(4):1439-1449.
39. Imahashi N, Inamoto Y, Ito M, et al. Clinical significance of hemophagocytosis in BM clot sections during the peri-engraftment period following allogeneic hematopoietic SCT. *Bone Marrow Transplant*. 2012; 47(3):387-394.
40. Ferris RL, Lu B, Kane LP. Too much of a good thing? Tim-3 and TCR signaling in T cell exhaustion. *J Immunol*. 2014;193(4):1525-1530.
41. Jin HT, Anderson AC, Tan WG, et al. Cooperation of Tim-3 and PD-1 in CD8 T-cell exhaustion during chronic viral infection. *Proc Natl Acad Sci U S A*. 2010; 107(33):14733-14738.
42. Ikehara Y, Yasunami Y, Kodama S, et al. CD4(+) Valpha14 natural killer T cells are essential for acceptance of rat islet xenografts in mice. *J Clin Invest*. 2000; 105(12):1761-1767.
43. Lin H, Nieda M, Rozenkov V, Nicol AJ. Analysis of the effect of different NKT cell subpopulations on the activation of CD4 and CD8 T cells, NK cells, and B cells. *Exp Hematol*. 2006;34(3):289-295.
44. Zeglen S, Zakliczynski M, Wozniak-Grygiel E, et al. Mixed cellular and humoral acute rejection in elective biopsies from heart transplant recipients. *Transplant Proc*. 2009; 41(8):3202-3205.
45. Grant CR, Holder BS, Liberal R, et al. Immunosuppressive drugs affect interferon (IFN)- $\gamma$  and programmed cell death 1 (PD-1) kinetics in patients with newly diagnosed autoimmune hepatitis. *Clin Exp Immunol*. 2017;189(1):71-82.



# RESEARCH, READ & CONNECT



We reach more than  
**6 hundred thousand readers each year**

**The first Hematology Journal in Europe**

Impressions YTD

**9,621,645**

Digital Readers

**4,431**

Total Audience

**554,484**

Worldwide rank

**7<sup>th</sup>**

Impact factor

**7.570**

Total citations

**16,255**



Journal of the Ferrata Storti Foundation

